ЖУРНАЛ
ЭКСПЕРИМЕНТАЛЬНОЙ И ТЕОРЕТИЧЕСКОЙ
ФИЗИКИ
АКАДЕМИЯ НАУК СССР

SOVIET PHYSICS

JETP

VOLUME 5 NUMBER 6

A Translation
of the
Journal of Experimental and Theoretical Physics
of the
Academy of Sciences of the USSR

Volume 32

DECEMBER 15, 1957

Published by the
AMERICAN INSTITUTE OF PHYSICS
INCORPORATED

SOVIET PHYSICS
JETP

A translation of the Journal of Experimental and Theoretical Physics of the USSR.

A publication of the

AMERICAN INSTITUTE OF PHYSICS

Governing Board

Frederick Seitz, *Chairman*
Allen V. Astin
Walter S. Baird
Jesse W. Beams
Hans A. Bethe
Raymond T. Birge
Richard H. Bolt
Franklin D. Dexter
Irvine C. Gardner
Samuel A. Goudsmit
Charles Kittel
Hugh S. Knowles
Winston E. Kock
R. Bruce Lindsay
William F. Meggers
Walter C. Michels
R. Ronald Palmer
Robert F. Paton
Joseph B. Platt
Ralph A. Sawyer
Henry D. Smyth
Mark W. Zemansky

Administrative Staff

Elmer Hutchisson
Director
Henry A. Barton
Associate Director
Mark W. Zemansky
Treasurer
Wallace Waterfall
Executive Secretary
Theodore Vorburger
Advertising Manager
Ruth F. Bryans
Publication Manager
Alice Mastro
Circulation Manager
Kathryn Setze
Assistant Treasurer
Eugene H. Kone
Director of Public Relations

American Institute of Physics Advisory Board on Russian Translations

Robert T. Beyer, *Chairman*
Dwight Gray, Morton Hamermesh, Vladimir Rojansky,
Freeman Dyson

Editor of Soviet Physics–JETP

J. George Adashko, Department of Electrical Engineering,
The City College of New York, Convent Avenue and
139th Street, New York, New York.

Soviet Physics is a monthly journal published by the American Institute of Physics for the purpose of making available in English reports of current Soviet research in physics as contained in the Journal of Experimental and Theoretical Physics of the Academy of Sciences of the USSR. The page size of Soviet Physics will be 7⅞" x 10½", the same as other Institute journals.

Transliteration of the names of Russian authors follows the system employed by the Library of Congress.

This translating and publishing project was undertaken by the Institute in the conviction that dissemination of the results of researches everywhere in the world is invaluable to the advancement of science. The National Science Foundation of the United States encouraged the project initially and is supporting it in large part by a grant.

The American Institute of Physics and its translators propose to translate faithfully all the material in the Journal of EXPERIMENTAL AND THEORETICAL PHYSICS OF THE USSR appearing after January 1, 1955. The views expressed in the translated material, therefore, are intended to be those expressed by the original authors, and not those of the translators nor of the American Institute of Physics.

Two volumes are published annually, each of six issues. Each volume contains the translation of one volume of the Journal of EXPERIMENTAL AND THEORETICAL PHYSICS OF THE USSR. New volumes begin in February and August.

Subscription Prices:

Per year (12 issues)	
United States and Canada	$60.00
Elsewhere	64.00
Back Numbers	
Single copies	$ 6.00

Subscriptions should be addressed to the American Institute of Physics, 335 East 45th Street, New York 17, New York.

Copyright by American Institute of Physics 1957

SOVIET PHYSICS

JETP

A translation of the Journal of Experimental and Theoretical Physics of the USSR.

SOVIET PHYSICS—JETP Vol. 5, No. 6, pp 1033-1339 DECEMBER 15, 1957

Production of π^+ Mesons in $p-p$ Collisions at 480–660 Mev.*

B. S. NEGANOV AND O. V. SAVCHENKO

Joint Institute for Nuclear Research

(Submitted to JETP editor October 21, 1956)

J. Exptl. Theoret. Phys. (U.S.S.R.) **32**, 1265-1275 (June, 1957)

The energy distributions of π^+ mesons from the reactions $p + p \rightarrow \pi^+ + n + p$ and $p + p \rightarrow \pi^+ + d$ have been measured at four laboratory system angles utilizing an external beam of 660 Mev protons. The differential cross section for π^+ meson production has been measured at eight laboratory system angles. The total cross section for the first reaction is (10.9 ± 1.1) mb and the angular distribution is proportional to $(0.66 \pm 0.14) + \cos^2\theta$. The excitation function of this reaction is given in the energy region 480–660 Mev approximately by the power law $0.67\,P_{\max}^{4.7}$ mb, where $P_{\max}$ is the maximum meson momentum in units of $m_{\pi^+}c$ in the center-of-mass system.

INTRODUCTION

MESON PRODUCTION in nucleon-nucleon collision is a more involved process than meson nucleon scattering or meson photoproduction on free nucleons. Thus, experiments on meson production in nucleon-nucleon collisions can yield important information on the characteristics of mesons and of the meson-nucleon interaction.

The reactions that lead to charged meson production in $p-p$ collisions at 600 Mev are

$$p + p \rightarrow \pi^+ + n + p; \qquad (1)$$

$$p + p \rightarrow \pi^+ + d. \qquad (2)$$

Production of two mesons which is energetically possible for proton energies above 600 Mev contributes only very little to the total cross section and is not considered in the present work. Lately there have appeared several papers on π^+ production in the energy region of this investigation. The reaction (2) was studied in detail in Ref. 1, using counter telescopes for the angles 30° to 90° in the center of mass system (c.m.s.). The excitation functions for this reaction were obtained in the energy range 510 to 660 Mev. In Ref. 2 reaction (1) was studied at an energy of 660 Mev in the same angular range by emulsion techniques.* The spectrum of the π^+ mesons was investigated in Ref. 3 with a magnetic spectrometer at an angle of 24° in the laboratory system (l.s.) at 660 and 560 Mev.

---

* This paper was presented at the High Energy Particle Conference in May, 1956, in Moscow.

* An error contained in Ref. 2 should be pointed out. In that paper the differential cross section was obtained using for the energy loss the formula $(dE/dR)_E = 0.067\,R_\pi^{0.419}$ which has been derived empirically from range–energy measurements in emulsions. This formula is valid for small energies. However, extrapolating it into the energy region around 170 Mev one will obtain values for $(dE/dR)_E$ which are for meson energies 100–150 Mev lower by 20–40% than the actual energy loss of mesons in copper which was used to slow down the π^+ mesons. After correcting for this error both the energy and the angular distributions obtained in Ref. 2 change and the agreement of the angular distributions of Ref. 2 with the ones obtained in the present work is considerably improved.

In the present work reactions (1) and (2) were studied at the angles 10° to 40° in the c.m.s. This angular region had not been investigated earlier. Furthermore additional information was obtained on the angular distribution of π^+ mesons from reaction (1) at angles 50° to 80° in the c.m.s., and the excitation function for this reaction was determined for the energies 480 to 660 Mev.

EXPERIMENTAL ARRANGEMENT

It follows from kinematical considerations that nucleons emerging from reaction (1) are restricted to certain angles in the l.s. For 660 Mev incoming protons this angle is about 50°. Since protons scattered elastically into large angles have small energies, it is possible to distinguish these from mesons at angles larger than 70° by means of a thin filter.

Experiments on π^+ production in the energy range 660–480 Mev became feasible after an external high intensity 657-Mev proton beam was produced with the synchrocyclotron of the Institute for Nuclear Problems of the U.S.S.R. Academy of Sciences. The proton beam passed through steel collimators inserted into the concrete shielding wall and fell on the target after passing through an ionization chamber (see Fig. 1). The average intensity at the target position was 3×10^8 protons/cm^2 sec and was monitored by the ionization chamber. The chamber was calibrated with respect to proton current in absolute terms by means of a Faraday cup. Proton energies below 657 Mev were obtained by placing polyethylene absorbers in the path of the beam before it passed through the collimators. The energy uncertainty at 500 Mev was ± 7 Mev.

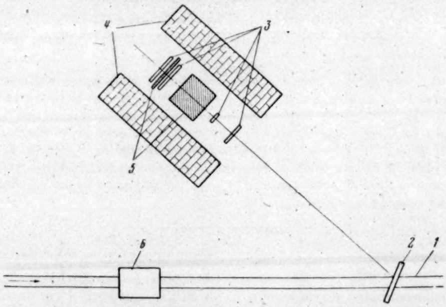

FIG. 1. Experimental setup. 1 – proton beam; 2 – target; 3 – scintillation counters; 4 – lead shield; 5 – copper or aluminum filters; 6 – monitor.

The π^+ production cross section on hydrogen at 60° –160° l.s. was obtained as the difference of charged particle yields from polyethylene and carbon targets, equal with respect to energy loss and with a thickness of about 1 g/cm^2. The excitation function was obtained with a liquid hydrogen target. The Dewar was made of glass. The effective target volume was defined by lead collimators which provided a shield for the detector against charged particles generated by the incoming protons in the glass walls of the Dewar.

The charged particles coming from the target were detected by a counter telescope. The first three scintillation counters were in coincidence, the fourth in anticoincidence. Between the second and the third counters was placed a copper or aluminum filter of different thickness. The interval of accepted ranges was given by the thickness of the filter placed between the third and the fourth counters. To produce a count a charged particle had to pass through the first three counters and stop in the filter between the third and the fourth counter. The first three counters consisted of 2 mm thick crystalline tolane (diphenyl acetylene) scintillators which were provided with special reflectors made of aluminum foil to increase the light collection efficiency. The counting efficiency of the telescope had a plateau of 200 v thus assuring a good stability of the setup. The efficiency of the telescope was determined by measuring the angular distribution of the charged particle yield from p–p collisions.

The integral

$$\int_0^{2\pi}\int_0^{\pi}\frac{1}{2}\frac{\partial\sigma}{\partial\omega}\sin\theta\,d\theta\,d\varphi \tag{3}$$

in the case of p–p collisions has to be equal to the total interaction cross section. Here $\partial\sigma/\partial\omega$ is the differential cross section for charged particle emission in the direction θ in the l.s. This is due to the fact that in the energy region of interest, where multiple meson production is still unimportant, only two charged particles are always formed in the final state of a p–p collision, because of charge conservation. In the present investigation the value obtained for the integral was (42.9 ± 1.5) mb, in good agreement with the total p–p cross section of (41.4 ± 0.6) mb obtained in Ref. 4. This shows that the efficiency of the counter telescope was close to 100% despite the small thickness of the scintillators. Because of the thinness of the counters it was possible to detect mesons with energies down to 15 Mev, and furthermore the number of chance coincidences was also decreased. These constituted the bulk of the background in the present experiment. By surrounding the counter telescope with a 10 cm lead shield the accidental counting rate was further reduced and the background then did not exceed 0.5% of the true counting rate.

EXPERIMENTAL RESULTS

The differential cross sections for π^+ meson production according to reactions (1) and (2) at an energy of 657 Mev were determined at eight angles in the l.s., running at full beam intensity. The results are given in Table 1. They include mesons with energies from 15 Mev in the l.s. up. The given cross sections include corrections due to decay in flight (6–3%) and to nuclear capture both in the target and in the scintillators (1.5%).

TABLE I. Differential cross sections in mb/sterad for mesons with energy greater than 15 Mev in the l.s.*

θ, lab system	160°	140°	123°	108°	95°	86°	70°	60°
$\left(\frac{\partial\sigma}{\partial\omega}\right)_{\text{lab}}$, $\frac{\text{mb}}{\text{sterad}}$	0.36 ±0.03	0.40 ±0.03	0.49 ±0.03	0.61 ±0.03	0.74 ±0.06	0.84 ±0.06	0.88 ±0.12	0.87 ±0.19

* The given errors are standard deviations from several independent runs.

Further, the energy distribution of π^+ mesons at primary energy of 657 Mev were determined for the angles 160°, 140°, 123°, and 108° in the l.s. The results were corrected for decay in flight, and for nuclear interactions and multiple scattering in the filters and scintillators of the counter telescope. The resulting counting efficiency for π^+ mesons is shown in Fig. 2 as a function of meson energy. The accuracy of these corrections was checked by comparing the number of mesons obtained by integrating the obtained spectrum with the number of mesons counted in the absence of a filter in the first three scintillators. The results of this comparison are summarized in Table 2.

From comparison of lines 2 and 3 of Table 2 one may conclude that the uncertainty in the counting efficiency for π^+ mesons does not exceed 10%. The energy distributions of the π^+ mesons after applying the corrections were normalized with respect to the total cross sections given in Table 1. The obtained spectra are shown in Fig. 3. The indicated

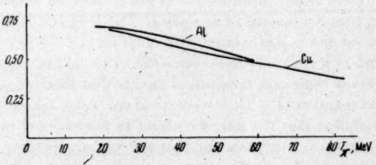

FIG. 2. Counting efficiency for π^+ mesons as a function of energy.

TABLE 2.

π^+ meson angle in the l.s.	160°	140°	123°	108°
Total number of mesons, N_1, from integrating the energy distributions	11300	7940	16090	18860
Number of mesons, N_2, counted in the first three scintillators	11200	8130	15840	16940
Ratio N_2/N_1	0.99±0.03	1.02±0.03	0.98±0.03	0.90±0.03

TABLE 3. Energy distribution of π^+ mesons from reactions (1) and (2).

E_p, Mev	485	521	557	584	597	609	621	633	646	657
$\left(\frac{\partial\sigma}{\partial\omega}\right)$ 95° l.s., in relative units	1.97 ±0.09	2.69 ±0.13	3.54 ±0.13	4.19 ±0.10	4.60 ±0.10	5.02 ±0.09	5.39 ±0.08	5.91 ±0.12	6,39 ±0,13	6.81 ±0.15

errors are the standard deviations due to counting statistics and the points are averages from two separate series of runs.

The excitation function for π^+ mesons from reactions (1) and (2) was obtained for a meson angle of 95° in the l.s. The results were corrected for the change of the ionization of protons at reduced energies, and for the admixture of slow particles to the beam generated in the polyethylene slabs which were used to slow down the protons. The latter correction was determined experimentally and did not exceed 4% under the most unfavorable conditions. The yield of mesons from reactions (1) and (2) for different proton energies is given in Table 3 in relative units.

DISCUSSION OF THE RESULTS

Each energy distribution of the π^+ mesons shown in Fig. 3 consists of two parts. The first one is broad and is associated with reaction (1); the second is a peak due to reaction (2). The dashed curves represent theoretical energy distributions for reaction (1). They were obtained under the assumption that the matrix element is proportional to the meson momentum and that one can neglect nucleon–nucleon interactions in the final state. Then the cross section is given by

$$\frac{\partial^2\sigma}{\partial E\,\partial\omega} \sim \frac{1}{\beta_\pi}\left[M\left(W-\sqrt{p^2+m^2}\right)-\frac{p^2}{4}\right]^{1/2} p^4, \tag{4}$$

where M and m are the nucleon and meson mass respectively, W is the kinetic energy of the protons in the c.m.s., and E, p, and β_π are the meson kinetic energy, momentum and velocity respectively also in the c.m.s. In deriving this formula the nucleons in the final state were assumed to be nonrelativistic. This is reasonable since for a primary energy of 660 Mev the maximum possible nucleon energy in the final state is 87 Mev. After transforming into the l.s. the theoretical cross sections were normalized to the experimental curves in the energy region where contributions from reaction (2) were fully excluded. The dash-dot curves were similarly calculated but with the assumption that the matrix element is independent of meson momentum. It is clearly evident that the other assumption leads to better agreement with the experiment.

The peak in the experimental distribution can now be separated out rather easily using the theoretical expression (4), taking into account the energy resolution of the detector. This is the dashed curve in Fig. 3. The curves shown on the right side for each angle in Fig. 3 have been obtained this way. The solid curves which have been drawn through the points represent the theoretical resolu-

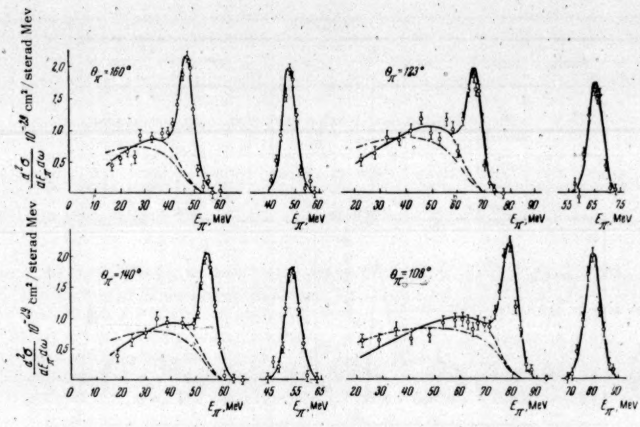

FIG. 3. Energy distributions of π^+ mesons from the reactions $p + p \rightarrow \pi^+ n + p$ and $p + p \rightarrow \pi^+ + d$; laboratory system energies and angles.

tion curves for the mesons from reaction (2). The form of the curves is given by

$$N(E) \sim \int_E^\infty \exp\left\{-\frac{(E_1 - E_0)^2}{\langle \Delta E^2 \rangle}\right\} \exp\left\{-\frac{(E_1 - E)}{\langle E \rangle}\right\} dE_1, \quad (5)$$

Here $<\Delta E^2>$ is the r.m.s. fluctuation of the meson energy including all factors contributing to the energy resolution of the setup; $< E > = < \Delta R > dE/dR$ with $< \Delta R >$ the average range shortening of the mesons in the filters due to multiple Coulomb scattering, and E_0 is the kinetic energy of the mesons from reaction (2).

The differential cross sections for meson production in reaction (2), obtained from the area under the peaks and transformed into the c.m.s., are given in Table 4.

The obtained points are plotted in Fig. 4, which also shows the points obtained in Ref. 1. One sees that the angular distribution given in Ref. 1 also holds for small angles. This shows that contributions of d-wave mesons in reaction (2) are unimportant even up to a proton energy of 660 Mev.

To obtain the angular distribution of the π^+ mesons from reaction (1) the meson energy distributions were transformed into the c.m.s., utilizing the fact that the expression

$$(1/p)(\partial^2\sigma / \partial E\, \partial\omega) \quad (6)$$

is an invariant. Here p and E are the meson momentum and energy respectively in the appropriate coordinate system. The meson energy distributions in

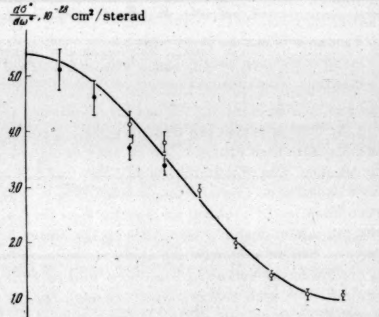

FIG. 4. Angular distribution of π^+ mesons from the reaction $p + p \rightarrow \pi^+ + d$; ● – results of this work; ○ – results from Ref. 1.

TABLE 4.

Angle, c.m.s.	10°	20°	30°	40°
$\left(\frac{\partial\sigma^*}{\partial\omega^*}\right)$, $\frac{\text{mb}}{\text{sterad}}$	0.51 ± 0.04	0.46 ± 0.03	0.37 ± 0.02	0.34 ± 0.02

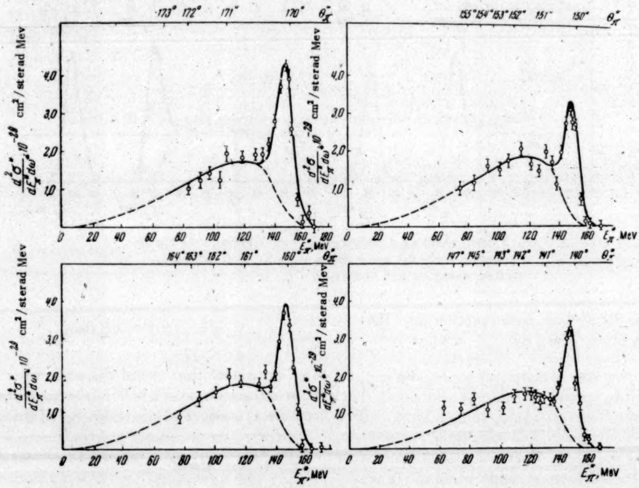

FIG. 5. Energy distribution of π^+ mesons from the reactions $p + p \rightarrow \pi^+ + n + p$ and $p + p \rightarrow \pi^+ + d$; center of mass angles and energies.

the c.m.s. from reactions (1) and (2) are plotted in Fig. 5. One sees that the mesons come out preferentially with high energy. The average energy of the mesons from reaction (1) is 110 Mev and 80% of the mesons have energies larger than 70 Mev. The transformation of such energy spectra from the l.s. into the c.m.s. depends very little on the meson energy, as can be seen from the scale of angles given at the top of the curves of Fig. 5, as well as from Table 5. The high energy part of the spectrum corresponds to an angular spread in the c.m.s. of ± 3°. Practically all mesons emitted in this angular spread were counted since the detector had an angular resolution of ± 2°. This peculiarity allows one to obtain the differential cross section in the c.m.s. by a measurement of the total meson yield in an arbitrary direction in the l.s. without first having to obtain the meson energy spectrum.

In Table 5, θ_π, E_π, θ_π^*, and E_π^* denote the angles and energies of the mesons in the l.s. and c.m.s. respectively.

In this manner the differential cross sections of π^+ meson production from reaction (1) were found for the angles 130° –100° in the c.m.s. According to the data of Ref. 1, reaction (2) does not contribute in this range. The differential cross section for the angles 171°, 162°, 152°, and 142° in the c.m.s. were obtained by integrating the smooth part of the respective energy spectra.

The low energy parts of the spectra inaccessible to the counter telescope were found by extrapolating the theoretical curves obtained by assuming a linear

TABLE 5.

E^*_π, Mev	$\theta_\pi = 60°$			E^*_π, Mev	$\theta_\pi = 80°$			$\theta_\pi = 108°$		
	E_π, Mev	θ^*_π	$\frac{d\cos\theta_\pi}{d\cos\theta^*_\pi}$		E_π, Mev	θ^*_π	$\frac{d\cos\theta_\pi}{d\cos\theta^*_\pi}$	E_π, MeV	θ^*_π	$\frac{d\cos\theta_\pi}{d\cos\theta^*_\pi}$
150	184	95°	0.72	150	130	116.5°	1.15	82	140°	2.06
90	111	99°	0.70	120	72	118°	1.15	61	141°	2.18
60	73	103°	0.69	70	59	124°	1.19	26	147°	2.59

dependence of the matrix element on the π^+ meson momentum. The uncertainty in the differential cross sections associated with the lack of knowledge of the actual energy spectra below the detection threshold is 5 to 15%, depending on angle.

The angular distribution of π^+ mesons created in reaction (2) is shown in Fig. 6. The curve in Fig. 6 corresponds to the expression

$$\partial\sigma^* / \partial\omega^* = (0.88 \pm 0{,}04)\,[(0.66 \pm 0{,}14) + \cos^2\theta^*_\pi] \cdot 10^{-27} \ \text{cm}^2/\text{sterad} \tag{7}$$

where the coefficients were obtained by a least-squares fit.

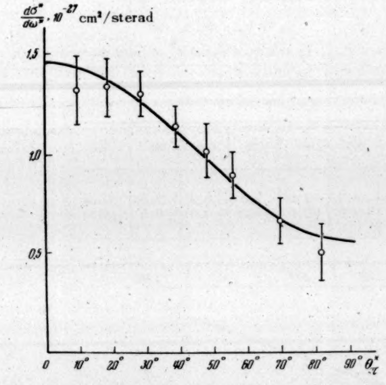

FIG. 6. Angular distribution of π^+ mesons from the reaction $p + p \to \pi^+ + n + p$.

The total cross section obtained by integrating (7) equals (10.9 ± 1.1) mb. In terms of the hypothesis of charge independence the cross section for reaction (1) is the sum of two independent parts[5]:

$$\partial\sigma / \partial\omega\,(p + p \to \pi^+ + n + p) = \partial\sigma_{10} / \partial\omega + \partial\sigma_{11} / \partial\omega, \tag{8}$$

where, according to Ref. 6, $\partial\sigma_{11}/\partial\omega$ is isotropic at 660 Mev and has a value ~ 0.28 cm²/sterad. Therefore we have

$$\partial\sigma^*_{10} / \partial\omega^* = (0.88 \pm 0.04)\,[(0.34 \pm 0.15) + \cos^2\theta^*_\pi] \cdot 10^{-27} \ \text{cm}^2/\text{sterad}. \tag{9}$$

Since the contribution of $\partial\sigma_{11}/\partial\omega$ to the differential cross section of reaction (1) for the angles 170° – 160° in the c.m.s. is only about 20%, the energy spectrum of π^+ mesons at these angles is almost completely that of $\partial\sigma_{10}/\partial\omega$. One thus notices a remarkable difference in the form of the energy distributions of π^+ and π^0 mesons the latter of which have been obtained in Ref. 7. The maximum in the π^0 spectrum is at lower energies and lies around 75 Mev. This can be understood qualitatively remembering that σ_{11} is due predominantly to transitions of the Pp kind. Assuming that the form of the energy spectrum associated with σ_{10} does not depend on the angle, as appears to be the case with π^0 mesons, then the full spectrum of mesons from reaction (1) should become softer when going from 180° to 90° in the c.m.s. In particular, it should be softer than the spectrum measured for 170° to 160° in the c.m.s. This softening is indeed noticeable in the spectrum for 140° c.m.s. (Fig. 5), where the ratio of the cross sections $(\partial\sigma_{11}/\partial\omega)/(\partial\sigma_{10}/\partial\omega)$ approaches 1/2. Together with the above linear dependence of the matrix element on meson momentum, the angular distribution (9) indicates that at 660 Mev π^+ mesons are created in reaction (1) in the p-state. A similar observation has been made earlier.[3] It is well known that the angular distribution of mesons associated with the transition ${}^1D_2 \rightarrow {}^3S_1p_2$ is proportional to

$$^1/_3 + \cos^2\theta. \qquad (10)$$

The fact that the obtained angular distribution for σ_{10} is close to (10) indicates that at 660 Mev the meson creation connected with σ_{10} is due to a ${}^1D_2 \rightarrow {}^3S_1p_2$. However, the results of the present work do not allow to exclude the possibility of transitions of the Pp kind leading to a similar angular distribution.

As mentioned earlier the excitation function of reaction (1) was obtained utilizing the circumstance that the transformation of the energy distributions does not strongly depend on the meson energy. It was shown in Ref. 5 that if the angular distribution in the c.m.s. has the form

$$A + \cos^2\theta, \qquad (11)$$

then the differential cross section at θ_0 = arccos $(1\sqrt{3})$ (55° or 125°) in the c.m.s. and the total cross section are connected by the relation

$$4\pi\,(\partial\sigma^* / \partial\omega^*)_{\theta_0} = \sigma_t. \qquad (12)$$

The angle θ_0 is called the isotropic angle. From the kinematics of reaction (1) one has in the energy region 510 to 660 Mev that the isotropic angle changes only by 1° if one considers mesons in the energy interval 0.5 $E_{\max}$ to $E_{\max}$. This energy interval contains 70 to 90% of all mesons. Furthermore, the transformation function for the solid angles from the l.s. to the c.m.s. for the same mesons changes only by 2% in the energy interval 510 to 660 Mev. These circumstances allow the determination of the excitation function of reaction (1) by using the meson yield as a function of proton energy as measured at 95° in the l.s. (~50° in the c.m.s.). The meson yield from reaction (2) was excluded according to the data of Ref. 1 where the excitation function was also obtained for 50° in the c.m.s. The results of the measurements were corrected for the change of the detection threshold with the c.m.s. energy of the mesons for decreasing proton energy. Since the angle 50° in the c.m.s. is not exactly the isotropic angle, the change of the angular distributions of the mesons from reaction (1) when going from 660 to 440 Mev proton energy[5] was also taken into account. The uncertainty in the total cross section due to these corrections at the lowest energy of 440 Mev did not exceed 15%. The excitation function normalized with respect to the total cross section at 657 Mev is given in Table 6.

The excitation function has also been plotted in Fig. 7. One sees that the excitation function is well represented by the power law

$$\sigma_t = 0{,}67\,P_{\max}^{4{,}7}\ \text{mb}, \qquad (13)$$

Here $P_{\max}$ is the maximum π^+ meson momentum in the c.m.s. in units $m_{\pi^+}c$.

TABLE 6. Energy distribution of π^+ mesons from reaction (1).

E_p, Mev	485	521	557	584	597	609	621	633	646	657
σ_t, mb	2.0 ±0.3	3.1 ±0.4	4.5 ±0.4	5.5 ±0.5	6.3 ±0.5	7.0 ±0.5	7.8 ±0.5	8.9 ±0.5	9.9 ±0.5	10.9 ±0.5

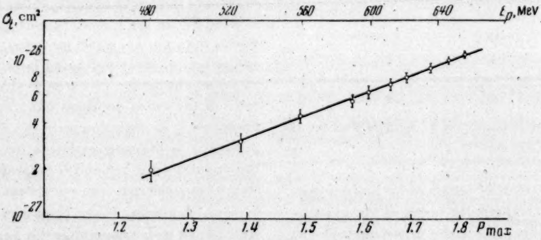

FIG. 7. Excitation function of the reaction $p + p \rightarrow \pi^+ + n + p$: $\sigma_t(p + p \rightarrow \pi^+ + n + p) = 0.67\,P_{\max}^{4.7}$ mb.

The excitation function for σ_{11} as measured in Ref. 6 has in the present energy region the form

$$\sigma_{11} = 0.11\, P_{\max}^{5.5}\ \text{mb}, \tag{14}$$

where $P_{\max}$ is the maximum momentum of the π^0 meson in units of $m_{\pi^0}c$. From the difference of $\sigma_t(p + p \rightarrow \pi^+ + n + p)$ and σ_{11} one obtains for σ_{10} a power law approximation:

$$\sigma_{10} = 0{,}55\, P_{\max}^{4,4}\ \text{mb}\cdot \tag{15}$$

Assuming a linear dependence of the matrix element on the meson momentum and neglecting the nucleon-nucleon interaction in the final state, one obtains for the excitation function of σ_{10} an expression of the form

$$\sigma_{10} \sim \frac{1}{v} \int\limits_0^{P_{\max}} \left[M\left(W - \sqrt{p^2 + m^2}\right) - \frac{p^2}{4} \right]^{1/2} p^4 dp \sim P_{\max}^{5,6}, \tag{16}$$

where v is the velocity of the incoming protons in the c.m.s.

Evidently the experimentally obtained excitation function changes slower with momentum. This can be explained by the nucleon-nucleon interaction in the final state and, probably, by the resonance character of the matrix element for the meson production. One will expect these factors to be important if the transition ${}^1D_2 \rightarrow {}^3S_1p_2$ should predominate since it is connected with the $T = 3/2$, $I = 3/2$ state of the meson-nucleon system.

The authors would like to express their gratitude to Professors M. G. Meshcheriakov and L. M. Soroko for discussions of the results of the present work.

---

[1] M. G. Meshcheriakov and B. S. Neganov, Dokl. Akad. Nauk SSSR, 100, 677 (1955).

[2] V. M. Sidorov, J. Exptl. Theoret. Phys. (U.S.S.R.), 31, 178 (1956); Soviet Phys. JETP 4, 22 (1957).

[3] Meshcheriakov, Zrelov, Vzorov, Neganov, and Shabudin, J. Exptl. Theoret. Phys. (U.S.S.R.), 31, 45 (1956); Soviet Phys. JETP 4, 60 (1957).

[4] Dzhelepov, Moskalev, and Medved', Dokl. Akad. Nauk SSSR, 104, 380 (1955).

[5] A. H. Rosenfeld, Phys. Rev. 96, 139 (1954).

[6] Iu. D. Prokoshkin and A. A. Tiapkin, J. Exptl. Theoret. Phys. (U.S.S.R.), 32, 750 (1957); Soviet Phys. JETP 5, 618 (1957).

[7] Iu. D. Baiukov and A. A. Tiapkin, J. Exptl. Theoret. Phys. (U.S.S.R.), 32, 953 (1957); Soviet Phys. JETP 5, 779 (1957).

Translated by M. Danos
264

SOVIET PHYSICS JETP VOLUME 5, NUMBER 6 DECEMBER 15, 1957

Reflection of Gamma-Rays From Bent Quartz Plates

O. I. SUMBAEV

All-Union Scientific Research Institute of Metrology

(Submitted to JETP editor October 16, 1956)

J. Exptl. Theoret. Phys. (U.S.S.R.) 32, 1276-1279 (April, 1957)

The wavelength dependence of the coefficient of reflection from the $13\bar{4}0$ planes of quartz crystal bent to a cylinder having a 2 meter radius was investigated on a two-meter crystal gamma-spectrometer. The quadratic character of this dependence was substantiated. It was shown that in theoretical examinations of this effect it is essential to take into account distortion of the reflecting planes. In the treatment, the plate is subdivided in thickness into a series of independently reflecting laminae, the thickness of which is less than the primary extinction distance. The crystal plate is found to behave as a mosaic crystal with small primary extinction. Thus the hitherto inexplicable quadratic dependence of the reflection coefficient on the wavelength finds a natural explanation.

IN INVESTIGATING the coherent reflection of x- and γ-rays from the $13\bar{4}0$ planes of quartz plates cut from an α-quartz single crystal so that the $13\bar{4}0$ planes were normal to the plane of the plate and the side edges were parallel to the optical axis of the crystal, Lind, West and DuMond[1] found that the dependence of the integrated reflection coefficient on the wavelength for plates elastically bent to a cylinder of 2 meters radius is close to quadratic. Their measurements of the integrated reflection coefficient for the same plate in the unstressed state led to a dependence close to the linear, *i.e.*, the dependence characteristic of ideal crystals. Lind *et al.* do not attempt to give an explanation of the observed effect noting only that "... the quartz might, however, become mosaic-like in structure in some elastically reversible way not now understood."

We felt it would be of interest to verify the quadratic dependence of the reflection coefficient on the wavelength discovered by Lind, West and DuMond and to find an explanation of the effect. The measurements were carried out on the two-meter crystal-diffraction spectrometer of the All-Union Scientific Research Institute of Metrology.[2] We investigated the reflection from the $13\bar{4}0$ planes of a $50 \times 30 \times 1.6$ mm plate of α-quartz cut and bent just as in the measurements of Lind, West and DuMond. We determined the ratio of the area under the spectral line to the number of pulses from the direct beam, due to photons of the same energy. This ratio Γ_i, as can readily be shown, is proportional to the integrated reflection coefficient. Figure 1 (curve *a*) shows the results of measurements at energies of 191 kev (In^{114}), 279 kev (Hg^{203}), 412 kev (Au^{198}) and 1190 kev (mean energy of the group of hard lines in the spectrum of Ta^{182}). It will be seen that a dependence of the form $\log \Gamma_i = c - n \log E$ obtains. Processing of the data by the method of least squares yields $n = 1.85 \pm 0.05$, where 0.05 is the mean square error. Analogous measurements with reflection from the $11\bar{2}4$ planes of α-quartz (the $50 \times 30 \times 0.8$ mm plate was cut so that the plane of the plate was perpendicular to the $11\bar{2}4$ planes) also led to a dependence very close to the quadratic (Fig. 1, curve *b*).

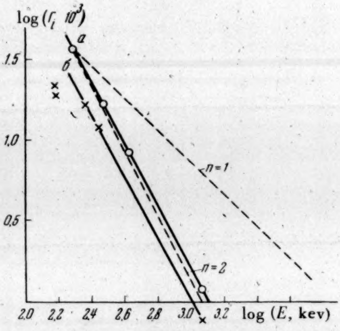

FIG. 1.

Lind, West and DuMond assumed that the initially flat reflecting planes remain plane when the plate is bent. This in general is not correct. Actually when a plate of arbitrary cross section is bent by the application of a bending moment M_1 acting in the *yoz* plane (Fig. 2) the displacements in the

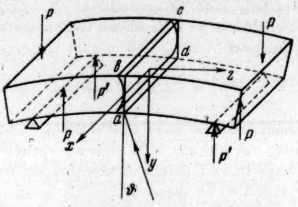

FIG. 2.

direction of the *z*-axis in the case of anisotropy of the general form are determined by the familiar relation[3]

$$W = (M_1 / 2I_1)[a_{35}xy + a_{34}y^2 + a_{33}y\,(2z - l)], \tag{1}$$

where M_1 is the effective bending moment, I_1 is the moment of inertia about the *x*-axis and the a_{ij}'s are strain coefficients. If a_{34} and a_{35} differ from zero, the cross sections are distorted by the bending into second-degree surfaces. With $a_{35} = 0$ the planes bend along the parabolas:

$$z = k_1 y^2, \quad k_1 = M_1 a_{34} / 2I_1.$$

If $a_{35} \neq 0$, Eq. (1) becomes invalid for cases of bending of the crystal plate between cylindrical mirrors or by application of moments by the method of Borovskii-Gil'varg.[4,5] Actually if $a_{35} \neq 0$, in addition to bending, the plate tends to twist. However, the design of the crystal holder prevents twisting with the result that in addition to the moment M_1 (couple *PP* in Fig. 2) the plate is subjected to a moment M_t opposing the torsion (forces *PP'* in Fig. 2). The deformation of a plate loaded in this manner is satisfactorily approximated by the following expression

$$W = \frac{a_{35}}{2\rho\,[a_{33} - a_{35}^2 / (a_{44}b^2 / a^2 + a_{55})]\,(a_{44}b^2 / a^2 + a_{55})} \times \left\{a_{45}\frac{b^2}{a^2}x^2 - \left[a_{45} - \frac{a_{34}}{a_{35}}\left(a_{44}\frac{b^2}{a^2} + a_{55}\right)\right]y^2 + 2\frac{b^2}{a^2}\,a_{44}xy\right\}, \tag{2}$$

which is rigorously valid for a plate of elliptic cross section (in which case *a* and *b* are the axes of the ellipse) bent to a cylinder of radius ρ. Neglecting the terms with b^2/a^2 (in our case $(b/a)^2 \approx 2.5 \times 10^{-3}$), we obtain

$$W = \frac{1}{2\rho\,(a_{33} - a_{35}^2 / a_{55})}\left(a_{34} - \frac{a_{45}}{a_{55}}a_{35}\right)y^2. \tag{3}$$

The coefficients in Eq. (3) must be expressed through constants in crystallographic coordinates. Then, for an α-quartz plate with working planes *hk*0, Eq. (3) assumes the form

$$W = -\frac{a_{14}^2}{\rho\,(a_{11}a_{44} - a_{14}^2 \sin^2 3\varphi)}\cos\varphi \sin 3\varphi \cos 2\varphi \cdot y^2, \tag{4}$$

where φ is the angle between the *y*-cut and principal (50 × 30) faces of the utilized plate. For plates cut as in our case ($13\bar{4}0$ working planes), $\varphi = 16°10'$ and Eq. (4) yields

$$W = -\,0.226 \times 10^{-3}\,y^2$$

with $a_{11} = 12.73 \times 10^{-7}$; $a_{14} = -\,4.23 \times 10^{-7}$; $a_{44} = 19.66 \times 10^{-7}$ cm²/kg (Ref. 3); $\rho = 200$ cm.

Thus, in this case, too, the reflecting planes proved to be bent and if we neglect displacements in the direction of the *x*- and *y*-axes the bent surface will be described by an equation of the form

$$z = k_2 y^2, \quad k_2 = -\,0.226 \times 10^{-3}\ \text{cm}^{-1}.$$

The width of the diffraction peak is related to the number *N* of planes participating in the reflection by the familiar expression

$$\Delta\vartheta = \tan\,\vartheta / \pi N, \tag{5}$$

where ϑ is the Bragg angle. The angle of the parabolic surface relative to the plane cross section *abcd* (Fig. 2) is $\Delta\vartheta' \approx \tan\Delta\vartheta' = 2k_2 y$. Congruous reflection can occur from planes for which $\Delta\vartheta'$ at the point of incidence does not exceed $\Delta\vartheta$. From the condition $\Delta\vartheta = \Delta\vartheta'$, and bearing in mind that

$$N = (y/d)\tan\vartheta,$$

where *d* is the interplanar distance between the reflecting planes, we obtain the following expression for the number of congruently reflecting planes:

$$N = \tan\,\vartheta / \sqrt{2\pi k_2 d}. \tag{6}$$

The thickness of the simultaneously reflecting lamina is given by

$$\Delta y = \sqrt{d / 2\pi k_2}. \tag{7}$$

Thus the plate is subvided in thickness into a series of independently reflecting laminae of thickness Δy. Let us assume that $\Delta y \ll t_x$, where t_x is the attenuation distance defined by the relation

$$t_x = [2r_0(F/v)\,pd\,\tan\vartheta]^{-1}, \tag{8}$$

where $r_0 = e^2/mc^2$, p is the polarization factor, F is the structure factor and v is the volume of the unit cell.

The intensity of reflection from the entire lamina will be proportional to

$$[r_0 p\,(F/v)\,\lambda\Delta y/\cos\vartheta]^2. \tag{9}$$

The width of the diffraction peak will obviously be

$$\Delta\vartheta_\Sigma = 2k_2 T, \tag{10}$$

where T is the thickness of the plate and the integrated reflection coefficient

$$R_\vartheta \sim 2k_2 T\left[r_0 p\left(\frac{F}{v}\right)\frac{\Delta y}{\cos\vartheta}\right]^2 \sim \frac{p^2}{\cos^2\vartheta}\,r_0^2\left(\frac{F}{v}\right)^2 dT\lambda^2. \tag{11}$$

This relation is identical with the expression for the integrated reflection coefficient for a mosaic crystal. Computing Δy from (7) with $k_2 = 0.226 \times 10^{-3}$ cm^{-1} and $d = 1.17 \times 10^{-8}$ cm, and t_x from (8) for $F\,(13\bar{4}0) = 21.0$, $v = 112$ A^3 (Ref. 1), $\lambda_{\max} = 2d \sin\vartheta = 0.1$ A, we obtain $\Delta y = 2.87 \times 10^{-3}$ cm and $t_x = 2.3 \times 10^{-2}$ cm, *i.e.*, we see that Δy is really appreciably smaller than t_x [Eq. (9) and the following are valid only under this condition]. From Eq. (10) with $T = 0.16$ mm we then obtain for the width of diffraction peak

$$\Delta\vartheta_\Sigma = 7.2 \times 10^{-5} \text{ radians.}$$

An examination analogous to that above shows that for a plate cut with the $11\bar{2}4$ planes perpendicular to the large faces the dependence of R_ϑ on the wavelength must also be quadratic.

Thus we see that the quadratic dependence of the reflection coefficient of an elastically bent quartz plate on the wavelength can be explained naturally without recourse to any additional hypotheses. The bent plate actually does become similar to a mosaic crystal in consequence of bending of the reflecting planes.

---

[1] Lind, West and DuMond, Phys. Rev. 77, 475 (1950).

[2] P. I. Lukirskii and O. I. Sumbaev, Izv. Akad. Nauk SSSR, Ser. Fiz. 20, 903 (1956).

[3] S. G. Lekhnitskii, *Theory of Elasticity of an Anisotropic Body*, GTTL, Moscow 1950.

[4] I. B. Borovskii, Dokl. Akad. Nauk. SSSR 72, 487 (1950).

[5] A. B. Gil'varg, Dokl. Akad. Nauk. SSSR 72, 489 (1950).

Translated by E. J. Rosen
265

SOVIET PHYSICS JETP VOLUME 5, NUMBER 6 DECEMBER 15, 1957

Determination of Mass of Slow Charged Particles in Photographic Plates

M. I. TRET'IAKOVA

P. N. Lebedev Physical Institute, Academy of Sciences U.S.S.R.

(Submitted to JETP editor December 27, 1956)

J. Exptl. Theoret. Phys. (U.S.S.R.) 32, 1280-1293 (June, 1957)

The accuracy of various methods of determination of the masses of slow charged particles stopped in photographic plates is examined. It is shown that for reliable identification of an individual particle it is not sufficient to determine its mass by only one method. Distributions in mass of slow charged particles ($E < 30$ Mev) produced by ~ 460 Mev protons are presented, the masses being determined by different methods. The mass and charge sign distributions have been obtained by the magnetic deflection-range method for slow particles ($E < 50$ Mev) created by cosmic rays at an altitude of ~ 9.5 km.

INTRODUCTION

THE DISCOVERY OF NEW unstable particles – heavy mesons and hyperons – in cosmic rays has made exceedingly important the determination of mass, charge, and fractional yield of the various particles. In connection with this, work on a systematic study of charged particles assumes great importance. Many investigations,[1-15] carried out with emulsions, Wilson cloud chambers, counters, or stripped emulsions have been devoted to a systematic study of the mass as of the stopped charged particles. The basic defect of these investigations was that particle identification was made on the basis of a single method of mass measurement, as a result of which experimental errors could lead to incorrect mass determinations in individual cases. An example of this is seen in Ref. 3 where a wide range of particle masses was obtained using emulsions.

With the aim of clarifying the dependability of various methods of mass determination of slow charged particles stopped in emulsions, and to find the conditions under which certain particle indentification may be made, we performed an experiment in which a C_2 emulsion was bombarded by 460 Mev protons, and studied the secondary particles which stopped in the emulsion.

The masses of slow charged particles were determined by three methods: a) using magnetic deflection and range (magnetic analysis, ρ and r); b) using grain counts and range (N, r); c) using scattering and range (α, r).

In examining the nature of slow charged particles created by cosmic rays at 9.5 km altitude, the basic method chosen to determine mass was magnetic analysis.[4] The principal advantage of this method, besides the higher accuracy in mass determination, is that the sign of the charge can be obtained independent of what happens at the end of the range. The use of emulsions sensitive to relativistic particles allowed observation of particles of arbitrary velocity. Whenever an "intermediate" mass ($m_\pi < m < m_p$) was found by magnetic deflection and range, the mass was determined in addition by two other methods – ionization and range, and scattering and range. This procedure turned out to be exceedingly important for reliable identification of the particle.

EXPERIMENTAL SETUP

Ilford C_2 plates with an emulsion thickness of 100 μ and a size 5×8 cm were bombarded by protons of ~ 460 Mev (first series of experiments). NIKFI-R plates with an emulsion thickness of 200 μ and a size 7.8×7.8 cm were bombarded by cosmic rays at altitude 9.5 km (second series of experiments). Photographic plates were bombarded in a magnetic field; control plates were bombarded without such field.

The setup used was similar to that described by Franzinetti.[4] Two plates were placed into a special container, emulsions facing each other at a distance of 3 mm, and located between the poles of an electromagnet in such a way that the field was perpendicular to the emulsion plane. During cosmic ray bombardment an 8 cm lead filter was placed above the plates and served as a meson generator. The temperature of the container during the experiment was held at 15 ± 5° C. The magnet provided a field of 27,000 Oersted. The maximum error in magnetic field measurement was 1%. Variations of the magnetic field during bombardment never exceeded

± 0.4%. The magnetic field was very homogeneous right out to the pole tips. If edge effects occurred, they were at less than 5 mm from the pole tips.

There were two aims in developing the emulsions: minimum distortion, and uniform development in depth. The C_2 plates were developed by the two bath method, the NIKFI-R plates by the temperature method. Before drying, the type R plates were soaked in 5% glycerine solution for two hours at 18° C. Drying took place in a closed cabinet at 18° C. These methods resulted in plates developed almost uniformly in depth, with only small distortions (noticeable distortions were observed less than 5 mm from the edges of the C_2 plates, and less than 10 mm from the edges of the R plates).

Scanning and track following was done with an MBI-2 microscope with magnification $10 \times 10 \times 1.5 = 150$. Notice was taken of all stopped particle tracks coming from the surface of the emulsion. The basic difficulty in microscopic examination of plates is finding the continuation of stopped particle tracks. In contrast to previous work[4-5] our search for the continuation of stopped particle tracks was made with a rotating table, which reduces the time by a factor of 3 – 4.

ERRORS IN THE DETERMINATION OF MASS BY VARIOUS METHODS

a) *Mass Determination by Magnetic Analysis and Range*

An analysis of the errors of this method is given in Ref. 4. The main sources of errors in this mass determination is the measurement of radius of curvature; the error in measurement of magnetic field strength is 1%, and the error in particle-range measurement is usually 2 – 3% and always less than 5%.

The radius of curvature can be expressed as:

$$\rho = R/2 \sin (\beta/2),$$

where R is the projection of the particle path in the space between the emulsions onto the emulsion plane, and β is the angle between the projections of tangents to the particle trajectory at the points of entry and exit from the emulsion onto a plane perpendicular to the magnetic field (or onto the emulsion plane). The error in the radius of curvature is determined by the error in measurement of β since $\Delta R/R \approx 0.01$. The error in β depends on distortion of the emulsions, scattering in the air space between emulsions, and scattering in the surface layers of the emulsion.

Under our experimental conditions the error in β due to the emulsion distortion gives an uncertainty of 0.1 – 0.3°. Since the C_2 plates were bombarded at normal atmospheric pressure, while the R plates were bombarded at 300 g/cm², the mass error caused by air scattering between the emulsions was 2 – 5% in the former case and 1 – 3% in the latter case. Most of the error in β is caused by multiple scattering of the particles in the surface layers of the emulsion. To reduce this error the direction of particle motion in the emulsion was measured with optimum cell length,[16] which for a range of 100 – 1500 μ is 8 – 25 μ and 14 – 40 μ for mesons and protons respectively. If one considers that the error in β is caused only by multiple scattering in the surface layers of the emulsion, then a theoretical value for the error can be obtained from the expression $\Delta\beta = \sqrt{2}\alpha_t$ where α_t is the theoretical value for the average multiple scattering angle between chords on a path length t_μ. To investigate the correspondence of this theoretical value and experiment we examined tracks in plates that had been bombarded without a magnetic field. In one pair of such plates there were 17 stopping tracks, in another pair there were 28 of which 6 were mesons. For each particle we obtained the ratio $\Delta\beta_{\text{exp}}/\Delta\beta_{\text{calc}}$, and then determined the average value of this ratio. It turned out that $\overline{\Delta\beta_{\text{exp}}/\Delta\beta_{\text{calc}}} = 0.6$ for the first case (17 tracks) and $\overline{\Delta\beta_{\text{exp}}/\Delta\beta_{\text{calc}}} = 0.7$ for the second case (28 tracks).* The error in β is thus determined by the expression

$$\Delta\beta = \sqrt{2} \times 0.7\, a_t \approx a_t.$$

It is important to note that all errors in β are contained in $\Delta\beta_{\text{exp}}$.

The mean-square values of mass errors for protons, deuterons and π-mesons as a function of range under the conditions of the present experiment are given in Table 1. The value of $\Delta m/m$ for $r = 10\,000\ \mu$ was calculated under the assumption that $R = 4$ cm; for all other ranges the experimental value of $\overline{R}$ was used. It is seen from Table 1 that in mass determination by the ρ, r method the error decreases with increasing range, since in general the longer range corresponds to a larger value of R.

---

*The ratio $\overline{\Delta\beta_{\text{exp}}/\Delta\beta_{\text{calc}}}$ deviates from unity because the track direction is measured at the center of gravity of the grain, while in the calculated $\Delta\beta$ the multiple scattering angle is taken between chords.

b) *Mass Determination by Ionization and Range*

The method is discussed in detail in Ref. 17.

For the C_2 plates mass was determined by examining the integral curves of the grain number $N(r)$ as a function of range. A calibrating curve was constructed from 13 proton tracks whose mass identification had been reliably made by the magnetic analysis-range method. The grains in a track were counted twice. Repeated measurement of the number of grains in a particular track by the same observer (a proton track of range 500 μ has about 550 grains) gave results which differed by 3 – 5%. Results of different observers differed by 5%. If a measurement was repeated after a long time interval, the spread in the number of grains reached 10%. Thus large subjective errors enter into the grain count. The [illegible] error in mass determination by grain count and range under the conditions of our experiments (range of examined particles $300\,\mu < r < 3000\,\mu$) is 35 – 25%.

TABLE I.

Range r, μ		100–500		500–1000		1000–2000	>2000	10000
$\bar{R}$, cm		0.5	1.0	1.0	1.4	1.8	> 2	4
$\frac{\Delta m}{m}$ %	p	—	~30	—	~22	~18	<16	~5
	d	—	~13	—	~13	~12	<12	~8
	π	~30	—	~15	—	~10	< 7	~4

In the type R plates ionization was measured either by the length density of gaps along the track or by a photometric device: The gap density was measured with a special apparatus constructed by A. I. Galaktionov, and the photometric measurements were made on a narrow slit instrument constructed along the ideas of A. E. Chudakov.*

In making measurements of the gap density for tracks inclined more than 20° in the undeveloped emulsion, a correction for the angle of the track was included.[18] In the photometric measurements corrections were applied for depth of the track in emulsion. The photometric method is an objective way of determining the relative ionization, although it can be used only for tracks inclined less than 5° in the emulsion.

Under the conditions of our experiments, fading and uneven development in depth of the emulsion had practically no effect. To eliminate variations due to emulsion sensitivity or development procedure, the calibrating track was always taken in the same plate as the unknown track. In selecting tracks for calibration it must be borne in mind, as shown by our data, that one-third of all heavy slow charged particles which stop in the emulsion are deuterons. (This holds also for particles coming from a single ray star produced in the emulsion.)

It is essential to note that in a steep track measurement of the ionization can differ considerably from the true value. For example if the track angle is 35° in the undeveloped emulsion then for a gap density measurement of 0.1 the actual value is 0.23, *i.e.*, almost 2.5 times larger. By using electron-sensitive emulsions, the (I, r) method allows under the best circumstances a proton mass determination of 6% for a 10 000 μ range, and for a heavy meson with $m = 1000\ m_e$ a mass determination of 10 – 7% for the range interval 5 – 10 mm.[17]

The method has poor sensitivity for separating the heavy stopped particles, since protons, deuterons and tritons have almost the same track density for ranges of a few millimeters.

c) *Mass Determination by Scattering and Range*

The multiple scattering along the track of a stopped particle was measured by the coordinate method. In the first series of measurements we used the constant cell method,[19] and in the second series the variable cell method.[2]

The error in mass determination of stopped charged particles is determined by the statistical error in the multiple scattering angle, and ranges from 50 to 20% under the circumstances of this experiment ($300\,\mu < r < 3000\,\mu$). Independent mass determination for μ-mesons using the constant-cell method gives an average mass value

---

*Articles in collaboration with these authors are in press (Prib. Tekhn. Experim.).

$$\overline{m}_{\mu} = (211 \pm 26)\, m_e$$

(10 μ-mesons from a $\pi - \mu$ decay).

In determining second differences by the variable cell method, we used for steep tracks third differences,[21] which allowed elimination of effects of emulsion distortion. The accuracy of various methods of mass determination for stopped charged particles as a function of particle range in electron sensitive emulsion is given in Table 2.

TABLE II. Relative error (in %) in mass determination of protons and π-mesons of various ranges in the emulsion.

Range r, μ	Protons			π-mesons		
	ρ, r	α, r	I, r*	ρ, r	α, r	I, r
100		—			—	
300	~30	50		30	50	
500		45			40	~20
1000	22	35		15	30	
2000	18	30		10	25	~15
3000	<16	25		< 7	20	~10
5000		22	~15		17	~ 7
10000	~5	17	~ 6	~ 4	13	~ 5

*Mass error depends significantly on emulsion sensitivity.

From a comparison of the various methods of mass determination for stopping charged particles it follows that the best accuracy for ranges less than 10 000 μ is given by the magnetic analysis – range method. Although the (I, r) method errors are comparable with the (ρ, r) method errors for ranges ~ 10 000 μ, the errors listed in the table for the I, r method were obtained with tracks inclined less than 10°, and the calibration was carried out with several tens of tracks. Under ordinary circumstances the error of the (I, r) method will be much greater, since it is necessary to examine much steeper tracks which pass through a series of emulsion layers. In such a case additional errors come about because of inclination, possible variation of sensitivity in different emulsion layers, variation in development, and errors in the calibration of each layer.

The magnetic analysis – range method is also very effective for the separation of heavy particles – protons, deuterons, and tritons. The mass determination error for deuterons and tritons in the (ρ, r) method depends only weakly on range, and is about 10 – 15%. The errors for the (ρ, r) method indicated in Table 2 can be reduced by increasing the space between emulsions, or by increasing the magnetic field strength. The range interval can be increased by using thicker emulsions. The time efficiency of the apparatus can be improved by increasing the dimensions of the polepieces.

EXPERIMENTAL RESULTS

First Series of Experiments

The mass of 48 particles was determined by the magnetic analysis – range method. Particles with ranges greater than 100 μ and with a projection of the path between emulsions onto the emulsion plane of more than 8 mm were examined. The mass of most of these particles was also determined by the grain count – range and scattering – range methods.

The distribution of particles by mass obtained by the various methods is shown in Fig. 1. As can be seen from Fig. 1, the mass determination error of slow charged particles ($E < 20$ Mev) using the magnetic analysis – range method is much smaller than with the other methods. This data is for particles with $m > m_p$. In Ref. 4 the analogous result is obtained for light mesons. The average values for proton and deuteron mass obtained by the (ρ, r) method are respectively $\overline{m}_p = (1850 \pm 70)\, m_e$ (27 particles) and $\overline{m}_d = (3630 \pm 130)\, m_e$ (14 particles).

The (N, r) and (α, r) methods were used to deter-

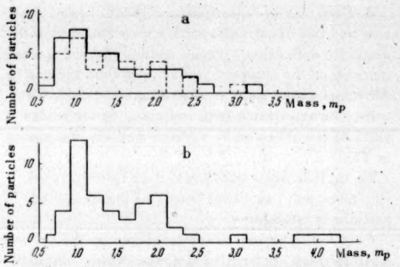

FIG. 1. Mass distribution of particles (first series of experiments): *a* – solid line – grain count and range; dashed line – scattering and range; *b* – magnetic deflection and range

mine the masses of 191 particles (only particles of range > 300 μ were examined). Analysis of the mass determination results by the three methods shows that the determination by magnetic deflection – range allows a positive identification of particle type in approximately 95% of the cases. If however the mass for a slow charged particle ($r < 2000\ \mu$) is determined by one of the methods [(N, r) or (α, r)], then the number of false identifications is 10 – 15%. Table 3 gives results for some of the cases where the mass determination by one method did not agree with that made by the other two methods.

It follows from the mass values and errors indicated in Table 3 that the probability that the particle is a deuteron is less than 1% for track 63, and less than 0.2% for track 158. A number of single scatterings were observed along track 209 which most likely raised the measured scatterings angle, and therefore lowered the mass. It therefore follows that positive identification of a particle requires mass measurement by more than one method. If two methods give the same result, the identification of the particle is almost positive. This applies to cases where the particle is brought to a stop by ionization loss. The results of the first series of experiments are given in Table 4, where the number and distribution of particle types found is shown.

TABLE III.

Track No.	Mass value (in m_p) obtained by the various methods			Range μ	Identification
	ρ, r	N, r	α, r		
63	1.12 ± 0.33	1.85 ± 0.45	0.81 ± 0.36	560	*p*
158	1.82 ± 0.50	1.00 ± 0.25	0.91 ± 0.40	553	*p*
209	1.90 ± 0.60	1.79 ± 0.50	0.370 ± 0.20	460	*d*

TABLE IV.

Particle type	Mass determination method			
	$\rho, r;\ a, r;\ N, r$		a, r and N, r for $r > 300\ \mu$	
	No. of particles*	% of all particles	No. of particles*	% of all particles
p	27 (5)	56.3	118 ± 9 (37)	61.5
d	14 (5)	29.2	58 ± 9 (16)	30.5
$m > m_d$	6 (2)	12.5	8 ± 1 (2)	4.3
μ and π	1	2	7	3.7

*The quantities in parentheses indicate the number of particles coming from stars in the emulsion.

Second Series of Experiments

The masses of 276 particles were determined by magnetic deflection and range. A histogram of the mass distribution is given in Fig. 2. The angular distribution of particles is given in Fig. 3. Let us examine each particle group in the histograms.

1. *Heavy Particles.* All positively charged parti-

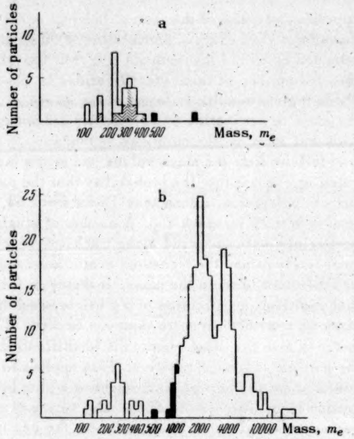

FIG. 2. Mass distribution of particles (second series of experiments): a – negative particles, b – positive particles. The crosshatched sections are negative π-mesons, the blackened section – particles with mass $m_\pi < m < m_p$.

cles with mass in the interval $11 - 2800\, m_e$ were considered protons, particles with $2800 - 4600\, m_e$ were considered deuterons, and particles with mass $4600 - 6600\, m_e$ were considered tritons. Particles with mass $> 6600\, m_e$ were considered heavier than tritons.* Average mass values obtained for protons, deuterons and tritons are respectively:
$\overline{m}_p = (1860 \pm 40)\, m_e$ from 120 cases,
$\overline{m}_d = (3610 \pm 50)\, m_e$ from 51 cases, and
$\overline{m}_t = (5700 \pm 180)\, m_e$ from 11 cases. The angular distribution of heavy particles is not isotropic. Examining the angular and energy distributions of the heavy particles it follows that most are knocked out of a nucleus by an incident nucleon, and do not come from an evaporation process.

2. *Light Particles.* Light particles are identified by taking account of the decay products, and can all be classified $\mu^\pm$ and $\pi^\pm$ mesons. The average mass values obtained are: $\overline{m}_\pi = (294 \pm 13)\, m_e$ (25 cases: 7 π^+ and 18 π^-) and $\overline{m}_\mu = (207 \pm 12)\, m_e$ (32 cases: 19 μ^+ and 13 μ^-).

3. *Particles of "Intermediate" Mass.* Seven positive and two negative particles were found by the magnetic deflection – range method to have a mass larger than the π-meson and smaller than the proton. All these cases were studied in great detail. The track characteristics with indicated decay modes and masses obtained by various methods are shown in Table 5.

We include some additional data for this table. By "track pair" is meant tracks of the examined particle in two plates.

Pair 150. The ionization measured on the primary particle track contradicts the mass value obtained by the (ρ, r) and (α, r) methods. Since the question of existence of particles with mass $500 - 600\, m_e$ is exceedingly important this case was studied further. Let us assume that the case represents the decay of a π-meson in flight. The angle between the π and μ mesons is 34 ± 5°. Grain density of the secondary particle track is $(60 \pm 5)/100\, \mu$. Such a density in a μ-meson track corresponds to a range of $2500 \pm 500\, \mu$. In order for an in-flight decay to yield a μ-meson of this energy, the π-meson must decay some $200 - 300\, \mu$ from the end of its range.

If one assumes that the π-meson has decayed in flight some $300\, \mu$ before the end of its range, then: 1) the ionization of the primary particle agrees with the assumption of a π-meson: 2) primary particle mass determined by the (α, r) method is $(175 \pm 90)\, m_e$; 3) primary particle mass determined by the (ρ, r) method is $(470 \pm 190)\, m_e$. Owing to the above, the case has been identified as decay of a π meson in flight. Under the conditions of the experiment, the probability of an in-flight π decay $\sim 300\, \mu$ before the end of range is about 1.5%.

It is essential to note that in the case of a decay or interaction of a particle in flight, the (α, r) method gives a mass value that is too high. This is also true for the (ρ, r) method. In such a case the additional method of mass determination must make use of the ionization.

Pair 23. The particle is identified as a proton. The probability of a proton having a measured mass $840\, m_e$ [obtained by the (ρ, r) method] under the conditions of the experiment [$m_p = (1860 \pm 40)\, m_e$, 120 cases], is 0.8%, *i.e.*, one case in 120, as actually observed.

Pair 30. The closeness of the particle mass to that of a proton, together with its negative charge, forced us to give this track pair very careful study. Measurement of scattering and ionization along the track showed that the direction of particle motion

---

*The boundaries of these intervals were chosen in such a manner that experimental error made it equally probable for a particle to be assigned to one group or the other near the boundary.

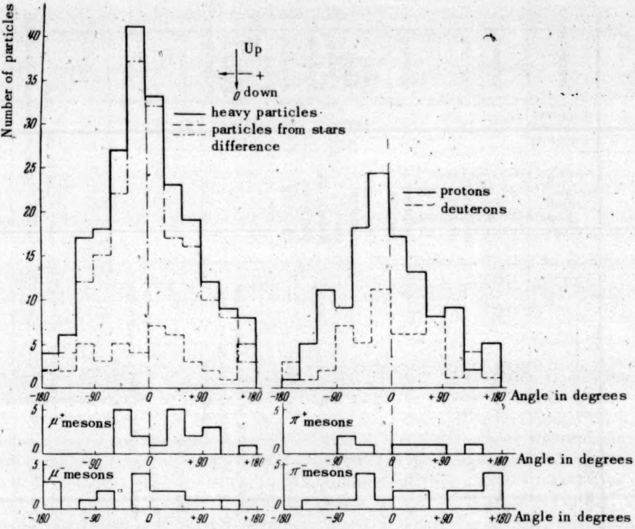

FIG. 3. Angular distribution of charged particles created by cosmic rays at an altitude of 9.5 km.

was opposite to that which had been assumed in the mass determination. In that case the particle charge will be positive.

Thus out of nine cases examined, only three particles turn out to be heavy mesons, all with positive charge and initial mass $900 - 1000 m_e$. It is possible to indicate several reasons for incorrect mass determination by the magnetic deflection – range method: scattering in the surface layers of the emulsion and in the space between emulsions, decay or interaction of the particle in flight near the end of its range, incorrect determination of particle motion direction (which is important for particles with $m \geqslant m_p$), and false coincidence (each member of a pair belongs to different particles).

Table 6 shows the number and fraction of each type of particle with allowance for definite identification in the "intermediate" mass region.

DISCUSSION OF THE RESULTS

1. *On the Certainty of Individual Particle Identification*

It follows from the experimental results of the present work that reliable identification of an individual particle can be made only if its mass is determined by several methods. This is particularly important in the identification of rare events (heavy mesons, or "new" particles). An analogous conclusion can be drawn from experiments performed with Wilson cloud chambers or counters. In Ref. 13, where a mass spectrometer was used, the sorting of particles by momentum and range produced three particles with mass in the interval $450 - 650 m_e$. However, additional mass determinations of these particles made by ionization and momentum showed that these particles were π-mesons which interacted in flight. The use of the additional ionization – range measurement together with the basic mass spectrometer method allowed a significantly higher certainty in the identification of heavy mesons, as well as a reduction in the experimental uncertainty for the fraction of such mesons.[15] It should also be noted that in many cases the estimated accuracy of mass determination should be reevaluated to disclose erroneous results or incorrect conclusions. We shall give some examples.

In Ref. 3, where photo emulsions were used, the number of charged particles with mass $600 - 1000 m_e$

TABLE V.

Pair No.	No. or pair and plate symbol		r, μ	Total path length in both tracks	β°	R, cm	ρ, cm	Mass value (in m_e))				Decay products	Minimum grains per 100 μ	Identification
								ρ, r	α, r	I, r	$\overline{m}$			
1	114* III, IV	+	217	525	5°	0.650	7.45	944±300	770±300	900±300	880±210	—	17	K-meson
2	145 III, IV	+	234	750	4°30′	0.610	7.76	1018±300 or 1018±780, if $m = m_\pi$	220±85	$m < m_\pi$		Relativistic particle	17	μ-meson
3	181 XI, XII	+	775	1520	6°11′	1.225	11.30	946+215	964±275	890±300	930+190	Relativistic particle	21	K-meson
4	150 XIX, XX	+	458	742	4°53′	0.480	5.64	580±145 or 580±215, if $m = m_\pi$	590±270	$m < m_\pi$	—	Gray decay particle track	22	Decay in flight π-meson
5	242 XIX, XX	+	452	987	5°	0.975	11.20	1200±420	710±270	$m_\pi < m < m_p$	955±250	Relativistic particle	22	K-meson
6	18 XXXVa, XXXVIa	—	123	404	7°6′	0.495	4.00	556+150 or 556+325, if $m = m_\mu$	245+90	$m \sim m_\pi$	—	3 prong star	31	π-meson
7	52 XXXVaXXXVIa	+	440	825	5°	0.750	8.60	870±365	Measurements of a and I show that the parts of the pair belong to different particles			—	31	False coincidence**
8	23 XIIIa, XIVa	+	385	883	6°	0.840	8.85	840±270	1875 ± 700		$m \sim m_p$	—	20	Proton
9	30 XIa, XIIa	—	296	592	3°	0.69	11.8	1625±740	Measurements of a and I along track show that particle has opposite direction of motion			—	20	—

---

*Absence of secondary particle tracks is due to low grain densities in tracks of relativistic particles and the high background on the plate.

** The probability for accidental coincidence under the conditions of the experiment is less than 0.5%, *i.e.*, 1 case in 276 tracks, as indeed observed.

TABLE VI.

Particle type	No. of particles	No. of particles created in emulsion	% relative to all particles	Remarks
p	124 ± 3	29	45	
d	50 ± 3	12	20.5	
$m > m_d$	28	5	10	
π^+	9	—	3	All particles suffer μ decay; one particle decays in flight
π^-	$20 (\pm 1)$	1	7.5	15 particles form stars
μ^+	22	4	8	20 cases of electron decay observed
μ^-	$14 (\pm 1)$	—	5	7 cases of electron decay observed
K^+ $(m \sim 950 m_e)$	3	1	~ 1	2 cases of a relativistic decay particle observed

was greater than the total number of π and μ mesons, a result which was not confirmed by further experimentation. The error of this result is due to overestimating the accuracy of mass determination by grain count and range (particles with range > 200 μ were examined). Independent mass determinations by the (l, r) and (α, r) methods, for heavy mesons formed by cosmic rays and stopped in the emulsion, gave results from 600 to $1700 m_e$ in individual cases; the mass-determination uncertainties given by the authors assumed the existence of several types of heavy mesons of different masses. However, it has since been well established that all heavy mesons have a mass $\sim 965 m_e$, with a maximum spread due to the different types of mesons of less than 0.5%.

The conclusions of the authors of Ref. 11, who used two cloud chambers and observed particles of mass 100 and $600 m_e$ in the soft component of cosmic rays 300 m above sea level, are in our opinion incorrect. This error is due to overestimating the accuracy with which the mass was determined by the (l, r) method under the conditions of their experiment

2. *Proportion of Heavy Mesons*

It is seen from Table 6 that at an altitude of 9.5 km positively charged heavy mesons with mass $\sim 1000 m_e$ comprise 2.5 ± 1.5% of the number of protons, or 10 ± 5% of the number of π-mesons.

In Franzinetti's work[4] (360 particles examined at ~ 3500 m) 7 particles were observed with $m_\pi < m < m_p$. The author states that all these cases may be due to experimental error. The use of only one method of mass determination did not allow the author to make positive identification in each case, and did not allow the separation of known heavy mesons from the 7 cases of "intermediate" mass particles with $m_\pi < m < m_p$. In work with emulsion stacks exposed in the stratosphere, taking account of the emulsion efficiency for the registration of heavy meson tracks (which according to Ref. 10 is 25 – 30%) the number of heavy mesons is 2.5 – 3% of the π-mesons.[9,10] These data pertain to particles stopped in the emulsion.

In Ref. 7 using a mass-spectrometer and a Wilson cloud chamber (mass was determined by two methods: momentum and range, and ionization and range), it was found that at 3200 m with a 9 cm lead filter the number of positively charged heavy mesons was 2.5% of the number of protons of the same range (range interval 2.5 – 4.5 cm Pb). In Ref. 12, using two cloud chambers (particle mass was determined by momentum and range), it was found that at 3250 m under an 8 cm lead filter the number of heavy mesons was 6 ± 4% of the number of π-mesons (range interval 10.5 – 22.5 g/cm^2).

Thus, from different experiments carried out at various altitudes it follows that at low and medium energies the number of stopped heavy mesons with mass $\sim 1000\, m_e$ is 1 – 5% of the number of protons, and 3 – 10% of the number of π-mesons.

Alikhanian *et al.*[6,7,15] report observations of particles with mass $\sim 550 m_e$. According to the most recent of these investigations,[15] done with a mass spectrometer and two cloud chambers, the number of particles of mass $(560 \pm 60) m_e$ is less than one percent of the number of μ-mesons in the same range interval. No stopped charged particles with mass

$500-600m_e$ were found in photoplates and emulsion stacks. If one assumes that such particles do exist in very small numbers, and if a positive particle decays to a slow π-meson, while a negative particle interacts and gives a star similar to a σ star from π-mesons, it is obviously very difficult to establish their existence from the decay products.

In our opinion the search for particles with mass $\sim 600m_e$ should be made in emulsions placed in a magnetic field. Since magnetic analysis allows higher accuracy for mass determination than other methods for slow charged particles, and besides results in a determination of particle mass and charge that is independent of decay processes, the use of the (ρ, r) method together with occasional use of the other methods will allow positive particle identification in the $600m_e$ region if such particles do exist. The use of plates will at the same time allow a study of the decay products.

3. *Proportion of Deuterons*

As indicated above, the magnetic deflection method allows the separation of heavy particles – protons, deuterons and tritons. From the data of the present work, the number of deuterons among slow particles stopped in the emulsion is 45 – 50% of the number of protons, and the number of tritons is $\sim$ 10% of the number of protons. From the data of Refs. 4 and 22, the number of deuterons stopped in the emulsion is 40 – 45% of the number of protons.

According to Refs. 23 – 25, where deuterons and tritons were not separated, the deuterons and tritons comprised $\sim$ 30% of the singly charged particles emitted from stars. Calculations by Le Couteur based on evaporation theory[26] give a similar number. However, the apparent agreement between experiment and evaporation theory is not necessarily real. For example, if one takes into account that the number of tritons is about 20% of the number of deuterons, then the actual number of deuterons as reported by all sources is about 40 – 50% of the number of protons; Le Couteur's figure is $\sim$ 20%.

The large emission of deuterons can possibly be explained as the result of non-evaporative processes where the particle is the result of a direct interaction between a nucleon and one or more nucleons in a nucleus. In this case an important part of deuteron formation is due to pickup of a nuclear nucleon by either the incident or scattered nucleon.[27,28] On the other hand, it has been shown by Migdal[29] that taking account of nucleon interactions in an evaporation process significantly increases the deuteron emission.

CONCLUSIONS

1. The mass determination error for slow charged particles stopped in an emulsion ($r < 10\ 000\,\mu$) is less for the magnetic deflection – range method than for the ionization – range method or the scattering – range method. Moreover, the magnetic field allows the particle charge to be determined.

2. In determining the mass of charged stopped particles by the magnetic deflection – range method, the errors were such that more than half (6 out of 9) the particles with "intermediate" ($m_\pi < m < m_p$) mass were incorrectly identified. If the mass of a slow charged particle is determined by another method – ionization – range or scattering – range, then identification of an "intermediate" mass is still more unlikely. From the analysis of our and other data, it follows that to identify reliably charged particles that constitute a very insignificant fraction of all particles observed (on the order of a few percent or less), the mass of such particles must be identified by several methods. Only if the results coincide can the identification be complete. In general, to find the proportion of heavy mesons, or to observe particles of unusual mass it is essential to determine the mass by several methods.

3. At an elevation of 9.5 km under 8 cm of lead the number of mesons with mass $\sim 1000m_e$ from among the stopped secondary particles caused by cosmic rays is 2.5 ± 1.5% of the number of protons. Particles with mass $500-600m_e$ are not observed. From the statistical information given in this paper it follows that the number of such particles, if they do exist, is less than 1% of the number of protons.

4. From both the 460 Mev proton data and the cosmic ray bombardments at 9.5 km it is seen that a large number of deuterons occurs among the slow charged secondary particles ($E < 50$ Mev). The number of deuterons is about half the number of protons.

In conclusion the author would like to express deep gratitude to her advisor Prof. N. A. Dobrotin, to Prof. M. G. Meshcheriakov and Prof. V. P. Dzhelepov for assistance in exposure of plates at the synchrocyclotron, to E. A. Brik, E. F. Vorob'ev, A. S. Kaliadin, and M. F. Solov'ev for scanning, to A. G. Novikov, S. F. Postnikov, P. P. Shishkov for construction of the apparatus and help in its operation, and to M. I. Podgoretskii and I. M. Gramenitskii for helpful discussions.

[1] Alikhanian, Morozov, Muskhelishvili, and Khrimian J. Exptl. Theoret. Phys. (U.S.S.R.) **18**, 673 (1948).

[2] A. I. Alikhanian, and A. I. Alikhanov, J. Exptl. Theoret. Phys. (U.S.S.R.) **21**, 1023 (1951).

[3] Alikhanian, Samoilovich, Gurevich, Babaian, and Gerasimov, J. Exptl. Theoret. Phys. (U.S.S.R.) **19**, 664 (1949).

[4] C. Franzinetti, Phil. Mag. **41**, 86 (1950).

[5] J. Barbour. Phys. Rev. **78**, 518 (1950).

[6] Alikhanian, Dadaian, and Shostakovich, Dokl. Akad. Nauk SSSR **82**, 693 (1952).

[7] A. Alikhanian and V. Kharitonov, Dokl. Akad Nauk SSSR **85**, 295 (1952).

[8] Amaldi, Fabri, Hoang, Lock. Scarci, Touscher, and Vitale. Suppl. Nuovo cimento **12**, 419 (1954).

[9] C. F. Powell. Suppl. Nuovo cimento **11**, 165 (1954).

[10] Baldo, Belliboni, Ceccarelli, Grilli, Sechi, Vitale, and Zorn, Nuovo cimento **1**, 1180 (1955).

[11] Inoki, Yasaki, and Matsukawa, Phys. Rev. **95**, 1565 (1954).

[12] M. S. Kozodaev and A. I. Filippov, Izv. Akad. Nauk SSSR, Fiz. Ser. **19**, 711 (1955).

[13] Liubimov, Eliseev, and Kocmachevskii, Izv. Akad. Nauk SSSR, Fiz. Ser. **19**, 720 (1955).

[14] H. Bridge, Nuovo cimento **1**, 874 (1955).

[15] Alikhanian, Shostakovich, Dadaian, Fedorov, and Deriagin, J. Exptl. Theoret. Phys. (U.S.S.R.) **31**, 955 (1956); Soviet Phys. JETP **4**, 817 (1957).

[16] W. T. Scott, Phys. Rev. **76**, 212 (1949).

[17] D. Morellet, Suppl. Nuovo cimento **1**, 209 (1955).

[18] P. E. Hodgson, Phil. Mag. **41**, 725 (1950).

[19] Y. Goldschmidt-Clermont, Nuovo cimento **7**, 331 (1950).

[20] Biswas, George, and Peters, Proc. Ind. Acad. Sci. **38**, 418 (1953).

[21] S. Biswas, George, Peters, and Swamy, Suppl. Nuovo cimento **12**, 369 (1954).

[22] Holtebekk, Isachsen, and Sörensen, Phil. Mag. **44**, 1037 (1953).

[23] N. Page, Proc. Phys. Soc. **A63**, 250 (1950).

[24] Harding, Lattimore, and Perkins, Proc. Roy. Soc. **A196**, 325 (1949).

[25] *Progress in Cosmic Ray Physics*, p 49, 1952.

[26] K. L. Le Couteur, Proc. Phys. Soc **A63**, 259, 498 (1950).

[27] G. F. Chew and M. L. Goldberger, Phys. Rev. **77**, 470 (1950).

[28] B. H. Bransden, Proc. Phys. Soc. **A65**, 738 (1952).

[29] A. B. Migdal. J. Exptl. Theoret. Phys. (U.S.S.R.) **28**, 3 (1955); Soviet Phys. JETP **1**, 2 (1955).

Translated by G. L. Gerstein
266

SOVIET PHYSICS JETP VOLUME 5, NUMBER 6 DECEMBER 15, 1957

Interaction of Nitrogen and Gold Nuclei

S. A. BARABOSHKIN, A. S. KARAMIAN AND G. N. FLEROV

(Submitted to JETP editor January 21, 1957)
J. Exptl. Theoret. Phys. (U.S.S.R.) 32, 1294-1297 (June, 1957)

The dependence of the cross sections on the energy of nitrogen ions has been determined for the reactions Au(N, 4*n*), Au(N, 5*n*) and Au(N, 6*n*). The irradiation was carried out at the internal test chamber of the cyclotron with monoenergetic ions accelerated up to 115 Mev. In accord with the theory of competitive processes, curves with pronounced peaks were obtained.

IRRADIATION OF GOLD WITH N^{14} ions, accelerated up to 100 – 130 Mev, produces highly excited Rn^{211} compound nuclei. The excitation energies involved amount to ~ 75 – 100 Mev. Such excitation of the nucleus should lead either to its disintegration into fragments, or to the "evaporation" of a certain number of nucleons – chiefly neutrons. In the latter case there are produced a number of isotopes of Rn, At, Po etc., which are either α-active or disintegrate through *K*-capture. In 1954 Burcham,[1] while studying the reaction products resulting from the irradiation of Au^{197} with accelerated ions of N^{14} and C^{13}, identified several Rn, At, and Po isotopes. He used the 150-cm cyclotron of the University of Birmingham to accelerate the N^{14} and C^{13} ions. Beams of accelerated multicharged ions with a continuous energy spectrum, decreasing sharply in the direction of higher energies, were obtained in this cyclotron. The maximum energies of the N^{14} and C^{13} ions at the ultimate radius were

130 and 110 Mev, respectively. The absence of a monoenergetic beam of multicharged ions made it impossible for him to obtain the energy dependence of the yields of reactions with emission of 4, 5 and 6 neutrons.

Using the source of multiply-charged ions developed by Morozov *et al.*,[2] an intense beam of 115-Mev monoenergetic N^{14} ions with charge 5 was obtained in the 150-cm cyclotron of the U.S.S.R. Academy of Sciences, and used for: 1) the study of the dependence of the cross sections on the energy of the nitrogen ions in the reactions Au (N, 4*n*), Au (N, 5*n*) and Au (N, 6*n*); 2) the determination of the absolute values of the cross sections of these reactions; 3) the determination of the principal mechanism of the interaction of heavy ions with gold nuclei. The latter case arose in connection with reported reactions[3] proceeding by means of partial penetration of nitrogen nuclei into the nuclei of the target and not by their complete fusion (grapeshot effect).

In the experiments the irradiation was carried out on piles consisting of 10 – 15 nickel foils on which thin gold layers were deposited. The piles were fastened at the internal test chamber of the cyclotron in front of the current collector (Fig. 1). The nickel foils were 1.5 – 2.0 μ thick, the gold layer on the foils comprised 0.1–0.3 mg/cm².

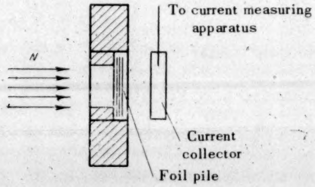

FIG. 1. Arrangement of the targets in the experiment

The energy lost by the beam in each foil was approximately 3 Mev. After irradiation the α-activity of the foils was measured during a time interval required for a unique separation of the half-lives. The α-particle were counted with the aid of an FEU-19 photomultiplier having a ZnS crystal and an amplitude discriminator. The discriminator bias used was the minimum necessary to eliminate the background produced by the superpositions of scintillations from the β-particles. The counting rates approached 10^4 pulses/min at a background of 1 – 2 pulses/min. The sensitivity of the apparatus was monitored by periodic measurement of the number of α-particles from a standard source (thick uranium foil). The solid angle of the count of the α-particles was determined experimentally.

In addition, some of the points on the excitation curve of the reaction (N, 5*n*) were obtained with the aid of photoplates, which were processed by T. F. Rasskazikhina.

The reactions were identified by the half-life periods of the α-active isotopes; moreover, the tabulated data of Ref. 4 and the results of Refs. 1 and 5, presented in Fig. 2 in the form of a schematic diagram, were taken as the base. From the schematic diagram it is evident that for the identification of the reactions (N, 4*n*), (N, 5*n*) and (N, 6*n*) the most convenient are the α-activities with the half-life periods of 108 min, 10.4 days and 25 min respectively. An essential factor in this method is the accuracy with which are determined the half-life periods and the branchings into α-disintegration and *K*-capture in the decay of the original isotopes Rn to At^{205}, At^{207}, and Po^{206}. Deviations in the values assumed for these quantities from the real values do not affect the form of the individual dependence curves of the cross sections on energy, but may lead to significant errors in the determination of the absolute values of the cross sections σ_{4n}, σ_{5n} and σ_{6n}. Therefore, in the cases where it was possible, refinements were made in some of the half-life periods and in the branchings of the α-disintegration and *K*-capture forks. For Rn^{206} and Po^{206} we have obtained half-life periods of 5.3 ± 0.1 min and 8.1 ± 0.5 days, respectively. The half-life periods of At^{207} and At^{205} in our experiments were in agreement with the data given in the schematic diagram. In several of the experiments it was possible to separate simultaneously from the disintegration curve the α-activities of Rn^{206} and Po^{206}, which permitted us to determine the branching in the disintegration fork of Rn^{206}. Considering, in accord with the schematic diagram, that At^{206} is completely disintegrated by *K*-capture, we have obtained for Rn^{206} a ratio K/α which is equal to 3.5 ± 0.2. It should be noted that this value was determined in several experiments differing in energy of the nitrogen ions by $\sim$ 15 Mev, and that within the limits of this accuracy compatible values were obtained for K/α. This result, evidently, substantiates the generatic relationship between Po^{206} and Rn^{206} and by the same token excludes the assumption regarding the formation of Po^{206} by means of partial penetration of nitrogen nuclei into Au^{197} nuclei.

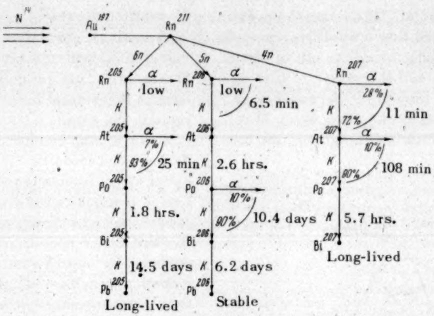
N14
Au 197
Rn 211
6n
5n
4n
Rn 205
α
low
Rn 206
α
low
6.5 min
Rn 207
α
28%
72%
11 min
K
At 205
α
7%
93%
25 min
At 206
2.6 hrs.
At 207
α
10%
90%
108 min
Po 205
1.8 hrs.
Po 206
α
10%
90%
10.4 days
Po 207
5.7 hrs.
Bi 205
14.5 days
Bi 206
6.2 days
Bi 207
Long-lived
Pb 205
Long-lived
Pb 206
Stable

FIG. 2. Decay scheme of the products of the reaction Au^{197} (M, xn) at $x = 4, 5$, and 6.

The variation of the cross sections of the reactions Au (N, $4n$), Au (N, $5n$) and Au (N, $6n$), which we have obtained, with the nitrogen-ion energy are given in Fig. 3. The characteristic course of the curves with the maxima is due to the presence of competitive reactions with emission of a different number of neutrons, as well as to the fission of the compound nucleus. The sharp decrease in the cross section of the reaction (N, $4n$) above 90 Mev can be explained by the fact that the reaction with emission of 5 neutrons predominates in this energy region. Analogously, the decrease in the cross section of the reaction (N, $5n$) above 100 Mev is determined by the fact that at these energies the reaction (N, $6n$) predominates. And, finally, the decrease in the cross section of the reaction (N, $6n$) above 110 Mev is brought about by the sharp increase in the cross section of fission of the composite nucleus.

In fact, the dependence on energy of the nitrogen ions of the total cross section of all the reactions with the emission of neutrons also has a characteristic maximum. Figure 4 shows this curve and its sum with the curve of the cross section of the fission of Au^{197} by nitrogen, which was borrowed from Ref. 6. The latter graph gives the energy dependence of the cross section of the formation of the compound nucleus Rn^{211} in the irradiation of gold by N^{14} ions. For comparison, the dependence of the "geometric" cross section calculated by the usual formula[7] for $r_0 = 1.55 \times 10^{-13}$ cm is given in the same figure.

As is evident from Fig. 4, the course of the cross section of the formation of the compound nucleus with subsequent fission or "evaporation" of neutrons is close to the theoretical. This result apparently indicates the comparatively low probability of the processes of partial penetration during the interac-

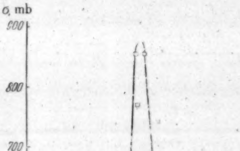

FIG. 3. Dependence of the cross sections of the reactions Au (N, $4n$), Au (N, $5n$) and Au (N, $6n$) on the energy of nitrogen ions. The arrows denote the points at which the cross sections are 0.2 and 8.0 *mb*.

tion of Au^{197} and N^{14} nuclei. Of course, the possibility cannot be excluded that a small portion of the observed activity is produced as a result of partial penetration. An analysis of the curves of Fig. 3 shows that the general form of the dependence on energy σ_{4n}, σ_{5n}, and σ_{6n} is the same as in other reactions at similar excitation energies of the composite nuclei.

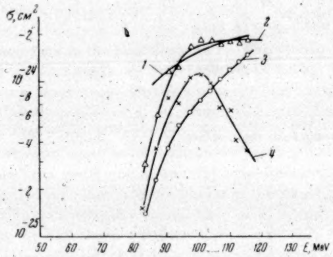

FIG. 4. Dependence on the energy of nitrogen ions of the cross sections: $\sum_{x=4}^{6}\sigma(\mathrm{N}, xn)$, $\sigma_{\text{fission}} + \sum_{x=4}^{6}\sigma(\mathrm{N}, xn)$, σ_{fission} and the theoretical cross section of the formation of the composite nucleus, calculated by the formula $\sigma_{\Gamma} = \pi R^2 [1-(B/E_N)]$: 1—$\sigma_\Gamma$, 2—$\sigma_f + \sum\sigma(xn)$, 3—$\sigma_f$, 4—$\sum\sigma(xn)$.

In 1956 Jackson[8] calculated the energy dependence of the cross sections of the reactions (p, xn) at $x = 1, 2, \ldots, 8$ in the irradiation of Bi^{206}, Pb^{206} and Pb^{208} for the range of proton energies 5 – 100 Mev. The author made the following assumptions: over the entire range of energies the temperature of the excited nucleus was considered constant and equal to 1.8 Mev; the nuclear radii were calculated by the formula $R = r_0 A^{1/3}$ at $r_0 = 1.35 \times 10^{-13}$ cm; the average energies of the neutron bonds in the above mentioned nuclei were assumed to be 7.3 Mev. The calculation took into account not only the neutrons emitted from the excited nuclei during the process of "evaporation", but also those knocked out as a result of direct nucleonic collisions between the protons and the nucleons of the target nuclei. It should be noted that, within the energy range of nuclear excitation in which we are interested, the role of the neutrons emitted as a result of a nuclear cascade is not large, therefore in its general formulation the theory can be applied also to pure "evaporation" processes. Jackson compared his calculations with the experimental data of Bell and Skarsgard.[9] This comparison has shown an agreement in the general form of the curves, but deviations in the details.

We have compared our data with the curves of Jackson and found that if we take into account the effect of the fission processes, the main difference lies in that our curves are shifted by ~ 10 – 15 Mev toward the higher energies. In this shift, apparently, is manifest the specific character of the reactions produced by multicharged ions, in particular, the formation of a "heated" compound nucleus with large angular momentum.

In the future, by an appropriate selection of the target nuclei irradiated by multicharged ions, we hope to obtain highly excited compound nuclei which will not break up into fragments. Such nuclei may serve as a good medium for the study of the processes of "evaporation" of nucleons from exited nuclei and the manifestation of the characteristics associated with excitation by multicharged ions.

We are grateful to academician I. V. Kurchatov for a number of valuable remarks during the discussion of the present paper. We also wish to express our thanks to the group of coworkers supervised by Iu. M. Pustovoit for ensuring good performance of the cyclotron during our experiments.

---

[1] W. E. Burcham, Proc. Phys. Soc. 67A, 555, 733 (1954).

[2] Morozov, Makov and Ioffe, Atom. Energiia 3, 272 (1957).

[3] Chackett, Fremlin and Walker, Phil. Mag. 45, 173 (1954).

[4] Hollander, Perlman and Seaborg, Revs. Mod. Phys. 25, 469 (1953).

[5] W. E. Burcham and B. C. Haywood, Proc. Phys. Soc. 69A, 862 (1956).

[6] Druin, Polikanov and Flerov, J. Exptl. Theoret. Phys. (U.S.S.R.) 32, 1298 (1957), Soviet Phys. 5, 1059 (1957) (this issue).

[7] G. Blatt and V. Weisskopf, *Theoretical Nuclear Physics*, IIL, 1954 (Russian translation).

[8] T. D. Jackson, Canad. Journ. of Phys. 34, 767 (1956).

[9] R. E. Bell and H. M. Skarsgard, Canad. Journ. of Phys. 34, 745 (1956).

Translated by Esther Rabkin
267

SOVIET PHYSICS JETP VOLUME 5, NUMBER 6 DECEMBER 15, 1957

Fission of Nuclei under the Influence of Accelerated Nitrogen Nuclei

V. A. DRUIN, S. M. POLIKANOV, G. N. FLEROV

(Submitted to JETP editor January 21, 1957)
J. Exptl. Theoret. Phys. (U.S.S.R.) 32, 1298-1304 (June 1957)

Experiments on fission induced in U^{235}, U^{238}, Bi, Au, Re, and Yb by accelerated nitrogen ions are described. The measurements were conducted with the aid of an ionization chamber. Graphs are presented showing the dependence of the fission cross sections for these nuclei on the nitrogen ion energy in the energy range from 70 to 110 Mev. The results obtained are analyzed from the viewpoint of influence of the parameter Z^2/A and of the excitation energy on the probability of fission.

---

1. INTRODUCTION

IN RECENT YEARS experiments have been conducted to investigate the fission of nuclei by light particles of high energy. These experiments have established many characteristics of such fission. It has been shown that in general there is symmetrical fission of the nucleus, and that the probability of fission is strongly dependent on the parameter Z^2/A (where Z is the nuclear charge, and A is the atomic weight). Nevertheless, it is difficult to obtain quantitative data on the dependence of the probability of fission on the excitation energy of the nucleus with various values of Z^2/A at high energies, since a cascade process occurs when the nuclei interact with high energy particles. This nuclear cascade process makes the nuclear excitation energy appear to be rather small and almost independent of the initial energy of the particle.

Calculations based on the Monte Carlo method and experimental data[1] indicate that a major part of the ejected nucleons in the nuclear cascade are protons. This leads to a large indeterminacy in the value of Z^2/A which is present after the nuclear cascade of the excited nucleus. Furthermore, this indeterminacy grows larger with increasing incident particle energy.

In light of the above it appears that quantitative data concerning the fission process can be obtained by the use of heavy accelerated ions such as nitrogen, oxygen, etc. Nuclear cascades do not appear in reactions produced by heavy incident nuclei, and the excitation energy of the resulting compound nucleus can be accurately determined if the energy of the incident particle is known. Thus, it is possible to change the excitation energy of the compound nucleus over a wide range by varying the energy of the incident particle. Also, the value of the parameter Z^2/A of the excited nucleus can be determined accurately.

Using nuclei with $Z < 83$ for targets, and employing nitrogen or oxygen nuclei as bombarding particles, one can study the fission of nuclei over a wide range of the parameter Z^2/A. It is worth noting that the study of fission in such nuclei as U, Np, Pu, etc., using accelerated heavy ions, is also of interest, since in these cases there can occur several specifically characteristic interactions of accelerated ions with the nuclei. Thus, it is presently well known that heavy ions, accelerated to moderate energies, can be successfully used for Coulomb excitation of the rotational levels of nuclei. When the accelerated heavy ions have sufficiently large energies, it will be found that in a certain number of cases the excitation energy of the nucleus exceeds the fission threshold because of the Coulomb interaction.

We give below experimental results on the fission cross sections of U^{235}, U^{238}, Bi, Au, and Yb under the influence of accelerated nitrogen ions, with respect to the energy of the nitrogen nuclei.

2. EXPERIMENTAL TECHNIQUE

Production of Accelerated Nitrogen Nuclei and Measurement of Their Energy

The accelerated nitrogen ions were produced in a cyclotron having pole pieces 150 cm. in diameter. The cyclotron was designed for the acceleration of ions with charge 5, produced directly in an ion source developed by P. M. Morozov, B. N. Makov and M. S. Ioffe. The nitrogen ion energy was 115 Mev at the final cyclotron radius. The measurements were carried out using the external beam in a cabin 12 meters away from the accelerator. Although no special measures were taken in bringing the beam out of the cyclotron chamber, a small portion of the accelerated ions of energy 70 to 115 Mev entered the outlet channel. Before the ion beam hit the target, it went through an aluminum foil 6 microns thick (which "stripped" the ions to a +7 charge state) and through a magnetic analyzer. For a given current, the magnetic analyzer would let through only ions of the corresponding fixed energy.

The ion beam intensity impinging on the target varied between 10^5 and 10^6 ions/second, depending on the ionic energy and state.

Recording of Fission Fragments

An ionization chamber was used to record the fission fragments. The nitrogen nuclei were admitted into the chamber through a thin metal foil window. The passage of nitrogen nuclei through the chamber raises the problem of distinguishing fission-fragment pulses from the pulses of nitrogen nuclei. Although the fission-fragment pulses are significantly larger than the nitrogen pulses, accidental superposition of the latter can produce pulses resembling those of fission fragments. A special chamber was therefore designed to permit strong attenuation of the nitrogen pulses. The chamber consisted of two compartments, separated by a thin metal foil (5 microns of nickel) which served as the collecting electrode. Both fission fragments and nitrogen nuclei caused ionization in the first compartment, but only nitrogen nuclei caused ionization in the second compartment. The dimensions of the compartments were so chosen that the nitrogen nuclei gave equal amounts of ionization in the two compartments.

The collecting electrode was at a potential of +200 volts with respect to the chamber casing. A supplementary electrode placed in the second compartment was at a potential of +400 volts, so that an electric field existed in the second compartment of equal magnitude but opposite direction to that in the first compartment. Thanks to this, the potentials induced on the collecting electrode as the result of the ionization caused by nitrogen ions in the first compartment were almost completely offset by the potentials of opposing sign induced by nitrogen ions in the second compartment. This scheme of compensation permitted reliable isolation of the fission-fragment pulses.

The chamber was filled with argon at a pressure of one atmosphere. A schematic drawing showing the construction of the chamber is given in Fig. 1.

The pulses from the chamber were passed to the grid of the first stage of a high-frequency linear amplifier, and after amplification, were recorded by a mechanical counter. A sample of typical results obtained with this chamber is given in Fig. 2.

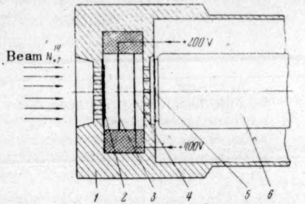

FIG. 1. Ionization chamber. 1 – chamber casing; 2 – investigated target material; 3 – collecting electrode; 4 – supplementary electrode; 5 – layer of ZnS; 6 – photomultiplier tube.

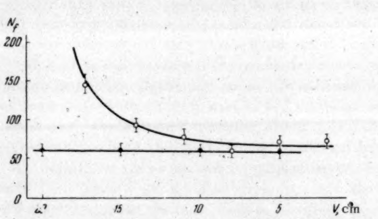

FIG. 2. Dependence of fission pulse count on the discriminator bias. ⦶ – for Re with nitrogen nuclei; ● – for U^{235} with thermal neutrons.

Recording of Nitrogen Ions

In order to determine the absolute fission cross section and to investigate the dependence of the fission cross section on the energy of the nitrogen ions, it is necessary to record the number of nitrogen ions which hit the target. With this aim in mind, the front and back walls of the chamber were made of thin metal foils, permitting the passage of the ion beam. A photomultiplier tube coated with a layer of ZnS was placed in contact with the back wall of the chamber to count the number of nitrogen ions. To decrease the loading on the photomultiplier, a collimator was placed in front of the ZnS. This collimator reduced the incident intensity by a factor of 800. After additional amplification, the pulses from the photomultiplier tube were passed to a counter having a discriminator. The system had a good plateau which stayed steady over a wide range of discriminator settings, and did not change with the passage of time. In a special experiment using alpha particles, it was established that the counting efficiency was practically 100%.

Targets

The targets consisted of discs of either aluminum 14 microns thick or nickel 6 microns thick, coated with a layer of the material being investigated (the diameter of the coated area was 30 millimeters). The gold and bismuth targets were prepared by diffusion of the metal in vacuo onto an aluminum foil; the targets of uranium and of a natural isotopic mixture of rhenium were diffused onto nickel, and the ytterbium targets were prepared on aluminum by electrolytic means.

The quantity of material on each target was determined by weighing (2 – 4 milligrams); in the case of U^{238} it was also determined by the emitted alpha-activity. The results by weighing in the case of U^{238} agreed satisfactorily with the results obtained by measuring alpha activity.

Experiments with the Internal Beam

The principal experiments were conducted with the external cyclotron beam. However, experiments were also carried out with the internal beam for U^{238}. In this case only the relative change of the fission cross section with respect to the energy of the nitrogen nuclei was studied. Fission fragments leaving the irradiated layer of uranium were gathered on tantalum plates which were positioned at an angle of 150 degrees with respect to the direction of the nitrogen ion beam. After a certain irradiation time, the beta-activity of the tantalum plates was measured. This beta-activity was proportional to the fission cross section. (It was assumed that for the energy interval 70 to 110 Mev of the nitrogen ions, the spectrum and angular distribution of the uranium fission fragments did not change materially. The agreement between results obtained with the internal and with the external beam supported this assumption.)

The thin uranium target (~0.6 mg/cm²) was attached directly to the current collector. This permitted the determination of the integral of the nitrogen ion beam current over the time of irradiation. The irradiation was carried out at a radius of 67 cm., and the measurement of the energy was accomplished with the aid of a nickel foil placed in front of the target. The experiments showed that the tantalum collecting plate gathers beta-active nuclei as well as fission fragments; these beta-active nuclei do not appear to be fission products, and are of only short duration. Apparently they are produced by the interaction of nitrogen ions with nickel, and reach the tantalum collectors by scattering. To avoid such contamination, the tantalum collectors were covered with nickel foils 2 microns thick. To exclude any activity being generated in the tantalum collecting plate by neutrons, an identical background plate was installed.

3. EXPERIMENTAL RESULTS

As a result of the experiments there were obtained data on the fission cross sections of U^{235}, U^{238}, Bi, Au, Re and Yb for various nitrogen ion energies. These data are presented graphically in Figs. 3 and 4.

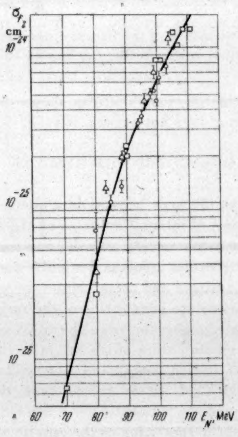

FIG. 3. Dependence of the fission cross-section on energy of the nitrogen nucleus: Δ – U^{238} with external beam; □ – U^{238} with internal beam; ○ – U^{235} with external beam.

The statistical errors of the measurements are shown on the graphs. Naturally, the absolute values of the cross sections are found with less accuracy, owing to errors in measuring the amount of material on the targets, in the counting efficiency for the nitrogen ions, etc. Analysis of the effect of these factors on the accuracy of the absolute val-

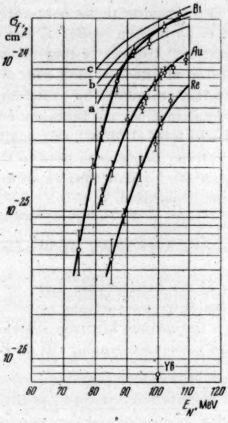

FIG. 4. Dependence of the fission cross section on the nitrogen nucleus energy for Bi, Au, Re and Yb.

ues of the fission cross sections shows that the maximum error does not exceed 15%.

4. DISCUSSION OF RESULTS

To analyze the experimental data one must know the mechanism of interaction between the nitrogen ions and the heavy nuclei; namely, one must know whether the process involves basically complete fusion of the nitrogen and target nuclei, or whether it involves particulate penetration of the target nucleus by the nitrogen nucleus. The first case leads to a highly excited state of the target nucleus, with a definite excitation energy and a known value of the parameter Z^2/A. In the second case, the excitation energy and the parameter Z^2/A are indeterminate, so that interpretation of the results is more complicated.

Experimental investigations[2, 3] of the interactions of multi-charged accelerated ions with heavy elements show that the basic process involves complete fusion of the interacting nuclei. From analysis of our experimental results we have concluded that the fission process is preceded by the formation of a highly excited nucleus with a known value of the excitation energy and of the parameter Z^2/A.

In the determination of the nuclear excitation energy, we took account of the nuclear recoil energy and of the change in the nuclear binding energy between the initial and final states of the nucleus. The latter correction was computed by the Weizsäcker formula

$$-E_{\text{B}}(Z, A) = -14.0\,A + 13.1\cdot A^{2/3} + \frac{77.3}{A}\left(\frac{A}{2} - Z\right)^2 + 0.584\,\frac{Z^2}{A^{1/3}} + \begin{cases} +34 & \text{for } Z \text{ odd, } A \text{ even} \\ -A^{3/4} & \text{for } Z \text{ even, } A \text{ even} \\ 0 & \text{for } A \text{ odd} \end{cases}$$

and amounted to 12, 17, and 22 Mev for rhenium, gold, and bismuth respectively.

Experimental investigation of the interaction of accelerated nitrogen ions with U^{235} and U^{238} nuclei showed that non-fission reactions occur with significantly lower probability than do fission reactions (by a factor of about 100). Therefore one can state that the curve given in Fig. 3 for U^{235} and U^{238} represents the dependence of the cross section for compound nucleus formation on the nitrogen ion energy. Since the probability of formation of the compound nucleus depends on the size of the Coulomb barrier, comparison of the curves for U^{235} and U^{238} indicates that the Coulomb barriers for these two nuclei are identical within the limits of experimental error.

The given results permit an estimate of the upper limit of the cross section for uranium fission resulting from Coulomb excitation by interaction with accelerated nitrogen ions. For a nitrogen ion energy of 70 Mev, this value is 7×10^{-27} cm.

The experimental results for Bi, Au, Re and Yb (Fig. 4) can be analyzed in order to clarify the influence on the probability of fission of the parameter Z^2/A and of the excitation energy which results from the nuclear reaction. The fission cross section is related to the probability of fission by the formula

$$\sigma_f = \sigma_c \cdot W_f, \qquad (1)$$

where σ_f is the fission cross section, σ_c is the cross section for formation of the compound nucleus, and W_f is the probability of fission. It can be seen from the formula that it is necessary to know both the cross section for fission of the excited nucleus and the cross section for formation of the compound nucleus in order to determine the probability of fission. Experimental investigation of the products of non-fissioning interactions of nitrogen nuclei with bismuth[4] show that for bismuth, as for uranium, the fission cross section practically coincides with the cross section for formation of a compound nucleus. For incident particle energies $E > 1.2\,E_{exc}$ (where E_{exc} is the nuclear Coulomb barrier energy) the cross section for formation of a compound nucleus agrees[5] to within 15% with the cross section calculated by the formula

$$\sigma_c \approx \pi (R_1 + R_2)^2\ [1 - (E_B / E)], \qquad (2)$$

where R_1 is the radius of the target nucleus and R_2 is the radius of the nitrogen nucleus. Moreover, the Coulomb barrier of the nucleus is found by the formula

$$E_{exc} = \frac{Z_1 Z_2}{r_0 \left(A_1^{1/3} + A_2^{1/3}\right)} \frac{(A_1 + A_2)}{A_1}, \qquad (3)$$

where Z_1 is the charge of the target nucleus, Z_2 is the charge of the nitrogen nucleus, A_1 is the atomic weight of the target nucleus and A_2 is the atomic weight of the nitrogen nucleus.

Fig. 4 shows the curves *a*, *b*, and *c*, calculated by formula (2) for Bi with values of r_0 equal to: 1.5×10^{-13} cm for curve *a*; 1.55×10^{-13} cm for curve *b*; and 1.6×10^{-13} cm for curve *c*. It is obvious that the theoretical curve calculated with $r_0 = 1.55 \times 10^{-13}$ cm best fits the experimental data for energies above 90 Mev.

The cross sections for formation of the compound nucleus for rhenium in the energy region above 85 Mev, and for gold above 90 Mev, were calculated by formula (2) using $r_0 = 1.55 \times 10^{-13}$ cm.

Figure 5 shows the dependence on the excitation energy of the probability of fission for the excited nuclei Th^{223} ($Z^2/A = 36.3$), Em^{211} ($Z^2/A = 35$) and for an isotopic mixture of Pb^{199} and Pb^{201} (average value of $Z^2/A = 33.6$), resulting from the complete fusion of the nitrogen nuclei with the nuclei of Bi, Au, and Re. Figure 6 shows the dependence of the probability of fission for the excited compound nucleus on the parameter Z^2/A with the given values of the excitation energy. It can be seen from the graphs that the probability of fission is strongly dependent on the value of Z^2/A of the excited nucleus.

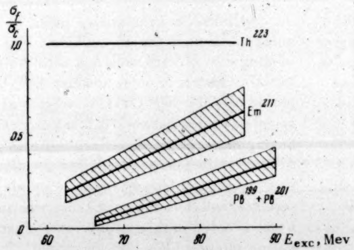

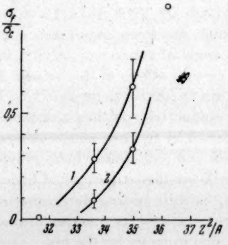

FIG. 5. Dependence of the probability of fission on the excitation energy E_{exc} for nuclei with various values of the parameter Z^2/A.

FIG. 6. Dependence of the probability of fission on the parameter Z^2/A for two different excitation energies: I–86 Mev; II–70 Mev.

The resulting values of the probability of fission fully determine the total probability of fission for the excited nuclei, but do not permit the establishment of the relation between high-temperature and emissive fission; that is, the relation between the number of fissions occurring upon the initial excitation of the nucleus and the number of fissions occurring after the first emission of several neutrons. To establish this relation, further investigations of the properties of strongly excited nuclei is necessary. Such an investigation, in combination with the data on probability of fission for the excited nuclei, will permit a more detailed study of the dependence of the relation Γ_f/Γ_n (Γ_f being the fission width and Γ_n being the neutron width) on the excitation energy and on the parameter Z^2/A.

We are indebted to Academician I. V. Kurchatov for many valuable comments made during discussion of the present work. To a group of associates led by Iu. M. Pustovoi we give our thanks for good cyclotron operation during our experiments.

[1] Belovitskii, Romanova, Sukhov, and Frank, J. Exptl. Theoret. Phys. (U.S.S.R.) 28, 729 (1956), Soviet. Phys. JETP 1, 581 (1955).

[2] W. E. Burcham, Proc. Phys. Soc. 67A, 555, 733 (1954).

[3] Baroboshkin, A. S. Karamian and G. N. Flerov, J. Exptl. Theoret. Phys. (U.S.S.R.) 32, 1294 (1957), Soviet Phys. JETP 5, 1055 (1957) (this issue).

[4] V. A. Karnauhov, Report, U.S.S.R. Acad. Sci. (1956).

[5] G. Blatt and V. Weisskopf, *Theoretical Nuclear Physics*, IIL, Moscow, 1954, Ch. VIII (Russ. Translation).

Translated by D. A. Kellogg
268

SOVIET PHYSICS JETP VOLUME 5, NUMBER 6 DECEMBER 15, 1957

Structure of Superconductors. X
Thermal, Microscopic and X-ray Investigation of the Bismuth–Palladium System

N. N. ZHURAVLEV
Moscow State University

(Submitted to JETP editor December 14, 1956)
J. Exptl. Theoret. Phys. (U.S.S.R.) 32, 1305-1312 (June, 1957)

A more accurate determination of the phase composition of alloys containing 43 – 54% by weight Pd is made, and the behavior of these alloys at low temperatures is explained. It is established that increase in the minimum interatomic distances in superconducting compounds of bismuth with palladium leads to an increase in T_c.

INVESTIGATION OF THE ALLOYS of bismuth with palladium has been undertaken in connection with the study of superconductivity, in view of the fact that certain alloys of this system become superconductors at low temperatures[1–4]. In this system superconductivity is thus manifested by compounds formed by two non-superconducting elements: bismuth and palladium. From previous microscopic and X-ray investigations of bismuth–palladium alloys, as well as from determinations of the melting temperatures for a series of these alloys. a tentative fusion diagram for the bismuth–palladium system has been constructed.[5] The crystalline structures of α- and β-Bi_2Pd and of BiPd have been determined,[6–9] and the low-temperature behavior of variously heat-treated alloys has been explained.[4,5,10] The present study was undertaken with the object of determining whether there is any connection between the atomic-crystalline structure of these alloys and their superconducting properties and with the further object of determining more precisely the phase composition of certain alloys and explaining their behavior at low temperatures.

THERMAL ANALYSIS

Chemically pure bismuth and palladium were employed in the preparation of the alloys; melting was accomplished in a resistance oven, in quartz capsules under an argon atmosphere. The heating and cooling curves were recorded with the aid of an automatic electronic potentiometer EPP-09 to temperatures of 200 – 400° C. The weights of the alloy samples ranged between 0.5 and 2 g. One curve having been recorded, the requisite amount of bismuth or palladium was added to the alloy; the latter was maintained for some time at an elevated temperature, and then the next curve was taken. Curves were recorded in this manner over a certain concentration interval (10 – 20% by weight), following which the alloy was replaced by a freshly-prepared mixture of bismuth and palladium, to avoid the accumulation of errors in the concentration.

The results obtained in this thermal analysis are represented graphically in Fig. 1. As palladium is added to the bismuth, the liquefaction temperature falls along *AB*. Beginning with ~ 5% by weight Pd, the liquefaction curve rises progressively along *BC*, and at 20.3% by weight Pd reaches a transition point at a temperature of 497°; at this temperature the compound Bi_2Pd liquefies with decomposition. The next branch of the liquefaction curve, *CDE*, beginning at 20.3% by weight Pd, rises as the palladium content of the alloys increases and reaches its peak at 33.8% by weight Pd, corresponding to the compound BiPd. Further addition of palladium

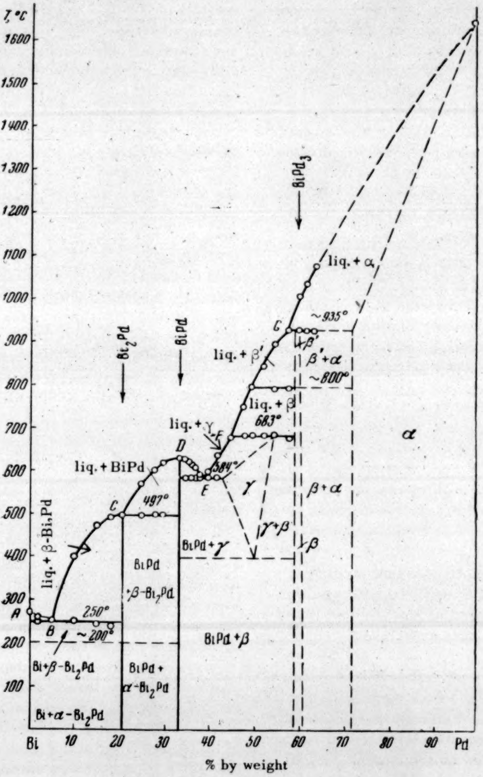

FIG. 1. Diagram of the Bi – Pd system.

causes the liquefaction curve to fall; eutectic points are found on the cooling curves at ~ 584°. The temperatures at which crystallization of the γ-phase becomes complete and the transition to the solid state occurs (eutectoid decomposition) could not be determined, owing to the inadequate sensitivity of the apparatus. The branch *EF* corresponds to initial precipitation of the γ-phase.

The compound $BiPd_3$ (β-phase) liquefies with decomposition at a temperature of 935°. The branch *FG* corresponds to initial precipitation of crystals of $BiPd_3$ (β-phase). On the cooling curves for alloys with concentrations of 55 and 58% by weight a weak thermal effect was observed at ~ 800° C which is related to a polymorphic transition of the compound $BiPd_3$ (β-phase). Thermal analysis was not carried out for the palladium-rich alloys, in view of their high melting temperatures.

Information is encountered in the literature regarding an X-ray study of the compound Pd_5Bi_3, which, according to the data of Ref. 11, crystallizes in two modifications: one high-temperature and the other low-temperature. For the high-temperature modification a structure of the type corresponding to nickel arsenide, with $a = 4.50 \pm 0.05$ kX and $c/a = 1.29$ is specified; for the low-temperature modification a low symmetry is indicated.

The results of our microscopic and X-ray studies in this composition range, however, show that in the temperature interval 400 – 680° C, there crystallizes a γ-phase having a rather large region of solubility and resembling the γ-phase of the antimony–palladium system,[12] rather than a compound having a definite stoichiometric composition (Pd_5Bi_3).

MICROSTRUCTURE AND X-RAY PHASE ANALYSIS

Investigation of the microstructure was carried out with alloys specially prepared for this purpose. The following etching agents were used in studying the microstructure: an aqueous mixture of KI + I, primarily for alloys containing large proportions of bismuth, and nitric acid and aqua regia, for alloys rich in palladium. The palladium-poor (hypoeutectic) alloys consist of bismuth and Bi_2Pd + Bi eutectic. Alloys containing less than 20.33% by weight Pd are composed of crystals of Bi_2Pd and Bi_2Pd + Bi eutectic. The number of precipitated Bi_2Pd crystals increases with increasing palladium concentration. Since Bi_2Pd can crystallize in two modifications,[7] alloys in this composition range when cooled rapidly from a temperature above 200° C consist of eutectic and Bi_2Pd crystals of the high-temperature modification (β-Bi_2Pd), while annealed alloys are composed of eutectic and Bi_2Pd crystals of the low-temperature modification (α-Bi_2Pd).

The temperature of the polymorphic transition in Bi_2Pd cannot be determined from the thermal analysis data, since the thermal effect, due to its small magnitude and the inadequate sensitivity of the apparatus, was not observed on the cooling curves. It may be presumed, however, that this temperature lies in the vicinity of 200° C, since alloys annealed at 350° C and then rapidly cooled from that temperature contain β-Bi_2Pd, while a β-Bi_2Pd alloy annealed for three hours at 195° C shows an intermediate condition, namely, an incomplete transition from the β to the α-modification is observed. The powder X-ray pattern obtained from such an alloy, characterized by a strong background, contains primarily the lines of α-Bi_2Pd. Metallographically, a unique structure is observed (Fig. 2), differing from the structures of the annealed and quenched alloys.

Alloys in the region between 20.33 and 32.8% by weight Pd are two-phase, and consist of crystals of Bi_2Pd and BiPd. Rapidly-cooled alloys consist of crystals of β-Bi_2Pd and BiPd. Annealed alloys consist of crystals of α-Bi_2Pd and BiPd. Powder X-ray patterns obtained from annealed and quenched alloys of the proper composition for BiPd (33.78% by weight Pd) are identical, precluding polymorphism in this compound.

Annealed alloys in the region from 32.8 to 33.8% by weight Pd are homogeneous, which suggests a small solubility of bismuth in BiPd. An attempt was made to confirm this metallographically-observed small solubility of bismuth in BiPd by X-ray methods. In the X-ray patterns obtained from polycrystalline samples of these alloys with radiations from copper in a chamber 86 mm in diameter no appreciable displacement of the back-reflected lines was observed. In alloys in the region from 33.8 to 43% by weight formation of a eutectic was observed, the eutectic point corresponding approximately to a concentration of 38% by weight Pd.

Hypoeutectic alloys rapidly cooled from a temperature above 400° consist of crystals of BiPd and BiPd + γ-phase eutectic (Fig. 3). Annealing of these alloys at temperatures below 400° leads to decomposition of the γ-phase. Figure 4 shows a photomicrograph of such an alloy, in which dark etched BiPd crystals can be seen in a matrix of BiPd + β-phase ($BiPd_3$) eutectoid. Ordinarily annealed hypereutectic alloys containing up to 43% by weight Pd consist of BiPd + γ-phase eutectic and γ-phase. Figure 5 shows a photomicrograph of a hypereutectic alloy, in which within the eutectic matrix there can be seen crystals of the γ-phase, surrounded by layers of the depleted eutectic. The presence of these layers gives some indication of variability in the composition of the γ-phase.

With rapid cooling, the formation of homogeneous alloys is observed in the region 43 – 54% by weight Pd, which implies the existence of a solid solution in this concentration interval. Varied heat treatment of alloys in this concentration region leads to variation of the alloy structure. Reducing the rate of cooling causes precipitation of the solid solution (γ-phase). Thus, for example, an alloy containing 48% by weight Pd when cooled with the capsule in the open air is found microscopically to have a homogeneous structure. Reducing the rate of cooling for this alloy leads to precipitation of a phase rich in palladium (β-phase) (Fig. 6). The structure of this alloy, with its characteristic alternation of light needles (more probably platelets) with dark zones, is similar to the structures found

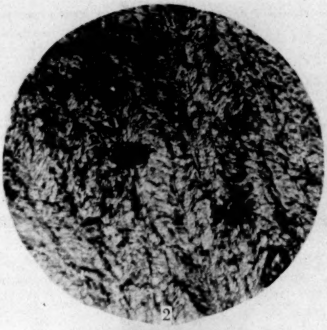

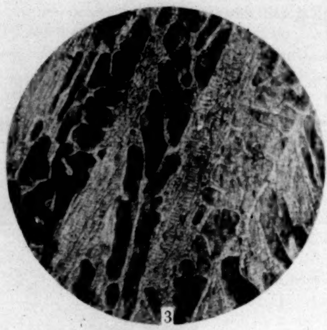

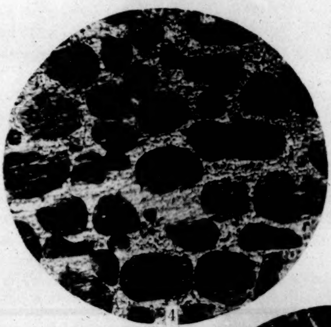

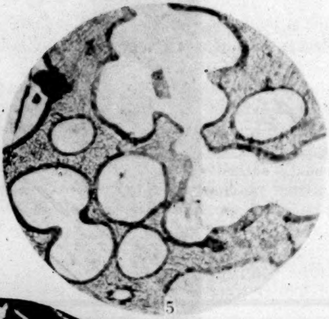

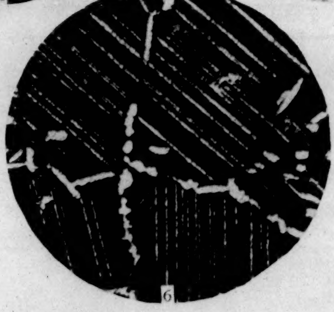

FIG. 2. Etched in KI + I; magnification 383×.

FIG. 3. Etched in KI + I; magnification 383×.

FIG. 4. Etched in KI + I; magnification 383×.

FIG. 5. Etched in KI + I; magnification 201×.

FIG. 6. Etched in HNO_3; magnification 201×.

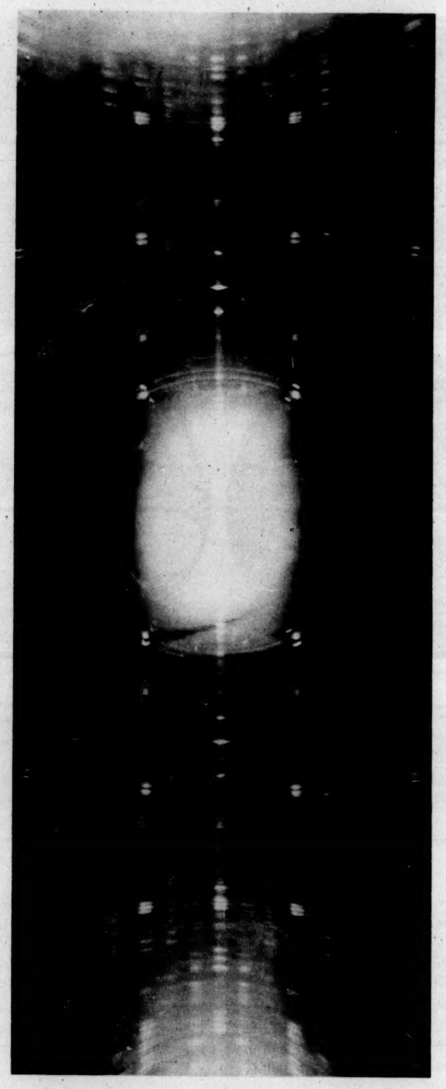

FIG. 7

in the analogous range of alloys in the antimony–palladium system, as reported in the work of Grigor'ev.[12] The light areas represent precipitation in the solid state of the palladium-rich phase (β-phase), while the dark matrix is the γ-phase. After prolonged annealing at a temperature of 250° C this structure changes sharply: the laminar formation is replaced by a typical pattern characteristic of eutectic mixtures containing, in addition, a certain amount of the superabundant component; *i.e.*, a structure similar to that represented in the photomicrograph in Fig. 4 is observed, in which, however, the number of BiPd crystals is smaller, in accordance with the composition. With insufficient annealing the decomposition of the γ-phase remains incomplete.

Powder X-ray patterns obtained for variously heat-treated alloys in this concentration range show against a strong background a small number of diffuse lines, from which it is difficult to determine definitely the phase composition of the alloy. Sharp lines were obtained only in the powder X-ray patterns for the γ-phase.

From a homogeneous alloy of composition 43.5% by weight Pd, cooled to the temperature of liquid air, segments were detached having the form of platelets with two well-formed plane surfaces giving ideal optical reflection. From the Laue and X-ray rotation patterns obtained with these crystalline concretions it was determined that the γ-phase crystallizes in a hexagonal lattice with constants $a = 7.75 \pm 0.05$ kX and $c = 5.85 \pm 0.05$ kX. The unit cell contains about 16 atoms of bismuth and palladium. The γ-phase has a super-lattice of the nickel arsenide type. For an alloy composition of 43.5% by weight Pd the pseudo-cell for the γ-phase has the parameters $a = 4.45$ and $c/a = 1.31$.

These γ-phase crystals were annealed for 8 hours at 250° C. X-ray rotation patterns were obtained from the annealed crystals (Fig. 7). In these X-ray rotation patterns, in addition to interference from the monocrystals, there appeared interference lines which were absent in the X-ray patterns for the un-annealed crystals. From the calculated interplanar distances and the intensities of the lines it was established that these correspond to two crystal lattices – BiPd and the low-temperature modifications of $BiPd_3$ (β-phase). Thus formation of two compounds as a result of annealing a homogeneous crystal of the γ-phase characterizes the eutectoid decomposition of this solid solution and confirms the metallographic data.

Alloys of composition corresponding to $BiPd_3$ (60.49% by weight Pd), both rapidly cooled and annealed, are metallographically homogeneous, but the powder X-ray patterns obtained for these alloys differ, from which it may be asserted that polymorphism occurs in this compound. This is confirmed by the differing solubilities of the annealed and quenched alloys in acids. Annealed alloys are more readily dissolved in HNO_3 than quenched alloys. It is probable that the compound $BiPd_3$ can exist over a certain concentration interval, since alloys containing 57% by weight Pd are nearly single-phase.

Alloys in the concentration interval from 60.49 to ~ 72% by weight palladium consist of crystals of a solid solution of bismuth in palladium and $BiPd_3$ (β-phase). With rapid cooling of the alloy, the solid solution of bismuth and palladium crystallizes in the form of dendrites, while annealed alloys are observed to contain crystals of irregular form. Alloys more rich in palladium, in the region up to 28% by weight Bi are found to be homogeneous after prolonged annealing, and represent a solid solution of bismuth and palladium. It has been established by X-ray methods that the maximum variation in the linear dimensions of the lattice for the solid mixture is about 3%.[7]

DENSITY, MICRO-HARDNESS AND TRANSITION TEMPERATURES FOR COMPOUNDS IN THE SUPERCONDUCTING STATE

The density σ_{hydr} of the compounds was determined for ingots weighing between 0.5 and 2.5 g by the method of hydrostatic suspension[13] in carbon tetrachloride ($\sigma_{\text{pycn}} = 1.585$ g/cm³) or bromoform ($\sigma_{\text{pycn}} = 2.885$ g/cm³).

Table 1 gives the densities σ_{hydr} and σ_X, the latter calculated from the X-ray data at room temperature.

The micro-hardness of the compounds was measured in the apparatus PMT-3, with a constant loading of 10 g on the indentor. The measurements were made on several samples from various melts, and the results were averaged. Table 1 also gives the average values of the micro-hardness and their limits of dispersion. For α and β-Bi_2Pd and the β and β' phases ($BiPd_3$) the scatter in the micro-hardness lies within the limits of error for the measurement, but for BiPd and the γ-phase it exceeds the limits of error, which may be explained by variation in the alloy composition and by anisotropy. For some of the ordinarily-annealed $BiPd_3$ samples the

TABLE 1

Compound	σ_{hydr}, g/cm^3	σ_X, g/cm^3	Average micro-hardness, kg/mm^2	Limits of variation in micro-hardness	T_c, °K
α-Bi_2Pd	11.5	11.65	170	140—200	1.7
β-Bi_2Pd	11.7	11.87	135	120—150	4.25
BiPd	12.5	12.56	200	130—270	3.7
γ-phase					
(composition 43.5% by weight Pd)	12.7	—	400	360—430	3.7—4
(composition 50.5% by weight Pd)	12.7	—	360	280—420	
$BiPd_3$ (β-phase)	12.8	—	230	185—280	—
$BiPd_3$ (β′-phase)	12.9	—	150	135—210	—

average values of the micro-hardness approached the micro-hardness for the γ-phase.

A study of the superconducting properties of bismuth–palladium alloys has been carried out by Alekseevskii, *et al.*,[1–4] at the Institute of Physical Problems, Academy of Sciences, U.S.S.R. Table 1 gives the temperatures T_c of the transition to the superconducting state for alloys of bismuth and palladium. The compounds α and β-Bi_2Pd and BiPd are superconductors. The transition to the superconducting state for the γ-phase at temperatures near T_c for BiPd may be occasioned by partial eutectoid decay in the samples, in which case the superconductivity of the latter would be due to the BiPd crystals, or, alternatively, T_c for the γ-phase may be near in value to T_c for BiPd. The compound $BiPd_3$ does not appear to be a superconductor.

DATA FROM THE STRUCTURAL STUDIES

1) The *low-temperature modification* α-Bi_2Pd crystallizes in a monoclinic lattice[6,7] with constants $a = 12.74 \pm 0.01$ A; $b = 4.25 \pm 0.02$ A; $c = 5.665 \pm 0.005$ A; $\beta = 102° 35' \pm 10'$. The unit cell is centered on the (001) face and contains four molecular masses, corresponding to 12 atoms. The space group C_{2h}^3, or $C\ 2/m$. The bismuth and palladium atoms are distributed in symmetry planes, in fourfold complexes (4*i*).

The structure of α-Bi_2Pd is of a new type.

Table 2 gives the interatomic distances, the coordinates of the atoms, and the number of neighbors.

TABLE 2

Atom	Complex	*x*	*y*	*z*	Number of neighbors	Interatomic distances, A
Bi I	4 i_1	0.156	0	0.321	4 Pd	2.78; 2.83; 2.83; 3.15
Bi II	4 i_2	0.076	1/2	0.796	3 Pd	2.90; 2.90; 2.87
Pd	4 i_3	0.226	0	0.820	7 Bi	2.78 2.83; 2.83; 2.90; 2.90; 2.97; 3.15

2) The *high-temperature modification* β-Bi_2Pd crystallizes in a tetragonal lattice[7] with constants $a = 3.362 \pm 0.001$ A; $c = 12.983 \pm 0.001$ A; the unit cell contains two molecular masses. The space group is D_{4h}^{17}, or $I4/mmm$. The two palladium atoms are located at the position 2(*a*), the four bismuth atoms at the position 4(*e*). The parameter for the bismuth atoms is $Z = 0.363$. The structure of β-Bi_2Pd is of a new type. The α and β-Bi_2Pd modifications are connected with each other structurally.

The interatomic distances are given in Table 3.

3) The *compound* BiPd crystallizes in an orthorhombic lattice[7,8] with constants $a = 7.203 \pm 0.001$ A; $b = 8.707 \pm 0.002$ A; $c = 10.662 \pm 0.001$ A. The unit cell is centered on the (001) face and contains

TABLE 3

Atoms	Experiment	Σ*R*
Bi — Bi	3.362	3.10
Bi — Bi	3.64	3.10
Bi — Pd	2.97	2.92

16 molecular masses, corresponding to 32 atoms. The space group is C_{2v}^{12}, or $Ccm2_1$. The structure of BiPd is of a new type having no center of symmetry.

The interatomic distances, the coordinates of the atoms, and the number of neighbors are listed in Table 4.

TABLE 4

Atom	Complex	x	y	z	Number of neighbors	Interatomic distances, A
Bi I	4a	0.108	0	0	7 Pd	2.93; 3.22; 2.96; 2.92; 2.92, 2.96; 2.96
					7 Bi	3.30; 3.55; 3.55; 3.76; 3.78; 3.78; 3.76
Pd I	4a	0.108	0	0.275	7 Bi	Coordinates of Pd relative to Bi the same as for Bi relative to Pd in the equivalent position
					2 Pd	2.70; 2.70
Bi II	4a	0.650	0	0	7 Pd	2.96; 2.90; 2.93; 2.92; 2.92; 2.96; 2.96
					7 Bi	3.30; 3.76; 3.76; 3.78; 3.78; 3.78; 3.78
Pd II	4a	0.650	0	0.275	7 Bi	Coordinates of Pd relative to Bi the same as for Bi relative to Pd in the equivalent position
					2 Pd	3.00; 3.00
Bi III	8a	0.125	0.274	0.722	7 Pd	2.92; 2.95; 2.92; 2.96; 2.93; 3.00; 3.02
					8 Bi	3.55; 3.76; 3.78; 3.76; 3.76; 3.78; 3.62; 3.78
Pd III	8a	0.125	0.274	0.447	7 Bi	Coordinates of Pd relative to Bi the same as for Bi relative to Pd in the equivalent position
					2 Pd	2.70; 3,00

CONCLUSION

The investigations carried out on alloys of bismuth with palladium have confirmed our previous tentative fusion diagram for the bismuth–palladium system. The position of the liquidus curve in the fusion diagram has been established, and the melting temperatures of the phases in the system have been determined with greater accuracy. In the concentration interval ~43 – 54% by weight Pd, the existence of a solid solution region analogous to the region in the antimony–palladium system has been confirmed.

The variation of the X-ray pattern with varying heat treatment of the alloy observed by the authors of Ref. 11 in their X-ray investigation of differently heat-treated alloys of composition corresponding to Pd_5Bi_3 (45.9% by weight Pd) has been interpreted erroneously. What these authors describe as the high-temperature modification of a compound Pd_5Bi_3 is in reality the γ-phase, which has a considerable range of solubility. The hexagonal cell with $a = 4.50$ and $c/a = 1.29$ cited by the authors is actually a pseudo-cell; owing to the presence of the super-lattice the true cell occupies a volume three times as large. What is referred to as the low-temperature modification of the compound Pd_5Bi_3 is really the product of the eutectoid decomposition of the γ-phase, consisting of a mixture of crystals of the two compounds BiPd and Bi_2Pd. The data obtained for this system indicate that superconductivity is manifested by compounds possessing extremely diverse types of crystal lattices, even including structures having no center of symmetry, as, for example, BiPd.[8]

TABLE 5

Compound	Minimum interatomic distances, A			
	T_c	Bi – Pd	Bi – Bi	Pd – Pd
α-Bi_2Pd	1.7	2.78	3.29	2.78
BiPd	3.7	2.92	3.30	2.70
β-Bi_2Pd	4.25	2.97	3.36	3.36

Analysis of the interatomic distances and comparison of these with the temperatures of the transitions to the superfluid state (Table 5) indicates that increase in the minimum interatomic distances in superconducting bismuth–palladium compounds leads to an increase in T_c.

I would like to take this opportunity to express my indebtedness to Prof. G. S. Zhdanov for his valued advice and instruction in the fulfillment of the present work.

---

[1] Alekseevskii, Brandt and Kostina, J. Exptl. Theoret. Phys. (U.S.S.R.) **21**, 951 (1951).

[2] N. E. Alekseevskii, J. Exptl. Theoret. Phys. (U.S.S.R.) **23**, 484 (1952).

[3] Alekseevskii, Brandt and Kostina, Izv. Akad. Nauk SSSR, Ser. Fiz. **16**, 233 (1952).

[4] Alekseevskii, Zhuravlev and Lifanov, J. Exptl. Theoret. Phys. (U.S.S.R.) **27**, 125 (1954).

[5] N. N. Zhuravlev and G. S. Zhdanov, Izv. Akad. Nauk SSSR Ser. Fiz. **20**, 708 (1956).

[6] Zevin, Zhdanov and Zhuravlev, J. Exptl. Theoret. Phys. (U.S.S.R.) **25**, 151 (1953).

[7] N. N. Zhuravlev and G. S. Zhdanov, J. Exptl. Theoret. Phys. (U.S.S.R.) **25**, 486 (1953).

[8] Kheiker, Zhdanov and Zhuravlev, J. Exptl. Theoret. Phys. (U.S.S.R) **25**, 651 (1953).

[9] G. S. Zhdanov, Trudy Inst. Kristallogr.; U.S.S.R. Acad. Sci. Publ. Hse. *10*, 231 (1954).

[10] Alekseevskii, Zhdanov, and Zhuravlev, Uch. Zap. MGU, Jubilee Collection of Physics Faculty.

[11] Schubert, Anderko, Kluge, Beeskow, Ibschner, Dorre and Esslinger, Naturwiss. **40**, 269 (1953).

[12] A. G. Grigor'ev, Izv. Inst. Platiny **1**, 32 (1929).

[13] E. M. Bronshtedt-Kupletskaya, *The Determination of the Specific Gravity of Minerals*, U.S.S.R. Acad. Sci. Publ. Hse., 1951, p. 43.

Translated by S. D. Elliott
269

SOVIET PHYSICS JETP VOLUME 5, NUMBER 6 DECEMBER 15, 1957

Structure of Superconductors. XI Investigation of Alloys of Bismuth with Platinum, Ruthenium, Osmium and Iridium

N. N. ZHURAVLEV AND L. KERTES
Moscow State University

(Submitted to JETP editor January 4, 1957)
J. Exptl. Theoret. Phys. (U.S.S.R.) 32, 1313-1318 (June, 1957)

Two superconducting compounds, BiPt and Bi_2Pt, are crystallized in the bismuth–platinum system. The compound Bi_2Pt crystallizes in two modifications, α and β. The appearance and disappearance of superconductivity in alloys of composition corresponding to Bi_2Pt may be explained by the presence of the high-temperature modification β-Bi_2Pt in these alloys. Bismuth does not form compounds with ruthenium, osmium or iridium by direct alloying.

INVESTIGATION OF THE ALLOYS of bismuth with platinum, ruthenium, osmium and iridium has been undertaken in connection with the study of superconductivity. A number of alloys of bismuth with elements in group VIII of the Mendeleev table become superconductors at low temperatures.[1–6]

1. THE BISMUTH–PLATINUM SYSTEM

It is known from data in the literature[7] that the solidification point for bismuth is lowered by approximately 2° by the addition of 0.2 – 1% by weight of platinum. It is suggested that the eutectic point corresponds to a concentration of less than 0.2% platinum. It is also known that when bismuth is alloyed with platinum two compounds are formed: BiPt and Bi_2Pt. The first has a structure of the type of nickel arsenide, with constants $a = 4.20$A, $c/a = 1.32$ (Refs. 8 and 9); for the second a structure of the type of pyrites is specified, with a constant $a = 6.683 \pm 0.005$A (Ref. 10). According to the data of Ref. 11, the compound BiPt becomes superconducting at 1.21° K, while from the data of Ref. 4 the transition occurs at ~ 2.4° K.

Samples of composition corresponding to Bi_2Pt give in some cases $T_c = 0.15°$ K, while in other cases they have no superconducting properties at all.[4] It is of interest to investigate the reason for such behavior in these alloys at low temperatures.

Thermal Analysis

Chemically pure bismuth and platinum were used in the preparation of the alloys. Melting was conducted in a resistance oven, in quartz capsules under an argon atmosphere. The heating and cooling curves were recorded with the aid of an electronic automatic potentiometer EPP-09 to temperatures of 200 – 400° C. The weights of the alloys lay between 0.5 and 1.5 g. After one heating and cooling curve had been recorded, the quantity of one or the other component needed to give the desired composition was added and another recording was made. Curves were recorded over a certain concentration interval (10 – 20% by weight), and then, to avoid accumulation of errors in the composition, the alloy was replaced by a freshly-compounded mixture of bismuth and platinum.

The results of the thermal analysis are presented in Fig. 1.

According to the data of Ref. 7 the addition of platinum lowers the melting temperature of bismuth by ~ 2° K. The EPP-09 apparatus does not have sufficient sensitivity to record a change in temperature within one-degree limits. For this reason we have not investigated the hypoeutectic alloys thermally. In the fusion diagram the melting point of bismuth *A* and the eutectic point *B* are very close to one another; with the scale used they coincide. From the eutectic point (~ 0.2% Pt) the liquefaction curve rises progressively along *BC* and at ~ 29% by weight Pt reaches a transition point at ~ 660°; at this temperature the compound Bi_2Pt melts with decomposition. The next segment of the liquefaction curve *CDE* beginning at ~ 29% by weight Pt rises as the platinum content of the alloy increases and reaches a maximum at 48.3% by weight Pt, corresponding to the compound BiPt. On the heating and cooling curves for alloys in the interval 11 – 32% by weight Pt a thermal effect is observed at ~ 390° having a large hysteresis which for a cooling rate of 20 – 25°/min reaches more than 100°. The magnitude of the hysteresis falls with increasing Pt content and reaches 20° for a composition corresponding to Bi_2Pt.

It is of interest to note that this thermal effect is not observed for alloys with platinum contents

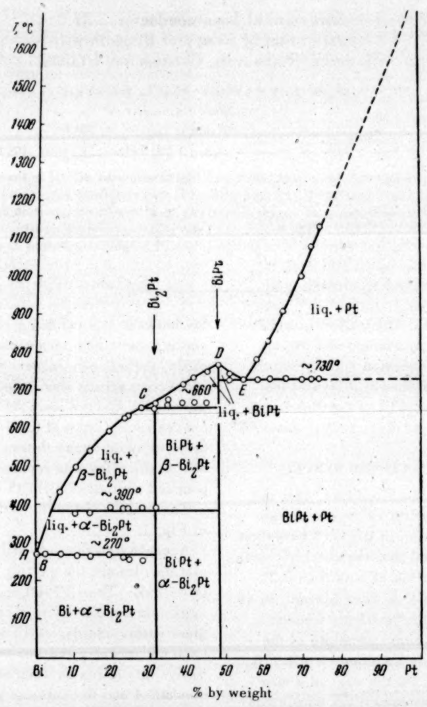

FIG. 1. Diagram of the Bi–Pt system

greater than that of the compound Bi_2Pt, although it should exist up to the concentration of BiPt. This can probably be explained by assuming that at these cooling rates the polymorphic transition does not take place in the solidified alloy. Further addition of platinum is accompanied by a fall in the liquefaction curve. Eutectic points are found on the cooling and heating curves at ~ 730°. From the point *E* onward the liquefaction curve rises steeply with increasing platinum content.

Microstructure and X-ray Phase Analysis

The investigation of the microstructure was carried out with alloys specially prepared for this purpose. In the study of the microstructure nitric acid and aqua regia were employed as etching agents. Alloys containing less than 31.84% by weight platinum consist of Bi_2Pt crystals and Bi_2Pt + Bi eutectic. The number of Bi_2Pt crystals precipitated increases as the platinum content rises. The compound Bi_2Pt crystallizes in two modifications with the temperature of the polymorphic transition ~ 390° Rapidly-cooled alloys in this composition interval at temperatures above 390° consist of eutectic and Bi_2Pt crystals of the high-temperature modification (β-Bi_2Pt), and annealed alloys of eutectic and Bi_2Pt crystals of the low-temperature modification (α-Bi_2Pt). Figure 2 shows a photomicrograph of an annealed alloy containing 8% by weight of platinum, in which light crystals of α-Bi_2Pt are visible in an

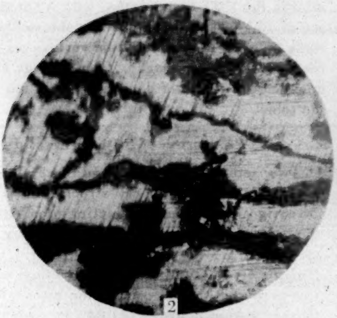

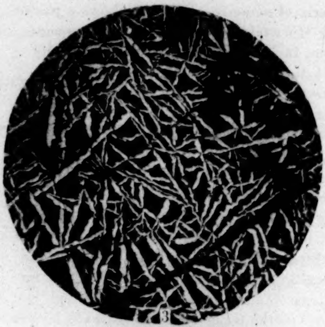

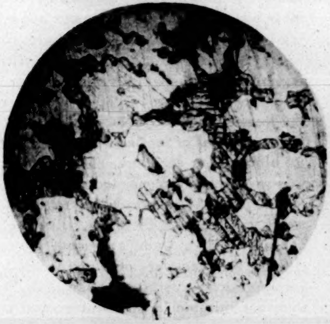

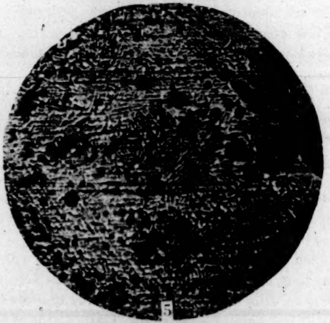

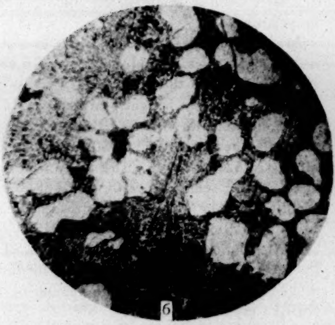

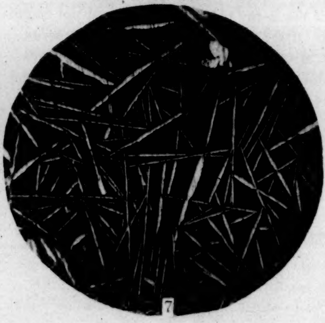

FIG. 2. Etched in HNO_3; magnification 86×.

FIG. 3. Etched in HNO_3; magnification 86×.

FIG. 4. Etched in HNO_3; magnification 201×.

FIG. 5. Etched in acid mixture (HNO_3 + HCl); magnification 440×.

FIG. 6. Etched in acid mixture (HNO_3 + HCl); magnification 200×.

FIG. 7. Etched in HNO_3; magnification 86×.

etched matrix of eutectic. Figure 3 shows a photomicrograph of a rapidly-cooled alloy of the same composition, in which needle-like (more probably tabular) crystals of β-Bi_2Pt can be seen in the etched eutectic matrix.

Alloys in the region between 31.8 and 48.3% by weight platinum are two-phase and consist of crystals of Bi_2Pt and of BiPt. Annealed alloys consist of crystals of α-Bi_2Pt and BiPt. Figure 4 shows a photomicrograph of an alloy containing 43% by weight of platinum, in which can be seen light BiPt crystals of irregular form and among them gray crystals of Bi_2Pt showing twinning lines similar to the lines observed for BiPd and Bi_2Pd.[12] The powder X-ray patterns obtained from annealed and rapidly-cooled alloys of the composition of BiPt (48.30% by weight Pt) are identical, which precludes polymorphism in this compound.

In alloys containing 48.3% by weight and higher of platinum, there is observed the formation of a BiPt + Pt eutectic (Fig. 5) with a eutectic point corresponding approximately to a concentration of 55% by weight platinum. Alloys more rich in platinum consist of crystals of platinum and BiPt + Pt eutectic. Figure 6 shows a photomicrograph of an alloy containing 70% by weight of platinum, in which light platinum crystals are visible in the eutectic matrix. A precision powder X-ray pattern was obtained, in a chamber 114 mm in diameter with radiations from copper, from platinum crystals separated from an alloy of this composition by dissolving the BiPt crystals in aqua regia. Calculation and indexing of the X-ray pattern showed that the magnitude of the lattice constant for the platinum crystals in the alloy agrees to within the limits of accuracy of the measurement with the constant for the initial pure platinum. This indicates a negligible solubility of bismuth in platinum, in contradistinction to the considerable solubility which we have found for bismuth in palladium,[12] as well as for antimony and lead[7] in palladium. Platinum, like rhodium,[13] does not dissolve bismuth.

Density and Micro-Hardness of the Compounds

The density σ_{hydr} of the compounds was determined with ingots weighing 0.5 – 1.5 g using the method of hydrostatic suspension[14] in carbon tetrachloride ($\sigma_{pycn} = 1.585$ gm/cm^3).

The densities σ_{hydr} and σ_X, the latter computed from X-ray data at room temperature, are listed in the table.

The micro-hardness of the compounds was measured in the PMT-3 apparatus, with a constant loading of 10 g on the indentor. Measurements were made on several samples from various melts, and the results were averaged. The average micro-hardness and its limits of dispersion are also listed in the table.

Production of β-Bi_2Pt Crystals

Two methods were employed to obtain β-Bi_2Pt crystals suitable for X-ray structural studies and investigation of superconducting properties: the method of production within a capillary, and the method of growth in a mother liquor. To obtain β-Bi_2Pt crystals using the first method an alloy was prepared whose composition corresponded closely to that of Bi_2Pt (31.84% by weight Pt). The alloy was placed within a quartz capsule terminating in a fine capillary (0.5 – 1 mm). The capsule was evacuated and placed within a tilting tubular resistance oven specially prepared for this purpose. The alloy was heated to 800 – 850° C, resulting in the formation of a droplet. The oven was swung into a vertical or inclined position, so that the droplet blocked the capillary. The tip of the capillary was wrapped in a dampened cotton pad (or immersed in water) and argon was admitted into the capsule; under this pressure the alloy filled the capillary, cooling rapidly. Using this method a number of β-Bi_2Pt samples were obtained in the form of aggregates of large crystals. These β-Bi_2Pt samples were not suitable for X-ray structural investigations, and were used in studying the superconducting properties.

In preparing crystals of β-Bi_2Pt by the second method alloys were employed having a composition richer in bismuth than that of Bi_2Pt. An alloy containing 8 – 10% by weight platinum was placed in a quartz capsule which was filled with argon. The alloy was heated to 700 – 750° and then cooled slowly to 420 – 450° C. The alloy was maintained at this latter temperature for several hours and then rapidly cooled. As a result of this heat treatment a two-phase alloy was obtained (Fig. 3) consisting of eutectic and deformed tabular crystals of β-Bi_2Pt. By selection of the rate of cooling for the alloy it proved possible to reduce the number of deformed β-Bi_2Pt crystals (Fig. 7).

The tabular β-Bi_2Pt crystals were separated from the alloy by dissolving the bismuth in dilute nitric acid. An interesting fact should be noted. If nitric acid of concentration greater than that necessary to dissolve the bismuth in the eutectic is used, not

Compound	σ_{hydr}, g/cm³	σ_X, g/cm³	Average micro-hardness, kg/mm²	Limits of variation in micro-hardness
α—Bi_2Pt	13.3	13.6	145	115—205
β—Bi_2Pt	12.9	—	90	85—105
BiPt	15.5	15.75	190	170—220

only the bismuth of the eutectic but also the bismuth in the compound will be dissolved. In etching the alloy a portion of the bismuth in the compound goes into solution. Such enrichment in platinum during the separation of Bi_2Pt crystals from the alloy has already been observed by Roessler.[15] Further increase in the concentration of the acid makes it possible to dissolve nearly all of the bismuth in the compound, leaving a residue of finely-divided platinum. Powder X-ray patterns obtained from this residue show extremely diffuse platinum lines. It is probably practicable, by such selective dissolving, to obtain a skeletal platinum catalyst similar to that described for copper and nickel in the dissertation of Kefeli.[16]

The tabular β-Bi_2Pt crystals separated from the alloy were not wholly suitable for X-ray structural investigations. From the Laue diagrams obtained with the X-ray beam directed perpendicular to the plane of the platelet it was established that the crystals have a hexagonal lattice.

2. ALLOYS OF BISMUTH WITH RUTHENIUM, OSMIUM AND IRIDIUM

Alloys of bismuth with ruthenium, osmium and iridium containing 80 – 90% by weight bismuth were prepared in quartz capsules under an argon atmosphere. Metallographic analysis of these alloys showed two-phase structures in all cases. Powder X-ray patterns were obtained for all of the alloys using copper radiation in a chamber 86 mm in diameter. The X-ray patterns showed lines of bismuth and of ruthenium, osmium or iridium, according to the alloy. In none of the X-ray patterns was any appreciable shifting of the back-reflected lines for one phase or the other observed.

The alloys were subjected to etching in nitric acid. There remained as a residue a grey powder in the case of the alloys of bismuth with ruthenium and iridium, and a dark blue powder in the case of the alloys of bismuth with osmium. From all of these powders X-ray patterns were obtained which showed that the etched powders consisted of ruthenium, iridium and osmium, respectively. Thus, bismuth does not form compounds with ruthenium, osmium or iridium by direct alloying.

CONCLUSION

Investigation of the alloys of bismuth with platinum has made it possible to construct a fusion diagram for the bismuth–platinum system. Two compounds are crystallized in the bismuth–platinum system: Bi_2Pt and BiPt. The compound Bi_2Pt melts with decomposition at a temperature $\sim$ 660° C and can exist in the two modifications α and β-Bi_2Pt, with the temperature of the polymorphic transition $\sim$ 390° C. The compound BiPt corresponds to a maximum in the fusion diagram, melts at $\sim$ 760° C, and forms a eutectic mixture with platinum.

The existence of the high-temperature modification β-Bi_2Pt explains the behavior of alloys of the composition of Bi_2Pt at low temperatures. The appearance of superconductivity in a rapidly-cooled alloy is due to the presence in the alloy of crystals of the superconducting high-temperature modification. The data obtained for the bismuth–platinum system do not as yet permit determination of the reason for the great diversity in T_c for the compound BiPt.

Investigation of the alloys of bismuth with ruthenium, osmium and iridium has shown that ruthenium, osmium and iridium do not form compounds when directly alloyed with bismuth. The data obtained for bismuth–iridium alloys provide confirmation of a previous investigation.[17]

We would like to take this opportunity to express our gratitude to Professor G. S. Zhdanov for his valued counsel and direction in the course of the present work, and to R. N. Kuz'min and A. I. Soklakov for their aid in carrying out the experiments.

[1] Alekseevskii, Brandt and Kostina, J. Exptl. Theoret. Phys. (U.S.S.R.) **21**, 951 (1951).

[2] Alekseevskii, Brandt and Kostina, Izv. Akad. Nauk SSSR, Ser. Fiz. **16**, 233 (1952).

[3] N. E. Alekseevskii, J. Exptl. Theoret. Phys. (U.S.S.R.) **23**, 484 (1952).

[4] N. E. Alekseevskii, J. Exptl. Theoret. Phys. (U.S.S.R.) **25**, 383 (1953).

[5] Alekseevskii, Zhuravlev and Lifanov, J. Exptl. Theoret. Phys. (U.S.S.R.) **27**, 125 (1954).

[6] Alekseevskii, Zhdanov and Zhuravlev, J. Exptl. Theoret. Phys. (U.S.S.R.) **28**, 237 (1955); Soviet Phys. JETP **1**, 99 (1955).

[7] M. Hansen, *The Structure of Binary Alloys;* Metallurgizdat, M.–L., 1951; p. 317 (J. Springer, Berlin, 1936; p. 324).

[8] E. Zintl and H. Kaiser, Z. anorg. u. allgem. Chem. **211**, 113 (1933).

[9] V. P. Glagoleva and G. S. Zhdanov, J. Exptl. Theoret. Phys. (U.S.S.R.) **25**, 284 (1953).

[10] H. I. Wallbaum, Z. Metallkunde **10**, 200 (1943).

[11] B. T. Matthias, Phys. Rev. **90**, 487 (1953).

[12] N. N. Zhuravlev and G. S. Zhdanov, J. Exptl. Theoret. Phys. (U.S.S.R.) **25**, 485 (1953).

[13] N. N. Zhuravlev and G. S. Zhdanov, J. Exptl. Theoret. Phys. (U.S.S.R.) **28**, 228 (1955); Soviet Physics JETP **1**, 91 (1955).

[14] E. M. Bronshtein-Kupletskaya, *The Determination of the Specific Gravity of Minerals*, U.S.S.R. Acad. Sci. Publ. Hse., 1951, pp. 43–55.

[15] F. Roessler, Z. anorg. u. allgem. Chem. 9, 68 (1895).

[16] L. M. Kefeli, Author's summary of doctoral dissertation, L. Ia. Karpov Physico-Chemical Institute, 1956.

[17] L. Wöhler and L. Metz, Z. anorg. u. allgem. Chem. **149**, 310 (1925).

Translated by S. D. Elliott
270

SOVIET PHYSICS JETP VOLUME 5, NUMBER 6 DECEMBER 15, 1957

The Penetrating Component of Extensive Cosmic Ray Showers in the Atmosphere

IU. N. VAVILOV, IU. F. EVSTIGNEEV, AND S. I. NIKOL'SKII

P. N. Lebedev Physical Institute, Academy of Sciences, U.S.S.R.

(Submitted to JETP editor January 12, 1957)
J. Exptl. Theoret. Phys. (U.S.S.R.) **32**, 1319-1327 (June, 1957)

We have investigated the spatial distribution of μ mesons arising from extensive air showers initiated by primary particles of various energies. It was found that within experimental errors the spatial distribution function for μ mesons did not depend on the energy of the primary particle. The number of μ mesons produced varied with the energy of the primary particle in such a way as to confirm the supposition, advanced previously, that the manner in which energy is distributed among the secondary particles in an elementary nuclear interaction changes at an energy of about 10^{15} ev.

IT HAS BEEN ESTABLISHED by many experiments[1] that the penetrating component in extensive air showers consists both of particles which react strongly with various nuclei, and those which do not (μ mesons). There are more of the latter (passive) particles than of the former (active) ones. In the following we describe the results of an investigation carried out in the summer and fall of 1954 at an altitude of 3860 m (Pamir) on the passive part of the penetrating component of showers.

1. EXPERIMENTAL SETUP

To study the spatial distribution of charged particles in extensive atmospheric showers, we investigated individual showers, using a large number of counters in a hodoscopic arrangement. For each shower of interest we found where the axis of the shower was, the spatial distribution of charged particles, and the total number of particles in the shower at the plane of observation. Penetrating par-

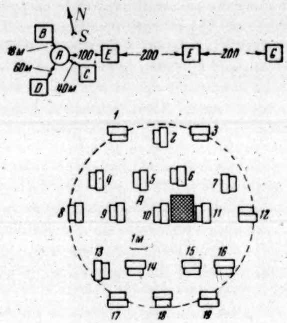

FIG. 1. Experimental arrangement for measuring the particle current density in extensive atmospheric showers whose axes fall near point A. The small arrow near B points north. The crosshatched rectangle near A denotes a detector for penetrating particles.

ticles were also detected at several points.

Figure 1 shows the general experimental setup. Nineteen groups of hodoscopic counters were distributed over a circle of radius 6 m. about the point A. Each group contained 24 counters of area 16 cm^2, and 24 counters of area 100 cm^2. The resolving time of the hodoscope channels was $(1-3) \times 10^{-5}$ sec. The axes of extensive air showers which passed near A could be located to within 1 m (taking into account the circular symmetry of the shower).

Figure 1 and table 1 show the number of hodoscope channels, the counter area feeding each channel, and the resolving time of the associated electronics. The number of counters at points B, C, D, as shown in Table 1, was enough to measure the current density of charged particles in showers involving $10^5 - 10^6$ particles. The counter area available at point E was sufficient to determine the current density of charged particles above E only in showers with about 10^6 particles. The charged particle current density in showers with fewer particles was obtained by assuming that showers with the same (total) number of particles have the same spatial distribution functions. Grouping together showers involving the same total number of particles and with the same axes, it is possible to find the probability of recording a particle at a given point, and hence the mean particle current density at a corresponding distance from the shower axis. The average current density of charged particles at points F and G, located 300 and 500 m from the center of the arrangement, was determined in a similar way.

In addition to the hodoscopic groups of counters

TABLE I.

Point	Distance from center, m	Counter area associated with one hodoscope channel, cm^2	Number of hodoscope channels	Resolving time of hodoscope, sec
B	18	22 100 330	24 24 24	$\sim10^{-5}$ $\sim10^{-5}$ $\sim10^{-5}$
C	40	22 100 330	24 24 36	$\sim10^{-5}$ $\sim10^{-5}$ $\sim10^{-5}$
D	60	100 330	24 48	$\sim10^{-5}$ $\sim10^{-5}$
E	100	22 330	24 48	$1\cdot10^{-5}$ $1\cdot10^{-5}$
F	300	22 100 4000	24 24 6	$\sim10^{-5}$ $\sim10^{-5}$ $2.5\cdot16^{-6}$
G	500	3000	8	$2.5\cdot10^{-6}$

used to measure the total charged particle current density, points *A*, *B*, *C*, *E*, and *G* had detectors of penetrating particles. The detectors at points *A*, *B*, and *C* (Fig. 2a) could distinguish between penetrating particles which did not interact strongly with nuclei (μ mesons) and electron showers formed in the material of the detector. The lead and iron absorbers surrounding the hodoscopic counters of the detector practically eliminated the possibility that electrons and photons from the air could reach these counters. Filters between the rows of counters allowed us to distinguish between electron showers and δ-showers produced by μ mesons. In detector *A*, one row of counters had an area of 0.48 m^2, the corresponding figures for detectors *B* and *C* being 0.36 m^2 and 0.72 m^2. The penetrating particle detectors at points *E* and *G* were simpler (Fig. 2b), since earlier measurements had shown that at such distances from the shower axis, there were no particles which interacted strongly with nuclei to produce showers. The counter area was 1.8 m^2 at point *E* and 2.4 m^2 at detector *G*.

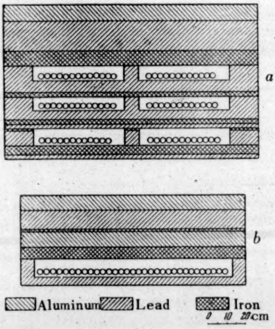

FIG. 2.

The hodoscopic arrangement described above was triggered by coincidences between the four groups of counters at the center of *A* (Fig. 1). The counter area in each of these groups was 400 cm^2. About 8000 extensive air showers were recorded in all. In about 1200 of these, the axis of the shower passed near *A*.

2. SPATIAL DISTRIBUTION OF μ MESONS IN SHOWERS

For the showers we observed, the μ meson current density was not large enough that it could be measured using the penetrating particle detectors described above. The average μ meson current density in showers with a given total number of particles was measured by counting the number of μ mesons passing through the detector in showers whose axes were all the same distance from the detector. The μ meson current density at this given distance from the shower axis can then be written

$$\rho_\mu(r) = (1/S)\ln(1 + m/n).$$

where *S* is the area covered by one row of detector counters, *m* is the number of μ mesons recorded, and *n* is the total number of showers observed in which the counters of the detector did not fire.

We observed events where the μ meson passed through the middle row of counters in Fig. 2a. In such cases, one counter of the middle row was discharged, and in addition a counter registered in at least one other row of the detector. When a μ meson passed through all three rows, the counters which registered were all found to lie on a straight line. When the μ meson passed between counters in the top or bottom rows, or went through the detector at an angle, or was absorbed in the material between the bottom and middle rows, then only two rows of the detector fired. All cases where two or more counters in the same row went off were due to δ-showers, or electron showers originating in the detector and were included neither in the *m* nor in the *n* of the above formula. Such showers, which originate in the detector, were excluded from consideration because when a big shower occurs in the detector it is not possible to say reliably whether a μ meson is present or not. Neglecting, then, the μ mesons which initiated δ-showers in the material, and taking electron showers in a detector to be statistically independent of the passage of a μ meson through that detector, we obtained, for each distance from the shower axis and for a given primary energy, the current density of μ mesons with enough energy ($\geq$ 440 Mev) to pass through the absorbers in the detector.

We measured the probabilities of recording δ-showers initiated both by μ mesons from the hard component of cosmic rays and by μ mesons associated with extensive air showers. Measurements were made with a detector of penetrating particles in a shaft whose depth was equivalent to 16 m of water. For all practical purposes, this eliminated that component of cosmic rays which interacts strongly with nuclei. The measurements showed that the probability of observing, in one row of the detector, a δ-shower initiated by a cosmic ray μ meson is $(7 \pm 0.6)\%$ of the total number of mesons passing through the detector. The corresponding probability for δ-showers initiated by μ mesons from extensive atmospheric showers was $(8 \pm 1)\%$. Since the probability of observing a δ-shower in at least one of the three layers of counters in the detector is about three times as large, the number of μ mesons passing through the detector unaccompanied by δ-showers was increased by 25% in calculating the μ meson current density.

In finding the μ meson current density at large distances from the shower axis, it was not necessary to exclude events where showers originated in the detector material. This is because even at 60 m from the shower core the number of particles which interact strongly with nuclei is only a few per cent of the number of μ mesons.[2] Hence at large distances from the shower core, both events where only one counter fired and events where counters in more than one row of the detector fired were taken to mean that a μ meson had passed through the detector. The number of the latter events ($\sim 10\%$) was about the same as the expected number of δ-showers, so that the difference in the criteria for selecting μ mesons did not distort the results.

Analysis of the experimental results leads to Fig. 3, which shows the current density of μ mesons with energy ≥ 440 Mev as a function of distance from the core in extensive atmospheric showers containing 5×10^4 to 10^6 ($\overline{\mathrm{N}} = 2 \times 10^5$) charged particles. In the measurements at 100 and 500 m, μ mesons with energy ≥ 390 Mev were counted, so that the current densities obtained experimentally at these distances were decreased by a factor obtained from the μ meson energy spectrum (at various distances from the core) given in Ref. 3. The correction was less than the statistical error at both 100 m and 500 m. It should also be mentioned that the detector which measured the μ meson current density at small distances from the shower axis was at the center of the setup, thus weighting the results in favor of showers with relatively few charged particles. This decreased the average μ meson current density at small distances from the shower axis.* In order to avoid this effect, the averaging was carried out over such a narrow range in the energy of the primary particle initiating the shower that the average energy in each interval was independent of where the shower axis fell.

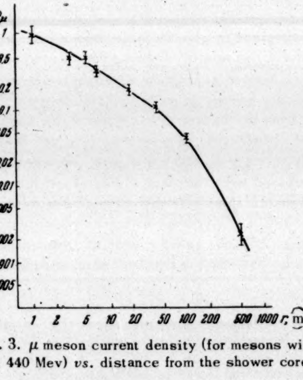

FIG. 3. μ meson current density (for mesons with energy $\geq$ 440 Mev) *vs.* distance from the shower core.

As has already been indicated in Ref. 4, the spatial distribution of μ mesons in extensive air showers cannot be completely explained by Coulomb scattering of the μ mesons from the nuclei of air atoms encountered in their progress through the atmosphere. The effect of the angular spread with which the π mesons are emitted in elementary nuclear interactions on the spatial distribution of μ mesons is more marked if one considers μ mesons of a fixed energy. Using the μ meson energy spectrum at various distances from the shower core given in Ref. 3, and the spatial distribution of μ mesons shown in Fig. 3, the mean square radius for the spread of μ mesons with energies 3.5 to 3.9 Bev turns out to be ≥ 300 m. The Coulomb scattering of μ mesons with the above energy and originating at a height of 10 km leads to an rms radius of 50 m, neglecting ionization losses. Ionization losses would only decrease this figure. This difference between the experimental rms radius of the spatial distribution and the rms radius obtained from Coulomb scattering calculations cannot be due to the earth's magnetic field. The expected lateral displacement from the shower axis is about $r \approx h300H'h/2E \approx 50$ m (E is the μ meson energy, H' the horizontal component of the earth's magnetic field, and h the height at which the μ mesons were formed). Finally, taking into account the angles at which the μ mesons from $\pi^{\pm}$ are emitted leads to a similar displacement.

Thus the angle at which π mesons are emitted in nucleon–nucleon interactions at high and very high energies must be taken into account to explain the spatial distributions of μ mesons. This is because all the other factors which tend to spread out the μ mesons lead to an rms radius for 3.5–3.9 Bev μ mesons of $\lesssim$ 100 m while experimentally the radius is $\geq$ 300 m.* It should be remembered that, unlike the situation with μ mesons, the spatial distribution of the electron–photon component in extensive atmospheric showers can be explained by Coulomb scattering of the electrons.[4] The angle at which π^0 mesons are emitted in nuclear interactions has no effect on the spatial distribution of electrons in the shower.

---

*This effect was neglected in Ref. 5, and consequently the distribution curve obtained there for small distances from the shower axis is distorted.

There are presumably two reasons for the fact that the angle of emission of π mesons has an appreciable effect on the spatial distributions of the penetrating component of extensive air showers, but not on the soft component. On one hand, μ mesons, the overwhelming majority of which come from $\pi^{\pm}$ mesons, have a considerably longer range than do the electron photon showers. The latter come from the decay of π^0 mesons having the same energy as the $\pi^{\pm}$ mesons leading to the μ meson component of extensive air showers. On the other hand, the shape of the spatial distribution function for electrons near the axis[6] indicates that π^0 mesons with an energy 10^{10} ev play a large role in the formation of the electron–photon component deep in the atmosphere. It is natural that mesons of such energy would be emitted from a nuclear interaction at smaller angles than the mesons producing the general current of μ mesons in the shower.

3. TOTAL NUMBER OF μ MESONS AS A FUNCTION OF ENERGY

If we assume that the spatial distribution of μ mesons does not depend on the energy of the primary particle, then we can compare the number of μ mesons in showers with varying numbers of charged particles. How valid is the above assumption? Figure 3 shows that for distances 0 – 40 m the spatial distribution varies as r^{-n}. Values of the exponent n for extensive atmospheric showers initiated by primary particles of various energies* are shown in Table 2. From the data in this table it is evident that the spatial distribution of μ mesons near the center of the shower is independent of the energy of the primary particle which started the shower (Fig. 4).

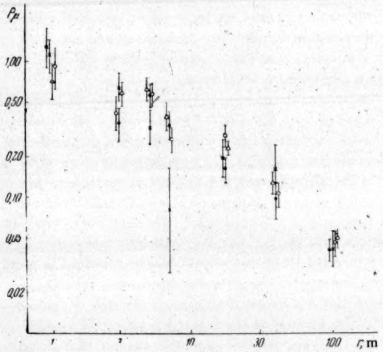

FIG. 4. Spatial distribution of μ mesons with energy more than 440 Mev in extensive showers with various (total) numbers of particles: × – 0.53 × 10^5; Δ – 1.5 × 10^5; ○ – 3.2 × 10^5; ● – 10^6. The μ meson current density is normalized relative to showers with 2 × 10^5 particles, using the number of μ mesons 100 m from the axis of the shower.

The statistical accuracy of our experimental data is insufficient to give reliable information about changes in the spatial distribution of μ mesons on the periphery of extensive atmospheric showers as the primary energy is varied. At distances of 100 – 500 m from the center of the shower the normalized spatial distribution of μ mesons is given by the formula $r^{-(1.8\pm0.2)}$ ($E_0 = 6 \times 10^{14}$ ev). This result can be compared with the data of Ref. 4, which were obtained at the same altitude as were our data (3860 m). In Ref. 4 the primary energies considered were more than 10^{17} ev, and the spatial distribution of μ mesons 200 – 800 m from the shower axis was measured. In complete agreement with our results, this spatial distribution was given by $r^{-(1.8\pm0.2)}$.

---

*Using our experimental data on the spatial distribution of 3.5 – 3.9 Bev μ mesons, and assuming that the $\pi^{\pm}$ mesons of corresponding energy are formed 2 – 8 km above the experimental setup, we can estimate the perpendicular momentum received by π mesons in the interaction with nuclei of particles of energy $\geq 10^{11}$ ev. The result is $1-3\mu c$, where μ is the mass of the π meson.

*In an earlier paper,[7] we took the coefficient of proportionality between the number of particles in the shower and the primary energy to be 5 × 10^{10} ev (at an altitude 3860 m). This estimate was based on calculations with a particular model of the nuclear cascade process. We now use the coefficient given by $E_0 = 2.5 \times 10^9 N$. The new value is based on an analysis of the absorption of extensive showers in the atmosphere.

Thus the spatial distribution of μ mesons does not change when the energy of the primary particle initiating the shower is increased by a factor of 200. This justifies our supposition that the spatial distribution of μ mesons in extensive atmospheric showers does not depend on the total number of particles.

The experimental data presently available do not give the total number of μ mesons with energy ≥ 440 Mev in an extensive atmospheric shower. This is because, even at the largest distances investigated, the μ meson current density, in the energy range given above, falls off slower than $1/r^2$. μ mesons with energies higher than 1 Bev have a narrower spatial distribution. The total number of such mesons can be obtained from the spatial distribution function in Fig. 3 and the data on the energy spectrum of μ mesons in extensive atmospheric showers (at various distances) given in Ref. 3. Figure 5 shows how the number of μ mesons with energy $\geq$ 1 Bev depends on the primary energy. From this graph it follows that in the energy (of the primary particle) range 10^{14} to 2×10^{15} ev the total number of μ mesons varies as $\sim E_0^{(0.62\pm0.12)}$.

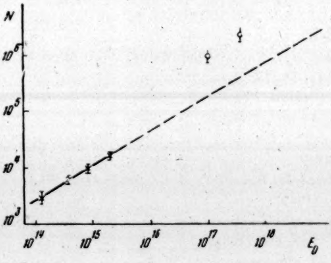

FIG. 5. The number of μ mesons with energy more than 1 Bev occurring in extensive showers initiated by primary particles of various energies. The crosses are experimental data from the present work, the circles are data from Ref. 4.

Our results on the relation between the number of μ mesons in the shower and the energy of the primary particle do not agree with the results of Ref. 9. The latter work was carried on at an altitude of 3260 m above sea level. The number of μ mesons N_μ was obtained as a function of the number of electrons, N_e for extensive atmospheric showers, by

TABLE II

Total number of charged particles in the shower	Energy of primary particle, ev	Meson current density in the total number of particles incident on one m² at various distances from the axis of the shower							
		1 m	3 m	5 m	7 m	18 m	40 m	100 m	n
$0.53\cdot10^5$	$1.3\cdot10^{14}$	0.5 ± 0.15	0.31 ± 0.07	0.15 ± 0.06	0.04 ± 0.04	0.08 ± 0.02	0.06 ± 0.02	0.02 ± 0.006	0.61 ± 0.1
$1.5\cdot10^5$	$3.7\cdot10^{14}$	0.6 ± 0.2	0.5 ± 0.09	0.51 ± 0.08	0.35 ± 0.08	0.19 ± 0.03	0.11 ± 0.02	0.043 ± 0.007	0.54 ± 0.12
$3.2\cdot10^5$	$8\cdot10^{14}$	1.2 ± 0.5	0.6 ± 0.18	0.8 ± 0.15	0.35 ± 0.09	0.38 ± 0.09	0.14 ± 0.03	0.062 ± 0.012	0.58 ± 0.12
$7.7\cdot10^5$	$1.9\cdot10^{15}$	3.3 ± 1.4	0.9 ± 0.3	1.5 ± 0.3	0.9 ± 0.2	0.4 ± 0.1	0.23 ± 0.05	0.11 ± 0.02	0.74 ± 0.11

varying the area of unshielded counters. It was found that $N_\mu \sim N_e^{0.87}$ in the energy interval 5×10^{14} to 8×10^{16} ev.

Our data pertain to an energy interval $10^{14} - 2 \times 10^{15}$ ev. To compare the two sets of data, we compare the total number of μ mesons with energy ≥ 1 Bev in extensive atmospheric showers, initiated by primary particles of energy $E_0 \approx 10^{15}$ ev with the number of μ mesons in showers initiated by primary particles of energy $E_0 = 10^{17}$ ev (Ref. 4). From Fig. 5 we see that in this energy interval the number of μ mesons varies as $E_0^{0.95\pm0.05}$ which agrees with Ref. 10. In the method of Ref. 9, the experimental data was averaged over a rather wide range of primary particle energies. The result quoted is thus the average of two different proportionality constants between the number of μ mesons and the number of electrons in the shower ($N_\mu \sim N_e^{0.6}$ and $N_\mu \sim N_e$).

The change in the relation between the number of μ mesons in the shower and the energy of the primary particle for $E_0 > 10^{15}$ ev agrees with the suggestion we made earlier,[7] on the basis of other data, that there is a change in the nature of the elementary nuclear interaction at an energy $\sim 10^{15}$ ev. Experimental data on the spatial distribution and vertical development of extensive atmospheric showers[11, 12] indicate that in the interaction of nuclei with nucleons of energy $10^{13} - 10^{14}$ ev, a large part of the energy is concentrated on one secondary particle. This is similar to the situation at $10^{10} - 10^{12}$ ev. This secondary particle, presumably a nucleon, maintains its energetically preferred role in the succeeding stages of the nuclear cascade process. This selection, in the first nuclear interaction, of an energetically preferred particle takes place in interactions with primary particles of energy up to $\sim 10^{15}$ ev. At energies higher than 10^{15} ev, the number of secondary particles carrying away most of the energy increases with increasing energy of the primary particle. If secondary nucleons with energy $\leq 10^{15}$ ev keep a large fraction of their energy in succeeding nuclear interactions, then one can regard an extensive atmospheric shower started by a primary particle of energy $> 10^{15}$ ev as approximately equivalent to a sum of showers, each started by particles of energy $> 10^{15}$ ev. In such a situation, the number of μ mesons must be approximately proportional to the energy of the primary particle, which is observed experimentally.

The measurements were made by a large staff at the Pamir Expedition of the Physics Institute, Academy of Sciences, U.S.S.R. The authors express their gratitude to all their comrades, and especially to O. I. Dovzhenko, V. M. Seleznev, and E. I. Tukish. The authors would also like to thank Prof. S. N. Vernov, Prof. N. A. Dobrotin and G. T. Zatsepin for valuable discussion of the results.

---

[1] Dobrotin, Zatsepin *et al.*, Uspekhi Fiz. Nauk **49**, 186 (1953).

[2] Vavilov, Nikol'skii and Sarantsev, J. Exptl. Theoret. Phys. (U.S.S.R.) **28**, 505 (1955); Soviet Phys. JETP **1**, 399 (1955).

[3] Dovzhenko, Nelepo and Nikol'skii, J. Exptl. Theoret. Phys. (U.S.S.R.) **32**, 463 (1957).

[4] Antonov, Vavilov, Zatsepin *et al.*, J. Exptl. Theoret. Phys. (U.S.S.R.) **32**, 227 (1957); Soviet Phys. JETP **5**, 172 (1957).

[5] Dobrotin, Zatsepin *et al.*, Nuovo cimento Suppl. **3**, 635 (1956).

[6] Dobrovol'skii, Nikol'skii *et al.*, J. Exptl. Theoret. Phys. (U.S.S.R.) **31**, 939 (1956); Soviet Phys. JETP **4**, 799 (1957).

[7] Nikol'skii, Vavilov, and Batov, Dokl. Akad. Nauk SSSR **111**, 71 (1956).

[8] K. Greisen, *Progress in Cosmic Ray Physics*, Vol. III, Amsterdam, 1956.

[9] Cocconi, Tongiorgi, and Greisen, Phys. Rev. **75**, 1963 (1949).

[10] Zatsepin, Rozental', *et al.*, Dokl. Akad. Nauk SSSR **69**, 341 (1949).

[11] Dobrotin, Zatsepin *et al.*, Izv. Akad. Nauk SSSR, Ser. Fiz. **19**, 666 (1955).

[12] V. V. Guzhavin and G. T. Zatsepin, J. Exptl. Theoret. Phys. (U.S.S.R.) **32**, 365 (1957); Soviet Phys. JETP **5**, 312 (1957).

Translated by R. Krotkov
271

SOVIET PHYSICS JETP VOLUME 5, NUMBER 6 DECEMBER 15, 1957

Pion Production in Zero Isotopic Spin Nuclei

A. G. MESHKOVSKII, IU. S. PLIGIN, IA. IA. SHALAMOV,
AND V. A. SHEBANOV

(Submitted to JETP editor February 6, 1957)
J. Exptl. Theoret. Phys. (U.S.S.R.) 32, 1328-1334 (June, 1957)

The energy spectra and differential cross section for the production of π^+ and π^- mesons in deuterium and of π^- mesons in carbon by 600-Mev protons were measured at 45°. Comparison of the data on the production of charged and neutral pions confirms the correctness for deuterium and carbon of the relation $d\sigma^+ + d\sigma^- = 2d\sigma^0$ which follows from the hypothesis of isotopic invariance for zero isotopic spin nuclei.

---

1. INTRODUCTION

THE HYPOTHESIS OF isotopic invariance leads to a number of relations among the cross sections of various interactions between nucleons and pions, nucleons, or nuclei. The experimental testing of these relations can provide valuable information concerning the accuracy with which this hypothesis is satisfied.

For pion production in nucleon-nucleon collisions the following relations exist among the total cross sections:[1-3]

$$\sigma(pn \to nn\pi^+) = \sigma(pn \to pp\pi^-), \tag{1}$$

$$\sigma(pp \to d\pi^+) = 2\sigma(pn \to d\pi^0), \tag{2}$$

$$\sigma(pp \to pn\pi^+) + 2\sigma(pn \to nn\pi^+) = 2[\sigma(pp \to pp\pi^0) + \sigma(pn \to pn\pi^0)]. \tag{3}$$

Relations (1) and (2) have been verified experimentally with 400-Mev nucleons.[4,5] Relation (1) has also been confirmed with neutrons at about 600 Mev (Ref. 6).

When pions are produced in collisions between nucleons and zero isotopic spin nuclei (H^2, He^4, C^{12}, N^{14}, *etc.*) we have the relation

$$\sigma^+ + \sigma^- = 2\sigma^0, \tag{4}$$

where σ^+, σ^- and σ^0 are the total or differential cross sections for π^+, π^- and π^0 production. This relation has thus far not been checked experimentally.

Prokoshkin and Tiapkin[7] recently measured the cross section for neutral pion production by 660-Mev protons on a few nuclei including deuterium and carbon. It thus became possible to check (4) for two isotopic spin zero nuclei by measuring the cross sections for π^+ and π^- production on these nuclei by 660-Mev protons. We have previously[8] obtained the π^+ production cross section in carbon at 45° by protons with this energy. In the present work we have measured the energy spectra and differential cross sections of the production of π^+ and π^- mesons in deuterium and of π mesons in carbon at the same angle. In this way the results of Prokoshkin and Tiapkin have been supplemented to provide the necessary information for the comparison of relation (4) with experiment.

2. EXPERIMENTAL METHOD

We worked with an external proton beam from the synchrocyclotron of the Joint Institute for Nuclear Research. The experimental method and a description of the apparatus are contained in our earlier papers.[8,9]

Pion production in deuterium was determined by the difference of counts from LiD and Li targets. Both targets were solid plates 1 cm thick. The carbon target was of special construction.[8]

It was shown[9] that the electron background in our apparatus could not exceed 2 to 3% of the total π^+ count. Since the π^- yield is considerably smaller than the π^+ yield it was necessary in the present work to estimate the electron background more accurately than previously.

The relative number of electrons was determined in two ways. In the first method, as previously, the number of registered electrons was taken to be the difference between counts from the paraffin and carbon targets when the direction of the magnetic field was such that negative particles were recorded. The electron count obtained in this manner clearly represented π^0 production in hydrogen nuclei in the paraffin target. To determine the electron background for a carbon target the count was multiplied by the ratio of the gamma-ray yields of carbon and hydrogen that was obtained at 33° in the laboratory system, which was close to our angle.[10] We have assumed that this ratio varies very little with energy since from the experiments on π^0 production it follows that the gamma-ray spectra are approximately the same for hydrogen and carbon.[11] The second method was a direct determination of the electron background, for which purpose a lead filter was placed close to the carbon target in the path of the particles before their entrance into the strong magnetic field. In the presence of the filter the counter telescope recorded almost no electrons so that the number of electrons could be determined from the counts with and without the filter.

The electron background was not measured for other targets; it was computed instead through multiplication of the result for the carbon target by the ratio of the gamma-ray yields of a given target and the carbon target. For this purpose we used the relative cross sections of gamma-ray production in different nuclei by 660-Mev protons at 33° in the laboratory system.[10]

For π^- energies beginning at 150 Mev the electron background was found to be insignificant. For example, for a carbon target and 160-Mev π^- mesons the electron background is 5% of the recorded negative particles. At lower π^- energies the electron background increases until it reaches 30% at 80 Mev. The values obtained for the electron background were taken into consideration in calculating the true number of pions produced in the targets.

3. RESULTS

Table 1 shows the π^+ and π^- energy spectra produced by 660-Mev protons on deuterium and carbon at 45°. The ion energies are given together with the corresponding differential cross sections $d^2\sigma^{\pm}/d\Omega\, dE$ in the laboratory system calculated for a single nucleus. Figures 1 and 2 are the spectra of π^+ and π^- production plotted from the data in Table 1.

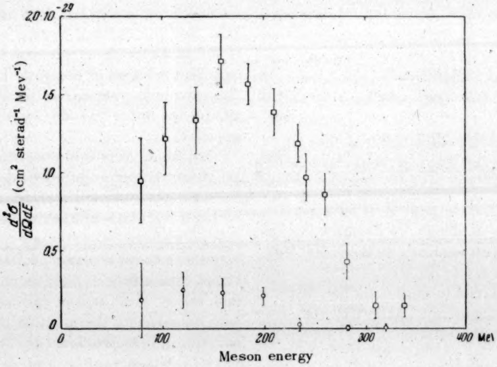

FIG. 1. Meson spectrum from deuterium: □ – π^+ mesons; ○ – π^- mesons

The results of integrating the spectra, that is, the differential cross sections $d\sigma^+/d\Omega$ and $d\sigma^-/d\Omega$ for π^+ and π^- production are given in Table 2. The result for π^+ mesons from carbon was taken from an earlier paper.[8] The table contains the calculated ratios $d\sigma^+/d\sigma^-$ of π^+ and π^- yields. The ratios obtained for the π^+ and π^- yields from deuterium and carbon are in good agreement with the results of other investigators who measured the relative π^+ and π^- yields at the same porton energy and at similar angles. At 24° Mescheriakov *et al.*[12] obtained $d\sigma_C^+/d\sigma_C^- = 7 \pm 0.8$ for carbon. At 90° Sidorov obtained $d\sigma_C^+/d\sigma_C^- = 5 \pm 0.7$ for carbon[6] and $d\sigma_d^+/d\sigma_d^- \approx 8$ for deuterium.[13]

4. DISCUSSION OF RESULTS

For the purpose of testing relation (4) in its differential form

$$d\sigma^+ + d\sigma^- = 2d\sigma^0 \qquad (5)$$

TABLE I.

Meson energy in Mev	$\frac{d^2\sigma^+}{d\Omega dE} \times 10^{29} \frac{\text{cm}^2}{\text{sterad-Mev}}$	Meson energy in Mev	$\frac{d^2\sigma^-}{d\Omega dE} \times 10^{30} \frac{\text{cm}^2}{\text{sterad-Mev}}$
	Deuterium		**Deuterium**
79	0.95 ± 0.27	79	1.80 ± 2.36
104	1.22 ± 0.23	120	2.46 ± 1.16
134	1.34 ± 0.21	159	2.26 ± 0.95
159	1.72 ± 0.17	199	2.07 ± 0.59
186	1.57 ± 0.13	234	0.25 ± 0.36
211	1.39 ± 0.15	282	0.04 ± 0.20
234	1.19 ± 0.12	320	0.05 ± 0.15
242	0.97 ± 0.15		
261	0.86 ± 0.13		
282	0.43 ± 0.11		Carbon
310	0.15 ± 0.09		
339	0.15 ± 0.07	79	3.89 ± 1.26
		120	5.79 ± 0.70
		159	5.06 ± 0.50
		199	3.81 ± 0.30
		234	2.58 ± 0.19
		282	1.18 ± 0.10
		320	0.63 ± 0.08

TABLE II.

Element	$d\sigma^+/d\Omega \times 10^{27}$ $\frac{\text{cm}^2}{\text{sterad}}$	$d\sigma^-/d\Omega \times 10^{27}$ $\frac{\text{cm}^2}{\text{sterad}}$	$d\sigma^+/d\sigma^-$
Deuterium	3.06 ± 0.34	0.38 ± 0.12	8.1 ± 2.7
Carbon	6.77 ± 0.62	1.00 ± 0.13	6.8 ± 1.1

we shall now combine the results obtained at 45° for deuterium and carbon with the data of Prokoshkin and Tiapkin on π^0 production.[7] Their work shows that the π^0 mesons produced by 660-Mev protons on deuterons are isotropically distributed in the center-of-mass system (c.m.s.) of the two colliding particles. Twice the value of the cross section in this system is $2\,d\sigma_d^0/d\Omega = (1.73 \pm 0.21) \times 10^{-27}$ cm^2 sterad^{-1}. Our data converted to the same system of coordinates give $d\sigma_d^+/d\Omega + d\sigma_d^-/d\Omega = (1.66 \pm 0.17) \times 10^{-27}$ cm^2 sterad^{-1}. A similar comparison for carbon in the laboratory system gives $2d\sigma_C^0/d\Omega = (7.20 \pm 0.70) \times 10^{-27}$ cm^2 sterad^{-1} and $d\sigma_C^+/d\Omega + d\sigma_C^-/d\Omega = (7.77 \pm 0.63) \times 10^{-27}$ cm^2 sterad^{-1}. Thus (5) is satisfied within the limits of experimental error for both deuterium and carbon.

At the same time it can be shown that the results of similar experiments[7,8,14] on π production in non-zero isotopic spin nuclei do not satisfy $d\sigma^+ + d\sigma^- = 2d\sigma^0$. Examples are provided by Li^7 and Be^9 with isotopic spin ½ in the ground state. For charged pions we have[8,14] $d\sigma_{\text{Li}}^+/d\Omega = (4.24 \pm 0.32) \times 10^{-27}$ cm^2 sterad^{-1}, $d\sigma_{\text{Li}}^-/d\Omega = (0.93 \pm 0.4) \times 10^{-27}$ cm^2 sterad^{-1}, $d\sigma_{\text{Be}}^+/d\Omega = (4.91 \pm 0.45) \times 10^{-27}$ cm^2 sterad^{-1} and $d\sigma_{\text{Be}}^-/d\Omega = (1.00 \pm 0.15) \times 10^{-27}$ cm^2 sterad^{-1}. Thus the sum $d\sigma^+/d\Omega + d\sigma^-/d\Omega$ is $(5.17 \pm 0.35) \times 10^{-27}$ cm^2 sterad^{-1} for Li and $(5.91 \pm 0.47) \times 10^{-27}$ cm^2 sterad^{-1} for Be, whereas[7] $2d\sigma_{\text{Li}}^0/d\Omega = (6.6 \pm 0.6) \times 10^{-27}$ cm^2 sterad^{-1} and $2d\sigma_{\text{Be}}^0/d\Omega = (6.8 \pm 0.6) \times 10^{-27}$ cm^2 sterad^{-1}. It must be mentioned that results for the cross sections $d\sigma_{\text{Li}}^{\pm}/d\Omega$ were obtained with specimens of natural lithium,[8,14] but this fact cannot seriously affect the comparison since there is only a relatively small amount of Li^6 in natural lithium.

The value which we obtained for the ratio $d\sigma^+/d\sigma^-$ in the case of deuterium will now be compared with theoretical result of Lapidus,[15] who evaluated the ratio for the pion energy range in which the pion-nucleon interaction involves predominantly states with isotopic spin $\frac{3}{2}$. His result for the ratio of the differential cross sections is $d\sigma_d^+/d\sigma_d^- = 11$. The fact that this value is close to the experimental result $d\sigma_d^+/d\sigma_d^- = 8.1 \pm 2.7$ indicates that in our case during the production of charged pions from $p-d$ collisions most of the final states of the pion-nucleon subsystem actually possess isotopic spin $T_{\pi N} = \frac{3}{2}$ and a smaller fraction have $T_{\pi N} = \frac{1}{2}$.

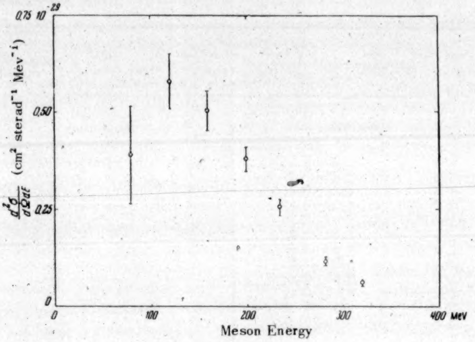

FIG. 2. π^- spectrum from carbon.

In π^+ production from $p-d$ collisions the reaction $pd \to H^3\pi^+$ is possible; this has been investigated with 340-Mev protons.[16] When the angle of ejection of the pions is 45° and the proton energy is 660 Mev the pion energy in the $pd \to H^3\pi^-$ reaction must be 343 Mev. Fig. 1 shows that relatively few π^+ mesons are in the spectral vicinity of 340 Mev. Thus in the total process of π^+ production from $p-d$ collisions at 45° the $pd \to H^3\pi^+$ reaction evidently plays only a small part.

Fig. 1 shows that the spectra of π^+ and π^- production from $p-d$ collisions differ markedly at high energies where the π^- yield falls off much more rapidly than that of the π^- mesons. A possible explanation of this result is the fact that since π^- mesons are produced in $p-d$ collisions through the reaction $pd \to ppp\pi^-$ the presence of three protons in the final state must be forbidden by the Pauli principle at relatively low proton beam energies. In connection with this explanation it is interesting to compare the probabilities of the reactions $pd \to ppp\pi^-$ and $pn \to pp\pi^-$, *i.e.*, the production of π^- mesons on the neutrons of deuterons and on free neutrons. The pion production cross section must clearly be smaller in the first case than in the second if there is partial forbiddenness of the first reaction.

In the energy region with which we are concerned there is no direct experimental information regarding the $pn \to pp\pi^-$ reaction, but the magnitude of $d\sigma(pn \to pp\pi^-)/d\Omega$ can be estimated by utilizing relation (3), which for the differential cross sections becomes[17]

$$d\sigma(pp \to pn\pi^+) + d\sigma(pn \to nn\pi^+) + d\sigma(pn \to pp\pi^-)$$
$$= 2[d\sigma(pp \to pp\pi^0) + d\sigma(pn \to pn\pi^0)]. \quad (6)$$

In this relation the cross section of the $pn \to nn\pi^+$ reaction can be expressed in terms of the $pn \to pp\pi^-$ cross section by means of the equality

$$\left.\frac{d\sigma(pn \to nn\pi^+)}{d\Omega}\right|_{\vartheta} = \left.\frac{d\sigma(pn \to pp\pi^-)}{d\Omega}\right|_{180^\circ-\vartheta}, \quad (7)$$

where the angle ϑ is in the c.m.s. Furthermore, since the 45° laboratory angle at which we performed our measurements is close to 90° in the c.m.s. we can quite accurately replace (7) with the equality $d\sigma(pn \to nn\pi^+) = d\sigma(pn \to pp\pi^-)$. Inserting this in (6) and utilizing available data[9,10] concerning the differential cross sections of the reactions $pp \to pp\pi^+$, $pp \to pp\pi^0$ and $pn \to pn\pi^0$ we obtain $d\sigma(pn \to pp\pi^-)/d\Omega = (0.32 \pm 0.10) \times 10^{-27}$ cm² sterad⁻¹, whereas our experimental result in the c.m.s. is $d\sigma_d^-/d\Omega = (0.18 \pm 0.06) \times 10^{-27}$ cm² sterad⁻¹. Thus the probability of π^- production on the neutron of a deuteron is actually smaller than the probability on a free neutron, although the large experimental errors do not at present permit us to obtain a reliable quantitative result.

We now make a similar comparison of π^+ production on deuteron nucleons and on free nucleons. The present work gives the result $d\sigma_d^+/d\Omega = (1.48 \pm 0.16) \times 10^{-27}$ cm² sterad⁻¹ in the c.m.s. of the two colliding nucleons. We also have[9]

$d\sigma_d^+/d\Omega = d\sigma(pp \rightarrow \pi^+)/d\Omega = (1.06 \pm 0.07) \times 10^{-27}$ cm^2 sterad^{-1} and, as mentioned previously, $d\sigma_n^+/d\Omega = d\sigma(pn \rightarrow pp\pi^-)/d\Omega = (0.32 \pm 0.10) \times 10^{-27}$ cm^2 sterad^{-1}. Hence $d\sigma_p^+/d\Omega + d\sigma_n^+/d\Omega = (1.38 \pm 0.12) \times 10^{-27}$ cm^2 sterad^{-1}, which is very close to the value of $d\sigma_d^+/d\Omega$. Thus π^+ production on deuteron nucleons possesses approximately the same probability as on free nucleons, which differs from the observed results for π^- production. This can be associated with the absence among the different $pd \rightarrow \pi^+ \ldots$ reactions of a $pd \rightarrow ppp\pi^-$ type reaction, which, as mentioned earlier, is partly forbidden.

The difference in shape between the π^+ and π^- spectra at high energies, which we observed in the case of deuterium, may also have a second cause besides the Pauli principle with respect to the $pd \rightarrow ppp\pi^-$ reaction. B. L. Ioffe has pointed out to us that π production at relatively high energies must involve the excitation of nucleons with relatively high kinetic energies, *i.e.*, nucleons of the beam, whereas at low π energies the excitation of target nucleons can also be involved. Since in $p-d$ experiments π^- mesons are produced only on target neutrons there must be a reduction of the π^- yield at high energies. This effect should of course be observed for other comples nuclei besides deuterium under proton bombardment. Confirmation is obtained in experiments on carbon which also show a difference of the π^+ and π^- spectra at high energies, as can be seen by comparing the spectrum in Fig. 2 with the π^+ spectrum obtained previously.[8] A similar distinction was detected earlier and subjected to thorough experimental investigation for beryllium and carbon by Meshcheriakov *et al.*[12]

In conclusion we wish to express our deep appreciation to Academician A. I. Alikhanov for his continued interest, and also to Iu. D. Prokoshkin, A. A. Tiapkin and L. L. Lapidus for fruitful discussions and communication of their results before publication.

---

[1] R. L. Garwin, Phys. Rev. **85**, 1044 (1952).

[2] A. M. L. Messiah, Phys. Rev. **86**, 430 (1952).

[3] J. M. Luttinger, Phys. Rev. **86**, 571 (1952).

[4] G. B. Yodh, Phys. Rev. **98**, 1330 (1955).

[5] R. A. Schluter, Phys. Rev. **96**, 734 (1954).

[6] V. M. Sidorov, J. Exptl. Theoret. Phys. (U.S.S.R.) **28**, 727 (1955); Soviet Phys. JETP **1**, 600 (1955).

[7] Iu. D. Prokoshkin and A. A. Tiapkin, J. Exptl. Theoret. Phys. (U.S.S.R.) **33**, 313 (1957), Soviet Phys. JETP **6**, (in press).

[8] Meshkovskii, Pligin, Shalamov, and Shebanov, J. Exptl. Theoret. Phys. (U.S.S.R.) **31**, 987 (1956); Soviet Phys. JETP **4**, 842 (1957).

[9] Meshkovskii, Pligin, Shalamov, and Shebanov, J. Exptl. Theoret. Phys. (U.S.S.R.) **31**, 560 (1956); Soviet Phys. JETP **4**, 404 (1956).

[10] Iu. D. Prokoshkin, *Symposium du CERN sur les accélérateurs de haute énergie et la physique des mésons π*, Genève, 1956, Vol. 2 p. 385.

[11] Baiukov, Kosodaev and Tiapkin, *Symposium du CERN*, 1956, Vol. 2 p. 398.

[12] Meshcheriakov, Vzorov, Zrelov, Neganov, and Shabudin, J. Exptl. Theoret. Phys. (U.S.S.R.) **31**, 55 (1956); Soviet Phys. JETP **4**, 79 (1957).

[13] V. M. Sidorov, *Symposium du CERN*, 1956, Vol. 2, 366.

[14] Meshkovskii, Shalamov, and Shebanov, J. Exptl. Theoret. Phys. (U.S.S.R.)**33**, 602 (1957); Soviet Phys. JETP **6**, (in press).

[15] L. I. Lapidus, J. Exptl. Theoret. Phys. (U.S.S.R.) **31**, 865 (1956); Soviet Phys. JETP **4**, 740 (1957).

[16] Frank, Bandtel, Madey and Moyer, Phys. Rev. **94**, 1716 (1954).

[17] Hove, Marshak and Pais, Phys. Rev. **88**, 1211 (1952).

Translated by I. Emin
272

SOVIET PHYSICS JETP VOLUME 5, NUMBER 6 DECEMBER 15, 1957

Angular and Energy Distributions of Photoprotons From Be^9 and C^{12}

I. V. CHUVILO AND V. G. SHEVCHENKO
The P. N. Lebedev Physical Institute, Academy of Sciences, U.S.S.R.

(Submitted to JETP editor February 9, 1957)
J. Exptl. Theoret. Phys. (U.S.S.R.) **32**, 1335-1339 (June, 1957)

Results of measurements of the angular and energy distributions of protons produced in the photodisintegration of Be^9 and C^{12} are presented. The gamma-ray source was a 265-Mev electron synchrotron. The protons were recorded on photographic plates. Analysis of the results leads to the conclusion that in the 60 – 80 Mev range the gamma rays interact mainly with separate structures produced within the nuclei.

WE HAVE INVESTIGATED the angular and energy distributions of photoprotons produced in C^{12} by bremsstrahlung with $E_{\gamma_{\max}} = 64$ and 84 Mev and in Be^9 by bremsstrahlung with $E_{\gamma_{\max}} = 68$ and 84 Mev. The electron synchrotron of the Physical Institute of the Academy of Sciences, U.S.S.R., provided gamma rays with a maximum energy of 265 Mev.

Fig. 1 is a diagram of the experimental arrangement. The proton beam passad through a collimator of 0.5 × 3 cm aperture. The target inside the vacuum chamber formed a 30° angle with the direction of the gamma-ray beam. The thickness of the graphite target was 113 mg/cm² and that of the beryllium target 58 mg/cm²; the impurity content did not exceed 0.3%. Paraffin and lead shielding eliminated neutron and gamma-ray backgrounds on the plates. The electron background was removed from the gamma-ray beam by a magnetic field of about 3000 oersteds. The radiation doses were determined by an ionization chamber monitor which was calibrated absolutely by an ionization chamber in the manner described by Lax.[1]

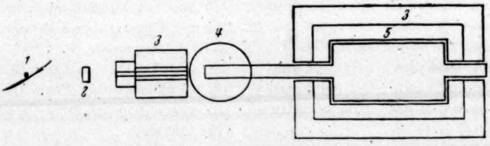

FIG. 1. Diagram of the experiment *1* – synchrotron; *2* – monitor; *3* – lead shield and collimator; *4* – magnet; *5* – graphite shield; *6* – camera.

The protons were registered on NIKFI (Cine-Photographic Research Institute) plates bearing 500 μ Ia-2 type emulsions placed in the camera at angles of 30, 45, 60, 75, 90, 120, and 150° with respect to the gamma-ray beam. The relative solid angles were calibrated with 3% accuracy by means of an alpha-ray source. The shift of the beam direction with respect to the target center was controlled by comparing the results on two plates at 90° which were placed symmetrically with respect to the target center. In addition, when the beam was focused on x-ray film its displacement from the target center did not exceed 0.2 – 0.3 mm. A correction was introduced for the shifting of the beam.

In scanning the plates we selected tracks proceeding from the irradiated portion of the target, beginning at the surface of the emulsion and corresponding to proton energies ⩾ 4 Mev. The energies of these protons were determined by using the range-energy curves for S-2 and Ia-2 emulsions, which practically coincide. The initial proton energy on leaving the target was determined from the absorber thickness with a correction for the target thickness. For the purpose of separating the various proton energy groups we used copper absorbers with thicknesses of 460, 560, 1000 and 1400 mg/cm². A correction was introduced for multiple proton scattering in the absorber.

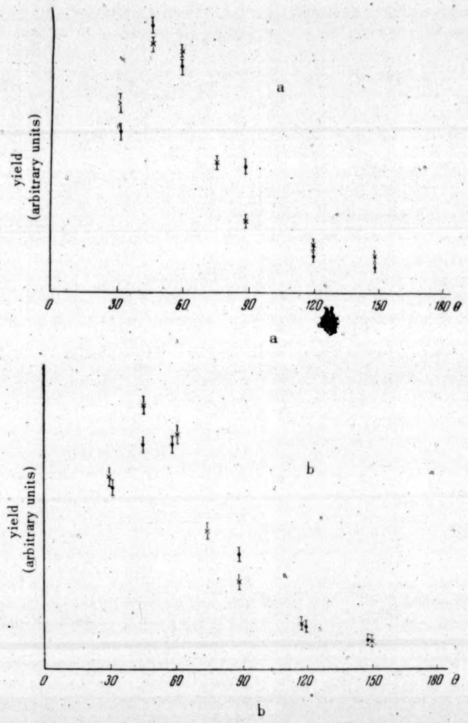

FIG. 2. Angular distributions of the photoprotons. *a*) Be^9: dots – $E_p > 20$ Mev, $E_{\gamma\,\max} = 68$ Mev; crosses – $E_p > 32$ Mev, $E_{\gamma\,\max} = 84$ Mev; *b*) C^{12}: dots – $E_p > 18$ Mev, $E_{\gamma\,\max} = 64$ Mev; crosses – $E_p > 26$ Mev, $E_{\gamma\,\max} = 84$ Mev.

The proton background was measured in the absence of the target. This was found to be 10 – 15% of the effect under investigation on plates forming angles of 30° and 150° with the beam and 3 – 4% on the other plates. The background consisted principally of 7-Mev protons.

Fig. 2 shows the angular distributions of the photoprotons. The marked asymmetry with respect to the 90° direction and the forward peaking from both beryllium and carbon can be explained most naturally by assuming that gamma rays of the given energies interact mainly with separate structures produced within the nuclei. This hypothesis is supported by the good agreement between the angular distribution of photoprotons from Be^9 (assuming a two-nucleon interaction mechanism) and from deuterons obtained with 60 and 80-Mev gamma rays.[2]

The above hypothesis is also supported by an analysis of the photoproton energy distribution for Be^9 (Fig. 3). The energy dependences of the cross sections for photodisintegration of the deuteron and Be^9 are in good agreement for protons of the same energies. The energy spectra are marked by characteristic bending at points which agree qualitatively as a function of the angle of proton flight with the corresponding points in the photoproton spectra of the deuteron.

A comparison of the photoproton production cross

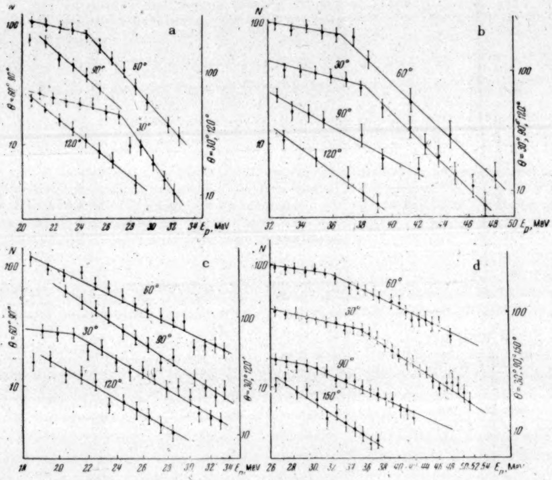

FIG. 3. Energy distribution of photoprotons (yield given in relative units): a – Be^9, $E_{\gamma\,\max} = 68$ Mev; b – Be^9, $E_{\gamma\,\max} = 84$ Mev; c – C^{12}, $E_{\gamma\,\max} = 64$ Mev; d – C^{12}, $E_{\gamma\,\max} = 84$ Mev.

sections of Be^9 and the deuteron gives $\sigma_{\text{Be}} = (0.8 \pm 0.2)A\sigma_d$ for $E_{\gamma\,\max} = 84$ Mev and $E_p = 32-38$ Mev and $\sigma_{\text{Be}} = (1.0 \pm 0.2)A\sigma_d$ for $E_{\gamma\,\max} = 68$ Mev and $E_p = 20-26$ Mev, where σ_{Be} is the cross section per effective quantum for Be^9 and σ_d is the cross section per effective quantum for the deuteron. Unfortunately the comparison could only be made by utilizing a rough theoretical estimate[3] of the absolute cross-section for the quasideuteron interaction ($\sigma_A = 1.6\,A\sigma_d$) neglecting the secondary processes, which can be important for gamma rays in the given energy range. It is noteworthy that the ratio of the deuteron and Be^9 photoproduction cross sections is constant within the limits of experimental error for the different proton energy groups when $E_{\gamma\,\max} = 68$ and 84 Mev. These results are thus also not inconsistent with the hypothesis that the quasideuteron interaction is predominant.

Let us turn now to the results obtained for carbon. The angular distribution and cross section for the photoproduction of 18 – 28 Mev protons in C^{12} by gamma rays with $E_{\gamma\,\max} = 64$ Mev are in poor agreement with the results obtained for the deuteron. It follows that although the reaction in the case of C^{12} also involves principally structures formed within the nucleus, either there is a two-nucleon absorption mechanism with a high (γ, np)-reaction threshold leading to the ejection of individual protons or the reaction involves more complex structures within the C^{12} nucleus. Such structures could be quasi alpha particles. The latter possibility is favored by the extremely large cross section of carbon decay into three alpha particles, which indicates a relatively large probability for the formation of quasi alpha particles within the C^{12} nucleus. The photodisintegration of C^{12} by gamma rays with $E_{\gamma\,\max} = 84$ Mev presents a different picture. A comparison of the experimental findings on the energy spectra and angular distributions of 26 – 36 Mev proton groups with corresponding data for the deuteron shows satisfactory agreement with the quasi-deuteron mechanism. The cross sections for C^{12} photoproton production and for deuteron photodisintegration give $\sigma_{\text{C}} = (1.1 \pm 0.2)A\sigma_d$, where σ_{C} is the carbon cross section per effective quantum. This relationship is similar to that obtained for the photodisintegration of Be^9. It is also of interest that the energy spectrum for C^{12} with $E_{\gamma\,\max} = 84$ Mev shows a maximum proton energy of 55 Mev, which gives a reaction energy of 28 Mev, thus agreeing with the energy of the

(γ, np) reaction in C^{12}. This indicates a small cross section for the (γ, p) reaction in carbon at the given energy. When C^{12} is irradiated with bremsstrahlung of $E_{\gamma_{\max}} = 64$ Mev the maximum proton energy corresponds to the energy threshold of the (γ, p) reaction, thus indicating that the latter reaction makes a considerable contribution to the total photoproton yield at the given excitation energy. Similar conclusions cannot be drawn for Be^9 because in this instance the thresholds of the (γ, p) and (γ, np) reactions practically coincide.

We converted the angular distributions to the center-of-mass system on the assumption that the principal contribution is made by the reactions $C^{12}(\gamma, p)B^{11}$ and $Be^9(\gamma, p)Li^8$ when ejection of a proton transfers recoil energy to the residual nucleus. These results can be approximated by curves of the form

$$a + b\sin^2\theta(1 + \gamma\cos\theta)^2.$$

In this analysis the relative amount of quadrupole absorption was found to be unsually large, amounting to 60 – 80% of the dipole contribution. This fact produces doubt as to the correctness of the scheme chosen to describe the interaction between quanta and the nuclei under consideration. A recalculation must be based on the above hypothesis that in the given energy range gamma rays interact with nuclei mainly through structures formed within the nucleus.

The extensive experimental results which are now available for light nuclei can be interpreted on the basis of theoretical concepts regarding the existence of structural units within the nuclei, *i.e.*, that a nucleon in a nucleus interacts not with all the other nucleons of the nucleus but only with those which are in definite states of motion with respect to the given nucleon (see Ref. 4, for example).

Our experimental data on photoprotons from Be^9 and C^{12} are in agreement with this hypothesis.

The authors are greatly indebted to Professor V. I. Veksler for a discussion of the results and wish to thank M. A. Balasheva, A. P. Lisitskaia and V. B. Solomakhina for their assistance.

---

[1] M. Lax, Phys. Rev. **72**, 61 (1947).
[2] L. Allen, Phys. Rev. **98**, 705 (1955).
[3] J. S. Levinger, Phys. Rev. **82**, 300 (1951).
[4] A. I. Baz', J. Exptl. Theoret. Phys. (U.S.S.R.) **31**, 831 (1956); Soviet Phys. JETP **4**, 704 (1957).

Translated by I. Emin
273

SOVIET PHYSICS JETP VOLUME 5, NUMBER 6 DECEMBER 15, 1957

Correlations in $\pi \to \mu \to e$-Decay

A. O. VAISENBERG AND V. A. SMIRNITSKII
Academy of Sciences, U.S.S.R.

(Submitted to JETP editor March 19, 1957)
J. Exptl. Theoret. Phys. (U.S.S.R.) **32**, 1340-1343, (June, 1957)

120 positrons from $\pi \to \mu \to e$ decays in emulsion were analysed by energy and by the angle between μ-meson and positron tracks. The observed distributions are in qualitative agreement with the two-component neutrino theory. If λ is the theoretical asymmetry parameter and α the fraction of the μ-mesons not depolarized by the emulsion, the measurements give the result $\alpha\lambda = 0.5 \pm 0.25$.

THIS PAPER DESCRIBES measurements of the positron energy and of the angle between μ-meson and positron tracks in $\pi^+ \to \mu^+ \to e^+$ decays in photographic emulsion. The problem arose from the observation by Lee and Yang[1] that a departure from parity conservation could lead to a correlation between the directions of μ-meson and electron. Landau[2] suggested that the interactions such as $\pi \to \mu \to e$ decay in which parity is not conserved are still invariant under "combined inversion," the combination of space-reflection with charge conjugation. He also showed that if the neutrino is polarized along its direction of motion and the antineutrino in the opposite direction (or vice versa), then the distribution in energy and angle of electrons emitted in $\pi \rightarrow \mu \rightarrow e$ decay has the form

$$dN = 2N\varepsilon^2 \{(3 - 2\varepsilon) + \lambda \cos\vartheta\,(2\varepsilon - 1)\}\, d\varepsilon\, d(\cos\vartheta). \tag{1}$$

Here ε is the ratio of the electron energy to the maximum possible energy, ϑ is the angle between the directions of μ-meson and electron, and λ is a constant of the theory, lying in the interval -1 to $+1$, and characterizing the degree of longitudinal polarization of the electron in $\mu \rightarrow e + \nu + \bar{\nu}$ decay. The formula shows that the correlation is small for $\varepsilon = 1/2$, changes sign at $\varepsilon = 1/2$, and increases strongly at the top of the spectrum. If $\lambda = 1$ (or -1), the electrons with maximum energy are all emitted forward (or all backward).

Garwin, Lederman and Weinrich[3] discovered the existence of an angular correlation of the form $(1 - \alpha \cos \vartheta)$ in $\pi^+ \rightarrow \mu^+ \rightarrow e^+$ decay in graphite and polyethylene, and they measured the magnetic moment of the μ-meson by observing the precession of the correlation axis in a magnetic field. But they did not observe the sharp increase in asymmetry from the middle to the top of the spectrum, which is characteristic of the two-component neutrino theory.

We here report only the preliminary results of observations which we have begun on the positron spectra and angular correlations in $\pi^+ \rightarrow \mu^+ \rightarrow e^+$ decay. Up to now we have observed 2334 $\pi - \mu$ decays in a systematic scan of a part of an emulsion block which we obtained from Prof. C. Powell. The block consists of 600 μ layers of Ilford G-5 emulsion, and was exposed in the stratosphere at a height of 28 km. From these decays we selected 120 cases in which the positron track-length is greater than 1 mm, so than an energy-measurement by the method of multiple scattering is possible. The selected events were also required to have the $\mu - e$ decay distant at least 100 μ from the emulsion surface and at least 1 cm from the edges. The scattering measurements were made twice (by two independent observers) for each track, by the coordinate method with cells of length 100 μ and 200 μ, and the usual checks on the correctness of the measurements were made. The results were not corrected for the effects of bremsstrahlung. The relation between second differences and electron energy was taken to be

$$E \approx 44/D_2^{(100)},$$

where E is the energy in Mev, and $D_2^{(100)}$ is the second difference measured in 100 μ cells. The distribution of visible track lengths was as follows:

Track length, mm	1—2	2—3	3—4	4—5	5—6	6
Number of tracks	62	31	15	6	5	1

The statistical error of the energy-measurements varies from 25% to 10% as the track-length varies from 1 mm to 6 mm.

The tracks of positrons and μ-mesons make small angles with the plane of the emulsion. The half-width of the distribution of these angles is less than 10° for positron and 15° for meson tracks. Hence we may assume without serious error that we observe the correlation for particles whose tracks lie in the emulsion plane.

The observed positron spectrum is shown in Fig. 1. It closely reproduces the positron spectrum observed in μ-e decay by previous observers.[4] The numbers in the histogram represent the angles ϑ measured in the emulsion plane. The inner (shaded) region of the histogram contains angles $\vartheta < 90°$, *i.e.*, those positrons which are emitted into the same half-plane as their parent μ-mesons. We separated from the spectrum the particles with energy exceeding 40 Mev, and selected those among them which made small angles with the μ-meson direction, obtaining the results shown in the table. The table shows a forward-backward asymmetry which is very large at small angles, not so large at wider angles, and agrees in magnitude with the asymmetry to be expected from Eq. (1).

When we look at the forward-backward asymmetry including all angles ($0 - 90°$ and $90 - 180°$), the effects are less marked but still noticeable. In particular, we may extract from the spectrum of Fig. 1 the following conclusions.

1. The total numbers of positrons are 54 forward and 66 backward.

2. The fraction of backward positrons increases significantly from 25 to 40 Mev. Counting positrons of energy greater than 25 Mev, the numbers are 49 forward and 59 backward. For energy greater than 40 Mev, the numbers are 20 forward and 31 backward.

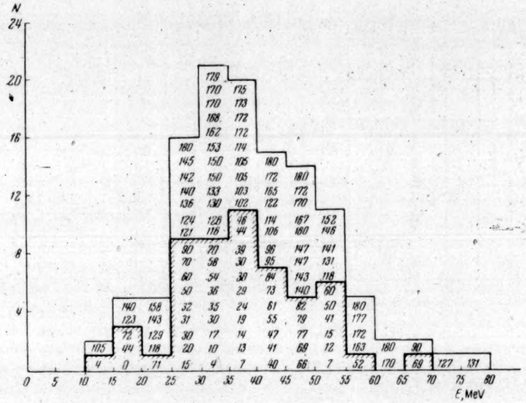

FIG. 1. Positron spectrum from $\pi \rightarrow \mu \rightarrow e$ decay.

Angles (degrees)	Direction	Number of positrons	Forward-backward ratio according to Eq. (1) with $\lambda = 1$.
0—10	Forward	1	1 : 4
170—180	Backward	9	
0—20	Forward	3	~1 : 4
160—180	Backward	14	
0—45	Forward	6	1 : 3.5
135—180	Backward	21	
45—90	Forward	14	1 : 1.6
90—135	Backward	10	

3. Of particles with energy greater than 55 Mev, 9 are backward and only 2 forward. The spectrum extends to these high energies because of the error in the energy measurements. From Eq. (1), the differential spectrum of backward-emitted positrons increases with energy like ε^2, while the spectrum of forward-emitted positrons decreases like $\varepsilon^2(1 - \varepsilon)$. Thus we should expect to find a high-energy tail to the backward positron spectrum only, and this is what is observed.

Fig. 2 shows a comparison of our data with Eq. (1). The continuous curves are integral energy spectra for forward and backward positrons, calculated for the plane angular ranges $0 - 20°$ and $160 - 180°$ (Fig. 2a), $0 - 45°$ and $135 - 180°$ (Fig. 2b), and $0 - 90°$ and $90 - 180°$ (Fig. 2c). The theoretical curves are calculated with $\lambda = -1$. In Figs. 2b and 2c, the backward experimental points are lower and the forward experimental points are higher than the theoretical curves. This is presumably a result of depolarization. If depolarization occurs, then the coefficient λ in Eq. (1) should be changed to $\alpha\lambda$, where α is the fraction of μ-mesons which is not depolarized. Our data give a determination of the quantity $\alpha\lambda$. A least squares fit to all our data, including all angles and energies, gives $\alpha\lambda = 0.50 \pm 0.25$. It should be mentioned that a least squares fit to the part of the data represented in Figs. 2a and 2b gives a rather higher value of $\alpha\lambda$. This is because the experimental points lie closer to the theoretical curves in Figs. 2a and 2b than they do in Fig. 2c. We defer any analysis of this phenomenon until we have collected a significantly larger number of measured decays.

The authors thank C. Powell for supplying the emulsions, A. I. Alikhanov for helping with the analysis, V. V. Vladimirskii, I. I. Gurevich and L. L. Gol'din for discussions and advice, N. V. Rabin, E. A. Kalganov and Z. V. Minervin for scanning and measuring, and V. F. Kuzichev, A. G. Avalishvili, and V. A. Titov for scanning the emulsions.

Note Added in Proof (May 7, 1957). We have subsequently measured energies and angles for 440 positrons from π-μ-e decay in a NIKFI-R emulsion exposed to the π^+ beam of the Dubna synchrocyclotron. Analysis of the total sample of 560 energies and

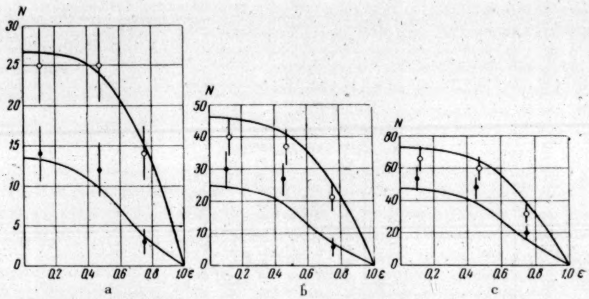

FIG. 2. Integral spectra of positrons from $\pi \to \mu \to e$ decay. a: solid circles, $\vartheta = 0-20^\circ$, open circles, $\vartheta = 160-180^\circ$; b: solid, $\vartheta = 0-45^\circ$, open, $\vartheta = 135-180^\circ$; c: solid, $\vartheta = 0-90^\circ$, open, $\vartheta = 90-180^\circ$. The curves show the theoretical distributions given by Eq. (1) with $\lambda = -1$.

angles shows that the asymmetry effect decreases from the top to the middle of the energy-spectrum and goes through zero in the range 20 – 30 Mev. This result is in complete agreement with Eq. (1) which is predicted by the two-component neutrino theory. A detailed analysis of the new data will be published later.

---

[1] T. D. Lee and C. N. Yang, Phys. Rev. **104**, 254 (1956).

[2] L. D. Landau, J. Exptl. Theoret. Phys. (U.S.S.R.) **32**, 405 (1957); Soviet Phys. JETP **5**, 336 (1957); L. D. Landau, Nuclear Physics **3**, 127 (1957).

[3] Garwin, Lederman and Weinrich, Phys. Rev. **105**, 1415 (1957).

[4] Bonetti, Levi-Setti, Panetti, Rossi, and Tomasini, Nuovo cimento **3**, 33 (1956).

[5] Bisucas, Ceccarelli and Crussard, Nuovo cimento **5**, 756 (1957).

Translated by F. J. Dyson
274

SOVIET PHYSICS JETP VOLUME 5, NUMBER 6 DECEMBER 15, 1957

Polarization of Electrons in β-Decay

A. I. ALIKHANOV, G. P. ELISEEV, V. A. LIUBIMOV
AND B. V. ERSHLER

(Submitted to JETP editor March 30, 1957)
J. Exptl. Theoret. Phys. (U.S.S.R.) 32, 1344-1349 (June, 1957)

Experiments have been made to test the law of conservation of parity by observing the longitudinal polarization of electrons in β-decay. It is found that the β-electrons have their spin directed opposite to their direction of motion. The degree of longitudinal polarization is equal to (v/c).

AFTER THE LAW of conservation of parity in weak interactions had been called in question[1,2] Landau[3] proposed the hypothesis of a two-component neutrino possessing only longitudinal polarization. He showed that in this case the electrons from β-decay would be emitted with a polarization of magnitude (v/c) along their direction of motion.

We have set up an experiment to observe the phenomenon predicted by Landau. To determine the polarization of β-decay electrons, we use the azimuthal asymmetry of the large-angle single scattering of a transversely polarized electron by a thin foil composed of a heavy element. Longitudinally polarized β-electrons are passed through crossed magnetic and electric fields. In the magnetic field the electron spins turn through an angle $\varphi = 300\, Hl/pc$. Here l is the path length in the magnetic field, measured in centimeters, p the electron momentum in ev/c, and H is the magnetic field in oersteds. The electric field is arranged so as to compensate the effect of the magnetic field on the particle orbits. Particles with velocity $\beta_0 = E/H$ travel in straight lines. Thus the crossed fields produce a transverse polarization of the electrons.

This method, well-known as the Wien velocity selector, was chosen for a variety of reasons.

1. The apparatus has a simple geometry with axial symmetry. Thus the chance of a spurious experimental asymmetry is reduced.

2. The spin of the electron can be rotated through any desired angle, and so the measurements can be made over a wide range of velocities.

3. When the directions of both magnetic and electric fields are reversed, the optics of the apparatus are unchanged while the sign of the azimuthal asymmetry is reversed. This allows a separation of true from spurious assymmetry.

4. When E and H are changed, the ratio $E/H = \beta_0$ being fixed, the energy-resolution of the apparatus changes very little. Since the polarization is proportional to $\beta = v/c$ and varies little with energy, any loss of energy-resolution has a small effect on the results and may give a large increase in the counting-rate.

The path of the electrons in the crossed fields measures 25 cm. The gap between the condenser-plates is 12 mm. When they emerge from the fields, the electrons are scattered by a gold foil making an angle of 45° with the beam direction. Electrons scattered through 90 ± 4° are detected by two Geiger counters in coincidence. Without breaking vacuum, the scatterer and the counters can be rotated through any angle about an axis coinciding with center of the beam. Between the counters there is an absorber which suppresses low-energy electrons.

We used a strontium-yttrium source of thickness 4 mg/cm² and intensity 4×10^8 disintegrations per second. The decay scheme is

$$_{38}\mathrm{Sr}^{90}\,(0^+)\xrightarrow[540\text{ Kev}]{\beta^-\,28y.}\,{}_{39}\mathrm{Y}^{90}\,(2^-)\xrightarrow[2260\text{ Kev}]{\beta^-\,64h.}\,{}_{40}\mathrm{Zr}^{90}\,(0^+).$$

Measurements were made with the energy in the neighborhood of 300 kev. The electric field was 18.3 kev/cm, and the magnetic field was $H = 79$ Oe, thus $\beta_0 = E/H = 0.775$. The angle through which the spins were turned was $\varphi \approx 50°$. The expected azimuthal asymmetries may be calculated from the data shown in Table 1. In a plane perpendicular to the spin direction, the expected azimuthal effect is

$$\delta_{\text{theor}} = \sum f(N)\,\Delta\beta \sin\varphi \Big/ \sum f(N) = 27.7\%.$$

The experimental results are shown in Table 2. One sees that (1) there is no asymmetry in the plane 0°–180° in which the spin is rotated, (2) asymmetry is observed in the plane 90°–270°, and changes

TABLE I. $\mathcal{E}$ is the electron kinetic energy in kev; $\beta = v/c$; $f(N)$ is the number of electrons of given energy which reach the counters in arbitrary units; $f(N)$ is the product of the energy-resolution curve of the apparatus, the probability that an electron of given energy will penetrate the absorber between the counters, the cross section for scattering the electron through 90°, and the energy-spectrum of the source; φ is the angle through which the electron spin turns in the magnetic field; Δ is the azimuthal asymmetry for a 100% transversely polarized electron. The values are taken from Ref. 8.

$\mathcal{E}$	200	250	300	350	400	450	500
$\beta=v/c$	0.70	0.74	0.78	0.81	0.83	0.84	0.86
$f(N)$	15	70	61	41	28	15	10
$\sin\varphi$	0.88	0.81	0.75	0.70	0.66	0.62	0.59
Δ	51.5	50	48.5	46.5	45	43.5	42
$\Delta\cdot\sin\varphi\cdot\beta$	31.7	30.0	28.4	26.4	24.6	22.7	21.3

TABLE II.

0	180	90	270	
129.7±5.7	132.7±5.8	150.1±3.9	125.2±4.0	Number of counts per minute. Field negative.
31.2±2.5	31.0±2.5	31.3±1.2	24.2±1.0	Background with no scatterer.
98.5±6.2	101.7±6.3	**118.8±4.0**	*101.0±4.1*	Effect
128.6±4.0	142.7±3.8	136.5±1.8	145.9±2.4	Number of counts per minute. Field positive.
29.8±2.2	34.2±2.4	37.4±1.1	27.5±1.1	Background with no scatterer.
98.6±4.8	108.5±4.2	*99.1±2.0*	**118.4±2.4**	Effect
200.3±7.8 207.0±7.3		199.0±3.6 237.2±4.2		Sum of effects with positive and negative field.

sign when the fields are reserved, and (3) the sign of the asymmetry indicates that electrons in β-decay are emitted with spins oriented in the direction opposite to their velocity, in agreement with the experimental result of Wu *et al.*[4]

The magnitude of the measured asymmetry is

$$\delta_{\text{obs}} = (17.4 \pm 2.6)\%.$$

Hence the degree of polarization of β-decay electrons appears to be

$$\beta(17.4 \pm 2.6)/27.7 = (0.63 \pm 0.09)\beta.$$

The gold scatterer which we used had a thickness of 0.537 mg/cm². To determine the ratio of multiple to single scattering in the foil, we used the criterion of Alikhanian, Alikhanov and Vaisenberg.[5] The intensity of single scattering should vary linearly with the foil thickness, and thus the excess intensity observed with thicker foils indicates the amount of multiple scattering. From the relative intensity of the scattering from foils of thickness 0.537 and 0.17 mg/cm², we deduce that the fraction of multiple scattering in the thicker foil is ~ 30%. Since the azimuthal asymmetry Δ varies strongly with the scattering angle and decreases sharply for angles less than 90°, the asymmetry will be small for multiply scattered electrons. Hence the measured value of the asymmetry should be increased by ~ 30%. In addition, the multiple scattering in a thick source produces a significant depolarization of electrons at a given energy. These corrections are so large that it is not possible to incorporate them in our final results, although the sign and the approximate magnitude of the corrections are known.

To reduce the depolarization in the source, and also to reduce the background and thus allow the use of a thin scattering foil, we made measurements of the polarization of electrons of energy ~ 1000 kev. In this energy range the electrons come from the $_{39}Y^{90}$ decay. The electric field was 20 kev/cm, and the magnetic field 71 Oe. Between the two coincidence counters there was an absorber (0.08 g/cm² Al + 0.08 g/cm² Cu) which stopped electrons of energy below 600 kev. The scatterer was a gold foil of thickness 1.9 mg/cm². The expected azimuthal asymmetry (see Table 3) was

$$\delta_{\text{theor.}} = \sum \Delta \sin\varphi \cdot \beta \cos\vartheta \cdot f(N) \Big/ \sum f(N) = 10.3\,\%.$$

TABLE III. Cos θ is the depolarization in the source; $\theta = \sqrt{\overline{\theta^2}}$ is the root-mean-square angle of multiple scattering.

$\mathcal{E}$	600	700	800	900	1000	1100	1200	1300	1400	1500	1600
$f(N)$	2	15	21	22	20	16	14	10	7	4	2
$\sin\varphi$	0.54	0.47	0.43	0.39	0.37	0.34	0.32	0.30	0.28	0.27	0.25
β	0.89	0.91	0.92	0.93	0.94	0.95	0.95	0.96	0.96	0.97	0.97
Δ	39	37	34	32	30	28	27	26	25	24	24
$\cos\theta$	0.91	0.94	0.94	0.96	0.96	0.97	0.97	0.97	0.98	0.98	0.98
$\Delta\beta \sin\varphi\cos\theta$	16	14.9	12.7	11.2	9.9	8.8	7.9	7.2	6.6	6.1	5.7

The experimental results are shown in Table 4. The azimuthal asymmetry, in the plane perpendicular to the plane of the spin rotation, is in this experiment

$$\delta_{\text{obs}} = (7.8 \pm 1.7)\,\%.$$

Observations with a thinner scatterer showed that multiple scattering is here only 6% of single. We thus find for the degree of polarization of 1000 kev electrons

$$(0.8 \pm 0.17)\,\beta.$$

In the energy-range around 1000 kev, the energy-resolution of the apparatus is poor. The number of scattered particles reaching the counters is practically independent of the applied fields, and is determined by the energy-spectrum of the source, the stopping-power of the absorber between the counters, and the scattering cross-section. This allowed us to make a control experiment with electrons of the same energy in zero electric and magnetic field. In this case the electrons remain longitudinally polarized, and no azimuthal asymmetry in scattering should be observed. The data in Table 4 show that in zero field there is indeed no azimuthal asymmetry (1.5 ± 3.5%).

The experiment was then repeated at an energy of ~ 300 kev with the same scatterer and a thinner source (~ 1.5 mg/cm²) in order to reduce the depolarization in the source. The observed degree of polarization was

$$(0.77 \pm 0.16)\,\beta,$$

definitely larger than the earlier result obtained with a thicker source. A comparison of the results at 300 kev and at 1000 kev shows that the polarization is proportional to (v/c), and the observed degree of polarization comes closer and closer to (v/c) as the experimental conditions are improved.

Our experiments on the polarization of electrons in β-decay, together with the experiments of Wu *et al.*[4] Lederman *et al.*[5] and of Vaisenberg and Smirnitskii,[6] demonstrate that parity is not conserved in weak interactions, and give strong evidence that the two-component neutrino theory proposed by Landau is in agreement with experiment.

The authors are deeply grateful to L. Ia. Suvorov, M. P. Anikina and V. D. Laptev for their painstaking and careful work in preparing the sources, to A. S. Kronrod for calculating the optics of the apparatus, and to M. E. Vishnevskii for much useful practical advice.

TABLE IV.

0	180	90	270	
31.7±0.7	32.8±0.7	33.2±0.4	30.7±0.4	**Number of counts per minute. Field negative.**
2.2±0.3	3.0±0.4	1.88±0.2	1.98±0.2	**Background with no scatterer.**
29.5±0.7	29.8±0.8	*31.3±0.4*	**28.7±0.5**	**Effect.**
31.6±0.9	31.1±0.9	30.6±0.4	31.9±0.4	**Number of counts per minute. Field positive.**
2.2±0.4	2.2±0.4	2.96±0,26	2.37±0,23	**Background with no scatterer.**
29.4±1.0	28.9±1.0	**27.6±0.5**	*29.6±0.5*	**Effect.**
58.4±1.3 59.2±1.3		60.9±0.6 56.3±0.6		**Sum of effects with positive and negative field.**
31.6±0.9	32.6±0.8	32.6±0.7	32.0±0.7	**Number of counts per minute. Zero field.**
2.7±0.4	2.7±0.3	2.9±0.4	2.8±0.3	**Background with no scatterer.**
28.9±1.0	29.9±0.9	29.7±0.8	29.2±0.8	**Effect.**

(Added April 9, 1957)

APPENDIX

New measurements have been made at 300 kev with a thin source and a thin scatterer ($0.17\ \text{mg/cm}^2$). The electrons were scattered at an angle (105 ± 4)°. The expected azimuthal asymmetry, including a 5% correction for depolarization in the source, was 36.2%. In this experiment the spurious asymmetry ($\sim$ 7%) in the spin rotation plane was measured by scattering the electrons with an aluminum foil, for which the theoretical asymmetry is less than 3%, and the results with the gold foil were corrected accordingly. The measured degree of polarization of the electrons was

$$(0.98 \pm 0.14)\beta.$$

Recently the group of S. Ia. Nikitin obtained similar results in our laboratory, confirming the longitudinal polarization of electrons in β-decay. Their method differed from ours in using a condenser bent through 108° to rotate the spins. They used Cu^{64} (forbidden decay) for their source.

After this work was finished, we learned from L. D. Landau that H. Frauenfelder had earlier obtained similar results. Frauenfelder's measurements were, as he himself said, qualitative in character. The method was similar to that used by Nikitin's group.

---

[1] T. D. Lee and C. N. Yang, Phys. Rev. 104, 254 (1956).

[2] L. D. Landau, J. Exptl. Theoret. Phys. (U.S.S.R.) 32, 405 (1957); Soviet Phys. JETP 5, 336 (1957).

[3] L. D. Landau, J. Exptl. Theoret. Phys. (U.S.S.R.) **32**, 407 (1957); Soviet Phys. JETP **5**, 337 (1957).

[4] Wu, Ambler, Hayward, Hoppes and Hudson, Phys. Rev. **105**, 1413 (1957).

[5] Alikhanian, Alikhanov and Vaisenberg, J. Phys. (U.S.S.R.) **9**, 280 (1945).

[6] Garwin, Lederman and Weinrich, Phys. Rev. **105**, 1415 (1957).

[7] A. O. Vaisenberg and V. A. Smirnitskii, J. Exptl. Theoret. Phys. **32**, 1340 (1957); Soviet Phys. JETP **5**, 1093 (1957) (this issue).

[8] H. A. Tolhoek, Revs. Mod. Phys **28**, 277 (1956); N. Sherman, Phys. Rev. **103**, 1601 (1956).

Translated by F. J. Dyson
275

SOVIET PHYSICS JETP VOLUME 5, NUMBER 6 DECEMBER 15, 1957

On the Structure of the Electron Spectrum in Lattices of the Tellurium Type

IU. A. FIRSOV

(Submitted to JETP editor April 29, 1956)
J. Exptl. Theoret. Phys. (U.S.S.R.) 32, 1350-1367 (June, 1957)

The general properties of the energy spectrum of an excess electron in a crystal with a lattice of the tellurium type are studied by group-theoretical methods, without resort to the approximation of weak or strong coupling. The possibility of contact between the zones in definite directions in the **k**-space is demonstrated. The effect of the spin-orbit interaction is investigated. It is shown that in semiconductors of this type there can be present two kinds of carriers of the same sign. Dispersion laws in the approximation quadratic in **k** are found on various assumptions about the location of the extrema of $E(\mathbf{k})$.

THE PROBLEM OF the energy spectrum of electrons in semiconductors is of extreme importance in the study of all the properties of semiconductors and, in particular, for the understanding of the kinetics of processes occurring in these materials. The complex structure of the electron spectrum in germanium was predicted theoretically and has been convincingly confirmed in relatively recent experiments on the cyclotron resonance.[1] There is every reason to suppose that, within the framework of the one-electron approximation, the effective mass by no means always has the properties of a tensor quality (for example, for holes in germanium[2]). Therefore it is of interest to see what information on this point can be obtained by considering the symmetry properties of the lattice.

The experiments of Shalyt obviously provide evidence that two kinds of holes are present in tellurium.[3] This is not possible in the simplified theory of the zone spectrum of tellurium recently proposed by Callen[4,5]. Moreover, the group-theoretical formula he used do not correspond to the actual structure of tellurium. Although some of the conclusions of Callen's work are also confirmed in our exact theory, the reasons for the occurrence of the effects in question are entirely different. But the considerations given by Callen on the origin of the zones do not encounter any contradictions, and we make use of them in the choice of the theoretical possibilities, which, as it will turn out, can occur.

1. METHOD OF TREATMENT

The method* we have used is based on general premises of group theory. The idea of the method is as follows: as is well known, the wave function of an electron in an ideal crystal can be written in the form $\Psi_{n\mathbf{k}} = e^{i\mathbf{k}\mathbf{r}}u_{n\mathbf{k}}$. The Schrödinger equation for the modulating factor takes the form:

$$\left[-\frac{\hbar^2}{2m}\frac{\partial^2}{\partial x_l^2} - i\frac{\hbar^2}{m}k_l\frac{\partial}{\partial x_l} + \frac{\hbar^2k^2}{2m} + U(\mathbf{r})\right]u_{n\mathbf{k}}(\mathbf{r}) = E_n(\mathbf{k})\,u_{n\mathbf{k}}(\mathbf{r}). \qquad (1)$$

Here summation is understood over the twice repeated indices l, and $U(\mathbf{r})$ is the self-consistent periodic potential. The function $U(\mathbf{r})$ possesses definite symmetry properties. We introduce the symmetry operators $\hat{G}_l$ such that $\hat{G}_l U(\mathbf{r}) = U(\mathbf{r}') = U(\mathbf{r})$, *i.e.*, such that the action of the operator $\hat{G}_l$ in the "coordinate" representation consists in taking the point **r** over into the point **r**$'$, *i.e.*,

---

* A more rigorous exposition of this method can be found in a paper by Seitz.[6]

$$\hat{G}_l \mathbf{r} = \mathbf{r}'. \tag{2}$$

It is clear that the required properties are possessed by the operators of translation by a whole number of lattice constants (we shall denote them by $\bar{\tau}_l = \mathbf{i}_0 x_l^0 + \mathbf{j}_0 y_l^0 + \mathbf{k}_0 z_l^0$), and also by rotation and reflection operators that take one atom in a crystal cell over into the position of another atom in the same or in another cell (we shall denote such operators by $\hat{\rho}_j$).

In addition there can exist so-called "open" symmetry elements, which reduce to rotations or reflections with subsequent translations. For such operators we shall use the notation

$$\{\hat{\rho}_j | \bar{\tau}_j\}. \tag{3}$$

If we write the Schrödinger equation in primed coordinates **r**$'$ and choose a new value of **k**$'$ such that its components along the new axes are equal to those of the old wave vector **k** in Eq. (1) along the unprimed axes, then this equation will have the same form as Eq. (1):

$$\left[-\frac{\hbar^2}{2m}\frac{\partial^2}{\partial x_l'^2} - i\frac{\hbar^2}{m}k_l\frac{\partial}{\partial x_l'} + \frac{\hbar^2 k^2}{2m} + U(\mathbf{r}')\right]u_{n\mathbf{k}}(\mathbf{r}') = E_n(k_1, k_2, k_3)\,u_{n,\mathbf{k}}(\mathbf{r}'). \tag{4}$$

Since Eqs. (1) and (4) are identical in form and possess the same transformation properties, their eigenvalues are equal. But in Eq. (4) the wave vector is written in terms of its components along the new axes, and if we write it in terms of components along the old axes we shall have from Eqs. (1) and (4):

$$E_n(k_1, k_2, k_3) = E_n(k_1', k_2', k_3'). \tag{5}$$

Let us go over to the unprimed coordinates in Eq. (4). The Laplacian operator and $U(\mathbf{r})$ are invariant with respect to our transformations. The application of the operator (3) to the coordinates gives:

$$x_l' = (\hat{\rho}_j)_{lm}\, x_m + x_l^0, \tag{6}$$

$$x_m = (\hat{\rho}_j^{-1})_{ml}\, x_l' + (\hat{\rho}_j^{-1}\bar{\tau}_j)_m. \tag{7}$$

Since $\dfrac{\partial}{\partial x_l'} = \dfrac{\partial x_i}{\partial x_l'}\dfrac{\partial}{\partial x_i}$, then $k_l\dfrac{\partial}{\partial x_l'} = k_l\dfrac{\partial x_i}{\partial x_l'}\dfrac{\partial}{\partial x_i} = k_i'\dfrac{\partial}{\partial x_i}$.

Consequently $k_i' = k_l\dfrac{\partial x_i}{\partial x_l'} = (\hat{\rho}_j^{-1})_{il}\,k_l$, *i.e.*, $\mathbf{k}' = (\hat{\rho}_j^{-1})\,\mathbf{k}$.

If we denote the Hamiltonian by $\hat{H}_{\mathbf{k}}$, then Eq. (4) in the unprimed coordinates will have the form:

$$\hat{H}_{\mathbf{k}'} u_{n\mathbf{k}}(\hat{G}_j\mathbf{r}) = E_n(k_1', k_2', k_3')\,u_{n\mathbf{k}}(\hat{G}_j\mathbf{r}). \tag{8}$$

If we understand the operators $\hat{G}_j$ to be taken in the representation with the functions $u_{n\mathbf{k}}(\mathbf{r})$ as the basis, then $u_{n\mathbf{k}}(\mathbf{r}) = \hat{G}_j u_{n\mathbf{k}}(\mathbf{r})$. Thus we have

$$\hat{H}_{\mathbf{k}'}\hat{G}_j\,u_{n\mathbf{k}}(\mathbf{r}) = E_n(\mathbf{k}')\,\hat{G}_j\,u_{n\mathbf{k}}(\mathbf{r}), \tag{9}$$

i.e., our operators do not commute:

$$\hat{G}_j\hat{H}_{\mathbf{k}} = \hat{H}_{\mathbf{k}'}\hat{G}_j. \tag{10}$$

We see that $\hat{G}_j u_{n\mathbf{k}}(\mathbf{r})$ is an eigenfunction of the Hamiltonian $\hat{H}_{\mathbf{k}'}$. But we have just seen that the eigenvalues for Eqs. (1) and (4) are the same, *i.e.*, the spectrum is symmetrical with respect to all the operators $\hat{\rho}_j$ as applied to the k-space:

$$E_n(\mathbf{k}') = E_n(\mathbf{k}), \quad \hat{G}_j u_{n\mathbf{k}}(\mathbf{r}) = u_{n\mathbf{k}'}(\mathbf{r}). \tag{11}$$

By the action of all the $\hat{\rho}_j$ on k we get in the k-space what is called the "star"[7] for the wave vector k remains invariant under the action of a cergroup of the operators $\hat{\rho}_j$, this group of operators is called the group of the wave vector k.[7] In this case there is commutability:

$$\hat{G}_j\hat{H}_{\mathbf{k}} = \hat{H}_{\mathbf{k}}\hat{G}_j. \tag{12}$$

We can now apply the general premises of group theory to the study of the electron spectrum, and, having compiled tables of the characters of the groups of various wave vectors, find out whether the zones coincide for a given value of the wave vector (*i.e.*, whether there is degeneracy). Such degeneracy occurs if for the group in question there exist representations of dimensionality greater than unity.

2. GROUPS OF SYMMETRY ELEMENTS FOR A LATTICE OF THE TELLURIUM TYPE

The space group of tellurium is D_3^6. Tellurium is a uniaxial crystal, with a structure consisting of a set of parallel chains of atoms. Within each of the infinite chains the atoms are connected by a screw axis of the third order directed along the principal axis of the crystal. The atoms of different chains are connected by simple axes of the second order and screw axes of the second order, located in planes perpendicular to the principal axis of the crystal.[8]

We adopt the following notations for the symmetry operators: $\hat{\rho}_3^1$ is the operator for a clockwise rotation around a third order screw axis, and its square $\hat{\rho}_3^2$ is the rotation in the counterclockwise direction; the operators of rotation around the second order axes are $\hat{\rho}_2^{(j)}$ (the upper index j corresponds to the number of the axis chosen); the operator for a translation along the principal axis is $\overline{\tau}_3$, and those for translations in the plane perpendicular to the principal axis are $\overline{\tau}_1$ (along the x axis) and $\overline{\tau}_2$.

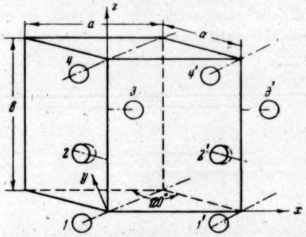

FIG. 1.

From Fig. 1, which shows the arrangement of the tellurium atoms in the crystal cell (there are three to a cell), and from Ref. 8, which gives the arrangement of the symmetry elements in the cell, we get the following expressions for the symmetry operators in the coordinate representation:

$$\hat{\rho}_3^1 = \begin{vmatrix} -1/2 & \sqrt{3}/2 & 0 \\ -\sqrt{3}/2 & -1/2 & 0 \\ 0 & 0 & 1 \end{vmatrix}; \quad \hat{\rho}_3^2 = \begin{vmatrix} -1/2 & -\sqrt{3}/2 & 0 \\ \sqrt{3}/2 & -1/2 & 0 \\ 0 & 0 & 1 \end{vmatrix};$$

$$\hat{\rho}_2^{(1)} = \begin{vmatrix} 1 & 0 & 0 \\ 0 & -1 & 0 \\ 0 & 0 & -1 \end{vmatrix}; \quad \hat{\rho}_2^{(2)} = \begin{vmatrix} -1/2 & \sqrt{3}/2 & 0 \\ \sqrt{3}/2 & 1/2 & 0 \\ 0 & 0 & -1 \end{vmatrix}; \quad \hat{\rho}_2^{(3)} = \begin{vmatrix} -1/2 & -\sqrt{3}/2 & 0 \\ -\sqrt{3}/2 & 1/2 & 0 \\ 0 & 0 & -1 \end{vmatrix} \tag{13a}$$

$$\overline{\tau}_1 = \mathbf{i}_0 a; \quad \overline{\tau}_2 = -\mathbf{i}_0 \frac{a}{2} + \mathbf{j}_0 \frac{\sqrt{3}}{2} a; \quad \overline{\tau}_3 = \mathbf{k}_0 b.$$

Then, according to the notation (3), the operator for a single step along a 3rd-order screw axis will be denoted by $\widetilde{C}_3^1 = \{\rho_3^1 \mid \overline{\tau}_3/3\}$. For the unit operator we write $E = \{\varepsilon \mid 0\}$. We write the operators for the three 2nd-order axes in the form:

$$U_2^{(1)} = \{\hat{\rho}_2^{(1)} \mid \overline{\tau}_3/3\}; \quad U_2^{(2)} = \{\hat{\rho}_2^{(2)} \mid 0\},$$
$$U_2^{(3)} = \{\hat{\rho}_2^{(3)} \mid 2\overline{\tau}_3/3\}. \tag{13}$$

We have presented only the principal symmetry elements. The word "principal" is used in the sense that all the remaining symmetry operations around other axes located inside the cell (according to Ref. 8 there are 15 of them in all) reduce to rotations around these "principal" axes, multiplied by principal translations.

From the meaning of the action of the operators that have been introduced we have the following multiplication law for them:

$$\{\hat{\rho}_h \mid \bar{\tau}_h\}\cdot\{\hat{\rho}_l \mid \bar{\tau}_l\} = \{\hat{\rho}_h \hat{\rho}_l \mid \bar{\tau}_h + \hat{\rho}_h \bar{\tau}_l\}, \qquad (14)$$

i.e., in the general case the operators do not commute. After the expressions for the operators in the "coordinate" representation are found, we can find for them the multiplication table (Table 1), which will be the same in all representations, including the representation of those Bloch functions $\Psi_{n,\mathbf{k}}$ that are solutions of the Schrödinger equation in which the Hamiltonian commutes with the group of operators described above. But in this last case it can turn out that some of the translations have the effect of unit elements, and the multiplication table takes a simpler form.

TABLE I

	E	$\tilde{C}_3^1$	$\tilde{C}_3^2$	$U_2^{(1)}$	$U_2^{(2)}$	$U_2^{(3)}$	T_1	T_2	T_3
E	E	$\tilde{C}_3^1$	$\tilde{C}_3^2$	$U_2^{(1)}$	$U_2^{(2)}$	$U_2^{(3)}$	T_1	T_2	T_3
$\tilde{C}_3^1$	$\tilde{C}_3^1$	$\tilde{C}^2$	T_3	$U_2^{(3)}$	$U_2^{(1)}$	$T_3U_2^{(2)}$	$T_1^{-1}T_2^{-1}C_3^1$	$T_1\tilde{C}_3^1$	$T_3\tilde{C}_3^1$
$\tilde{C}_3^2$	$\tilde{C}_3^2$	T_3	$T_3\tilde{C}_3^1$	$T_3U_2^{(2)}$	$U_2^{(3)}$	$T_3U_2^{(1)}$	$T_2\tilde{C}_3^2$	$T_2^{-1}T_1^{-1}\tilde{C}_3^2$	$T_3\tilde{C}_3^2$
$U_2^{(1)}$	$U_2^{(1)}$	$U_2^{(2)}$	$T_3^{-1}U_2^{(3)}$	E	$\tilde{C}_3^1$	$T_3^{-1}\tilde{C}_3^2$	$T_1U_2^{(1)}$	$T_2^{-1}T_1^{-1}U_2^{(1)}$	$T_3^{-1}U_2^{(1)}$
$U_2^{(2)}$	$U_2^{(2)}$	$T_3^{-1}U_2^{(3)}$	$T_3^{-1}U_2^{(1)}$	$T_3^{-1}\tilde{C}_3^2$	E	$T_3^{-1}\tilde{C}_3^1$	$T_2U_2^{(2)}$	$T_1U_2^{(2)}$	$T_3^{-1}U_2^{(2)}$
$U_2^{(3)}$	$U_2^{(3)}$	$U_2^{(1)}$	$U_2^{(2)}$	$\tilde{C}_3^1$	$\tilde{C}^2$	E	$T_2^{-1}T_1^{-1}U_2^{(3)}$	$T_2U_2^{(3)}$	$T_3^{-1}U_2^{(3)}$

3. ON THE BRILLOUIN ZONE FOR LATTICES OF THE TELLURIUM TYPE

It is well known that the shape of the first Brillouin zone can be found from the condition

$$(\mathbf{k}/2\pi)\boldsymbol{\tau}_i = n_i \quad (n_i = 0.1). \qquad (15)$$

From Eq. (15) we have

$$\frac{\mathbf{k}}{2\pi} = n_1 \frac{[\boldsymbol{\tau}_2\boldsymbol{\tau}_3]}{[\boldsymbol{\tau}_1[\boldsymbol{\tau}_2\boldsymbol{\tau}_3]]} + n_2 \frac{[\boldsymbol{\tau}_3\boldsymbol{\tau}_1]}{[\boldsymbol{\tau}_1[\boldsymbol{\tau}_2\boldsymbol{\tau}_3]]} + n_3 \frac{[\boldsymbol{\tau}_1\boldsymbol{\tau}_2]}{[\boldsymbol{\tau}[\boldsymbol{\tau}_{12}\boldsymbol{\tau}_3]]}. \qquad (15\text{a})$$

Taking (13 a) into account we get

$$\frac{\mathbf{k}}{2\pi} = \frac{n_1}{a}\left(\mathbf{i}_0 + \frac{1}{\sqrt{3}}\mathbf{j}_0\right) + \frac{n_2}{a}\frac{2}{\sqrt{3}}\mathbf{j}_0 + \frac{n_3}{b}\mathbf{k}_0. \qquad (15\text{b})$$

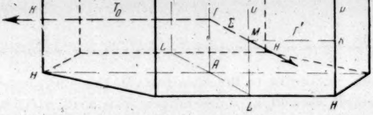

FIG. 2.

If k varies over the range $-\pi \leq \mathbf{k}\boldsymbol{\tau} \leq \pi$, then

$$\mathbf{k}_1^{\mathrm{gr}} = \pm\frac{\pi}{a}\left(\mathbf{i}_0 + \frac{1}{\sqrt{3}}\mathbf{j}_0\right), \quad \mathbf{k}_2^{\mathrm{gr}} = \pm\frac{2}{a}\frac{\pi}{\sqrt{3}}\mathbf{j}_0;$$

$$\mathbf{k}_3^{\mathrm{gr}} = \mathbf{k}^{\mathrm{gr}} - \mathbf{k}_2^{\mathrm{gr}} = \pm\frac{\pi}{a}\left(\mathbf{i}_0 - \frac{1}{\sqrt{3}}\mathbf{j}_0\right); \qquad (16)$$

$$\mathbf{k}_4^{\mathrm{gr}} = \pm\frac{\pi}{b}\mathbf{k}_0.$$

TABLE II

Designation of special point	Components of wave vector along axes	Designation of special point	Components of wave vector along axes
Γ	$0,\ 0,\ 0$	T'	$k_x,\ 2\pi/\sqrt{3}\,a, 0$
A	$0,\ 0,\ \pi/b$	S'	$k_x,\ 2\pi/\sqrt{3}\,a,\ \pi/b$
K	$4\pi/3a,\ 0,\ 0$	Λ	$0,\ 0,\ k_z$
H	$4\pi/3a,\ 0,\ \pi/b$	P	$4\pi/3a,\ 0,\ k_z$
M	$2\pi/\sqrt{3}\,a, 0,\ 0$	T_0	$k_x,\ 0,\ 0$
L	$2\pi/\sqrt{3}\,a, 0,\ \pi/b$		

Thus the first Brillouin zone has the shape of a hexagonal prism. We adopt the usual[9, 10] designations for the special points. Table 2 shows the values of the wave vector corresponding to the special points, in terms of components along the axes.

4. CONSTRUCTION OF TABLES OF CHARACTERISTICS FOR GROUPS BELONGING TO WAVE VECTORS

If we choose as basis functions the oscillating Bloch factors $u_{n\mathbf{k}}(\mathbf{r})$, then all translations will act as unit elements, *i.e.*, with respect to this basis the group will be isomorphic to D_3 and we can make use of well known results.[11] Thus for the point $\Gamma(\mathrm{k} = 0)$ two-fold degeneracy is possible (because the group has a representation of the second order), *i.e.*, at this point some of the zones come together in pairs. If for the point A we take as basis functions the $u_{n\mathbf{k}_A}(\mathbf{r})$, then we shall have:

$$U_2^{(i)}\hat{H}_{\mathbf{k}_A} = \hat{H}_{-\mathbf{k}_A}U_2^{(i)}; \quad \widetilde{C}_3^1\hat{H}_{\mathbf{k}_A} = \hat{H}_{\mathbf{k}_A}\widetilde{C}_3^1. \tag{17}$$

But since $\mathbf{k}_A$ and $-\mathbf{k}_A$ differ by $2\pi/b$, and we are using the concept of the reduced wave vector, we can also include all the $U_1^{(i)}$ in the group of the wave vector, along with $\widetilde{C}_3^1$ and $\widetilde{C}_3^2$. The table of characters for the Bloch oscillating factor $u_{n,\mathbf{k}_A}$ will be the same as for $u_{n,0}$.

Similar results are also obtained for the points K and H. Thus there can be contacts between zones at the points Γ, A, K, H. For the points L, M, T_0, T', S the group of the wave vectors will be E and $U_2^{(1)}$. This is the point group C_2,[11] and since here the multiplicity of the representations does not exceed unity, there is no degeneracy at these points. For the points Λ and P the group of the wave vector is E, $\widetilde{C}_3^1$, $\widetilde{C}_3^2$, *i.e.*, a group isomorphic to C_3.[11]

In the case in which the symmetry elements include "open" ones (screw axes, slip planes), the space group is not a simple product of a point group by a group of translations, and the groups for which the $\Psi_{n,\mathbf{k}}$ are taken as basis are not isomorphic to the corresponding point groups. (For example, this occurs for the case of the hexagonal close-packed lattice D_{6h}^4 and for the germanium lattice[9, 10] D_h^7). For the point Γ we have $\Psi_{n,0} = u_{n,0}$; the results obtained can also be referred to the new basis. For the point A we have $\psi_{n,\mathbf{k}_A} = e^{i\pi/b}u_{n,\mathbf{k}_A}$. In this case

$$(\widetilde{C}_3^1)^3\psi_{n,\mathbf{k}_A} = \{\varepsilon\,|\,\overline{\tau}_3\}\psi_{n,\mathbf{k}_A} = -\psi_{n,\mathbf{k}_A}.$$

We write $\{\varepsilon|\overline{\tau}_3\} = T_3$. Now $(T_3)^2 = E$ (where E is the unit element). But $\{\varepsilon|\overline{\tau}_1\}$ and $\{\varepsilon|\tau_2\}$ act as unit elements, *i.e.*, the multiplication table takes a simplified form. We can now divide the elements into classes, using the following property:

$$A_i^{-1}BA_i = C_i. \tag{18}$$

If A_i runs through all the elements of the group, then B and all the C_i obtained by this operation belong to one class. It is not hard to verify that there are six classes (we shall denote them by K_j):

$$K_1 = E; \quad K_2 = T_3; \quad K_3 = \widetilde{C}_3^1, T_3\widetilde{C}_3^2;$$

$$K_4 = \widetilde{C}_3^2, T_3\widetilde{C}_3^1;$$

$$K_5 = U_2^1, T_3U_2^{(2)}, T_3U_2^{(3)}; \quad K_6 = T_3U_2^{(1)}, U_2^{(2)}, U_2^{(3)}.$$

Thus we shall have six representations. To find their dimensionalities we make use of the fact that

$n = \Sigma m_i^2$ where m_i is the dimensionality of the ith representation and n is the number of elements in the group. We get four one-dimensional representations and two with two dimensions. To construct the table of characters we use the following theorem[12]

$$\left(h_i\chi_i^{(d)}/\chi_E^{(d)}\right)\cdot\left(h_j\chi_j^{(d)}/\chi_E^{(d)}\right)=\sum_l a_{ijl}h_l\chi_l^{(d)}/\chi_E^{(d)}. \tag{19}$$

Here h_i is the number of elements in the ith class, and $\chi_i^{(d)}$ is the character of the elements of the ith class in the representation d. The coefficient a_{ijl} is the number of times the class K_l is contained in the products of all elements of the class K_i by all elements of the class K_j. Since the multiplication table of the elements is known, we can find the coefficients a_{ijl} and get the system of equations for the $\chi_j^{(d)}$. By solving this system we get Table 3. In this table we must take the last three representations, where the action of T_3 is equivalent to multiplication by -1. The first three representations relate to $u_{n,\mathbf{k}_A}$. From Table 3 it follows that $\Psi_{n,\mathbf{k}_A}$ that we have determined the degree of degeneracy at the point A correctly. Similar results are obtained for the points K and H, because

$$T_1\psi_{n,\mathbf{k}_H}=\omega^2\psi_{n,\mathbf{k}_H};\quad T_2\psi_{n,\mathbf{k}_H}=\omega^2\psi_{n,\mathbf{k}_H};$$
$$T_1T_2\psi_{n,\mathbf{k}_H}=\omega\psi_{n,\mathbf{k}_H};\quad \omega=e^{i2\pi/3}, \tag{20}$$

i.e., the elements T_1T_2, T_1 and T_2 commute with all the elements of the group, and inclusion of them in the groups of the wave vectors for the points K and H would lead to a trivial tripling of the number of representations obtained (Table 3), by multiplying the characters already found by 1, ω, ω^2. Such considerations show that the results for the points K are similar to those for the point Γ.

5. THE DOUBLE-VALUED GROUPS FOR TELLURIUM

For the construction of the double-valued representations, which give the transformations of spinors, we can use the artifice proposed by Bethe.[13] For the case in which the $u_{n,\mathbf{k}}$ are taken as the basis, the groups in question are isomorphic to certain point groups, so that we can use the double-valued groups obtained for the latter.[11] If the $\Psi_{n,\mathbf{k}}$ are taken as the basis, we must introduce the following consideration. We shall assume that

$$(\hat{\rho}_3^1)^3=\delta;\quad (\hat{\rho}_2^{(i)})^2=\delta,\quad (\delta)^2=\varepsilon.$$

Then

$$(\widetilde{C}_3^1)^3=\{\delta\mid\bar{\tau}_3\};\quad(\widetilde{C}_3^1)^6=\{\varepsilon\mid 2\bar{\tau}_3\};$$
$$(U_2^{(i)})^2=\{\delta\mid 0\};\quad (U_2^{(i)})^4=\{\varepsilon\mid 0\}. \tag{21}$$

TABLE III

	K_1	K_2	K_3	K_4	K	K_6
A_1''	1	1	1	1	1	1
A_2''	1	1	1	1	—1	—1
A_3''	2	2	—1	—1	0	0
A_1	1	—1	—1	1	1	—1
A_2	1	—1	—1	1	—1	1
A_3	2	—2	1	—1	0	0

TABLE IV Таблица 4

	E	T_3	$Q=-\{\delta\|0\}$	QT_3	$\widetilde{C}_3^1$ $T_3Q\widetilde{C}_3^2$	$T_3\widetilde{C}_3^2$ $Q\widetilde{C}_3^1$	$T_3\widetilde{C}_3^2$ $Q\widetilde{C}_3^1$	$\widetilde{C}_3^1$ $Q\widetilde{C}_3^2$	$U_2^{(1)}$ $T_3U_2^{(2)}$ $T_3U_2^{(3)}$	$QU_2^{(1)}$ $QT_3U_2^{(2)}$ $QT_3U_2^{(3)}$	$T_3U_2^{(1)}$ $U_2^{(2)}$ $U_2^{(3)}$	$QT_3U_2^{(1)}$ $T_3U_2^{(2)}$ $T_3U_2^{(3)}$
A_1'	1	—1	—1	1	1	1	—1	—1	i	$-i$	$-i$	i
A_2'	1	—1	—1	1	1	1	—1	—1	$-i$	i	i	$-i$
A_3'	2	—2	—2	2	—1	—1	1	1	0	0	0	0

But the relations (21) are insufficient for the construction of the complete multiplication table of the elements, which is necessary for the determination of the characters. In the Appendix it is shown that it suffices to know any two non-trivial multiplication rules, whereupon all the others can be found. Using the relation (18) and the law of multiplication of the elements, we can divide the elements into classes and use the theorem (19) to find the characters. In this connection it must be noted that our operators have the same action on the coordinates as before, although they act differently on the spinors (*cf.* Appendix). By these considerations we get Table 4. For the points H the results are similar to those obtained previously.

6. GENERAL PROPERTIES OF THE ZONE STRUCTURE

Using the results that have been obtained, we consider the problem of contacts between the zones. What happens with the two-dimensional representation Γ_3 if we place ourselves at the point Λ? Using the table of characters for the groups of these wave vectors, we reduce Γ_3 into irreducible representations of the group of Λ (*i.e.*, we reduce the representation E of the group D_3 in terms of representations of the group C_3).[3] We have:

$$\Gamma_3 = \Lambda_2 + \Lambda_3. \tag{22}$$

Since Λ_1 and Λ_2 are complex conjugate representations, they belong to a large number of pairs of complex conjugate functions. But because of the symmetry with respect to time inversion[11, 14] any pair of complex conjugate functions belongs to a single energy level, *i.e.*, in the absence of a magnetic field we will have contacts of the zones along the entire z axis in the k space. This conclusion is also valid for points of the type P. Along all other directions in the k space the degeneracy is removed, and there is no contact of zones (apart from the possibility of an accidental degeneracy). If we take into account the spin-orbit interaction, these results are somewhat changed. As is well known,[15] the operator for the spin-orbit interaction has the form:

$$(\hbar / 4m^2c^2)\,[\nabla U(\mathbf{r})\,\hat{p}]\,\hat{\sigma}. \tag{23}$$

In the case of degeneracy we seek the ψ-function in the form:

$$u = a_1u_1S_{1/2} + a_2u_1S_{-1/2} + a_3u_2S_{1/2} + a_4u_2S_{-1/2}, \tag{24}$$

where u will transform according to the representation $A \times D_{1/2}$, if u_1 and u_2 transform according to the representation A and the "free" spinor $(S_{1/2}, S_{-1/2})$ according to $D_{1/2}$. To find out whether the degeneracy is removed, we must reduce $A \times D_{1/2}$ into irreducible double-valued representations of the symmetry group of the given Hamiltonian. The characters for $D_{1/2}$ can be found by taking the traces of the matrices $\begin{vmatrix} \alpha & \beta \\ \gamma & \delta \end{vmatrix}$, which give the transformations of the "free" spinors.[11] We have

$$\hat{\rho}_3^1 = \begin{vmatrix} e^{i\pi/3} & 0 \\ 0 & e^{i\pi/3} \end{vmatrix}; \quad \hat{\rho}_2^{(1)} = \begin{vmatrix} 0 & i \\ i & 0 \end{vmatrix} \quad etc. \tag{25}$$

i.e., $\chi(\hat{\rho}_3^1) = 1, \ \chi(\hat{\rho}_3^2) = -1, \ \chi(\hat{\rho}_2^{(i)}) = 0.$

After some simple algebraic transformations, we get:

$$\begin{aligned} \Gamma_3 \times D_{1/2} &= \Gamma_1' + \Gamma_2' + \Gamma_3'; \\ K_3 \times D_{1/2} &= K_1' + K_2' + K_3', \\ A_3 \times D_{1/2} &= A_1' + A_2' + A_3'; \\ H_3 \times D_{1/2} &= H_1' + H_2' + H_3'. \end{aligned} \tag{26}$$

We recall that Γ_3 and K_3 are identical to E in the group D_3, and Γ_3' and K_3' are identical to E_2' in the group D_3'; Γ_1' and Γ_2', K_1' and K_2' are identical with E' in the group D_3' (*cf.* Ref. 11).

Since in all of the equations (26) the two first primed double-valued representations are complex conjugates, they can be combined into one. Thus, at the points Γ, A, K, H the two-fold degeneracy is removed. Furthermore,

$$\Lambda_2 \times D_{1/2} = \Lambda_1' + \Lambda_3' \text{ and } \Lambda_3 \times D_{1/2} = \Lambda_1' + \Lambda_2'. \tag{27}$$

Here Λ_2' and Λ_3' are conjugates, arose from a single level, and therefore can be united in a single representation of doubled dimensionality (in virtue of the symmetry of the spinors with respect to time reversal[16, 17]). Thus in this case also the two-fold degeneracy is removed.

Thus, if we neglect the spin-orbit interaction, among the infinite set of zones there are pairs of zones that are in contact with each other along the directions in the k space that have been indicated above. Although one cannot draw a unique conclusion as to whether contact occurs between the two last valence p zones in tellurium, there is such a possibility. According to Callen, these p zones are in general contact along all directions in the k space, which excludes the possibility of the presence of two kinds of holes in tellurium. From the above considerations it follows that the contact occurs only along certain directions in the **k** space, and then the dispersion law $E(\mathbf{k})$ can be different in the two p zones, *i.e.*, the effective masses of the carriers in these zones can be different. A choice between the existing possibilities can be made either by comparison with experiment, or else by resorting to Callen's idea about the origin of the zones in tellurium,[4] assuming that his arguments provide evidence in favor of overlapping of the p zones (but not their complete contact). If in zeroth approximation the edges of the valence zones coincide, then they have their extrema in common, and they necessarily lie on the lines of contact or near them. As we have seen, the spin-orbit interaction removes the degeneracy, and the lower edges of the zones do not coincide, *i.e.*, as the temperature rises there will be an increase of the relative number of those current carriers that are in the state corresponding to the energetically higher zone. If the holes in the lower zone have different effective masses from those in the upper zone, then at low temperatures these holes alone will play an effective part in processes; but at higher temperatures, when the numbers of carriers of the two kinds is approximately the same, the course of a process can be mainly determined by the properties of the other holes. Just such properties in tellurium are proposed by Shalyt for one of the possible explanations of his experiments.[3]

The results are valid for arbitrary values of the wave vector **k** [we agree to reckon **k** from the point of the extremum for $E(\mathbf{k})$]. To be more specific, let us obtain in analytic form the dispersion law $E(\mathbf{k})$ in the approximation quadratic in **k**, for various particular assumptions about the locations of the extrema.

7. THE DISPERSION LAW FOR LOCATION OF THE EXTREMA AT THE POINTS Γ, *A*, *K*, *H*

We assume that an extremum occurs at one of these points. For the non-degenerate case (representations of types A_1 and A_2 in the notation of Ref. 11) the dispersion law has the form:[2]

$$E = D_{jj}^{\alpha\beta} k^\alpha k^\beta, \tag{28}$$

where
$$D_{jj}^{\alpha\beta} = \frac{\hbar^2}{2m}\delta_{\alpha\beta} + \frac{\hbar^2}{m^2}\sum_i \frac{p_{ji}^\alpha p_{ij}^\beta}{E_j(\mathbf{k}_0) - E_i(\mathbf{k}_0)},$$
$$p_{ji}^\alpha = -i\hbar \int u_{j,\mathbf{k}_0} \frac{\partial}{\partial_\alpha} u_{i,\mathbf{k}_0}\, d\tau,$$

and $\mathbf{k}_0$ is the point around which the resolution is carried out. This is the equation of an ellipsoid. It is not hard to see that this will be an ellipsoid of revolution around the z axis, because from the symmetry properties of the spectrum it follows that $E(\mathbf{k}) = E(\mathbf{k}')$ if $\mathbf{k}' = \hat{\rho}_i^1\mathbf{k}$. For the point Γ this will be a single ellipsoid (Fig. 3, *a*); for the points *A*, *K*, *H* the pictures are more peculiar, and are shown in Fig. 3, *b*, *c*, *d*.

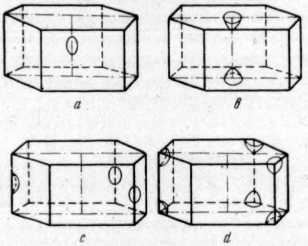

FIG. 3.

Of more interest is the case of two-fold degenerate states (representations of type E in the notation of Ref. 11), for which the dispersion law is determined by the equation:[2]

$$\begin{vmatrix} D_{11}^{\alpha\beta}k^\alpha k^\beta - E & D_{12}^{\alpha\beta}k^\alpha k^\beta \\ D_{21}^{\alpha\beta}k^\alpha k^\beta & D_{22}^{\alpha\beta}k^\alpha k^\beta - E \end{vmatrix} = 0. \tag{29}$$

The coefficients D are determined in a way similar to that shown in Eq. (28). All told there are 24 unknown coefficients. We can reduce this number, knowing the law of transformation of u_1 and u_2 under the action of the symmetry operators. Obviously:

$$\widetilde{C}_3^1 u_1 = (\widetilde{C}_3^1)_{11}u_1 + (\widetilde{C}_3^1)_{12}u_2;$$
$$\widetilde{C}_3^1 u_2 = (\widetilde{C}_3^1)_{21}u_1 + (\widetilde{C}_3^1)_{22}u_2$$

and similarly for the operators $\widetilde{C}_3^2$, $U_2^{(1)}$, $U_2^{(2)}$, $U_2^{(3)}$. We must find the two-rowed matrices corresponding to these operators in the representation of the Bloch oscillating factors u_1 and u_2. For this it suffices to use the operator multiplication law obtained in the coordinate representation, but valid in any representation, and the orthogonality rules for matrix elements[11]

$$\sum_G G_{ik}^\alpha (G_{lm}^\beta)^* = (p/f_\alpha)\,\delta_{\alpha\beta}\delta_{il}\delta_{km}. \tag{30}$$

Here α and β are indices labelling irreducible representations, f_α is the dimensionality of representation α, *p* is the number of elements in the group, and G^{α}_{jk} are the elements of the matrix corresponding to the element *G* in the representation α. In this way one can show that u_1 and u_2 transform like *x* and *y* under the action of the operators of the group D_3 in the case in which the first 2nd order axis makes the angle φ with the *x* axis, *i.e.*,

$$E=\begin{vmatrix}1&0\\0&1\end{vmatrix};\quad \widetilde{C}_3^1=\begin{vmatrix}1/2&\sqrt{3}/2\\-\sqrt{3}/2&1/2\end{vmatrix};$$

$$U_2^{(1)}=\begin{vmatrix}\cos 2\varphi&\sin 2\varphi\\-\sin 2\varphi&\cos 2\varphi\end{vmatrix}\ \ etc. \tag{31}$$

Using the law of transformation of the functions under the action of the operators of the group D_3, one can verify that:

$$p^z_{1a}=p^z_{2a}=p^z_{1b}=p^z_{2b}=0;$$

$$p^y_{1a}=p^y_{2a}=p^x_{1b}=p^y_{2b}=0;$$

$$p^z_{11'}=p^z_{22'}=0;\quad p^x_{12'}=p^x_{21'}=p^y_{11'}=p^y_{22'}=0;$$

$$p^x_{1a}=p^y_{2a};\quad p^x_{2b}=-p^x_{1b};\quad p^z_{12'}=-p^z_{21'}; \tag{32}$$

$$p^x_{11'}=-p^x_{22'}=-p^y_{12'}=-p^y_{21'}.$$

Here the index *a* labels functions transforming according to the representation A_1, the index *b* those belonging to the representation A_2; the indices 1 and 1′, 2 and 2′, and also *l* and *l*′ label functions transforming by various two-rowed representations *E*. We get the dispersion law in the form:

$$\begin{vmatrix}-A_1k_x^2-Ak_yk_z+A_3k_z^2+A_2(k_x^2+k_y^2)-E & -A_1k_xk_y-Ak_xk_z\\ -A_1k_xk_y-Ak_xk_z & -A_1k_y^2+Ak_yk_z+A_3k_z^2+A_2(k_x^2+k_y^2)-E\end{vmatrix}=0;$$

$$A_1=\frac{\hbar^2}{m^2}\sum_a\frac{|p^x_{1a}|^2}{E_a-E}-\frac{\hbar^2}{m^2}\sum_b\frac{|p^y_{1b}|^2}{E_b-E};\quad A_3=\frac{\hbar^2}{2m}-\frac{\hbar^2}{m^2}\sum_l\frac{|p^z_{12'}|^2}{E_l-E};$$

$$A_2=\frac{\hbar^2}{2m}-\frac{\hbar^2}{m^2}\sum_l\frac{|p^x_{11'}|}{E_l-E}-\frac{\hbar^2}{m^2}\sum_b\frac{|p^y_{1b}|^2}{E_b-E}; \tag{33}$$

$$A=\frac{\hbar^2}{m^2}\sum_l\frac{p^y_{12'}p^z_{2'1}+p^z_{12'}p^y_{2'1}}{E_l-E}.$$

Solving the quadratic equation for *E*, we get:

$$E=A_3k_z^2+\left(A_2-\frac{A_1}{2}\right)(k_x^2+k_y^2)\pm\left[\frac{A_1^2}{4}(k_x^2+k_y^2)^2+A^2k_z^2(k_x^2+k_y)-AA_1(k_y^2-3k_x^2)k_yk_z\right]^{1/2}. \tag{34}$$

It is not hard to see that the radicand is equal to

$$\left|\frac{A_1}{2}(k_x+ik_y)^2+iAk_z(k_x-ik_y)\right|^2,$$

i.e., it is always positive, and consequently *E* is real.

In addition the solution is invariant with respect to $\hat{\rho}_2^{(1)}$, since the action of this operator reduces to the replacements $k_y\to -k_y$, $k_z\to -k_z$, and with respect to $\hat{\rho}_3^1$, since this results in multiplying k_x+ik_y by $\omega=e^{i2\pi/3}$ and k_x-ik_y by $\omega^2=e^{i4\pi/3}$. Thus our spectrum satisfies the needed requirements of symmetry and reality. Keeping in mind that

$$k_x=k\sin\vartheta\cos\varphi,\quad k_y=k\sin\vartheta\sin\varphi,$$

$$k_z=k\cos\vartheta,$$

we rewrite Eq. 34 in the form:

$$E=k^2\left\{A_3\cos^2\vartheta+\left(A_2-\frac{A_1}{2}\right)\sin^2\vartheta\pm\right.$$

$$\pm\left[\sin^2\vartheta\left(\frac{A_1^2}{4}\sin^2\vartheta+A^2\cos^2\vartheta\right.\right.$$

$$\left.\left.\left.-A_1A\sin\vartheta\cos\vartheta\cos 3\varphi\right)\right]^{1/2}\right\}. \tag{35}$$

Let us investigate the place of contact of the zones for the case in which the radicand vanishes.

First case:

$$\sin^2\vartheta = 0,$$

i.e., there will be contact of the zones along the z axis, as follows from our earlier general arguments.

Second case:

$$\frac{A_1^2}{4}\sin^2\vartheta + A^2\cos^2\vartheta - AA_1\sin\vartheta\cos\vartheta\cos 3\varphi = 0.$$

For $\vartheta \neq \pi/2$ we get:

$$\tan^2\vartheta = 2\frac{A}{A_1}[\cos 3\varphi \pm (\cos^2 3\varphi - 1)^{1/2}]. \qquad (36)$$

For contact of the zones it is necessary that the solution (36) be real, *i.e.*, $\cos 3\varphi = \pm 1$. Consequently, the solutions (36) will be:

$$\varphi_{\text{extr}} = 0, \quad 2\pi/3, \quad 4\pi/3; \quad \tan(\vartheta_{\text{extr}}) = 2A/A_1,$$

$$\varphi_{\text{extr}} = \pi/3, \quad \pi, \quad 5\pi/3; \quad \tan(\vartheta_{\text{extr}}) = -2A/A_1. \qquad (37)$$

Along these directions an additional contact of the zones will occur. This is an accidental degeneracy occurring only in the approximation quadratic in **k**. Let us denote the angle-dependent factor in Eq. (35) by $m^{\pm}(\vartheta, \varphi)$ (the signs ± correspond to the sign of the root). According to Eq. (35) we have two kinds of carriers of the same sign, with masses m^+ and m^- which are already not tensor quantities. A change of sign of m^+ or m^- for certain values of ϑ φ would mean that we obtained a resolution near a point of inflection, which in the present work is in general of no interest. Therefore we shall assume that the parameters A, A_1, A_2, A_3 are such that this case does not occur. For the points A, K, H we get exactly similar results, with the single exception that at these points there will appear a characteristic pattern of repetition, analogous to the situation shown for nondegenerate states in Fig. 3, *a–d*.

8. THE DISPERSION LAW FOR EXTREMA AT THE POINTS Λ, P

It was shown in Sec. 4 that in this case the group of the wave vector isiisomorphic to C_3. Then:

$$\overset{*}{u}_1 = u_2; \quad \widetilde{C}_3^1 u_1 = \omega u_1; \quad \widetilde{C}_3^1 u_2 = \omega^2 u_2.$$

For these points

$$\int \overset{*}{u}_j (\partial/\partial x \pm i\partial/\partial y)\, u_j d\tau = 0,$$

because $u_j u_j^*$ is invariant with respect to C_3^1 and $(\partial/\partial x \pm i\partial/\partial y)$ is multiplied by ω or ω^2. In a similar way we get:

$$\int \overset{*}{u}_1 (\partial/\partial x + i\partial/\partial y)\, u_{2'}\, d\tau$$

$$= \int \overset{*}{u}_2 (\partial/\partial x - i\partial/\partial y)\, u_{1'}\, d\tau = 0.$$

Proceeding in the same way, one can verify that

$$\begin{gathered} p^x_{11'} = p^y_{11'} = p^x_{22'} = p^y_{22'} = p^z_{12'} = p^z_{2'1} = 0; \quad p^z_{1a} = p^z_{2a} = 0; \\ p^x_{21'} = ip^y_{21'}; \quad p^x_{12'} = -ip^y_{12'}; \quad p^x_{1a} = ip^y_{1a}; \quad p^x_{2a} = -ip^y_{2a}; \quad p^z_{11'} = -(p^z_{22'})^*. \end{gathered} \qquad (38)$$

Here the index a is affixed to functions that transform according to the representation Λ_1 (*i.e.*, for which the operation C_3^1 amounts to a factor ω). By a procedure like that of Sec. 1, we get the dispersion equation:

$$\begin{vmatrix} A(k_x^2 + k_y^2) + Bk_z^2 - E & A_{12}(k_x + ik_y)^2 + B_{12}k_z(k_x - ik_y) \\ A_{12}(k_x - ik_y)^2 + \overset{*}{B}_{12}(k_z + ik_y) & A(k_x^2 + k_y^2) + Bk_z^2 - E \end{vmatrix} = 0, \qquad (39)$$

where

$$A = \frac{\hbar^2}{2m} - \frac{\hbar^2}{m^2}\sum_a \frac{|p^x_{1a}|^2}{E_a - E} - \frac{\hbar^2}{m^2}\sum_j \frac{|p^x_{12'}|^2}{E_j - E}; \quad A_{12} = \frac{\hbar^2}{m^2}\sum_a \frac{|p^x_{1a}|^2}{E_a - E};$$

$$B = \frac{\hbar^2}{2m} - \frac{\hbar^2}{m^2}\sum_j \frac{|p^z_{11'}|^2}{E_j - E};$$

$$B_{12} = -\frac{\hbar^2}{m^2}\sum_j \frac{p^x_{12'}\, p^z_{2'2} + p^x_{1'2}\, p^z_{11'}}{E_j - E} = B'_{12} + iB''_{12}.$$

In the problem of the contact of zones we get analogous results, the only difference being that now

$$\tan(\vartheta_{\mathrm{extr}}) = -|B_{12}|/A_{12},$$

$$\cos 3\varphi_{\mathrm{extr}} = \pm B''_{12}/|B_{12}|.$$

The dispersion law depends on five parameters and has the form:

$$E = Bk_z^2 + A(k_x^2 + k_y^2) \pm [A_{12}^2(k_x^2 + k_y^2)^2 + |B_{12}|^2 k_z^2 (k_x^2 + k_y^2) + 2\,\mathrm{Re}\,(A_{12}B_{12}^* k_z (k_x + ik_y)^3)]^{1/2}. \tag{40}$$

9. THE SPIN-ORBIT INTERACTION

The Schrödinger equation for an "excess" electron in the crystal, including relativistic effects, if we neglect the displacement of the entire spectrum by amounts of the order of $(v/c)^2$ times the separation between zones, has the form:

$$\left\{H_{\mathbf{k}} + \frac{\hbar^2}{4m^2c^2}[\nabla U(\mathbf{r})\,\mathbf{k}]\,\hat{\sigma} + \frac{\hbar}{4m^2c^2}[\nabla U(\mathbf{r})\,\hat{p}]\,\hat{\sigma}\right\} u_{n\mathbf{k}}(\mathbf{r}) = E_n(\mathbf{k})\, u_{n\mathbf{k}}(\mathbf{r}). \tag{41}$$

We introduce the spin functions $S_{1/2} = \begin{pmatrix}1\\0\end{pmatrix}$ and $S_{-1/2} = \begin{pmatrix}0\\1\end{pmatrix}$; then:

$$\begin{aligned}
[\nabla U\mathbf{k}]\,\hat{\sigma}S_{1/2} &= S_{1/2}\left(\frac{\partial U}{\partial x}k_y - \frac{\partial U}{\partial y}k_x\right) + S_{-1/2}\left[-ik_z\left(\frac{\partial U}{\partial x} + i\frac{\partial U}{\partial y}\right) + i\frac{\partial U}{\partial z}(k_x + ik_y)\right],\\
[\nabla U\mathbf{k}]\,\hat{\sigma}S_{-1/2} &= -S_{-1/2}\left(\frac{\partial U}{\partial x}k_y - \frac{\partial U}{\partial y}k_x\right) + S_{1/2}\left[ikz\left(\frac{\partial U}{\partial x} - i\frac{\partial U}{\partial y}\right) - i\frac{\partial U}{\partial z}(k_x - ik_y)\right].
\end{aligned} \tag{42}$$

The action of $[\nabla U\hat{p}]\hat{\sigma}$ is similar, but k_i must be replaced by $-i\hbar\partial/\partial x_i = \hat{p}_i$.

In order that there be an extremum at the point $\mathbf{k}_0$, we must have:

$$\int u_j^* \nabla u_{j'} d\tau = 0, \quad (s', j'|[\nabla U\mathbf{k}]\,\hat{\sigma}|s, j) = 0. \tag{43}$$

The second of the conditions (43) is automatically fulfilled in crystals with a center of inversion.[13] In our case it is not fulfilled. This means that the extremum is displaced from the point $\mathbf{k}_0$. For degenerate states we shall seek the function in the form:

$$u = a_1u_1S_{1/2} + a_2u_2S_{1/2} + a_3u_1S_{-1/2} + a_4u_2S_{-1/2}. \tag{44}$$

A. *The points* Γ, *A*, *K*, *H*.

A consideration of the selection rules of the matrix elements of the operators $[\nabla U\mathbf{k}]\hat{\sigma}$ and $[\nabla U\hat{p}]\hat{\sigma}$ for the two-rowed representations of the points Γ, *A*, *K*, *H* enables us to obtain the dispersion law in the form of the vanishing of the determinant

$$\begin{gathered}
\|\alpha_{ik}\| = 0;\\
\alpha_{11} = -A_1k_x^2 - Ak_yk_z + \gamma k_y - E'; \qquad \alpha_{12} = -A_1k_xk_y - Ak_xk_z - \gamma k_x + i\varkappa,\\
\alpha_{13} = i\gamma k_z; \quad \alpha_{14} = -\gamma k_z; \quad \alpha_{21} = -A_1k_xk_y - Ak_xk_z - \gamma k_x - i\varkappa,\\
\alpha_{22} = -A_1k_y^2 + Ak_zk_y - \gamma k_y - E', \quad \alpha_{23} = -\gamma k_z, \quad \alpha_{24} = -i\gamma k_z;\\
\alpha_{31} = -i\gamma k_z, \quad \alpha_{32} = -\gamma k_z, \quad \alpha_{33} = -A_1k_x^2 - Ak_yk_z - \gamma k_y - E', \quad (45)\\
\alpha_{34} = -A_1k_xk_y - Ak_xk_z - \gamma k_x - i\varkappa; \quad \alpha_{41} = -\gamma k_z, \quad \alpha_{42} = i\gamma k_z,\\
\alpha_{43} = -A_1k_yk_x - Ak_xk_z - \gamma k_x + i\varkappa, \quad \alpha_{44} = -A_1k_y^2 + Ak_yk_z + \gamma k_y - E'.
\end{gathered} \tag{45}$$

Here

$$i\varkappa = \frac{\hbar}{4m^2c^2}\int u_1^*\left(\frac{\partial U}{\partial y}\hat{p}_x - \frac{\partial U}{\partial x}\hat{p}_y\right)u_2 d\tau;$$

$$\gamma = \frac{\hbar^2}{4m^2c^2}\int u_1^* \frac{\partial U}{\partial x} u_1 d\tau.$$

For $\mathbf{k} = 0$ the determinant breaks up into two:

$$\begin{vmatrix} E & -i\varkappa \\ i\varkappa & E \end{vmatrix} = 0, \qquad \begin{vmatrix} E & i\varkappa \\ -i\varkappa & E \end{vmatrix} = 0, \tag{46}$$

i.e., at the point $\mathbf{k} = 0$, $E = \pm|\varkappa|$ and there is a splitting; therefore we can rewrite Eq. (45), using as basis functions those that satisfy Eq. (46):

for $E = -|\varkappa|$

$$u'_{\mathrm{I}} = 2^{-1/2}(u_1 + iu_2)S_{1/2}; \quad u''_{\mathrm{I}} = 2^{-1/2}(u_1 - iu_2)S_{-1/2},$$

for $E = |\varkappa|$

$$u'_{11} = 2^{-1/2}(u_1 - iu_2) S_{1/2};\; u''_{11} = 2^{-1/2}(u_1 + iu_2) S_{-1/2}.$$

This corresponds to a canonical transformation by means of the operator $\hat{A}$:

$$\hat{A} = \begin{vmatrix} 1 & i & 0 & 0 \\ 0 & 0 & 1 & -i \\ 1 & -i & 0 & 0 \\ 0 & 0 & 1 & i \end{vmatrix} \tag{47}$$

Transforming the determinant (45) and expanding it, we get the equation:

$$(E'^2 - \varkappa^2 - |d|^2)^2 = 4k_z^2\gamma^2 [(E' - |\varkappa|)^2 + A^2 (k_x^2 + k_y^2)^2], \tag{48}$$

where

$$|d|^2 = \frac{A_1^2}{4} (k_x^2 + k_y^2)^2 + (A^2k_z^2 + \gamma^2)(k_x^2 + k_y^2) - AA_1 (k_y^2 - 3k_x^2) k_y k_z,$$
$$E' = E - A_3k_z^2 - \left(A_2 - \frac{A_1}{2}\right)(k_x^2 + k_y^2). \tag{49}$$

First case:

For $A_ik^2 \gg \gamma k$, $A_ik^2 \gg |\varkappa|$ we get $E' = \pm |d|$, which is the same as Eq. (34).

Second case:

If $\gamma k \ll |\varkappa|$, $A_ik^2 \ll |\varkappa|$, where A_i is the largest of the parameters, then for $k_z \sim \gamma/A_i$ we have: $A_ik^2 \sim \gamma^2/A_i$, *i.e.*, the terms γk and $A_i k^2$ are of the same order of smallness. But $\gamma^2/A_i \ll |\varkappa|$, *i.e.*, the off-diagonal terms in the determinant are small in comparison with $2|\varkappa|$, and therefore we can neglect them and solve the two 2nd order determinants

$$\begin{vmatrix} -|\varkappa| - E' & 2ik_z\gamma \\ -2ik_z\gamma & -|\varkappa| - E' \end{vmatrix} = 0,$$
$$\begin{vmatrix} |\varkappa| - E' & 0 \\ 0 & |\varkappa| - E' \end{vmatrix} = 0. \tag{50}$$

independently. As the equipotential surfaces we have two ellipsoids of revolution, with their centers displaced along the k_z axis by $4\gamma/A_3$:

$$E_{1,2} = |\varkappa| - 2\gamma^2 / A_3 + (A_2 - A_1/2)(k_x^2 + k_y^2) + A_3 (k_z \pm \gamma / A_3)^2. \tag{51}$$

Thus, in agreement with the general conclusions of Sec. 6, the effective masses of the carriers at low temperatures are different from their values for high temperatures. The points *A*, *H*, *K* differ in showing a characteristic repetition pattern, analogous to the situation shown in Fig. 3, *a–d*. For nondegenerate states of type A_1 or type A_2 (Ref. 11) we have not obtained any significant results, because in this case all the matrix elements of the spin-orbit interaction operator are zero.

B. Points of Types Λ and P

By a similar argument we get the secular equation

$$\begin{gathered} \|\beta_{ik}\| = 0; \\ \beta_{11} = \varkappa - E', \quad \beta_{12} = ik_z\delta, \quad \beta_{13} = i\gamma (k_x - - ik_y), \\ \beta_{14} = A_{12} (k_x + ik_y)^2 + B_{12}k_z (k_x - ik_y) + i\delta (k_x - ik_y), \\ \beta_{21} = - ik_z\delta_{14}, \quad \beta_{22} = \varkappa - E', \quad \beta_{24} = i\gamma (k_x + ik_y), \\ \beta_{23} = A_{12}^* (k_x - ik_y)^2 + B_{12}^* k_z (k_x + ik_y) + i\delta^* (k_x + ik_y), \\ \beta_{31} = i\gamma (k_x + ik_y), \quad \beta_{33} = - \varkappa - E', \quad \beta_{34} = 0, \\ \beta_{32} = A_{12} (k_x + ik_y)^2 + B_{12}k_z (k_x - ik_y) - i\delta (k_x - ik_y), \\ \beta_{41} = A_{12}^* (k_x - ik_y)^2 + B_{12}^* k_z (k_x + ik_y) - i\delta^* (k_x + ik_y), \\ \beta_{42} = - i\gamma (k_x - ik_y), \quad \beta_{43} = 0, \quad \beta_{44} = - \varkappa - E'. \end{gathered} \tag{52}$$

Here

$$E' = E - Bk_z^2 + A (k_x^2 + k_y^2); \quad \varkappa = \frac{\hbar}{4m^2c^2} \int u_1^* \left(\frac{\partial U}{\partial x} \hat{p}_y - \frac{\partial U}{\partial y} \hat{p}_x \right) u_1 d\tau;$$
$$\delta = \frac{\hbar^2}{4m^2c^2} \int u_1^* \left(\frac{\partial U}{\partial x} - i \frac{\partial U}{\partial y} \right) u_2 d\tau; \quad \gamma = \frac{\hbar^2}{4m^2c^2} \int u_1^* u_1 \frac{\partial U}{\partial z} d\tau.$$

For $E \gg |\varkappa|$ we get the results already known from Sec. 2. For the opposite case $E \ll |\varkappa|$ we can solve independently two 2nd-order determinants; *i.e.*, we get

$$E_1 = |\varkappa| - \frac{|\delta|^2}{B} + A(k_x^2 + k_y^2) + B\left(k_z \pm \frac{|\delta|}{B}\right)^2;$$
$$E_2 = -|\varkappa| + A(k_x^2 + k_y^2) + Bk_z^2. \qquad (53)$$

(We note that γ and $\varkappa$ are real, and δ is an imaginary quantity.)

The interpretation of the results goes just as in case *A*. For the one-dimensional representations of type Λ_1 the inclusion of the spin-orbit interaction does not lead to any new results, since all the matrix elements are zero.

C. Other Cases of Location of the Extrema

For all points other than Γ, *A*, *K*, *H*, Λ, *P* there exist only one-dimensional representations, *i.e.*, at such points the zones are not in contact, and thus the dispersion law has the form (28), *i.e.*, the equipotential surfaces will be ellipsoids. A special feature is that because of the symmetry of the spectrum with respect to D_3 in the **k** space the number of extremal points is increased by multiplication and can be as large as six (if they do not lie on any symmetry element). For points of type *T* there will be three ellipsoids of revolution; for points *S* there will be repetition like that shown in Fig. 3, *a–d*. For points of type Σ we have six ellipsoids of revolution, etc.

CONCLUSION

In presenting our results we would like to remark that on the basis of the experimental data existing at present, according to which the effective masses of the holes are different for high and low temperatures, one can draw the conclusion that for hole-type tellurium the case of zones in contact is realized and the extrema are located at some or other of the points Γ, *A*, *H*, *K*, Λ, *P*. This same case is also obviously realized for electron-type tellurium.[5] The results found are valid for arbitrary lattices with space groups D_3^{4-7}, *i.e.*, also for selenium. The whole question comes down to just where the extrema are located, and whether the last valence zones are in contact. The positions of the extrema can be found either by numerical calculations, which despite all their elaborateness cannot at present pretend to great accuracy, or by comparison with experiment of the conclusions that follow from the various possible forms of the spectrum. The latter approach appears the more promising, and in this way the writer has been able to obtain expressions for the magnetic susceptibility coefficient[19] and for the cyclotron resonance frequency.

In conclusion the writer considers it his duty to thank Prof. A. I. Ansel'm for a discussion of the results and for his constant interest in the work.

APPENDIX

For the ordinary point groups we have:

$$\hat\rho_3^1\,\hat\rho_2^{(1)} = \hat\rho_2^{(3)}, \quad \hat\rho_3^1\,\hat\rho_2^{(2)} = \hat\rho_2^{(1)}.$$

From geometrical considerations it is clear that these rules must be satisfied with accuracy up to a multiplication by δ, so that we must have one of the four possibilities

$$\hat\rho_3^1\,\hat\rho_2^{(1)} = \delta\hat\rho_2^{(3)}, \quad \hat\rho_3^1\,\hat\rho_2^{(2)} = \delta\hat\rho_2^{(1)}, \qquad \text{(I)}$$
$$\hat\rho_3^1\,\hat\rho_2^{(1)} = \delta\hat\rho_2^{(3)}, \quad \hat\rho_3^1\,\hat\rho_2^{(2)} = \hat\rho_2^{(1)}, \qquad \text{(II)}$$
$$\hat\rho_3^1\,\hat\rho_2^{(1)} = \hat\rho_2^{(3)}, \quad \hat\rho_3^1\,\hat\rho_2^{(2)} = \delta\hat\rho_2^{(1)}, \qquad \text{(III)}$$
$$\hat\rho_3^1\,\hat\rho_2^{(1)} = \hat\rho_2^{(3)}, \quad \hat\rho_3^1\,\hat\rho_2^{(2)} = \hat\rho_2^{(1)}. \qquad \text{(IV)}$$

For case I: $\hat\rho_3^1 = \hat\rho_2^{(3)}\hat\rho_2^{(1)} = \hat\rho_2^{(1)}\hat\rho_2^{(2)}$, or, multiplying Eq. (I) by $\delta\hat\rho_3^1$ on the left, we get:

$$\hat\rho_3^1\,\hat\rho_2^{(3)} = (\hat\rho_3^1)^{-1}\hat\rho_2^{(1)}, \quad \textit{i.e.}, \quad (\hat\rho_2^{(1)}\hat\rho_2^{(2)})^{-1}\cdot\hat\rho_2^{(1)} = \delta\hat\rho_2^{(2)}.$$

Thus we have:

$$\hat\rho_3^1\,\hat\rho_2^{(3)} = \delta\hat\rho_2^{(2)}. \qquad (1)$$

Taking the reciprocals of (I) and (1), we have:

$$\hat\rho_2^1\,\hat\rho_3^2 = \hat\rho_2^{(3)}; \quad \hat\rho_2^{(2)}\hat\rho_3^2 = \hat\rho_2^{(1)}; \quad \hat\rho_2^{(3)}\,\hat\rho_3^2 = \hat\rho_2^{(2)}. \qquad (2)$$

Multiplying Eq. (2) by $\hat\rho_3^1$ on the right, we get:

$$\hat\rho_2^{(3)}\hat\rho_3^1 = \delta\hat\rho_2^{(1)}; \quad \hat\rho_2^{(1)}\hat\rho_3^1 = \delta\hat\rho_2^{(2)}; \quad \hat\rho_2^{(2)}\hat\rho_3^1 = \delta\hat\rho_2^{(3)}. \qquad (3)$$

Taking the reciprocals of (3), we have:

$$\hat\rho_3^2\,\hat\rho_2^{(3)} = \hat\rho_2^{(1)}; \quad \hat\rho_3^2\,\hat\rho_2^{(1)} = \hat\rho_2^{(2)}; \quad \hat\rho_3^2\,\hat\rho_2^{(2)} = \hat\rho_2^{(3)}. \qquad (4)$$

Multiplying Eqs. (I) and (1) on the right by $\hat\rho_2^{(1)}$, $\hat\rho_2^{(2)}$, $\hat\rho_2^{(3)}$ respectively, we get:

$$\hat\rho_2^{(3)}\hat\rho_2^{(1)} = \hat\rho_3^1; \quad \hat\rho_2^{(1)}\hat\rho_2^{(2)} = \hat\rho_3^1; \quad \hat\rho_2^{(2)}\hat\rho_2^{(3)} = \hat\rho_3^1. \qquad (5)$$

Taking the reciprocals of (5), we see that:

$$\hat\rho_2^{(1)}\hat\rho_2^{(3)} = \delta\hat\rho_3^2; \quad \hat\rho_2^{(2)}\hat\rho_2^{(1)} = \delta\hat\rho_3^2; \quad \hat\rho_2^{(3)}\hat\rho_2^{(2)} = \delta\hat\rho_3^2. \qquad (6)$$

It is not hard to verify that with these rules of multiplication $\hat\rho_2^{(1-3)}$ go into one class, and $\delta\hat\rho_2^{(1-3)}$ into another class, and in addition $\hat\rho_3^1$ and $\delta\hat\rho_3^2$ form one class and $\delta\hat\rho_3^1$ and $\hat\rho_3^2$ another. For the cases (II) – (IV) this would not occur, and therefore they are not realized.

The fulfillment of the conditions mentioned above is necessary. In fact: $\delta\hat\rho_3^2$ and $\hat\rho_3^1$ must go into one class, since there is an element that changes the direction of the 3rd order screw axis into its opposite; $\hat\rho_2^{(j)}$ and $\delta\hat\rho_2^{(i)}$ cannot go into a single class, because there is no element in the group that takes one 2nd order axis over into the other and at the same time changes the direction of the axis into its opposite. It is well known that the elements $\{\hat\rho_l \mid \bar\tau_l\}$ and $\{\hat\rho_m \mid \bar\tau_m\}$ belong to one class, if there is an element $\{\hat\rho_k \mid \bar\tau_k\}$ such that the relation

$$\{\hat\rho_k \mid \bar\tau_k\} \cdot \{\hat\rho_l \mid \bar\tau_l\} = \{\hat\rho_m \mid \bar\tau_m\} \cdot \{\hat\rho_k \mid \bar\tau_k\}. \qquad (7)$$

holds.

Recalling that our operators act on the coordinates as before, we get the following limitations on $\bar\tau_m$ and $\bar\tau_l$:

$$\bar\tau_k + \bar\rho_k \bar\tau_l = \bar\tau_m + \hat\rho_m \bar\tau_k. \qquad (8)$$

Taking, for example, $\hat\rho_l = \hat\rho_3^1$, $\hat\rho_m = \delta\hat\rho_3^2$ and noting that the action of δ on $\bar\tau$ is equivalent to multiplication by a unit element and that these rotations are conjugate by the use of $\hat\rho_2^{(i)}$, we shall have: $\hat\rho_2^{(i)}\tau_l = \tau_m$, or $\tau_l = -\bar\tau_m$. Thus there go into one class the elements

$$\{\hat\rho_3^1 \mid \bar\tau_3/3\} \text{ and} \{\varepsilon \mid -\bar\tau_3\} \cdot \{\delta\hat\rho_3^2 \mid 2\bar\tau_3/3\},$$

and into the other class

$$\{\varepsilon \mid \bar\tau_3\} \cdot \{\hat\rho_3^1 \mid \tau_3/3\} \text{ and } \{\delta\hat\rho_3^2 \mid 2\bar\tau_3/3\}.$$

Carrying through a similar consideration, we get 12 classes. Knowing the multiplication law of the elements, we find that of the classes, and, using Ref. 19, we find the table of characters (Table 4).

---

[1] Dresselhaus, Kip, and Kittel, Phys. Rev. **98**, 368 (1955).

[2] J. M. Luttinger and W. Kohn, Phys. Rev. **97**, 869 (1955).

[3] S. S. Shalyt, Izv. Akad. Nauk SSSR, Ser. Fiz. (in press).

[4] H. Callen, J. Chem. Phys. **22**, 518 (1954).

[5] A. Nussbaum, Phys. Rev. **94**, 337 (1954).

[6] F. Seitz, Ann. of Math. **37**, 17 (1936).

[7] Bouckaert, Smoluchowski, and Wigner, Phys. Rev. **50**, 58 (1936).

[8] *Internationale Tabellen zur Bestimmung von Krystalstrukturen*, Erster Band, Berlin 1935.

[9] C. Herring, J. Franklin Inst. **233**, 525 (1942).

[10] R. J. Elliott, Phys. Rev. **96**, 266 (1954).

[11] L. Landau and E. Lifshitz, *Quantum Mechanics*, OGIZ, Moscow, 1948.

[12] A. Speiser, *Die Theorie der Gruppen von Endlicher Ordnung*, Berlin 1937.

[13] H. Bethe, Ann. d. Phys. **3**, 131 (1929).

[14] C. Herring, Phys. Rev. **52**, 361, 365 (1937).

[15] A. I. Akhiezer and V. B. Berestetskii, *Quantum Electrodynamics*, GITTL, Moscow 1953.

[16] E. Wigner, Göttinger Nachr. 1932, p. 546.

[17] H. Kramers, Proc. Acad. Sci. Amsterdam **33**, 952 (1930).

[18] R. Karplus and J. M. Luttinger, Phys. Rev. **95**, 1154 (1954).

[19] Iu. A. Firsov, J. Tech. Phys. (U.S.S.R.) (in press).

Translated by W. H. Furry
276

SOVIET PHYSICS JETP VOLUME 5, NUMBER 6 DECEMBER 15, 1957

Theory of Diffuse Scattering of X-Rays and Thermal Neutrons in Solid Solutions. II.

Microscopic Theory

M. A. KRIVOGLAZ

Institute of Metal Physics of the Academy of Sciences, Ukrainian SSR

(Submitted to JETP editor May 13, 1956)

J. Exptl. Theoret. Phys. (U.S.S.R.) 32, 1368-1381 (June, 1957)

Diffuse scattering of x-rays and thermal neutrons by composition and order fluctuations in solid solutions is considered. For disordered solutions and ordered solutions of *AB* stoichiometric composition the calculations have been carried out taking into account interaction between atoms lying in coordinative spheres separated by arbitrarily large distances. A method is indicated for the determination of the ordering energy for various coordinative spheres from the experimental distribution of the background intensity. Anomalously high diffuse scattering near points of phase transition of the second order and near critical points on the decay curve is considered.

TWO TYPES OF APPROACH are possible in the investigation of scattering of x-rays and of slow neutrons by solid solutions. Usually in calculating the intensity of scattered radiation the interference pattern formed by secondary waves scattered by various atoms is first obtained for a given configuration of atoms at the various lattice points, and then an average is taken over the various possible configurations (see, for example, Refs. 1 – 8). In this approach the intensity of scattered radiation turns out to be expressed in terms of the correlation parameters for the occupancy of the different lattice points by atoms of a given kind. The formulae obtained in this way are convenient for calculating the intensity of scattered radiation when the distant order and the correlation parameters are known, and also for the solution of the inverse problem, that of determining the correlation parameters from the distribution of intensity of diffuse scattering as given by experiment. However, as a result of the fact that the calculation of correlation parameters for different coordinative spheres as functions of the temperature, of the composition of the solution, and of parameters characterizing the interaction energies of the crystal is, as a rule, difficult, this method of investigating the scattering is less convenient for the determination of the intensity of the scattered radiation as a function of the quantities enumerated above. The dependence of the intensity of diffuse scattering on the temperature and on the concentration has been found for a one-dimensional lattice. For a three-dimensional crystal a calculation of this type has been carried out in the nearest neighbor approximation only for the case of high temperatures when the correlation in the solution is not great. The very interesting case when the temperature of the solution is of the same order of magnitude as the temperature of transition into the ordered state was not considered.

Another method which was introduced by Einstein[9] for treating the problem of light scattering is considerably more convenient for the investigation of the dependence of the intensity of scattering on the temperature, on the composition and on the constants of the interatomic interaction. The crystal is regarded as a periodic structure consisting of effective atoms which is responsible for the appearance of lines (or spots) on an x-ray photograph. Fluctuations of composition and long range order which give rise to diffuse scattering of waves are superimposed on this periodic structure. The probability of fluctuations depends in an essential way on the temperature, on the composition and on the energy parameters and this permits one to relate these quantities in a simple manner to the intensity of diffuse scattering of x-rays or of neutrons. This method was applied for the first time to the scattering of x-rays by Landau[10] who considered scattering by fluctuations in the degree of long range order in crystals of molecular type near a point of phase transition of the second order. The scattering by solid solutions, which in addition to fluctuations of long range order also have fluctuations in composition with the correlation between these fluctuations being important, was investigated by the present author[11] (this paper will be referred to as I). In Refs. 10 and 22 scattering was considered to be due to fluctuations extending over a large number of lattice constants, which permits one to carry out a phenomenological investigation without making use of a concrete model for the crystal. However, in view of the fact that the x-ray wavelengths are of the same order as the lattice constants, the above large scale fluctuations are associated with diffuse scattering through angles close either to the directions of Bragg scattering or to the incident beam. In order to find the intensity of scattering at arbitrary angles it is necessary to consider fluctuations whose dimensions are of the same order as the lattice constant. The calculation of probabilities of such fluctuations can no longer be carried out by means of the thermodynamic theory of solutions and a concrete statistical model of the solution must be used which necessarily must contain a number of simplifying assumptions. At the same time the use of such a model makes it possible to relate the intensity of diffuse scattering to the constants of the atomic interaction.

In this paper the intensity of the scattered radiation is determined with the aid of the usual statistical model of a solid solution in which the energy of the crystal is represented as the sum of the interaction energies of different atom pairs. Just as in I, the background associated with the geometric (statistical and thermal) lattice distortions will not be considered, *i.e.*, only that part of the diffuse scattering will be investigated which is determined by the distribution (which is to some extent random) of the various kinds of atoms among the crystalline lattice points. The presentation will be given in terms of x-ray scattering. However, the results obtained will equally well apply to the scattering of thermal neutrons if in place of atomic factors for the scattering of x-rays one substitutes the neutron scattering factors averaged over the isotopes and takes into account the fact that in addition to the background considered here there exists in the case of neutron scattering a background associated with the random distribution of isotopes and with neutron scattering dependent on nuclear spins (see, for example, Ref. 8). Although the solution model used here is a very approximate one the method developed below may also be applied to more accurate models whenever they might be introduced.

1. GENERAL EXPRESSION FOR THE INTENSITY OF SCATTERING BY A SOLID SOLUTION

Almost all the known solid solutions of metals have in the disordered state crystalline lattices in which the elementary cell contains only one atom. A lattice of such type may be decomposed into n geometrically identical sublattices similarly situated with respect to each other (containing lattice points of a given kind) in such a way that each atom interacts only with the nearest atoms of other sublattices and does not interact with atoms at lattice points of its own sublattice. By choosing a sufficiently large n one can take into account the interaction with atoms situated in distant coordinative spheres.

The distribution of atoms among the lattice points of the binary solution $A-B$ may be characterized by the set of quantities p_{Ais} equal to unity or zero depending on whether the sth point of the ith sublattice is occupied by atom A or B respectively. Within the framework of the kinematic scattering theory the intensity of scattering of monochromatic x-rays by a single crystal with a given distribution of atoms may be written when expressed in electronic units in the form

$$I = \left| \sum_{i=1}^{n} \sum_{s=1}^{N_0} (f_A p_{Ais} + f_B p_{Bis}) \exp(i\mathbf{q}\mathbf{R}_{is}) \right|^2. \quad (1)$$

Here $N_0 = N/n$ is the number of atoms in a sublattice, $\mathbf{q} = \mathbf{k}_2 - \mathbf{k}_1$ is the difference between the propagation vectors of the scattered and incident waves, $\mathbf{R}_{is} = \mathbf{R}_i + \mathbf{R}_s$ is the vector drawn from the origin of coordinates to the sth lattice point of the ith sublattice, $p_{Bis} = 1 - p_{Ais}$, f_A and f_B are the atomic scattering factors of atoms A and B corresponding to the vector $\mathbf{q}$. The expression $f_A p_{Ais} + f_B p_{Bis}$, which changes in going over from one lattice point to another, can be written in the form of a sum of the term $f_A p_{Ai} + f_B p_{Bi}$ (p_{Ai} and p_{Bi} are the probabilities that the lattice points of the ith sublattice are occupied by atoms A and B) averaged over the lattice points of the given sublattice, and of the deviation $(p_{Ais} - p_{Ai})(f_A - f_B)$ from the average value. The square of the term corresponding to the purely periodic distribution of "average atoms"

$$I_1 = \left| \sum_{i=1}^{n} (f_A p_{Ai} + f_B p_{Bi}) \exp(i\mathbf{q}\mathbf{R}_i) \right|^2 \times \left| \sum_{s=1}^{N_0} \exp(i\mathbf{q}\,\mathbf{R}_s) \right|^2, \quad (2)$$

determines the intensity of the sharp lines (situated at $\mathbf{q} = 2\pi\mathbf{K}_n$ where $\mathbf{K}_n$ are the vectors of the reciprocal lattice) which will not be discussed below. The cross term disappears in the limit of an infinite crystal. The square of the second term is determined by the deviation of the actual distribution of the atoms among the lattice points from the average distribution and describes the diffuse scattering. The intensity of this scattering is equal to

$$I_2 = N_0^2 |f_A - f_B|^2 \left| \sum_{i=0}^{n} p_{\mathbf{q}i} \right|^2, \tag{3}$$

where

$$p_{\mathbf{q}i} = \frac{1}{N_0} \sum_{s=1}^{N_0} (p_{Ais} - p_{Ai}) \exp(i\,\mathbf{qR}_{is}) \tag{4}$$

and in the rest of this section we shall take **q** to be a reduced vector. We shall label the atomic planes perpendicular to the vector **q** by the index *f*. If **q** is not perpendicular to any system of atomic planes then the crystal may be divided into "infinitely thin" layers perpendicular to **q** which can also be labelled by the index *f*. The numbers of lattice points belonging to one of the sublattices are the same for the various parallel planes containing lattice points of this sublattice. We denote this number by ν. In summing over lattice points lying in one plane (layer) the exponential factor in (4) remains constant. Therefore in the summation (4) p_{Ais} may be replaced by the average density p_{Ai}^f of atoms *A* on the lattice points of the *i*th sublattice in the *f*th plane. Further, if the *Z* axis is chosen parallel to the vector **q**, then the expression (4) takes on the following form:

$$p_{\mathbf{q}i} = \frac{\nu}{N_0} \sum_{f_i=1}^{N_0/\nu} (p_{Ai}^f - p_{Ai}) \exp(iqZ_{if}). \tag{5}$$

Thus, in accordance with (3) and (5) the background intensity is determined by the deviation of the densities p_{Ai}^f in the various planes from the average density, *i.e.*, by the distribution of the fluctuations in the distribution of atoms *A* among the lattice points of the various sublattices. The probability of a given distribution of fluctuation is proportional to exp $(-R/kT)$ where the minimun work *R* required to produce such a fluctuation is equal to

$$\begin{aligned} R = {} & \frac{1}{2} \sum_i \sum_f \frac{\partial^2 \varphi}{\partial p_{Ai}^{f2}} (p_{Ai}^f - p_{Ai})^2 \\ & + \sum_{i<j} \sum_{f,g} \frac{\partial^2 \varphi}{\partial p_{Ai}^f \partial p_{Aj}^g} (p_{Ai}^f - p_{Ai})(p_{Aj}^g - p_{Aj}) \\ & + \sum_i \sum_{f<g} \frac{\partial^2 \varphi}{\partial p_{Ai}^f \partial p_{Ai}^g} (p_{Ai}^f - p_{Ai}^g)(p_{Ai}^g - p_{Ai}). \end{aligned} \tag{6}$$

Here φ is the thermodynamic potential of the crystal. The second derivatives of the thermodynamic potential with respect to the densities of atoms *A* in planes not containing lattice points the interaction between which is being taken into account are equal to zero. As a result of this the last term in (6) disappears when the crystal is broken up into sublattices as indicated, while in the second term only those terms are retained which correspond to planes the atoms of which interact with each other. The derivatives with respect to concentrations in atomic planes appearing in (6) are related to the derivatives with respect to the usual concentrations referring to the whole crystal by the expressions

$$\frac{\partial^2 \varphi}{\partial p_{Ai}^{f2}} = \frac{\nu}{N_0} \frac{\partial^2 \varphi}{\partial p_{Ai}^2}; \qquad \frac{\partial^2 \varphi}{\partial p_{Ai}^f \partial p_{Aj}^g} = \frac{\nu}{N_0} \frac{z'}{z} \frac{\partial^2 \varphi}{\partial p_{Ai} \partial p_{Aj}}, \tag{7}$$

where *z* is the total number of lattice points of the *j*th sublattice closest to the given lattice point of the *i*th sublattice situated in the *f*th plane, while *z'* is the number of such points of the *j*th sublattice contained in the *g*th plane.

In accordance with (3) and (5), to determine the background intensity one must know not the spatial distribution of the quantities p_{Ai}^f, but the Fourier components of this distribution. Therefore it is more convenient to calculate directly the average values of the squares and the products of the Fourier components of the quantities p_{Ai}^f, p_{Aj}^g. The expansion into a Fourier series of the difference $p_{Ai}^f - p_{Ai}$ has the form

$$p_{Ai}^f - p_{Ai} = \sum_k [r_{ik} \exp(ikZ_{if}) + r_{ik}^* \exp(-ikZ_{if})], \tag{8}$$

with $0 < k < 2\pi/\Delta Z$ where ΔZ is the distance between adjacent atomic planes (layers). Substituting (8) and (7) into (6) and taking it into account that $k(Z_{ig} - Z_{if}) = \mathbf{k}\mathbf{a}_{\xi ij}$, where the vector **k** is directed along the *Z* axis, $\mathbf{a}_{\xi ij}$ is the vector drawn from a lattice point of the *i*th sublattice situated in the *f*th plane to one of the nearest lattice points of the *j*th sublattice in the *g*th plane, we obtain

$$\begin{aligned} R = {} & \sum_i \frac{\partial^2 \varphi}{\partial p_{Ai}^2} \sum_{\mathbf{k}} r_{i\mathbf{k}} r_{i\mathbf{k}}^* \\ & + \frac{1}{z} \sum_{i<j} \frac{\partial^2 \varphi}{\partial p_{Ai} \partial p_{Aj}} \sum_{\xi=1}^{z} \sum_{\mathbf{k}} \cos \mathbf{a}_{\xi ij} \mathbf{k} \, (r_{i\mathbf{k}} r_{j\mathbf{k}}^* + r_{i\mathbf{k}}^* r_{j\mathbf{k}}). \end{aligned} \tag{9}$$

Thus the expression for the minimum work breaks up into terms $R_{\mathbf{k}}$ corresponding to different **k**. Therefore the expression for the distribution of the probabilities for the Fourier components of the fluctuations will correspondingly break up into a product of factors corresponding to the individual components. The distribution of the probabilities of fluctuations in the qth Fourier component which, in accordance with (3) and (5), determines the background intensity has the form

$$w \sim \exp\left(-\frac{R_{\mathbf{q}}}{kT}\right) = \tag{10}$$

$$\exp\left\{-\sum_{i=1}^{n} a_{ii}\left(r'^{2}_{i\mathbf{q}} + r''^{2}_{i\mathbf{q}}\right) - \sum_{i\neq j=1}^{n} a_{ij}\left(r'_{i\mathbf{q}}r'_{j\mathbf{q}} + r''_{i\mathbf{q}}r''_{j\mathbf{q}}\right)\right\},$$

where

$$a_{ii} = \frac{1}{kT}\frac{\partial^2\varphi}{\partial p^2_{Ai}};$$

$$a_{ij} = \frac{1}{zkT}\frac{\partial^2\varphi}{\partial p_{Ai}\partial p_{Aj}}\sum_{\xi=1}^{z}\cos \mathbf{a}_{\xi ij}\mathbf{q} \quad (i\neq j), \tag{11}$$

while $r'_{i\mathbf{q}}$ and $r''_{i\mathbf{q}}$ denote the real and the imaginary parts of the complex quantity $r_{i\mathbf{q}}$. With the aid of formula (10) one may determine the average values of the squares and of the products of Fourier components belonging to different sublattices

$$\frac{1}{2}\overline{\left(r_{i\mathbf{q}}r^{*}_{j\mathbf{q}} + r^{*}_{i\mathbf{q}}r_{j\mathbf{q}}\right)} = \bar{b}_{ij}. \tag{12}$$

Here the quantites b_{ij} form a matrix inverse to the matrix a_{ij} which is determined by formula (11), and (12) is applicable both for $i \neq j$ and for $i = j$. It follows from (3), (5), (8) and (12) that the intensity of diffuse scattering may be expressed in terms of the quantities b_{ij} in the following manner:

$$I_2 = N_0^2\,|f_A - f_B|^2\sum_{i,j=1}^{n} b_{ij}. \tag{13}$$

Thus, in order to determine the background intensity it is necessary to know the thermodynamic potential of the solution as a function of the variables p_{Ai} to calculate the matrix a_{ij} with the aid of formulas (11), and then to find the sum of all the matrix elements of the inverse matrix b_{ij}.

The sum $\sum_{i,j=1}^{n} b_{ij}$ may be obtained in a number of cases without carrying out the inversion of the matrix a_{ij}, but by directly finding the sum of the matrix elements of the inverse matrix. Assume that the sum of the matrix elements of each row of the matrix a_{ij} does not depend on the row index and is equal to A:

$$\sum_{i=1}^{n} a_{si} = A. \tag{14}$$

Then the sum of all the matrix elements of the inverse matrix will be equal to

$$\sum_{i,k=1}^{n} b_{ik} = n / A. \tag{15}$$

2. SCATTERING BY DISORDERED SOLID SOLUTIONS

Let us determine the intensity of diffuse scattering by a disordered solution with a crystalline lattice in which the elementary cell contains only one atom, taking into account interactions between pairs of atoms separated by arbitrary distances. For this purpose we pick out within the crystal a polyhedron containing a sufficiently large number of elementary cells to allow us to neglect the interaction of an atom at the center of the polyhedron with atoms outside its boundaries. We shall consider that each lattice point within this polyhedron belongs to its own sublattice, so that the number of sublattices is equal to the number n of lattice points within the polyhedron. Each atom will not interact with the atoms of its own sublattice and will interact with one atom of each of the other sublattices. Therefore for the calculation of the background intensity we can use the method described in the preceding section, and we shall have in the summation (11) for a_{ij} $(i \neq j)$ only one term corresponding to the given i and j $(z = 1)$. In a crystalline lattice whose elementary cell contains only one lattice point all the lattice points are equivalent, and the systems of vectors drawn from a given lattice point to all the other lattice points are the same independently of which lattice point is chosen as the initial one. Further, in a disordered solution the derivatives $\partial^2\varphi/\partial p_{Ai}\partial p_{Aj}$ depend only on the distance between the nearest lattice points of the ith and the jth sublattices (and also on the direction of the vector joining them) but do not depend on the nature of these sublattices. Therefore the same matrix elements appear in the different rows of the matrix a_{ij}, although they may occur in a different order. Therefore, formula (15) may be used for the calculation of the sum of the matrix elements of the inverse matrix, and in accordance with (13)–(15) and (11) the intensity of the diffuse scattering from a disordered solution is

$$I_2 = N\,|f_A - f_B|^2 \Big[x_0 + \sum_{l=1}^{\infty} x_l \sum_{\varkappa_l = 1}^{z_l} \cos \mathbf{a}_{\varkappa l}\mathbf{q} \Big]^{-1}. \qquad (16)$$

Here l is the index of the coordinative sphere,* $\varkappa_l$ are indices of the lattice points of this sphere, z_l is the coordination number corresponding to the lth sphere, $\mathbf{a}_{\varkappa l}$ is a vector drawn from the central lattice point to the lattice point with the index $\varkappa_l$ in the lth coordinative sphere, and

$$x_0 = \frac{1}{N_0 kT}\,\frac{\partial^2 \varphi}{\partial p_{A1}^2}; \quad x_l = \frac{1}{N_0 kT}\,\frac{\partial^2 \varphi}{\partial p_{A1}\partial p_{Ail}}. \qquad (17)$$

In order to be able to use formula (16) we must know the thermodynamic potential of the solution as a function of the variables p_{Ail}. In the model of the solution which we have adopted at high temperatures when correlation in the solution is not important we have

$$\begin{aligned} \varphi = -\frac{N_0}{2} \sum_{j=1} \sum_{\substack{i_l=1 \\ (i_l \neq j)}}^{n} \{ & p_{Aj} p_{Ail} v_{AAl} \\ & + [p_{Aj}(1-p_{Ail}) + p_{Ail}(1-p_{Aj})] v_{ABl} \\ & + (1-p_{Aj})(1-p_{Ail}) v_{BBl} \} \\ + N_0 kT \sum_{i_l=1}^{n} & [p_{Ail} \ln p_{Ail} + (1-p_{Ail}) \ln (1-p_{Ail})], \end{aligned} \qquad (18)$$

where v_{AAl}, v_{ABl} and v_{BBl} are the interaction energies taken with reversed sign for the atom pairs AA, AB and BB when one of the atoms is at some lattice point j while the other atom of the crystal is at the lattice point $\varkappa_l$ at a distance equal to the radius of the lth coordinative sphere. It follows from (17) and (18) that at high temperatures

$$\begin{gathered} x_0 = 1/c(1-c); \quad x_l = w_l/kT, \\ w_l = 2v_{ABl} - v_{AAl} - v_{BBl}, \end{gathered} \qquad (19)$$

where c is the concentration of atoms A in solution, while w_l is the energy of ordering for the lth coordinative sphere.

Expression (18) is valid only at high temperatures if $l|w_l|/kT \ll 1$ for all l. In the case of arbitrary temperature one may obtain an expression for φ if the concentration of one of the components of the solution is sufficiently small ($c \ll 1$). According to Ref. 12, we have in this case

$$\begin{aligned} \varphi = -\frac{1}{2} N \sum_{i_l=2}^{n} v_{BBl} - N_0 \sum_{j=1}^{n} p_{Aj} \sum_{i_l=1}^{n} (v_{ABl} - v_{BBl}) \\ + kTN_0 \sum_{i=1}^{n} [p_{Ail} \ln p_{Ail} \\ + (1-p_{Ail}) \ln (1-p_{Ail})] \\ - N_0 kT \sum_{j<i_l=1}^{n} p_{Aj} p_{Ail} \Big[\exp\Big(-\frac{w_l}{kT}\Big) - 1 \Big]. \end{aligned} \qquad (20)$$

In the above

$$x_0 = 1/c(1-c); \quad x_l = 1 - \exp(-w_l/kT). \qquad (21)$$

It follows from (16), (19) and (21) that according to I, both when the temperature is increased and when the concentration of one of the components of the solution is made to approach zero, when the solution becomes ideal or weak, the distribution of background approaches the uniform Laue background $I_2 = N|f_A - f_B|^2 c(1-c)$.

If only the interaction with the same atoms of the first coordinative sphere ($w_1 = w$; $w_l = 0$ for $l \neq 1$) is important, then for a decaying solution ($w < 0$) the maxima of the ratio $I_2/|f_A - f_B|^2$ lie near the reflections corresponding to the principal lines and to the incident beam (where the sum $\Sigma \cos \mathbf{a}_\varkappa \cdot \mathbf{q} = z$), while the minima lie near reflections corresponding to superstructure lines (where the above sum is negative). Conversely, for a solution undergoing ordering ($w > 0$) the maxima of the ratio $I_2/|f_A - f_B|^2$ lie near reflections corresponding to superstructure lines, while the minima lie near the principal lines. In the nearest neighbor approximation it also follows from (16) and (21) that at low concentration of one of the components the inhomogeneity of the background is more sharply pronounced for decaying solutions (for the same $|w|/kT$).

The quantities x_l occuring in (16) may be found from experiment if the experimental distribution of the background intensity is known for different $\mathbf{q}$. Indeed, by taking the components of the vectors $\mathbf{a}_{\varkappa l}$ and $\mathbf{q}$ respectively along the basic vectors of the crystalline lattice and along the vectors $\mathbf{b}_\alpha$ of the reciprocal lattice

---

*For the same distance between the central and the $\varkappa_l$th lattice points the quantities x_l may, generally speaking, be different. In such a case we shall take the coordinative sphere to be subdivided into several coordinative spheres of the same radius for which the x_l are the same, while z_l denote the coordination numbers for such coordinative spheres.

$$\mathbf{a}_{\varkappa l} = \sum_{\alpha=1}^{3} \mathbf{d}_\alpha n_{\varkappa l \alpha}; \quad \mathbf{q} = \sum_{\alpha=1}^{3} \mathbf{b}_\alpha k_\alpha$$

it is possible to write the above ratio in the form of a three-dimensional Fourier series

$$\frac{N|f_A - f_B|^2}{I_2} = x_0 + \sum_{n_{\varkappa l\alpha}=-\infty}^{\infty} x_l \exp\left(i \sum_{\alpha=1}^{3} n_{\varkappa l\alpha} k_\alpha\right), \tag{22}$$

where $n_{\varkappa l\alpha}$ take on all the integral values from $-\infty$ to ∞ for each α. Carrying out the Fourier transformation we obtain

$$x_0 = \frac{1}{8\pi^3} \int_0^{2\pi}\int_0^{2\pi}\int_0^{2\pi} \frac{N|f_A - f_B|^2}{I_2} dk_1 dk_2 dk_3;$$
$$x_l = \frac{1}{8\pi^3} \int_0^{2\pi}\int_0^{2\pi}\int_0^{2\pi} \frac{N|f_A - f_B|^2}{I_2} \cos\left(\sum_{\alpha=1}^{3} n_{\varkappa l\alpha} k_\alpha\right) dk_1 dk_2 dk_3, \tag{23}$$

where the numbers $n_{\varkappa l\alpha}$, $\alpha = 1, 2, 3$ correspond to some lattice point in the lth coordinative sphere.* In using formulas (23) it should be kept in mind that other parts of diffuse scattering which are not considered here (associated with thermal vibrations, geometric distortions, *etc.*) must be excluded, and do not enter into I_2. The method for the experimental determination of the functions $I_2(k_1, k_2, k_3)$ is given in Cowley's paper.[6]

Thus with the aid of formulas (23), (19) and (21) it is possible to calculate the energies of ordering w_e for different coordinative spheres from the experimental values of the background intensity for various crystal orientations and for various scattering angles (various k_α) obtained in the case of scattering by a solution at high temperature or having a low concentration of one of the components. The use of solutions with a low concentration of one of the components is more convenient in the case of negative w_e since in this case the quantities $|x_l|$ are sufficiently large at low temperatures.

The case when the correlation in solution is not small can be investigated by means of the approximation in which only the interaction with neighboring atoms is taken into account. It should be emphasized that in this case, as before, the correlation in all the coordinative spheres is taken into account, and not only in the occupancy of neighboring lattice points. We shall consider first solutions whose crystalline lattices may be broken up into two sublattices with the same number of lattice points in such a way that each lattice point is surrounded only by lattice points of the other sublattice (for example solutions with a body-centered cubic lattice, or with a simple cubic lattice). After denoting the concentrations of atoms A in these two sublattices by $p_A^{(1)}$ and $p_A^{(2)}$ we shall find that in the nearest neighbor approximation formula (16) for the intensity of diffuse scattering from a disordered crystal takes on the form

$$I_2 = N|f_A - f_B|^2 \left[a_1 + a_2 \sum_{\varkappa=1}^{z} \cos \mathbf{a}_\varkappa \mathbf{q}\right]^{-1}. \tag{24}$$

Here

$$a_1 = \frac{2}{NkT} \frac{\partial^2 \varphi}{\partial p_A^{(1)2}}, \qquad a_2 = \frac{2}{zNkT} \frac{\partial^2 \varphi}{\partial p_A^{(1)} \partial p_A^{(2)}},$$

z is the coordination number of the first coordinative sphere, while $\mathbf{a}_\varkappa$ are vectors drawn from the central lattice point to the lattice points of this sphere. The quantities a_1 and a_2 may be calculated in the nearest neighbor approximation if use is made of the expression for the thermodynamic potential in the form of an expansion in powers of w/kT where w is the energy of ordering for the first coordinative sphere. Expansions for structures of the type under consideration have been obtained by Chang.[13] By differentiating the series obtained by him for the thermodynamic potential we shall obtain the following expansions for a_1 and a_2 in the case of disordered solutions:

$$a_1 = \frac{1}{f} + zf\left(\frac{w}{kT}\right)^2 - zf(1-4f)\left(\frac{w}{kT}\right)^3 - f\left[-\frac{z}{12}(7 - 72f + 180f^2) + \frac{y}{2} f(1-6f)\right]\left(\frac{w}{kT}\right)^4 + \cdots \tag{25}$$

$$a_2 = \frac{w}{kT} - \frac{1}{2}(1-4f)\left(\frac{w}{kT}\right)^2 + \frac{1}{6}(1-6f)^2\left(\frac{w}{kT}\right)^3 - (1-4f)\left[\frac{1}{24}(1-12f)^2 + \left(\frac{y}{z} - 1\right) f^2\right]\left(\frac{w}{kT}\right)^4 + \cdots. \tag{26}$$

Here $f = c(1 - c)$, $y = 24$ for the simple cubic lattice and $y = 96$ for the body centered cubic lattice. The terms proportional to $(w/kT)^5$ and $(w/kT)^6$ give small corrections to the expansions (25) and (26).

---

*The integration in (23) is carried out over the volume of an elementary cell in the space of the reciprocal lattice. This integration obviously can be taken over the volume of any arbitrary cell.

In the case of high temperatures formulae (24), (25 and (26) lead to the following expression for the back ground intensity:

$$I_2 = N\,|f_A - f_B|^2\, c(1-c)\left[1 + \frac{w}{kT}\, c(1-c) \sum_{\varkappa=1}^{z} \cos \mathbf{a}_\varkappa \mathbf{q}\right]^{-1}. \tag{27}$$

Up to quadratic terms this expression coincides with the expression for I_2 obtained by Lifshitz[9] (for a simple cubic lattice).

In the structures under consideration sharp Bragg reflections corresponding to principal lines occur at values of the quantity $\mathbf{k}_1 - \mathbf{k}_2$ for which the conditions $\mathbf{q}\cdot\mathbf{a}_\varkappa = 2\pi m_\varkappa$ are satisfied, where $m_\varkappa$ are integers. The conditions $\mathbf{q}\cdot\mathbf{a}_\varkappa = \pi(2m_\varkappa + 1)$ correspond to the superstructure lines. Near these values of the vector $\mathbf{q}$ one can expand $\cos \mathbf{a}_\varkappa\cdot\mathbf{q}$ in powers of the vector $\mathbf{q}'$ which represents the amount that must be added to $\mathbf{q}$ to obtain the value for which a given principal or superstructure Bragg reflection occurs. If we limit ourselves to quadratic terms we obtain:

$$I_2 = N\,|f_A - f_B|^2 \left[a_1 + z a_2 \mp \frac{a_2}{2} \sum_{\varkappa=1}^{z} (\mathbf{a}_\varkappa \mathbf{q}')^2\right]^{-1}, \tag{28}$$

where the upper sign corresponds to a principal line and the lower to a superstructure line.

It was shown in I [see formulae (15) and (21) of Ref. I] that at temperatures somewhat greater than the temperature of ordering (in solutions undergoing ordering) or the temperature of decay (in decaying solutions) the background intensity near superstructure or principal lines respectively is anomalously large. If the composition of the solution corresponds to the maximum temperature of ordering or decay, then for cubic crystals the expression for the background intensity has the form

$$I_2 = N\,|f_A - f_B|^2 \beta \left[\frac{T - T_0}{T_0} + \gamma q'^2\right]^{-1}, \tag{29}$$

where T_0 is the temperature of ordering or decay respectively.

Expressions of the same type for solutions of stoichiometric composition are obtained in the statistical theory from formulae (25), (26) and (28) if one takes into account the fact that according to Chang[13] the temperature T_0 of such a solution is determined by the relation

$$\frac{w}{kT_0} = \pm \frac{4}{z}\left[1 + \frac{1}{z} + \frac{4}{3}\frac{1}{z^2} + \left(\frac{y}{z} + 2\right)\frac{1}{z^3} + \cdots\right]$$

(the plus sign corresponds to the ordering and the minus sign to the decaying solution) and if one expands $a_1 \pm z a_2$ in powers of $1/z$. Moreover the statistical theory permits one to calculate the quantities β and γ which appeared in the thermodynamic theory as parameters. Expansions of these quantities in powers of $1/z$ have the form

$$\beta = \frac{1}{4}\left[1 + \frac{1}{z} + \frac{5}{3}\frac{1}{z^2} + 3\left(\frac{y}{z} + 1\right)\frac{1}{z^3} + \cdots\right];$$
$$\gamma = \frac{1}{6}\left[1 + \frac{2}{z} + \frac{14}{3}\frac{1}{z^2} + \left(4\frac{y}{z} + \frac{32}{3}\right)\frac{1}{z^3} + \cdots\right]a^2, \tag{30}$$

where $a = |\mathbf{a}_\varkappa|$. Thus the parameter γ is of order $a^2/4$ and $\beta \sim 1/3$.*

In order to discuss in the nearest neighbor approximation solutions with a face-centered cubic lattice, one should break up this lattice into four simple sublattices each of which contains one of the lattice points of the elementary cell of the original lattice. In this case the given lattice point has for its nearest neighbors only lattice points of other sublattices, so that the formulas given above may be utilized. The intensity of diffuse scattering by a disordered crystal is given, as before, by formula (24), but the expressions for the quantities a_1 and a_2 appearing in this formula have a somewhat different form. Making use of the expression for the thermodynamic potential of the solution with a face-centered cubic lattice[12] in the for of an expansion in powers of w/kT we obtain

$$a_1 = 1/f + 12f\,(w/kT)^2 - 12f\,(w/kT)^3 + \cdots, \tag{31}$$

$$a_2 = w/kT - {}^1/_2\,(1 - 4f)\,(w/kT)^2 + {}^1/_6\,(1 + 12f - 60f^2)\,(w/kT)^3 + \cdots. \tag{32}$$

These expansions can be used at temperatures considerably higher than the temperature of ordering of a solution with a face-centered cubic lattice (in a decaying solution with $c \sim \frac{1}{2}$ formulae (31) and (32) are approximately valid right up to the temperature of decay).

---

*In Ref. 5 a conclusion is reached that at a phase transition of the second order the background intensity has only a weak maximum and anomalously large scattering should not be observed. This erroneous conclusion is connected with the unjustified extension to a three-dimensional crystal of the formula derived by Obraztsov[5] for a linear chain (where, as is well known, there is no phase transition to the ordered state).

3. SCATTERING BY ORDERED SOLID SOLUTIONS

In the case of an ordered solution of arbitrary composition the sums of the matrix elements belonging to the various rows of the matrix (11) are, generally speaking, not the same, so that one cannot use formula (15) for the determination of the sum $\sum_{i,j=1}^{n} b_{ij}$, but one must invert the matrix a_{ij}. If in an ordered solution there is the same number of lattice points of the first and the second kind, and if each of the lattice points is surrounded only by lattice points of the other kind, then in the nearest neighbor approximation one should choose lattice points of the first and second kinds for sublattices into which the crystal must be broken up in order to be able to apply the formulas of Sec. 1. By inverting the second order matrix a_{ij} determined by formulae (11) we shall obtain from (13) the following expression for the background intensity:

$$I_2 = N\,|f_A - f_B|^2 \Big[a_1 + a_2 \sum_{\varkappa=1}^{z} \cos \mathbf{a}_\varkappa \mathbf{q} - M\Big]^{-1}, \tag{33}$$

where

$$a_1 = \frac{1}{NkT}\left(\frac{\partial^2\varphi}{\partial p_A^{(1)^2}} + \frac{\partial^2\varphi}{\partial p_A^{(2)^2}}\right); \quad a_2 = \frac{2}{zNkT}\,\frac{\partial^2\varphi}{\partial p_A^{(1)}\,\partial p_A^{(2)}};$$

$$M = \frac{1}{(NkT)^2}\left(\frac{\partial^2\varphi}{\partial p_A^{(1)^2}} - \frac{\partial^2\varphi}{\partial p_A^{(2)^2}}\right)^2 \Big/ \Big[a_1 - a_2 \sum_{\varkappa=1}^{z} \cos \mathbf{a}_\varkappa \mathbf{q}\Big]. \tag{34}$$

Thus, in the nearest neighbor approximation the dependence of I_2 on the direction of the beam, on the angle of scattering, and on the wavelength is determined by the sum $\Sigma \cos \mathbf{a}_\varkappa \cdot \mathbf{q}$. If the coordinate axes in the cubic crystal are directed along the cubic axes, then this sum for a simple cubic lattice is given by $2(\cos aq_x + \cos aq_y + \cos aq_z)$ while for a body centered cubic lattice

$$4 \cos \frac{\sqrt{3}}{3}\, aq_x \cdot \cos \frac{\sqrt{3}}{3}\, aq_y \cdot \cos \frac{\sqrt{3}}{3}\, aq_z.$$

Expressions for a_1, a_2, and for the numerator in M may be written in the form of an expansion in powers of w/kT if one starts out with Chang's[13] expansion for φ. On carrying out a differentiation we obtain

$$\begin{aligned} a_1 = \frac{v}{2u} + \frac{z}{2} v \left(\frac{w}{kT}\right)^2 - \frac{z}{2} vs \left(\frac{w}{kT}\right)^3 &+ \Big[\frac{z}{24}(7v - 36v^2 + 180vu) \\ &- \frac{y}{4}(v^2 - 2u - 6uv)\Big]\left(\frac{w}{kT}\right)^4 + \cdots, \end{aligned} \tag{35}$$

$$\begin{aligned} a_2 = \frac{w}{kT} - \frac{1}{2} s \left(\frac{w}{kT}\right)^2 + \frac{1}{6}(1 - 6v + 36u)\left(\frac{w}{kT}\right)^3 \\ - \Big[\frac{1}{24}(1 - 12v + 120u) + \frac{y}{z} u\Big] s \left(\frac{w}{kT}\right)^4 + \cdots, \end{aligned} \tag{36}$$

$$\begin{aligned} \frac{1}{NkT}\left(\frac{\partial^2\varphi}{\partial p_A^{(1)^2}} - \frac{\partial^2\varphi}{\partial p_A^{(2)^2}}\right) = \\ -\frac{t}{2}\Big\{\frac{1}{u} + z\left(\frac{w}{kT}\right)^2 - zs\left(\frac{w}{kT}\right)^3 \\ + \Big[\frac{z}{12}(7 - 36v + 180u) \\ + \frac{y}{2}(-v + 6u)\Big]\left(\frac{w}{kT}\right)^4 + \cdots\Big\}. \end{aligned} \tag{37}$$

Here

$$\left.\begin{aligned} v &= p_A^{(1)}(1 - p_A^{(1)}) + p_A^{(2)}(1 - p_A^{(2)}) \\ &= 2c(1 - c) - \frac{\eta^2}{2}; \\ u &= p_A^{(1)} p_A^{(2)}(1 - p_A^{(1)})(1 - p_A^{(2)}) \\ &= \left(c^2 - \frac{\eta^2}{4}\right)\Big[(1 - c)^2 - \frac{\eta^2}{4}\Big]; \\ s &= (1 - 2p_A^{(1)})(1 - 2p_A^{(2)}) = (1 - 2c)^2 - \eta^2; \\ t &= p_A^{(1)}(1 - p_A^{(1)}) - p_A^{(2)}(1 - p_A^{(2)}) = (1 - 2c)\,\eta, \end{aligned}\right\} \tag{38}$$

where η is the degree of long range order defined by the relations

$$p_A^{(1)} = c + {}^1/_2\,\eta; \quad p_A^{(2)} = c - {}^1/_2\,\eta.$$

The quantity t becomes zero for a solution of stoichiometric composition $c = \frac{1}{2}$ and for a disordered solution. In this case according to (37) $M = 0$ (within the framework of the model adopted this conclusion is valid not only in the nearest neighbor approximation, but also taking into account the interaction with more distant atoms) and formula (33) for the background intensity becomes considerably simpler. We note that in this case the expansions (35) and (36) coincide with the expansions (25) and (26) for a disordered solution if in the latter one replaces $f \to p_A^{(1)}(1 - p_A^{(1)})$; $w/kT \to -w/kT$; $\alpha_2 \to -\alpha_2$.

In agreement with I near the temperature of ordering the intensity of diffuse scattering becomes anomalously large close to the superstructure lines. For $c = \frac{1}{2}$ the expression for I_2 is found to be the same as (29) if in this formula $(T - T_0)/T_0$ is replaced by $2(T_0 - T)/T_0$.

In solutions of stoichiometric composition AB in which lattice points of the first kind are surrounded by lattice points of the second and first kinds in the same way in which lattice points of the second kind are surrounded by lattice points of the first and second kinds (crystals of the type of NaCl, β-brass, AuCu etc.) one can investigate the scattering without making use of the nearest neighbor approximation. In order to do this one must break up the crystal into n sublattices as was done in the preceding section for disordered lattices. When this is done $n/2$ sublattices will consist of lattice points of the first kind and the same number of sublattices will consit of lattice points of the second kind. In the case of solutions of stoichoimetric composition AB the derivatives $\partial^2\varphi/\partial p_{Ai}^2$ are the same for different i, and for the structures under consideration the sum of the matrix elements belonging to any given row of the matrix (11) does not depend on the row index. Therefore the sum of all the b_{ij} may be computed by means of formula (15). Thus, in the case under consideration, just as in the case of disordered solutions, the intensity of diffuse scattering is given by formula (16). However, in this formula one must now regard lattice points of different kinds, even if they are situated at the same distance, as belonging to different coordinative spheres, so that z_ε is equal to the number of lattice points of a given kind situated at a definite distance from the central lattice point (see also the first footnote of this article).

The quantities x_0 and x_l appearing in formula (16) may be found in the case of low temperatures, considerably lower than the temperature of ordering, if the solution is in an almost completely ordered state. In this case according to Krivoglaz[12] the thermodynamic potential is equal to

$$\varphi = \varphi' + kTN_0 \sum_{i=1}^{n} [p_{Ai} \ln p_{Ai} + (1 - p_{Ai}) \ln (1 - p_{Ai})] - kTN_0 \Bigg[\sum_{i_l < j = 1}^{n/2} (1 - p_{Ail})(1 - p_{Aj})(e^{-w_l/kT} - 1)$$
$$+ \sum_{i_l < j = n/2+1}^{n} p_{Ail} p_{Aj} (e^{-w_l/kT} - 1) + \sum_{i_l = 1}^{n/2} \sum_{j = n/2+1}^{n} (1 - p_{Ail}) p_{Aj} (e^{w_l/kT} - 1) \Bigg]. \tag{39}$$

Here φ' depends linearly on p_{Ai}, and the energies w_l correspond, as before, to a given pair of lattice points of sublattices i and j. Taking the first sublattice to consist of lattice points of the first kind, and taking into account the fact that for $c = \frac{1}{2}$ $p_{Ai} = \frac{1}{2}(1 + \eta)$ we obtain

$$x_0 = 1 / p_{A1}(1 - p_{A1}) = 4/(1 - \eta^2), \tag{40}$$
$$x_l = 1 - \exp(-w_l/kT), \tag{41}$$

if the lth coordinative sphere about a lattice point of the first sublattice consists of lattice points of the first kind, and

$$x_l = \exp(w_l/kT) - 1, \tag{42}$$

if the lth coordinative sphere consists of lattice points of the second kind.* Formulas (23), (41) and (42) enable us to determine the energies of ordering for different coordinative spheres in an almost completely ordered solution from data on the distribution of background intensity.

In the case of solutions AB in which each lattice point is surrounded only by lattice points of the other kind (of the type of NaCl, or β-brass) it follows from (16), (40) and (42) that in the nearest neighbor approximation the background intensity at low temperatures is equal to

$$I_2 = \frac{1}{4} N |f_A - f_B|^2 (1 - \eta^2) \times \left[1 + \frac{1 - \eta^2}{4} (e^{w/kT} - 1) \sum_{\varkappa=1}^{z} \cos \mathbf{a}_\varkappa \mathbf{q} \right]^{-1}. \tag{43}$$

As $T \to 0$, η approaches unity exponentially:[12] $1 - \eta \approx 2 \exp(-zw/kT)$. Therefore the second term in the denominator of (43), which is associated with correlation and which leads to an increase in the background near the superstructure lines, decreases exponentially as $\exp[-(z - 2)w/kT]$ as the temperature is reduced and the inhomogeneity of the background disappears in agreement with I. The quantity I_2 itself also decreases exponentially like $\exp(-zw/2kT)$ (in a completely ordered crystal the intensity of diffuse scattering of the type under consideration is evidently equal to zero). It can be easily shown that for solutions having a structure of the type under consideration whose composition differs somewhat from the stoichiometric composition with $c = \frac{1}{2}$ the value of I_2 at very low temperatures is equal to

---

*Here we consider lattice points of different kinds, corresponding to the same value of ρ_l, as belonging to different coordinative spheres.

$$I_2 = N\,|f_A - f_B|^2 \Big\{ c(1-c) - \frac{\eta^2}{4} - \Big(c^2 - \frac{\eta^2}{4}\Big)\Big[(1-c)^2 - \frac{\eta^2}{4}\Big] \times (e^{w/kT} - 1) \sum_{\varkappa=1}^{z} \cos \mathbf{a}_\varkappa \mathbf{q} \Big\}. \tag{44}$$

In the case of almost completely ordered solutions with a face centered crystal lattice having a layered structure of the type of AuCu and of stoichiometric composition it follows from (16), (40), (41) and (42) that in the nearest neighbor approximation

$$I_2 = \frac{1}{4} N\,|f_A - f_B|^2 \Big\{ 1 + \frac{1-\eta^2}{4} \Big[(1 - e^{-w/kT}) \sum_{\varkappa_1=1}^{4} \cos \mathbf{a}_{\varkappa_1} \mathbf{q} + (e^{w/kT} - 1) \sum_{\varkappa_2=1}^{8} \cos \mathbf{a}_{\varkappa_2} \mathbf{q} \Big] \Big\}^{-1} (1 - \eta^2), \tag{45}$$

where the index $\varkappa_1$ labels vectors drawn between lattice points of the same kind while $\varkappa_2$ labels those drawn between lattice points of different kinds. It may be seen from formula (45) that even if one neglects the usually small tetragonality of crystals of the symmetry type under consideration (a difference, in the length of the vectors $\mathbf{a}_{\varkappa_1}$ and $\mathbf{a}_{\varkappa_2}$), nevertheless the directions (100) perpendicular to the planes containing lattice points of one kind, and the directions (010) and (001) which lie in these planes turn out not to be equivalent with respect to x-ray scattering.

For solutions of the type AuCu whose composition differs slightly from a stoichiometric one it is easy to carry out at low temperatures the inversion of the matrix a_{ij} making use of the fact that in this case the non-diagonal matrix elements are considerably smaller than the diagonal ones. As a result of this we shall obtain from (11), (13) and (39)

$$I_2 = N\,|f_A - f_B|^2 \Big\{ c(1-c) - \frac{\eta^2}{4} - \Big[1 - \exp\Big(-\frac{w}{kT}\Big)\Big]\Big[\Big(c(1-c) - \frac{\eta^2}{4}\Big)^2 + (1 - 4c(1-c))\frac{\eta^2}{4}\Big] \sum_{\varkappa_1=1}^{4} \cos \mathbf{a}_{\varkappa_1} \mathbf{q} - \Big[\exp\Big(\frac{w}{kT}\Big) - 1\Big]\Big(c^2 - \frac{\eta^2}{4}\Big)\Big[(1-c)^2 - \frac{\eta^2}{4}\Big] \times \sum_{\varkappa_2=1}^{8} \cos \mathbf{a}_{\varkappa_2} \mathbf{q} \Big\} \tag{46}$$

In an analogous manner it is possible to obtain the intensity of diffuse scattering from almost completely ordered solutions with a face centered cubic lattice of the type AuCu_3

$$I_2 = N\,|f_A - f_B|^2 \Big\{ c(1-c) - \frac{3}{16}\eta^2 - \frac{1}{2}\Big(c - \frac{\eta}{4}\Big)\Big(1 - c + \frac{\eta}{4}\Big)\Big[\Big(c + \frac{3}{4}\eta\Big) \times \Big(1 - c - \frac{3}{4}\eta\Big)(e^{w/kT} - 1) + \Big(c - \frac{\eta}{4}\Big)\Big(1 - c + \frac{\eta}{4}\Big)(1 - e^{-w/kT})\Big] \sum_{\varkappa=1}^{1} \cos \mathbf{a}_\varkappa \mathbf{q} \Big\}. \tag{47}$$

We note that formulas (45) – (47) which have been derived for almost completely ordered solutions hold over a considerable range of the existence of an ordered phase in solutions of the type of AuCu and AuCu_3, since in these solutions the phase transition into the ordered state must necessarily be a phase transition of the first order,[14] and the degree of long range order usually increases as a result of the transition to a value close to unity.

I take this opportunity to express my gratitude to A. A. Smirnov for his interest in this work and for discussion of results.

---

[1] M. Laue, Ann. Phys. 78, 167 (1925).

[2] I. M. Lifshitz, J. Exptl. Theoret. Phys. (U.S.S.R.) 8, 959 (1938).

[3] I. M. Lifshitz, J. Exptl. Theoret. Phys. (U.S.S.R.) 9, 500 (1939).

[4] A. A. Smirnov and S. V. Vonsovskii, Jour. of Phys. (U.S.S.R.) 5, 263 (1941); A. A. Smirnov and B. V. Paduchev, J. Exptl. Theoret. Phys. (U.S.S.R.) 21, 541 (1951).

[5] Iu. N. Obraztsov, J. Exptl. Theoret. Phys. (U.S.S.R.) 8, 593 (1938).

[6] J. M. Cowley, J. Appl. Phys. 21, 24 (1950).

[7] Warren, Averbach, and Roberts, J. Appl. Phys. 22, 1493 (1951).

[8] Danilenko, Krivoglaz, Matysina, and Smirnov, Fiz. Metal. i Metalloved. (Physics of Metals & Metal Working) 4, 28 (1957).

[9] A. Einstein, Ann. Phys. 33, 1275 (1910).

[10] L. D. Landau, J. Exptl. Theoret. Phys. (U.S.S.R.) 7, 1232 (1937).

[11] M. A. Krivoglaz, J. Exptl. Theoret. Phys. (U.S.S.R.) 31, 625 (1956); Soviet Phys. JETP 4, 293 (1957).

[12] M. A. Krivoglaz, J. Phys. Chem. (U.S.S.R.) in press.

[13] T. S. Chang, J. Chem. Phys. 9, 169 (1941).

[14] E. M. Lifshitz, J. Exptl. Theoret. Phys. (U.S.S.R.) 11, 255 and 259 (1941).

Translated by G. M. Volkoff
277

SOVIET PHYSICS JETP VOLUME 5, NUMBER 6 DECEMBER 15, 1957

Interaction between Current Carriers and *F*-centers and the Acoustic Vibrations of the Lattice in Ionic Crystals

M. F. DEIGEN AND V. L. VINETSKII
Institute of Physics, Academy of Sciences, Ukrainian SSR

(Submitted to JETP editor July 7, 1956)
J. Exptl. Theoret. Phys. (U.S.S.R.) 32, 1382-1392 (June, 1957)

Interaction between an "excess" electron in an ionic crystal with optical and acoustical vibrations of the lattice is considered. Account of interaction with acoustical vibrations leads to a reduction of the energy of the system and to a change in the effective mass of the current carrier in comparison with the polaron. The wave functions, the energies of the ground and excited states of the *F*-centers and the parameters of the *F*-absorption band are computed with account of the "condenson" interaction. A comparison of the polaron and condenson effects in ionic crystals is given.

THE INTERACTION of the "excess" electron with optical vibrations in an ionic dielectric leads to the appearance of "polaron" states.[1] The effective mass of the current carrier in such crystals – the polarons – can differ appreciably from the effective mass of the "band" electron. In polaron theory the interaction with acoustical vibrations was not excluded in the zeroth approximation, but was considered as a reason for the scattering of polaron waves.[2] As an excitation potential, use was made of the micropotential assumed by Bloch, Brillouin and Bethe.[3] Such a consideration is valid for those crystals in which the corrections to the energy (as a result of consideration of the interaction with the acoustical vibrations of the lattice) are significantly smaller than the spacing of the energy levels of the polaron. However, the effect of the interaction with acoustical vibrations of the lattice is not small in a whole series of ionic crystals with strong homopolar coupling. Hence, consideration of this interaction in the zeroth approximation of the theory is a necessity.

Such a consideration is given below. We chose a potential of the deformation type as the interaction potential for the electron with the acoustical vibrations of the lattice. This potential was hypothesized by Pekar and one of the authors of this paper,[4] and is the condenson potential.* The energy terms and wave functions of the system were computed by the variational method and by an adiabatic approximation. The effective mass of the current carrier was computed; it differs from the effective mass of the polaron. In this same approximation, the quantum states of the *F*-center were considered and the parameters of the *F*-absorption band were obtained. A comparison of the magnitude of the condenson and polaron effects in ionic crystals is given.

---

* This potential was proposed independently by Bardeen and Shockley.[10]

I. HAMILTONIAN OF THE SYSTEM. GROUND STATES OF THE CRYSTAL WITH AN "EXCESS" ELECTRON (VARIATIONAL METHOD)

Making use of the results of Refs. 1, 4, 5, the Hamiltonian of the crystal – "excess" electron system can be written in the following fashion:

$$\hat{H} = -\frac{\hbar^2}{2\mu_0}\Delta + V_p(\mathbf{r}) + V_k(\mathbf{r}) + \hat{H}_{\text{op}\parallel} + \hat{H}_{\text{ac}}, \tag{1}$$

$$V_p(\mathbf{r}) = e\int \frac{\mathbf{P}(\mathbf{r}')(\mathbf{r}-\mathbf{r}')}{|\mathbf{r}-\mathbf{r}'|^3}\,d\tau' \tag{2}$$

$\mathbf{P}(\mathbf{r})$ is the inertial part of the separate polarization of the dielectric by the field of the electron:

$$V_k(\mathbf{r}) = a(u_{11} + u_{22} + u_{33}), \tag{3}$$

u_{kk} are the diagonal components of the deformation tensor of the dielectric; a is the coupling constant of the electron with the acoustical vibrations of the lattice; $\hat{H}_{\text{op}\parallel}$ and $\hat{H}_{\text{ac}}$ are the Hamiltonians of the longitudinal optical and acoustical vibrations, respectively, of the lattice; μ_0 is the effective mass of the band electron. In Eq. (1) we have omitted the Hamiltonian of the transverse optical vibrations of the lattice, since, in the macroscopic approximation used here, the electron is not excited by these vibrations.[1]

The Hamiltonian (1), after substitution of (2) and (3), can be transformed to

$$\hat{H} = -\frac{\hbar^2}{2\mu_0}\Delta + e\int\frac{\mathbf{P}(\mathbf{r}_1)(\mathbf{r}-\mathbf{r}_1)}{|\mathbf{r}-\mathbf{r}_1|^3}\,d\tau_1 + a(u_{11}+u_{22}+u_{33}) + \frac{\hbar\omega}{2}\sum_k (q_k^2 - \partial^2/\partial q_k^2) + \frac{1}{2}\sum_{\varkappa\alpha}\hbar\omega_{\varkappa\alpha}(q_{\varkappa\alpha}^2 - \partial^2/\partial q_{\varkappa\alpha}^2), \tag{4}$$

where q_k, $q_{\varkappa\alpha}$ are the generalized coordinates of the normal vibrations, k and $\varkappa$ are the number of the optical and acoustical vibrations; ω is the limiting frequency of the optical vibrations; $\omega_{\varkappa\alpha}$ are the frequencies of the corresponding acoustical vibrations, α is the number of the acoustical branch of the vibrations.

The ground state of the system is determined from the absolute minimum of the functional

$$\overline{H} = \int \Psi^*(\mathbf{r}\ldots q_k \ldots q_{\varkappa\alpha})\,\hat{H}\,\Psi(\mathbf{r}\ldots q_k\ldots q_{\varkappa\alpha}\ldots)\,d\tau\,dq_1\,dq_2, \quad dq_1 = \prod_k dq_k;\ dq_2 = \prod_\alpha\prod_\varkappa dq_{\varkappa\alpha} \tag{5}$$

with the additional normalization condition

$$\int|\Psi|^2\,d\tau\,dq_1\,dq_2 = 1.$$

The minimized function is put in product form:

$$\Psi(\mathbf{r}\ldots q_k\ldots q_{\varkappa\alpha}\ldots) = \psi(\mathbf{r})\,\Phi(\ldots q_k\ldots)\prod_\alpha F_\alpha(\ldots q_{\varkappa\alpha}\ldots). \tag{6}$$

Substitution of (6) in (5), and variation with respect to Φ and to F_α lead to a system of equations for Φ and F_α

$$\begin{gathered}\Big(\sum_k H_k\Big)\Phi = \lambda\Phi;\ \Big(\sum_\varkappa H_{\varkappa\alpha}\Big)F_\alpha = \lambda_\alpha F_\alpha,\\ H_k = \frac{1}{2}\hbar\omega\,[(q_k - q_k^0)^2 - \partial^2/\partial q_k^2] - \frac{c}{8\pi}D_k^2[\psi],\\ H_{\varkappa\alpha} = \frac{1}{2}\hbar\omega_{\varkappa\alpha}\,[(q_{\varkappa\alpha} - q_{\varkappa\alpha}^0)^2 - \partial^2/\partial q_{\varkappa\alpha}^2] - \frac{a^2}{2\rho}K_{-\varkappa}^2[\psi]\cos^2\theta_\alpha/f_\alpha^2,\\ q_k^0 = (c/4\pi\hbar\omega)^{1/2}D_k[\psi],\ q_{\varkappa\alpha}^0 = (\rho\hbar\omega_{\varkappa\alpha})^{-1/2}aK_{-\varkappa}[\psi]\cos\theta_\alpha/f_\alpha,\end{gathered} \tag{7}$$

$c = 1/n^2 - 1/\varepsilon$; ε is the dielectric constant of the crystal, n = optical index of refraction; $f_\alpha = \omega_{\varkappa\alpha}/|\varkappa|$; ρ = density of the crystal, θ_α is the angle between the vectors $\varkappa$ and $\mathbf{q}_{\varkappa\alpha}$:

$$D_k[\psi] = e\int |\psi(\mathbf{r})|^2 \frac{(\mathbf{r}_1-\mathbf{r})}{|\mathbf{r}_1-\mathbf{r}|^3}\chi_k(\mathbf{r}_1)\,d\tau\,d\tau_1, \quad K_{-\varkappa}[\psi] = -\int |\psi(\mathbf{r})|^2 \chi_{-\varkappa}(\mathbf{r})\,d\tau, \tag{8}$$

χ_k and $\chi_\varkappa$ are basic functions to which the expansion of the vectors of the specific polarization of the dielectric $\mathbf{P}(\mathbf{r})$ and the displacement of the medium $\mathbf{u}(\mathbf{r})$ reduce.[1]

The eigenfunctions and the eigenvalues of Eq. (7) have the form

$$\begin{gathered}\Phi = \prod_k \exp\left\{-\frac{1}{2}(q_k - q_k^0)^2\right\} H_{n_k}(q_k - q_k^0), \quad E = \hbar\omega\sum_k\left(n_k + \frac{1}{2}\right) - \frac{c}{8\pi}D_k^2[\psi],\\ F_\alpha = \prod_\varkappa \exp\left\{-\frac{1}{2}(q_{\varkappa\alpha} - q_{\varkappa\alpha}^0)^2\right\} H_{n_\varkappa}(q_{\varkappa\alpha} - q_{\varkappa\alpha}^0)\\ E_\alpha = \sum_\varkappa \hbar\omega_{\varkappa\alpha}\left(n_\varkappa + \frac{1}{2}\right) - \frac{a^2}{2\rho}K_{-\varkappa}^2[\psi]\frac{\cos^2\theta_\alpha}{f_\alpha^2},\end{gathered} \tag{9}$$

n_k and $n_\varkappa$ are the quantum numbers of the oscillators, H_n are the Tschebycheff-Hermite polynomials of order n.

Use of Eqs. (9) allows us to represent the functions $\overline{H}$ in the form

$$\overline{H} = J[\psi] + \hbar\omega\sum_k\left(n_k + \frac{1}{2}\right) + \sum_{\varkappa\alpha}\hbar\omega_{\varkappa\alpha}\left(n_\varkappa + \frac{1}{2}\right), \tag{10}$$

where $J[\psi]$ is a function depending only on $\psi(\mathbf{r})$:

$$J[\psi] = \frac{\hbar^2}{2\mu_0}\int|\nabla\psi|^2\,d\tau - \frac{c}{8\pi}\sum_k D_k^2[\psi] - \frac{a^2}{2\rho}\sum_{\varkappa\alpha} f_\alpha^{-2}\cos^2\theta_\alpha K_{-\varkappa}^2[\psi]. \tag{11}$$

The procedure for further calculations requires a knowledge of the explicit form of the dependence of the quantities $\cos\theta_\alpha$ and f_α on $\varkappa$. For crystals with a lattice of the type NaCl, these dependencies can be found by making use of the results of Tolpygo.[6] It follows from his work that

$$\cos^2\theta_\alpha = \frac{[(k_1 + k_2 s_\alpha)z - (k_3 + k_4 s_\alpha)]^2}{Y_\alpha(k_1 + k_2 s_\alpha)^2 + (k_3 + k_4 s_\alpha)^2 - 2z(k_1 + k_2 s_\alpha)(k_3 + k_4 s_\alpha)}.$$

Here $k_1, k_2, \ldots, z$ are constants depending on the parameters of the crystal,

$$Y_\alpha = n_x^2/(n_x^2 - s_\alpha)^2 + n_y^2/(n_y^2 - s_\alpha)^2 + n_z^2/(n_z^2 - s_\alpha)^2, \quad \mathbf{n} = \boldsymbol{\varkappa}/|\boldsymbol{\varkappa}|,$$

s_α is a root of the cubic equation:

$$n_x^2/(n_x^2 - s) + n_y^2/(n_y^2 - s) + n_z^2/(n_z^2 - s) + z = 0.$$

The roots s_α (α = 1, 2, 3) correspond to the three branches of acoustic vibrations:

$$f_\alpha = v_\alpha el/\sqrt{\mu d},$$

μ is the reduced mass of the two ions of opposite sign, d is the shortest distance between them;

$$l = (\mu_1 + \mu_2)/[0{,}69557 - 4(a_{11} + a_{22})],$$

$\mu_i = m_i/\mu$ (i = 1, 2), m_i is the mass of the ion, a_{11} and a_{22} are functions of the parameters of the crystal;

$$v_\alpha^2 = 1 + 2zs_\alpha.$$

It is appropriate to approximate the quantity

$$B = \sum_\alpha B_\alpha = \sum_\alpha v_\alpha^{-2}\cos^2\theta_\alpha \tag{12}$$

by the expression

$$B = (c_0 + c_4 Y_4 + c_6 Y_6 + c_8 Y_8 + c_{10} Y_{10})^2, \tag{13}$$

where Y_i is a spherical function which is invariant relative to a rotation about the coordinate axes by $\pi/2$, and reflection from the coordinate planes.[9]

The coefficients c_i were determined by comparison of Eqs. (12) and (13) at five different points. The smoothness of the approximation is verified at seven other points.

The chosen approximation gives an error of the order of 10%. Changing from summation to integration in Eq. (11), we can write

$$J[\psi] = \frac{\hbar^2}{2\mu_0}\int |\nabla\psi|^2 d\tau - \frac{e^2 c}{2}\int \frac{\psi^2(1)\,\psi^2(2)}{r_1 - r_2}\,d\tau_1\,d\tau_2$$

$$-\frac{a^2}{2\rho}\frac{L^3}{8\pi^3}\int_0^\infty K_{-\varkappa}^2[\psi]\,\varkappa^2\,d\varkappa\int_0^{\pi/2}\sin\vartheta\,d\vartheta\int_0^{2\pi} B(\vartheta,\varphi)\,d\varphi,$$

L^3 is the volume of the fundamental cell of the crystal. $J[\psi]$ is minimized with respect to $\psi(r)$ by means of the approximating function

$$\psi_0(r) = (\alpha^3/7\pi)^{1/2}(1+\alpha r)\,e^{-\alpha r}. \qquad (14)$$

Use of (14) and (8) and rather tedious calculations permit us to determine $J[\psi]$ as a function of the parameter α of the approximation:

$$J_0[\alpha] = \frac{1}{14}\left\{\frac{3\hbar^2}{\mu_0}\alpha^2 - 3e^2 c\alpha - a^2\frac{\mu l Q_0 d}{\rho e^2}\frac{437}{2^9\cdot 7\pi^2}\alpha^3\right\},$$

$$Q_0 = \int_0^{\pi/2}\sin\vartheta\,d\vartheta\int_0^{2\pi} B(\vartheta,\varphi)\,d\varphi. \qquad (15)$$

The extremum condition $dJ_0/d\alpha = 0$ allows us to find the expression α corresponding to a minimum of the functional α_m:

$$\alpha_m = \hbar^2 e^2 g_0\left(1 - \sqrt{1 - \mu_0 c/\hbar^4 g_0}\right), \qquad (16)$$

$$g_0 = (2^9\cdot 7\pi^2/437)\,\rho/\mu a^2\mu_0 Q_0 l d. \qquad (17)$$

Expressions (15)–(17) determine the minimal value of the functional.

The above calculation can be carried as far as numerical results only for certain crystals, for which the dependence of f_α and $\cos\vartheta_\alpha$ on $\varkappa$ is known. Therefore, the approximate consideration of the ground state of the current carrier in polar crystals is of interest, under the assumption that the crystal is isotropic. In this case, using the results of Refs. 1 and 5, we can write the function $J[\psi]$ in the form

$$J[\psi] = \frac{\hbar^2}{2\mu_0}\int |\nabla\psi|^2 d\tau$$
$$-\frac{e^2 c}{2}\int\frac{\psi^2(1)\,\psi^2(2)}{r_1 - r_2}\,d\tau_1 d\tau_2 - \frac{a^2}{2(K + 4\mu/3)}\int\psi^4 d\tau. \qquad (18)$$

Here K and μ are the moduli of uniform compression and shear, respectively.

Using Eq. (14) as an approximating function, we get

$$J_0[\alpha] = \frac{3}{14}\frac{\hbar^2}{\mu_0}\alpha^2 - \frac{3}{14}e^2 c\alpha - \frac{437\,a^2}{49\cdot 2^9\pi(K + 4\mu/3)}\alpha^3. \qquad (19)$$

The condition $dJ_0/d\alpha = 0$ leads in this case to an expression for α_m analogous to Eq. (16), but with a value of g_0 different from Eq. (17):

$$g_0 = (2^8\cdot 7\pi/437)(K + 4\mu/3)/\mu_0 a^2 e^2. \qquad (20)$$

2. ENERGY OF THE FUNDAMENTAL STATE AND THE WAVE FUNCTION OF A SYSTEM IN THE ADIABATIC APPROXIMATION. EFFECTIVE MASS OF THE CURRENT CARRIER.

In the adiabatic approximation the energy of the system is computed in two ways: first, the configuration of the ions is fixed by giving the totality of the normal coordinates P_k; u_k or q_k, $q_\varkappa$. The state of the conduction electron corresponding to this configuration is determined by the equation

$$\left[-\frac{\hbar^2}{2\mu_0}\Delta + V_p(\mathbf{r}) + V_k(\mathbf{r})\right]\psi(\mathbf{r}) = E_0\psi(\mathbf{r}). \qquad (21)$$

Here $V_p(\mathbf{r})$ and $V_k(\mathbf{r})$ are expressed by Eqs. (2) and (3). The value of E_0 which is found enters as a component part in the energy of the "heavy" subsystem.

It is appropriate to replace Eq. (21) by the equivalent variational principle

$$E_0(\ldots P_k \ldots u_\varkappa \ldots) = \min_\psi\left\{\frac{\hbar^2}{2\mu_0}\int|\nabla\psi|^2 d\tau + \int V_p(\mathbf{r})\,|\psi|^2 d\tau + \int V_k(\mathbf{r})\,|\psi|^2 d\tau\right\}.$$

The total energy of the conduction electron in the longitudinal acoustic and optical vibrations is equal to

$$H = E_0(\ldots P_k \ldots u_\varkappa \ldots) + H_{\mathrm{op}} + H_{\mathrm{ac}}. \tag{22}$$

Solution of the Schrödinger equation with Hamiltonian (22) is very difficult in the general case. However, it is possible to find the solution for the equilibrium configuration of the ions, for which the potential energy of the ions is a minimum. This potential energy can be written in the form

$$F(\psi \ldots P_k \ldots u_\varkappa \ldots) = E_0(\ldots P_\varkappa \ldots u_\varkappa \ldots) + \sum_k \frac{2\pi}{c_k} P_k^2 + \frac{\rho}{2} \sum_\varkappa \omega_\varkappa^2 u_\varkappa^2.$$

Here the second and third terms are the potential energies of the optical and acoustical vibrations of the ions. Let us assume that the crystal is isotropic.

Minimizing F with respect to P_k and $u_\varkappa$, we get

$$P_k = c_k D_k / 4\pi; \quad u_\varkappa = -aK_{-\varkappa} / |\varkappa| (K + 4\mu/3). \tag{23}$$

Substitution of (23) reduces F to the functional $J[\psi]$ [Eq. (18)] which depends only on $\psi(\mathbf{r})$. Minimizing $J[\psi]$ was carried out above. The solutions obtained refer to an electron in a polaron-condenson well,* the center of which is at the origin of the coordinates. However, the current carrier can be localized at any point of the crystal. For a polaron-condenson with center at the point ξ, the equilibrium solution is obtained by a translation of the quantities $\psi_0(\mathbf{r})$, $\mathbf{P}_0(\mathbf{r})$, $\mathbf{u}_0(\mathbf{r})$, $V_{p0}(\mathbf{r})$ and $V_{k0}(\mathbf{r})$ through the vector $\boldsymbol{\xi}$. In complete analogy with Ref. 1, we represent the polarization $\mathbf{P}$ and the displacement $\mathbf{u}$ at an arbitrary point in the crystal in the form

$$\mathbf{P}(\mathbf{r}) = \mathbf{P}_0(\mathbf{r} - \xi) + \mathbf{P}'(\mathbf{r}); \quad \mathbf{u}(\mathbf{r}) = \mathbf{u}_0(\mathbf{r} - \xi) + \mathbf{u}'(\mathbf{r}),$$

where $\mathbf{P}'(\mathbf{r})$ and $\mathbf{u}'(\mathbf{r})$ can be regarded as small perturbations of the polarization and displacement, respectively, at those places in space where the polaro-condenson is localized, and where the terms $\mathbf{P}_0(\mathbf{r} - \boldsymbol{\xi})$ and $\mathbf{u}_0(\mathbf{r} - \boldsymbol{\xi})$ are large. In the rest of space, far from the polaro-condenson, $\mathbf{P}_0(\mathbf{r} - \boldsymbol{\xi})$ and $\mathbf{u}_0(\mathbf{r} - \boldsymbol{\xi})$ are small and the polarization and the displacement are defined by the vectors $\mathbf{P}'(\mathbf{r})$ and $\mathbf{u}'(\mathbf{r})$. In the zeroth approximations, the terms $\mathbf{P}'(\mathbf{r})$ and $\mathbf{u}'(\mathbf{r})$ are omitted; then the solution of Eq. (21) will be $\psi_0(\mathbf{r} - \boldsymbol{\xi})$. Introducing the terms $\mathbf{P}'(\mathbf{r})$ and $\mathbf{u}(\mathbf{r})$ as small perturbations, and making use of perturbation theory, we compute the energy of the electron in the first approximation. It is shown to be equal to

$$E(\ldots P_k \ldots u_\varkappa \ldots) = \frac{\hbar^2}{2\mu_0} \int |\nabla\psi|^2 d\tau - \int \mathbf{P}(\mathbf{r}) D_0(\mathbf{r} - \xi)\, d\tau + a \sum_\varkappa u_\varkappa |\varkappa| K_{-\varkappa}(\xi), \tag{24}$$

$$K_{-\varkappa}(\xi) = -\int [\psi_0(r - \xi)]^2 \chi_{-\varkappa}(r)\, d\tau.$$

Substituting Eqs. (23) and (24) in Eq. (22), and making use of the relation

$$\omega_\varkappa^2 = (K + 4\mu/3)\varkappa^2/\rho,$$

we get

$$H = J[\psi] + \sum_k \frac{2\pi}{c_k} P_k'^2 + \sum_k \frac{2\pi}{c_k \omega_k^2} \dot{P}_k^2 + \frac{1}{2}(K + 4\mu/3) \sum_\varkappa u_\varkappa'^2 \varkappa^2 + \frac{\rho}{2} \sum_\varkappa \dot{u}_\varkappa^2. \tag{25}$$

Introducing the notation

$$2\pi P_k^2 / c_k \omega_k^2 = \varphi_{1k}^2; \quad \rho u_\varkappa^2 / 2 = \varphi_{2k}^2; \quad 2\pi P_{k\xi}^2 / c_k \omega_k^2 = \varphi_{1k\xi}^2; \quad \rho u_{\varkappa\xi}^2 / 2 = \varphi_{2k\xi}^2, \tag{26}$$

---

* Such a development will be called hereinafter a polaro-condenson.

we can rewrite Eq. (25) in the form

$$H = J[\psi] + \sum_{\alpha=1}^{2} \sum_{k} [\dot{\varphi}_{\alpha k}^{2} + (\varphi_{\alpha k} - \varphi_{\alpha k \xi})^{2} \omega_{\alpha k}^{2}].$$

Transforming to canonically conjugate coordinates,

$$g_{\alpha k} = \dot{\varphi}_{\alpha k} \sqrt{2 / \hbar\omega_{\alpha k}}; \quad q_{\alpha k} = \varphi_{\alpha k} \sqrt{2\omega_{\alpha k} / \hbar}$$

and replacing $g_{\alpha k}$ by the operator $-i\partial/\partial q_{\alpha k}$, we get

$$H = J[\psi] + \frac{1}{2} \sum_{\alpha=1}^{2} \sum_{k} \hbar\omega_{\alpha k} [(q_{\alpha k} - q_{\alpha k \xi})^{2} - \partial^{2} / \partial q_{\alpha k}^{2}]. \quad (27)$$

We can determine the quantity ξ, which enters into Eq. (27), from the condition

$$\partial E(\ldots P_k \ldots u_\varkappa \ldots \xi) / \partial \xi_i = 0 \quad (i = 1, 2, 3),$$

which, with the use of the notation (26) and Eq. (23), can be written in the following form:

$$\sum_{\alpha} \sum_{k} \varphi_{\alpha k} \omega_{\alpha k}^{2} \partial \varphi_{\alpha k \xi} / \partial \xi_i = 0. \quad (28)$$

We can determine ξ in another manner; let us approximate φ_α by the function $\varphi_{\alpha\xi}$ by means of the method of least squares, and so choose ξ_i that the integral $\sum_{\alpha} \int (\varphi_\alpha - \varphi_{\alpha\xi})^{2} d\tau$ will be a minimum. In this case, in place of the condition (28), we get

$$\sum_{\alpha} \sum_{k} \varphi_{\alpha k} \partial \varphi_{\alpha k \xi} / \partial \xi_i = 0. \quad (29)$$

In a way similar to that used by Pekar,[7] we select (for the determination of ξ) an equation intermediate to (28) and (29):

$$\sum_{\alpha} \sum_{k} \varphi_{\alpha k} \omega_{\alpha k} \partial \varphi_{\alpha k \xi} / \partial \xi_i = 0$$

or, in normal coordinates

$$\sum_{\alpha} \sum_{k} q_{\alpha k} \partial q_{\alpha k \xi} / \partial \xi_i = 0. \quad (30)$$

By use of the method developed by Pekar, we can obtain a series of auxiliary relations which are necessary for what follows.

Defining the operators $\hat{\omega}_{1k}$ and $\hat{\omega}_{2k}$ by means of the relation

$$\hat{\omega}_{1k} \chi_k(r) = (\omega_0 + k^2\omega_1) \chi_k(r), \quad \hat{\omega}_{2k} \chi_k(r) = -k\chi_{-k}(r),$$

we can show that

$$\sum_{\alpha} \int [\hat{\omega}_{\alpha}^{n_1} \varphi_\alpha(r - \xi)] [\hat{\omega}_{\alpha}^{n_2} \varphi_\alpha(r - \xi)] d\tau = \sum_{\alpha} \int \varphi_\alpha(r) \hat{\omega}_{\alpha}^{n} \varphi_\alpha(r) d\tau.$$

We differentiate this equation with respect to ξ_i, recalling that $n_1 = n_2 = n/2$:

$$\sum_{\alpha} \int \frac{\partial \psi_\alpha(r - \xi)}{\partial \xi_i} \hat{\omega}_{\alpha}^{n} \varphi_\alpha(r - \xi) d\tau = 0,$$

and then differentiate with respect to ξ_j:

$$\sum_{\alpha} \int \frac{\partial \varphi_\alpha(r - \xi)}{\partial \xi_i} \frac{\partial \hat{\omega}_{\alpha}^{n} \varphi_\alpha(r - \xi)}{\partial \xi_j} = -\sum_{\alpha} \int \frac{\partial^2 \varphi_\alpha(r - \xi)}{\partial \xi_i \partial \xi_j} \hat{\omega}_{\alpha}^{n} \varphi_\alpha(r - \xi) d\tau = O_{ij}^{(n)}.$$

Thanks to the spherical symmetry of the functions $\varphi_\alpha(r)$ and $\hat{\omega}_{\alpha}^{n} \varphi_\alpha(r)$, $O_{ij}^{(n)} = \delta_{ji} O^{(n)}$. The total differential of Eq. (30) is then

$$\sum_{\alpha k} dq_{\alpha k} \partial q_{\alpha k \xi} / \partial \xi_i + \sum_{\alpha k} \sum_{j=1}^{3} q_{\alpha k} (\partial^2 q_{\alpha k \xi} / \partial \xi_i \partial \xi_j) d\xi_j = 0. \quad (31)$$

It is easy to show that

$$\sum_{\alpha k} \sum_{j} q_{\alpha k} \partial^2 q_{\alpha k \xi} / \partial \xi_i \partial \xi_j = -\frac{2}{\hbar} \delta_{ij} O^{(1)}.$$

Here we can transform Eq. (31) to the form

$$\frac{\partial q_{\alpha k\xi}}{\partial \xi_l} = \frac{2}{\hbar} O^{(1)} \frac{\partial \xi_l}{\partial q_{\alpha k}} \quad \text{or} \quad \frac{\partial \xi_l}{\partial q_{\alpha k}} = \frac{\hbar}{2O^{(1)}} \frac{\partial q_{\alpha k\xi}}{\partial \xi_l}.$$

These formulas allow us to establish the validity of the following equations:

$$\sum_{\alpha k} \sum_{j=1}^{3} \hbar\omega_{\alpha k} \frac{\partial \xi_l}{\partial q_{\alpha k}} \frac{\partial \xi_j}{\partial q_{\alpha k}} \frac{\partial^2}{\partial \xi_l \partial \xi_j} = \frac{\hbar^2 O^{(2)}}{2(O')^2} \sum_{j=1}^{3} \frac{\partial^2}{\partial \xi_j^2}, \tag{32a}$$

$$\sum_{\alpha k} \sum_{ij} \hbar\omega_{\alpha k} \frac{\partial \xi_j}{\partial q_{\alpha k}} \left(\frac{\partial}{\partial \xi_j} \frac{\partial \xi_i}{\partial q_{\alpha k}}\right) \frac{\partial}{\partial \xi_i} = \frac{\hbar^3}{4(O^1)^2} \sum_{\alpha k i j} \omega_{\alpha k} \frac{\partial q_{\alpha k\xi}}{\partial \xi_j} \frac{\partial^2 q_{\alpha k\xi}}{\partial \xi_i \partial \xi_j} \frac{\partial}{\partial \xi_j}. \tag{32b}$$

In the case of spherical symmetry of the function φ_α, Eq. (32b) will vanish.

The solution to Schrödinger's equation with operator $\hat{H}$ is sought in the form

$$\Psi(\ldots q_{\alpha k} \ldots) = U(\xi_1, \xi_2, \xi_3) \exp\left\{-\frac{1}{2} \sum_{\alpha k} (q_{\alpha k} - q_{\alpha k\xi})^2\right\},$$

the $q_{\alpha k}$ enter directly into Ψ, and are also contained in the ξ_i. We denote by $\frac{\partial}{\partial^* q_{\alpha k}}$ differentiation only with respect to the $q_{\alpha k}$ which do not enter into the ξ_i. In this case,

$$\frac{\partial^2}{\partial q_{\alpha k}^2} = \frac{\partial^2}{\partial^* q_{\alpha k}^2} + \frac{\partial \xi_i}{\partial q_{\alpha k}} \frac{\partial \xi_j}{\partial q_{\alpha k}} \frac{\partial^2}{\partial \xi_i \partial \xi_j} + \frac{\partial \xi_j}{\partial q_{\alpha k}} \left(\frac{\partial}{\partial \xi_j} \frac{\partial \xi_i}{\partial q_{\alpha k}}\right) \frac{\partial^2}{\partial \xi_i} + \frac{\partial \xi_i}{\partial q_{\alpha k}} \frac{\partial^2}{\partial \xi_i \partial^* q_{\alpha k}} + \frac{\partial \xi_i}{\partial q_{\alpha k}} \frac{\partial^2}{\partial^* q_{\alpha k} \partial \xi_i}. \tag{33}$$

Taking (30) into account, we can show that

$$\partial^2 \Psi / \partial \xi_i \partial^* q_{\alpha k} = 0, \qquad \partial^2 \Psi / \partial^* q_{\alpha k} \partial \xi_i = \Psi \partial q_{\alpha k\xi} / \partial \xi_i. \tag{34}$$

Considering Eqs. (27), (32a), (32b), (33) and (34), we get

$$H\Psi = \left\{J[\psi] + \frac{1}{2} \sum_{\alpha k} \hbar\omega_{\alpha k} - \frac{3}{2} \hbar \frac{O^{(2)}}{O^{(1)}} - \frac{\hbar^2}{2M} \Delta_\xi \right\} \Psi,$$

$$M = 2(O^1)^2 / O^{(2)}.$$

Thus the energy of the ground state of the polarocondenson is

$$H = J[\psi_0] + \frac{1}{2} \sum_{\alpha k} \hbar\omega_{\alpha k} - {}^3/_2\, \hbar (O^{(2)} / O^{(1)}). \tag{35}$$

It is easy to verify that for the polaron in the absence of dispersion of the optical frequencies, Eq. (35) takes the form

$$H = J[\psi_0] + \frac{\nu - 3}{2} \hbar\omega_0,$$

which coincides with the result of Ref. 1. Here ν is the general number of polarized longitudinal normal vibrations of the crystal in the volume L^3.

Computation of the integrals $O^{(1)}$ and $O^{(2)}$ permits us to express the effective mass of the polarocondenson explicity in terms of the parameters of the crystal. The integrals pertaining to the optical vibrations were computed earlier. Computation of the integrals pertaining to the acoustical vibrations lead to the following expression for the effective mass of the current carrier in an ionic crystal:

$$M = \frac{[437\cdot 70\, \pi^2 c e^2 E^2 + 183\cdot 128\, a^2 \sqrt{E\rho}\, \omega\alpha]^2 \alpha^3}{147\cdot 64 \pi^3 \omega^2 E^4 [49\cdot 437\, \pi c e^2 E + 43\cdot 147\, a^2 \alpha^2]} 10^{-2},$$

where α is determined by Eqs. (16) and (20), $E = K + 4\mu/3$.

3. INTERACTION OF THE ELECTRON OF THE F-CENTER WITH THE ACOUSTICAL VIBRATIONS OF THE LATTICE. COMPARATIVE ESTIMATE OF THE POLARON AND CONDENSON EFFECTS IN IONIC CRYSTALS.

The Hamiltonian of the F-centers – crystal system, analogous to Eq. (4), can be written in the form

$$\hat{H} = -\frac{\hbar^2}{2\mu_0} \Delta + e \int \frac{\mathbf{P}(\mathbf{r}_1)(\mathbf{r} - \mathbf{r}_1)}{|\mathbf{r} - \mathbf{r}_1|^3} d\tau_1 + a(u_{11} + u_{22} + u_{33}) - \frac{ze^2}{\varepsilon r} + \frac{\hbar\omega}{2} \sum_k (q_k^2 - \partial^2/\partial q_k^2) + \sum_{\varkappa\alpha} \frac{\hbar\omega_{\varkappa\alpha}}{2} (q_{\varkappa\alpha} - \partial^2/\partial q_{\varkappa\alpha}^2).$$

The result differs from Eq. (4) by the term $-ze^2/\varepsilon r$, which represents the energy of interaction of the electron with the Coulomb field of the defect.

With the aid of computations similar to those carried out in the first part of the work, we obtain for the energy of the ground state of the F-center in crystals of the type NaCl an expression similar to Eq. (10), in which $J[\psi]$ is equal to

$$J[\psi] = \frac{\hbar^2}{2\mu_0}\int |\nabla\psi|^2 d\tau - \frac{ze^2}{\varepsilon}\int\frac{|\psi|^2}{r}d\tau - \frac{e^2c}{2}\int\frac{\psi^2(1)\,\psi^2(2)}{(r_1-r_2)}d\tau_1\,d\tau_2 - \frac{a^2}{2\rho}\frac{L^3}{8\pi^3}\int K^2_{-\varkappa}[\psi]\,\varkappa^2\,d\varkappa\,B(\vartheta,\ \varphi)\sin\vartheta d\vartheta d\varphi.$$

Making use of the function (14), we obtain

$$J(\alpha) = \frac{1}{14}\left\{\frac{3\hbar^2}{\mu_0}\alpha^2 - \frac{3e^2}{\varepsilon}(3z+\varepsilon c)\,\alpha - a^2\frac{\mu l Q_0 d}{\rho e^2}\frac{437\alpha^3}{2^9\cdot 7\pi^2}\right\}, \tag{36}$$

$$\alpha_m = \hbar^2 e^2 g_0\left(1-\sqrt{\frac{\mu_0(3z+\varepsilon c)}{\hbar^4\varepsilon g_0}}\right), \tag{37}$$

where g_0 is defined by Eq. (17).

Calculation of the $2p$ state of the F-center is performed in an entirely similar way; the approximating function was chosen in the form

$$\varphi_{2p}(r) = \beta^{5/2}\pi^{-1/2}e^{-\beta r}\,r\cos\vartheta.$$

The energy of the excited state is determined by the expression

$$H_1 \doteq J[\beta] + \hbar\omega\sum_k\left(n'_k+\frac{1}{2}\right) + \sum_{\varkappa\alpha}\hbar\omega_{\varkappa\alpha}\left(n'_{\varkappa\alpha}+\frac{1}{2}\right),$$

where

$$\begin{gathered} J_1[\beta] = \frac{1}{2}\left\{\frac{\hbar^2}{\mu_0}\beta^2 - \frac{e^2}{\varepsilon}(z+0{,}3914\varepsilon c)\,\beta - a^2\frac{\mu l d}{\rho e^2}\frac{1}{2^9\pi^2}(14Q_0-42Q_2+45Q_4)\,\beta^3\right\}, \\ \beta = \hbar^2 e^2 g_1\left\{1-\sqrt{1-(\mu_0/\varepsilon\hbar^4)(z+0{,}3914\varepsilon c)/g_1}\right\}, \end{gathered} \tag{38}$$

$$Q_k = \int_0^{\pi/2}\cos^k\vartheta\sin\vartheta d\vartheta\int_0^{2\pi}B(\vartheta,\ \varphi)\,d\varphi, \qquad g_1 = 2^9\pi^2\rho/3\mu_0 a^2\mu l d\,(14Q_0-42Q_2+45Q_4). \tag{39}$$

According to Ref. 8, the frequency of the maximum of the absorption band of the local centers is computed from the equation

$$\hbar\Omega_{\max} = |J_0 - J_1| + {}^1\!/_2\,a\hbar\omega + \hbar\sigma_1. \tag{40}$$

The half width of the corresponding absorption band, in the limiting cases of high and low temperatures, is determined by the expressions

$$\delta = 2\sqrt{2\ln 2}\sqrt{kT(a_0\hbar\omega+2\hbar\sigma_1)}, \quad \delta^0 = 2\sqrt{2\ln 2}\sqrt{{}^1\!/_2(\hbar\omega)^2a_0+\hbar^2\sigma_2}, \tag{41}$$

where

$$a_0 = \sum_k (q^0_{k1s} - q^0_{k2p})^2; \quad \sigma_1 = \frac{1}{2} \sum_{\varkappa\alpha} (q^0_{\varkappa\alpha 1s} - q^0_{\varkappa\alpha 2p})^2 \, \omega_{\varkappa\alpha}; \quad \sigma_2 = \frac{1}{2} \sum_{\varkappa\alpha} (q^0_{\varkappa\alpha 1s} - q^0_{\varkappa\alpha 2p})^2 \, \omega^2_{\varkappa\alpha}.$$

The quantity $a_0\hbar\omega/2$ was computed in Ref. 1; calculations that are cumbersome, but that present no difficulties in principle, let us determine $\hbar\sigma_1$ and $\hbar^2\sigma_2$:

$$\begin{gathered} \hbar\sigma_1 = \frac{a^2\mu \, ld \, \alpha^3}{2\pi^2\rho e^2} \left\{ \frac{437}{2^9 \cdot 49} Q_0 + \frac{1}{2^9} \frac{1}{v^3} (14Q_0 - 42Q_2 + 45Q_4) \right. \\ \left. - \frac{1}{28\,(v+1)^7} [(7v^4 + 49v^3 + 66v^2 + 28v + 4)\, Q_0 - 3v^2 (7v^2 + 49v + 12)\, Q_2] \right\}, \end{gathered} \tag{42}$$

$$\begin{gathered} \hbar^2\sigma_2 = \frac{a^2\hbar \sqrt{l\mu d}\, \alpha^4}{2\pi^3\rho e} \left[\frac{183}{7^3 \cdot 10} Q'_0 + \frac{1}{70v^4} (7Q'_0 - 28Q'_2 + 36Q'_4) \right. \\ - \frac{4}{7} \left\{ \frac{(21v^8 + 288v^6 - 270v^4 - 48v^2 + 9)\, Q'_0 - 12(7v^8 + 192v^6 + 165v^4 - 4v^2)\, Q'_2}{6\,(v^2-1)^6} \right. \\ \left. \left. + \frac{6v^2 \ln v}{(v^2-1)^7} [(-9v^6 - 3v^4 + 13v^2 - 1)\, Q'_0 + (54v^6 + 150v^4 + 38v^2 - 2)\, Q'_2] \right\} \right], \end{gathered} \tag{43}$$

where

$$v = \alpha/\beta; \quad Q'_k = \int_0^{\pi/2} \cos^k \vartheta \sin \vartheta \, d\vartheta \int_0^{2\pi} \Big(\sum_\alpha B_\alpha v_\alpha \Big) \, d\varphi.$$

In the approximation in which the crystal is considered isotropic, Eqs. (36), (38), (42), and (43) take the form

$$\begin{gathered} J[\alpha] = \frac{3\hbar^2}{14\mu_0} \alpha^2 - \frac{3e^2}{14\varepsilon} (3z + \varepsilon c)\, \alpha - \frac{437}{49 \cdot 2^9 \pi} \frac{a^2}{(K + 4\mu/3)} \alpha^3, \\ J[\beta] = \frac{\hbar^2}{2\mu_0} \beta^2 - \frac{e^2}{2\varepsilon} (z + 0{,}3914\varepsilon c)\, \beta - \frac{9}{2^9\pi} \frac{a^2}{(K + 4\mu/3)} \beta^3, \\ \hbar\sigma_1 = \frac{a^2\alpha^3}{K + 4\mu/3} \left\{ 0{,}00555 - 0{,}0227 \frac{27v^2 + 14v + 2}{(v+1)^7} + \frac{1}{v^3} 0{,}00560 \right\}, \\ \hbar^2\sigma_2 = \frac{a^2\alpha^4}{\sqrt{\rho\,(K + 4\mu/3)}} \left\{ 0{,}00540 + 0{,}00704 \frac{1}{v^4} + 0{,}00965 \frac{1}{(v^2-1)^7} [(v^2 - 1)(7v^8 \right. \\ \left. + 480v^6 + 930v^4 + 32v^2 - 9) - 12v^2 \ln v \,(27v^6 + 141v^4 + 77v^2 - 5)] \right\}. \end{gathered} \tag{44}$$

Here α is determined from (37) and (20), and β from (39), but with a different value of g_1:

$$g_1 = 2^8\pi\,(K + 4\mu/3)/27\mu_0 a^2 e^2.$$

The theory contains two parameters, a and μ_0. Their determination is possible by comparison of the theoretically computed values of δ and $\hbar\Omega_{\max}$ with the corresponding experimental parameters of the F-band.

The best agreement of the theoretical and experimental data for the alkali halide crystals, considered in Ref. 1, is obtained if we set $a = 0$, which demonstrates the small value of the condenson effect in these crystals.

Unfortunately, the absence of a complete set of experimental data for other crystals compels us to limit ourselves only to estimates.

The most favorable of the crystals known to us in regard to the experimental data is Cu_2O. But even here information is lacking on the dispersion of the vibration frequencies of the lattice. For this reason, we restrict ourselves to a comparative estimate of the polaron and condenson effects in the approximation in which the crystal is regarded as isotropic. Availing ourselves of the data[9] for F bands, and of the expressions (40) and (41), we can determine μ_0/m and a approximately:

$$\mu_0/m \approx 0.9; \quad |a| \approx 7\ \text{eV}.$$

From these parameters we estimated the polaron and condenson terms in (19) and (44). It turned out that for the polaro-condenson the magnitude of the condenson term amounted to about 10% of the total energy, while for the F-center, to about 25%.

The values of the effective masses of the bound electron and the current carrier change appreciably in comparison with the corresponding values obtained without regard to the condenson effect. Thus μ_0/m appeared to be two times smaller than the value in Ref. 1, while $M/m = 7.63$ instead of 9.69 as in Ref. 1.

---

[1] S. I. Pekar, *Studies on the Electronic Theory of Crystals*, GITTL, 1951.

[2] Iu. E. Perlin, J. Exptl. Theoret. Phys. (U.S.S.R.) 21, 547 (1951).

[3] H. A. Bethe and A. Sommerfeld, *Electron Theory of Metals*, ONTI, 1938 (Russ. transl.).

[4] M. F. Deigen and S. I. Pekar, J. Exptl. Theoret. Phys. (U.S.S.R.) 21, 803 (1951).

[5] M. F. Deigen, J. Exptl. Theoret. Phys. (U.S.S.R.) 31, 504 (1956); Soviet Phys. JETP 4, 424 (1957).

[6] K. B. Tolpygo, Trudy, Physical Inst. Academy of Sciences, Ukrainian SSR 6, (1954).

[7] S. I. Pekar, J. Exptl. Theoret. Phys. (U.S.S.R.) 27, 411 (1954).

[8] M. A. Krivoglaz and S. I. Pekar, Trudy, Physical Inst., Academy of Sciences, Ukrainian SSR 4, 37 (1953).

[9] B. Schönwald, Ann. Phys. 15, 395 (1932).

[10] W. Shockley, *Theory of Electronic Semiconductors*, IIL, 1955 (Russ. transl.).

Translated by R. T. Beyer
278

SOVIET PHYSICS JETP VOLUME 5, NUMBER 6 DECEMBER 15, 1957

Dispersion Relations for Photoproduction of Pions on Nucleons*

A. A. LOGANOV AND A. N. TAVKHELIDZE

(Submitted to JETP editor July 24, 1956)
J. Exptl. Theoret. Phys. (U.S.S.R.) 32, 1393-1403 (June, 1957)

Dispersion relations are derived for pion photoproduction reactions on nucleons. The spin and isotopic structure of the reaction amplitude is established, and the unobservable energy range is separated. It is shown that the dispersion relations are inhomogeneous.

FORMAL SCATTERING THEORY, based on the unitarity and asymmetry of the scattering matrix, leads to an expression for the amplitude in terms of phase shifts. The values of the phase shifts depend on the dynamics of the collision process. Since the character of the dynamics of the process is not taken into account in the formulation of the formal scattering theory, it is natural that the values of the phases remain unknown in such an analysis. The determination of phase shifts from experimental data is of great interest, for it permits a deeper study of the character of the meson-nucleon collisions. Using the charge-independence hypothesis in the s- and p-wave approximation it becomes possible to find several possible sets of phase shifts for the meson-nucleon collisions. This ambiguity can be eliminated using the causality principle. In fact, Goldberger[1] has found the Hermitian and anti-Hermitian portions of the forward-scattering amplitude to be connected by dispersion relations that lead to a correct choice of phase shifts for the meson-nucleon collision processes.

N. N. Bogoliubov* developed general principles for the derivation of dispersion relations for a great variety of scattering processes. His method is essentially based on analyticity theorems that follow from the principle of causality.

In the present article we shall use the Bogoliubov method to derive dispersion relations for the photoproduction of mesons on nucleons.[3]

---

*Paper delivered at the All-Union Conference on Physics of High Energy Particles on May 15, 1956.

* Reported by N. N. Bogoliubov to many seminars on theoretical physics in the V. A. Steklov Mathematics Institute in January 1956.

1. AMPLITUDE OF THE PHOTOPRODUCTION REACTION

Let us denote by $\varphi_\rho^{(-)}(q)$, the operator for the annihilation of a meson of type ρ ($\rho = 1, 2, 3$), and by $a_\nu^{(+)}(k)$ the operator of photon production ($\nu = 0, 1, 2, 3$). The matrix element for the photoproduction reaction can then be written with the aid of the S-matrix formalism in the form

$$S(\alpha, k; \omega, q) = (2\pi)^3 < \Phi^*_{p's'} \varphi_\rho^{(-)}(q) S a_\nu^{(+)}(k) \Phi_{ps} > . \tag{1.1}$$

Here Φ denotes the amplitude of the state of the scatterer, and the indices α and ω, which pertain to the initial and final states respectively, include all the quantum numbers that characterize the system with the exception of the momenta of the photon and meson.

Since

$$\begin{aligned} A_\nu(x) &= \frac{1}{(2\pi)^{3/2}} \int \frac{d\mathbf{k}}{\sqrt{2k^0}} \{e_{\nu\lambda}(\mathbf{k})\, a_\lambda^{(+)}(\mathbf{k})\, e^{ikx} + e_{\nu\lambda}(k)\, a_\lambda^{(-)}(\mathbf{k})\, e^{-ikx}\}, \\ \varphi_\rho(x) &= \frac{1}{(2\pi)^{3/2}} \int \frac{d\mathbf{q}}{\sqrt{2q^0}} \{\varphi_\rho^{(+)}(\mathbf{q})\, e^{iqx} + \varphi_\rho^{(-)}(\mathbf{q})\, e^{-iqx}\}, \end{aligned} \tag{1.2}$$

we have

$$[\varphi_\rho^{(-)}(\mathbf{q}), \varphi_\rho(x)] = \frac{(2\pi)^{-3/2}}{\sqrt{2q^0}} e^{iqx}, \quad [A_\mu(x), a_\nu^{(+)}(\mathbf{k})] = \frac{(2\pi)^{-3/2}}{\sqrt{2k_0}} e_\mu^\nu e^{-ikx} \tag{1.3}$$

and consequently

$$[\varphi_\rho^{(-)}(\mathbf{q}), S] = \frac{(2\pi)^{-3/2}}{\sqrt{2q^0}} \int e^{iqx} \frac{\delta S}{\delta \varphi_\rho(x)}\, dx, \quad [S, a_\nu^{(+)}(\mathbf{k})] = \frac{(2\pi)^{-3/2}}{\sqrt{2k^0}} e_\mu^\nu \int e^{-iky} \frac{\delta S}{\delta A_\mu(y)}\, dy. \tag{1.4}$$

Transposing the creation operators in (1.1) to the extreme left position, and the annihilation operators to the extreme right, we obtain with the aid of (1.4)

$$S(\alpha, k; \omega, q) = \sum_\mu e_\mu^\nu S_{\mu\rho}. \quad S_{\mu\rho} = \frac{1}{\sqrt{4k^0 q^0}} \int e^{i(qx-ky)} \left\langle \Phi^*_{p's'} \frac{\delta^2 S}{\delta\varphi_\rho(x)\, \delta A_\mu(y)} \Phi_{ps} \right\rangle dx\, dy. \tag{1.5}$$

We shall assume that Φ_{ps} describes a scatterer in the lower energy state. No spontaneous processes can occur therefore, and

$$S\Phi_{ps} = \Phi_{ps}, \tag{1.6}$$

or from the unitarity of the S-matrix

$$S^+ \Phi_{ps} = \Phi_{ps}. \tag{1.7}$$

Taking (1.7) into account, we can rewrite (1.5) as

$$S_{\mu\rho} = \frac{1}{\sqrt{4k^0 q^0}} \int e^{i(qx-ky)} \langle \Phi^*_{p's'} \frac{\delta^2 S}{\delta\varphi_\rho(x)\, \delta A_\mu(y)} S^+ \Phi_{ps} \rangle. \tag{1.8}$$

Let us introduce the operators

$$j_\rho(x) = i \frac{\delta S}{\delta\varphi_\rho(x)} S^+, \quad i_\mu(y) = i \frac{\delta S}{\delta A_\mu(y)} S^+ \tag{1.9}$$

and call them respectively the meson-current $j_\rho(x)$ and electromagnetic-current $i_\mu(y)$ operators. These operators are Hermitian. In fact

$$j_\rho^+(x) = -iS\delta S^+ / \delta\varphi_\rho(x),$$

but since $S^+S = 1$,

$$S\frac{\delta S^+}{\delta\varphi_\rho(x)} = -\frac{\delta S}{\delta\varphi_\rho(x)}S^+$$

and consequently

$$j_\rho^+(x) = j_\rho(x). \tag{1.10}$$

Analogously

$$i_\mu^+(x) = i_\mu(x). \tag{1.11}$$

Variation of (1.9) leads to

$$\frac{\delta^2 S}{\delta A_\mu(y)\,\delta\varphi_\rho(x)}S^+ = -j_\rho(x)\,i_\mu(y) - i\frac{\delta j_\rho(x)}{\delta A_\mu(y)},\quad \frac{\delta^2 S}{\delta A_\mu(y)\,\delta\varphi_\rho(x)}S^+ = -i_\mu(y)\,j_\rho(x) - i\frac{\delta i_\mu(y)}{\delta\varphi_\rho(x)}. \tag{1.12}$$

Subtracting one equation from the other, we get

$$\delta i_\mu(y)/\delta\varphi_\rho(x) - \delta j_\rho(x)/\delta A_\mu(y) = -i\,[j_\rho(x)\,i_\mu(y) - i_\mu(y)\,j_\rho(x)]. \tag{1.13}$$

Changing to the Heisenberg representation, we write

$$\langle\Phi^*_{p's'}\,j_\rho(x)\,i_\mu(y)\,\Phi_{ps}\rangle = \langle\Psi^*_{p's'}\,J_\rho(x)\,I_\mu(y)\,\Psi_{ps}\rangle. \tag{1.14}$$

Here J and I are the current operators in the real-particle representation, and Ψ_{ps} – the amplitude of state of the nucleon in the same representation. Let us assume that the energy-momentum operator in this system has a complete set of eigenfunctions, denoted by $\Psi_{n,\,k_n}$. The index $\mathbf{k}_n$ denotes the momentum of the system, and n represents the remaining quantum numbers that determine the state of the system. The energy of the nth state of the system will be

$$E_n = \sqrt{M_n^2 + \mathbf{k}_n^2}. \tag{1.15}$$

From the assumption of the completeness of the system we can write

$$\langle\Psi^*_{p's'}\,J_\rho(x)\,I_\mu(y)\,\Psi_{ps}\rangle = \frac{1}{(2\pi)^3}\sum_n\int d\mathbf{k}_n\,\langle\Psi^*_{p's'}J_\rho(x)\,\Psi_{n,\,k_n}\rangle\,\langle\Psi^*_{n,\,k_n}\,I_\mu(y)\,\Psi_{ps}\rangle. \tag{1.16}$$

Translational-invariance considerations permit representation of the operators J_ρ and I_μ in the following form

$$J_\rho(x) = e^{i\hat{P}x}\,J_\rho(0)\,e^{-i\hat{P}x},\quad I_\mu(y) = e^{i\hat{P}y}\,I_\mu(0)\,e^{-i\hat{P}y}. \tag{1.17}$$

Inserting (1.17) into (1.16) and recalling that $\Psi_{n,\,k_n}$ are eigenfunctions of the operator $\hat{P}$ we get

$$\begin{gathered}\langle\Psi^*_{p's'}\,J_\rho(x)\,I_\mu(y)\,\Psi_{ps}\rangle = (2\pi)^{-3}\sum_n\int d\mathbf{k}_n\,\langle\Psi^*_{p's'}\,J_\rho(0)\,\Psi_{n,\,k_n}\rangle\langle\Psi^*_{n,\,k_n}I_\mu(0)\,\Psi_{ps}\rangle\\ \times\exp\left\{-ik_n(x-y) + \frac{i}{2}(p+p')(x-y) + \frac{i}{2}(p'-p)(x+y)\right\},\quad k_n\cdot x = x^0\sqrt{M_n^2+\mathbf{k}_n^2} - \mathbf{k}_n\mathbf{x}.\end{gathered} \tag{1.18}$$

Introducing the notation

$$F_{\mu\rho}^{ps;\,p's'}(x-y)=(2\pi)^{-3}\sum_n\int d\mathbf{k}_n\langle\Psi^{*}_{p's'}J_\rho(0)\Psi_{n,\,k_n}\rangle\langle\Psi^{*}_{n,\,k_n}I_\mu(0)\Psi_{ps}\rangle$$
$$\times\exp\left\{-ik_n(x-y)+\frac{i}{2}(p+p')(x-y)\right\}, \tag{1.19}$$

we can rewrite (1.18) as

$$\langle\Psi^{*}_{p's'}J_\rho(x)I_\mu(y)\Psi_{ps}\rangle=e^{i(p'-p)(x+y)/2}F_{\mu\rho}^{ps;\,p's'}(x-y). \tag{1.20}$$

Analogously, translational-invariance considerations lead to

$$\langle\Phi^{*}_{p's'}\frac{\delta^2S}{\delta A_\mu(y)\,\delta\varphi_\rho(x)}S^{+}\Phi_{ps}\rangle=e^{i(p'-p)(x+y)/2}V_{\mu\rho}^{ps;\,p's'}(x-y), \tag{1.21a}$$

$$\langle\Phi^{*}_{p's'}\frac{\delta i_\mu(y)}{\delta\varphi_\rho(x)}\Phi_{ps}\rangle=e^{i(p'-p)(x+y)/2}W_{\mu\rho}^{ps;\,p's'}(x-y), \tag{1.21b}$$

$$\langle\Phi^{*}_{p's'}i_\mu(y)j_\rho(x)\Phi_{ps}\rangle=e^{i(p'-p)(x+y)/2}F_{\rho\mu}^{ps;\,p's'}(y-x). \tag{1.21c}$$

Let us establish certain relationships between the functions F, V, and W. It follows from (1.20) and (1.21) that

$$F_{\mu\rho}^{*ps;\,p's'}(x)=F_{\rho\mu}^{p's';\,ps}(-x). \tag{1.22}$$

Using (1.12) and (1.13) we get

$$V_{\mu\rho}^{ps;\,p's'}(x)=-iW_{\mu\rho}^{ps;\,p's'}(x)-F_{\rho\mu}^{ps;\,p's'}(-x), \tag{1.23a}$$

$$W_{\mu\rho}^{ps;\,p's'}(x)-W_{\rho\mu}^{ps;\,p's'}(-x)=-i\,[F_{\mu\rho}^{ps;\,p's'}(x)-F_{\rho\mu}^{ps;\,p's'}(-x)], \tag{1.23b}$$

$$W_{\mu\rho}^{*ps;\,p's'}(x)=W_{\mu\rho}^{p's';\,ps}(x). \tag{1.23c}$$

According to (1.21a), Eq. (1.8) can be written as

$$S_{\mu\rho}=(4k^0q^0)^{-1/2}\int dx\,dy\exp\left\{\frac{i}{2}(k+q)(x-y)+\frac{i}{2}(q-k)(x+y)+\frac{i}{2}(p'-p)(x+y)\right\}V_{\mu\rho}^{ps;\,p's'}(x-y), \tag{1.24}$$

from which we obtain after integrating over $(x+y)$

$$S_{\mu\rho}=i\,(2\pi)^4(4k^0q^0)^{-1/2}\delta(p'-p+q-k)\,T_{\mu\rho}^{ps;\,p's'}\left(\frac{k+q}{2}\right), \tag{1.25}$$

where

$$T_{\mu\rho}^{ps;\,p's'}\left(\frac{k+q}{2}\right)=-i\int e^{i(k+q)x/2}V_{\mu\rho}^{ps;\,p's'}(x)\,dx.$$

2. AUXILIARY REACTION AMPLITUDE AND ITS PROPERTIES

The expression (1.25) is too complicated for investigation. Let us introduce the amplitude

$$\mathfrak{M}(\alpha,k;\omega,q)=-i\,(4k^0q^0)^{-1/2}\sum_\mu e_\mu^\nu\int e^{i(qx-ky)}\langle\Phi^{*}_{p's'}\frac{\delta i_\mu(y)}{\delta\varphi_\rho(x)}\Phi_{ps}\rangle\,dx\,dy, \tag{2.1}$$

which, on the basis of (1.21c), can be rewritten

$$\begin{aligned}\mathfrak{M}(\alpha, k; \omega, q) = &-i\,(4k^0q^0)^{-1/2} \sum_{\mu} e_{\mu}^{\nu} \int dx\, dy \cdot \exp\Big\{\frac{i}{2}(x+y)(q-k) \\ &+ \frac{i}{2}(k+q)(x-y) + \frac{i}{2}(p'-p)(x+y)\Big\} W_{\mu\rho}^{ps;\,p's'}(x-y).\end{aligned} \tag{2.2}$$

Integrating over $(x + y)$ we get

$$\begin{aligned}\mathfrak{M}(\alpha, k; \omega, q) &= i\,(2\pi)^4 (4k^0q^0)^{-1/2}\, \delta(p'-p+q-k) \sum_{\mu} e_{\mu}^{\nu} M_{\mu\rho}^{ps;\,p's'}\left(\frac{k+q}{2}\right), \\ M_{\mu\rho}^{ps;\,p's'}\left(\frac{k+q}{2}\right) &= -\int e^{i(k+q)x/2}\, W_{\mu\rho}^{ps;\,p's'}(x)\, dx.\end{aligned} \tag{2.3}$$

We shall show that in the observed region (real momenta, positive energies) the amplitudes T and M are equal. Subtracting (2.3) from (1.25) and taking (1.23a) into account, we get

$$T_{\mu\rho}^{ps;\,p's'}\left(\frac{k+q}{2}\right) - M_{\mu\rho}^{ps;\,p's'}\left(\frac{k+q}{2}\right) = i\int e^{i(k+q)x/2}\, F_{\rho\mu}^{ps;\,p's'}(-x)\, dx. \tag{2.4}$$

Inserting the expression (1.19) for F into (2.4) we get by elementary computations

$$\begin{aligned} &T_{\mu\rho}^{ps;\,p's'}\left(\frac{k+q}{2}\right) - M_{\mu\rho}^{ps;\,p's'}\left(\frac{k+q}{2}\right) \\ &= 2\pi i \sum_{n} \langle \Psi_{p's'}^{*} I_{\mu}(0)\, \Psi_{n,\,k_n} \rangle \langle \Psi_{n,\,k_n}^{*} J_{\rho}(0)\, \Psi_{ps} \rangle\, \delta\left(\sqrt{M_n^2 + \mathbf{k}_n^2} + \frac{k^0+q^0}{2} - \frac{p^0+p^{0\prime}}{2}\right), \\ &\mathbf{k}_n = (\mathbf{p} + \mathbf{p}' - \mathbf{q} - \mathbf{k})/2.\end{aligned} \tag{2.5}$$

It can be shown that the argument of the δ-function is greater than zero in the observed region.

Actually, using the energy-momentum conservation laws

$$k^0 - p^{0\prime} = q^0 - p^0, \quad \mathbf{p}' - \mathbf{k} = \mathbf{p} - \mathbf{q},$$

we get

$$\sqrt{M_n^2 + \mathbf{k}_n^2} + \frac{k^0+q^0}{2} - \frac{p^0+p^{0\prime}}{2} = \sqrt{M_n^2 + (\mathbf{p}-\mathbf{q})^2} + \sqrt{\mu^2 + \mathbf{q}^2} - \sqrt{M^2 + \mathbf{p}^2}.$$

Since $M_n \gg M$, to prove the above statement it is necessary to show that

$$\sqrt{M^2 + (\mathbf{p}-\mathbf{q})^2} > \sqrt{M^2 + \mathbf{p}^2} - \sqrt{\mu^2 + \mathbf{q}^2}.$$

The correctness of this inequality is readily proved by squaring both sides. Thus, T and M are equal in the real-amplitude region.

We shall operate hereinafter in a coordinate system in which

$$\mathbf{p} + \mathbf{p}' = 0. \tag{2.6}$$

Using the energy and momentum conservation laws

$$\mathbf{k}^2 = \mu^2 + \mathbf{q}^2; \quad \mathbf{k} - \mathbf{q} = -2\mathbf{p},$$

we get

$$^1/_2\,(\mathbf{k} - \mathbf{q}) = -\mathbf{p}; \quad ^1/_2\,(\mathbf{k} + \mathbf{q}) = \lambda\mathbf{e} - (\mu^2 / 4\mathbf{p}^2)\,\mathbf{p}, \tag{2.7}$$

where λ is arbitrary. The vector **e** is orthogonal to the vector **p**. Hence

$$\mathbf{k} = \lambda\mathbf{e} - (1 + \mu^2 / 4\mathbf{p}^2)\,\mathbf{p}, \quad \mathbf{q} = \lambda\mathbf{e} + (1 - \mu^2 / 4\mathbf{p}^2)\,\mathbf{p}. \tag{2.8}$$

The quantity λ can be expressed in terms of the meson energy E as follows:

$$E^2 = \lambda^2 + (1 + \mu^2 / 4\mathbf{p}^2)^2\,\mathbf{p}^2. \tag{2.9}$$

Having made the above remarks concerning the chosen coordinate system, we turn to the study of the properties of the amplitude M. Let us represent the amplitude M in the form

$$M_{\mu\rho}^{ps;\,p's'} = D_{\mu\rho}^{ps;\,p's'} + i\,A_{\mu\rho}^{ps;\,p's'}, \tag{2.10}$$

where

$$D_{\mu\rho}^{ps;\,p's'} = \frac{1}{2}(M_{\mu\rho}^{ps;\,p's'} + M_{\rho\mu}^{*p's';\,ps}), \quad A_{\mu\rho}^{ps;\,p's'} = \frac{1}{2i}(M_{\mu\rho}^{ps;\,p's'} - M_{\rho\mu}^{*p's';\,ps}). \tag{2.10a}$$

Inserting the expression (2.3) for M into (2.10a) and taking the properties (1.23) into account, we get

$$A_{\mu\rho}^{ps;\,p's'}\left(\frac{k+q}{2}\right) = {}^1/_2\int e^{i(k+q)x|2}\,\{F_{\mu\rho}^{ps;\,p's'}(x) - F_{\rho\mu}^{ps;\,p's'}(-x)\}, \tag{2.11}$$

$$D_{\mu\rho}^{ps;\,p's'}\left(\frac{k+q}{2}\right) = -{}^1/_2\int e^{i(k+q)x|2}\,\{W_{\mu\rho}^{ps;\,p's'}(x) + W_{\rho\mu}^{ps;\,p's'}(-x)\}. \tag{2.12}$$

Let us introduce functions X and Y such that

$$X_{\nu\rho}^{ps;\,p's'}\left(\frac{k+q}{2}\right) = \sum_{\mu} e_{\mu}^{\nu}\,D_{\mu\rho}^{ps;\,p's'}\left(\frac{k+q}{2}\right), \tag{2.13}$$

$$Y_{\nu\rho}^{ps;\,p's'}\left(\frac{k+q}{2}\right) = \sum_{\mu} e_{\mu}^{\nu}\,A_{\mu\rho}^{ps;\,p's'}\left(\frac{k+q}{2}\right). \tag{2.14}$$

Using (2.11) and (2.12), as well as the invariance of the reaction amplitude under reflection of momenta, we can obtain the following important relations

$$P_{ss'}\,X_{\nu\rho}^{*ps;\,p's'}\left(\frac{k^0+q^0}{2};\ \frac{\mathbf{k}+\mathbf{q}}{2}\right) = X_{\nu\rho}^{ps;\,p's'}\left(-\frac{k^0+q^0}{2},\ \frac{\mathbf{k}+\mathbf{q}}{2}\right), \tag{2.15}$$

$$P_{ss'}\,Y_{\nu\rho}^{*ps;\,p's'}\left(\frac{k^0+q^0}{2},\ \frac{\mathbf{k}+\mathbf{q}}{2}\right) = -Y_{\nu\rho}^{ps;\,p's'}\left(-\frac{k^0+q^0}{2},\ \frac{\mathbf{k}+\mathbf{q}}{2}\right). \tag{2.16}$$

$P_{ss'}$ is the spin commutation operator. In fact

$$Y_{\nu\rho}^{*ps;\,p's'}\left(\frac{k+q}{2}\right) = +{}^1/_2\int e^{-i(k+q)x|2}\,\{F_{\mu\rho}^{*ps;\,p's'}(x) - F_{\rho\mu}^{*ps;\,p's'}(-x)\}\,e_{\mu}^{\nu}\,dx.$$

taking (1.22) into account, this expression can be rewritten as

$$Y^{*ps;\,p's'}_{\nu\rho}\left(\frac{k+q}{2}\right) = -{}^1/_2\int e^{-i(k+q)x/2}\,\{F^{p's';\,ps}_{\mu\rho}(x) - F^{p's';\,ps}_{\rho\mu}(-x)\}\,e^{\nu}_{\mu}\,dx. \tag{2.17}$$

Comparing (2.17) with (2.14) and taking into account the invariance of the reaction amplitude under reflection of the momenta,

$$\mathbf{k}\to-\mathbf{k},\quad \mathbf{q}\to-\mathbf{q},\quad \mathbf{p}\to-\mathbf{p},\quad \mathbf{p}'\to-\mathbf{p}'\quad (\mathbf{p}=-\mathbf{p}'),$$

one can readily check the correctness of (2.16) in the chosen coordinate system. Analogously, one can prove (2.15).

Equations (2.15) and (2.16) can be used to make up the combinations

$$(1\pm P)\,X^{ps;\,p's'}_{\nu\rho} = X^{ps;\,p's'}_{\nu\rho} \pm P_{ss'}\,X^{*ps;\,p's'}_{\nu\rho}, \tag{2.18}$$

$$(1\pm P)\,Y^{ps;\,p's'}_{\nu\rho} = Y^{ps;\,p's'}_{\nu\rho} \pm P_{ss'}\,Y^{*ps;\,p's'}_{\nu\rho}, \tag{2.19}$$

which have the following parity properties relative to E:

$$\begin{aligned}&(1+P)\,X^{ps;\,p's'}_{\nu\rho} \text{ — even},\\ &(1-P)\,X^{ps;\,p's'}_{\nu\rho} \text{ — odd},\\ &(1+P)\,Y^{ps;\,p's'}_{\nu\rho} \text{ — odd},\\ &(1-P)\,Y^{ps;\,p's'}_{\nu\rho} \text{ — even},\end{aligned} \tag{2.20}$$

3. ROLE OF BOUND STATES IN PHOTOPRODUCTION PROCESSES

It is important to study the role of the bound states in photoproduction processes, since this problem is related to the analysis of the unobservable energy region in the dispersion relations. In our chosen reference system $\mathbf{p}+\mathbf{p}'=0$, the photoproduction threshold is $|\mathbf{p}| + \mu^2/4|\mathbf{p}|$. Let us consider the energy region in which $E < |\mathbf{p}| + \mu^2/4|\mathbf{p}|$ and where consequently bound states can be produced. Substituting (1.19) into (2.11) and integrating with respect to x, we get

$$\begin{aligned}Y^{ps;\,p's'}_{\nu\rho}\left(\frac{k+q}{2}\right) = {}&\pi\sum_{\mu,n} e^{\nu}_{\mu}\,\langle\Psi^{*}_{p',\,s'}J_{\rho}(0)\,\Psi_{n,\,\lambda\mathbf{e}-\varepsilon\mathbf{p}}\rangle\langle\Psi^{*}_{n,\,\lambda\mathbf{e}-\varepsilon\mathbf{p}}I_{\mu}(0)\,\Psi_{ps}\rangle\\ &\times\delta\left(\sqrt{M^2+\mathbf{p}^2}+E-\sqrt{M^2+\lambda^2+\varepsilon^2\mathbf{p}^2}\right),\\ &-\pi\sum_{\mu,n} e^{\nu}_{\mu}\,\langle\Psi^{*}_{p',\,s'}I_{\mu}(0)\,\Psi_{n,\,-\lambda\mathbf{e}+\varepsilon\mathbf{p}}\rangle\langle\Psi^{*}_{n;\,-\lambda\mathbf{e}+\varepsilon\mathbf{p}}J_{\rho}(0)\,\Psi_{ps}\rangle\,\delta\left(\sqrt{M^2+\mathbf{p}^2}-E-\sqrt{M_n^2+\lambda^2+\varepsilon^2\mathbf{p}^2}\right),\end{aligned} \tag{3.1}$$

($\varepsilon = \mu^2/4\mathbf{p}^2$). By virtue of the smallness of the coupling constant e (electric charge), the energy of the interaction with the electromagnetic field can be considered as a perturbation. This makes possible an expansion in terms of the eigenstates of the energy-momentum vector of the meson-nucleon system.

Bearing the above approximation in mind and taking it into account that there are no bound states whatever in the meson-nucleon system between M and $M+\mu$, it is possible to show (for small scatterer momenta $\mathbf{p}^2 < M\mu/2$) that in the energy range

$$0 < E < \frac{M\mu+\mu^2/4-\mathbf{p}^2}{\sqrt{M^2+\mathbf{p}^2}} \tag{3.2}$$

the quantity $Y^{ps;\,p's'}_{\nu\rho}\left(\frac{k+q}{2}\right)$ can be written as

$$Y^{ps;\,p's'}_{\nu\rho}(E,\lambda\mathbf{e}) = -\pi\frac{M^2-\mu^2/4}{M^2+p^2}\sum_{\mu s''} e^{\nu}_{\mu}\langle\Psi^{*}_{p's'}I_{\mu}(0)\,\Psi_{-\lambda\mathbf{e}+\varepsilon\mathbf{p},\,s''}\rangle \times \langle\Psi^{*}_{-\lambda\mathbf{e}+\varepsilon\mathbf{p},\,s''}J_{\rho}(0)\,\Psi_{ps}\rangle\,\delta\left(E-\frac{\mathbf{p}^2+\mu^2/4}{\sqrt{M^2+\mathbf{p}^2}}\right). \tag{3.3}$$

In fact, let us consider the δ-function of expression (3.1). It is easy to show that the δ-singularities of these functions at $M_n = M$ will occur at the energies

$$E_1 = -\frac{\mathbf{p}^2+\mu^2/4}{\sqrt{M^2+\mathbf{p}^2}}\ \text{and}\ E_2 = \frac{\mathbf{p}^2+\mu^2/4}{\sqrt{M^2+\mathbf{p}^2}}$$

for the first and second δ-functions respectively. If $M_n \neq M$, *i.e.*, $M_n \geq M + \mu$, the δ-singularities of these functions will occur at energies

$$E_1' \geqslant \frac{M\mu+\mu^2/4-\mathbf{p}^2}{\sqrt{M^2+\mathbf{p}^2}}\ \text{and}\ E_2' \leqslant -\frac{M\mu+\mu^2/4-\mathbf{p}^2}{\sqrt{M^2+\mathbf{p}^2}}$$

for the first and second δ-functions respectively.

If $p^2 < M\mu/2$ (small scatterer momenta), it is easy to see that $E_2 < E_1'$ and consequently we have (3.3) in the region (3.2).

Let us consider the mean values of the currents contained in (2.13). By way of example let us calculate the mean value of the meson-current $J_\rho(0)$, and analogously compute the mean value of the electromagnetic-current. We have

$$\langle\Psi^{*}_{p's'}J_{\rho}(x)\,\Psi_{ps}\rangle = e^{i(p'-p)x}\langle\Psi^{*}_{p's'}J_{\rho}(0)\,\Psi_{ps}\rangle$$

and on the other hand

$$\langle\Psi^{*}_{p's'}J_{\rho}(x)\,\Psi_{ps}\rangle = i\,\langle\Phi^{*}_{p's'}\frac{\delta S}{\delta\varphi_{\rho}(x)}\Phi_{ps}\rangle.$$

Introducing the Fourier transform

$$\varphi_{\rho}(x) = (2\pi)^{-4}\int e^{iqx}\varphi_{\rho}(q)\,dq$$

and considering that

$$\frac{\delta S}{\delta\varphi_{\rho}(q)} = (2\pi)^{-4}\int e^{iqx}\frac{\delta S}{\delta\varphi_{\rho}(x)}\,dx,$$

we get

$$i\,\langle\Phi^{*}_{p's'}\frac{\delta S}{\delta\varphi_{\rho}(q)}\Phi_{ps}\rangle = \langle\Psi^{*}_{p's'}J_{\rho}(0)\,\Psi_{ps}\rangle\,\delta(q-p+p').$$

The latter expression can be represented symbolically in the form of the following sum of diagrams:

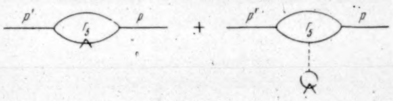

Here Γ_5 is the strongly-bound portion. Had there been three meson lines in place of the symbol Γ, the sum under consideration would have been

$$\mathfrak{G}^{\rho}_{5}(p,p',q)\,\Delta^{\rho}_{c}(q).$$

Since in our case there is no free meson line, the resulting expression must be multiplied in addition by $(\mu^2 - q^2)$. Using the normalization condition for the Green function at $p'^2 = M^2$, $p^2 = M^2$, $q^2 = \mu^2$, and also the energy-momentum conservation law, we obtain as a final expression

$$\langle\Psi^{*}_{p's'}J_{\rho}(0)\,\Psi_{ps}\rangle = g\,\langle\bar{u}_{s'}(p')\,\gamma^5\tau_{\rho}u_s(p)\rangle, \tag{3.4}$$

where g is the renormalized pseudoscalar coupling constant between the meson and nucleon fields. In the case of the electromagnetic field

$$\langle\Psi^{*}_{p's'}I_{\mu}(0)\,\Psi_{ps}\rangle = \langle\bar{u}_{s'}(p')\left\{e\frac{1+\tau_3}{2}\gamma^{\mu}+\frac{1}{2}\hat{\mu}\,[(k\cdot\gamma),\gamma^{\mu}]\right\}u_s(p)\rangle. \tag{3.5}$$

Here e is the renormalized electron charge and

$$\hat{\mu} = \mu_p\frac{1+\tau_3}{2}+\mu_n\frac{1-\tau_3}{2}, \tag{3.6}$$

μ_p and μ_n are the anomalous magnetic moments of the proton and neutron respectively. Using (3.4) to (3.6), we can rewrite (3.3) as

$$Y_{\nu\rho}^{ps;\,p's'}(E,\lambda e) = -\pi\frac{M^2-\mu^2/4}{M^2+p^2}\,g\sum_{s'',\,\mu}e_\mu^\nu\langle\bar{u}_{s'}(-\mathbf{p})\Big\{e\frac{1+\tau_3}{2}\gamma^\mu$$

$$+\frac{1}{2}\hat{\mu}\,[k\gamma),\gamma^\mu]\Big\}u_{s''}(p'')\rangle\langle\bar{u}_{s''}(p'')\gamma_5\tau_\rho u_s(p)\rangle\,\delta(E-E_2),$$

$$\mathbf{p}'' = -\lambda\mathbf{e} + \varepsilon\mathbf{p}.$$

4. MATRIX STRUCTURE OF THE PHOTOPRODUCTION AMPLITUDE

From consideration of the relativistic and gradient invariances, the photoproduction reaction amplitude can be rewritten as:[4]

$$R_{\nu\rho} = \sum_s \hat{\Omega}_\rho^s\bar{u}(p')\,P_{\alpha\beta}^s(k,p,p',\gamma)\,u(p)\,e_\alpha^\nu k_\beta,$$

$$R_{\nu\rho} = X_{\nu\rho} + iY_{\nu\rho}, \qquad (4.1)$$

where $P_{\alpha\beta}^s$ is an anti-symmetric (relative to α and β) tensor of second rank. In the pseudoscalar theory one can write the following four linearly independent operators

$$\hat{P}_{\alpha\beta}^s = \begin{cases}\gamma_5(p_\alpha p'_\beta - p_\beta p'_\alpha), & \gamma_5(\gamma_\alpha p_\beta - \gamma_\beta p_\alpha),\\ \gamma_5(p'_\alpha\gamma_\beta - \gamma_\alpha p'_\beta). & \gamma_5(\gamma_\alpha\gamma_\beta - \gamma_\beta\gamma_\alpha).\end{cases} \qquad (4.2)$$

$\hat{\Omega}^s$ stands for the isotopic spin operators. In a system consisting of nucleon, pion, and electromagnetic fields, the only matrices that participate in the description of the interaction are the matrices τ_ρ in the coupling between the nucleon and pion fields, and the electric-charge matrix $\frac{1}{2}(1+\tau_3)$ in the coupling between the nucleon and electromagnetic fields. Since the initial state of a photoproduction process is the nucleon plus electromagnetic field and the final state is the nucleon plus meson field, the most general expression for the reaction amplitude in isotopic space can be written as

$$\hat{\Omega}_\rho^s = \Omega_1^s\delta_{3\rho} + \Omega_2^s\tau_\rho + \Omega_3^s\frac{i}{2}[\tau_3,\tau_\rho]. \qquad (4.3)$$

Inserting (4.2) into (4.1), the expression for the photoproduction amplitude, for transverse polarization and for the system of coordinates chosen by us ($\mathbf{p}+\mathbf{p}'=0$), can be written as

$$\hat{R}_{\nu\rho} = (\boldsymbol{\sigma}\boldsymbol{\pi}_\nu)\hat{R}_\rho^1 + \boldsymbol{\sigma}(\mathbf{k}-\mathbf{q})\hat{R}_\rho^2$$

$$+\boldsymbol{\sigma}[[\mathbf{k}\boldsymbol{\pi}^\nu]\mathbf{q}]\hat{R}_\rho^3 + [\mathbf{kq}]\,\boldsymbol{\pi}_\nu\hat{R}_\rho^4, \qquad (4.4)$$

where the $\hat{R}_\rho^i$ have a matrix structure in isotopic space, analogous to (4.3). Since $\mathbf{k}$ and $\mathbf{q}$ can be expressed in terms of the vectors $\mathbf{e}$ and $\mathbf{p}$ [see (2.8)], the reaction amplitude can be represented as

$$\hat{R}_{\nu\rho} = (\boldsymbol{\sigma}\boldsymbol{\pi}^\nu)\hat{L}_\rho^1 + (\boldsymbol{\sigma}\mathbf{p})(\mathbf{p}\boldsymbol{\pi}^\nu)L_\rho^2$$

$$+\lambda(\boldsymbol{\sigma}\mathbf{e})(\mathbf{p}\boldsymbol{\pi}^\nu)\hat{L}_\rho^3 + \lambda[\mathbf{pe}]\boldsymbol{\pi}^\nu\hat{L}_\rho^4, \qquad (4.5)$$

where the $\hat{L}_\rho^i$ have a matrix structure analogous to (4.3).

5. DISPERSION RELATIONS

It was shown in Ref. 2 that

$$S_\mathbf{e}\hat{R}_{\nu\rho} = \hat{R}_{\nu\rho}(\lambda\mathbf{e}) + \hat{R}_{\nu\rho}(-\lambda\mathbf{e}), \quad \mathfrak{A}_\mathbf{e}\hat{R}_{\nu\rho} = \frac{1}{\lambda}(\hat{R}_{\nu\rho}(\lambda\mathbf{e}) - \hat{R}_{\nu\rho}(-\lambda\mathbf{e})) \qquad (5.1)$$

are analytic functions in the upper half-plane. To use the generalized Cauchy theorem and to write down the dispersion relations, it is necessary to make certain assumptions concerning the rate of growth of the photoproduction amplitude at infinity. Since the degree of reaction amplitude growth is a dynamic factor, it cannot be obtained from any kinematic considerations. We shall assume henceforth that the degree of growth of the photoproduction amplitude is zero.

Based on the above assumption, one can use the Cauchy theorem to write for the combination (5.1) the following dispersion relations:

$$S_\mathbf{e}R_{\nu\rho}(E,\lambda\mathbf{e}) = \frac{1}{\pi i}\,\mathrm{Vp}\int_{-\infty}^{+\infty}\frac{S_\mathbf{e}R_{\nu\rho}(E',\lambda'\mathbf{e})}{E'-E}\,dE' + C, \qquad (5.2a)$$

$$\mathfrak{A}_{\mathbf{e}} R_{\nu\rho}(E, \lambda\mathbf{e}) = \frac{1}{\pi i} \operatorname{Vp} \int_{-\infty}^{+\infty} \frac{\mathfrak{A}_{\mathbf{e}} R_{\nu\rho}(E', \lambda'\mathbf{e})}{E' - E} \, dE', \tag{5.2b}$$

or, separating the Hermitian parts of (5.2a) and (5.2b), we obtain a dispersion relation that connects the Hermitian part of the amplitude $X_{\nu\rho}$ with the anti-Hermitian part $Y_{\nu\rho}$:

$$S_{\mathbf{e}} X_{\nu\rho}(E, \lambda\mathbf{e}) = \frac{1}{\pi} \operatorname{Vp} \int_{-\infty}^{+\infty} \frac{S_{\mathbf{e}} Y_{\nu\rho}(E', \lambda'\mathbf{e})}{E' - E} \, dE' + \operatorname{Re} \hat{C}, \tag{5.3a}$$

$$\mathfrak{A}_{\mathbf{e}} X_{\nu\rho}(E, \lambda\mathbf{e}) = \frac{1}{\pi} \operatorname{Vp} \int_{-\infty}^{+\infty} \frac{\mathfrak{A}_{\mathbf{e}} Y_{\nu\rho}(E', \lambda'\mathbf{e})}{E' - E} \, dE'. \tag{5.3b}$$

Using (2.16) in the dispersion relations (5.3a) and (5.3b), one can eliminate the region of negative energies and rewrite these expressions as

$$S_{\mathbf{e}} X_{\nu\rho}^{ps;\, p's'}(E, \lambda\mathbf{e}) = \frac{1}{\pi} \operatorname{Vp} \int_{0}^{+\infty} dE' \left[\frac{S_{\mathbf{e}} Y_{\nu\rho}^{ps;\, p's'}(E', \lambda'\mathbf{e})}{E' - E} + \frac{P_{ss'} S_e Y_{\nu\rho}^{*ps;\, p's'}(E', \lambda'\mathbf{e})}{E' + E} \right] + \operatorname{Re} \hat{C}. \tag{5.4a}$$

$$\mathfrak{A}_{\mathbf{e}} X_{\nu\rho}^{ps;\, p's'}(E, \lambda\mathbf{e}) = \frac{1}{\pi} \operatorname{Vp} \int_{0}^{+\infty} dE' \left[\frac{\mathfrak{A}_{\mathbf{e}} Y_{\nu\rho}^{ps;\, p's'}(E', \lambda'\mathbf{e})}{E' - E} + \frac{P_{ss'} \mathfrak{A}_{\mathbf{e}} Y_{\nu\rho}^{*ps;\, p's'}(E', \lambda'\mathbf{e})}{E' + E} \right]. \tag{5.4b}$$

According to (4.5), the most general expression for energy-independent constant can be written as

$$\operatorname{Re} \hat{C} = \hat{C}_1(p^2)\, \boldsymbol{\sigma\pi}^{\nu} + \hat{C}_2(p^2)\, (\boldsymbol{\sigma}\mathbf{p})\, (\mathbf{p}\boldsymbol{\pi}^{\nu}), \tag{5.5}$$

where $\hat{C}_1$ and $\hat{C}_2$ have an isotopic structure analogous to (4.3). Using (3.3) and (5.5), the dispersion relation (5.4a) can be represented as

$$\begin{aligned} S_e X_{\nu\rho}^{ps;\, p's'}(E, \lambda e) = {} & -\frac{M^2 - \mu^2/4}{M^2 + \mathbf{p}^2} \sum_{\mu s''} \pi_{\mu}^{\nu} \left\{ \frac{S_e \langle \Psi_{p's'}^{*} I_{\mu}(0) \Psi_{p''s''} \rangle \langle \Psi_{p''s''} J_{\rho}(0) \Psi_{ps} \rangle}{E_2 - E} \right. \\ & \left. + S_e \frac{\langle \Psi_{ps'}^{*} J_{\rho}(0) \Psi_{p''s''} \rangle \langle \Psi_{p''s''}^{*} I_{\mu}(0) \Psi_{p's} \rangle}{E_2 + E} \right\} \\ & + \frac{1}{\pi} \operatorname{Vp} \int_{\frac{M\mu + \mu^2/4 - \mathbf{p}^2}{\sqrt{M^2 + \mathbf{p}^2}}}^{\infty} dE' \left[\frac{S_e Y_{\nu\rho}^{ps;\, p's'}(E', \lambda' e)}{E' - E} + \frac{P_{ss'} S_e \overline{Y}_{\nu\rho}^{*ps;\, p's'}(E', \lambda' c)}{E' + E} \right] + \hat{C}_1'(p^2)(\boldsymbol{\sigma\pi}^{\nu}) + \hat{C}_2(p^2)(\boldsymbol{\sigma}\mathbf{p})(\mathbf{p}\boldsymbol{\pi}^{\nu}). \end{aligned} \tag{5.6}$$

A complete analysis of the dispersion relations is given in Ref. 6.

In conclusion I wish to express deep gratitude to Academician N. N. Bogoliubov, under whose guidance the work was performed, and also to B. M. Stepanov for evaluating this work.

Note added in proof (May 27, 1957). The results obtained in this article show that the dispersion relations given by B. L. Ioffe for the photoproduction processes [J. Exptl. Theoret. Phys. (U.S.S.R.) 31, 583 (1956); Soviet Phys. JETP 4, 534 (1957)] are in error.

---

[1] M. L. Goldberger, Phys. Rev. 99, 979 (1955).

[2] Bogoliubov, Medvedev, and Polivanov, *Dispersion Relations*, Gostekhizdat, 1957 (in press).

[3] A. A. Logunov and B. M. Stepanov, Dokl. Akad. Nauk SSSR 110, 368 (1957); Soviet Phys. "Doklady" 1, 552 (1956). Logunov, Stepanov, and Tavkhelidze, Dokl. Akad. Nauk SSSR 112, 45 (1957); Soviet Phys. "Doklady" 2, 12 (1957).

[4] Koba, Katani, and Nakai, Progr. Theoret. Phys. 6, 849 (1951).

[5] G. F. Chew and F. E. Low, Phys. Rev. 101, 1579 (1956).

[6] A. A. Logunov and A. N. Tavkhelidze, Nuclear Physics (in press).

Translated by J. G. Adashko
279

SOVIET PHYSICS JETP VOLUME 5, NUMBER 6 DECEMBER 15, 1957

Application of the Dirac-Fock-Podol'skii Method to a Mechanical Many-Body Problem

I. G. FIKHTENGOL'TS

(Submitted to JETP editor July 28, 1956)
J. Exptl. Theoret. Phys. (U.S.S.R.) 32, 1404-1411 (June, 1957)

The general form of all the classical integrals of the motion and the generalized expression for the inertial mass of a body, in the relativistic many-body problem, are established with the aid of the many-time formalism. The results are applied to a system of interacting electric charges and to a system of bodies interacting gravitationally.

THE TREATMENT of the relativistic many-body problem is physically more coherent if the motion of the bodies is described by four-dimensional rather than by three-dimensional vectors. In view of this, we shall describe each of the n bodies of the system not merely by its three spatial coordinates x_i, y_i, z_i ($i = 1, 2, \ldots, n$) but also by its time coordinate t_i. Correspondingly, we shall also apply the term "four-dimensional" to all functions and relations in which the motion of the bodies is described by four-dimensional vectors. Such a method was applied first in quantum electrodynamics in the work of Dirac, Fock, and Podol'skii,[1] and later in classical electrodynamics in the work of Markov.[2] In the present article this method is applied to the mechanical n-body problem.

The system of bodies is supposed isolated, and only the translational motion of the bodies is considered; no account is taken of the dependence of this motion on their shape and other parameters (the bodies are supposed spherically symmetric, and the distances between them are supposed much greater than their linear dimensions).

Treatment of the many-body problem from a purely mechanical point of view is naturally approximate, and permissible only when radiation may be neglected. Therefore we assume that the speeds of the mechanical motion are small in comparison with the speed of light, and we retain only quantities of order $\dot{\mathbf{r}}_i^2/c^2$ in the case of electrical interaction, and only quantities of order $\dot{\mathbf{r}}_i^4/c^4$ in the case of gravitational interaction between the bodies ($\dot{\mathbf{r}}_i^2$ is the square of the velocity of translational motion of the ith body).

1. THE FOUR-DIMENSIONAL EQUATIONS OF MOTION OF A SYSTEM OF BODIES, AND THEIR INTEGRALS

The equations of motion in which each body is described by means of its own time can be written in the form

$$d\mathscr{P}_{\nu i}/dt = \mathscr{T}_{\nu i} \; (\nu = 0, 1, 2, 3; \; i = 1, 2, \ldots, n). \tag{1}$$

Here

$$\mathscr{P}_{0i} = -c^{-1}\partial\mathscr{L}/\partial\dot{x}_{0i}, \quad \mathscr{P}_{ji} = \partial\mathscr{L}/\partial\dot{x}_{ji}, \tag{2}$$

$$\begin{gathered} \mathscr{T}_{0i} = -c^{-1}\partial\mathscr{L}/\partial x_{0i}, \\ \mathscr{T}_{ji} = \partial\mathscr{L}/\partial x_{ji} \; (j = 1, 2, 3), \end{gathered} \tag{3}$$

where $\mathscr{L}$ is the four-dimensional Lagrangian function (to be determined later), dependent on the variables t, $x_{\nu i}$, and $\dot{x}_{\nu i}$; t is the independent variable, for which we use the proper time of the coordinate system; $x_{0i} = t_i$ is the time coordinate, and $x_{1i} = x_i$, $x_{2i} = y_i$, $x_{3i} = z_i$ are the spatial coordinates, of the ith body in the chosen coordinate system. A superior dot indicates differentiation with respect to the variable t.

To establish relations between the general integrals of the four-dimensional equations (1) and the groups of transformations with respect to which these equations are invariant, we change from the variables t and $x_{\nu i}$ in Eqs. (1) to new variables τ

and $q_{\nu i}$, by setting

$$\tau = \tau(t, \alpha), \; q_{\nu i} = q_{\nu i}(t, x_{\nu i}, \alpha), \tag{4}$$

where α is a parameter, and where

$$(\tau)_{\alpha=0} = t, \; (q_{\nu i})_{\alpha=0} = x_{\nu i}. \tag{5}$$

By following the references,[3–6] it is not hard to show that when the four-dimensional equations (1) are invariant with respect to a one-parameter group of transformations, determined by relations (4) and (5), the equations (1) have the following integral corresponding to this group:

$$\Big(\sum_{i=1}^{n}\sum_{\nu=0}^{3}\frac{\partial\mathscr{L}}{\partial\dot{x}_{\nu i}}\dot{x}_{\nu i} - \mathscr{L}\Big)\Big(\frac{\partial\tau}{\partial\alpha}\Big)_{\alpha=0}$$

$$-\sum_{i=1}^{n}\sum_{\nu=0}^{3}\frac{\partial\mathscr{L}}{\partial\dot{x}_{\nu i}}\Big(\frac{\partial q_{\nu i}}{\partial\alpha}\Big)_{\alpha=0} + \Big(\frac{\partial f}{\partial\alpha}\Big)_{\alpha=0} = \text{const}, \tag{6}$$

where the function f is determined by the relation

$$\mathscr{L}\Big(\tau, q_{\nu i}, \frac{dq_{\nu i}}{d\tau}\Big)\frac{d\tau}{dt} - \mathscr{L}(t, x_{\nu i}, \dot{x}_{\nu i})$$

$$= \frac{d}{dt} f(t, x_{\nu i}, \alpha), \text{ with } \tau = \tau(t, \alpha), \quad q_{\nu i} = q_{\nu i}(t, x_{\nu i}, \alpha), \tag{7}$$

in accordance with the form of the function $\mathfrak{L}$ and of the transformation (4). In formula (6) it is understood that $\mathfrak{L}$ is the untransformed function $\mathfrak{L}(t, x_{\nu i}, \dot{x}_{\nu i})$.

Existence of a function f that satisfies the condition (7) is equivalent to the requirement that the four-dimensional equation (1) be invariant with respect to the group of transformations (4). In particular, such a function f obviously exists when the function $\mathfrak{L}$ itself is invariant with respect to the group of transformations being considered; for then the left side of Eq. (7) is by definition zero, and therefore $f = \text{const}$. It follows that when the function $\mathfrak{L}$ is invariant with respect to a certain group of transformations, the function f may be set equal to zero in the integral (6) corresponding to this group of transformations.

We assume that the sets of quantities $\mathfrak{P}_{\nu i}$ and $\mathfrak{J}_{\nu i}$ ($\nu = 0, 1, 2, 3$) constitute four-dimensional vectors with respect to the Lorentz transformations; we deduce that the Lagrangian function $\mathfrak{L}$ in which we are interested, and in which the motion of the bodies is described by four-dimensional vectors, must be invariant with respect to these transformations. It is of importance that the function $\mathfrak{L}$ must also be invariant with respect to a change of the origin and scale of the proper time of the coordinate system. By setting first $\tau = t + \alpha$, $q_{\nu i} = x_{\nu i}$ and then $\tau = (1 + \alpha)t$, $q_{\nu i} = x_{\nu i}$ in the integral (6), we deduce that invariance of the four-dimensional $\mathfrak{L}$ with respect to a change of origin and scale of the proper time of the coordinate system is equivalent to the supposition that the function $\mathfrak{L}$ identically satisfies the equation

$$\sum_{i=1}^{n}\sum_{\nu=0}^{3}(\partial\mathscr{L}/\partial\dot{x}_{\nu i})\,\dot{x}_{\nu i} - \mathscr{L} = 0, \tag{8}$$

i.e., is a homogeneous function of the first degree in the variables $\dot{x}_{\nu i}$. From (1) and (8) it also follows that the four-dimensional function $\mathfrak{L}$ must not depend explicitly on the variable t.

Together with the conditions already imposed on the four-dimensional function $\mathfrak{L}$, it is necessary that when every $x_{0i} = t$ this function reduce to the ordinary Lagrangian function L of the mechanical system under consideration, *i.e.*, that the following equality be satisfied:

$$\mathscr{L}|_{x_{0i}=t} = L. \tag{9}$$

We shall call the function L, as distinguished from the function $\mathfrak{L}$, three-dimensional (we shall apply the term "three-dimensional" to all functions and relations in which the motion of the bodies is described by three-dimensional vectors).

It is not hard to show that conditions (8) and (9) and the requirement that the function $\mathfrak{L}$ be invariant with respect to Lorentz transformations completely determine this function. However, indeterminacy of the three-dimensional function L entails a corresponding indeterminacy of its four-dimensional analog $\mathfrak{L}$.

In what follows, we shall consider only such functions as satisfy conditions (8) and (9) and are Lorentz-invariant. In accordance with this, all integrals of the four-dimensional equations (1) that are consequences of the invariance of the equations with respect to Lorentz transformations can be put into the following very simple form, in conformity with formula (6):

$$\sum_{i=1}^{n}\sum_{\nu=0}^{3}\frac{\partial\mathscr{L}}{\partial\dot{x}_{\nu i}}\Big(\frac{\partial q_{\nu i}}{\partial\alpha}\Big)_{\alpha=0} = \text{const}. \tag{10}$$

By starting from relations (10) and, in the Lorentz transformations, making each of the ten parameters in turn different from zero (and the rest equal to zero), we get the four-dimensional analogs of all ten of the usual integrals of motion of an isolated system of bodies. From the invariance of the function $\mathcal{L}$ with respect to a shift of origin of the time coordinates x_{0i}, a shift of origin of the spatial coordinates x_{1i}, x_{2i}, x_{3i}, a rotation of the spatial axes, and a change to a reference system moving with constant velocity with respect to the original system, there follow respectively: the energy integral

$$\sum_{i=1}^{n} \partial\mathcal{L}/\partial\dot{x}_{0i} = \text{const}, \tag{11}$$

three momentum integrals

$$\sum_{i=1}^{n} \partial\mathcal{L}/\partial\dot{x}_{ji} = \text{const}\ (j = 1, 2, 3), \tag{12}$$

three angular-momentum integrals

$$\sum_{i=1}^{n} \left(\frac{\partial\mathcal{L}}{\partial\dot{x}_{ji}} x_{hi} - \frac{\partial\mathcal{L}}{\partial\dot{x}_{hi}} x_{ji}\right) = \text{const} \quad (j = 1, 2, 3;\ h = 1, 2, 3) \tag{13}$$

and three integrals of motion of the center of inertia

$$\sum_{i=1}^{n} \left(\frac{\partial\mathcal{L}}{\partial\dot{x}_{ji}} x_{0i} + \frac{1}{c^2}\frac{\partial\mathcal{L}}{\partial\dot{x}_{0i}} x_{ji}\right) = \text{const}\ (j = 1, 2, 3) \tag{14}$$

for the four-dimensional equations of motion (1).

Thus, by constructing the four-dimensional Lagrangian function $\mathcal{L}$ of the mechanical problem under consideration, it is possible to find for each body, according to formula (2), its energy-momentum vector $\mathcal{P}_{\nu i}$ ($\nu = 0, 1, 2, 3$); the set of quantities

$$\mathcal{P}_{\nu} = \sum_{i=1}^{n} \mathcal{P}_{\nu i}\, (\nu = 0, 1, 2, 3)$$

constitutes the conserved energy-momentum vector of the whole system of bodies, and the set of quantities

$$\mathcal{N}_{\mu\nu} = \sum_{i=1}^{n} (x_{\mu i}\overset{*}{\mathcal{P}}_{\nu i} - x_{\nu i}\overset{*}{\mathcal{P}}_{\mu i})$$

$$\times (\mu = 0, 1, 2, 3;\ \nu = 0, 1, 2, 3),$$

where

$$\overset{\bullet}{\mathcal{P}}_{0i} = \mathcal{P}_{0i}/c,\ \overset{\bullet}{\mathcal{P}}_{ji}\mathcal{P}_{ij}\ (j = 1, 2, 3;\ i = 1, 2, \ldots, n)$$

constitutes the conserved antisymmetric tensor of angular momentum and of the motion of the center of inertia.

Since $\mathcal{P}_{0i}$ is the time component of the four-dimensional energy-momentum vector of the ith body, we deduce that the quantities

$$\mathcal{E}_i = c\mathcal{P}_{0i} \text{ and } \mathcal{M}_i = \mathcal{P}_{0i}/c \tag{15}$$

may be interpreted respectively as the four-dimensional analogs of the total energy and of the inertial mass of the ith body.

Upon setting every $x_{0i} = t$ in formulas (15), we get generalized expressions for the total energy

$$E_i = -\partial\mathcal{L}/\partial\dot{x}_{0i}\big|_{x_{01} = x_{02}\cdots x_{0n} = t} \tag{16}$$

and for the inertial mass

$$M_i = -\frac{1}{c^2}\frac{\partial\mathcal{L}}{\partial\dot{x}_{0i}}\bigg|_{x_{01} = x_{02} = \cdots = x_{0n} = t} \tag{17}$$

of the ith body in the ordinary (three-dimensional) treatment of the many-body problem.

Thus for an isolated body moving with velocity $\dot{\mathbf{r}}$, the four-dimensional Lagrangian function has the form

$$\mathcal{L} = -\overset{\circ}{m}c^2\sqrt{\dot{x}_0^2 - \dot{\mathbf{r}}^2/c^2},$$

where $\overset{\circ}{m}$ is the rest mass of the body and x_0 is its time coordinate; accordingly,

$$E = \overset{\circ}{m}c^2/\sqrt{1 - \dot{\mathbf{r}}^2/c^2},\ M = \overset{\circ}{m}/\sqrt{1 - \dot{\mathbf{r}}^2/c^2}.$$

In the more general case, when the motion of a system of interacting bodies is considered, the relation (17) gives a generalized expression for the inertial mass of a body. Like the energies E_i, the inertial masses M_i are functions of time and depend in an essential way on the nature of the interaction of the bodies. We note that despite the indeterminacy of the function $\mathcal{L}$, which is connected with the indeterminacy of the function L, relation (17) uniquely defines the quantity M_i.

Along with the establishment of generalized expressions for the inertial mass of a body, the passage to a many-time formalism gives a possibility of pointing out the general form of all the classical integrals of motion in the ordinary (three-dimensional) treatment of the many-body problem. Upon setting every $x_{0i} = t$ in the integrals (11) to (14), we have: the energy integral

$$\sum_{i=1}^{n} E_i = \text{const}, \qquad (11^*)$$

the momentum integrals

$$\sum_{i=1}^{n} P_{ji} = \text{const}, \qquad (12^*)$$

the angular-momentum integrals

$$\sum_{i=1}^{n} (x_{ji}P_{hi} - x_{hi}P_{ji}) = \text{const} \qquad (13^*)$$

and the integrals of motion of the center of inertia

$$\sum_{i=1}^{n} P_{ji}t - \sum_{i=1}^{n} M_i x_{ji} = \text{const}. \qquad (14^*)$$

In these formulas, as usual,

$$P_{ji} = \partial L / \partial \dot{x}_{ji}.$$

In addition, by virtue of the homogeneity condition (8),

$$\sum_{i=1}^{n} E_i = \sum_{i=1}^{n} \sum_{j=1}^{3} \frac{\partial L}{\partial \dot{x}_{ji}} \dot{x}_{ji} - L,$$

as was to be expected.

From (12*) and (14*) it follows, in particular, that for every isolated system of bodies

$$\sum_{i=1}^{n} P_{ji} = \frac{d}{dt} \sum_{i=1}^{n} M_i x_{ji}, \qquad (18)$$

so that for the relativistic coordinates of the center of inertia

$$X_j = \sum_{i=1}^{n} M_i x_{ji} \Big/ \sum_{i=1}^{n} M_i \quad (j = 1,2,3)$$

the Newtonian equations

$$d^2 X_j / dt^2 = 0.$$

remain valid.

2. SYSTEM OF INTERACTING ELECTRIC CHARGES

To formulate the four-dimensional equations of motion of a system of interacting electric charges, it is sufficient to find the four-dimensional Lagrangian function $\mathfrak{L}$ of the problem.

To terms of order $\dot{\mathbf{r}}_i^2/c^2$, the required four-dimensional Lagrangian function may be expressed in the form

$$\mathscr{L} = -\sum_{i} m_i c^2 \sqrt{\dot{x}_{0i}^2 - \frac{\dot{\mathbf{r}}_i^2}{c^2}} - \frac{1}{2} \sum_{i \neq k} \frac{e_i e_k}{S_{ik}} \mathcal{U}_{ik}, \qquad (19)$$

$$S_{ik} = \sqrt{(\mathbf{r}_i - \mathbf{r}_k)^2 - c^2 (x_{0i} - x_{0k})^2}, \qquad (20)$$

$$\mathcal{U}_{ik} = \sqrt{\dot{x}_{0i}\dot{x}_{0k} - c^{-2} (\dot{\mathbf{r}}_i \dot{\mathbf{r}}_k) - c^{-2} \mathcal{A}_{ik} / S_{ik}^2} \qquad (21)$$

and

$$\mathcal{A}_{ik} = [(\dot{\mathbf{r}}_i (\mathbf{r}_i - \mathbf{r}_k)) - c^2 \dot{x}_{0i} (x_{0i} - x_{0k})]$$

$$\times [(\dot{\mathbf{r}}_k (\mathbf{r}_i - \mathbf{r}_k)) - c^2 \dot{x}_{0k} (x_{0i} - x_{0k})]. \qquad (22)$$

In these formulas, m_i is the rest mass, e_i the charge, and $\mathbf{r}_i$ the radius vector of the ith particle. The summation over indices i and k is from 1 to n.

It is immediately evident that (19) is Lorentz-invariant, satisfies the homogeneity condition (8), and reduces for all $x_{0i} = t$ to the known (three-dimensional) Lagrangian function L (*cf.*, for example, Refs. 5 and 7) of a system of electric charges.

From the fact that for a system of interacting electric charges there exists a four-dimensional function $\mathfrak{L}$, satisfying all the requirements of Sec. 1, it follows that for such a system all the deductions of that section are valid.

The integrals of motion of a system of electric charges have been treated in complete detail in Refs. 5 and 7, and therefore we shall not concern ourselves with them here. We pause to consider only the total energy and the inertial mass of a particle.

By starting from the relation (16) and the explicit form of the function $\mathfrak{L}$ [*cf.* (19)], we arrive at the following expression for the total energy E_i of an electrically interacting particle, to terms of order $\dot{\mathbf{r}}_i^2/c^2$:

$$E_i = \frac{m_i c^2}{\sqrt{1-\dot{\mathbf{r}}_i^2/c^2}} + \frac{1}{2}\sum_k{}' \frac{e_i e_k}{|\mathbf{r}_i - \mathbf{r}_k|}\Big(1 + \frac{1}{2c^2}(\dot{\mathbf{r}}_i \dot{\mathbf{r}}_k) + \frac{1}{2c^2}\frac{(\dot{\mathbf{r}}_i(\mathbf{r}_i - \mathbf{r}_k))(\dot{\mathbf{r}}_k(\mathbf{r}_i - \mathbf{r}_k))}{|\mathbf{r}_i - \mathbf{r}_k|^2}\Big). \tag{23}$$

The prime on the summation emphasizes that the summation index takes all values from 1 to n except one ($k \neq i$).

We get the magnitude of the inertial mass M_i of the same particle by dividing (23) by c^2. Thus to terms of order $\dot{\mathbf{r}}_i^2/c^2$, we have (*cf.* also Ref. 8)

$$M_i = \frac{m_i}{\sqrt{1-\dot{\mathbf{r}}_i^2/c^2}} + \frac{1}{2c^2}\sum_k{}' \frac{e_i e_k}{|\mathbf{r}_i - \mathbf{r}_k|}. \tag{24}$$

Formula (24) is the generalization of the well-known Einstein expression for inertial mass to the case of interacting electric charges.

3. SYSTEM OF BODIES INTERACTING GRAVITATIONALLY

To formulate the four-dimensional equations of motion of a system of bodies in the case of gravitational interaction, it is sufficient, as for a system of interacting electric charges, to find the four-dimensional Lagrangian function of the problem.

To terms of order $\dot{\mathbf{r}}_i^2/c^2$, the required four-dimensional Lagrangian function may be expressed in the form

$$\mathscr{L} = -\sum_i m_i c^2 \sqrt{\dot{x}_{0i}^2 - \frac{\dot{\mathbf{r}}_i^2}{c^2}} + \frac{1}{2}\sum_{i \neq k} \frac{\gamma m_i m_k}{S_{ik}}\Big(U_{ik} - \frac{1}{c^2}\sum_l{}' \frac{\gamma m_l}{S_{il}} U_{il}\Big). \tag{25}$$

Here

$$U_{ik} = [\dot{x}_{0i}\dot{x}_{0k} - c^{-2}(\dot{\mathbf{r}}_i \dot{\mathbf{r}}_k) - (\mathscr{A}_{ik}/c^2 S_{ik}^2) + 3c^{-2}\mathscr{B}_{ik}^2],$$

$$\mathscr{B}_{ik}^2 = (\dot{\mathbf{r}}_i - \dot{\mathbf{r}}_k)^2 - c^2(\dot{x}_{0i} - \dot{x}_{0k})^2,$$

S_{ik} and $\mathscr{A}_{ik}$ have the previous meanings (20) and (22).

It is evident that the function (25) is invariant with respect to Lorentz transformations, satisfies the homogeneity condition (8), and reduces for all $x_{0i} = t$ to the known (three-dimensional) Lagrangian function L (*cf.*, for example, Ref. 9) of our problem.

From the fact that for a system of bodies interacting gravitationally there exists a four-dimensional function $\mathscr{L}$, satisfying all requirements of Sec. 1, it follows that for such a system of bodies all the deductions of that section are valid. We consider some of them.

By starting from the relation (16) and the explicit form of the function $\mathscr{L}$ [*cf.* (25)], we get an expression for the total energy E_i of the ith particle in the case of gravitational interaction, to terms of order $\dot{\mathbf{r}}_i^2/c^2$. We get the magnitude of the inertial mass M_i of the same particle by dividing E_i by c^2. Thus to terms of order $\dot{\mathbf{r}}_i^4/c^4$ we get [*cf.* also Ref. 9]:

$$M_i = \frac{m_i}{\sqrt{1-\dot{\mathbf{r}}_i^2/c^2}} - \frac{1}{2c^2}\sum_k{}' \frac{\gamma m_i m_k}{|\mathbf{r}_i - \mathbf{r}_k|}\Big(1 + \frac{1}{2c^2}(\dot{\mathbf{r}}_i \dot{\mathbf{r}}_k) + \frac{1}{2c^2}\frac{(\dot{\mathbf{r}}_i(\mathbf{r}_i - \mathbf{r}_k))(\dot{\mathbf{r}}_k(\mathbf{r}_i - \mathbf{r}_k))}{|\mathbf{r}_i - \mathbf{r}_k|^2} - \frac{3}{2c^2}(\dot{\mathbf{r}}_i - \dot{\mathbf{r}}_k)^2 - \frac{1}{c^2}\sum_l{}' \frac{\gamma m_l}{|\mathbf{r}_i - \mathbf{r}_l|}\Big). \tag{26}$$

Formula (26) is the generalization of the well-known Einstein expression for inertial mass to the case of gravitational interaction of the bodies.

Remembering that the relations of Sec. 1 hold whenever the four-dimensional function $\mathscr{L}$ satisfies the necessary general requirements, we easily get for the system of bodies under consideration, with the aid of the expression (26) for the inertial mass M_i, the momentum integrals [*cf.* (18) and (12*)] and the integrals of motion of the center of inertia [*cf.* (18) and (14*)] to terms of order $\dot{\mathbf{r}}_i^4/c^4$. (The second derivatives with respect to the variable t, which enter into the correction terms in M_i, are easily eliminated with the aid of the equations of motion, which are known to terms of order $\dot{\mathbf{r}}_i^2/c^2$.) Consequently, by using the general relations of Sec. 1, we can easily increase the accuracy of six of the integrals of motion as compared with the accuracy of the Lagrangian function L. As for the energy and angular-momentum integrals, increase of their accuracy requires a corresponding increase of the accuracy of the Lagrangian function itself. All these relations were established to terms of order $\dot{\mathbf{r}}_i^2/c^2$ in Ref. 9, already cited.

In closing, we pause to consider the relation between the inertial and the ponderable mass of a body. By virtue of (26), the inertial mass of a body depends on its rest mass, on the velocity of the body as a whole, and on the nature of the interaction of this body with all the other bodies. The inertial masses of interacting electric charges, according to (24), depend also on the values of the charges. From expressions (24) and (26) it follows that the inertial masses agree with the rest masses only in the first (Newtonian) approximation.

As for the ponderable mass ("gravitational charge") of a body, it follows from the Einstein gravitational equations that, except for the choice of the unit of measurement, the ponderable mass of a body always coincides with its rest mass. The experiments of Eötvös and the nondependence of the motion of a body (of small mass) in a fixed gravitational field upon the value of its mass lead to the same conclusion. But since the inertial mass of a body coincides with its rest mass only in the Newtonian approximation, therefore the equality between the ponderable and inertial masses of a body also holds only in the Newtonian approximation.

If we take account of the fact that (*cf.* Ref. 10) the motion of a body of finite (not small) mass in a gravitational field – which in this case is not fixed – depends on the value of the mass even in the first (Newtonian) approximation, we arrive at the conclusion that the problem of the dependence of the motion of a body on its mass does not reduce to the problem of the relation between the inertial mass of a body and its ponderable mass.

From the above discussion it follows, in particular, that the physical basis of the Einstein equivalence principle is not an equality between the ponderable and inertial masses, which holds only in the Newtonian approximation, but an equality of the ponderable mass ("gravitational charge") of a body to its rest mass.

---

[1] Dirac, Fock, and Podolsky, Physik. Z. Sowjetunion 2, 468 (1932).

[2] M. Markov, J. Phys. (U.S.S.R.) 7, 42 (1943).

[3] E. Noether, Gött. Nachr. 235 (1918).

[4] E. L. Hill, Revs. Modern Phys. **23**, 253 (1951).

[5] V. A. Fock, *Theory of Space, Time, and Gravitation*, 1955.

[6] R. Courant and D. Hilbert, *Methoden der mathematischen Physik*, Vol. I.

[7] L. Landau and E. Lifshitz, *Field Theory*, 1948.

[8] I. G. Fikhtengol'ts, J. Exptl. Theoret. Phys. (U.S.S.R.) **21**, 648 (1951).

[9] I. G. Fikhtengol'ts, J. Exptl. Theoret. Phys. (U.S.S.R.) **20**, 233 (1950).

[10] I. G. Fikhtengol'ts, J. Exptl. Theoret. Phys. (U.S.S.R.) **32**, 1098 (1957); Soviet Phys. JETP **5**, 893 (1957).

Translated by W. F. Brown, Jr.
280

SOVIET PHYSICS JETP VOLUME 5, NUMBER 6 DECEMBER 15, 1957

Excitation of Rotational States in α-Decay of Even-Even Nuclei

V. M. STRUTINSKII

(Submitted to JETP editor August 10, 1956; resubmitted December 15, 1956)
J. Exptl. Theoret. Phys. (U.S.S.R.) 32, 1412-1420 (June, 1957)

The relative probability of excitation of rotational states in the α-decay of deformed even-even nuclei is computed. The deformation parameter of the nucleus is determined by comparison with the probability for transition to the 2 + state. The values of the deformation parameter and relative probability of transition to a 4 + rotational state obtained in this way are compared with the experimental data.

THE EXCITATION of the rotational states of a nucleus in α-decay can be produced either by the interaction of the α-particle with the non-spherical field of nuclear forces, or by the interaction of the α-particle with the Coulomb field of the non-spherical daughter nucleus. The rotation of the nucleus plays an essential role.[1] The decay of even-even nuclei turns out to be especially simple when the quantity of motion of the whole system is equal to zero. In this case the Schrödinger equation for the system: α-particle + deformed daughter nucleus is greatly simplified – in the Hamiltonian of the system one can exclude the rotational coordinates of the core. For even-even nuclei, the Schrödinger equation in spherical coordinates has the form[1]

$$\frac{\hbar^2}{2m}\frac{\partial^2 u}{\partial r^2} - \hbar^2\left(\frac{1}{2mr^2}+\frac{1}{J}\right)\hat{l}^2 u = (V-E)\,u, \qquad (1)$$

where $\psi(\mathbf{r}) = u(\mathbf{r})/r$ is the wave function of the system and depends only on the coordinates $\mathbf{r}$ of the α-particle relative to a coordinate system fixed in the nucleus; m is the mass of the α-particle, J the nuclear moment of inertia, E the energy of the system (equal to the energy of the α-particle at infinity, at the transition to the ground state of the daughter nucleus), $\hat{l}^2$ is the operator of the square of the angular momentum:

$$\hat{l}^2 = -\frac{1}{\sin\vartheta}\frac{\partial}{\partial\vartheta}\sin\vartheta\frac{\partial}{\partial\vartheta},$$

where ϑ is the angle with respect to the nuclear symmetry axis. In the expression of $\hat{l}^2$ the term $\hat{l}_z^2$ – which contains differenciation with respect to the azimuthal angle φ, has been omitted because the wave function does not depend on φ. If the wave function did contain states with non-zero projections of the angular momentum on the symmetry axis, the nucleus would rotate close to the symmetry axis. This is impossible because the moment of inertia with respect to the symmetry axis is zero ($J_z = 0$, $J_x = J_y = J$).

As it will be shown below, the angular dependence of the wave function is determined, for large distances from the nucleus, principally by the anisotropy of the Coulomb barrier and by the effects of nuclear rotation and centrifugal forces. The effect of nuclear interaction comes as an unknown boundary condition on the nuclear surface and has a relatively small influence on the intensity distribution in the α-spectrum.

In the region outside the nucleus, let us expand the wave function into the quasi-classical series:

$$u = \exp\{\hbar^{-1}[S_0(\mathbf{r}) + \hbar S_1(\mathbf{r}) + \ldots]\}. \qquad (2)$$

The method of successive approximations gives for S_1 and S_2 the equations:

$$(\partial y/\partial x)^2 + 4(1/x^2+\beta)\,\eta(1-\eta)(\partial y/\partial\eta)^2 = v - 1, \qquad (3)$$

$$\frac{\partial y}{\partial x}\frac{\partial S_0}{\partial x} + 4\left(\frac{1}{x^2}+\beta\right)\eta(1-\eta)\frac{\partial S_1}{\partial\eta}\frac{\partial y}{\partial\eta} = -\frac{1}{2}\frac{\partial^2 y}{\partial x^2} + \frac{1}{2}\left(\frac{1}{x^2}+\beta\right)\hat{l}_\eta^2 y, \qquad (4)$$

where the following notation has been introduced

$$v(\mathbf{x}) = V(\mathbf{r})/E;\ \mathbf{x} = \mathbf{r}/R_0;\ \beta = mR_0^2/J;$$

$$S_0 = -\hbar k_0 R_0 y(\mathbf{x});\ k_0 = \sqrt{2mE}/\hbar,$$

$\eta = \sin^2\vartheta$ for $\alpha > 0$ (prolate nucleus) and $\eta = \cos^2\vartheta$ for $\alpha < 0$ (oblate nucleus). It is assumed that the nuclear deformation is small and that, therefore, the nuclear surface can be described by the following equation which is exact up to the terms of the order α^2

$$R(\vartheta) = R_0 (1 - {}^1/_5\alpha^2 + \alpha P_2(\cos\vartheta))$$
$$\text{or} \quad x(\eta) = x_0 - \varepsilon\eta, \tag{5}$$

where $\varepsilon = {}^2/_3|\alpha|$, α being the nuclear deformation parameter, while $x_0 = 1 + |\alpha|\gamma - \alpha^2/5$ is the major semi-axis of the nucleus. The parameter γ is equal to 1 for a prolate nucleus, and to ½ for an oblate nucleus. R_0 is the radius of s sphere of volume equal to the nuclear volume: $R_0 = r_0 A^{1/3}$.

Let us expand the functions y, S_1 and v in a power series of η:

$$y = \sum_n y_n\eta^n; \; S_1 = \sum_n z_n(x)\eta^n; \; v = \sum_n v_n(x)\eta^n. \tag{6}$$

From (3) and (4), we obtain the following equations for y_n and z_n:

$$y'_m + 2m(2 - \delta_{1m})(x^{-2} + \beta) y_1 y_m / y'_0 = g_m(x), \tag{7}$$
$$z'_m + 4m(x^{-2} + \beta) y_1 z_m / y'_0 = h_m(x), \tag{8}$$

where δ_{ab} is the Kronecker symbol. The functions g_m and h_m have the following values for $m = 0$, 1, and 2:

$$g_0 = \sqrt{v_0 - 1}/y'_0, \; h_0 = [-y''_0 - 4(x^{-2} + \beta) y_1]/2y'_0,$$
$$g_1 = v_1/2y'_0, \; h_1 = [-y'_1 z'_0 - {}^1/_2 y''_1$$
$$+ 8(x^{-2} + \beta)(y_2 + {}^3/_8 y_1)]/y'_0, \tag{7'}$$
$$g_2 = [-(y'_1)^2 + 4y_1^2(\beta + x^{-2})]/2y'_0.$$

Here

$$v_0 = b(x^{-1} + 0.4\gamma\varepsilon x^{-3});$$
$$v_1 = -0.6\,\varepsilon b x^{-3}; \; b = 2Ze^2/R_0E;$$

all the v_m with $m > 1$ are set equal to zero because, in what follows, we will take into account only the quadrupole potential of the nucleus.

The functions g_m always contain $y_{m'}$ with $m' < m$, so that Eq. (7) can be solved consecutively. The same holds for Eq. (8) because the right hand side on the mth equation (8) contains only those $z_{m'}$ for which $m' < m$. The solution of Eq. (7) for $m > 1$, as well as the solution of any of the equations (8), can be written in the form

$$\begin{matrix} y_m \\ z_m \end{matrix} = \exp(-4mF(x)) \left\{ \begin{matrix} y_m(x_0) \\ z_m(x_0) \end{matrix} + \int_{x_0}^{x} \begin{matrix} q_m(t) \\ h_m(t) \end{matrix} \exp(4mF(t))\, dt \right\}, \quad F(x) = \int_{x_0}^{x} \left(\frac{1}{x^2} + \beta\right) \frac{y_1^2}{y'_0}\, dx. \tag{9}$$

For $m = 1$, Eq. (7) is the Ricatti equation

$$y'_1 + 2(x^{-2} + \beta) y_1^2 / y'_0 = v_1 / 2y'_0, \tag{10}$$

and its solution can be found in a general form.

Let us take the boundary condition for the solution of Eq. (3) in the form $S_0(\mathbf{r}) = \text{const} = 0$ on the surface of the nucleus, or $y[x(\eta), \eta] = 0$. Expanding the left hand side of this equality in a power series of the small quantity $\varepsilon\eta$ and equating to zero the coefficients of η^m we obtain the boundary condition for the function y_m at the point x_0:

$$+ \sum_{i_l = 1}^{n/2} \cdot \sum_{j = n/2+1}^{n} (1 - p_{Ail}) p_{Aj} (e^{w_l / kT} - 1) \Bigg] . \tag{11}$$

The values of the functions y_m at the point x_0 for $m \leqslant 2$ are:

$$y_0(x_0) = 0, \; y_1(x_0) = \varepsilon y'_0(x_0),$$
$$y_2(x_0) = \varepsilon y'_1(x_0) - {}^1/_2\varepsilon^2 y''_0(x_0). \tag{11'}$$

The boundary condition chosen for the wave function is, of course, not exact. However, if the true wave function is a smooth function of ϑ on the surface of the nucleus, the possible inaccuracy of the boundary condition on the nuclear surface will lead to an error in $y_m(x_0)$ of the order of $1/k_0R$ (boundary condition (11) gives for $y_1(x_1)$ a value of the order of $\varepsilon\varkappa/k_0$, where $\varkappa$ is the value of the wave vector of the α-particle in the neighborhood of the nuclear surface). This error is not substantial, because the angular dependence of the wave function in the neighborhood of the sphere of exit from underneath the barrier depends very weakly on the boundary condition on the sphere $x = x_0$. Indeed, the function $F(x)$ of Eq. (9) is positive and monotonically increasing with x in the whole region under the barrier. Therefore, at large distances from the nucleus, the first term in Eq. (9) (which depends on the boundary condition) is strongly attenuated by the exponential factor. This result has a simple physical meaning: close to the nuclear surface, only small angles are important: $\vartheta \lesssim \vartheta^* = (\varepsilon\varkappa R_0)^{-1/2}$. This is true for the functions y_m for $m > 1$. It is easy to convince oneself that, at large distances, y_1 depends also weakly on the boundary condition, but only if $y_1(x_0)$

is not too small. The reason is the following: close to the nuclear surface the wave packet contains α-particle states and, correspondingly, nuclear states with high angular momenta: $l \lesssim 2\,\varepsilon\varkappa R_0$ (see Appendix). During further passage through the barrier, the packet smears out owing to the concurrent action of the nucleus, of the centrifugal forces, and of the quadrupole potential. The first two effects are proportional to the square of the angular momentum, *i.e.*, during passage through the barrier, the smearing of the packet increases as the angular distribution of the α-particles in the neighborhood of the nucleus gets sharper, *i.e.*, as $y_1(x_0)$ increases. As will be shown in the Appendix, it is for the same reason that the anisotropy of the wave function cannot be very large at large distances. In practice, the half width of the wave function cannot be less that 40 – 50°.

One cannot set up a correct boundary condition for the functions z_m, because these functions are of the same order of magnitude as the possible inaccuracy of the boundary condition. However, if one takes into account that at large distances the functions z_m depend also weakly on the boundary condition, one can set them equal to zero on the sphere $x = x_0$.

It is easy to see that with such a boundary condition for the functions z_m, and with boundary condition (11) for the function y_m the expansion of the wave function in a power series of $\eta = \sin\vartheta$ or $\cos\vartheta$ is at the same time an expansion in the parameter ε. Indeed, as it can be seen from Eq. (11), the boundary condition on the functions y_m has the property that $y_m(x_0)$ is of the order of ε^m [see also (7′) and (11′)]. The same is true for the right-hand sides of (7). It follows that the solution of these equations themselves will diminish as ε^m. The same holds for the functions z_m with the boundary condition $z_m(x_0) = 0$.* Let us note that the function $F(x)$ in (9) is, for small deformations, proportional to ε, and that all that has been said above about the weak dependence of the angular distribution of α-particles at large distances on the conditions at the nuclear surface is true only for dedormations which are not too small: the function $F(x)$ must be, in the neighborhood of the sphere of exit from underneath the barrier, of the order of unity (actually F turns out to be equal to 0.2 – 0.4). The relative probability of excitation of a rotational state of the daughter nucleus with spin I is equal to

$$\xi_I = \frac{(2I+1)\left(\int\limits_0^\pi \sin\vartheta\, d\vartheta\, \psi(\vartheta)\, P_I(\cos\vartheta)\right)^2}{\int\limits_0^\pi \sin\vartheta\, d\vartheta\, \psi(\vartheta),} \tag{12}$$

where $P_I(\cos\vartheta)$ is the Legendre polynomial and for $\psi(\vartheta)$ one can take the wave function in the neighborhood of the sphere of exit from underneath the barrier. In order to determine $\psi(\vartheta)$ in first approximation with respect to α, one has to solve the Ricatti equation (10). In this approximation we simply have

$$\psi(\vartheta) \sim \exp\left\{-a\begin{pmatrix}\sin^2\vartheta\\ \cos^2\vartheta\end{pmatrix}\right\},\quad a = k_0 R_0 y_1(x)^*,$$

and the integrals in (12) can be evaluated in a general manner. For an oblate nucleus we obtain:

$$\xi_2 = \frac{5}{16}\{3e^a\chi^{-1}(\sqrt{a}) - 3a^{-1} - 2\}^2,$$

$$\chi(a) = \int\limits_0^a e^{t^2}\,dt. \tag{13}$$

The solution of the Ricatti equation can be simplified if one takes into account that the contribution of the quadrupole potential is small* with respect to the contribution of the term proportional to y_1^2.* The accuracy of the first approximation is, however, not sufficient, because ξ_I is a sharp function of α and, if the determination of the wave function is not accurate enough, the error in ξ_I can be too large. Because of this, the wave function has been computed taking into account terms of the order α^2 in the quasi-classical part (in S_0) and a term of the order α in the quantum correction.† The wave function has the form

---

*The solutions of the mth equations of (7) and (8) and the functions y_m and z_m contain also terms of order higher than ε^m. These terms are substantial at large distances from the nucleus.

*Formally, v_1 of (10) is a small quantity of lower order, but since the quadrupole potential falls off rapidly with distance, its contribution at large distances becomes numerically small relative to the contribution of the term containing y_1^2.

†An actual calculation of terms of higher order (y_3 and z_3) for the case of the decay of U^{234} and $\alpha = 0.15$ has shown that the contribution from these terms is indeed small (the correction to the exponent is $\lesssim 0.1$); practically, one can therefore limit oneself to the terms mentioned.

$$\psi \sim \exp\left\{-a_1\frac{\sin^2\vartheta}{\cos^2\vartheta}-a^2\frac{\sin^4\vartheta}{\cos^4\vartheta}\right\},$$

$$\alpha \gtreqless 0,\quad a_1 = k_0Ry_1 - z_1,\quad a_2 = k_0R_0y_2,$$

$(a_2/a_1 \sim \varepsilon)$. For $y_{1,2}$ and z_1, their value at the point $x^* = b - 1$ was used, *i.e.*, somewhat short of the exit sphere. One has to do that because in the immediate neighborhood of the exit sphere the quasi-classical approximation is not valid. But one can show that in the region $x \geqslant x^*$ the angular dependence of the wave function is practically constant.

The calculations were performed on an *M*-2 electronic computer. Equations (7) and (8) were solved using variable increments chosen to make the accuracy of the functions at the point x^* of the order of 10^{-3}. The integrals in Eq. (12) were computed for $l = 2$ and 4 using Simpson's rule with a spacing of 1/512. The probability of transition into a state $l \geqslant 6$ was not determined because the probability of transition into these states depends appreciably on the boundary condition as well as on other factors which are difficult to take into account (the octupole potential and higher order potentials, a more accurate characteristic of the nuclear shape, the finite dimensions of the α-particle, *etc.*)

The calculation was performed for all the even-even nuclei mentioned in the reviews, Refs. 1 and 2, for $r_0 = 1.2$, 1.3, and 1.4×10^{-13} cm, for positive and negative values of α from 0.05 to 0.25 in steps of 0.05. In order to illustrate the convergence of the series, the dependence of the functions y_1, y_2 and z_1 on α at the point $x^* = b - 1$ has been plotted on Fig. 1. The series converges faster at smaller distances from the nucleus. The parameter involved in Eq. (7) and (8) (the energy E and the rotational constant $B = \hbar^2/2J$) and the experimental value of ξ_2 and ξ_4 were determined from the compiled experimental data.[2,3] The experimental values of these parameters are tabulated together with the results of the calculations. The references to the experimental work are given in the mentioned reviews and are therefore not shown in the table. The value of ξ_4 given for the case of decay of Ra^{226} is obtained from Ref. 4.

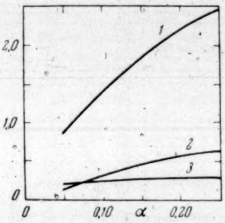

FIG. 1. Plot illustrating the convergence of the series. Decaying nucleus Pu^{236}, $r_0 = 1.4 \times 10^{-13}$ cm. Curve 1 – $k_0R_0y_1(x^*)$, 2 – $k_0R_0y_2(x^*)$, 3 – $z_1(x^*)$. The relative order of the functions y_1, y_2 and z_1 is α, α^2 and α, respectively.

The values of α tabulated in the third column were obtained by comparison with the experimental value of the relative probability of transition into the state with $l = 2$. For each nucleus and each sign of deformation the upper column corresponds to $r_0 = 1.4 \times 10^{-13}$ cm and the lower to $r_0 = 1.2 \times 10^{-13}$ cm. The difference between these values of r_0 is small and one cannot practically make a choice between them. For $r_0 = 1.3 \times 10^{-13}$ cm the value of α is always in between the values corresponding to $r_0 = 1.4 \times 10^{-13}$ and 1.2×10^{-13} cm. These values of α are not tabulated. For an oblate nucleus with a given deformation, the probability of transition into a 2+ state is always considerably smaller than for a prolate nucleus. For an oblate nucleus with any value of $\alpha \leqslant 0.25$, ξ_2 is, in most of the cases, smaller than its experimental value. On the other hand, the quadrupole moment data indicate a small deformation ($\alpha \lesssim 0.20$); therefore, the data on intensity distribution in the α-spectrum exclude the assumption of oblate nuclei. This is in agreement with the experimental results on $\alpha - \gamma$ angular correlation in the case of α-decay of Am^{241} from which it follows that the nuclei Am^{241} and Np^{237} are prolate.*[5]

The few exceptions are the nuclei for which the probability of transition into a 2+ state is relatively small (isotopes of Rn, Cm, and Cf). The assumption that these nuclei are oblate can be made to agree – generally speaking – with the intensity distribution of the α-spectrum although this yields deformations. The quadrupole moment data on these nuclei would permit one to make a definite conclusion about their shape. The table shows the negative values of α only in those cases for which the assumption on oblate nucleus can be made to agree with the intensity of transition into the 2+ state.

---

*An adiabatic rotation of the nucleus was assumed in Ref. 5. This assumption does not agree with what actually happens, but one can show that the nuclear rotation does not substantially change the relative phase between the $l = 2$ and $l = 0$ waves, a phase which is important for the determination of the sign of the deformation.

Daughter nucleus	E, Mev; B, kev; ξ_2 (exp.)	α	α_Q	ξ_4 (calc.)	ξ_4 (exp.)
Rn^{220}	5.68 40 0.05	+0.07 +0.08 −0.14 −0.15		10^{-4} $7 \cdot 10^{-5}$	
Rn^{222}	4.78 31 0.06	+0.08 0.10 −0.15 0.20		$5 \cdot 10^{-5}$ $3 \cdot 10^{-5}$	
Ra^{222}	6.34 18.2 0.27	+0.13 0.15		$4 \cdot 10^{-3}$	$8 \cdot 10^{-3}$
Ra^{224}	5.42 14 0.40	+0.17 0.20		10^{-2}	$2.8 \cdot 10^{-3}$
Ra^{226}	4.68 11.2 0.30	+0.15 0.17		$6 \cdot 10^{-3}$	$2.6 \cdot 10^{-3}$
Ra^{228}	3.99 10 0.32	+0.17 0.21		$6 \cdot 10^{-3}$	
Th^{226}	5.89 11.6 0.45	+0.17 0.20		$1.4 \cdot 10^{-2}$	
Th^{228}	5.32 10 0.47	+0.18 0.21		$1.6 \cdot 10^{-2}$	$4.4 \cdot 10^{-3}$
Th^{230}	4.76 8.7 0.31	+0.14 0.15		$6 \cdot 10^{-3}$	$4 \cdot 10^{-3}$
Th^{232}	4.50∼8.3 ∼0.37	+0.16 0.18	0.07[6]	10^{-2}	
Th^{234}	4.18∼8.3 ∼0.30	+0.14 0.15		$6 \cdot 10^{-3}$	
U^{230}	6.19∼8.3 0.16	+0.08 0.09			
U^{232}	5.75 7.5 0.25	+0.10 0.12	U^{233} 0.17 [7]	$4 \cdot 10^{-3}$	
U^{234}	5.50 7.8 0.39	+0.14 0.16	U^{235} 0.12 [7]	10^{-2}	$1.2 \cdot 10^{-3}$
U^{236}	5.16 7.5 0.32	+0.13 0.15		$8 \cdot 10^{-3}$	$1.2 \cdot 10^{-3}$

Daughter nucleus	E, Mev; B, kev ξ_2 (exp.)	α	α_Q	ξ_4 (calc.)	ξ_4 (exp.)
U^{238}	4.90 7.3 0.25	+0.12 0.13	0.11 [7] 0.07 [6]	$3 \cdot 10^{-3}$	
Pu^{238}	6.11 7.3 0 36	+0.12 0.13		10^{-2}	$5 \cdot 10^{-4}$
Pu^{240}	5.80 7.2 0.33	+0.12 0.13		$1.3 \cdot 10^{-2}$	
Cm^{242}	6.75 7.0 0.28	+0.10 0.11 −0.20 0.25		$6 \cdot 10^{-3}$ $1.5 \cdot 10^{-2}$	$>10^{-3}$
Cm^{246}	6.15 6.2 0.11	+0.07 0.08 −0.09 0.10		$2 \cdot 10^{-3}$ $1.5 \cdot 10^{-3}$	
Cm^{248}	6.12 6,2 0,11	+0.07 0.08 −0.12 0.14		10^{-3} 10^{-3}	
Cf^{250}	7.22 7.0 0.18	+0.08 0.08 −0.12 0.14		$4 \cdot 10^{-3}$ $3 \cdot 10^{-3}$	$>3 \cdot 10^{-3}$

The fourth column (α_Q) of the table shows the values of α determined from quadrupole moments obtained from experiments on Coulomb excitation of rotational levels, for $r_0 = 1.4 \times 10^{-13}$ cm. The parameter α_Q is obtained using the formula:[8]

$$Q_0 = \tfrac{6}{5} Z R_0^2 \alpha_Q .$$

At the present time the quadrupole moment of the following even-even nuclei has been measured: Th^{232} ($Q_0 = 5.6$ barns[6]) and U^{238} ($Q_0 = 6.9$ barns[6] and 9.5 barns[7]). The table shows both values for U^{238}. $Q_0 = 6.9$ barns corresponds to $\alpha = 0.07$. This value differs appreciably from the α determined from α-decay. The discrepancy is also very large in the case of Th^{232}. In the other case, the deformation parameter has been determined from the quadrupole moment of the neighboring odd isotopes.[7] These isotopes are shown in the table. The dependence of the deformation parameter on the quadrupole moment agrees qualitatively with the measured nuclear quadrupole moments. The following columns list the calculated and experimental values of the transition probability into the 4+ state. In all the cases the agreement with the experimental data on decay into a 4+ state is satisfactory. The discrepancy between the experimental and the theoretical values of ξ_4 is within reasonable limits and can be fully accounted for by the inaccuracy of the boundary condition (it is shown in the appendix that the inaccuracy of the boundary condition can change ξ_4 by a factor of $\sim e$). Fig. 2 shows the dependence of ξ_2 on α for the decays of Cm^{242} (experimental value $\xi_2 = 0.35$) and Ra^{222}, for $r_0 = 1.4 \times 10^{-13}$ cm (for the latter nucleus the intensity of transition into a 2+ state has not been determined experimentally). Let us note that the curves showing the dependence of ξ_2 on α turn out to be close to each other for all the isotopes of the same element, but are quite different for different elements.

Generally speaking, the nuclear deformation can also be determined from the absolute probability of

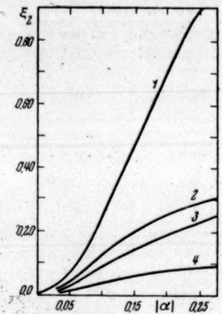

FIG. 2. Relative probability of transition into an $I = 2$ state *vs.* deformation of the daughter nucleus. The following parent nuclei are shown: 1 – Cm^{242}, $\alpha > 0$; 2 – Cm^{242}, $\alpha < 0$; 3 – Ra^{222}, $\alpha > 0$; 4 – Ra^{222}, $\alpha < 0$.

α-decay – the presence of deformation leads to an increase of the Coulomb barrier penetrability. This effect is, however, relatively small as compared to the spherical case (the decay probability increases by a factor of ~ 10). The factor in front of the exponential is determined either with the same accuracy or less accurately; this method does not, therefore, permit the determination of the deformation with any accuracy.

In conclusion the author expresses his gratitude to C. B. Mostinskaia who carried out the calculations with an electronic computer.

APPENDIX

1. DEPENDENCE OF THE WAVE FUNCTION ON THE BOUNDARY CONDITION AT THE NUCLEAR SURFACE

In the neighborhood of the nucleus one can neglect the curvature of the α-particle orbit. On a sphere Σ surrounding the nucleus, of radius $x_0 = 1 + \alpha$ equal to the major semi-axis of the nucleus (we consider prolate nuclei), the wave function can be written in the form

$$\psi\big|_\Sigma = \chi(\vartheta)\exp\left\{-\int_{x_0-\Delta x}^{x_0} \varkappa\, dx\right\} \simeq \chi(\vartheta)\exp\{-\varkappa R_0 \Delta x(\vartheta)\}, \qquad (A.1)$$

where $\chi(\vartheta) \equiv \chi[x(\eta), \eta]$ is the wave function at the nuclear surface and $\Delta x(\vartheta) = \varepsilon \sin^2 \vartheta$. Let us expand the function (A.1) is Legendre polynomials:

$$\psi\big|_\Sigma = \sum_l a_l P_l(\cos\vartheta), \qquad (A.2)$$

$$a_l \sim (2l+1)\int_0^\pi \psi\big|_\Sigma P_l(\cos\vartheta)\sin\vartheta\, d\vartheta.$$

Only small angles are important in (A.2), because practically $\varepsilon\varkappa R \sim 4-5 \gg 1$. Substituting, in the exponent, ϑ^2 for $\sin^2\vartheta$ and a Bessel function for the Legendre polynomial, we find:

$$a_l \sim (2l+1)\int_0^\infty e^{-c\vartheta^2} J_0\left[\left(l+\frac{1}{2}\right)\vartheta\right]\vartheta\, d\vartheta \sim (2l+1)\exp[-l(l+1)/4c], \qquad (A.3)$$

where $c = \varepsilon\varkappa R + \delta$, δ being a correction due to the function $\chi(\vartheta)$. If the function $\chi(\vartheta)$ is not too abrupt, $\delta \lesssim 1$. The quadrupole potential can be neglected in the analysis of the dependence of the intensity of rotational state excitation on the boundary condition. In the region under the barrier one can therefore write the wave function in the form

$$\psi(x,\vartheta) = \sum_l a_l R_l(x) P_l(\cos\vartheta), \qquad (A.4)$$

where R_l are the usual Coulomb radial functions $[R_l(x_0) = 1]$. The relative probability of excitation of a spin I rotational level is equal to

$$\xi_I = a_I^2 \frac{R_I^2(x^*)}{R_0^2(x^*)} \approx (2I+1)\exp\left[-I(I+1)\left(\frac{1}{2c}+d\right)\right] \approx (2I+1) \times \exp\left\{-I(I+1)\left(\frac{1}{2\varepsilon\varkappa R_0}+\frac{\delta}{2(\varepsilon\varkappa R_0)^2}+d\right\}, \qquad (A.5)$$

$$d \approx \frac{1}{k_0R_0}\int_{x_0}^{x^*}\frac{(\beta+x^{-2})}{(v_0-1)^{1/2}}dx = \frac{1}{k_0R_0}\left(\frac{2}{\sqrt{b}}+\frac{\pi}{2}\beta b\right).$$

For most nuclei $\beta \sim 0.1$, $b \sim 5$. Here $d = 1.5/k_0R_0$. The factor $\delta/2(\varepsilon\varkappa R_0)^2$ which depends on the boundary condition on the nuclear surface is substantial for $l \gtrsim \sqrt{2\varepsilon\varkappa R_0}$. For $\delta \lesssim 1$ and $I = 2$, the correction which is due to the inaccuracy of the boundary condition does not exceed $\sim 20\%$. For $I = 4$, the ξ_I calculated with an approximate boundary condition can be several times larger or smaller than the true value. The probability of transition into higher states depends appreciably on the boundary condition.

2. MINIMUM ANGULAR WIDTH OF THE WAVE FUNCTION

The action of centrifugal forces and the energy loss of the α-particle (nuclear rotation) lead to a finite width of the wave function on the sphere of exit from underneath the barrier, even for a δ-function distribution of α-particles on the sphere Σ. The intensities of the fine-structure lines in the α-spectrum for a deformed nucleus cannot, therefore, exceed the values given by the simple Gamow formula, which does not take into account the nuclear deformation. The minimum width of the wave function can be obtained either by using formula (A.5), putting $c = \infty$, or directly from Eq. (10), by letting $v_1 = 0$ and $y_1(x_0) = \infty$ in the Ricatti equation. We obtain

$$y_1(x^*)\big|_{\max} = \left[2\int_{x_0}^{x^*} \frac{(\beta + x^{-2})}{(v_0 - 1)^{1/2}} \right]^{-1} = \frac{1}{2\, d k_0 R_0}. \quad \text{(A.6)}$$

The angular half width ϑ^* of the wave function is determined from $\sin\vartheta^* \approx \sqrt{k_0 R_0 y_1(x^*)}$; for the values of d mentioned above and for $k_0 R_0 \approx 8$, it is equal to $\sim 40^\circ$. As can be seen from Eq. (10), the quadrupole potential can only decrease the value of $y_1(x^*)$ and leads, therefore, to an additional increase of the angular width of the wave function and to a decrease of the probability of transition into excited rotational states.

---

[1] V. M. Strutinskii, J. Exptl. Theoret. Phys. (U.S.S.R.) **30**, 411 (1956); Soviet Phys. **3**, 450 (1956).

[2] F. Asaro and I. Perlman, Ann. Rev. Nucl. Sci. **4**, 157 (1954).

[3] Gol'din, Novikova, and Peker, Usp. Fiz. Nauk **59**, 459 (1956).

[4] Harbottle, McKeown, and Sharff-Goldhaber, Phys. Rev. **103**, 1776 (1956).

[5] V. M. Strutinskii, Dokl. Akad. Nauk SSSR **104**, 524 (1955).

[6] Davis, Divatia, Lend, and Moffat, Phys. Rev. **103**, 1801 (1956).

[7] J. O. Newton, Physica **22**, 1129 (1956).

[8] A. Bohr and B. Mottelson, Kong. Dansk. Vid. Sels. mat. fys. medd **27**, No. 16 (1953), Probl. Sovr. fiz. **9** (1956).

Translated by E. S. Troubetskoy
281

SOVIET PHYSICS JETP VOLUME 5, NUMBER 6 DECEMBER 15, 1957

Motion of a Charge Parallel to the Axis of a Cylindrical Channel in a Dieletric

L. S. BOGDANKEVICH AND B. M. BOLOTOVSKII
P. N. Lebedev Institute of Physics, Academy of Sciences, U.S.S.R.

(Submitted to JETP editor July 14, 1956; resubmitted December 21, 1956)
J. Exptl. Theoret. Phys. (U.S.S.R.) 32, 1421-1428 (June, 1957)

The field produced by a charge moving parallel to the axis of a cylindrical channel in a dielectric is determined. The field and energy losses of the charge are computed for various assumptions concerning the medium.

THE PASSAGE OF A CHARGE along a channel in a dielectric was first considered by Ginzburg and Frank.[1] These authors calculated the field produced by a point charge moving with uniform motion along the axis of a cylindrical channel of radius a, filled with a dielectric $\varepsilon_1(\omega)$ in a medium of dielectric constant $\varepsilon_2(\omega)$.

Problems connected with the passage of a charge along the axis of a channel in a dielectric have also been treated by Bohr,[2] Schoenberg,[3] Huybrechts,[3,5] and Sitenko[6] (problems of this type have also been considered in Ref. 7).

In problems concerning the generation of electromagnetic radiation, focusing of charged particles in a cylindrical channel, and the theory of Cerenkov counters, it is of interest to consider the case in which the charge moves in the channel along a straight line parallel to the axis rather than along the axis itself.

1. We consider an infinite cylindrical channel in an isotropic medium of dielectric constant $\varepsilon_2(\omega)$. It will be assumed that the space inside the channel is filled with an isotropic dielectric with dielectric constant $\varepsilon_1(\omega)$. The radius of the channel is denoted by a. We consider a charge which moves with uniform motion along a line parallel to the axis of a channel at a distance r_0. The equations for the electromagnetic field potentials are as follows:

$$\Delta\varphi = -\frac{4\pi\rho}{\varepsilon},$$

$$\Delta\mathbf{A} - \frac{\varepsilon}{c^2}\frac{\partial^2\mathbf{A}}{\partial t^2} = -\frac{4\pi}{c}\mathbf{j} + \frac{\varepsilon}{c}\,\mathrm{grad}\,\frac{\partial\varphi}{\partial t}. \qquad (1)$$

In what follows we shall choose the potential gauge to make $\mathrm{div}\,\mathbf{A} = 0$. In Eq. (1) $\varepsilon = \varepsilon_1$ inside the channel and $\varepsilon = \varepsilon_2$ outside. We introduce the cylindrical coordinates r, φ, and z with the z axis parallel to the channel axis. The angle φ is measured from the plane which passes through the axis of the channel and the line of motion of the charge. Then, in Eq. (1) the charge density ρ is given by:

$$\rho = e\delta(\mathbf{r} - \mathbf{r}_0)\,\delta(z - vt). \qquad (2)$$

Here $\mathbf{r}_0$ is the projection of the radius vector of the particle on the plane $z = \text{const}$, while $\mathbf{r}$ is the projection of the radius vector of the point of observation on the same plane. In the present problem it is convenient to represent $\delta(\mathbf{r} - \mathbf{r}_0)$ in the following form:

$$\delta(\mathbf{r} - \mathbf{r}_0) = \frac{1}{2\pi}\sum_{m=-\infty}^{m=\infty} e^{im\varphi}\int_0^\infty J_m(kr)\,J_m(kr_0)\,k\,dk, \qquad (3)$$

where $J_m(x)$ is a Bessel function of order m and φ is the angle between $\mathbf{r}$ and $\mathbf{r}_0$. For $\delta(z - vt)$ we use the usual representation

$$\delta(z - vt) = \frac{1}{2\pi v}\int e^{i\omega(z-vt)/v}\,d\omega. \qquad (4)$$

Taking account of (3) and (4), Eq. (2) can be rewritten in the form

$$\rho = \frac{e}{(2\pi)^2 v}\sum_{m=-\infty}^{m=\infty} e^{im\varphi} \times \int J_m(kr)\,J_m(kr_0)\,e^{i\omega(z-vt)/v}k\,dk\,d\omega. \qquad (5)$$

Hereinafter, when the limits of integration are not given explicitly, the integration over k is taken from 0 to ∞ while the integration over ω is taken from $-\infty$ to $+\infty$.

We find the solution for the first equation in (1). The expression for ρ in (5) is an expansion in the eigenfunctions of the Laplacian operator in cylindrical coordinates. This facilitates the determination of the particular solution φ_{inhom} of the inhomogeneous equation. If we write ρ in the form

$$\rho = \frac{e}{(2\pi)^2 v}\sum_{m=-\infty}^{m=\infty}\int \rho_m(r, z, \varphi, t, k, \omega)\,k\,dk\,d\omega, \qquad (6)$$

then from Eq. (5), ρ_m satisfies the equation $\Delta\rho_m = \lambda\rho_m$, *i.e.*, it is an eigenfunction of the Laplacian operator with eigenvalues $\lambda = -(k^2 + \omega^2/v^2)$. Whence it follows that

$$\varphi = \frac{e}{\pi v}\sum_{m=-\infty}^{m=\infty} e^{im\varphi}\int\frac{J_m(kr)\,J_m(kr_0)}{\varepsilon(\omega)\,(k^2 + \omega^2/v^2)}\,e^{i\omega(z-vt)/v}k\,dk\,d\omega. \qquad (7)$$

The integration over k in Eq. (7) is performed without difficulty. We obtain

$$\varphi = \frac{e}{\pi v}\sum_{m=-\infty}^{m=\infty} e^{im\varphi}\int e^{i\omega(z-vt)/v}\,\varphi_{m\,\text{inhom}}(r, \omega)\,d\omega, \qquad (8)$$

$$\varphi_{m\,\text{inhom}} = \begin{cases} \dfrac{1}{\varepsilon_1(m)}K_m\left(\dfrac{|\omega|}{v}r\right)I_m\left(\dfrac{|\omega|}{v}r_0\right) & r > r_0 \\ \dfrac{1}{\varepsilon_1(\omega)}I_m\left(\dfrac{|\omega|}{v}r\right)K_m\left(\dfrac{|\omega|}{v}r_0\right) & r < r_0. \end{cases} \qquad (9)$$

Here, I_m and K_m are Bessel functions of imaginary argument. Eq. (8) gives the particular solution of the inhomogeneous equation inside the channel. To this solution it is necessary to add a solution of the homogeneous equation which satisfies the boundary conditions at $r = a$.

To the solution in (9) we add the function $\varphi_{m\,\text{hom}}$ which satisfies

$$\varphi_{m\,\text{hom}} = \begin{cases} \dfrac{\alpha_m}{\varepsilon_1}I_m\left(\dfrac{|\omega|}{v}r_0\right)I_m\left(\dfrac{|\omega|}{v}r\right) & r < a \\ \gamma_m K_m\left(\dfrac{|\omega|}{v}r\right) & r > a. \end{cases} \qquad (10)$$

The boundary conditions at $r = a$

$$\varphi_{1m} = \varphi_{2m}, \quad \varepsilon_1\partial\varphi_{1m}/\partial r = \varepsilon_2\partial\varphi_{2m}/\partial r$$

yield

$$\alpha_m = \frac{(\varepsilon_2 - \varepsilon_1) K_m(|\omega| a/v) K'_m(|\omega| a/v)}{\varepsilon_1 K_m(|\omega| a/v) I'_m(|\omega| a/v) - \varepsilon_2 I_m(|\omega| a/v) K'_m(|\omega| a/v)}; \tag{11}$$

$$\gamma_m = \frac{(v/\omega a) I_m(|\omega| r_0/v)}{\varepsilon_1 K_m(|\omega| a/v) I'_m(|\omega| a/v) - \varepsilon_2 I_m(|\omega| a/v) K'_m(|\omega| a/v)}.$$

Thus the potential of the longitudinal field is completely determined. The expansion of the potential is of the form given in (8) where instead of $\varphi_{m\,\mathrm{inhom}}$ we must use $\varphi_{m\,\mathrm{inhom}} + \varphi_{m\,\mathrm{hom}}$.

We now ascertain the vector potential **A** for the transverse field. First we find the particular solution for the inhomogenous equation

$$\Delta \mathbf{A} - \frac{\varepsilon}{c^2}\frac{\partial^2 \mathbf{A}}{\partial t^2} = -\frac{4\pi}{c}\mathbf{j} + \frac{\varepsilon}{c}\,\mathrm{grad}\,\frac{\partial \varphi}{\partial t}.$$

The solution of this equation is conveniently represented in the form

$$\mathbf{A}_{\mathrm{inhom}} = \mathbf{A}_{\mathrm{I}} + \mathbf{A}_{\mathrm{II}}, \tag{12}$$

$$\mathbf{A}_{\mathrm{I}} = \frac{e}{\pi c}\sum_{m=-\infty}^{m=+\infty} e^{im\varphi}\int e^{i\omega(z-vt)/v}\,\mathbf{A}_{m\mathrm{I}}(r,\omega)\,d\omega,$$

$$\begin{aligned}
A_{mz\mathrm{I}} &= \frac{1}{\varepsilon_1\beta^2}\left[K_m\left(\frac{|\omega|}{v}r\right)I_m\left(\frac{|\omega|}{v}r_0\right) - \varkappa_1^2 K_m\left(\frac{|\omega|}{v}\varkappa_1 r\right)I_m\left(\frac{|\omega|}{v}\varkappa_1 r_0\right)\right],\\
A_{mr\mathrm{I}} &= -\frac{i}{\varepsilon_1\beta^2}\left[K'_m\left(\frac{|\omega|}{v}r\right)I_m\left(\frac{|\omega|}{v}r_0\right) - \varkappa_1 K'_m\left(\frac{|\omega|}{v}\varkappa_1 r\right)I_m\left(\frac{|\omega|}{v}\varkappa_1 r_0\right)\right],\\
A_{m\varphi\mathrm{I}} &= \frac{mv}{\omega r}\frac{1}{\varepsilon_1\beta^2}\left[K_m\left(\frac{|\omega|}{v}r\right)I_m\left(\frac{|\omega|}{v}r_0\right) - K_m\left(\frac{|\omega|}{v}\varkappa_1 r\right)I_m\left(\frac{|\omega|}{v}\varkappa_1 r_0\right)\right],\\
\varkappa_1 &= \sqrt{1-\varepsilon_1\beta^2},\quad \omega > 0,\quad r > r_0,\quad r < a.
\end{aligned} \tag{13}$$

Equation (13) applies for $\omega > 0$, $r > r_0$. For $r < r_0$, the expressions for $\mathbf{A}_m$ are obtained from (13) by replacing I_m with K_m, K'_m with I'_m, and K_m with I_m. For example, for $r < r_0$, $\omega > 0$:

$$A_{mr\mathrm{I}} = -\frac{i}{\varepsilon_1\beta^2}\left[I'_m\left(\frac{|\omega|}{v}r\right)K_m\left(\frac{|\omega|}{v}r_0\right) - \varkappa_1 I'_m\left(\frac{|\omega|}{v}\varkappa_1 r\right)K_m\left(\frac{|\omega|}{v}\varkappa_1 r_0\right)\right].$$

When $\omega < 0$, the complex conjugate of the expression is used. In this case, if $\varepsilon_1\beta^2 > 1$,

$$\varkappa_1 = \begin{cases} +i\sqrt{\varepsilon_1\beta^2 - 1} & \omega > 0\\ -i\sqrt{\varepsilon_1\beta^2 - 1} & \omega < 0\end{cases}$$

The expressions in (13) also apply when $r > a$; in this case ε_1 is replaced by ε_2.

The term $\mathbf{A}_{\mathrm{II}}$ is determined by the expression

$$\mathbf{A}_{\mathrm{II}} = \frac{e}{\pi c}\sum_{m=-\infty}^{m=+\infty} e^{im\varphi}\int e^{i\omega(z-vt)/v}\,\mathbf{A}_{m\mathrm{II}}(r,\omega)\,d\omega,$$

where

$$A_{mz\mathrm{II}} = \begin{cases} \dfrac{\alpha_m}{\varepsilon_1\beta^2} I_m\left(\dfrac{|\omega|}{v}r_0\right) I_m\left(\dfrac{|\omega|}{v}r\right) & r < a,\\[2ex] \dfrac{\gamma_m}{\beta^2} K_m\left(\dfrac{|\omega|}{v}r\right) & r > a,\end{cases} \qquad A_{mr\mathrm{II}} = \begin{cases} -i\,\dfrac{\alpha_m}{\varepsilon_1\beta^2} I_m\left(\dfrac{|\omega|}{v}r_0\right) I'_m\left(\dfrac{|\omega|}{v}r\right) & r < a\\[2ex] -i\,\dfrac{\gamma_m}{\beta^2} K'_m\left(\dfrac{|\omega|}{v}r\right) & r > a,\end{cases}$$

$$A_{m\varphi\mathrm{II}} = \begin{cases} \dfrac{mv}{\omega r}\dfrac{\alpha_m}{\varepsilon_1\beta^2} I_m\left(\dfrac{|\omega|}{v}r_0\right) I_m\left(\dfrac{|\omega|}{v}r\right) & r < a\\[2ex] \dfrac{mv}{\omega r}\dfrac{\gamma_m}{\beta^2} K_m\left(\dfrac{|\omega|}{v}r\right) & r > a.\end{cases} \tag{14}$$

Equations (13) and (14) yield the particular solution of the inhomogeneous equation inside and outside the channel.

We now find the general solution for the homogeneous equation. It is necessary to find the general expression for the "cylindrical" vector, *i.e.*, the vector which satisfies the following equation in a cylindrical coordinate system:

$$\mathbf{\Lambda}_{\text{hom}} = 0, \quad \operatorname{div} \mathbf{\Lambda}_{\text{hom}} = 0.$$

It is easily shown that this vector can be written in the form

$$\mathbf{A}_{\text{hom}} = \frac{e}{\pi c} \sum_{m=-\infty}^{m=\infty} e^{im\varphi} \int e^{i\omega(z-vt)/v} \mathbf{A}_{m\,\text{hom}}(r,\ \omega)\, d\omega,$$

$$A_{mz\,\text{hom}} = \begin{cases} \dfrac{-\varkappa_1^2}{\varepsilon_1\beta^2} \lambda_{1m} I_m\left(\dfrac{|\omega|}{v}\varkappa_1 r_0\right) I_m\left(\dfrac{|\omega|}{v}\varkappa_1 r\right) & r < a \\ -\dfrac{\varkappa_2^2}{\varepsilon_2\beta^2} \lambda_{2m} I_m\left(\dfrac{|\omega|}{v}\varkappa_2 r_0\right) K_m\left(\dfrac{|\omega|}{v}\varkappa_2 r\right) & r > a, \end{cases}$$

$$A_{mr\,\text{hom}} = \begin{cases} \dfrac{i\varkappa_1}{\varepsilon_1\beta^2} I_m\left(\dfrac{|\omega|}{v}\varkappa_1 r_0\right)\left[\lambda_{1m} I_m'\left(\dfrac{|\omega|}{v}\varkappa_1 r\right) + \dfrac{mv}{\omega r}\dfrac{\theta_{1m}}{\varkappa_1} I_m\left(\dfrac{|\omega|}{v}\varkappa_1 r\right)\right] & r < a \\ \dfrac{i\varkappa_2}{\varepsilon_2\beta^2} I_m\left(\dfrac{|\omega|}{v}\varkappa_2 r_0\right)\left[\lambda_{2m} K_m'\left(\dfrac{|\omega|}{v}\varkappa_2 r\right) + \dfrac{mv}{\omega r}\dfrac{\theta_{2m}}{\varkappa_2} K_m\left(\dfrac{|\omega|}{v}\varkappa_2 r\right)\right] & r > a \end{cases} \tag{15}$$

$$A_{m\varphi\,\text{hom}} = \begin{cases} -\dfrac{\varkappa_1}{\varepsilon_1\beta^2} I_m\left(\dfrac{|\omega|}{v}\varkappa_1 r_0\right)\left[\dfrac{mv}{\omega r}\dfrac{\lambda_{1m}}{\varkappa_1} I_m\left(\dfrac{|\omega|}{v}\varkappa_1 r\right) + \theta_{1m} I_m'\left(\dfrac{|\omega|}{v}\varkappa_1 r\right)\right] & r < a \\ \dfrac{-\varkappa_2}{\varepsilon_1\beta^2} I_m\left(\dfrac{|\omega|}{v}\varkappa_2 r_0\right)\left[\dfrac{mv}{\omega r}\dfrac{\lambda_{2m}}{\varkappa_2} K_m\left(\dfrac{|\omega|}{v}\varkappa_2 r\right) + \theta_{2m} K_m'\left(\dfrac{|\omega|}{v}\varkappa_2 r\right)\right] & r > a. \end{cases}$$

The coefficients λ_{1m}, λ_{2m}, θ_{1m} and θ_{2m} must be determined from the continuity conditions on E_z, E_φ, E_r and H_z at the edge of the channel. These conditions yield four equations for the coefficients. For brevity we shall use the following notation

$$I_m\left(\frac{|\omega|}{v} a\right) = I, \quad I_m\left(\frac{|\omega|}{v}\varkappa_1 r_0\right) = I_{\varkappa_1}, \quad K_m\left(\frac{|\omega|}{v}\varkappa_1 a\right) = K_1,$$
$$K_m\left(\frac{|\omega|}{v} a\right) = K, \quad I_m\left(\frac{|\omega|}{v}\varkappa_2 r_0\right) = I_{\varkappa_2}, \quad K_m\left(\frac{|\omega|}{v}\varkappa_2 a\right) = K_2,$$
$$I_m\left(\frac{|\omega|}{v}\varkappa_1 a\right) = I_1.$$

Then,

$$\lambda_{1m} = \frac{1}{D}\left[(\varkappa_1\varkappa_2)^2 (\varkappa_1 I_1 K_2' - \varkappa_2 I_1' K_2)(\varkappa_1\varepsilon_2 K_1 K_2' - \varkappa_2\varepsilon_1 K_2 K_1') - \left(\frac{mv}{\omega a}\right)^2 I_1 K_1 K_2^2 (\varepsilon_2 - \varepsilon_1)^2 \beta^2\right],$$

$$\lambda_{2m} = \frac{1}{D}\left[\varkappa_1^3\varkappa_2\varepsilon_2 \frac{v}{\omega a}\frac{I_{\varkappa_1}}{I_{\varkappa_2}} (\varkappa_1 I_1 K_2' - \varkappa_2 I_1' K_2)\right] - 1;$$

$$\theta_{1m} = \frac{1}{D}\left[m\left(\frac{v}{\omega a}\right)^2 \varkappa_2^2\varepsilon_1(\varepsilon_1 - \varepsilon_2)\beta^2 K_2^2\right];$$

$$\theta_{2m} = \frac{1}{D}\left[m\left(\frac{v}{\omega a}\right)^2 \varkappa_1^2\varepsilon_2(\varepsilon_1 - \varepsilon_2)\beta^2 I_1 K_2 \frac{I_{\varkappa_1}}{I_{\varkappa_2}}\right];$$

$$D = (\varkappa_1\varkappa_2)^2 (\varkappa_1 I_1 K_2' - \varkappa_2 I_1' K_2)(\varepsilon_1\varkappa_2 K_2 I_1' - \varepsilon_2\varkappa_1 I_1 K_2') + \left(\frac{mv}{\omega a}\right)^2 (I_1 K_2)^2 (\varepsilon_2 - \varepsilon_1)^2 \beta^2. \tag{16}$$

Equations (13), (14), (15) and (16) determine completely the vector potential of the transverse field which satisfies the boundary conditions. If, in we set $r_0 = 0$ the formulas obtained earlier for φ and $\mathbf{A}$ these equations pertain to the motion of a charge along the axis of a channel of radius a. This procedure is easily carried out, noting that

$$I_m(0) = \begin{cases} 1 & m = 0 \\ 0 & m \neq 0, \end{cases}$$

while $mI_m(0) = 0$ for any m. As is to be expected, the formulas for φ and $\mathbf{A}$ go over to expressions for the potentials obtained in Refs. 1 and 7 in which the motion of a charge along the axis of a channel in a dielectric was considered.

2. Using the gauge which is obtained from the condition $\operatorname{div}\mathbf{A} = 0$, it is possible to divide the field into a longitudinal part and a transverse part. For example,

$$E_{z\,\text{long}} = -\frac{\partial\varphi}{\partial z}, \quad E_{z\,\text{tr}} = -\frac{1}{c}\frac{\partial A_z}{\partial t} \tag{17}$$

In what follows, it will be of interest to find the energy lost by the charge in the excitation of the transverse field in the medium, in particular, the loss due to Cerenkov radiation. This energy loss can be determined in terms of the reaction on the charge itself of the transverse field created by the charge

$$eE_{z\text{tr}} = \frac{e^2}{\pi v^2}\sum_{m=0}^{\infty} a_m \int \frac{i\omega}{\varepsilon_1}\Big\{ I_m\Big(\frac{|\omega|}{v} r_0\Big)\Big[K_m\Big(\frac{|\omega|}{v} r_0\Big) + \alpha_m I_m\Big(\frac{|\omega|}{v} r_0\Big)\Big] - \varkappa_1^2 I_m\Big(\frac{|\omega|}{v}\varkappa_1 r_0\Big)\Big[K_m\Big(\frac{|\omega|}{v}\varkappa_1 r_0\Big) + \lambda_{1m} I_m\Big(\frac{|\omega|}{v}\varkappa_1 r_0\Big)\Big]\Big\} d\omega, \tag{18}$$

where $a_m = 1$ for $m = 0$ and $a_m = 2$ for $m \neq 0$.

For values of ω which satisfy $\varepsilon_1(\omega) = 0$, the expression under the integral sign has no singularity. This is to be expected since the losses at the frequencies for which $\varepsilon_1(\omega) = 0$ are characteristic only of the longitudinal field.

To compute the dependence of the energy integral on r_0, we consider the case analyzed by Ginzburg and Frank,[1] *i.e.*, the motion of a charge inside a hollow channel when

$$\varepsilon_1 = 1, \ \varepsilon_2\beta^2 > 1.$$

Since $\varkappa_1 = \sqrt{1 - \beta^2} > 0$, I_m and K_m are real functions; hence the energy loss (18) for the present case can be expressed as follows:

$$eE_{z\text{tr}} = -\frac{e^2}{\pi v^2}(1-\beta^2)\sum_{m=0}^{\infty} a_m \times \int_{\varepsilon_2\beta^2>1} \lambda_{1m} I_m^2\Big(\frac{|\omega|}{v}\varkappa_1 r_0\Big) i\omega\, d\omega,$$

where λ_{1m} is determined from (16).

If the departure of the charge from the axis of the channel is small, the energy integral is simplified if I_m is expanded in powers of r_0

$$\begin{aligned} eE_{z\text{tr}} = &-\frac{e^2}{\pi v^2}(1-\beta^2)\int_{\varepsilon_2\beta^2>1} \lambda_{10} i\omega\, d\omega \\ &-\frac{e^2}{\pi v^2}(1-\beta^2)\, r_0^2 \int_{\varepsilon_2\beta^2>1} \frac{\lambda_{10}+\lambda_{11}}{2} i\omega^3 d\omega. \end{aligned} \tag{19}$$

Using well-known relations for Bessel functions, it may be shown that the first term in (19) coincides with the expression obtained in Ref. 1. The second term in (19) is proportional to r_0^2. This dependence on r_0 at small r_0 indicates that when the charge moves along the axis of the channel the loss is either a maximum or a minimum. The coefficient λ_{11} [*cf.* (16)] is a complicated complex function and, in the general case, an investigation of the expression in (19) is difficult.

3. [illegible] consider the motion of a charge in the particular case in which the second medium is a metal with infinite conductivity. This case is characterized by $\varkappa_2 \to \infty$ and $\varepsilon_2 \to -\infty$.

It is easy to show that in the case at hand (18) goes over to the expression

$$eE_{z\,\text{tr}} = -\frac{e^2}{2v^2}\operatorname{Re}\sum_{m=0}^{\infty} a_m \int_{\varepsilon_1\beta^2>1} \frac{1-\varepsilon_1\beta^2}{\varepsilon_1}\, \frac{J_m^2(|\omega||\varkappa_1| r_0/v)\, N_m(|\omega||\varkappa_1| a/v)}{J_m(|\omega||\varkappa_1| a/v)}\, i\omega\, d\omega. \tag{20}$$

The loss integral is determined by the residues at the poles of the expression under the integral. Because of the poles the integrals become series and the continuous spectrum is replaced by a discrete spectrum characteristic of a waveguide.

Actually a pole is found when $J_m\Big(\frac{|\omega|}{v}\sqrt{\varepsilon_1\beta^2 - 1}\, a\Big) = 0$, *i.e.*, for values $\omega = \omega_{ms}$, for which $\frac{|\omega_{ms}|}{v}\sqrt{\varepsilon_1(\omega_{ms})\beta^2 - 1}\, a = \mu_{ms}$ where μ_{ms} is the sth root of the Bessel function of mth order. The following expression is obtained for the loss due to Cerenkov radiation:

$$eE_{z\,\mathrm{tr}} = -\frac{2e^2}{a^2}\sum_{m,s} a_m \frac{\mu_{ms}}{\omega_{ms}} \tag{21}$$

$$\times\left[\frac{d}{d\omega}\left(\frac{|\omega|}{v}\sqrt{\varepsilon_1\beta^2-1}\,a\right)\right]^{-1}_{\omega=\omega_{ms}} \frac{1}{\varepsilon_1(\omega_{ms})}\frac{J_m^2(\mu_{ms}r_0/a)}{J_m'^2(\mu_{ms})}.$$

If the material with which the wave guide is filled is dispersionless, that is, if $\varepsilon_1 = \mathrm{const} > 1/\beta^2$, the loss can be written in a simpler form

$$eE_z = -\frac{4e^2}{a^2\varepsilon_1}\sum_{s=1}^{\infty}\left[\frac{1}{2}\frac{J_0^2(\mu_{0s}r_0/a)}{J_0'^2(\mu_{0s})} + \sum_{m=1}^{\infty}\frac{J_m^2(\mu_{ms}r_0/a)}{J_m'^2(\mu_{ms})}\right]. \tag{22}$$

Eq. (22) was obtained by a different method in Ref. 8. If the charge moves along the axis the formula for the loss due to Cerenkov radiation goes over to the expression first obtained by Akhiezer, Liubarskii, and Fainberg:

$$eE_{z\,\mathrm{tr}} = -\frac{2e^2}{a^2}\frac{1}{\varepsilon_1}\sum_{s=1}^{\infty} J_1^{-2}(\mu_{0s}) \quad \text{for} \quad \varepsilon_1\beta^2 > 1.$$

Using Eq. (22) we can determine the magnitude of the Cerenkov-radiation loss as a function of r_0. The Cerenkov loss is a maximum when $r_0 = 0$. Actually, it is easy to show that in this case, when $r_0 = 0$

$$d\,(eE_{z\,\mathrm{tr}})/dr_0 = 0, \quad d^2(eE_{z\,\mathrm{tr}})/dr_0^2 < 0.$$

When $r_0 = a$, the loss is equal to zero.

4. The case of a charge which does not move along the axis allows an analysis of the radial force which acts on the charge. A charge moving in a channel with $\varepsilon_1\beta^2 < 1$, will radiate into the outer medium. The radiation reaction in non-central motion will be directed not only along the line of motion of the charge but also in the radial direction. From simple physical considerations, it is clear that if the radiation of the charge is directed into the external medium, the charge should experience a recoil force in the direction of the axis. However, in addition to the radiation reaction, there are also so-called "image" forces which arise as a result of the presence of the boundary. It is impossible to separate the effect of the image force from the reaction on the Cerenkov radiation.

We now find the conditions for which the charge is focused towards the axis. We write the radial component of the force which acts on the charge

$$F_r = eE_r + \frac{e}{c}[\mathbf{v}\times\mathbf{H}]_r,$$

$$F_r = -\frac{e^2}{\pi v^2}\sum_{m=0}^{\infty} a_m \int\frac{\varkappa_1^3}{\varepsilon_1} I_m\left(\frac{|\omega|}{v}\varkappa_1 r_0\right)$$

$$\times\left[K_m'\left(\frac{|\omega|}{v}\varkappa_1 r_0\right) + \lambda_{1m} I_m'\left(\frac{|\omega|}{v}\varkappa_1 r_0\right)\right]\omega\,d\omega.$$

$$a_0 = 1,\ a_m = 2 \text{ for } m \neq 0$$

It is obvious that a contribution to the radial force is given only by terms with λ_{1m} under the integral. Hence,

$$F_r = -\frac{e^2}{\pi v^2}\sum_{m=0}^{\infty} a_m$$

$$\times \operatorname{Re}\int\frac{\varkappa_1^3}{\varepsilon_1}\lambda_{1m} I_m\left(\frac{|\omega|}{v}\varkappa_1 r_0\right) I_m'\left(\frac{|\omega|}{v}\varkappa_1 r_0\right)\omega\,d\omega. \tag{23}$$

The sign of F_r is determined by the sign of Re λ_{1m} since I_m and I_m' are positive real functions. As has been indicated above, λ_{1m} is a complicated function and in the general case it is impossible to ascertain the sign of the radial force. In the particular case of the emission of waves whose wavelength is much smaller than the radius of the channel, $|\omega|\varkappa_1 a/v \gg 1$, it is possible to make use of the asymptotic form of the Bessel function and the expression for λ_{1m} is simplified considerably.

For $|\omega|\varkappa_1 a/v \to \infty$:

$$\lambda_{1m} = \pi e^{-2|\omega|\varkappa_1 a/v}\,\frac{\varepsilon_1^2 t^2 - \varepsilon_2^2\varkappa_1^2 + 2i\varkappa_1 t\varepsilon_1\varepsilon_2}{\varepsilon_1^2 t^2 + \varepsilon_2^2\varkappa_1^2},$$

where $t^2 = \varepsilon_2\beta^2 - 1$ and $\varkappa_1^2 = 1 - \varepsilon_1\beta^2$. From the expression for λ_{1m} it is obvious that Re $\lambda_{1m} > 0$ when

$$\varepsilon_1^2 t^2 > \varepsilon_2^2\varkappa_1^2.$$

In this case the charge experiences a focusing force.

5. It is well known that when a charged particle moves uniformly in an infinite cylindrical channel in which the conditions for Cerenkov radiation are satisfied while the Cerenkov radiation cannot be excited in the medium external to the channel, *i.e.*, when $\varepsilon_1\beta^2 > 1$ and $\varepsilon_2\beta^2 < 1$, the spectrum of the radiation in the channel will exhibit a discrete character, in contrast to the continuous spectrum radiated by a particle in an unbounded medium.

The equation for the frequency spectrum has been obtained by Bolotovskii for the case in which the charged particle moves along the axis of the channel:[7]

$$\begin{aligned}&\varepsilon_1 \sqrt{1-\varepsilon_2\beta^2}\, K_0\left(\frac{|\omega|}{v} a \sqrt{1-\varepsilon_2\beta^2}\right)\\ &\quad\times J_0'\left(\frac{|\omega|}{v} a \sqrt{\varepsilon_1\beta^2-1}\right)\\ &+\varepsilon_2 \sqrt{\varepsilon_1\beta^2-1}\, J_0\left(\frac{|\omega|}{v} a \sqrt{\varepsilon_1\beta^2-1}\right)\\ &\quad\times K_0'\left(\frac{|\omega|}{v} a \sqrt{1-\varepsilon_2\beta^2}\right)=0\end{aligned} \tag{24}$$

In the short-wave range, *i.e.*, when $\omega\sqrt{1-\varepsilon\beta^2}\, a/v \gg 1$, Eq. (24) can be simplified considerably if the asymptotic expressions for the Bessel functions are used

$$\tan\left(\frac{|\omega|}{v} a \sqrt{\varepsilon_1\beta^2-1}-\frac{\pi}{4}\right)=-\frac{\varepsilon_2}{\varepsilon_1}\sqrt{\frac{\varepsilon_1\beta^2-1}{1-\varepsilon_2\beta^2}}, \tag{25}$$

this expression is similar to that derived by Frank for this case from simple physical considerations.[10]

For practical purposes it is of interest to analyze the radiation spectrum when a charged particle moves parallel to the axis of a cylindrical channel but at a distance r_0 from the axis. Using (16), the dispersion equation for this case can be written as follows:

$$\begin{aligned}&s^2\varkappa_2^2\,[\varepsilon_1\varkappa_2K_2J_1'+\varepsilon_2 sJ_1K_2']\,[-sJ_1K_2'-\varkappa_2J_1'K_2]\\ &\quad+(mv/\omega a)^2J_1^2K_2^2(\varepsilon_2-\varepsilon_1)^2\beta^2=0,\end{aligned} \tag{26}$$

where for brevity, we have introduced the notation

$$s^2=\varepsilon_1\beta^2-1,\quad \varkappa_2^2=1-\varepsilon_2\beta^2,$$

$$K_2=K_m\left(\frac{|\omega|}{v}a\varkappa_2\right),\ J_1=J_m\left(\frac{|\omega|}{v}as\right).$$

This equation has discrete roots. In the radiation of short waves, just as in (25), the asymptotic form of the Bessel function can be used and the dispersion equation can be written:

$$\tan\left(\frac{|\omega|}{v}as-\frac{m\pi}{2}-\frac{\pi}{4}\right)=\frac{-s\varkappa_2(\varepsilon_1+\varepsilon_2)+s\varkappa_2(\varepsilon_1-\varepsilon_2)\sqrt{1+4(mv/\omega a)^2\varepsilon_1/s^4\varkappa_2^2}}{2\varepsilon_1\varkappa_2^2}. \tag{27}$$

When $m = 0$, (27) goes over to (25). The expression in the right-hand part of (27) can be called the change of phase of the mth harmonic in total internal reflection. It is interesting to note that the equation which determines the eigen-frequency of the Cerenkov radiation produced by a particle moving with a velocity close to the velocity of light in the case where the external medium is a metal has exactly the same form as that pertaining to a Cerenkov counter, in which the radiation undergoes total internal reflection at the boundaries (for example, $\varepsilon_2 = 1$). Actually, the metal is characterized by $\varepsilon_2 \to -\infty$, $\varkappa_2 \to \infty$ while in the second case $\varepsilon_2 = 1$, $\beta = 1$, *i.e.*, $\varkappa_2 \to 0$. The dispersion equation (27) in both cases assumes the form

$$\tan\left(\frac{|\omega|}{v}as-\frac{m\pi}{2}-\frac{\pi}{4}\right)\to\infty,$$

$$i.e.,\ \frac{|\omega|}{v}as-\frac{m\pi}{2}+\frac{\pi}{4}=\pi n,$$

where $n = 0, 1, 2, \ldots$ Hence, the radiation spectrum produced by a parallel beam of relativistic particles is the same in a silvered and non-silvered Cerenkov counter.

---

[1] V. L. Ginzburg and I. M. Frank, Dokl. Akad. Nauk SSSR **56**, 699 (1947).

[2] A. Bohr, cited in N. Bohr, *The Passage of Atomic Particles Through Matter* (Moscow, 1950, Russian translation).

[3] M. Schoenberg, Nuovo cimento **9**, 270 (1952).

[4] M. Schoenberg, Nuovo cimento **9**, 372 (1952).

[5] H. Huybrechts and M. Schoenberg, Nuovo cimento **9**, 764 (1952).

[6] A. G. Sitenko, J. Tech. Phys. (U.S.S.R.) **23**, 2200 (1953).

[7] M. Bolotovskii, Dissertation, Institute of Physics, Academy of Sciences (1954).

[8] Cestmir Muzikar, Czech. J. Phys. **5**, 1, 9 (1955).

[9] Akhiezer, Liubarskii and Fainberg, Dokl. Akad. Nauk SSSR **73**, 55 (1950).

[10] I. M. Frank, Usp. Fiz. Nauk **58**, 111 (1956).

Translated by H. Lashinsky
282

SOVIET PHYSICS JETP VOLUME 5, NUMBER 6 DECEMBER 15, 1957

Optical Model of the Interaction of Nucleons with Nuclei in the Resonance Region of the Compound Nucleus

V. M. AGRANOVICH AND A. S. DAVYDOV

(Submitted to JETP editor August 17, 1956)
J. Exptl. Theoret. Phys. (U.S.S.R.) 32, 1429-1436 (June, 1957)

A study is made of the energy dependence of the real and imaginary parts of the effective potential of the optical model, with all states of the compound nucleus taken into account. An interpretation is given of the broad resonances in the interaction of neutrons with nuclei.

INTRODUCTION

IN PAPERS of Brueckner, Watson, and their collaborators[1] a basis has been given for the optical model of the interaction of low-energy nucleons with nuclei, which had been introduced by Feshbach, Porter, and Weisskopf[2] to explain the scattering by nuclei of neutrons of energies up to 3 Mev. In the optical model the interaction of a nucleon with a nucleus, which involves the many-body problem, is reduced to a consideration of the motion of the nucleon in a certain complex effective potential $V(1+i\zeta)$. Here the results of the interaction of the nucleon with the nucleus are separated into the elastic scattering (caused by the real part of the potential) and all other processes, which go through the stage of the compound nucleus (caused by the imaginary part of the potential). The imaginary part of the optical potential is determined by the coupling between the one-nucleon excited states and the many-particle excitations of the compound nucleus.

A study of the energy dependence of the real and imaginary parts of the effective potential is of great interest, especially in the range of energies corresponding to those at which isolated resonances are observed in the cross-sections. This problem has already been studied in a paper by Brueckner, Eden, and Francis.[3] In that paper, however, only the two-particle states of the compound system are considered; it is shown that in the energy range corresponding to two-particle excitations of the compound system the real and imaginary parts of the effective potential undergo considerable changes.

In the present paper an attempt is made to study the energy dependences of the real and imaginary parts of the effective potential with the inclusion of all states of the compound nucleus. Unlike what was found in Ref. 3, we do not get a rapid variation of the real part of the potential in the energy range corresponding to the isolated resonances in the reaction cross-sections. Even the imaginary part of the potential increases relatively smoothly with the energy outside the isolated resonances and in the region of overlapping levels. In the region of isolated resonances the imaginary part of the effective potential rises sharply.

In order not to complicate the problem by inclusion of the Coulomb interaction, we consider only the interaction of a neutron with the nucleus.

1. ENERGY DEPENDENCE OF THE REAL PART OF THE OPTICAL POTENTIAL

According to the optical model[1] the real part of the effective interaction potential of a neutron and a nucleus is given by

$$V(r) = \mathrm{Re} \sum_{\alpha=1}^{A} \langle t_\alpha \rangle, \tag{1.1}$$

where $<t_\alpha>$ denotes the average, over the wave function φ_0 of the ground state of the target nucleus A, of the operator of the interaction of pairs, which is determined by the integral equation

$$t_\alpha = v_\alpha + v_\alpha D^{-1} t_\alpha, \tag{1.2}$$

where v_α is the interaction of the incident nucleon with the αth nucleon of the target nucleus; the operator D is given by

$$D = E - H_A - K_n + i\eta, \tag{1.3}$$

where E is the energy of the system, H_A is the Hamiltonian operator of the nucleus A, K_n is the operator for the kinetic energy of the relative motion of neutron and nucleus, and η is a small positive number, which assures the presence of outgoing waves only in the scattering. After the integrations have been carried out one must let η go to zero.

By direct substitution one can verify by the use of the operator identity

$$D^{-1} + D^{-1}v_\alpha (D - v_\alpha)^{-1} \equiv (D - v_\alpha)^{-1},$$

that the operator equation (1.2) has the solution

$$t_\alpha = v_\alpha + v_\alpha (D - v_\alpha)^{-1} v_\alpha. \qquad (1.4)$$

In the approximation of the optical model the wave function χ_ϵ of the incident neutron must satisfy the Schrödinger equation

$$[\varepsilon - K_n + V(r)]\,\chi_\varepsilon(r) = 0,$$

where ε is the energy of the relative motion of neutron and nucleus.

Let us determine the dependence of the mean value of the real part of the optical potential

$$\overline{V} = (\chi_\varepsilon(r), \quad V(r)\,\chi_\varepsilon(r)). \qquad (1.5)$$

on the energy ε of the relative motion. Substituting Eq. (1.1) into Eq. (1.5) and taking into account Eq. (1.4), we get

$$\overline{V} = \operatorname{Re} \sum_{\alpha=1}^{A} \{(\Phi_{0\varepsilon}, v_\alpha \Phi_{0\varepsilon})$$

$$+ (\Phi_{0\varepsilon}, v_\alpha (D - v_\alpha)^{-1} v_\alpha \Phi_{0\varepsilon})\}, \qquad (1.6)$$

where $\Phi_{0\epsilon} = \varphi_0 \chi_\epsilon(r)$.

We are interested in the behavior of the expression (1.6) in the energy range corresponding to the resonances in the cross-sections for nuclear reactions. We introduce the wave functions X_λ and energies E_λ of the compound nucleus $A + 1$ by means of the Schrödinger equation

$$HX_\lambda = E_\lambda X_\lambda, \qquad (1.7)$$

where

$$H = H_A + K_n + \sum_{\alpha=1}^{A} v_\alpha \qquad (1.8)$$

is the Hamiltonian operator of the total system.

With natural boundary conditions the solutions (1.7) for $E_\lambda > 0$ correspond to disintegrating states. Because of the large lifetimes of the states of the compound nucleus in comparison with the lifetimes of single particle excitations, we shall make the approximation of assuming that the E_λ are real and that the X_λ form a complete normal orthogonal system of functions for the compound nucleus. Then we can write

$$v_\alpha \Phi_{0\varepsilon} = \sum_\lambda R_\lambda^\alpha(\varepsilon)\, X_\lambda,$$

$$R_\lambda^\alpha(\varepsilon) = (X_\lambda, v_\alpha \Phi_{0\varepsilon}). \qquad (1.9)$$

Now we can write

$$(D - v_\alpha)^{-1} v_\alpha \Phi_{0\varepsilon} = \sum_\lambda R_\lambda^\alpha(\varepsilon)\,(D - v_\alpha)^{-1} X_\lambda. \quad (1.10)$$

Introducing the matrix $f_{\lambda\mu}^\alpha(\varepsilon)$ by the equation

$$(D - v_\alpha)^{-1} X_\lambda = \sum_\mu f_{\lambda\mu}^\alpha(\varepsilon)\, X_\mu, \qquad (1.11)$$

we bring Eq. (1.10) into the form

$$(D - v_\alpha)^{-1} v_\alpha \Phi_{0\varepsilon} = \sum_{\lambda,\mu} R_\lambda^\alpha(\varepsilon)\, f_{\lambda\mu}^\alpha(\varepsilon)\, X_\mu. \quad (1.12)$$

To determine the matrix $f_{\lambda\mu}^\alpha(\varepsilon)$ we apply to both sides of Eq. (1.11) the operator

$$D - v_\alpha \equiv E - H + \sum_{\beta \neq \alpha} v_\beta + i\eta;$$

then, taking account of Eq. (1.7), we get

$$X_\lambda = \sum_\mu f_{\lambda\mu}^\alpha(\varepsilon) \Big\{E - E_\mu + i\eta + \sum_{\beta \neq \alpha} v_\beta\Big\} X_\mu.$$

Multiplying this equation by $X_{\lambda_1}^*$ and integrating over all variables of the compound nucleus, we get the equation

$$\sum_\mu f_{\lambda\mu}^\alpha(\varepsilon)\, \{(E - E_\lambda + i\eta)\, \delta_{\mu\lambda_1} + Q_{\mu\lambda_1}^\alpha\} = \delta_{\lambda\lambda_1}, \quad (1.13)$$

where

$$Q_{\mu\lambda}^\alpha \equiv \Big(X_\lambda, \sum_{\beta \neq \alpha} v_\beta X_\mu\Big). \qquad (1.14)$$

Assuming that the nondiagonal matrix elements $Q_{\lambda\mu}$ are smaller in absolute value than the diagonal elements, we can solve Eq. (1.13) for $f_{\lambda\mu}$. Then, substituting Eq. (1.12) into Eq. (1.6) and taking into account Eq. (1.9), we get

$$\bar{V} = \mathrm{Re} \sum_{\alpha} \Big\{ (\Phi_{0\varepsilon}, v_{\alpha}\Phi_{0\varepsilon}) + \sum_{\lambda} \frac{|R_{\lambda}^{\alpha}(\varepsilon)|^2}{E - E_{\lambda} + Q_{\lambda\lambda}^{\alpha} + i\eta} - \sum_{\lambda \neq \mu} \frac{R_{\lambda}^{\alpha}(\varepsilon)}{E - E_{\lambda} + Q_{\lambda\lambda}^{\alpha} + i\eta} Q_{\lambda\mu}^{\alpha} \frac{R_{n}^{*\alpha}(\varepsilon)}{E - E_{\mu} + Q_{\mu\mu}^{\alpha} + i\eta} \Big\}. \tag{1.15}$$

From Eq. (1.14) we see that $Q_{\lambda\lambda}^{\alpha}$ is the average energy of interaction of one nucleon with $A - 1$ nucleons in the compound nucleus in the state X_{λ}. Consequently, $Q_{\lambda\lambda}^{\alpha} < 0$ and its absolute value is some tens of millions of electron volts. Thus it follows from Eq. (1.15) that for energies of relative motion $\varepsilon < 30$ Mev the real part of the potential (1.15) varies smoothly with the energy. At energies of the relative motion greater than 30 Mev the excitation energy of the compound nucleus falls in the region of the continuous spectrum, and the imaginary part of the optical potential becomes so appreciable that the concept of single-particle states becomes less justified.

2. THE IMAGINARY PART OF THE EFFECTIVE INTERACTION POTENTIAL BETWEEN NEUTRON AND NUCLEUS

The imaginary part (ζV) of the potential in the optical model of nuclear interactions describes all processes that go through the stage of the compound nucleus. In obtaining Eq. (1.1) we took into account only the coherent scattering of the neutrons inside the nuclear matter. Therefore the imaginary part $\mathrm{Im} \sum_{\alpha} \langle t_{\alpha} \rangle$ gives only the decay of the state $\Phi_{0\epsilon}$ owing to the presence of outgoing waves. A special argument is required for the calculation of the imaginary part of the potential caused by transitions into states of the compound nucleus with the same energy.

If the probability per unit time for a transition from a single-particle excitation $\Phi_{0\epsilon}$ into excitations of the compound nucleus is denoted by Γ, then the imaginary part ζV of the potential for the optical model is given in terms of Γ by the relation

$$2(\chi_{\varepsilon}, \zeta V \chi_{\varepsilon}) = \hbar\Gamma. \tag{2.1}$$

The system consisting of the nucleus A and the neutron is described in the optical model by the Hamiltonian

$$H_0 = H_A + K_n + V(r), \tag{2.2}$$

where H_A is the Hamiltonian of the target nucleus, K_n is the operator for the kinetic energy of the relative motion of nucleus and neutron, and $V(r)$ is given by Eq. (1.1). Let us denote by $E_{n\epsilon}$ and $\Phi_{n\epsilon}$ respectively the eigenvalues and eigenfunctions of this operator. Here $E_{n\epsilon} = E_n + \varepsilon$, and

$$\Phi_{n\varepsilon} = \varphi_n \chi_{\varepsilon}, \quad H_A \varphi_n = E_n \varphi_n,$$

$$[K_n + V(r)] \chi_{\varepsilon} = \varepsilon \chi_{\varepsilon}.$$

Using Eq. (2.2), we can write the complete Hamiltonian of the system, Eq. (1.8), in the form

$$H = H_0 + H', \tag{2.3}$$

$$H' = \sum_{\alpha} \{v_{\alpha} - \mathrm{Re}\langle t_{\alpha} \rangle\}. \tag{2.4}$$

The operator (2.4), which represents the difference between the complete Hamiltonian and the Hamiltonian of the optical model, is the cause of the formation of the compound nucleus, in which the excitation energy is distributed over a large number of degrees of freedom.

In order to calculate the transition probability Γ we shall look for a solution of the time-dependent Schrödinger equation

$$i\hbar \partial \Psi / \partial t = (H_0 + H') \Psi \tag{2.5}$$

in the form

$$\Psi = a(t) \Phi_{0\varepsilon} \exp\{-iE'_{0\varepsilon} t/\hbar\} + \sum_{n,\xi}{}' b_{n\xi}(t) \Phi_{n\xi} \exp\{-iE'_{n\xi} t/\hbar\} \tag{2.6}$$

with the initial conditions

$$a(0) = 1, \quad b_{n\xi}(0) = 0, \tag{2.7}$$

and where

$$E'_{n\xi} = E_{n\xi} + (\Phi_{n\xi}, H'\Phi_{n\xi}). \tag{2.8}$$

Substituting Eq. (2.6) into Eq. (2.5), we get (for $t < \Gamma^{-1}$) the system of equations

$$\begin{aligned} i\hbar\, da/dt &= \sum_{n\xi}{}' (\Phi_{0\varepsilon}, H'\Phi_{n\xi})\, b_{n\xi} \exp\{i(E'_{0\varepsilon} - E'_{n\xi}) t/\hbar\}, \\ i\hbar\, db_{n\xi}/dt &= a(\Phi_{n\xi}, H'\Phi_{0\varepsilon}) \exp\{i(E'_{n\xi} - E'_{0\varepsilon}) t/\hbar\} + \ldots \end{aligned} \tag{2.9}$$

We solve the system (2.9) with the initial conditions (2.7) by the substitution

$$a(t) = \exp\{-\Gamma t/2\}.$$

Then in the usual way we get

$$b_{n\xi} = (\Phi_{n\xi}, H'\Phi_{0\varepsilon}) \times \frac{\exp\{-i(E'_{0\varepsilon} - E'_{n\xi} - i\Gamma\hbar/2)\,t/\hbar\} - 1}{E'_{0\varepsilon} - E'_{n\xi} - i\Gamma\hbar/2},$$

$$\Gamma = \frac{2i}{\hbar}\sum_{n\xi}{}' \,|(\Phi_{0\varepsilon}, H'\Phi_{n\xi})|^2 \times \frac{1 - \exp\{i(E'_{0\varepsilon} - E'_{n\xi} - i\Gamma\hbar/2)\,t/\hbar\}}{E'_{0\varepsilon} - E'_{n\xi} - i\Gamma\hbar/2}. \qquad (2.10)$$

Introducing the number of states $\omega(E)dE$ in the energy interval dE, we can go in Eq. (2.10) from the sum to an integral; then

$$\Gamma = \frac{2\pi}{\hbar}\,|(\Phi_{0\varepsilon}H'\Phi_{n_0\xi_0})|^2\,\omega(E_{n_0\xi_0}), \qquad (2.11)$$

where $E_{n_0\xi_0} \approx E_{0\epsilon}$.

To find the energy dependence of Γ in the region of the resonances of the compound nucleus, we expand the function $\Phi_{0\epsilon}$ in terms of the complete set of the functions X_λ of the operator (2.3),

$$\Phi_{0\varepsilon} = \sum_\lambda A_{\lambda,0\varepsilon}X_\lambda. \qquad (2.12)$$

It is easy to verify that the expansion coefficients are given by the formula

$$A_{\lambda,0\varepsilon} = (\Phi_{0\varepsilon}, H'X_\lambda)/(E_\lambda - E_{0\varepsilon}). \qquad (2.13)$$

From the normalization of the functions X_λ and $\Phi_{n\xi}$ we have the equations

$$\sum_{n,\xi} A_{\lambda,n\xi}A^*_{\lambda',n\xi} = \delta_{\lambda\lambda'}; \quad \sum_\lambda A_{\lambda,n\xi}A_{\lambda,n'\xi'} = \delta_{nn'}\delta_{\xi\xi'}. \qquad (2.14)$$

Substituting Eq. (2.12) into Eq. (2.11) and using Eq. (2.13), we get

$$\Gamma = \frac{2\pi}{\hbar}\left|\sum_\lambda \frac{(\Phi_{0\varepsilon}, H'X_\lambda)(X_\lambda, H'\Phi_{n_0\xi_0})}{E_\lambda - E_{0\varepsilon}}\right|^2 \omega(E_{n_0\xi_0}). \qquad (2.15)$$

In the region of overlapping resonances the sum over λ can be replaced by an integral; then

$$\Gamma = \frac{2\pi}{\hbar}\left|\int \frac{(\Phi_{0\varepsilon}, H'X_\lambda)(X_\lambda, H'\Phi_{n_0\xi_0})}{E_\lambda - E_{0\varepsilon}}\,\omega(E_\lambda)\,dE_\lambda\right|^2 \times \omega(E_{n_0\xi_0}). \qquad (2.16)$$

If, on the other hand, the energy $E_{0\epsilon}$ falls in the region of isolated resonances, for example $E_{0\epsilon} \approx E_\lambda$, then in the sum over λ in Eq. (2.15) only one term will be important; consequently,

$$\Gamma \approx \frac{2\pi}{\hbar}\left|\frac{(\Phi_{0\varepsilon}, H'X_\lambda)(X_\lambda, H'\Phi_{n_0\xi_0})}{E_\lambda - E_{0\varepsilon}}\right|^2 \omega(E_{n_0\xi_0}) + \Gamma_0, \qquad (2.17)$$

where Γ_0 is the part of Γ that is weakly energy dependent.

To calculate Γ from Eqs. (2.15) and (2.17) one must know the wave functions X_λ and $\Phi_{n\xi}$ and the energy dependence of the density of states $\omega(E)$.

Under certain simplifying assumptions, an estimate of the quantity Γ is made in the following section. Here we only remark that the expressions (2.16) and (2.17) make it possible to draw qualitative conclusions about the energy dependence of Γ. Namely, in the region of isolated resonances of the compound nucleus the energy dependence of Γ is of a resonance character. Outside the isolated resonances and in the region of overlapping resonances the quantity Γ increases with the energy, mainly owing to the change of the density of states $\omega(E)$. It must be noted, however, that our arguments are valid only for not too high excitation energies (ε < 50 Mev).

3. INTERPRETATION OF THE BROAD RESONANCES IN THE INTERACTION OF NEUTRONS WITH NUCLEI

The quantity $\hbar\Gamma$ defined by Eq. (2.15) characterizes the width of the single-particle levels of the nucleus. Therefore $\hbar\Gamma$ is to be compared with the experimentally observed widths (~ 2 Mev) of the broad maxima of the scattering cross-sections of low-energy (~ 5 Mev) neutrons averaged over the resonances.

For an estimate of the quantity Γ in the region of closely spaced resonances, using Eq. (2.13) we put Eq. (2.15) in the following form:

$$\hbar\Gamma = 2\pi\omega(E_{n_0\xi_0}) \Big| \sum_{\lambda} A_{\lambda,0\varepsilon} A_{\lambda,n_0\xi_0} (E_\lambda - E_{n_0\xi_0}) \Big|^2 .$$

Now, neglecting off-diagonal terms of alternating sign, we get

$$\hbar\Gamma \approx 2\pi\omega(E_{n_0\xi_0}) \sum_{\lambda} | A_{\lambda,0\varepsilon} |^2 | A_{\lambda,n_0\xi_0} |^2 (E_\lambda - E_{n_0\xi_0})^2 .$$

Introducing the density of states $\omega(E_\lambda)$ of the compound nucleus, we can replace the summation over λ by an integral over the energy. Then

$$\hbar\Gamma \approx 2\pi\omega(E_{n_0\xi_0}) \times \int | A_{\lambda,0\varepsilon} |^2 | A_{\lambda,n_0\xi_0} |^2 (E_\lambda - E_{n_0\xi_0})^2 \omega(E_\lambda)\, dE_\lambda . \tag{3.1}$$

In this same approximation the orthogonality condition (2.14) is written in the form

$$\int A_{\lambda,n\xi} A^{*}_{\lambda,n'\xi'} \omega(E_\lambda)\, dE_\lambda = \delta_{nn'}\delta_{\xi\xi'} . \tag{3.2}$$

To estimate the value of Γ we assume that the energy dependence of $|A_{\lambda,0\epsilon}|^2 \omega(E_\lambda)$ can be represented by the expression

$$| A_{\lambda,0\varepsilon} |^2 \omega(E_\lambda) = \frac{B}{\Omega_{0\varepsilon}} \exp\left\{ -\left(\frac{E_\lambda - E_{0\varepsilon}}{\Omega_{0\varepsilon}} \right)^2 \right\}, \tag{3.3}$$

where B is determined from the condition (3.2). Then

$$B = 2\pi^{-1/2} [1 + \Phi(x)]^{-1}, \tag{3.4}$$

$$\Phi(x) = \frac{2}{\sqrt{\pi}} \int_0^x e^{-t^2} dt, \quad x \equiv E_{0\varepsilon}/\Omega_{0\varepsilon}. \tag{3.5}$$

The quantity $\Omega_{0\epsilon}$ is expressed in terms of the value of the "second moment" W^2 introduced in the paper of Lane, Thomas, and Wigner[4]

$$W^2 \equiv \sum_{\lambda} (E_\lambda - E_{0\varepsilon})^2 | A_{\lambda,0\varepsilon} |^2 . \tag{3.6}$$

Going from sum to integral and inserting (3.3), we get

$$W^2 = \frac{\Omega_{0\varepsilon}^2}{2[1 + \Phi(x)]} \left\{ 1 + \Phi(x) - \frac{2x}{\sqrt{\pi}} e^{-x^2} \right\}. \tag{3.7}$$

From Eq. (3.7) it follows that for $x < 1$ and for $x > 1$

$$\Omega_{0\varepsilon}^2 = 2W^2 . \tag{3.8}$$

On the other hand, substituting Eq. (2.13) into Eq. (3.6), we have

$$W^2 = \sum_{\lambda} | (\Phi_{0\varepsilon}, H'X_\lambda) |^2 = (\Phi_{0\varepsilon}, (H')^2 \Phi_{0\varepsilon}), \tag{3.9}$$

where, according to Eqs. (2.4) and (1.4), the operator H' is given by

$$H' = \sum_{\alpha} (v_\alpha - \langle v_\alpha \rangle) - \operatorname{Re} \sum_{\alpha} \langle v_\alpha (D - v_\alpha)^{-1} v_\alpha \rangle . \tag{3.10}$$

Substituting Eq. (3.3) into Eq. (3.1) and using the equations $E_{0\epsilon} \approx E_{n_0\xi_0}$, $\Omega_{0\epsilon} \approx \Omega_{n_0\xi_0}$, we can write

$$\hbar\Gamma = \frac{8\omega(E_{n_0\xi_0})}{\Omega_{0\varepsilon}^2 [1 + \Phi(x)]^2} \times \int_0^\infty \omega^{-1}(E) (E - E_{0\varepsilon})^2 \exp\left\{ -\frac{2(E - E_{0\varepsilon})^2}{\Omega_{0\varepsilon}^2} \right\} dE . \tag{3.11}$$

Equation (3.11) gives the width of a "giant" resonance in the neutron scattering cross-section (in the region of overlapping levels of the compound nucleus) and its dependence on the energy. To estimate the value of $\hbar\Gamma$ and its dependence on the energy $E_{0\epsilon}$ it is necessary to know the energy dependence of the density of states $\omega(E)$. According to the statistical model of the nucleus

$$\omega(E) = c \exp\left(\sqrt{bE}\right), \tag{3.12}$$

where the parameters c and b are functions of the mass number A. According to Ref. 5, satisfactory agreement with experimental values of the density of levels is obtained with the choice $b = 0.14(A - 12)$ for nuclei with mass numbers in the range $15 < A < 70$.

Equation (3.12) is inconvenient for analytical calculation, and therefore we set

$$\omega(E) = a \exp\{\beta E\} \tag{3.13}$$

and choose the coefficient β in such a way that in the range $7 < E < 30$ Mev, which is most important in the integral (3.11), Eq. (3.13) gives about the same increase of the levels as does Eq. (3.12).

For nuclei with mass numbers close to 60 we can take $\beta = 0.3$. It must, of course, be kept in mind that in the interaction of neutrons of energy less than 3 Mev with nuclei only those states of the compound nucleus are excited that have spins differing from that of the original nucleus by ± ½. Equation (3.12) refers to all possible levels of the compound nucleus. Therefore the energy dependence of the density of levels with a definite spin value must be given by a value of β less than 0.3.

Substituting Eq. (3.13) into Eq. (3.11), we find after simple calculations

$$\hbar\Gamma = \frac{2\sqrt{2}\,\Omega_{0\varepsilon}}{[1+\Phi(x)]^2}\int\limits_{-x\sqrt{2}}^{\infty} y^2 \exp\{-y(y+2a)\}\,dy,$$

$$a \equiv \frac{\beta\Omega_{0\varepsilon}}{2\sqrt{2}}. \qquad (3.14)$$

For $\beta = 0$ and, consequently, for $a = 0$, using Eq. (3.8) and $x < 1$, we have

$$\hbar\Gamma = (\sqrt{\pi}\,\Omega_{0\varepsilon}/\sqrt{2})[1+\Phi(x)]^{-2} \approx W_{0\varepsilon}.$$

This value agrees with that obtained in the paper of Lane, Thomas, and Wigner on the basis of the assumption that $\hbar\Gamma = W_{0\epsilon}$, which leads as follows from their calculation, to the excessive value $\hbar\Gamma = W_{0\epsilon} = 23$ Mev. It must, however, be noted that in the calculation of $W_{0\epsilon}$ in Ref. 4 account was taken only of the terms

$$\sum_{\alpha}(v_\alpha - \langle v_\alpha\rangle).$$

in the operator W' of Eq. (3.10).

If we adopt for $W_{0\epsilon}$ the value 23 Mev obtained in Ref. 4, then according to Eq. (3.8) $\Omega_{0\epsilon} \approx 32$ Mev. When the inequality $x \equiv \frac{E_{0\epsilon}}{32} < 1$ is satisfied, it follows from Eq. (3.14) that

$$\hbar\Gamma \approx 2\sqrt{2}\,\Omega_{0\varepsilon}\int\limits_{0}^{\infty} y^2 \exp\{-y(y+2a)\}\,dy. \qquad (3.15)$$

It follows from Eq. (3.15) that the value $\hbar\Gamma = 2.5$ Mev is obtained, if we set $\beta \approx 0.13$. But if $\Omega_{0\epsilon} = 20$ Mev, we must take $\beta = 0.2$.

[1] N. Francis and K. Watson, Phys. Rev. **92**, 291 (1953); K. Brueckner, Phys. Rev. **96**, 508 (1954); **97**, 1353 (1955); K. Brueckner and C. Levinson, Phys. Rev. **97**, 1344 (1955); R. Eden and N. Francis, Phys. Rev. **97**, 1366 (1955); Brueckner, Eden, and Francis, Phys. Rev. **98**, 1445 (1955); **99**, 76 (1955).

[2] Feshbach, Porter, and Weisskopf, Phys. Rev. **96**, 448 (1954).

[3] Brueckner, Eden, and Francis, Phys. Rev. **100**, 891 (1955).

[4] Lane, Thomas, and Wigner, Phys. Rev. **98**, 693 (1955).

[5] J. Heidmann and H. A. Bethe, Phys. Rev. **84**, 274 (1951).

Translated by W. H. Furry
283

SOVIET PHYSICS JETP VOLUME 5, NUMBER 6 DECEMBER 15, 1957

Contribution to the Theory of Exchange Collisions between Fast Nucleons and Deuterons*

L. I. LAPIDUS

Joint Institute for Nuclear Research

(Submitted to JETP editor August 28, 1956)

J. Exptl. Theoret. Phys. (U.S.S.R.) 32, 1437-1441 (June, 1957)

It is shown that, under some general assumptions regarding the nucleon-nucleon scattering amplitude, comparison of the experimental data on exchange scattering of fast nucleons by deuterons with the results of computations carried out in the impulse approximation can be of aid in the phase shift analysis of scattering of neutrons by protons. The phase shift analysis carried out by Klein does not agree with the experimental data on the exchange scattering.

1. THE RESULTS OF EXPERIMENTS with unpolarized nucleons do not give the possibility to determine the spin dependence of nuclear forces. This determination requires experiments with polarized nucleons.

A few years ago, Pomeranchuk,[1] Chew,[2] and Shmushkevich[3] pointed out another way to get information on the spin dependence of nuclear forces. If one investigates the angular dependence of fast protons from exchange collisions of high energy neutrons with deuterons and compares it with the results of calculations in the impulse approximation, one can obtain some information on the spin dependence of exchange forces between the neutron and the proton.

Assuming that, for angles close to 180° ($\theta = 0°$), the amplitude for nucleon-nucleon collision has the form

$$M = a' + b'\boldsymbol{\sigma}_1\boldsymbol{\sigma}_2 = a + b(1 + \boldsymbol{\sigma}_1\boldsymbol{\sigma}_2)/2 = a + bP_S \tag{1}$$

(P_s is the spin exchange operator), and that the functions a and b do not depend on the spin. Pomeranchuk has shown how it is possible to obtain information on the magnitudes a and b from the experimental data on exchange *n-d* scattering. The spins of the particles of the deuteron being parallel, the appearance of fast particles, in the conditions where the momentum $\mathbf{k}_f$ of the fast proton after collision is close to the momentum $\mathbf{k}_i$ of the impinging neutron, is possible only as a consequence of exchange collisions without any spin exchange.

In order to draw more detailed conclusions on the cross section ratio for *n-d* and *n-p* collisions, Chew had to make a series of additional assumptions on the character of nuclear forces.

The theory of Pomeranchuk is in qualitative agreement with the experimental data[4,5] on exchange scattering of 380 Mev neutrons by deuterons. In the general case, however, when (1) is replaced by the relationship[6,7]

$$\begin{gathered} M = \alpha + \beta(\boldsymbol{\sigma}_1\mathbf{n})(\boldsymbol{\sigma}_2\mathbf{n}) + \gamma_1(\boldsymbol{\sigma}_1\mathbf{P})(\boldsymbol{\sigma}_2\mathbf{P}) + \gamma_2(\boldsymbol{\sigma}_1\mathbf{K})(\boldsymbol{\sigma}_2\mathbf{K}) + \mu(\boldsymbol{\sigma}_1 + \boldsymbol{\sigma}_2, \mathbf{n}) \\ \mathbf{n} = [\mathbf{k}_i\mathbf{k}_f]/|[\mathbf{k}_i\mathbf{k}_f]|, \quad \mathbf{P} = (\mathbf{k}_i + \mathbf{k}_f)/|\mathbf{k}_i + \mathbf{k}_f|, \quad \mathbf{K} = (\mathbf{k}_i - \mathbf{k}_f)/|\mathbf{k}_i - \mathbf{k}_f|, \end{gathered} \tag{2}$$

the expression for exchange scattering cross section becomes, as shown by Pomeranchuk, unwieldy and a simple interpretation of the experimental results becomes impossible.

It is shown in the present paper that, under certain general assumptions concerning M, one can still use the experimental data on exchange scattering of 300 to 400 Mev nucleons by deuterons with small momentum transfer to obtain additional information on the scattering of neutrons by protons for the phase shift analysis of the *n-p* scattering data.

2. The five quantities α, β, γ_1, γ_2, and μ of (2) depend, generally speaking, on the energy of the colliding nucleons as well as on the scattering angle. After averaging over the initial spins and summing over the final spins, the differential *n-p* scattering cross section (in the center-of-mass system) can be expressed in terms of these functions in the following way:

---

*Delivered at the All-Union Conference on High-Energy Particle Physics, May 16, 1956.

$$d\sigma_{np}/do = {}^1/_4 \mathrm{Sp} M^+M = |\alpha|^2 + |\beta|^2 + |\gamma_1|^2 + |\gamma_2|^2 + 2|\mu|^2. \tag{3}$$

For the differential cross section for exchange collision between neutrons and deuterons we have (in the laboratory system):[3]

$$\begin{aligned}\sigma_{nd} do\, d\mathfrak{f} = 8\frac{k_f}{k_i}\{{}^1/_6[4|\alpha|^2 + 4|\beta|^2 + 4|\gamma_1|^2 + 4|\gamma_2|^2 + 10|\mu|^2 \\ + {}^1/_2|\alpha+\beta+\gamma_1+\gamma_2|^2]\left|\int \Phi_{\mathfrak{f}}^t \exp\{-i\varkappa\rho\}\varphi_0 d\rho\right|^2 + {}^1/_6[{}^1/_2|\alpha-\beta-\gamma_1-\gamma_2|^2 \\ + |\alpha-\beta|^2 + |\gamma_1-\gamma_2|^2 + 2|\mu|^2]\left|\int \Phi_{\mathfrak{f}}^s \exp\{-i\varkappa\rho\}\varphi_0 d\rho\right|^2\}\frac{d\mathfrak{f}}{(2\pi)^3}do,\end{aligned} \tag{4}$$

where φ_0 represents the deuteron ground state wave function, $\Phi_{\mathfrak{f}}^t$ and $\Phi_{\mathfrak{f}}^s$ are functions which describe the motion of two particles with a relative momentum $\mathfrak{f}$

$$\Phi_{\mathfrak{f}}^t(r) = 2^{-1/2}(e^{i\mathfrak{f}\mathbf{r}} - e^{-i\mathfrak{f}\mathbf{r}}),$$

$$\Phi_{\mathfrak{f}}^s(r) = 2^{-1/2}(e^{i\mathfrak{f}\mathbf{r}} + e^{-i\mathfrak{f}\mathbf{r}}) + (1 - e^{-i2\delta_0})e^{-ifr}/\sqrt{2}ifr, \quad \cot\delta_0 = -\sqrt{\frac{\varepsilon}{E}}.$$

Denoting by S_1 the coefficient of the first integral in (4) and by S_2 the coefficient of the second integral, and performing an approximate integration over $d\mathfrak{f}$, we have the following expression[3] for the differential cross section for fixed-angle scattering of a fast particle:

$$\frac{d\sigma_{nd}}{do} = 4\cos\theta\left\{(S_1+S_2) - (S_1-S_2)\frac{1}{\theta}\sqrt{\frac{2\varepsilon}{E}}\arctan\left(\theta\sqrt{\frac{E}{2\varepsilon}}\right)\right\}. \tag{5}$$

This expression does not depend on the relative motion of the two slow nucleons. In view of what follows, let us present M in a somewhat different form:

$$\begin{aligned}M = BS + C(\boldsymbol{\sigma}_1 + \boldsymbol{\sigma}_2, \mathbf{n}) + \{{}^1/_2 G[(\boldsymbol{\sigma}_1\mathbf{K})(\boldsymbol{\sigma}_2\mathbf{K}) + (\boldsymbol{\sigma}_1\mathbf{P})(\boldsymbol{\sigma}_2\mathbf{P})] \\ + {}^1/_2 H[(\boldsymbol{\sigma}_1\mathbf{K})(\boldsymbol{\sigma}_2\mathbf{K}) - (\boldsymbol{\sigma}_1\mathbf{P})(\boldsymbol{\sigma}_2\mathbf{P})] + N(\boldsymbol{\sigma}_1\mathbf{n})(\boldsymbol{\sigma}_2\mathbf{n})\}T.\end{aligned} \tag{6}$$

Here

$$S = {}^1/_4(1 - \boldsymbol{\sigma}_1\boldsymbol{\sigma}_2), \quad T = {}^1/_4(3 + \boldsymbol{\sigma}_1\boldsymbol{\sigma}_2)$$

are the singlet and triplet projection operators.

The functions B, C, ... of (6) can be expressed in terms of α, β, ... of (2). In order to obtain this relationship, let us transform (2) into the form (6), using relations of the type

$$(\boldsymbol{\sigma}_1\mathbf{n})(\boldsymbol{\sigma}_2\mathbf{n})T = (\boldsymbol{\sigma}_1\mathbf{n})(\boldsymbol{\sigma}_2\mathbf{n}) + S$$

etc., and the inequality

$$(\boldsymbol{\sigma}_1\mathbf{P})(\boldsymbol{\sigma}_2\mathbf{P}) + (\boldsymbol{\sigma}_1\mathbf{K})(\boldsymbol{\sigma}_2\mathbf{K}) + (\boldsymbol{\sigma}_1\mathbf{n})(\boldsymbol{\sigma}_2\mathbf{n}) = (\boldsymbol{\sigma}_1\boldsymbol{\sigma}_2),$$

which is valid for three mutually-orthogonal arbitrary vectors **P**, **K** and **n**. We get

$$\begin{aligned}\alpha = {}^1/_4(B + N + G), \gamma_1 = {}^1/_4(G - N - B - 2H), \beta = -{}^1/_4(G - N + B - 2N), \\ \gamma_2 = {}^1/_4(G - N - B + 2H), \quad \mu = C.\end{aligned} \tag{7}$$

In the center-of-mass system of the colliding nucleons, we have

$$S_1 + S_2 = {}^1\!/_4 \mid B \mid^2 + {}^1\!/_4 \mid G - N \mid^2 + {}^1\!/_2 \mid N \mid^2 + {}^1\!/_2 \mid H \mid^2 + 2 \mid C \mid^2 = d\sigma_{np} / do, \tag{8}$$

$$6\,(S_1 - S_2) = 4\,(d\sigma_{np}/do) + \operatorname{Re} N^* (G - N - B) - \mid H \mid^2 - {}^1\!/_4 \mid B + G - N \mid^2. \tag{9}$$

Using (8) and (9), the expression (5) for the transverse cross section for exchange *n-d* collisions can be presented in the following form (in the laboratory system)

$$\begin{aligned}\frac{d\sigma_{nd}}{do} = \Big[1 - \frac{2}{3\theta}\sqrt{\frac{2\varepsilon}{E}}\operatorname{arc\,tan}\Big(\theta\sqrt{\frac{E}{2\varepsilon}}\Big)\Big]\frac{d\sigma_{np}}{do} - {}^2\!/_3 \cos\theta\, [\operatorname{Re} N^* (G - N - B) \\ - \mid H \mid^2 - {}^1\!/_4 \mid B + G - N \mid^2]\, \frac{1}{\theta}\sqrt{\frac{2\varepsilon}{E}}\operatorname{arc\,tan}\Big(\theta\sqrt{\frac{E}{2\varepsilon}}\Big),\end{aligned} \tag{10}$$

which becomes for $\theta = 0^\circ$ ($\theta_n = 180^\circ$)

$$\frac{d\sigma_{nd}\,(0^\circ)}{do} = \frac{1}{3}\,\frac{d\sigma_{np}\,(180^\circ)}{do} - \frac{2}{3}\,[\operatorname{Re} N^* (G - N - B) - \mid H \mid^2 - {}^1\!/_4 \mid B + G - N \mid^2]_{\theta_n = 180^\circ}. \tag{11}$$

It is interesting to compare the expressions for the exchange *n-d* collision cross-section with the corresponding expressions for exchange collisions of π-mesons with deuterons. For the π-N scattering, the matrix M can be written in the form $M = A + B(\boldsymbol{\sigma}\mathbf{n})$, where the functions $A(\theta)$ and $B(\theta)$ can be expressed in the following way:[8]

$$\begin{aligned} A\,(\theta) &= \frac{1}{k}\sum_l [(l + 1) \exp\{i\delta_l^+\} \sin\delta_l^+ + l \exp\{i\delta_l^-\} \sin\delta_l^-]\, P_l\,(\theta), \\ B\,(\theta) &= \frac{1}{ik}\sum_l [\exp\{i\delta_l^+\} \sin\delta_l^+ - \exp\{i\delta_l^-\} \sin\delta_l^-]\, P_l^1\,(\theta). \end{aligned} \tag{12}$$

In the same impulse approximation, one obtains for the cross section for exchange scattering of π-mesons by deuterons[9]

$$\frac{d\sigma}{do}(\pi^- - d \mid \pi^0\, 2n) = \frac{d\sigma}{do}(\pi^- p \mid \pi^0 n) - (\mid A \mid^2 + {}^1\!/_3 \mid B \mid^2)\,\frac{2\alpha}{\mid \mathbf{k}_i - \mathbf{k}_f \mid}\operatorname{arc\,tan}\frac{\mid \mathbf{k}_i - \mathbf{k}_f \mid}{2\alpha}. \tag{13}$$

This process of interaction of π-mesons with deuterons leads to the formation of two slow identical nucleons in the final state. Because of the Pauli principle, the cross section for this process is characterized by a considerable decrease of the cross section for meson-deuteron interaction compared with the cross section for meson-nucleon interaction in the region of small angles of the outgoing fast particle. A similar decrease of the cross section for the case of exchange *n-d* scattering is given by the first term of (10). The presence of the term in square brackets in (10) and (11) and the absence of analogous expressions in (13) are explained by the absence of spin dependence in the π-N interaction for $\theta \to 0^\circ$ and by the presence of spin dependence in (2) and (6) even for $\theta = 0^\circ$ and $\theta = 180^\circ$.

3. In Refs. 1 – 3 the functions α, β, ... were left arbitrary and no further analysis was possible without making additional assumptions.

Using the work of Wright[10] one can, as in the case of the π-N interaction, express these functions in terms of the phase shifts for nucleon-nucleon scattering and of Legendre polynomials and their derivatives (notation of Ref. 10):*

$$B = \frac{1}{2ik}\sum_l \alpha_{l,\,0}^N (2l+1)\, P_l = \frac{1}{2}\,[B_1\,(\theta) + B_0\,(\theta)] = \frac{1}{2ik}\Big\{\sum_{l=2k} \alpha_{l,\,0}^N (2l + 1)\, P_l + \sum_{l=2k+1} \alpha_{l,\,0}^N (2l + 1)\, P_l\Big\},$$

---

* Similar expressions were obtained by R. M. Ryndin and by Stech and Bakke.[11]

$$C=\frac{1}{2}\frac{\sin\theta}{4k}\left\{\sum_l\left[\beta_1^{l+1}\frac{(2l+3)}{l+1}P'_l-\beta_2^{l+1}\frac{(2l+3)}{l+2}P'_{l+2}-\alpha^N_{l,1}\frac{(2l+1)}{l(l+1)}P'_l\right]-\alpha^N_{0,1}\right\}=\frac{1}{2}[C_1(\theta)+C_0(\theta)],$$

$$N={}^1/_2[N_1(\theta)+N_0(\theta)],\quad H={}^1/_2[H_1(\theta)+H_0(\theta)],\quad G-N={}^1/_2[G_1(\theta)-N_1(\theta)+G_0(\theta)-N_0(\theta)]. \tag{14}$$

The isotopic invariance of nucleon-nucleon interaction is taken into account in the second halves of these equations. The matrix $M_1 = M_{T=1}$ is meant to be the M-matrix for p-p scattering without electromagnetic effects. The quantities B_0, C_0, N_0, and G_0 contain the contribution of the n-p state with $T = 0$. The functions B_1, C_1, N_1, and G_1 do not reverse signs as one makes the substitution $\theta \rightleftarrows \pi-\theta$, but the signs of the functions B_0, C_0, H_0, N_0 and G_0 are reversed by the substitution.

The functions B, N, H and $G-N$ are involved in (10) and (11) in combinations which are different from the combinations involved in the expression for the scattering cross section of an unpolarized beam by an unpolarized target; the investigation of exchange n-d scattering gives therefore additional information on the spin dependence of exchange forces between the neutron and proton. If one compares (10) and (11) with the expressions for the functions $D(\theta)$ and $R(\theta)$ which characterize the change of polarization after scattering a polarized beam by an unpolarized target:[12,13]

$$(d\sigma_{np}/do)(1-D(\theta))={}^1/_4|G-N-B|^2+|H|^2,$$

$$(d\sigma_{np}/do)\,R(\theta)={}^1/_2\,\mathrm{Re}\,[(G-N+B)N^*+(G-N-B)H^*]\cos\frac{\theta}{2}+\mathrm{Im}\,[C^*(G-N+B)]\sin\frac{\theta}{2}, \tag{15}$$

it becomes clear that the experiments on exchange n-d scattering are, in the impulse approximation framework, close to the experiments on triple nucleon scattering. In this fashion, the experimental data on exchange n-d scattering together with the results of experiments with polarized nucleons can be used to obtain information on the spin dependence of the amplitude of exchange n-p scattering for the phase shift analysis of the n-p scattering data.

4. The experimental data of V. Dzhelepov, Kazarinov, and Fliagin[4,5] on exchange collision of 380 Mev neutrons with deuterons indicate a considerable decrease of the fast proton yield at angles close to 0°. The ratio $\sigma_{nd}(0)/\sigma_{np}(0)$ is 0.2 ± 0.035. Within the framework of Pomeranchuk's investigation,[1] this indicates a considerable probability of spin exchange in the exchange n-p collision. Using (11), the principal result of the experiment can be presented in the form

$$[\mathrm{Re}\,N^*(G-N-B)-|H|^2-{}^1/_4|B+G-N|^2]\,|_{\theta_n=180^\circ}={}^1/_5\,d\sigma_{np}(180^\circ)/do. \tag{16}$$

From the point of view of phase shift analysis, the expression (16) picks out, from among all the scattering phase shifts which agree with the experimental data on unpolarized n-p scattering cross section and on the polarization in n-p collisions, only those phase shifts which agree with the experimental data on n-d scattering. From the same point of view, there is another source of independent information on n-p scattering; it is the investigation of the polarization of the fast nucleons formed in exchange n-d collisions. For small momentum transfer, the polarization of fast nucleons can, in the impulse approximation, be expressed in terms of the amplitude of n-p scattering. The expression for the polarization differs from the corresponding expression for the case of collisions of a neutron with a free proton in the region of small angles.

If the functions B, C, ... are expressed in terms of the nucleon-nucleon scattering phase shifts, the comparison of the n-p scattering data with expressions of the type (10) show the applicability of the impulse approximation in similar problems, when the impinging particle interacts with a bound particle. For the same purpose, it can be profitable to compare the results of calculations with the experimental data on the exchange pion-deuteron collisions. In this case the situation is simplified by the fact that the meson-nucleon scattering phase shifts are now determined with a sufficient reliability.

The literature does not contain any uniquely determined n-p scattering phase shifts for the high energy region. If one still uses the phase shift analysis of Klein[14] for 330 Mev neutrons, the ratio $\sigma_{nd}(0)/\sigma_{np}(0)$ turns out to be close to unity. This is in strong contradiction with the experimental data on exchange n-d scattering, probably due principally to the fact that Klein's analysis (which underestimates the role of states with $L \geq 2$) agrees badly with the experimental data on *n-p* scattering in the angular region close to 180°.

The author is thankful to V. P. Ddzelepov, Iu. M. Kazarinov, and B. M. Golovin for profitable discussion and interest in the work.

---

[1] I. Ia. Pomeranchuk, Dokl. Akad. Nauk SSSR **78**, 249 (1951). J. Exptl. Theoret. Phys. (U.S.S.R.) **21**, 1119 (1951).

[2] G. Chew, Phys. Rev. **84**, 710 (1951).

[3] I. M. Shmushkevich, Report to the Academy of Sciences, U.S.S.R. (1953).

[4] V. P. Dzhelepov, Thesis, Institute for Nuclear Problems of the Academy of Sciences, U.S.S.R. (1954).

[5] Dzhelepov, Kazarinov and Fliagin, Dokl. Akad. Nauk SSSR **100**, 655 (1955).

[6] R. H. Dalitz, Proc. Phys. Soc. (London) **A65**, 175 (1952). L. Wolfenstein and J. Ashkin, Phys. Rev. **85**, 947 (1952).

[7] I. M. Shmushkevich, Thesis, Leningrad Physico-Technical Institute (1953).

[8] J. V. Lepore, Phys. Rev. **79**, 137 (1950).

[9] V. B. Berestetskii and I. Ia. Pomeranchuk, Dokl. Akad. Nauk SSSR **81**, 1019 (1951).

[10] S. Courteney Wright, Phys. Rev. **99**, 996 (1955).

[11] F. Bakke and B. Stech, Z.Physik **144**, 219 (1956).

[12] L. Wolfenstein, Phys. Rev. **96**, 1654 (1955).

[13] R. Oehme, Phys. Rev. **98**, 147 216 (1955).

[14] C. Klein, Nuovo cimento **2**, 38 (1955).

Translated by E. S. Troubetskoy
284

SOVIET PHYSICS JETP VOLUME 5, NUMBER 6 DECEMBER 15, 1957

On the Magnetic Properties of Superconductors of the Second Group

A. A. ABRIKOSOV

Institute of Physical Problems, Academy of Sciences, U.S.S.R.

(Submitted to JETP editor November 15, 1956)
J. Exptl. Theoret. Phys. (U.S.S.R.) **32**, 1442-1452 (June, 1957)

A study is made of the magnetic properties of bulk superconductors for which the parameter $\varkappa$ of the Ginzburg-Landau theory is greater than $1/\sqrt{2}$ (superconductors of the second group). The results explain some of the experimental data on the behavior of superconductive alloys in a magnetic field.

THE AUTHOR[1] has already noted that the quasi-microscopic Ginzburg-Landau theory[2] of superconductivity leads to the conclusion that there exist two groups of superconductors. For the first of these groups, the parameter $\varkappa$ entering into the Ginzburg-Landau theory is less than $1/\sqrt{2}$, and for the second group it is greater than $1/\sqrt{2}$.

This parameter $\varkappa$ determines to a great extent the surface energy at the normal – superconducting interface. It has already been mentioned,[2] in particular, that the calculated surface energy of a superconductor with $\varkappa > 1/\sqrt{2}$ is negative. Thus superconductors of the second group should have properties very different from those of the first group.

For pure metal, $\varkappa$ is found to be small. For instance for mercury, $\varkappa = 0.16$. In view of this, Ginzburg and Landau considered only the case in which $\varkappa \ll 1/\sqrt{2}$.

It has been shown by Zavaritskii,[3] however, that the properties of pure metal thin films condensed at liquid-helium temperatures are not described by such a theory. Zavaritskii and the present author have therefore suggested that such films correspond to $\varkappa > 1/\sqrt{2}$, and that superconductors can thus be divided into two groups. The critical field for superconductors of the second group has already been calculated[1] as a function of the film thickness. The agreement obtained with Zavaritskii's experimental data was not bad.

In the present work, a more detailed investigation of the magnetic properties of bulk superconductors of the second group (a cylinder in a longitudinal field) is undertaken. The results obtained show that $\varkappa > 1/\sqrt{2}$ for a large number of superconducting alloys whose magnetic properties had not previously been well understood.*

1. TRANSITION TO THE NORMAL STATE

It was shown by Ginzburg and Landau[2] that if $\varkappa > 1/\sqrt{2}$, the superconductivity is maintained at fields greater than H_{cm} at which equilibrium could exist between the normal and superconducting states. At fields higher than H_{cm}, a state with $\Psi = 0$ is unstable, and superconducting sections with $\Psi \neq 0$ may arise. It was shown[1] that this instability continues to some value H_{c2}, which for a bulk superconductor is $\varkappa\sqrt{2}H_{cm}$. At this value of the field the superconductor undergoes transition to the normal state by means of a second-order phase transition. In this section we shall investigate the properties of a superconductor in the neighborhood of the transition point, that is

$$\varkappa - H_0 / \sqrt{2}H_{cm} \ll \varkappa. \tag{1}$$

The Ginzburg-Landau equations (in units previously used by the author,[2] and to be used henceforth),† can be written

$$\left(\frac{i\nabla}{\varkappa} + \mathbf{A}\right)^2 \Psi = \Psi - \Psi \,|\Psi|^2, \tag{2}$$

$$-\operatorname{curl}\operatorname{curl}\mathbf{A} = |\Psi|^2\mathbf{A} + \frac{i}{2\varkappa}(\Psi^*\nabla\Psi - \Psi\nabla\Psi^*). \tag{3}$$

We shall assume that the superconductor fills all space, and that the external field H_0 is directed along the z axis. Let the potential A be directed along the y axis.

Close to the transition point $|\Psi|^2 \ll 1$, so that in the first approximation we may neglect the influence of Ψ on the field. We then obtain

$$H = \mathrm{const} = H_0, \quad A = H_0 x. \tag{4}$$

We note that the point $x = 0$ may be located anywhere in space. Let us now go on to Eq. (2). Inserting (4) into the equation for Ψ, neglecting the term $|\Psi|^2\Psi$ and considering Ψ to be a function of x only in the first approximation, we obtain the oscillator type of equation

$$d^2\Psi / dx^2 - \varkappa^2 (1 - H_0^2 x^2)\Psi(x) = 0, \tag{5}$$

as found previously.[2] This equation has solutions when $H_0 = \varkappa/(2n + 1)$. In particular, the largest value $H_0 = \varkappa$ corresponds to

$$\Psi = \exp\{-\varkappa^2 x^2 / 2\}. \tag{6}$$

In addition to such solutions, Eq. (2) is satisfied by the function

$$\exp\left\{iky - \frac{\varkappa^2}{2}\left(x - \frac{k}{\varkappa^2}\right)^2\right\}. \tag{7}$$

Since the point $x = 0$ has no special properties, the conditions will be exactly the same at all points of space, and it is natural to pick Ψ in the form

$$\Psi = \sum_{n=-\infty}^{\infty} C_n e^{ikny}\psi_n(x),$$
$$\psi_n(x) = \exp\left[-\frac{\varkappa^2}{2}\left(x - \frac{kn}{\varkappa^2}\right)^2\right] \tag{8}$$

with arbitrary coefficients k and C_n.

This form of Ψ is a solution of the linear equation, and refers in facts to $H_0 = \varkappa$. In order to find a solution for $H_0 < \varkappa$, let us take into account the nonlinear terms in the equations. We find the approximation of interest by inserting A from Eq. (4) with $H_0 = \varkappa$, and Ψ from Eq. (8) into Eq. (3). This leads to

$$\frac{\partial^2 A}{\partial x^2} = \sum_{n,m} C_n C_m^* e^{i(n-m)ky}\left[\varkappa k - \frac{(n+m)k}{2\varkappa}\right]\psi_n(x)\psi_m(x),$$
$$-\frac{\partial^2 A}{\partial x\,\partial y} = \frac{ik}{2\varkappa}\sum_{n,m} C_n C_m^* e^{i(n-m)ky}(n-m)\psi_n(x)\psi_m(x). \tag{9}$$

It can be shown easily that

$$H = \partial A / \partial x = H_0 - |\Psi|^2 / 2\varkappa; \tag{10}$$

$$A = H_0 x - \frac{1}{2\varkappa}\int |\Psi|^2 dx, \tag{11}$$

is a solution of this equation, where Ψ is given by Eq. (8), and H_0 is some still undetermined constant. It will be shown later that this constant is equal to the external field strength.

Let us now consider Eq. (2) in the following approximation. We insert into it Eq. (11), and take account of the term $\Psi|\Psi|^2$. We shall assume in this approximation that the function is still of the form of Eq. (8), but we shall add small terms $\psi_n^{(1)}(x)$ to all the $C_n\psi_n(x)$. The equations for these small terms are of the form

---

*The suggestion that $\varkappa$ may be greater than $1/\sqrt{2}$ for alloys was first made by L. D. Landau.

†We note that in these units $H_{cm} = 1/\sqrt{2}$.

$$\left(\frac{kn}{\varkappa}-\varkappa x\right)^2\psi_n^{(1)}-\frac{1}{\varkappa^2}\frac{d^2\psi_n^{(1)}}{dx^2}-\psi_n^{(1)}=2(\varkappa-H_0)\varkappa\left(x-\frac{nk}{\varkappa^2}\right)C_n\psi_n(x)+$$
$$+\sum_{p,\,m}C_pC_m^*C_{n-p+m}\left\{\left[x-\frac{k}{\varkappa^2}\left(n-\frac{p-m}{2}\right)\right]\psi_{n-p+m}(x)\int^x\psi_p(x')\,\psi_m(x')\,dx'-\psi_p(x)\,\psi_m(x)\,\psi_{n-p+m}(x)\right\}. \tag{12}$$

Thus $\psi_n^{(1)}$ is a solution of an inhomogeneous equation. But in order for such a solution to exist, it is necessary that the right side of the equation be orthogonal to the solution of the corresponding homogeneous equation. The solution of the homogeneous equation is just the function $\psi_n(x)$. Performing the necessary integration, we obtain the following condition:

$$\left(\frac{1}{2\varkappa^2}-1\right)\sum_{p,\,m}C_pC_m^*C_{n-p+m}\exp\left\{-\frac{k^2}{2\varkappa^2}\left[(p-n)^2+(m-n)^2\right]\right\}+\frac{\varkappa-H_0}{\varkappa}C_n=0. \tag{13}$$

Let us multiply this equation by C_n^* and sum over n. It is easily verified that we then obtain

$$\frac{\varkappa-H_0}{\varkappa}\overline{|\Psi|^2}+\left(\frac{1}{2\varkappa^2}-1\right)\overline{|\Psi|^4}=0, \tag{14}$$

where Ψ is the function of Eq. (8). Thus H_0 enters into Ψ in the form of a coefficient.

The quantity H_0 can be expressed in terms of the magnetic induction. According to (10) and (14), we have

$$B=\overline{H}=H_0-\overline{|\Psi|^2}/2\varkappa=H_0-(\varkappa-H_0)/(2\varkappa^2-1)\beta, \tag{15}$$

where

$$\beta=\overline{|\Psi|^4}/(\overline{|\Psi|^2})^2 \tag{16}$$

is independent of H_0.

Let us now calculate the free energy. According to Ginzburg and Landau,[2] the free energy is

$$\frac{F_{sH}-F_{s0}}{H_{cm}^2/4\pi}=\int dV\left\{\frac{1}{2}-|\Psi|^2+\frac{|\Psi|^4}{2}+H^2+\left(-\frac{i\nabla\Psi}{\varkappa}-\mathbf{A}\Psi\right)\left(\frac{i\nabla\Psi^*}{\varkappa}-\mathbf{A}\Psi^*\right)\right\}. \tag{17}$$

If we now make use of (2) and (3) and neglect the surface integral, which is of no importance to us, we obtain

$$\frac{F_{sH}-F_{s0}}{H_{cm}^2/4\pi}=\int\left(H^2-\frac{|\Psi|^4}{2}+\frac{1}{2}\right)dV. \tag{18}$$

The free energy per unit volume is proportional to the average of the integrand. Denoting this average by F_1 and writing it in terms of B, we obtain

$$F_1=\frac{1}{2}+B^2-\frac{(\varkappa-B)^2}{1+(2\varkappa^2-1)\beta}. \tag{19}$$

For a given B this quantity will be minimum when β has its lowest value.

We note that (13) can be written in the form

$$\partial\beta/\partial C_n^*=0, \tag{13'}$$

becoming equivalent to the condition that β is a minimum. It is seen from (16) that β cannot be less than unity.

The condition that Ψ be periodic in x is the following simple recursion relation for the C_n:

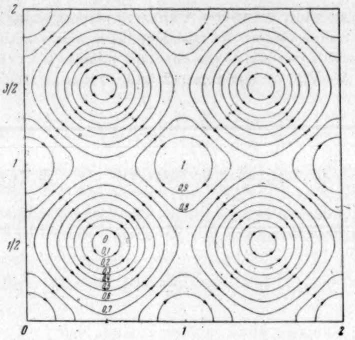

$$C_{n+N} = C_n. \tag{20}$$

The general analysis of the problem of choosing the coefficients is extremely complicated, but there is no reason to suppose that the actual value of N is a very large number. It would seem that the lowest energy corresponds to the simplest case* $N = 1$. In this case β is given by

$$\beta = \frac{k}{\varkappa\sqrt{2\pi}}\left(\sum_n \exp\left\{-\frac{k^2}{2\varkappa^2}n^2\right\}\right)^2.$$

The minimum value of β is obtained when $k = \varkappa\sqrt{2\pi}$, and is equal to

$$\psi = \left(\sum_n e^{-\pi n^2}\right)^2 = \vartheta_3^2(0, 1) = 1.18. \tag{21}$$

Then Ψ is

$$\Psi = Ce^{-\varkappa^2x^2/2}\vartheta_3[\sqrt{2\pi}\,\varkappa i\,(x+iy);\ 1]. \tag{22}$$

It can be shown from the properties of the function ϑ_3 that rotation by 90° multiplies Ψ by the phase factor $e^{i\varkappa^2 xy}$, but does not change it otherwise. Thus $|\Psi|^2$ has the symmetry of a square lattice. When $x = y = (1/\varkappa)\sqrt{\pi/2}$, the function Ψ vanishes. According to (10), H attains its maximum value H_0 at these points.

We shall now show that H_0 is equal to the field strength. As is well known, the field strength is $4\pi\,\partial\bar{F}/\partial B$ (in the usual units). This leads to a relation between H and B which is identical with Eq. (15). In order to perform the comparison with experiment (this will be done in Sec. 3) more conveniently, the latter can be rewritten in terms of the function $M(H_0)$,

$$-4\pi M/(H_{c2} - H_0) = 1/1.18\,(2\varkappa^2 - 1), \tag{23}$$

where M and H can be taken in the usual units. We note that the magnetic moment is proportional to the first power of $H_{c2} - H_0$.

Equation (23) is the macroscopic characterization of the behavior of a bulk sample in an external field. As for the microscopic structure of the field penetration, collecting the results described above we obtain the following picture. In a plane perpendicular to the field direction, the structure is periodic with the symmetry of a square lattice. The field varies between its maximum value H_0 and its minimum value given by

$$H_{\min} = H_0 - (H_{c2} - H_0)\sqrt{2}/(2\varkappa^2 - 1). \tag{24}$$

When the applied field strength H_0 is increased, the field between the maxima increases up to values equal to $H = H_0 = \varkappa$.

The field and current distribution is shown in the figure. The lines correspond to $|\Psi|^2 = \text{const}$ (normalized to $|\Psi|^2_{\max} = 1$) or equivalently, to $H = \text{const}$. These are then the streamlines (their directions being given by the arrow).

2. THE BEGINNING OF FIELD PENETRATION INTO A SUPERCONDUCTOR

In the preceding section we concluded that in the neighborhood of the transition point to the normal state, superconductors of the second group are in a special state which is neither normal nor superconducting, and differs significantly from the intermediate state which may arise in noncylindrical bulk samples. Let us call this the mixed state. One naturally wonders how this state changes as the field is decreased, and where and how the transition to superconductivity occurs.

If we direct our attention to the experimental

---

*In addition to this case, which will be seen later to lead to a square lattice, we considered the example of a triangular lattice. The side of the triangle is $(1/\varkappa)\sqrt{8\pi/3\sqrt{3}}$. By numerical integration, however, we were able to show that this lattice corresponds to a larger value of β, namely $\beta = 1.32$ (see also the next section).

$B(H_0)$ curves for alloys,[4] we see that this transition can be both a first and a second order phase transition. It would seem (see Sec. 3) that the first order phase transition occurs when $\varkappa$ is not very large, whereas the second order transition occurs when $\varkappa \gg 1$. It is extremely difficult to explain this on theoretical grounds, since this would require solving Eqs. (2) and (3) without any simplifying assumptions.

Let us consider only the simplest case of a second order phase transition, which would seem, as has already been mentioned, to take place when $\varkappa$ is not too small.

Let us start with a determination of the transition point. It is natural to assume that when the field first begins to penetrate, the structure of this penetration is again of the lattice type, although with a very large period. At the lattice points the field will have its maximum value, and will practically vanish between them. Thus the field penetration pattern is that of separated filaments. This pattern reminds one of the distribution of superfluidity in helium II by the creation of vortex filaments, as proposed by Onsager[5] and Feynman.[6] The similarity is even greater when one analyzes the behavior of the Ψ function in the neighborhood of these filaments in greater detail. When one considers the situation at fields close to H_{c2}, one sees easily that in the neighborhood of those points where Ψ vanishes and the field is maximum, the phase of the Ψ function is* θ, where θ is the polar angle, and thus changes by 2π in going once around such a point. It is natural to suppose that the phase behaves in the same way in the neighborhood of separate filaments when the separation between them is large. As will be seen later, the Ψ function vanishes also in the center of a filament. This behavior of the Ψ function, in particular of its phase, has been suggested by Feynman in application to vortices in helium II.

When the filaments are sufficiently separated, they can be considered independent of each other, and each filament can be treated separately. In this case, the problem has cylindrical symmetry. Let us introduce the modulus and phase of the Ψ function

$$\Psi = fe^{i\varphi} \qquad (25)$$

and consider the vector $\mathbf{A}$ directed perpendicular to the radius vector. We introduce the scalar quantity Q, which is equal to the absolute value of the vector $\mathbf{A} - \nabla\varphi/\varkappa$. Equations (2) and (3) then become

$$-\frac{1}{\varkappa^2 r}\frac{d}{dr}\left(r\frac{df}{dr}\right) + Q^2 f = f - f^3, \qquad (26)$$

$$\frac{d}{dr}\left[\frac{1}{r}\frac{d}{dr}(rQ)\right] = Qf^2. \qquad (27)$$

The field H is given by

$$H = -\frac{1}{r}\frac{d}{dr}(rQ). \qquad (28)$$

The statement of the problem requires that $f \to 1$, $H \to 0$, $Q \to 0$ as $r \to \infty$. Further, we have assumed that for a separate filament $\varphi = \theta$. But this leads to $\nabla_\theta\varphi = \partial\varphi/r\partial\theta = 1/r$. In other words, $Q \to 1/\varkappa r$ as $r \to 0$. According to the theory of Onsager and Feynman the superfluid velocity v_s in helium II diminishes in the same way, with increasing distance from the center of the filament.

In addition, it is of course necessary to require that f be everywhere bounded. These conditions uniquely determine the solution of (26) and (27). In general, however, this solution can be obtained only by numerical integration, and this must be performed separately for each value of $\varkappa$.

When $\varkappa \gg 1$, the solution is considerably simplified. We note for this purpose that the distance over which Q should have a large variation is $r \sim 1$. As for f, it varies to a large extent at distances $r \sim 1/\varkappa$. In view of this, one may assume that f has already attained the value $f = 1$ in Eq. (26), from which we immediately obtain

$$Q = K_1(r)/\varkappa, \qquad (29)$$

where K_1 is the Hankel function of imaginary argument. Further, we note that $Q = 1/\varkappa r$ when $r \ll 1$. Inserting this into the equation for f we obtain

$$\frac{1}{\varkappa^2}\left[\frac{1}{r}\frac{d}{dr}\left(r\frac{df}{dr}\right) - \frac{1}{r^2}f\right] = f^3 - f. \qquad (30)$$

At distances $r \gg 1/\varkappa$, the solution of this equation is $f^2 = 1 - 1/\varkappa^2 r^2$, and when $r \ll 1/\varkappa$, the solution is $f = Cr$, where C is a constant which can be obtained by numerical solution of (30).

Let us now calculate ε, the free energy per unit length of a filament. To do this we must evaluate the integral

---

* In the neighborhood of such a point with coordinates (x_1, y_1), Ψ is proportional to $(x - x_1) + i(y - y_1)$.

$$\varepsilon = 2\pi\int_0^\infty\left(H^2+\frac{1-f^4}{2}\right)r\,dr$$

$$=\pi\int_0^\infty\left[(1-f^4)\,r-f^2\frac{d}{dr}(r^2Q^2)\right]dr. \tag{31}$$

If we note that the integrand decays exponentially when $r \gg 1$, and assume that $\ln\varkappa \gg 1$, it is easily seen that the important contribution to the integral will be from the interval $1/\varkappa \ll r \ll 1$, and we then obtain

$$\varepsilon = (2\pi/\varkappa^2)\ln\varkappa.$$

Numerical integration of (30) and (31) makes it possible to obtain a correction to $\ln\varkappa$, so that we finally obtain

$$\varepsilon = (2\pi/\varkappa^2)(\ln\varkappa + 0.081). \tag{32}$$

In order that the formation of filaments be energetically possible, the field strength H_0 must be such that $F_1 - 2H_0B$ be negative. If the filament density, *i.e.*, the number of filaments crossing a unit area, be denoted by n, we have

$$F_1 = n\varepsilon, \qquad B=\overline{H}=n\int H\,dS=n\oint \mathbf{A}\,d\mathbf{l}. \tag{33}$$

In view of the fact that the contour of integration extends to $r = \infty$, and that at these large distances $Q = 0$, we conclude that $\mathbf{A} = \nabla\varphi/\varkappa$, which means that its absolute value is $1/\varkappa r$. Thus

$$B = 2\pi n/\varkappa. \tag{34}$$

It follows from this that the filaments start being formed when the field strength H_0 attains the value

$$H_{c1} = \varepsilon\varkappa/4\pi. \tag{35}$$

This formula is valid for arbitrary $\varkappa$ on the assumption that the phase transition is of second order. When $\varkappa \gg 1$, we obtain

$$H_{c1} = (1/2\varkappa)(\ln\varkappa + 0.08). \tag{36}$$

It is interesting to note that at the center of the filament the field is about twice H_{c1} in the given case. Indeed, according to Eq. (27) we have

$$H(0) = \int_0^\infty Qf^2\,dr = (\ln\varkappa - 0{,}18)/\varkappa. \tag{37}$$

From (35) it is seen that H_{c1} is independent of n, and that an arbitrary number of filaments may be formed in this approximation for $H_0 > H_{c1}$. In order to find the function $n(H_0)$, and therefore $B(H_0)$, we must take account of the interaction between the filaments.

This is easily done if $\varkappa \gg 1$. Indeed, in this case the region in which f differs from unity ($r \sim 1/\varkappa$) is small compared with the distances at which the interaction between the filaments takes place ($r \sim 1$). In view of this, the filament centers will play the role of singularities in the solution, and their detailed structure will not be of importance. It is not difficult to see that the equation for the field together with the conditions at the centers of the filaments can be written in the form

$$\Delta H - H = -(2\pi/\varkappa)\sum_m \delta(\mathbf{r}-\mathbf{r}_m), \tag{38}$$

where the $\mathbf{r}_m$ are the coordinates of the centers of the filaments. The solution of this equation is

$$H = \frac{1}{\varkappa}\sum_m K_0(|\mathbf{r}-\mathbf{r}_m|). \tag{39}$$

The energy can be written in the form

$$F_1 = \overline{H^2+(\nabla H)^2} = \overline{H(H-\Delta H)}$$

$$= \frac{2\pi n}{\varkappa^2}\sum_m K_0(|\mathbf{r}_m|), \tag{40}$$

where the $\mathbf{r}_m$ are calculated from one of the filament centers. The term corresponding to $\mathbf{r}_m = 0$ should be replaced by Eq. (32). The quantity n and the periodicity of the lattice, which enter into (40), can be expressed in terms of the magnetic induction B by Eq. (34). For a square lattice we obtain

$$F_1 = \frac{\varkappa B}{2\pi}\varepsilon + \frac{B}{\varkappa}\sum_{l^2+m^2\geqslant 1} K_0\left(\sqrt{\frac{2\pi(l^2+m^2)}{\varkappa B}}\right). \tag{41}$$

It is, however, possible that the lattice is actually not a square one or that its symmetry changes as the field is varied. Therefore the problem should be dealt with more carefully. The most probable structure which one can assume instead of the square one is the triangular one. For such a lattice one easily obtains

$$F_1 = \frac{\varkappa B}{2\pi}\varepsilon + \frac{B}{\varkappa}\sum_{l^2+m^2+lm\geqslant 1} K_0\left(\sqrt{\frac{4\pi(l^2+m^2+lm)}{\sqrt{3}\varkappa B}}\right). \tag{42}$$

By comparing the asymptotic form of this expression for small B with asymptotic form of (41),

$$F_{1\Delta} \approx \frac{\varkappa B}{2\pi}\varepsilon + 6\frac{B}{\varkappa}\sqrt{\frac{\pi}{2}}\left(\frac{\sqrt{3}\varkappa B}{4\pi}\right)^{1/4}\exp\left(-\sqrt{\frac{4\pi}{\sqrt{3}\varkappa B}}\right), \tag{43}$$

$$F_{1\Box} \approx \frac{\varkappa B}{2\pi}\varepsilon + 4\frac{B}{\varkappa}\sqrt{\frac{\pi}{2}}\left(\frac{\varkappa B}{2\pi}\right)^{1/4}\exp\left(-\sqrt{\frac{2\pi}{\varkappa B}}\right),$$

one sees clearly that for sufficiently small B there should be a transition to the triangular modification. The value of H_0 at the transition point is determined by setting the free energy for a given field strength equal to $F_1 - 2H_0B$, and is

$$H_1' = H_{c1} + 0.0394/\varkappa. \tag{44}$$

This transition is clearly a first order phase transition. The induction undergoes a jump from $B_1 = 0.286/\varkappa$ to $B_2 = 0.294/\varkappa$. At fields greater than H_1', the square lattice is more favorable, which justifies to some degree the assumption made in the previous section.

We note that the transition takes place in the immediate neighborhood of H_{c1}, and that the discontinuity in the induction is so small (about 3%) that it would be extremely difficult to observe it on a $B(H_0)$ curve.

It is not difficult to see that when $H = H_{c1}$, the $B(H_0)$ curve has a vertical tangent. Indeed, when $H = H_{c1}$, the H_0-dependence of B is determined primarily by the term $H_0 \sim \exp[-(4\pi/\sqrt{3}\varkappa B)^{1/2}]$, and $dH_0/dB \to 0$ as $B \to 0$. In the other limiting case, when $\varkappa B \gg 1$, the various terms of the sum of Eq. (41) have arguments which lie close to each other, so that the sum can be replaced by an integral. This gives $F_1 \approx B^2$, and $H_0 \approx B$. Thus as H_0 is increased, the curve asymptotically approaches the straight line $B = H_0$. This goes on until the distance between the filaments becomes of the order of $1/\varkappa$, *i.e.*, until $H_0 \sim \varkappa$.

The dependence of $\varkappa B$ on $(H_0 - H_{c1})$ is given by the universal function

$$\varkappa(H_0 - H_{c1}) = \frac{1}{4}\sum_{x_{l,m}\neq 0}[2K_0(x_{l,m}) + x_{l,m}K_1(x_{l,m})],$$

$$\text{where } x_{l,m} = \sqrt{4\pi(l^2+m^2+lm)/\sqrt{3}\varkappa B} \quad \text{for } \varkappa(H_0 - H_{c1}) < 0.0394,$$
$$x_{l,m} = \sqrt{2\pi(l^2+m^2)/\varkappa B} \quad \text{for } \varkappa(H_0 - H_{c1}) > 0.0394. \tag{45}$$

We note that $(\partial B/\partial H_0)_T$ is always positive, which indicates that the situation discussed is stable.[7]

For very large values of $\varkappa$ Eq. (35) can be used to find H_{c1}. To do this one must solve (26) and (27) numerically, after which ε is calculated from (31). On the other hand, finding $B(H_0)$ in this case requires solving a separate and very complex problem.

To conclude this section, let us turn our attention to the intermediate state in noncylindrical speciments (or cylinders in nonparallel fields). It is most interesting that no intermediate state arises in specimens for which $\varkappa \gg 1$. One obtains instead a uniform pattern of a mixed state (in ellipsoidal samples). When the transition in the field H_{c1} is of the first order, however, an intermediate state does arise.

3. COMPARISON OF THEORY AND EXPERIMENT

No detailed data exist currently on the magnetic properties of superconducting alloys. The only work which is more or less suitable for comparison with the theory is that of Shubnikov, Khotkevich, Shepelev, and Riabinin,[4] performed in 1937. Let us compare the theoretical results with the data of this work.

If we are to speak of general qualitative characteristics, we must first note that starting at some alloy concentration, the $B(H_0)$ curve indicates a region of partial field penetration; this corresponds to the conclusion reached above on the existence of a mixed state. This region is bounded by the two field strengths H_{c1} and H_{c2}, and although the transition from the superconducting state to the mixed one can be either of first or of second order, the transition to the normal state must definitely be of first order. In the neighborhood of H_{c2}, the $B(H_0)$ curve is linear. All this is in agreement with the results of Sec. 1. Further, if the alloy concentration is sufficiently high, the transition at H_{c1} seems also to be of second order. According to the

Alloy composition	T°K	H_{c_2}	H_{cm}	$\varkappa\sqrt{2}$	tan α (theory)	tan α (exp.)	H_{c1} (theory)	H_{c1} (exp.)
Pure Pb	4.24		540	0.22÷0.36				
Pb + 2.5% Tl	4.22	704	596	1.18	2.12	2.2	—	510
	1.92	1100	846	1.3	1.21	1.2	—	740
Pb + 5% Tl	4.22	1010	561	1.8	0.38	0.38	—	430
	1.82	1730	854	2	0.27	0.27	—	600
Pb + 15% Tl	4.22	2170	534	4.07	0.054	0.052	150	230
	1.76	3760	762	4.9	0.036	0.036	210	310
Pb + 30% Tl	4.22	2840	575	4.94	0.036	0.033	150	170
	1.70	4460	756	5.9	0.025	0.023	190	240
Pb + 50% Tl	4.22	2270	370	6.14	0.023	0.02	90	110
	2.3	4270	520	8.2	0.013	0.014	120	150
Pb + 2% In	4.22	983	604	1.6	0.51	0.45	—	530
	1.95	1520	842	1.8	0.37	0.3	—	730
Pb + 8% In	4.22	2400	563	4.26	0.049	0.045	170	220
	1.75	3780	812	4.7	0.041	0.043	240	310

theory, at this point the $B(H_0)$ curve has a vertical tangent, and then begins gradually to approach the straight line $B = H_0$. This conclusion also more or less agrees with the experimental curves.

Going on to a quantitative comparison, we note that the two parameters H_{cm} and $\varkappa$ which enter into the theory must be determined from the experimental curves. This can be done by finding the upper critical field H_{c2} and the area under the curve of the magnetic moment $B(H_0) - H_0$, where H_0 is the field strength. In fact from the definition of H_{cm}, we have

$$\frac{1}{2} H_{cm}^2 = \int_0^\infty [H_0 - B(H_0)]\, dH_0 = \int_0^{H_{c2}} [H_0 - B(H_0)]\, dH_0. \tag{46}$$

Of course in order that H_{cm} defined in this way have meaning, it is necessary that the experimental $B(H_0)$ curve be that for equilibrium. When we know H_{cm}, we can find $\varkappa$ from the equation $H_{c2} = \varkappa\sqrt{2}H_{cm}$.

The values of H_{cm} and $\varkappa$ obtained in this way can be used to compare the magnetic moment in the neighborhood of the upper critical field H_{c2} with experiment. According to Sec. 1, the dependence of M on H_0 is given by Eq. (23).

We can compare with experiment, in addition to M, Eq. (36) for the first critical field.

The results of such comparison are given in the Table.* One should bear in mind that the accuracy with which the slope of the magnetic moment curve is determined in the neighborhood of H_{c2} (let us denote the ratio in Eq. (23) by tan α) and H_{c1} from the curves of Shubnikov, *et al.*[4] is no greater than 15%. It is seen from the table that the data for tan α are in very good agreement with the theory. The values of tan α vary from specimen to specimen by a factor as high as 150, and the theory always gives the correct value within the above-mentioned limits.

The situation with respect to H_{c1} is somewhat worse. Although the theoretical values are always of the same order of magnitude as the experimental ones, they lie too low in all cases. It should be borne in mind, however, that the values of $\varkappa$ dealt with here are not very large compared to unity, and this can lead to a systematic error in determining H_{c1} from (35), an equation which is valid only when $\varkappa \gg 1$. It is not difficult to see in which direction the theoretical value must be corrected in order to account for the fact that $\varkappa$ is not very large. This can be done by making the natural assumption that $H_{c1} = H_{cm}$ when $\varkappa = 1/\sqrt{2}$. Instead of this, insertion of $\varkappa = 1/\sqrt{2}$ into Eq. (36) leads to a negative value of H_{c1}. Thus for values of $\varkappa$ which are not very large, the actual theoretical value of H_{c1} should be greater than that given by (36). In principle, it is also possible to perform a comparison between experiment and Eq. (45) for $B(H_0)$ in the neighborhood of H_{c1}. This equation, however, is in principle valid only for $\varkappa \gg 1$, so that only a qualitative comparison is possible; this has already been done at the beginning of this section. Furthermore, the experimental curves in this region are measured with very low accuracy, so that a quantitative comparison is not really very meaningful. We note here that according to the experimental data, when $\varkappa$ is close to $1/\sqrt{2}$ the transition to the mixed state would seem to be a first order phase transition. In this case the concept of isolated filaments does not correspond at all to the mixed state at the transition point.

---

*It is significant here that the theory remains applicable for temperatures far from T_c. As fields close to H_{c2}, this conclusion is strictly correct, since Ψ is small in this region. Recently, however, Ginzburg[8] has presented arguments which tend to show that the theory is applicable also for arbitrary fields and temperatures.

In order to investigate the dependence of H_{cm} and $\varkappa$ on the concentration, let us compare their values at a fixed temperature of 4.2°. For comparison, the table gives the data also for pure lead at the same temperature, taken from Lock.[9] It is seen from the table that H_{cm} hardly depends on the concentration (except for the 50% Pb-Tl alloy). The variation is no greater than 11% and has no apparent regularity. However, $\varkappa$ increases regularly with increasing concentration, and varies for Pb-Tl alloys from 1.18 at 2.5% Tl to 6.14 at 50% Tl.

Some years ago Pippard[10] made the interesting suggestion that there exists in superconductors a certain characteristic length (the coherence length) which determines the "range of order" of the superconducting electrons. This length characterizes the minimum distance at which the number of superconducting electrons may change significantly. It may, for instance, refer to the thickness of the transition layer between the normal and superconducting phases.

According to the theory of the previous sections, the quantity $\delta/\varkappa$ should play the role of such a length. This length determines the thickness of the transition layer in the intermediate state.[2] If we bear in mind that $\varkappa = (\sqrt{2}e/hc)H_{cm}\delta^2$, then it is clear that the characteristic length is proportional to $1/\sqrt{\varkappa}$. According to Pippard, this length should depend strongly on the impurity concentration. At high concentrations it should be of the order of the mean free path of an electron in the metal. It is seen from the table that this concept is not in disagreement with the experimental data.

The results described show that the quasi-microscopic theory is able to describe many of the regular properties of superconducting alloys. Thus these regular properties arise primarily not because macroscopic regions with relatively large values of T_c and H_{cm} arise in the alloy, as has been thought previously, but from the destruction of electron order at distances small compared with the penetration thickness δ.

It is true, of course, that macroscopic inhomogeneities may be of importance. Without even going into the fact that a strong inhomogeneity can change the overall pattern, we note that such a phenomenon as the remanent magnetic moment cannot be described by the present theory and is more probably a result of such inhomogeneities. The structure of the field penetration itself should be extremely sensitive to inhomogeneities, so that in real substances it would hardly be in the form of a regular lattice.

In conclusion I take this opportunity to express my gratitude to Academician L. D. Landau and N. V. Zavaritskii for valuable comments and discussion of the work.

---

[1] A. A. Abrikosov, Dokl. Akad. Nauk SSSR **86**, 489 (1952).

[2] V. L. Ginzburg, L. D. Landau, J. Exptl. Theoret. Phys. (U.S.S.R.) **20**, 1064 (1950).

[3] N. N. Zavaritskii, Dokl. Akad. Nauk SSSR **86**, 501 (1952).

[4] Shubnikov, Khotkevich, Shepelev, and Riabinin, J. Exptl. Theoret. Phys. (U.S.S.R.) **7**, 221 (1937).

[5] L. Onsager, Nuovo cimento **6**, Supp. 2, 249 (1949).

[6] R. P. Feynman, *Progress in Low Temperature Physics I* (North Holland Publish. Co., Amsterdam, 1955).

[7] V. P. Silin, J. Exptl. Theoret. Phys. (U.S.S.R.) **30**, 197 (1956); Soviet Phys. JETP **3**, 123 (1956).

[8] V. L. Ginzburg, J. Exptl. Theoret. Phys. (U.S.S.R.) **30**, 593 (1956), Soviet Phys. JETP **3**, 621 (1956).

[9] J. M. Lock, Proc. Roy. Soc. (London) A **208**, 391 (1951).

[10] A. B. Pippard, Proc. Cambridge Phil. Soc. **47**, 617 (1951); Proc. Roy. Soc. (London) A **216**, 547 (1953).

Translated by E. J. Saletan
285

SOVIET PHYSICS JETP VOLUME 5, NUMBER 6 DECEMBER 15, 1957

The Structure of Shock Waves in a Plasma

V. D. SHAFRANOV
Academy of Sciences, U.S.S.R.

(Submitted to JETP editor November 24, 1956)
J. Exptl. Theoret. Phys. (U.S.S.R.) 32, 1453 (1957)

The structure of shock waves in a plasma is investigated, taking account of the difference between the electron and the ion temperatures. The following cases are considered: a) nostationary shock wave in which the exchange of energy between electrons and ions may be neglected; b) stationary shock wave; c) stationary shock wave in a strong magnetic field.

THE STRUCTURE OF SHOCK WAVES in a plasma has been investigated in a number of works.[1-3] However, in all of these works it was assumed that the electron and ion temperatures were the same. In fact, however, shock waves in a plasma are characterized just by a difference between the electron and ion temperatures.

As is shown below, shock waves in a plasma without a magnetic field have the following structure. In addition to the usual density jump in a shock wave, there is a region of smooth temperature change. In front of the jump there is a region of raised electron temperature due to the high electron thermal conductivity. Behind the jump there is a comparatively broad region in which equalization of the electron and ion temperatures takes place (Figs. 1, 2).

If the plasma is located in a magnetic field parallel to the plane of the discontinuity, the electron thermal conductivity is strongly lowered and the heated region in front of the density jump is absent. Only the region of temperature equalization behind the jump exists (Fig. 3).

The width of the transition region is considerably greater than the mean free path. Therefore, it can be described by the equations of hydrodynamics, for any shock wave intensity. The structure of the jump itself will not interest us.

1. In the present article we consider a two-component plasma consisting of electrons (mass m, charge $-e$) and ions of one type (mass M, charge ze). The system of equations describing such a plasma consists of Maxwell's equations and the hydrodynamic equations:[4]

$$\partial n_\alpha / \partial t = -\operatorname{div} n_\alpha \mathbf{v}_\alpha, \tag{1}$$

$$\begin{aligned} m_\alpha n_\alpha \frac{d\mathbf{v}_\alpha}{dt} &= -\nabla p_\alpha + (\mathbf{div}\, \pi)_\alpha \\ &+ e_\alpha n_\alpha \left(\mathbf{E} + \frac{1}{c} \mathbf{v}_\alpha \times \mathbf{H}\right) + \mathbf{R}_\alpha, \end{aligned} \tag{2}$$

$$\frac{n_\alpha}{\gamma - 1} \frac{dT_\alpha}{dt} + p_\alpha \operatorname{div} \mathbf{v}_\alpha + \operatorname{div} \mathbf{q}_\alpha - \pi_{\alpha lk} \frac{\partial v_{\alpha l}}{\partial x_k} = Q_\alpha \tag{3}$$

where $\alpha = e, i$ refers to electrons and ions respectively, and the subscript i will be suppressed henceforth; $p_\alpha = n_\alpha T_\alpha$; m_α is the mass of the charge; $(\operatorname{div} \pi)_k = \partial \pi_{lk} / \partial x_l$; $\gamma = 5/3$ is the ratio of heat capacities.

Using the equation of continuity and Maxwell's equations, the last two equations may be written in the form

$$\left.\begin{aligned} &\frac{\partial (Mn\mathbf{v})}{\partial t} = -\mathbf{div}\,\Pi + zen\left(\mathbf{E} + \frac{1}{c}\mathbf{v} \times \mathbf{H}\right) - \mathbf{R}, && (4) \\ &\frac{\partial}{\partial t}\left(\frac{Mnv^2}{2} + \frac{nT}{\gamma - 1}\right) = -\operatorname{div}\left\{\mathbf{v}\left(\frac{Mnv^2}{2} + \frac{\gamma}{\gamma - 1} nT - \pi\right) + \mathbf{q}\right\} + \\ &\qquad + zen\,\mathbf{vE} - \mathbf{vR} + Q, && (5) \end{aligned}\right\} \text{ ions}$$

$$\left.\begin{aligned} &\frac{\partial (m, n_e\mathbf{v}_e)}{\partial t} = -\mathbf{div}\,\Pi_e - en_e\left(\mathbf{E} + \frac{1}{c}\mathbf{v}_e \times \mathbf{H}\right) + \mathbf{R}, \qquad (6) && (6) \\ &\frac{\partial}{\partial t}\left(\frac{mn_ev_e^2}{2} + \frac{n_eT_e}{\gamma - 1}\right) = -\operatorname{div}\left\{\mathbf{v}_e\left(\frac{mn_ev_e^2}{2} + \frac{\gamma}{\gamma - 1} n_eT_e - \pi_e\right) + \mathbf{q}_e\right\} - \\ &\qquad - en_e\mathbf{v}_e\mathbf{E} + \mathbf{v}_e\mathbf{R} + Q_e\,. && (7) \end{aligned}\right\} \text{ electrons}$$

where

$$\Pi_{kl} = p\delta_{kl} + Mnv_k v_l - \pi_{kl}, \quad (\mathbf{v}\pi)_k \equiv v_l \pi_{lk},$$

π_{kl} is the viscosity tensor, and **R** is the frictional force of electrons and ions. In the absence of a magnetic field (and for $z = 1$)*

$$\mathbf{R} = 0{,}5\,\frac{mn_e}{\tau_e}(\mathbf{v} - \mathbf{v}_e) - 0{,}7\, n_e \nabla T_e,$$

In a strong magnetic field (to within $mc/eH\tau_e$)

$$\mathbf{R} = (mn_e/\tau_e)(\mathbf{v} - \mathbf{v}_e);$$

Q_e and Q represent liberation of heat in the electron and ion gases,[6]

$$Q = \frac{3m}{M}\frac{n_e}{\tau_e}(T_e - T)\,[^6], \quad Q_e = -\mathbf{R}(\mathbf{v} - \mathbf{v}_e) - Q;$$

$\mathbf{q}_e$ and $\mathbf{q}$ are the thermally conducting electron and ion fluxes. In the absence of a magnetic field

$$\mathbf{q}_e = -\varkappa_e \nabla T_e, \qquad \mathbf{q} = -\varkappa \nabla T,$$

$$\varkappa_e = \xi_e(z)\, n_e T_e \tau_e / m, \quad \varkappa = \xi(z)\, n T\tau / M,$$

$$\tau_e = 3\sqrt{m}T_e^{3/2} / 4\sqrt{2\pi}\lambda z^2 e^4 n,$$

$$\tau = 3\sqrt{M}T^{3/2} / 4\sqrt{\pi}\lambda z^4 e^4 n,$$

where ξ_e and ξ are coefficients of order unity, $\xi_e(1) = 3.16$, $\xi(1) = 3.92$, and

$$\lambda = \frac{1}{2}\ln\left(\frac{T_e T}{T_e + T}\right)^3 \frac{1}{e^6 n}$$

is the well known Coulomb logarithm, which can be considered constant.

By adding (4) to (6) and (5) to (7) we obtain the laws of conservation of momentum and energy of the entire system

$$\frac{\partial}{\partial t}\left(Mn\mathbf{v} + mn_e\mathbf{v}_e + \frac{1}{4\pi c}\mathbf{E}\times\mathbf{H}\right)$$

$$= -\operatorname{div}(\Pi + \Pi_e - T), \tag{8}$$

$$\frac{\partial}{\partial t}\left(\frac{Mnv^2}{2} + \frac{mn_e v_e^2}{2} + \frac{nT}{\gamma - 1} + \frac{n_e T_c}{\gamma - 1} + \frac{H^2 + E^2}{8\pi}\right)$$

$$= -\operatorname{div}\left\{\mathbf{v}\left(\frac{Mnv^2}{2} + \frac{\gamma}{\gamma - 1}nT - \pi\right) + \mathbf{q}\right. \tag{9}$$

$$\left. + \mathbf{v}_e\left(\frac{mn_e v_e^2}{2} + \frac{\gamma}{\gamma - 1}n_e T_e - \pi_e\right) + \mathbf{q}_e + \frac{c}{4\pi}\mathbf{E}\times\mathbf{H}\right\},$$

where

$$T_{kl} = \frac{1}{4\pi}(H_k H_l + E_k E_l) - \frac{H^2 + E^2}{8\pi}\delta_{kl}.$$

2. For our problem, the most significant properties of the plasma are: a) quasi-neutrality, b) large difference between the masses of the ions and electrons. The criterion of quasi-neutrality is, as is well known, the smallness of the Debye length d with respect to the characteristic distance of the given problem. In a shock wave, this characteristic distance is the width of the discontinuity, determined by the mean free path of the particles l. The relative density of charges in the discontinuity $(n_e - zn)/n_e \approx d^2/l^2 \approx 10^{-7}n/T^3$ is small at temperatures $T \gtrsim 10^5$ degrees for all reasonable densities. Therefore, inside the discontinuity as well as outside, the electron and ion charge densities, and consequently also their velocities, can be considered equal: $n_e = zn$, $v_e = v$. The mass difference leads to a difference in the mechanisms through which the particles are heated. In a shock wave, the basic mechanisms for ions are dissipation processes in the discontinuity, transferring part of the kinetic energy of motion with respect to the discontinuity $Mv^2/2$ into energy of thermal motion. Since the velocities of the electrons and ions are equal, the kinetic energy of the electrons $mv^2/2$ is negligible with respect to the ion energy as well as the energy of thermal motion T which is of the same order of magnitude. Electrons in the jump may be heated by adiabatic compression, by acceleration in the electric field of the ions, and directly by elastic collisions with ions. Clearly, the electron temperature will generally differ from the ion temperature.

Furthermore, because of the large mass difference, energy transfer during collisions between one type of particle and the other is small (approximately the mass ratio times the energy of the particles). Therefore, the width x of the region in which temperature equalization takes place is a factor of M/m greater than the distance through which the electrons are displaced between collisions: $x \approx v\tau_e M/m$, or is a factor of $\sqrt{M/m}$ greater than the mean free path: $x \approx l\sqrt{M/m}$ (since $v \approx \sqrt{T/M}$). For a shock wave formed in a system with small dimensions, for example, in a gaseous discharge, this region may be of fundamental interest.

---

*The second terms in R arises from thermal diffusion. The numerical value of the coefficient of thermal diffusion for a fully ionized plasma is given, for example, in Ref. 5.

3. In the examination of the structure of a shock wave in the absence of a magnetic field, an essential factor is the high thermal conductivity of the electronic component of the plasma, associated with the mass difference. Actually, the mean free paths of electrons and ions for small z and comparable temperatures are of the same order of magnitude, but the thermal velocity of the electrons is greater by a factor of $\sqrt{M/m}$. Consequently, the electron coefficient of thermal conductivity $\varkappa_e \approx l\sqrt{T/m}$ is also a factor of $\sqrt{M/m}$ greater than the ion coefficient $\varkappa \approx l\sqrt{T/M}$. As a result, the electron temperature in the shock wave does not have a discontinuity, in spite of the existence of a density jump (one may speak of an "isoelectrothermal" jump). The hydrodynamic equations describing the structure of the transition layer outside the density jump differ from the corresponding equations describing the transition layer in the case of an isothermal jump (Ref. 7 p. 421) in that the density of energy flux due to electron thermal conductivity enters into the equation expressing the constancy of the energy flux. Furthermore, since the electron and ion temperatures differ, one more equation is added [it is convenient to take the heat transfer equation for ions (3)]

$$\frac{\varkappa}{j}\frac{dT_e}{dx} = \frac{\gamma}{\gamma-1}(\Theta-\Theta_1) + {}^1/{}_2 M(v^2 - v_1^2),$$

$$n\Theta - n_1\Theta_1 + Mj(v - v_1) = 0, \tag{10}$$

$$\frac{nv}{\gamma-1}\frac{dT}{dx} + nT\frac{dv}{dx} = \frac{3m}{M}\frac{zn(T_e - T)}{\tau_e}.$$

where $\Theta = T + zT_e$, $j = nv = \text{const}$. The electric field due to the separation of charges may be found from the equation of motion of the electrons (2),

$$eE = -\frac{1}{n}\frac{d(nT_e)}{dx} - \frac{1}{n}R_x. \tag{11}$$

Small terms of the order of $\sqrt{m/M}$ and of higher order have been omitted. These equations are rigorous for a stationary shock wave and are applicable to nonstationary waves if the characteristic time of the variable quantities exceeds the time required by particles to pass through the transition layer: $t > x/v \sim \tau_e\sqrt{M/m}$.

To integrate Eq. (10) we must know the conditions in the density jump. These conditions may be obtained from the hydrodynamic equations in the usual way, taking account of the constancy of the electron temperature. They reduce to the following. In the density jump, an electric double layer is formed, which corresponds to a jump of the electric potential. Therefore, the condition that the energy flux density be constant has the form for ions (see Eq. 5),

$$\frac{\gamma}{\gamma-1}(T_{20} - T_{10}) + \frac{1}{2}M(v_{20}^2 - v_{10}^2) + ze(\varphi_{20} - \varphi_{10}) = 0. \tag{12}$$

The subscripts 10 and 20 refer to the values of quantities in the jump on different sides of the discontinuity. The magnitude of the potential jump may be determined from the following considerations. Since the directed motion of the electrons is negligible in comparison with the thermal motion, the electrons in the jump have a Maxwell-Boltzmann distribution, and consequently, their density is $n = \text{const}\cdot\exp(e\varphi/T_{e0})$. Hence,

$$e(\varphi_{20} - \varphi_{10}) = T_{e0}\ln(n_{20}/n_{10}), \tag{13}$$

where T_{e0} is the temperature of the electrons in the jump. The same condition may be obtained directly from Eq. (11). Equations (10) – (13) are the complete solution of the problem of the structure of a shock wave in a plasma.

We will consider two cases. In the first case there is no exchange of energy between the electrons and ions behind the wave front. Such conditions are realized approximately when the wave front has moved from the point of its formation through a distance less than that required for temperature equalization. The shock wave has the following structure. Between region 1 of the undisturbed gas and the density jump, there is a transition region in which the density varies smoothly from n_1 to n_{10}, the ion temperature from T_1 to T_{10}, and the electron temperature from T_{e1} to $T_{e0} = T_{e2}$. Furthermore, the density and the ion temperature are changed by the jump from n_{10} to $n_{20} = n_2$, and from T_{10} to $T_{20} = T_2$, respectively. The values of p_2, n_2, v_2, Θ_2, are connected with p_1, n_1, v_1, Θ_1, and the ratio of the velocity of the front to the velocity of sound $M_1 = \sqrt{Mv_1^2/\gamma\Theta_1}$ through the usual equations for an ideal gas (Ref. 5, p. 408). The results of a numerical integration of system (10) are shown in Fig. (1) for $M_1 = 6$, $z = 1$. The wave is moving from the right to the left. The density scale is based on the density n_1 in the undisturbed plasma, the temperature scale is based on $\Theta_2/2$, the length scale is based on $3.16\, v_2 \tau_2 \sqrt{2M/m}\, \Theta_2^2/4M^2 v_1^4$, where τ_2 is the time between collisions of ions for $n = n_2$, $T = \Theta_2/2$. Conditions in the isoelectrothermal jump for $z = 1$ and various M_1, obtained by numerical integration of Eq. (10), are given in Table 1. For $M_1 < 1.12$, there is no discontinuity. As $M_1 \to \infty$, the ion temperature in the wave increases proportionately to M_1^2, while the electron temperature approaches a constant limit. In this case, our equations lose their meaning since our assertion that the width of the transition region considerably exceeds the width of the jump is violated. Actually, the width of the transition region may be estimated by comparing the electron heat fluxes $nv dT_e/dx$, and $-\varkappa_e d^2 T_e/dx^2$ with the transfer of energy by ions $nmT/M\tau_e$, whence $x \approx v\tau_e T_e M/Tm$. The width of the jump is of the order of the mean free path of the ions $l \approx \sqrt{T/M}\,\tau$. We require $x \gg l$, or $T_e > T(m/M)^{1/3} z^{-4/3}$. This condition is fulfilled at $z = 1$, for example, only for $M \lesssim 7$. In stronger shock waves, the electrons in the discontinuity will be able to attain temperatures of the order of $T_e \approx T_2 (m/M)^{1/3} z^{-4/3}$ by collisions with ions.

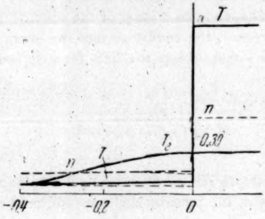

FIG. 1.

TABLE I. Conditions in the jump in the nonstationary mode.

M_1	1.12	1.5	2	3	4	6	8	$M_1 \gg 1$
$n_2/n_1 = 4M_1^2/(3+M_1^2)$	1.18	1.71	2.29	3.00	3.37	3.69	3.82	4
n_{10}/n_1	1.18	1.14	1.11	1.08	1.06	1.04	1.03	$1+3.66M_1^{-2}$
$\Theta_2/2T_1 = (5M_1^2-1)\times$ $\times(M_1^2+3)/16M_1^2$	1.12	1.49	2.08	3.67	5.86	12.12	20.9	$0.31\ M_1^2$
Te_0/T_1	1.10	1.36	1.73	2.51	3.29	4.78	5.97	13.2
T_{10}/T_1	1.14	1.21	1.28	1.35	1.37	1.33	1.26	1
T_{20}/T_1	1.14	1.62	2.43	4.83	8.43	19.5	35.8	$0.625\ M_1^2$

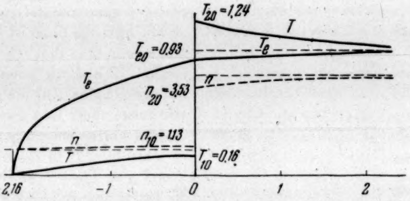

FIG. 2.

In the second case, we consider a stationary shock wave. The temperatures of the electrons and ions on both sides of the front and far from it are equal. In this case, the density jump is divided into two regions in each of which there is a gradual variation of density and ion temperature from the values n_1, n_2 and T_1, T_2 respectively, to the values n_{10}, n_{20}, and T_{10}, T_{20} in the jump, connected by relations (10) – (13). The electron temperature varies continuously from $T_{e1} = \Theta_1/2$ to $T_{e2} = \Theta_2/2$, with the value $T_e = T_{e0}$ in the jump. The derivative dT_e/dx is discontinuous in the jump. The results of a numerical integration of equations (10) – (13) for $z = 1$, $M_1 = \infty$, are shown in Fig. (2). Because of the strong dependence of $\varkappa_e$ on T_e, the electron temperature front is

TABLE II. Conditions in the jump in a stationary shock wave.

M_1	1.20	1.3	1.5	1.8	3	4	6	7	$M_1 \gg 1$
n_{10}/n_1	1.23	1.22	1.21	1.18	1.15	1.143	1.136	1.135	1.131
n_{20}/n_1	1.23	1.36	1.62	1.93	2.72	3.03	3.29	3.35	3.526
T_{e0}/T_1	1.17	1.25	1.43	1.74	3.44	5.48	11.3	15.1	$0.29\, M_1^2$
T_{10}/T_1	1.19	1.23	1.29	1.37	1.73	2.71	3.16	3.83	$0.05\, M_1^2 + 1.2$
T_{20}/T_1	1.19	1.32	1.58	1.99	4.26	6.97	14.7	19.7	$0.387\, M_1^2$

steep and extends far ahead. The conditions in the isoelectrothermal jump are given in Table 2 for finite M_1. For $M_1 < 1.20$, all quantities in the shock wave vary slowly, without discontinuities.

4. Let us assume that a magnetic field H exists in the plasma, directed along the z-axis, parallel to the plane of the discontinuity. The shock wave moves in the negative direction along the x-axis. The structure of the shock wave is quite dependent on the magnitude of the magnetic field since the latter has a strong influence on the thermal conductivity. For the examination of effects associated with a magnetic field, we will consider the limiting case of a strong magnetic field for which $\Omega^2\tau^2 > 1$, $\Omega_e^2\tau_e^2 \gg 1$ ($\Omega = zeH/Mc$, $\Omega_e = eH/mc$). These conditions signify that the radius of the Larmor circle along which a charge moves in a plane perpendicular to the magnetic field does not exceed the mean free path for ions, and is considerably less than the mean free path for electrons. The coefficient of electron thermal conductivity is strongly lowered in this case (by factor of $\Omega_e^2\tau_e^2$), and is less than the ion thermal conductivity approximately by a factor of $z^{-2}\sqrt{M/m}$. As regards the viscosity, the component of the viscosity tensor of interest to us π_{xx}, equal to $(4\eta/3)\, dv/dx$ at $H = 0$ ($\eta \approx nT\tau$), is changed by the coefficient only slightly. In particular, for $\Omega^2\tau^2 \gg 1$, it is decreased by a factor of four. This result may be explained as follows. The component of the tensor π_{zz} remains the same as for $H = 0$: $\pi_{zz} = 2\eta(\partial v_z/\partial z - \frac{1}{3}\operatorname{div} \mathbf{v})$. For a monatomic gas, which the plasma appears to be, $\pi_{xx} + \pi_{yy} + \pi_{zz} = 0$. As a result of axial symmetry, $\pi_{xx} = \pi_{yy}$, and consequently, $\pi_{xx} = -\eta(\partial v_z/\partial z - \frac{1}{3}\operatorname{div} \mathbf{v})$. In the present case, $\partial/\partial y = \partial/\partial z = 0$, and $\pi_{xx} = (\frac{1}{3})\eta\, dv/dx$.

Hence, the width of the discontinuity, as in the usual non-ionized gas, is of the order of the mean free path. As when $H = 0$, temperature changes of the electrons and ions passing through the discontinuity are not equal, and the exchange of energy between them is retarded. Therefore, except for the discontinuity, there is a comparatively broad transition region in which temperature equalization takes place. In the case of ideal conductivity, the equations describing the structure of the shock wave in the transition region have the form

$$\frac{H^2}{4\pi n} + \frac{Mv^2}{2} + \frac{\gamma}{\gamma-1}\Theta = \frac{H_2^2}{4\pi n_2} + \frac{Mv_2^2}{2} + \frac{\gamma}{\gamma-1}\Theta_2\,,$$

$$\frac{H^2}{4\pi} + Mnv^2 + n\Theta = \frac{H_2^2}{4\pi} + Mn_2v_2^2 + n_2\Theta_2\,;$$

$$nv = n_2v_2;\quad Hv = H_2v_2, \tag{14}$$

$$\frac{nv}{\gamma-1}\frac{dT_e}{dx} + nT_e\frac{dv}{dx} + \frac{3m}{M}\frac{n(T_e - T)}{\tau_e} = 0\,.$$

The condition in the discontinuity which permits us to determine the electron and ion temperatures separately is easily obtained by noting that an adiabatic compression is the only significant mechanism for the heating of electrons in the discontinuity. Therefore,

$$T_{e0} = T_{e1}(n_{20}/n_1)^{\gamma-1}.$$

Since the change of density is bounded, $n_{20}/n_1 \leqslant (\gamma + 1)/(\gamma - 1)$, the increase of electron temperature is insignificant ($T_{e0} \leqslant 2.5T_{e1}$ for $\gamma = \frac{5}{3}$).

The solution of the first two equations of system (14) in the transition region is tribial

$$v = \text{const} = v_2;\quad H = \text{const} = H_2;$$

$$\Theta = \text{const} = \Theta_2.$$

The variation of the electron and ion temperatures behaves according to the last of equations (14) in which we must set $dv/dx = 0$, and according to the condition $zT_e + T = \Theta_2$. Letting $\Theta_2/(z + 1)$ be the unit temperature, and $x_1 = v_2\tau_2\sqrt{M/2m}\, z^2/(z + 1)$ the unit length, where τ_2 is taken at $n = n_2$ and $T = \Theta_2/(z + 1)$, we obtain the solution of this equation in the form

$$x = \frac{1}{2} \ln \frac{1+\sqrt{T_e}}{1-\sqrt{T_e}} \frac{1-\sqrt{T_{e0}}}{1+\sqrt{T_{e0}}} - \sqrt{T_e}\left(1+\frac{T_e}{3}\right) + \sqrt{T_{e0}}\left(1+\frac{T_{e0}}{3}\right). \tag{15}$$

The functions $T(x)$, $T_e(x)$, $\Theta(x)$ for $z = 1$, $M_1 = \infty$ are shown in Fig. (3). These curves are not assumed to be highly accurate, since as a result of the low electron temperature in the discontinuity, the exchange of energy in the discontinuity becomes substantial. The behavior of all the quantities in the discontinuity may be obtained for weak waves by including the terms in the viscosity $(\eta/3n)\, dv/dx$ and $-(\eta/3)\, dv/dx$ in the left hand sides of the first and second equations respectively of system (14).

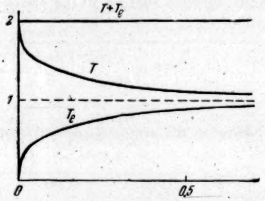

FIG. 3.

In conclusion, we thank Academician M. A. Leontovich for his guidance and S. I. Braginskii for discussions concerning this work. We also thank the mathematics group under the direction of G. I. Biriuk and N. A. Grechina for carrying out the numerical calculations.

---

[1] J. F. Denisse and Y. Rocard, J. Phys. Rad. 12, (1951).

[2] W. Marshall, Proc. Roy. Soc. 233, 367 (1955).

[3] H. K. Sen, Phys. Rev. 102, 5 (1956).

[4] S. I. Braginskii (in press).

[5] R. Landshof, Probl. Sovr. Fiz. 2, (1956).

[6] L. D. Landau, J. Exptl. Theoret. Phys. (U.S.S.R.) 7, 203 (1937).

[7] L. D. Landau and E. M. Lifshitz, *Mechanics of Continuous Media*, Gostekhizdat, 1953.

Translated by D. Lieberman
286

SOVIET PHYSICS JETP VOLUME 5, NUMBER 6 DECEMBER 15, 1957

On the Angular Distribution of Deuterons from the $Be_4^9(pd)Be_4^8$ Reaction

D. P. GRECHUKHIN

(Submitted to JETP editor September 24, 1956)
J. Exptl. Theoret. Phys. (U.S.S.R.) 32, 1460-1463 (June, 1957)

It is shown that even at proton energies ≥ 8 Mev the main contribution is from the region within the Be_4^9 nucleus. This significantly modifies the deuteron angular distribution, good agreement with experiment being obtained for proton energies of ≈ 22 Mev with a Be_4^8 radius $r_0 = 5 \times 10^{-13}$ cm.

WHEN ANALYZING the angular distribution of deuterons from the $Be_4^9(pd)Be_4^8$ reaction on the basis of the theoretical angular distribution from the $Be_4^8(pd)Be_4^9$ stripping reaction and the principle of detailed balance, difficulties arise related to the choice of the nuclear radius r_0. This is determined by agreement between the theoretical and experimental distribution curves at some single point. For nuclei that are not too light, the radius r_0 for the stripping reaction (using Butler's formula for the angular distribution) is given by $r_0 = (1.2A^{1/3} + 1.7) \times 10^{-13}$ cm, where A is the atomic weight of the target nucleus. This value of r_0 is in good agreement with that obtained by scattering of neutrons with energy $E \geq 1$ Mev by nuclei. For light nuclei the value of r_0 is found to be larger than that given by the above formula. Thus, for instance, for the direct and inverse reactions on Li_3^7, B_5^{10}, B_5^{11}, the nuclear radii lie in the interval between 4.5×10^{-13} and 5×10^{-13} cm,[1,2] and depend extremely weakly on the incident particle energies. For the $Be_4^9(dp)Be_4^{10}$ reaction at a deuteron energy of 3.6 Mev, the radius r_0 is found to be 6.1×10^{-13} cm.

At a proton energy $E_p \simeq 16-22$ Mev, however, in order to obtain agreement between the theoretical and experimental deuteron distributions from the

(pd) reaction on Be$_4^9$, it is necessary to choose r_0 for Be$_4^8$ in the interval between 3×10^{-13} and 2×10^{-13} cm, which is in sharp disagreement both with r_0 values for neighboring nuclei and for Be$_4^9$ for low deuteron energies.[1] Reynolds and Standing[1] conclude from this that r_0 must depend on the proton energy.

Previously Gordon[3] had suggested that this sharp decrease of r_0 is related to the increase in the contribution from the region within the nucleus as E_p increases. He did not, however, present any numerical calculations. We present below a calculation of the angular distribution of deuterons from the Be$_4^9$$(pd)Be_4^8$ reaction with the same assumptions as those made by Butler.[4] It is shown that the region within the Be$_4^8$ nucleus contributes fundamentally to the process when $E_p \geq 8$ Mev for all angles θ. This situation gives rise to many additional difficulties, since it is necessary to account for proton scattering by Be$_4^8$ and deformation of the deuteron wave functions due to interaction with this nucleus. For proton energies $E_p > V$ (where V is the potential well depth of the interaction of the proton or deuteron with Be$_4^8$), plane waves and an expansion in terms of the parameter V/E_p may be used for the zeroth approximation. Then good agreement between the theoretical and experimental distributions is obtained for $E_p = 22$ Mev when we choose $r_0 = 5 \times 10^{-13}$ cm and the radius of action of nuclear forces equal to 1.05×10^{-13} cm.

For lower proton energies the plane wave approximation is too rough, and the distortion of the waves must be accounted for. Such calculations are at present being performed and will be published elsewhere.

The decay of Be$_4^8$ into two α-particles leads to no difficulties, since the half-life $\tau_1 \approx 10^{-14}$ sec of Be$_4^8$ is much greater than the time $\tau_2 \approx r_0/v_p \approx 10^{-20}$ sec of the process.

ANGULAR DISTRIBUTION OF DEUTERONS IN THE PLANE WAVE APPROXIMATION

As is well known, Be$_4^9$ is a loosely bound system analogous to the deuteron (the binding energy of the neutron in Be$_4^9$ is $\varepsilon = 1.63$ Mev). This makes it possible to develop the theory of stripping of Be$_4^9$ in the same way as was done by Butler for deuteron stripping.[4] The approximate nature of Butler's assumptions is well known (they have been discussed more than once in the literature), but experiment continues to give good agreement with Butler's theory.

In order to investigate the question of which region is important in the reaction under consideration, it is sufficient to perform the calculation in the plane wave approximation, neglecting the interaction of the proton or deuteron with the Be$_4^8$ nucleus.

We shall describe the state of the Be$_4^8$ $+ n + p$ system in terms of the coordinate system $\mathbf{R}$, $\mathbf{r}_1$, ρ_1, or $\mathbf{R}$, $\mathbf{r}_2$, ρ_2, where

$$\mathbf{R} = \frac{M_a\mathbf{R}_a + M_n\mathbf{R}_n + M_p\mathbf{R}_p}{M}, \quad \mathbf{r}_1 = \mathbf{R}_n - \mathbf{R}_a; \; \rho_1 = \frac{\mathbf{R}_n M_n + \mathbf{R}_a M_a}{M_n + M_a} - \mathbf{R};$$

$$\mathbf{r}_2 = \mathbf{R}_n - \mathbf{R}_p; \; \rho_2 = \frac{\mathbf{R}_p M_p + \mathbf{R}_n M_n}{M_p + M_n} - \mathbf{R}; \; M = M_a + M_n + M_p.$$

Here $\mathbf{R}_a$, $\mathbf{R}_p$, and $\mathbf{R}_n$ are the radius vectors of the Be$_4^8$ nucleus (index a), the proton (index p), and the neutron (index n), respectively. We describe the wave function of the system before the reaction in terms of the coordinates $\mathbf{R}$, $\mathbf{r}_1$, ρ_1, and after the reaction in terms of the coordinates $\mathbf{R}$, $\mathbf{r}_2$, ρ_2. We then join the functions at the surface $|\mathbf{r}_2| = r_{20}$ of the second bound system, where in our case r_{20} is simply the radius of action of nuclear forces and varies between 1.05×10^{-23} and 1.7×10^{-23} cm.

The method of calculation is entirely analogous to Butler's,[4] so that we shall not go into detail. Butler has shown that the angular distribution $S(\theta)$ for stripping is given by the integral

$$\frac{1}{r^2}\Phi_{l_2 m_2}(r_2) = \int \psi(\mathbf{r}_1)\, Y^*_{l_2 m_2}(\theta_{\mathbf{r}_2} \psi_{\mathbf{r}_2})\, \psi_{\mathbf{k}_1}(\rho_1)\, \psi^*_{k_2}(\rho_2)\, d\Omega_{\mathbf{r}_2} d\rho_2$$

(we have omitted the spin functions and indices). Here $\psi(\mathbf{r}_1)$ is the wave function of the relative motion of the neutron in Be_4^9, $\psi_{\mathbf{k}_1}(\rho_1)$ is the wave function of the relative motion of the proton and Be_4^9 in the initial state, $\psi_{\mathbf{k}_2}(\rho_2)$ is the wave function of the relative motion of the deuteron and Be_4^8 (the system in the final state), l_2 is the orbital angular momentum of the neutron in the final state (in the present case the final nucleus is a deuteron, so that $l_2 = 0$), and we choose $\psi_{\mathbf{k}_1}$ and $\psi_{\mathbf{k}_2}$ in the form of plane waves.

After some operations we obtain the angular distribution function in the form

$$S(\theta_{\mathbf{k}_1\mathbf{k}_2}) = |Q_{l_1}(x_1)|^2 \, |I_{l_2} j_{l_2}(x_2) - II_{l_2} x_2 j_{l_2+1}(x_2)|^2;$$

$$x_1 = \left| \left(\frac{M_p}{M}\right)^{1/2} \left(\frac{M_a}{M_a + M_n}\right) \frac{\sqrt{2(M_a + M_n)W_1}}{h}\, \mathbf{n}_1 - \left(\frac{M_p + M_n}{M}\right)^{1/2} \frac{\sqrt{2M_aW_2}}{\hbar}\, \mathbf{n}_2 \right| r_0;$$

$$x_2 = \left| \left(\frac{M_p}{M}\right)^{1/2} \frac{\sqrt{2(M_a + M_n)W_1}}{\hbar}\, \mathbf{n}_1 - \left(\frac{M_p^2}{M(M_p + M_n)}\right)^{1/2} \frac{\sqrt{2M_aW_2}}{\hbar}\, \mathbf{n}_2 \right| r_{20};$$

Here $\mathbf{n}_1$ and $\mathbf{n}_2$ are unit vectors in the directions of $\mathbf{k}_1$ and $\mathbf{k}_2$, respectively, $W_1 = E_p(M_a + M_n)/M$, $W_2 = W_1 + Q$, Q is the energy released by the reaction, r_0 is the Be_4^8 radius in the $\mathrm{Be}_4^8 + n$ system, r_{20} is the radius at which the functions are joined and lies between 1.05×10^{-13} and 1.7×10^{-13} cm, j is the spherical Bessel function of half-integer index,

$$I_{l_2} = \sum_{q=0}^{l_2} \frac{(l_2+q)!\,[l_2+q+k_nr_{20}]}{q!\,(l_2-q)!\,(2k_nr_{20})^q}, \quad II_{l_2} = \sum_{q=0}^{l_2} \frac{(l_2+q)!}{-q)!\,(2k_nr_{20})^q},$$

and k_n is the wave number of the relative motion of the neutron in the bound state in the final system.

In the case of the (pd) reaction,

$$I_{l_2} = (k_dr_{20}), \quad II_{l_2} = 1. \quad k_d = 0{,}23 \cdot 10^{13}\ \mathrm{cm}^{-1},$$

so that

$$S(\theta_{\mathbf{k}_1\mathbf{k}_2}) = |Q_{l_1}(x_1)|^2 \, |(k_dr_{20})\, j_0(x_2) - x_2 j_1(x_2)|^2;$$

$$Q_{l_1}(x_1) = \int_0^\infty R_{l_1}(r_1)\, j_{l_1}(x_1r_1/r_0)\, r_1^2 dr_1,$$

where R_{l_1} is the radial part of the neutron wave function in the Be_4^9 system. This function can be obtained only for specific models. We shall make use of the wave function used by Guth and Mullin[5] in calculating the cross section for the (γn) reaction for gamma energies between 1.7 and 4 Mev, namely

$$R_{l_1}(r_1) = \begin{cases} A_1 j_1(\beta r_1) & \text{for } r_1 \leqslant r_0, \\ B_1(1+\alpha r_1)(\alpha r_1)^{-2} e^{-\alpha(r_1 - r_0)} & \text{for } r_1 \geqslant r_0, \end{cases}$$

$$B_1 = -A_1 \sin\beta r_0; \ \beta = [2\mu\hbar^{-2}(V-\varepsilon)]^{1/2}; \ \alpha = \sqrt{2\mu\varepsilon/\hbar}; \ \mu = 8M_n/9,$$

where $V = 12.16$ Mev is the interaction potential well depth of $\mathrm{Be}_4^8 + n$, $r_0 = 5 \times 10^{-13}$ cm, and $\varepsilon = 1.63$ Mev. Inserting this function into the integral, we obtain

$$Q_{l_1} = Q_1 + Q_2 = \frac{0.267x_1j_0(x_1) + 0.236j_1(x_1)}{11.5 - x_1^2} + \frac{0.32x_1j_0(x_1) - 0.242j_1(x_1)}{1.77 + x_1^2}$$

The dependence of these quantities on x_1 is given in Figs. 1 and 2. Here Q_1 is the contribution from the region $r_1 \leq r_0$, and Q_2 is the contribution from the region outside the nucleus $r_1 \geq r_0$. It is clearly seen that Q_1 is of the same order as Q_2 even for small values of x_1, so that

$$1.75 \leqslant x_1 \leqslant 6.3 : |Q_1| \geqslant |Q_2|.$$

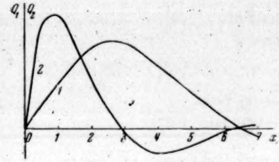

FIG. 1. *1* – plot of $Q_1(x_1)$ (in arbitrary units); *2* – plot of $Q_2(x_1)$.

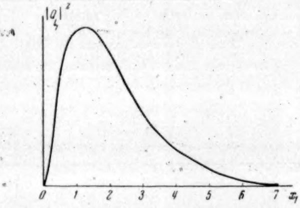

FIG. 2. Plot of $|Q_1(x_1)|^2$ (in arbitrary units).

In the $Be_4^9(pd)Be_4^8$ reaction, the interval over which x_1 varies depends on the proton energy:

$$E_p = 2\text{ Mev}\quad 0.92 \leq x_1 \leq 3.57;\quad x_1 = 1.7 \text{ for } \theta = 50^\circ$$
$$E_p = 3.6\text{ Mev}\quad 1.05 \leq x_1 \leq 4.5\;;\quad x_1 = 1.7 \text{ for } \theta = 33^\circ$$
$$E_p = 8\text{ Mev}\quad 1.37 \leq x_1 \leq 6.0\;;\quad x_1 = 1.7 \text{ for } \theta = 14^\circ$$
$$E_p = 22\text{ Mev}\quad 2.16 \leq x_1 \leq 10.4\;;$$

thus, even at proton energies $E_p \simeq 8$ Mev, the contribution of the internal region of the Be_4^9 nucleus is significant and comparable with the contribution of the external region. Therefore the angular distribution obtained in the plane wave approximation cannot be used for energies of the order of the potential well depth. The proton distribution as obtained by Butler's theory should lead to large differences between the experimental and theoretical deuteron distribution curves, and these are indeed observed in the form of the sharp difference in the values of r_0 for low and high energies. (Let us bear in mind that r_0 is usually determined from the position of the first maximum in the distribution, which means that for our reaction it is determined from the data for $\theta \sim 25^\circ$ and $E_d \approx 3.6$ Mev, where the contribution from the external region is still most significant.)

When $E_p \gg V$ one may neglect the deformation of the function in the zeroth approximation in V/E_p, and calculate the angular distribution with plane waves. The angular distribution for $E_p = 22$ Mev is shown in Fig. 3. Here the reaction parameters are taken as $r_0 = 5 \times 10^{-13}$ cm (rather than 2×10^{-13} cm, as elsewhere[1,3]), $r_{20} = 1.05 \times 10^{-13}$ cm, and $r_{20} = 1.7 \times 10^{-13}$ cm. The distribution obtained is in good agreement with experiment. It is important to note that the angular distribution is determined basically by the factor $|Q_{l_1}|^2$, and since the wave functions of the proton and deuteron enter primarily into the slowly varying second factor, this may explain the independence of the shape of the angular distribution on the proton energy.

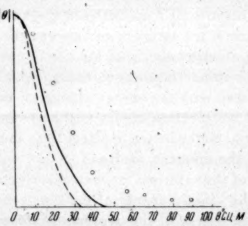

FIG. 3. Angular distribution of deuterons (arbitrary units) obtained in the plane wave approximation. The solid curve corresponds to $r_{20} = 1.05 \times 10^{-13}$ cm, and the dotted curve to $r_{20} = 1.7 \times 10^{-13}$ cm; the proton energy is 22 Mev in the laboratory coordinate system. The circles give the experimental angular distribution.[6]

[1] J. B. Reynolds and K. G. Standing, Phys. Rev. **101**, 158 (1956).

[2] J. R. Holt and T. N. Marsham, Proc. Phys. Soc. **A66**, 1032 (1953).

[3] M. M. Gordon, Phys. Rev. **99**, 1625 (1955).

[4] S. T. Butler, Proc. Roy. Soc. **A208**, 559 (1951).

[5] E. Guth and C. J. Mullin, Phys. Rev. **76**, 234 (1948).

[6] B. L. Cohen, E. Newman, *et al.*, Phys. Rev. **90**, 323 (1953).

Translated by E. J. Saletan

SOVIET PHYSICS JETP VOLUME 5, NUMBER 6 DECEMBER 15, 1957

Interaction Energy of Atoms For Small Nuclear Separations

O. B. FIRSOV

(Submitted to JETP editor September 24, 1956)
J. Exptl. Theoret. Phys. (U.S.S.R.) 32, 1464-1469 (June, 1957)

As is well known, the Thomas-Fermi equation for electrons can be obtained by minimizing a certain functional of the spatial density distribution. At the same time a functional of a certain function of the coordinates is established, such that its maximum value gives the same electron energy. It is shown for two nuclei that if one inserts into these functionals the sum of the electron densities and the sum of f functions which cause the single-nucleus functionals to be, respectively, minimum and maximum, then the relative difference between these functionals will not exceed 5%. The electron energies then lie between the two values of these functionals.

---

1. MINIMIZATION PRINCIPLE

FOR SEPARATIONS less than the dimensions of a Bohr orbit $\sim 10^{-8}$ cm between the nuclei of interacting atoms, the interaction between the external parts of the electron shells of the atoms contributes a term to the atomic interaction energy which is small compared with the energy change of the internal parts of the electron shells of the system. Thomas-Fermi methods are applicable to the internal parts of the electron shells.

Because of the relation between the electron density ρ and the kinetic energy of the electrons, the total electron energy of the system of interacting atoms is given by (see, for instance, Gombas[1])

$$e^{-2}H = \frac{3}{5}\lambda\int \rho^{5/3}\,dv - \int\sum_i \frac{Z_i}{r_i}\rho\,dv + \iint\frac{\rho(\mathbf{r})\,\rho(\mathbf{r}')\,dv\,dv'}{|\mathbf{r}-\mathbf{r}'|}, \qquad (1)$$

where $\lambda = (3\pi^2)^{2/3}h^2/2me^2 \approx 2.5\times 10^{-8}$ cm, and $Z_i e$ are the nuclear charges. We shall henceforth take the electron charge e equal to unity; r_i is the distance to the ith nucleus. The first term on the right of Eq. (1) is the kinetic energy of the electrons according to the Thomas-Fermi model, the second is the interaction energy of the electrons with the nuclei, and the third is the interaction energy among the electrons.

The density ρ is found by minimizing H. Variation of H with respect to ρ gives

$$\lambda\rho_0^{2/3} = \sum\frac{Z_i}{r_i} - \int\frac{\rho_0(\mathbf{r}')\,dv}{|\mathbf{r}-\mathbf{r}'|}. \qquad (2)$$

The electric potential φ is given by

$$\varphi = \sum\frac{Z_i}{r_i} - \int\frac{\rho(\mathbf{r}')\,dv'}{|\mathbf{r}-\mathbf{r}'|}, \qquad (3)$$

$$\nabla^2\varphi = -4\pi\sum Z_i\delta(\mathbf{r}-\mathbf{r}_i) + 4\pi\rho. \qquad (4)$$

It follows from Eq. (2) that

$$\varphi_0 = \lambda\rho_0^{2/3}, \qquad (5)$$

$$\nabla^2\varphi_0 = -4\pi\sum Z_i\delta(\mathbf{r}-\mathbf{r}_i) + 4\pi\lambda^{-3/2}\varphi_0^{3/2}. \qquad (6)$$

Equation (6) is the Thomas-Fermi equation for an arbitrary number of nuclei (for a neutral system no subsidiary condition is needed in performing the variation).

If the solution of Eq. (2) is found, then it can be used to simplify $H = H_0$,

$$H_0 = \frac{\lambda}{10}\int\rho_0^{5/3}\,dv - \frac{1}{2}\int\sum\frac{Z_i}{r_i}\rho_0\,dv. \qquad (7)$$

If $\rho = \rho_0 + \delta\rho$, $\delta\rho \ll \rho_0$, then from Eq. (2) we obtain

$$H = H_0 + \frac{1}{3}\lambda\int\rho_0^{-1/3}(\delta\rho)^2\,dv + \frac{1}{2}\iint\frac{\delta\rho(\mathbf{r})\,\delta\rho(\mathbf{r}')\,dv\,dv'}{|\mathbf{r}-\mathbf{r}'|}. \qquad (8)$$

From Eq. (8) it is seen that what is added to H_0 is essentially positive, so that H_0 is the minimum value of H. We note that $H_0 < 0$. This can be seen by inserting Eq. (2) into Eq. (7), obtaining

$$H_0 = -\frac{2}{5}\int\sum\frac{Z_i}{r_i}\rho_0\,dv - \frac{1}{10}\iint\frac{\rho_0(\mathbf{r})\,\rho_0(\mathbf{r}')\,dv\,dv'}{|\mathbf{r}-\mathbf{r}'|} \qquad (9)$$

$$H_0 = -\frac{2}{5}\int \lambda\rho_0^{5/3} dv - \frac{1}{2}\int \frac{\rho_0(\mathbf{r}')\,\rho_0(\mathbf{r})\,dv dv'}{|\mathbf{r}-\mathbf{r}'|}. \quad (10)$$

2. MAXIMIZATION PRINCIPLE

Let us now consider another functional of some function f, namely

$$H_1 = -\frac{1}{4\pi}\int\left[\frac{1}{2}(\nabla f)^2 + \frac{8\pi}{5\lambda^{3/2}}\left(\sum\frac{Z_i}{r_i} - f\right)^{5/2}\right]dv. \quad (11)$$

We shall consider only real H_1, so that $f < \Sigma Z_i/r_i$ (this inequality may involve some other external potential on the right side), and shall require f to vanish at infinity.* Finally, we shall take the positive root for $(\ldots)^{5/2}$. Then clearly $H_1 < 0$ and can take on arbitrarily large negative values depending on f.

The maximum value of H_1 is given by the condition

$$\delta H_1 = 0, \quad (12)$$

which leads to the following equation for $f = f_0$:

$$\nabla^2 f_0 + 4\pi\lambda^{-3/2}\left(\sum(Z_i/r_i) - f_0\right)^{3/2} = 0. \quad (13)$$

Now let $f = f_0 + \delta f$, $\delta f \ll f_0$. Then

$$\begin{aligned} H_1 &= H_{10} \\ &- \frac{1}{4\pi}\int\left[(\nabla f_0\cdot\nabla\delta f) - 4\pi\lambda^{-3/2}\left(\sum\frac{Z_i}{r_i} - f_0\right)^{3/2}\delta f\right]dv \\ &- \frac{1}{4\pi}\int\left[\frac{1}{2}(\nabla\delta f)^2 + 3\pi\lambda^{-3/2}\left(\sum\frac{Z_i}{r_i} - f_0\right)^{1/2}(\delta f)^2\right]dv. \end{aligned} \quad (14)$$

Since

$$\int(\nabla f_0\cdot\nabla\delta f_0)\,dv = \int\nabla(\nabla f_0\cdot\delta f)\,dv - \int\nabla^2 f_0\cdot\delta f\,dv.$$

the first integral on the right side can be replaced by a surface integral at infinity and vanishes in view of the conditions on f and δf. Therefore the second term in (14) becomes

$$\frac{1}{4\pi}\int\left[\nabla^2 f_0 + 4\pi\lambda^{-3/2}\left(\sum\frac{Z_i}{r_i} - f_0\right)^{3/2}\right]\delta f\,dv$$

and vanishes in view of Eq. (13). Thus the addition to H_{10} [*i.e.*, the last term in Eq. (14)] is essentially negative, so that when we set $f = f_0$ the value of H_1 is indeed maximal.

The function $\Sigma\,(Z_i/r_i) - f_0$, as is easily seen from Eq. (13), satisfies

$$\begin{aligned} \nabla^2\left(\sum\frac{Z_i}{r} - f_0\right) &= -4\pi\sum Z_i\delta(\mathbf{r}-\mathbf{r}_i) \\ &+ 4\pi\lambda^{-3/2}\left(\sum\frac{Z_i}{r_i} - f_0\right)^{3/2}, \end{aligned} \quad (15)$$

which is identical with Eq. (6) for $\varphi_0(\mathbf{r})$. Since the boundary conditions for $\varphi_0(\mathbf{r})$ (that is, vanishing at infinity) are the same as those for $(\Sigma Z_i/r_i - f_0)$, we have

$$\sum Z_i/r_i - f_0 = \varphi_0. \quad (16)$$

From (3) and (5) it follows that

$$f_0 = \int\frac{\rho_0(\mathbf{r}')\,dv'}{|\mathbf{r}-\mathbf{r}'|} = \sum\frac{Z_i}{r_i} - \lambda\rho_0^{2/3},\quad \nabla^2 f_0 = -4\pi\rho_0. \quad (17)$$

From Eq. (11) H_1 can be written in the form

$$H_1 = \frac{1}{8\pi}\int f\nabla^2 f\,dv - \frac{2}{5}\int\left(\sum\frac{Z_i}{r_i} - f\right)^{5/2}\lambda^{-3/2}dv. \quad (18)$$

Inserting $f = f_0$ and using Eq. (17), *i.e.*,

$$\nabla^2 f_0 = -4\pi\rho_0,\quad f_0 = \sum\frac{Z_i}{r_i} - \lambda\rho_0^{2/3},$$

we have

$$\begin{aligned} H_{10} &= -\frac{1}{2}\int\left(\sum\frac{Z_i}{r_i} - \lambda\rho_0^{2/3}\right)\rho_0 dv - \frac{2}{5}\lambda\int\rho_0^{5/3}dv \\ &= \frac{\lambda}{10}\int\rho_0^{5/3}dv - \frac{1}{2}\int\sum\frac{Z_i}{r_i}\rho_0\,dv = H_0, \end{aligned} \quad (19)$$

which is the same as H_0 as given by Eq. (7). Thus H_0 is the absolute minimum for H and the absolute maximum for H_1.

If $f \neq f_0$, then $H_1 < H_0$. The function f can be associated in an arbitrary way with ρ, so long as Eq. (17) is satisfied in the limiting case $f \to f_0$ and $\rho \to \rho_0$. For instance, we may set

$$f = a\int\frac{\rho(\mathbf{r}')\,dv'}{|\mathbf{r}-\mathbf{r}'|} + (1-a)\left(\sum\frac{Z_i}{r_i} - \lambda\rho_0^{2/3}\right),$$

where a is an arbitrary constant.

3. ON THE PHYSICAL MEANING OF THE MINIMAL AND MAXIMAL VARIATIONAL PRINCIPLES

As is well known, Eq. (1) for H is an approximation for the quantum mechanical H given by

---

*If $f = \Sigma Z_i/r_i$, then $H_1 = -\infty$.

$$e^{-2}H=\frac{\hbar^2}{2me^2}\int\sum_k|\nabla_k\Psi|^2\prod_k dv_k$$
$$-\int\sum_k\sum_i\frac{Z_i}{r_{ik}}|\Psi|^2\prod_k dv_k \qquad (20)$$
$$+\frac{1}{2}\int\sum_{k\neq k'}\frac{|\Psi|^2}{r_{kk'}}\prod_k dv_k$$

(summation and multiplication are over k from 1 to ΣZ_i).

In Eq. (20) H is the mathematical expectation value of the system for arbitrary Ψ. The requirement that H be an extremum in Eq. (20) leads to one of the possible energy values of the system given by the Schrödinger equation. Only for the ground state (with minimum energy) and for electrons satisfying the Pauli exclusion principle, however, does Eq. (20) reduce approximately to Eq. (1) with $\rho=\rho_0$. If $\rho\neq\rho_0$, Eq. (1) can hardly be considered the energy of the system without additional assumptions, since a given ρ does not in general determine the Ψ function. Nevertheless, the variational principle for Eq. (1) is a consequence of the general variational principle for (20), since the relation between the kinetic energy and the density, as well as the relation between the last terms of Eqs. (1) and (20) is satisfied not only by the ground-state Ψ.

As for the maximization principle for H_1 defined by Eq. (11), the physical meaning of the f function depends on the way f is associated with the density ρ, and as has already been mentioned, this association is to some extent arbitrary. Thus although when $\rho\neq\rho_0$ we may somewhat conventionally call H as defined by Eq. (1) the energy of the system, when $f\neq f_0$ it is hardly possible to assign any physical meaning to H_1 as defined by Eq. (11).

Nevertheless, the existence of a maximization principle for H_1 and a minimization principle for H makes it possible to establish both a lower and upper bound for H_0. In order actually to calculate the exact value of $H=H_0=H_1$, it is necessary to solve either the nonlinear integral equation (2) or the nonlinear differential equation (6), which even for two nuclei presents great calculational difficulties even with the use of an electronic computer. The functional close to the extremum is not very sensitive to small variations in the function on which it depends. Making use of this fact we may vary ρ over a more or less well chosen class of functions, obtaining an approximate value for H_0 by requiring that H be a minimum for this class. However even this operation involves calculations which are too ponderous in view of the complexity of Eq. (1). Several authors[1] have calculated H for two centers with $\rho=\rho_{01}(r_1)+\rho_{02}(r_2)$ (Hund[1] has performed the same calculation with a more complicated function for the special cases of N_2 and F_2). In all of these cases the only accurate assertion possible is that "H_0 is less than the calculated value of H." How much less, one can only guess. We now have available another accurate assertion: "H_0 is greater than the calculated value of H_1." Thus if we set $H_0\approx(H+H_1)/2$, the error in H_0 is no greater than $\pm(H-H_1)/2$.

4. THE TWO-CENTER PROBLEM

Let us evaluate the possible error in calculating H_0 by using $\rho=\rho_{01}(r_1)+\rho_{02}(r_2)$ in H, where ρ_{01} and ρ_{02} are the solutions of Eq. (2) for each atom separately.

In view of Eq. (2) we have

$$\int\frac{\rho_{0i}(\mathbf{r}')\,dv'}{|\mathbf{r}-\mathbf{r}'|}=\frac{Z_i}{r_i}-\lambda\rho_{01}^{2/3}(r_i). \qquad (21)$$

Inserting (21) into Eq. (1) we obtain

$$H=\lambda\int\left[\frac{3}{5}(\rho_{01}+\rho_{02})^{2/3}-\frac{1}{2}(\rho_{01}^{2/3}+\rho_{02}^{2/3})\right](\rho_{01}+\rho_{02})\,dv$$
$$-\frac{1}{2}\int\left(\frac{Z_1}{r_1}+\frac{Z_2}{r_2}\right)(\rho_{01}+\rho_{02})\,dv. \qquad (22)$$

In order now to obtain an expression for H_1, let us set, analogously, $f=f_{01}(r_1)+f_{02}(r_2)$, where f_{01} and f_{02} are solutions of Eq. (13) for each atom separately.

Then in view of Eq. (17) we have

$$f_{0i}=Z_i/r_i-\lambda\rho_{0i}^{2/3};\qquad \frac{1}{4\pi}\nabla^2 f_{0i}=-\rho_{0i}. \qquad (23)$$

Inserting $f=f_{01}+f_{02}$ into (18) and making use of Eq. (23), we obtain

$$H_1=\lambda\int\left[\frac{1}{2}(\rho_{01}+\rho_{02})-\frac{2}{5}(\rho_{01}^{2/3}+\rho_{02}^{2/3})^{3/2}\right](\rho_{01}^{2/3}+\rho_{02}^{2/3})\,dv$$
$$-\frac{1}{2}\int\left(\frac{Z_1}{r_1}+\frac{Z_2}{r_2}\right)(\rho_{01}+\rho_{02})\,dv. \qquad (24)$$

In order to compare (22) and (24), it is convenient to introduce the quantity

$$\alpha=(\rho_{01}-\rho_{02})/(\rho_{01}+\rho_{02}),\quad -1<\alpha<1. \qquad (25)$$

Then

$$H = \int \xi(\alpha)\, \frac{1}{2}\left(\lambda\rho_{01}^{2/3} + \lambda\rho_{02}^{2/3}\right)(\rho_{01} + \rho_{02})\, dv - \frac{1}{2}\int \left(\frac{Z_1}{r_1} + \frac{Z_2}{r_2}\right)(\rho_{01} + \rho_{02})\, dv, \tag{26}$$

$$H_1 = \int \eta(\alpha)\, \frac{1}{2}\left(\lambda\rho_{01}^{2/3} + \lambda\rho_{02}^{2/3}\right)(\rho_{01} + \rho_{02})\, dv - \frac{1}{2}\int \left(\frac{Z_1}{r_1} + \frac{Z_2}{r_2}\right)(\rho_{01} + \rho_{02})\, dv, \tag{27}$$

where

$$\xi(\alpha) = 1.2\left[\left(\frac{1+\alpha}{2}\right)^{5/3} + \left(\frac{1-\alpha}{2}\right)^{5/3}\right]^{-1} - 1, \qquad \eta(\alpha) = 1 - 0.8\left[\left(\frac{1+\alpha}{2}\right)^{5/3} + \left(\frac{1-\alpha}{2}\right)^{5/3}\right]^{2/3}. \tag{28}$$

Some values of $\xi(\alpha)$ and $\eta(\alpha)$ are given in the following table: Clearly, ξ and η are even functions of α.

α	0	0.1	0.2	0.3	0.4	0.5	0.6	0.7	0.8	0.9	1
ξ	−0.048	−0.047	−0.044	−0.038	−0.028	−0.017	−0.002	+0.016	0.042	0.090	0.200
η	−0.132	−0.129	−0.124	−0.115	−0.101	−0.084	−0.061	−0.031	+0.008	+0.074	0.200
$\xi - \eta$	0.084	0.082	0.080	0.077	0.073	0.067	0.059	0.047	0.034	0.016	0.000

We now note that according to (21)

$$\varphi_{01} = \lambda\rho_{01}^{2/3} < Z_1 / r_1, \quad \varphi_{02} = \lambda\rho_{02}^{2/3} < Z_2 / r_2. \tag{29}$$

Therefore

$$\int \frac{1}{2}\left(\lambda\rho_{01}^{2/3} + \lambda\rho_{02}^{2/3}\right)(\rho_{01} + \rho_{02})\, dv < \frac{1}{2}\int \left(\frac{Z_1}{r_1} + \frac{Z_2}{r_2}\right)(\rho_{01} + \rho_{02})\, dv. \tag{30}$$

Since the absolute values of ξ and η are no greater than 0.2, the last integral in both Eqs. (26) and (27) is at least five times greater than the first integrals in these equations. Therefore the last integrals in (26) and (27) effectively determine the magnitudes of H and H_1, and therefore also of H_0. From Eq. (30) and the table for ξ and η,

$$H - H_1 < 0{,}084 \int \frac{1}{2}\left(\lambda\rho_{01}^{2/3} + \lambda\rho_{02}^{2/3}\right)(\rho_{01} + \rho_{02})\, dv$$

$$< 0{,}08 \int \left(\frac{Z_1}{r_1} + \frac{Z_2}{r_2}\right)(\rho_{01} + \rho_{02})\, dv,$$

since $\xi - \eta \leqslant 0.084$. Therefore H differs from H_0 by no more than +8% and the mean $(H + H_1)/2$ differs from H_0 by no more than 4%.

We have determined here the upper limit of the error, which is actually much smaller. In order to calculate it, H and H_1 must be calculated with the appropriate Z_1 and Z_2 and with the nuclear separation R. The value of $\xi - \eta$ is about 0.08 only if $\rho_{01} \approx \rho_{02}$, and is smaller in all other cases. Therefore $H - H_1$ becomes larger as Z_2 and Z_1 approach each other, and as R becomes smaller. In the limit $Z_2 = Z_1$ and $R = 0$, the calculation of H and H_1 is simply performed (since this case $\rho_{01} = \rho_{02}$) using the well known relations

$$\frac{3}{5}\lambda \int \rho_{0i}^{5/3}\, dv = -H_{0i} = C\,\frac{Z_i^{7/3}}{\lambda}; \qquad \int \frac{Z_i}{r_i}\rho_{0i}\, dv = \frac{7}{3}\,C\,\frac{Z_i^{7/3}}{\lambda}.$$

$$H = -0.048 \cdot 2\int \lambda\rho_{01}^{5/3}\, dv - 2\int \frac{Z_1}{r_1}\rho_{01}\, dv = -4.83\,C\,\frac{Z_1^{7/3}}{\lambda},$$

$$H_1 = -0.132 \cdot 2\int \lambda\rho_{01}^{5/3}\, dv - 2\int \frac{Z_1}{r_1}\rho_{01}\, dv = -5.11\,C\,\frac{Z_1^{7/3}}{\lambda}.$$

When $Z_2 = Z_1$ we must set $Z = 2Z_1$ in H_0, so that

$$H_0 = -2^{7/3} C Z_1^{7/3}/\lambda = -5.04 C Z_1^{7/3}/\lambda.$$

Thus

$$\frac{H - H_0}{H_0} = 4.17\,\%, \quad \frac{H_0 - H_1}{H_0} = 1.38\,\%,$$

$$\frac{{}^1/_2\,(H + H_1) - H_0}{H_0} = 1.38\,\%.$$

---

[1] P. Gombas, *Statistical Theory of the Atom and its Applications*, (Russian translation of *Statistische Theorie des Atoms und Ihre Anwendungen*, Springer-Verlag, Vienna, 1949). IIL, Moscow, 1951.

Translated by E. J. Saletan
288

SOVIET PHYSICS JETP VOLUME 5, NUMBER 6 DECEMBER 15, 1957

On the Exciton Mechanism for Capture of Current Carriers in Homopolar Semiconductors

V. L. BONCH-BRUEVICH
Moscow State University

(Submitted to JETP editor October 2, 1956)
J. Exptl. Theoret. Phys. (U.S.S.R.) 32, 1470-1478 (June, 1957)

Capture of charge carriers by structural defects, in which energy is transferred to small radius excitons, is investigated. The temperature dependence of recombination coefficients is determined.

1. INTRODUCTION

THE PROBLEM OF THE MECHANISM for capture of current carriers by impurity centers is still unsolved. This statement is particularly applicable to the mechanism for carrying off the energy which is liberated during the localization of a carrier which makes a transition from a band to an impurity level. Until recently it was implicitly assumed that this energy is given directly to the lattice, which undergoes a deformation during an electron transition of this type. Only recently it has been shown[1-4] that this possibility is by no means the only one, and that the so-called radiationless transitions can (at least, in their first stage) also proceed without participation by the lattice, but rather via a redistribution of the energy within the many-electron system itself. In Refs. 1 – 3 this redistribution was caused by the presence of another carrier, to which the liberated energy was transferred. Reference 4 pointed out that for a radiationless transition it is sufficient for the energy to be transferred to any neutral excitation of the many-electron system, and treated th[illegible]ocess of capture with excitation of plasma oscillations. In all these cases, the conversion of the excitation energy into heat (*i.e.*, conversion into phonons) occurs only in a later, much slower stage of the proces[illegible]

In the present paper we shall treat the [illegible]on" mechanism for capture, in which the liberated energy goes into the formation of "Frenkel excitons" (*i.e.*, excitons of small radius and, consequently, rather high dissociation energy). The inverse process – the ionization of impurity centers by exciton impact – was discussed earlier by Lashkarev[5] and Zhuze and Ryvkin,[6] and treated quantitatively by Toyozawa[7] (*cf.* also Ref. 18). However, there are various contradictory points in Ref. 7. In the first place, in the formulation of the problem given there, the interaction of the electrons with the exciton field is not at all small, whereas a weak coupling method is used in the calculation. In addition, even if we disregard this main objection, the specific computations in Ref. 7 are applicable only to traps which are sufficiently shallow to be described by the "hydrogen" model. All of these considerations have compelled us once again to consider the exciton mechanism for capture, using for this purpose the consistent many-electron theory of semiconductors developed earlier.[8] In accordance with many well known experimental results, we shall consider the capture of current carriers by deep traps. Calculation of the absolute value of the capture cross section turns out to be extremely difficult; however, its temperature dependence can be determined quite well, as we shall show later.

In order to emphasize the essentially "intra-electronic" character of this phenomenon, we shall treat the problem without including the interaction of excitons with the lattice. As is well known,[9–10] inclusion of the interaction with the lattice gives rise to important features of the exciton spectrum; however, the interaction of the electrons with one another still plays the major role in the process in which we are interested.

2. INITIAL EQUATIONS

As shown in Ref. 8, on the basis of the general theory of excitations in many-electron systems developed in Ref. 11, the wave functions of excited states of a homopolar semiconductor can be represented as*

$$\psi_m = L_m \psi_0, \tag{2.1}$$

$$L_m = \sum_{\alpha_1, \ldots, \alpha_m} \sum_{\beta_1 \ldots \beta_m} \varphi_m (\alpha_1, \ldots, \alpha_m, \beta_m, \ldots, \beta_1)\, a^*_{\alpha_1} \ldots a^*_{\alpha_m} a_{\beta_m} \ldots a_{\beta_1}, \tag{2.2}$$

where a^*_α, a_β are the Fermi operators for creation and annihilation of particles in states α and β; ψ_0 is the wave function of the ground state of the system, for which (by definition) the occupation numbers are $N(\beta) = 1$, $N(\alpha) = 0$. The index α denotes the set of quantities **g**, *a*, *s*, which give respectively the number of the elementary cell, the number of the atom in the cell, and the atomic quantum numbers,† and the spin quantum number. Similarly, $\beta = \{\mathbf{f}, b, t\}$, where **f**, *b*, *t* have the same significance as **g**, *a*, *s*, respectively. The function φ_m is the wave function of a system with *m* pairs of elementary excitations; for states of low excitation (for which *m* is small compared to the total number of atoms in the lattice) it can be written as a determinant of the functions φ_1 referring to the various energy values λ_1. The functions are given by the equations

$$\sum_{\alpha'} \Big\{ A(\alpha; \alpha') + 2 \sum_{\beta''} B(\alpha, \beta''; \beta'', \alpha') \Big\} \varphi_1(\alpha'; \beta) - \sum_{\beta'} \Big\{ A(\beta'; \beta) + 2 \sum_{\beta''} B(\beta', \beta''; \beta''; \beta) \Big\} \varphi_1(\alpha; \beta') - 2 \sum_{\alpha', \beta'} B(\alpha, \beta'; \beta, \alpha') \varphi_1(\alpha'; \beta') = \lambda_1 \varphi_1(\alpha; \beta). \tag{2.3}$$

A and *B* are the matrix elements of the additive and binary parts of the Hamiltonian, respectively, calculated with the system of orthogonalized "quasi-atomic" functions ψ_α, ψ_β; the quantity $B(\alpha_1, \alpha_2; \beta_2, \beta_1)$ is antisymmetric in the indices α_1 and α_2, β_2 and β_1. In Ref. 8 it was shown that Eq. (2.3) has solutions which describe excess electrons and holes which behave qualitatively like the "non-interacting electrons" of the standard band theory (hereinafter we shall for brevity simply talk of electrons). As shown in Ref. 11, this formulation of the problem is approximate, and valid only if the quantities $B(\alpha_1, \alpha_2; \alpha, \beta)$, $B(\alpha, \beta; \beta_1, \beta_2)$ are small compared with the other matrix elements of the Hamiltonian. Matrix elements of the type indicated connect states with different values of *m*, so that they give rise to creation and annihilation of elementary excitations and in particular to recombination of excess electrons and holes. If we treat quantities of the type of $B(\alpha, \beta; \beta_1, \beta_2)$ as small perturbations, it is easy to get the corresponding transition probabilities. In the first approximation only transitions with unit change of *m* are possible. In particular, the transition probability (per unit time) from $m = 1$ to $m = 2$ is

$$P(1 \to 2) = (2\pi / \hbar) \, |H_{21}|^2 \, \delta(\lambda_2 - \lambda_1), \tag{2.4}$$

where (remembering that the ground state energy of the system is taken to be zero),

$$H_{21} = 2 \sum_{\alpha_1, \alpha_2} \sum_{\beta_1, \beta_2} \bar{\varphi}_2 (\alpha_1, \alpha_2; \beta_2, \beta_1) \times \Big\{ \sum_\alpha [\varphi_1(\alpha; \beta_1) B(\alpha_1, \alpha_2; \beta_2, \alpha)] - \varphi_1(\alpha; \beta_2) B(\alpha_1, \alpha_2; \beta_1, \alpha)] + \sum_\beta [\varphi_1(\alpha_2; \beta) B(\beta, \alpha_1; \beta_2, \beta_1) - \varphi_1(\alpha_1; \beta) B(\beta, \alpha_2; \beta_2, \beta_1)] \Big\}. \tag{2.5}$$

For compactness, we have omitted the "quantum

---

[*] For the conditions of applicability of this representation of the wave functions of excited states, *cf.* Ref. 11.

[†] Unlike Ref. 8, in the present paper we take account of all the excited atomic states; *i.e.*, the system of basic functions which is used in making the transition to the second-quantized representation is complete.

numbers" characterizing the functions φ_1 and φ_2. The functions φ_1 and φ_2 must be normalized as follows:

$$\sum_{\alpha,\beta} |\varphi_1(\alpha;\beta)|^2 = 1, \tag{2.6}$$

$$4\sum_{\alpha_1,\alpha_2}\sum_{\beta_1,\beta_2} |\varphi_2(\alpha_1,\alpha_2;\beta_2,\beta_1)|^2 = 1. \tag{2.7}$$

We note that the calculation of the transition probability is of interest not only for the problem of recombination of current carriers, but also for estimating the degree of applicability of the method; it is clear that the method is applicable only if the lifetime of a current carrier is large compared to other characteristic times which describe the behavior of the electron system. Actually this is the case.

3. UNPERTURBED PROBLEM. EXCITONS OF SMALL RADIUS

We first consider the unperturbed problem (2.3). As shown in Ref. 8, Eq. (2.3) has two types of solution describing, respectively, a free electron and a hole, and an exciton. The solutions of the first type were investigated in general in Ref. 8. Neglecting the interaction between the free electron and hole, they have the form

$$\varphi_1(\alpha;\beta) = \varphi_n(\alpha)\varphi_p(\beta),\ \lambda_1 = \lambda_n + \lambda_p \tag{3.1}$$

(the indices *n* and *p* refer to electron and hole), where

$$\begin{aligned}\varphi_n(\alpha) &= \chi_n^{k,\mu}(a)\,S_\sigma(s)\,F_n^k(\mathbf{g}),\\ \varphi_p(\beta) &= \chi_p^{l,\nu}(b)\,S_\tau(t)\,F_p^l(\mathbf{f}).\end{aligned} \tag{3.2}$$

Here **k**, **l** are the quasi-momenta of electron and hole, σ and τ indices giving their spins, μ and ν various discrete quantum numbers (*e.g.*, the band number, *etc.*). The functions F_n and F_p are plane waves in the ideal lattice; in a non-ideal lattice they are wave functions in either the continuous or discrete spectrum for a quasi-particle moving in the field of the structural defect. (In this case the quasi-momenta **k** or **l** do not occur.) In the case of deep traps (located in the middle of a forbidden band) the functions of the discrete spectrum fall off very rapidly with distance from the trap. It is easy to see that the only important values of the quasi-momenta are those close to zero (if they are measured from the points corresponding to minima on the surfaces of constant energy). Actually, **k** and **l** enter into (3.2) and (2.5) either through the energies λ_n and λ_p, or in the combinations $ka/\hbar$, $la/\hbar$, where a is a characteristic length which determines the rate at which the "localized" function F falls off. Also essential here is the usual assumption that exchange integrals containing quasi-atomic functions referring to different centers fall off rapidly. Upon averaging over the equilibrium distribution we get quantities of order

$$a/L \ll 1,\ kT/J \ll 1, \tag{3.3}$$

where L is the "thermal" wavelength of the current carrier; J is the ionization energy of the deep trap (*i.e.*, the difference between the energy of the system when the carrier is at the bottom of the corresponding band and when it is in the trapping level). The inequalities (3.3) comprise the basic approximation used in the present paper. Wherever possible, the quantities which appear on the left in (3.3) will be set equal to zero.

We now turn to exciton-type solutions of (2.3). A complete investigation of these solutions is hardly meaningful at present, since we cannot say too much about the coefficients in (2.3) without making crude assumptions about models. However, for our purposes it is sufficient merely to establish the fact that excitons of small radius (of the order of the lattice constant) exist. To do this, we limit the class of functions $\varphi_1(\alpha;\beta)$ by the condition $\varphi_1(\alpha;\beta) \sim \Delta(\mathbf{g}-\mathbf{f})$ (Δ is the delta function). Then Eq. (2.3) describes the joint motion of the electron and the hole (*i.e.*, the motion of the exciton), and the dissociation energy of the exciton is greater (*i.e.*, the energy of the system is less) than on the hydrogen model. Since Eq. (2.3) was gotten from a variational principle, the true minimum of the energy, which would be obtained if we did not limit the class of functions φ_1 by the auxiliary condition given above, lies even lower, and the functions corresponding to it also decrease rapidly with increasing $|\mathbf{g}-\mathbf{f}|$ (because all "smooth" functions are described by the hydrogen model of the exciton). Thus (2.3) has exciton solutions of the form

$$\begin{aligned}\varphi_1(\alpha;\beta) = G^{-1/2}\exp\left\{-\frac{i}{\hbar}d\left(\mathbf{K},\frac{\mathbf{g}+\mathbf{f}}{2}\right)\right\}\\ \times\Phi_{K,\rho}(\mathbf{g}-\mathbf{f};a,b)\,S_{\sigma\tau}(s,t),\ \lambda_1 = \lambda_{\mathbf{exc}}(\mathbf{K},\rho,\sigma,\tau),\end{aligned} \tag{3.4}$$

where **K** is the quasi-momentum of the exciton, d the lattice constant, ρ the set of discrete quantum numbers, G the number of elementary cells in the fundamental volume of the crystal, and Φ a function which drops rapidly with increasing $|\mathbf{g} - \mathbf{f}|$.

The solutions (3.4) correspond to free excitons, not localized on a defect. It is known (*cf.* for example, Ref. 12) that local exciton levels in the vicinity of a structural defect can also occur. The latter are obviously described by functions of the form

$$\varphi_1(\alpha; \beta) = S_{\sigma\tau}(s, t)\, \Phi_\rho(\mathbf{g}, a; \mathbf{f}, b),\ \lambda = \lambda_{\mathbf{exc}}(\rho, \sigma, \tau), \tag{3.5}$$

where Φ drops rapidly with increasing $|\mathbf{g}|$ and $|\mathbf{f}|$. (We are considering a structural defect of atomic type, located at the origin of coordinates.)

It is extremely important that in such a formulation of the problem the states describing both the exciton and the free electron and hole are obtained from solutions of the same equation. It is also important to remark that excited states are taken into account in (2.3), so that we are considering all those effects which, in the phenomenological treatment of the problem, are described by means of the dielectric constant. Thus the excitons which we are discussing here are real excitons, observable in experiment, and not the virtual excitons which in Toyozawa's[7] treatment give rise to the dielectric constant of the crystal.* This is precisely the point of basic difference between the theory presented in the present paper and that of Ref. 7.

4. TRANSITION PROBABILITY

For the calculation of the transition probability it is convenient (though not necessary) to specialize the system somewhat. We shall consider a semiconductor containing structural defects of atomic type (impurity atoms, vacancies, *etc.*). We shall assume that in the ground state the corresponding local levels are filled. The structural defects may be either neutral or charged, depending on the nature of the sample and the particular defect, and also on the content and composition of other impurities. We shall treat the capture of free holes. Then the initial state is described by a wave function ψ_1, where $\varphi_1(\alpha; \beta)$ is a function of the type of (3.1) (describing a free electron and hole). The final state is ψ_2, where φ_2 corresponds to the presence of a free electron, a hole localized on the defect, and an exciton. In accordance with our remarks in Sec. 2, this means that φ_2 has the form (N is a normalization factor):

$$\varphi_2^{\lambda_2}(\alpha_1, \alpha_2; \beta_2, \beta_1) = \frac{1}{4\sqrt{N}}\{\varphi_1^{\lambda_1'}(\alpha_1; \beta_1)\, \varphi_1^{\lambda_1''}(\alpha_2; \beta_2)$$

$$- \varphi_1^{\lambda_1'}(\alpha_1; \beta_2)\, \varphi_1^{\lambda_1''}(\alpha_2; \beta_1) + \varphi_1^{\lambda_1''}(\alpha_1; \beta_1)\, \varphi_1^{\lambda_1'}(\alpha_2; \beta_2) - \varphi_1^{\lambda_1''}(\alpha_1; \beta_2)\, \varphi_1^{\lambda_1'}(\alpha_2; \beta_1)\}, \tag{4.1}$$

$$\lambda_2 = \lambda_1' + \lambda_1''; \quad \lambda_1' = \lambda_n + \lambda_p, \quad \lambda_1'' = \lambda_{\mathbf{exc}}, \tag{4.2}$$

while the functions φ_1 in (4.1) have the form of either (3.1), (3.2) (for λ_1'), or (3.4), (3.5) (for λ_1''). The free electron, which is present in both the initial and final states, is included because, by the very nature of the construction of the function (2.1), excitations occur only subject to conservation of the total charge of the system. This electron, however, does not participate in the process of capture of the hole (as long as we do not consider the process of collisional recombination which, by the way could also be investigated by the method given here). Therefore, only the last two terms in the matrix element (2.5) are important; in addition, in our case we can neglect exchange between electrons (but not between holes). Then, using the antisymmetry of B, we obtain

$$H_{21} = -2N^{-1/2} \sum_{\alpha_1, \alpha_2} \sum_{\beta_1, \beta_2} \bar{\varphi}_1^{\lambda_1'}(\alpha_1; \beta_1)\, \bar{\varphi}_1^{\lambda_1''}(\alpha_2; \beta_2) \times \varphi_1^{\lambda_1}(\alpha_1; \beta)\, B(\beta, \alpha_2; \beta_2, \beta_1), \tag{4.3}$$

(λ_1 is the energy of the system in the initial state). The matrix element $B(\beta, \alpha_2; \beta_2, \beta_1)$ has the form:[8]

$$B(\beta, \alpha_2; \beta_2, \beta_1) = \delta_{tt_2}\delta_{s_2t_1} G'_{ba_2;\, b_2b_1}(\mathbf{f}, \mathbf{g}_2;\ \mathbf{f}_2\mathbf{f}_1) - \delta_{tt_1}\delta_{s_2t_2} G''_{ba_2;\, b_2b_1}(\mathbf{f}, \mathbf{g}_2; \mathbf{f}_2, \mathbf{f}_1), \tag{4.4}$$

where G' and G'' are integrals containing the Coulomb potential and quasi-atomic functions.

Substituting (4.4) and the functions φ_1 in (4.3) and summing over α_1, we find, within the approximation given by (3.3),

---

*In crystals of the germanium type, the difference between the two kinds of excitons is by no means small, since the dielectric constant is 16!

$$H_{21} = -N^{-1/2} \sum_{b, b_1, b_2, a_2} \sum_{\mathbf{f}, \mathbf{g}_2} \bar{\chi}_p^{\nu_1}(b_1)\, \bar{\Phi}_{K,\rho}(a_2; b_2)\, \chi_p^{\nu}(b)$$
$$\times \exp\left[\frac{i}{\hbar} d(\mathbf{K}, \mathbf{g}_2)\right] F_p(\mathbf{f}) \{\delta_{\tau_1\sigma_2}\delta_{\tau_2\tau} G'_{ba_2;b_2b_1}(\mathbf{f}, \mathbf{g}_2; \mathbf{g}_2, 0)$$
$$- \delta_{\tau_1\tau}\delta_{\sigma_2\tau_2} G''_{ba_2;b_2b_1}(\mathbf{f}, \mathbf{g}_2; \mathbf{g}_2, 0)\} \qquad (4.5)$$

(where $F_p(\mathbf{f})$ is the hole wave function in the continuous spectrum for zero quasi-momentum).

No satisfactory explicit evaluation of the sum (4.5) is possible. However, this is not necessary for our purposes since, by virtue of the approximation (3.3) (*i.e.*, for deep traps), no quantities appear which depend on the quasi-momentum of the captured hole (and which would, when averaged over the equilibrium distribution of holes, lead to a dependence of the transition probability on temperature). What is of interest is the dependence of the transition probability on the quasi-momentum of the emitted exciton (*i.e.*, in the final analysis, on the depth of the trap). This dependence can be determined if $dK/\hbar \ll 1$, *i.e.*, if the depth of the trap is sufficiently close to the minimum energy of excitation of the exciton. Actually, it is easy to verify that G' is always an exchange integral, while G'' is either an exchange or a Coulomb integral, depending on the values of $\mathbf{f}$ and $\mathbf{g}_2$. In the first case, only small values of $\mathbf{g}_2$ are important, and consequently $\exp[id(\mathbf{K}, \mathbf{g}_2)/\hbar] \approx 1$. In the second case the corresponding sum can be approximately replaced by an integral which is easily evaluated, since the main contributions to it come from large distances r for which the Coulomb integral is $\sim 1/r$. Thus we get:

$$H_{21} \cong \delta_{\tau_1\sigma_2}\delta_{\tau_2\tau} a(\nu_1, \nu, \rho) -$$
$$- \delta_{\tau_1\tau}\delta_{\sigma_2\tau_2}\{(\hbar / dK)^2 b(\nu_1, \nu, \rho) + c(\nu_1, \nu, \rho)\}, \qquad (4.6)$$

where a, b, c are constants having the dimensions of an energy.

Formula (4.6) is valid for non-localized excitons. If localized excitons are emitted, then we must use the wave function (3.5) instead of (3.4). The corresponding quantity H_{21} can also be written in the form of (4.6) by setting $b = 0$.

We thus find for the transition probability

$$P(1 \to 2)$$
$$= (2\pi/\hbar)\,\delta(\lambda_{\mathbf{exc}} - J - \lambda_p)\{\delta_{\tau_1\sigma_2}\delta_{\tau_2\tau} |a(\nu_1, \nu, \rho)|^2$$
$$+ \delta_{\tau_1\tau}\delta_{\sigma_2\tau_2} |(\hbar / dK)^2 b(\nu_1, \nu, \rho) + c(\nu_1, \nu, \rho)|^2$$
$$+ \delta_{\sigma\tau}\delta_{\tau\tau_1}\delta_{\tau\tau_2}[a(\nu_1, \nu, \rho)((\hbar / dK)^2 \bar{b}(\nu_1, \nu, \rho) \qquad (4.7)$$
$$+ \bar{c}(\nu_1, \nu, \rho)) + \text{comp. conj.}]\}.$$

It is easily seen that the last two terms in the curly brackets refer only to emission of excitons with zero spin, while the first term corresponds to emission of excitons with arbitrary spin.

For the further development, it is convenient to make some sort of assumption concerning the shape of the spectrum of the free exciton. The simplest form is

$$\lambda_{\mathbf{exc}} = \lambda_0(\rho) + K^2 / 2M(\rho), \qquad (4.8)$$

where λ_0 and M are constants which in general depend on the spin of the exciton.

We must emphasize that the basis for this approximation is much poorer than that of all the preceding approximations; however we must remember that it affects only the dependence of the effective cross section on the depth of the trap but does not affect the temperature dependence of the recombination coefficient.

If we now sum over the quasi-momentum of the exciton (for the case of emission of non-localized excitons) and also over the spins and other quantum numbers of the quasi-particles in the final state, we get the effective capture cross section for holes, σ_p:

a) with emission of non-localized excitons of spin one (V_0 is the volume of the elementary cell, and v the velocity of the captured hole):

$$\sigma_p = (V_0^2 / \hbar^4 v) \sum_\rho M^{3/2} (J + \lambda_p - \lambda_0)^{1/2} A_\nu(\rho); \qquad (4.9)$$

b) with emission of non-localized excitons of spin zero,

$$\sigma_p \cong (V_0^2 / \hbar^4 v) \sum_\rho \frac{\hbar^4 B_\nu(\rho)}{d^4 M^{1/2} (J + \lambda_p - \lambda_0)^{3/2}}; \qquad (4.10)$$

c) with emission of localized excitons of arbitrary spin,

$$\sigma_p = (V_0/\hbar v) \sum_{\rho} C_\nu(\rho)\, \delta\,[\lambda_{\mathrm{exc}}(\rho) - J - \lambda_p]. \tag{4.11}$$

Here A, B, C are constants having dimensions of the square of an energy; the subscript ν indicates the "type" of hole.

5. RECOMBINATION COEFFICIENTS. CONCLUDING REMARKS

The quantities of experimental interest are not the capture cross sections themselves, but rather the recombination coefficients c_n and c_p, which are defined[12] as the average values of $\sigma_n v$ and $\sigma_p v$ over the equilibrium distribution of current carriers in the respective bands. On the basis of (4.9) – (4.11) we get:

a) with emission of non-localized excitons of spin one,

$$c_p = \frac{V_0^2}{2\hbar^4}\Big\{\sum_{\rho,\,\lambda_0(\rho)<J} M^{1/2}(J-\lambda_0)^{1/2} A_\nu/\rho + \sum_{\rho,\,\lambda_0(\rho)>J} M^{1/2}(\lambda_0 - J)^{1/2} A'_\nu(\rho) \exp\Big(-\frac{\lambda_0 - J}{kT}\Big)\Big\}; \tag{5.1}$$

b) with emission of non-localized excitons of spin zero,

$$c_p = \frac{V_0^2}{2d^4}\Big\{\sum_{\rho,\,\lambda_0(\rho)<J} \frac{B_\nu(\rho)}{M^{1/2}(J-\lambda_0)^{3/2}} + \sum_{\rho,\,\lambda_0(\rho)>J} \frac{B'_\nu(\rho)(\lambda_0 - J)^{1/2}}{M^{1/2}(kT)^2} \exp\Big(-\frac{\lambda_0 - J}{kT}\Big)\Big\}; \tag{5.2}$$

c) with emission of localized excitons,

$$c_p = \frac{V_0}{\hbar (kT)^{3/2}} \sum_{\rho,\,\lambda_{\mathrm{exc}}(\rho)\geqslant J} C_\nu(\rho)(\lambda_{\mathrm{exc}} - J)^{1/2} \exp\Big(-\frac{\lambda_{\mathrm{exc}} - J}{kT}\Big). \tag{5.3}$$

These same formulas (with different constants, of course) also hold for c_n.

We emphasize that actually only the first terms in the series (5.1) – (5.3) are important, since for the small radius excitons which we are considering the levels for internal motion are relatively widely separated from one another. We may therefore assume approximately that, for example for the emission of non-localized excitons,

$$c_p = \mathrm{const}, \quad \text{if} \quad \lambda_0 < J, \qquad c_p \sim \exp\Big(-\frac{\lambda_0 - J}{kT}\Big), \quad \text{if} \quad \lambda_0 > J, \tag{5.4}$$

where const denotes a quantity independent of temperature, while λ_0 is the minimum energy of a "real" exciton.

The apparent discrepancy for $J = \lambda_0$ has, of course, no real significance: actually for $J = \lambda_0$ small quantities of the type which we neglected before are left in the denominator. However, the theory actually does give a resonant increase in the capture cross section and the recombination coefficients when $J \approx \lambda_0$. This conclusion could be checked experimentally, if we could succeed in observing the exciton absorption of light in crystals of the type considered here (or if we studied processes of capture of excitons in molecular crystals). We should emphasize that from the mere existence of exciton states it does not necessarily follow that there is exciton absorption of light; also the probability of this process may turn out to be small.

The order of magnitude of the constants which appear in (5.1) – (5.3) depends essentially on the specific model for the capturing center, so that it is exceedingly difficult to evaluate. Nevertheless it can be shown that if there is no Coulomb repulsion between the current carrier and the structure defect, then even with the strictest assumptions the capture cross section turns out to be not less than 10^{-16} cm^2 (and actually this estimate is on the low side, possibly even by a large factor).

Of particular interest for comparison with experiment is the temperature dependence of the recombination coefficients. As we see from (5.1) – (5.3), for capture with emission of non-localized excitons, c_n and c_p are independent of temperature (to terms of order a^2/L^2 and kT/J), as soon as $\lambda_0 < J$. On the other hand, for $\lambda_0 > J$ and also for emission of localized excitons there is an exponential rise of the recombination coefficients upon heating. A dependence of this type has actually been observed in germanium alloyed with copper[14] and with nickel;[15] in the first case the observations are on capture of electrons, in the second they are for both electrons and holes. The latter case is especially interesting, since considerations associated with the presence of a Coulomb barrier can hardly apply here: the holes are captured by negatively charged traps.

We note that if capture with emission of localized excitons actually plays an important role, then the corresponding traps should serve not only as recombination centers but also as attachment levels (with a short time constant). In fact, as soon as the energy liberated during capture of the current carrier remains localized near the capturing center, there is a considerable probability for the inverse transition to occur with ejection of the localized carrier into the corresponding band. (This remark applies not only to the exciton mechanism for capture, but in general to all cases where the liberated energy is at least temporarily localized near the trap. This may, for example, also be the case for capture with transfer of the energy to local lattice oscillations which are generated in the neighborhood of the defect.[15])

If the local exciton levels lie below all the others, then the ratio of the probabilities for the various effects of the trap should depend markedly on temperature. In fact, if the exciton manages to go over from the localized to the free state (for example, by virtue of its interaction with the lattice), then the trap functions essentially as a recombination center; in the contrary case (where the average time for transition of the exciton into a non-localized form is large compared to the lifetime of the carrier in the trap), the trap plays the part of an attachment level.* Since under our conditions the probability of a transition of the exciton into the continuous spectrum is proportional to exp $\{-\Delta\lambda/kT\}$, where $\Delta\lambda$ (> 0) is the distance between the bottom of the exciton band and the local exciton level, it is clear that heating should result in stronger "recombinational" action of the capturing center. Careful treatment of the interaction of the exciton with the lattice is essential for a more detailed investigation of this question. However, we emphasize that our whole discussion applies only to attachment levels with a short time constant. The nature of the levels on which current carriers "sit" for a few seconds or even more[16,17] cannot of course be explained in this way.

We remark in conclusion that, as is now completely clear, radiationless electron transitions can be the result of a variety of different causes: the energy can be transferred directly to the lattice, to another current carrier, to plasma oscillations, or finally to excitons. The second and third of the processes listed are relatively easy to distinguish, since the corresponding recombination coefficients depend specifically on the concentration of current carriers. As for the first and fourth possibilities, they apparently can be distinguished only by the temperature dependence of their recombination coefficients. It therefore seems to us that the investigation of the concentration and temperature dependence of recombination coefficients is one of the most urgent problems for experiment.

---

* From this it also follows that there is, in general, no sharp dividing line between attachment levels and recombination centers; there can be a continuous transition from one type to the other.

---

[1] L. Pincherle, Proc. Phys. Soc. B68, 319 (1955).
[2] N. Sclar and E. Burstein, Phys. Rev. **98**, 1757 (1955).
[3] J. W. Ostrowski and L. Sosnowski, Bull. Pol. Acad. Sc. **2**, 385 (1954).
[4] V. L. Bonch-Bruevich, Izv. Akad. Nauk SSSR, Ser. Fiz. **21**, 87 (1957).
[5] V. E. Lashkarev, Memorial Volume for Academician S. I. Vavilov, U.S.S.R. Academy of Sciences Press, Moscow, 1952, p. 324.
[6] V. P. Zhuze and S. M. Ryvkin, Dokl. Akad. Nauk SSSR **77**, 241 (1953).
[7] Y. Toyozawa, Progr. Theor. Phys. **12**, 421 (1954).
[8] V. L. Bonch-Bruevich, Physics Reports of the Lvov State University 1 (6), 59 (1955).
[9] A. S. Davydov, *Theory of Light Absorption in Molecular Crystals*, Ukrainian Academy of Sciences Press, Kiev, 1951.
[10] E. I. Rashba, *Optics and Spectroscopy* **2**, 88 (1957).
[11] V. L. Bonch-Bruevich, J. Exptl. Theoret. Phys. (U.S.S.R.) **25**, 417 (1955).
[12] W. Shockley and W. T. Read, Phys. Rev. **87**, 835 (1952).
[13] R. M. Baum and J. F. Battey, Phys. Rev. **98**, 923 (1955).
[14] J. F. Battey and R. M. Baum, Phys. Rev. **100**, 1634 (1955).
[15] I. M. Lifshitz, J. Exptl. Theoret. Phys. (U.S.S.R.) **17**, 1076 (1947).
[16] J. A. Hornbeck and J. R. Haynes, Phys. Rev. **97**, 311 (1955).
[17] J. R. Haynes and J. A. Hornbeck, Phys. Rev. **100**, 606 (1955).
[18] A. G. Samoilovich and V. M. Kondratenko, J. Exptl. Theoret. Phys. (U.S.S.R.) **31**, 596 (1956); Soviet Phys. JETP **4**, 481 (1957).

Translated by M. Hamermesh

SOVIET PHYSICS JETP VOLUME 5, NUMBER 6 DECEMBER 15, 1957

On the Rarita–Schwinger Method in the Theory of Particles of Half-Integral Spin

E. E. FRADKIN
Leningrad State Pedagogical Institute

(Submitted to JETP editor October 10, 1956)
J. Exptl. Theoret. Phys. (U.S.S.R.) **32**, 1479-1482 (June, 1957)

The possibility of generalizing the Rarita–Schwinger method of setting up the Lagrangian for particles with large spins ($s > 3/2$) is examined. It is shown that the result obtained by Moldauer and Case is valid only for particles of spin 3/2.

IN A WORK ON THE THEORY of particles with high half-integral spin, Rarita and Schwinger[1] have shown in spinor-tensor form a method for constructing the Lagrangian without additional quantities, and have given the Lagrangian for spin-3/2 particles in explicit form.

In a recently published work, Moldauer and Case[2] give a Lagrangian which, according to these authors, gives the correct equations for particles with arbitrary half-integral spin $s = n + 1/2$, where $n = 1, 2, 3, \ldots$. On the basis of equations which follow from the variation of their Lagrangian including interactions with the electromagnetic field, conclusions are reached with regard to the magnetic moment of particles with spin $s = n + 1/2$ and the quadrupole moment of particles with spin 3/2 and 5/2.

We shall show in this note that the Lagrangian density given by Eq. (1.7) of Moldauer and Case,[2] as well as their field equations (1.9) and subsidiary conditions (1.10) which include interactions with the electromagnetic field are correct only for particles with spin 3/2 and may not be extended to particles with higher spins. Therefore their results for magnetic and quadrupole moments can be considered valid only for particles with spin* 3/2.

The Lagrangian function as given by Moldauer and Case is

$$L = \Psi^{+}_{\varkappa\nu_2\ldots\nu_n}\Big[(\gamma_\mu\partial_\mu + m)\,\delta_{\varkappa\lambda} + A(\gamma_\varkappa\partial_\lambda + \gamma_\lambda\partial_\varkappa) + \left(\frac{3}{2}A^2 + A + \frac{1}{2}\right)\gamma_\varkappa\gamma_\rho\partial_\rho\gamma_\lambda - (3A^2 + 3A + 1)\,m\gamma_\varkappa\gamma_\lambda\Big]\Psi_{\lambda\nu_2\ldots\nu_n}, \tag{1}$$

where

$$\partial_\mu = \partial/\partial x_\mu\ (\mu = 1, 2, 3, 4);\quad x_1 = x,$$

$$x_2 = y,\quad x_3 = z,\ x_4 = it;\quad \hbar = c = 1;$$

$\Psi_{\nu_1,\nu_2\ldots\nu_n}$ is an nth rank spin tensor symmetric with respect to all its indices ($\nu_i = 1, 2, 3, 4$);

$$\Psi^{+}_{\nu_1\nu_2\ldots,\nu_n} = (-1)^r\,\Psi^{*}_{\nu_1\nu_2\ldots\nu_n}\gamma_4,$$

where r is the number of times the index 4 occurs in $\nu_1, \nu_2, \ldots, \nu_n$; A is a real parameter which may take on arbitrary values other than $-1/2$.

For free particles, L as given by Eq. (1) should lead to the Dirac equation

$$(\gamma_\mu\partial_\mu + m)\,\Psi_{\nu_1\nu_2\ldots\nu_n} = 0 \tag{2}$$

with the subsidiary conditions

$$\gamma_\lambda\Psi_{\lambda\nu_2\ldots\nu_n} = 0,\quad \partial_\lambda\Psi_{\lambda\nu_2\ldots\nu_n} = 0. \tag{3}$$

We have previously[3] used such a Lagrangian to describe particles with spin 3/2. In the same article we have shown the relation between the equations obtained by variation of the Lagrangian of Eq. (1) with $n = 1$, and the other known forms of writing the equations for spin-3/2 particles, namely the Fierz-Pauli-Gupta equations,[4,5] the Petras equations,[6] and the Gel'fand-Iaglom equations;[7] in addition, we discuss the question of allowable linear transformations of the spin-3/2 equations. It is found that the arbitrariness in the coefficient A is related to the arbitrariness in normalizing the metric in the spin-1/2 subspace. The transformation

$$\Psi_\nu = \Psi'_\nu + k\gamma_\nu\gamma_\lambda\Psi'_\lambda, \tag{4}$$

where

$$k = (A' - A)/2(2A + 1)\qquad (k \neq -1/4), \tag{5}$$

---

*At the same time, of course, part of the Moldauer and Case[2] article which deals with constructing the equations for the independent components of free-particle wave functions with spin $n + 1/2$ in Hamiltonian form is undoubtedly correct, since it is based on the free-particle equations established in the work of Rarita and Schwinger.[1]

leads to the transition from one value of A to another* A'. In the special case $A = -1/3$ the Lagrangian density of Eq. (1) is that given by Rarita and Schwinger.[1]

In order to derive the equations for particles with spin greater than $3/2$, when $n \geqslant 2$, it is important to note that the symmetry of $\Psi_{\nu_1\nu_2\ldots\nu_n}$ with respect to all its tensor indices leads to the fact that the variations $\delta\Psi^+_{\nu_1\nu_2\ldots\nu_n}$ are not independent.

It is particularly important to account for the symmetry of $\Psi^+_{\varkappa\nu_2\ldots\nu_n}$ with respect to the index $\varkappa$ when performing the variation of L. When the variation of Eq. (1) is correctly performed, it leads to the following field equations for particles with spin $s = n + 1/2$:

$$\begin{aligned}
&(\gamma_\mu\partial_\mu + m)\Psi_{\nu_1\nu_2\ldots\nu_n} + \frac{1}{n}A(\gamma_{\nu_1}\partial_\lambda\Psi_{\lambda\nu_2\ldots\nu_n} + \gamma_{\nu_2}\partial_\lambda\Psi_{\nu_1\lambda\nu_3\ldots\nu_n} + \ldots\\
&\quad + \gamma_{\nu_n}\partial_\lambda\Psi_{\nu_1\nu_2\ldots\nu_{n-1}\lambda} + \gamma_\lambda\partial_{\nu_1}\Psi_{\lambda\nu_2\ldots\nu_n} + \gamma_\lambda\partial_{\nu_2}\Psi_{\nu_1\lambda\nu_3\ldots\nu_n} + \ldots\\
&\ldots + \gamma_\lambda\partial_{\nu_n}\Psi_{\nu_1\nu_2\ldots\nu_{n-1}\lambda}) + \frac{1}{n}B(\gamma_{\nu_1}\gamma_\rho\partial_\rho\gamma_\lambda\Psi_{\lambda\nu_2\ldots\nu_n} + \gamma_{\nu_2}\gamma_\rho\partial_\rho\gamma_\lambda\Psi_{\nu_1\lambda\nu_3\ldots\nu_n} + \ldots\\
&\ldots + \gamma_{\nu_n}\gamma_\rho\partial_\rho\gamma_\lambda\Psi_{\nu_1\nu_2\ldots\nu_{n-1}\lambda}) + \frac{1}{n}Cm(\gamma_{\nu_1}\gamma_\lambda\Psi_{\lambda\nu_2\ldots\nu_n} + \gamma_{\nu_2}\gamma_\lambda\Psi_{\nu_1\lambda\nu_3\ldots\nu_n} + \ldots\\
&\qquad\qquad \ldots + \gamma_{\nu_n}\gamma_\lambda\Psi_{\nu_1\nu_2\ldots\nu_{n-1}\lambda}) = 0,
\end{aligned} \tag{6}$$

where we have written

$$B = {}^3/_2 A^2 + A + {}^1/_2, \quad C = -(3A^2 + 3A + 1). \tag{7}$$

Let us first note that the form of (6) depends strongly on the value of n, so that it is impossible to obtain an equation of a single form for arbitrary n, as was done by Moldauer and Case. Secondly, for $n \geqslant 2$, *i.e.*, for free particles with spin $s \geqslant 5/2$, it is not only impossible to obtain the subsidiary conditions (3) with the coefficients given by Eq. (7), but in general, with any values of A, B, and C.

Detailed investigation shows that so many algebraic conditions must be fulfilled by A, B, and C that for values of n higher than 1 the number of equations is greater than the number of unknowns, and the equations become inconsistent. The mistake made by Moldauer and Case[2] is that they did not take account of symmetry in varying L.

Let us consider the question of the applicability of the Rarita–Schwinger method to particles with spin $5/2$. We may attempt to extend L as given by Eq. (1). The most general Lagrangian density with no additional quantities for particles with spin $5/2$, which leads to first-order equations is of the form

$$\begin{aligned}
L = \Psi^+_{\varkappa\nu}\{(\gamma_\mu\partial_\mu + m)\delta_{\varkappa\lambda} + 2a_1(\gamma_\varkappa\partial_\lambda + \gamma_\lambda\partial_\varkappa) + 2a_2\gamma_\varkappa\gamma_\rho\partial_\rho\gamma_\lambda + 2a_3 m\gamma_\varkappa\gamma_\lambda\}\Psi_{\lambda\nu}\\
+ 2a_4(\Psi^+_{\varkappa\varkappa}\partial_\lambda\gamma_\nu\Psi_{\lambda\nu} + \Psi^+_{\varkappa\nu}\partial_\varkappa\gamma_\nu\Psi_{\lambda\lambda}) + \Psi^+_{\varkappa\varkappa}(a_5\gamma_\rho\partial_\rho + a_6 m)\Psi_{\lambda\lambda}.
\end{aligned} \tag{8}$$

When

$$2a_1 = A, \quad 2a_2 = B, \quad 2a_3 = C, \quad a_4 = a_5 = a_6 = 0 \tag{9}$$

the function of Eq. (8) becomes the Lagrangian density of Eq. (1) for $n = 2$.

To obtain the subsidiary conditions (3) for free particles it becomes necessary, as a consequence of the field equations which follow from the Lagrangian density of Eq. (8), to operate with $\gamma_\varkappa$ and $\partial_\varkappa$ and sum over $\varkappa$ and then to operate with $\delta_{\nu\varkappa}$, $\partial_\nu\gamma_\varkappa$, and $\partial_\nu\partial_\varkappa$ and sum over $\varkappa$ and ν. We then obtain two sets of equations. The first two operations give two differential equations for $\gamma_\lambda\Psi_{\lambda\nu}$, $\partial_\lambda\Psi_{\lambda\nu}$, $\Psi_{\lambda\lambda}$, $\partial_\rho\partial_\lambda\Psi_{\lambda\rho}$ and $\partial_\rho\gamma_\lambda\Psi_{\lambda\rho}$. The three final operations lead to equations of the form

$$\begin{aligned}
&A_{33}\Psi_{\lambda\lambda} + A_{35}\partial_\rho\gamma_\lambda\Psi_{\lambda\rho} = 0,\\
&A_{43}\Psi_{\lambda\lambda} + A_{44}\partial_\rho\partial_\lambda\Psi_{\lambda\rho} + A_{45}\partial_\rho\gamma_\lambda\Psi_{\lambda\rho} = 0,\\
&A_{53}\Psi_{\lambda\lambda} + A_{54}\partial_\rho\partial_\lambda\Psi_{\lambda\rho} + A_{55}\partial_\rho\gamma_\lambda\Psi_{\lambda\rho} = 0,
\end{aligned} \tag{10}$$

where the A_{ik} (with $i, k = 1, 2, 3, 4, 5$) are certain expressions containing differential operators and depending on the coefficients $a_1 - a_6$ as parameters.

---

*This makes the results for the quadrupole moment of spin-$3/2$ particles as obtained by Moldauer and Case seem even stranger, as it depends on the unspecified parameter A, and thus on the choice of the representation.

The condition that under which the system (10) has the only required vanishing solution is that the operator determinant of the set of equations become a nonzero constant. This requirement leads to three algebraic equations for the coefficients $a_1 - a_6$ and to the condition ($m \neq 0$)

$$(1+6a_3)(1+2a_3+4a_6) \neq 0. \qquad (11)$$

Inserting

$$\Psi_{\lambda\lambda} = 0, \quad \partial_\rho \gamma_\lambda \Psi_{\lambda\rho} = 0, \quad \partial_\rho \partial_\lambda \Psi_{\lambda\rho} = 0,$$

into the equations obtained with the aid of the first two operations, we obtain

$$\begin{aligned} A_{11}\gamma_\lambda \Psi_{\lambda\nu} + A_{12}\partial_\lambda \Psi_{\lambda\nu} &= 0, \\ A_{21}\gamma_\lambda \Psi_{\lambda\nu} + A_{22}\partial_\lambda \Psi_{\lambda\nu} &= 0. \end{aligned} \qquad (12)$$

From the condition that the system (12) has only a vanishing solution, we obtain two other algebraic equations for the coefficients a_1, a_2, and a_3. Solving the five equations obtained, we obtain the coefficients a_2, a_3, a_4, a_5, and a_6 as functions of the arbitrary parameter a_1:

$$\begin{aligned} a_2 &= {}^1/_4\,(5a_1^2 + 2a_1 + 1); \\ a_3 &= -{}^1/_8\,(15a_1^2 + 10a_1 + 3); \\ a_4 &= -{}^1/_8\,(5a_1^2 + 6a_1 + 1); \\ a_5 = a_6 &= {}^1/_{16}\,(15a_1^2 + 10a_1 - 1). \end{aligned} \qquad (13)$$

Condition (11), however, is not fulfilled for any value of a_1. The determinant of (10) vanishes identically and therefore there exists no set of values for the coefficients $a_1, \ldots, a_6$ for which both sets (10) and (12) have simultaneously only vanishing solutions, *i.e.*, the subsidiary conditions (3) cannot follow from the L function of Eq. (8).*

We can thus conclude that the Rarita–Schwinger method does not give positive results for spin-$^5\!/_2$ particles. One may suppose that this is related to the fact that in analogy with the spin-$^3\!/_2$ case, the Lagrangian function for spin-$^5\!/_2$ particles should have two arbitrary parameter related to the choice of normalization in the subsidiary subspaces with spin ½ and spin $^3\!/_2$. It was just this number of arbitrary coefficients which appeared in the Lagrangian function for spin-$^5\!/_2$ particles as constructed previously by the author[8] using a method involving subsidiary quantities of lower rank.

In conclusion, the author expresses his deep gratitude to S. V. Izmailov for valuable discussion.

---

[1] W. Rarita and J. Schwinger, Phys. Rev. **60**, 61 (1941).

[2] P. A. Moldauer and K. M. Case, Phys. Rev. **102**, 279 (1956).

[3] E. E. Fradkin and S. V. Izmailov, Uch. Zap. (Scient. Notes), Leningrad, A. I. Gertsen State Pedag. Inst. **141**, 88 (1956) (in press).

[4] M. Fierz and W. Pauli, Proc. Roy. Soc. **A173**, 211 (1939).

[5] S. N. Gupta, Phys. Rev. **95**, 1334 (1954).

[6] M. Petras, Czech, Phys. Jl. **5**, 160 (1955).

[7] I. M. Gel'fand and A. M. Iaglom, J. Exptl. Theoret. Phys. (U.S.S.R.) **18**, 703 (1948).

[8] E. E. Fradkin, J. Exptl. Theoret. Phys. (U.S.S.R.) **20**, 27 (1950).

Translated by E. J. Saletan
290

*If we turn to L of Eq. (1) ($n = 2$), then setting $a_4 = a_5 = a_6 = 0$ in agreement with Eq. (9) we obtain two incompatible equations for $a_1 = A/2$.

SOVIET PHYSICS JETP VOLUME 5, NUMBER 6 DECEMBER 15, 1957

On The Statistical Interpretation of Quantum Theory

R. L. STRATONOVICH
Moscow State University

(Submitted to JETP editor October 12, 1956)
J. Exptl. Theoret. Phys. (U.S.S.R.) 32, 1483-1495 (June, 1957)

We consider various principles of operator arrangements as basis for a statistical interpretation. An extremely concise expression for the distribution of trajectories in functional space is obtained, using the action functional, for the case of the ground state. The bichronological arrangement in time is a Markov process, and a continuous distribution density is found for it.

THERE ARE THREE STAGES in the probability interpretation of quantum theory. The first stage is the usual interpretation of the absolute square of the wave function as a probability density. The second stage is the search for a joint distribution for physical quantities, corresponding to non-commuting operators, at a given time.[1,2] If we want to consider the evolution in time, it is not sufficient to limit ourselves to a calculation of the change with time of these distributions. Moreover, it is of some general interest to study joint multiple distributions which correspond to different times and which take into account the correlation between states at different times. The consideration of such distributions forms the third stage of the problem mentioned at the beginning, and we shall consider it here from first principles. Thus the subject of the investigation of the present paper will be closely related to a paper by Feynman,[3] but in contradistinction to the latter our work is based upon the idea that the shape of the distribution should follow simply from an accepted "principle of arranging" operators. This fact plays a systematic role, and makes it in particular possible to show a relation between the papers of Feynman[3] and Moyal[1] and also to indicate another possible space-time interpretation.

1. PRINCIPLES OF OPERATOR ARRANGEMENTS AND THEIR ROLE IN A STATISTICAL INTERPRETATION

One can easily determine the probability density distribution $w(a)$ of a physical quantity a corresponding to an operator A, if one uses the quantum rule for averaging. For a given state described by a wave function Ψ (or, more generally, by any matrix density) we have

$$w(a) = \langle\delta(A-a)\rangle \equiv (\Psi, \delta(A-a)\Psi). \qquad (1)$$

This definition is connected with the considerations that the usual statistical method of averaging $\int F(a)\,w(a)\,da$ should agree with the quantum average $\langle F(A)\rangle$.

The evaluation of expression (1) can, of course, be reduced to calculating the averages of the exponential function or of powers,

$$\begin{aligned} w(a) &= \frac{1}{2\pi}\int e^{-iaI}\langle e^{iAI}\rangle\, dI \\ &= \frac{1}{2\pi}\int e^{-iaI}\sum\frac{(iI)^n}{n!}\langle A^n\rangle\, dI. \end{aligned} \qquad (2)$$

The integral of the exponent can be interpreted as the integral showing how to treat the characteristic function $\langle(\exp(iAI))\rangle$.

One can prove that expression (1) is non-negative, but this is not important for our discussion. The fact is that for a comprehensive statistical interpretation of quantum theory (that is, for a consideration of joint distributions of quantities corresponding to non-commuting operators) one must apparently inevitably allow the possibility of local negative values of the distribution density, without this, however, leading to negative probabilities for integral operations which are connected to physical measurements. This should still be a small price to pay for the possibility to use for typical quantum phenomena the classical presentation and the usual probability theory. Unfortunately, the situation is to a large degree still complicated because of the involved nature of the distributions; we shall return to this below.

The generalization of Eq. (1) for the case of non-commuting operators A_1, A_2, ... has the form

$$w(a_1, a_2, \ldots) = \langle\delta(A_1-a_1)\,\delta(A_2-a_2)\ldots\rangle, \qquad (3)$$

but now the question arises in what order the operators under the average sign will act. The determination of this order in Eq. (3) is equivalent to the determination of the order of operation of the operators in the characteristic function $\langle \exp i (A_1 l_1 + A_2 l_2 + \ldots) \rangle$ or in the compound moments $\langle A_{n_1} A_{n_2} \ldots \rangle$.

We denote by Pr any principle of operator arrangement. To be precise, let Pr fix the coefficients $c(i, \ldots, l)$ in the expansion

$$\mathrm{Pr}\, A_{n_1} \ldots A_{n_s} = \sum c(i, \ldots, l)\, A_{n_i} \ldots A_{n_l} \; (s = 2, 3 \ldots) \tag{4}$$

for all possible permutations of the operators A ($i, \ldots, l$ is a permutation of the numbers $1, \ldots, s$). These coefficients must satisfy the conditions

$$\sum c(i, \ldots, l) = 1; \quad c(i, \ldots, l) \geqslant 0. \tag{4a}$$

The operators under the Pr-sign can be rearranged. The action on a function of operators is defined by the action on each term of its Taylor expansion.

If we choose any one ordering principle Pr, we can use it to determine the characteristic function of a multiple distribution

$$\Theta(l_1, l_2, \ldots) = \langle \mathrm{Pr} \exp i (A_1 l_1 + A_2 l_2 + \ldots) \rangle, \tag{5}$$

the distribution density $\langle \mathrm{Pr}\, \delta(A_1 - a_1)\, \delta(A_2 - a_2) \ldots \rangle$, correlation functions *etc.*, *i.e.*, on the basis of this principle we can construct a complete statistical picture.

The difficulty connected with the large number of possible choices for Pr is mitigated by the fact that in actual cases one can show that there are only a small number of specific rules for arranging operators which should especially be preferred (because of symmetry, relativistic invariance, or other reasons). One cannot, however, attain a sufficiently simple principle, and one must take into account several "preferable" statistical pictures and their interconnection. We shall consider below separately the various cases of distribution principles and the distribution laws connected with them.

The simplest ordering principle occurs if in all products $A_{n_1} A_{n_2} \ldots$ one of the operators acts always either before or after another, and on the right hand side of Eq. (4) there is only one term. One can then assign to the operators Feynman's index s (which is such that a smaller value of s corresponds to earlier action).[4] In particular, if we identify s with the time t, we shall have the chronological arrangement Pr = P. The chronological arrangement leads to a simple result in the Heisenberg representation, when all the operators taken at one particular time commute (the non-commutability of the coordinates and the momenta is not taken into account as one can express the momenta as derivatives with respect to the coordinates).

It is convenient to denote the reverse way of arranging the operators ($s = -t$) by Pr = P*. An advantage of the chronological and antichronological arrangements is their simplicity and relativistic invariance; the disadvantage is that real functions of Hermitian operators will, generally speaking, correspond to non-Hermitian operators. Also the probability density corresponding to them is complex.[5]

One can avoid this defect by going over to the arrangement principle

$$\mathrm{Pr}^{(1)} = {}^1/_2 (\mathrm{P} + \mathrm{P}^*). \tag{6}$$

Another corrected mode of expansion, which is also based upon the P and P* arrangements, can most conveniently be formulated by its application to the exponential function

$$\mathrm{Pr}^{(2)} \exp \sum A_i u_i = \mathrm{P}^* \left[\exp \frac{1}{2} \sum A_i u_i\right] \mathrm{P} \left[\exp \frac{1}{2} \sum A_i u_i\right]. \tag{7}$$

A natural generalization of this arrangement principle is given by the equation

$$\mathrm{Pr}^{(2n)} \exp \sum A_i u_i = \left\{\mathrm{P}^* \left[\exp \frac{1}{2n} \sum A_i u_i\right] \mathrm{P} \left[\exp \frac{1}{2n} \sum A_i u_i\right]\right\}^n. \tag{8}$$

In the limit $n \to \infty$ we get the completely symmetrical ordering

$$\mathrm{Pr}^{(s)} \exp \sum A_i u_l = \exp \sum A_i u_l. \tag{9}$$

From Eqs. (7) to (9) one can determine the operation of Pr on other functions, for instance by differentiating with respect to $u_{n_1}, u_{n_2}, \ldots$, and subsequently putting these arguments equal to zero we can find $\mathrm{Pr}\, A_{n_1} A_{n_2} \ldots$.

Below we shall consider the distributions and characteristic functionals, which we shall mark by an index in brackets, corresponding to the above forms of arranging operators.

The symmetrical arrangement (9) is convenient for considering linear transformations of operators. It was used in Ref. 1 for a statistical interpretation of quantum states at a fixed time. By applying it to the coordinate and momentum operators one obtained in that paper the Wigner distribution, which could, however, equally easily have been obtained from the $\mathrm{Pr}^{(2)}$ arrangement.

Among the ordering principles (7) to (9) introduced by us the bichronological principle $\mathrm{Pr}^{(2)}$, which we shall denote by R, plays a special role as it is bilinear in P, just as the quantum average value is bilinear in the wave function. For a state described by the vector ψ, the characteristic functional $\left\langle \mathrm{R} \exp \int A(t)\, u(t)\, dt \right\rangle$ is the absolute square of the vector $\mathrm{P}[\exp \int A u\, dt/2]\,\psi$. As a counterpart to R we have the principle R′ corresponding to a characteristic functional $\Theta^{(\mathrm{R}')}$ which is the square of the vector $\mathrm{P}^*[\exp \int A u\, dt/2]\,\psi$. In the majority of cases $\Theta^{(\mathrm{R}')}$ and $\Theta^{(\mathrm{R})}$ are connected according to the equation $\Theta^{(\mathrm{R}')}[u(t)] = \Theta^{(\mathrm{R})}[u(-t)]$; this equation is satisfied as long as for at least one time t and one representation the matrix elements of the operators $A(t)$, of the energy and of the state operator ρ are real.

2. THE CASE OF LINEAR EQUATIONS OF MOTION

Let us consider a different type of distribution corresponding to the above mentioned ordering principles, for instance, the case of quantum systems subject to linear equations of motion, *i.e.*, systems for which the Lagrangian depends linearly and quadratically on the dynamical variables q [in the case of many discrete degrees of freedom $q = q_1, q_2, \ldots$; in the case of fields $q = \varphi(x)$].

In field theory this case corresponds to free fields, which we assume to be boson-fields. Under those circumstances the commutators of the dynamical variables are c-numbers which simplifies matters considerably. The fact is that if repeated commutators of A and B vanish the following formulas hold,

$$e^A e^B = e^B e^{A+[A,\,B]}; \quad e^{A+B} = e^B e^{A+[A,\,B]/2} \tag{10}$$

By applying these formulas several times we are able to find the following correlation between the characteristic functionals $\langle \mathrm{Pr} \exp \int q u\, dt \rangle$ for the trajectory $q(t)$ corresponding to the principles P, R, $\mathrm{Pr}^{(s)}$,

$$\Theta^{(R)}[u(t)] = \Theta^{(s)}[u(t)]$$
$$= \Theta^{(P)}[u(t)] \exp \frac{1}{2} \iint\limits_{t' > t} [q(t), q(t')]\, dt\, dt' \tag{11}$$

Thus for the case of linear equations of motion the symmetrical arrangement gives the same result as the bichronological one. Furthermore, in those cases $q(t)$ is expressed in terms of the initial operators $q(t_0)$, $q'(t_0)$ by means of the same linear transformations as in the classical case. If we substitute this expression into the exponent $\langle \exp \int q u\, dt \rangle \equiv \Theta^{(s)}[u]$, we see that $\Theta^{(s)}[u]$ can be expressed in terms of the symmetrical initial characteristic function by classical means. Expressed differently, if we start from a Wigner distribution, the time evolution taking into account all multiple distribution laws will not differ from the classical one. As far as the momentaneous distribution in phase space is concerned, this fact was noted in Ref. 1.

Let us consider the correlation function

$$k_{qq}(t, t') = \langle \mathrm{Pr}\, q(t)\, q(t') \rangle - \langle q(t) \rangle \langle q(t') \rangle.$$

Symmetrizing the integral in the exponent (11) we find

$$k_{qq}^{(P)}(t, t') = k_{qq}^{(s)}(t, t')$$
$$+ \frac{1}{2} \operatorname{sgn}(t' - t)\, [q(t'), q(t)]. \tag{12}$$

Other correlation functions $k_{(n)\,q}$ $(n = 3, 4, \ldots)$ (higher semi-invariants) are the same for P and $\mathrm{Pr}^{(s)}$.

The results obtained here can directly be generalized to the case of free quantum fields corresponding, for instance, to a Lagrangian $2L = \varphi^{\lambda} \varphi_{\lambda} - m^2 \varphi^2$. Also we must substitute $\varphi(x)$ for $q(t)$ in (11) and (12) and take into account that

$$\varepsilon(x', x)\, [\varphi(x'), \varphi(x)] = 2i\hbar \bar{\Delta}(x', x) \quad (c = 1).$$

Some initial distributions will give a relativistically invariant correlation function

$$k_{\varphi\varphi}^{(s)}(x, x') = k\Delta^{(1)}(x, x'); \qquad k_{\varphi\varphi}^{(P)} = k\Delta^{(1)} + i\hbar\bar{\Delta}, \tag{13}$$

where $\Delta^{(1)}$ and $\bar{\Delta}$ are the well-known singular functions. If these initial distributions are also normalized we have

$$\Theta^{(s)}[u(x)] = \exp \frac{k}{2} \iint \Delta^{(1)}(x, x')\, u(x)\, u(x')\, dx\, dx'. \tag{14}$$

The ground state corresponds to $k = \hbar/2$ and

$$\hbar^{-1} k_{\varphi\varphi}^{(P)} = \frac{1}{2} \Delta^{(1)} + i\bar{\Delta} = \Delta^F.$$

Having taken the integral inversion one can calculate the distribution densities $w^{(s)}$ and $w^{(P)}$ of various multiplicities, including continuous ones.

The distribution in functional space for the case of the chronological arrangement is closely connected to Feynman's Lagrangian form. We give as an example the probability functional $w^{(P)}[q(t)]$ for a finite time interval $0 \leqslant t \leqslant T$ in the case of a harmonic oscillator having a normalized distribution and a correlation function

$$k_{qq}^{(P)}(t, t') = k\cos\omega(t-t') - \frac{i\hbar}{2m\omega}\sin\omega|t-t'|. \tag{15}$$

The dispersion k of the coordinate fluctuations is connected with Θ (which is the absolute temperature multiplied by Boltzmann's constant) through the relation $2km\omega = \hbar/\tanh(\hbar\omega/2\Theta)$. Defining

$$\begin{aligned} a &= m\omega/\tanh(\omega T + i\hbar\omega/\Theta); \\ b &= m\omega/\sinh(\omega T + i\hbar\omega/\Theta) \end{aligned} \tag{16}$$

the result of the calculations is in the form

$$\begin{aligned} & w_{0T}^{(P)}[q(t)] \\ & = N^{-1}\exp\frac{i}{\hbar}\left\{\sum_{j=0}^{n-1}\frac{n.\varepsilon}{2}\left[\left(\frac{q(t_{j+1})-q(t_j)}{\varepsilon}\right)^2\right.\right. \\ & \left.\left. -\omega^2 q^2(t_j)\right] - \frac{a}{2}[q^2(0)+q^2(T)] + bq(0)q(T)\right\}. \end{aligned} \tag{17}$$

The sum in the exponent in (17) is the action integral $\int_0^{T-\varepsilon} L[q(t+\varepsilon), q(t)]\,dt$. Equation (17) is the Lagrangian form of the thermodynamic Gibbsian quantum ensemble cooresponding to a temperature Θ.

3. THE CHRONOLOGICAL ARRANGEMENT IN THE CASE OF ARBITRARY EQUATIONS OF MOTION

When the equations of motion are nonlinear, the commutator $[q(t), q(t')]$ will be a c-number only in first order in $t-t'$ (the operator supplement is proportional to $(t-t')^2$). In the nonlinear case, therefore, the results of the previous section are correct for small time intervals to the first order in their duration. This is sufficient to conclude that the Wigner distribution for $q(t)$, $\dot{q}(t)$ follows equally easily from the R as from the $\mathrm{Pr}^{(s)}$ arrangement. However, to determine the distributions involving considerable time intervals we must put our considerations upon a new basis. To begin with we restrict ourselves to the chronological arrangement.

1. We try to determine the density $w^{(P)}(q(t_1), \ldots, q(t_n))$ of the joint distribution of the coordinates at the times $t_1, \ldots, t_n$. If to be definite we put $t_n \geqslant \ldots \geqslant t_1$ we have

$$\begin{aligned} & w^{(P)}(q_1, \ldots q_n) \\ & = (\Psi^*\delta(q(t_n)-q_n)\ldots\delta(q(t_1)-q_1)\Psi), \end{aligned} \tag{18}$$

where Ψ is the state vector in the Heisenberg representation. We choose as a basis the eigenvectors of the operators $q(t)$. If we go over to a new representation we write Eq. (18) in the form

$$\begin{aligned} w^{(P)}(q_1, \ldots, q_n) = \int\cdots\int \Psi^*(q_n', t_n)\,\delta(q_n'-q_n)U(q_n', t_n; q_{n-1}', t_{n-1})\ldots\delta(q_1'-q_1)\,\Psi(q_1', t_1) \\ \times dq_1'\ldots dq_n'. \end{aligned} \tag{19}$$

where $q_k' = q'(t_k)$, $\Psi(q'(t), t) = (q'(t)|\,)$ is the state vector in the $q(t)$-representation, and $U(q''(t_1), t_1; q'(t), t) = (q''(t_1)|q'(t))$ is the unitary operator $U(t_1, t)$ of the transition from one time to another. After integrating we have

$$\begin{aligned} & w^{(P)}(q_1, \ldots, q_n) \\ & = \Psi^*(q_n, t_n)\,U(q_n, t_n; q_{n-1}, t_{n-1})\ldots \\ & \ldots U(q_2, t_2; q_1, t_1)\,\Psi(q_1, t_1). \end{aligned} \tag{20}$$

Dividing the segment $(0, T)$ into increasingly smaller sections by the points $t_k = \varepsilon k$ $(\varepsilon = T/n)$ we can make the transition to a distribution in functional space. As shown by Feynman,[3] we have

$$\begin{aligned} & U(q\;(t'), t'; q(t), t) = \mathrm{const}\int\ldots \\ & \int\exp\left\{\frac{i}{\hbar}\int_t^{t'-\varepsilon} L[q(t+\varepsilon), q(t)]\,dt\right\}dt\prod_{t+\varepsilon}^{t'-\varepsilon} dq(t), \end{aligned} \tag{21}$$

where $t' > t$, and where $L[q(t+\varepsilon), q(t)]$ is the Lagrangian in which we have replaced $\dot{q}(t)$ by $[q(t+\varepsilon) - q(t)]/\varepsilon$. By virtue of (20) and (21) the functional probability for a trajectory $q(t)$ in the interval $(0, T)$ will have the form

$$w_{0T}^{(P)}[q(t)] = N^{-1}\Psi^{*}(q(T),T)\exp\left\{\frac{i}{\hbar}\int_{0}^{T-\varepsilon} L[q(t+\varepsilon), q(t)]dt\right\}\Psi(q(0), 0). \tag{22}$$

The normalizing factor N has a direct meaning only for the final subdivision.

2. The operator (21) can, as is well-known, be written in the form

$$U(q', t'; q, t) = \sum_{n}\psi_n(q')\exp\left\{-\frac{i}{\hbar}(t'-t)E_n\right\}\psi_n^{*}(q). \tag{23}$$

where ψ_n is the eigenfunction of the energy operator H corresponding to an eigenvalue E_n. We now take in (21) and (23) the limit $t' - t \to \infty$; strictly speaking, the operator U is not defined in that limit. To be able to go to the limit we replace H by $(1-i\mu)H$ where $i\mu$ is small and imaginary. This change corresponds to replacing the Lagrangian $L = T - U$ by

$$L_{\mu} = (1-i\mu)^{-1}T - (1-i\mu)U \approx L + i\mu H, \tag{24}$$

which expresses the assumption of weak dissipative effects. After this substitution E_n goes over into $(1-i\mu)E_n$ and we have

$$U_{\mu}(t'-t) \to \psi_0 \exp\left\{-\frac{i}{\hbar}(t'-t)E_0\right\}\psi_0^{*} \quad \text{for} \quad t'-t \to \infty. \tag{25}$$

In agreement with equations (21) and (25) we can write for the wave function of the ground state

$$\psi_0(q(t)) = N^{-1/2}\int\ldots\int\exp\left\{\frac{i}{\hbar}\int_{-\infty}^{t-\varepsilon} L[q(t+\varepsilon), q(t')]\,dt'\right\}\prod_{-\infty}^{t-\varepsilon} dq(t). \tag{26}$$

where the lower limit $T_1 = -\infty$ must be understood in the following sense: first of all we replace L by L_{μ} while T_1 is still finite; after that we let T_1 go to $-\infty$ simultaneously changing the coefficient $N^{-1/2}$ which depends on T_1 and $q(T_1)$; finally we let $\mu \to 0$. In Ref. 6 a different formula was used,

$$\psi_0 = \text{const}\lim_{T\to\infty}\int\cdots\int\exp\left\{\frac{S_T}{\hbar}\right\}\Pi\, dq(t)\left(S_T = \int_{-T}^{t} L\,dt'\right). \tag{27}$$

If the factor is properly chosen the function ψ_0 will be the action function as can be seen, for instance, from Eq. (27). If we take this into account and substitute (26) into (22) we are led to the conclusion that in the case of the ground state the distribution $w_{0T}^{(P)}[q]$ for the trajectory $q(t)$ in the interval $[0, T]$ is equal to the integral of $\exp\frac{i}{\hbar}\int_{-\infty}^{\infty} L\,dt$ over the trajectories outside that interval. Hence it follows naturally that in the case of the ground state the "complete" distribution density for trajectories along the infinite line $-\infty < t < \infty$ is equal to

$$w^{(P)}[q(t)] = N^{-1}\exp\left\{\frac{i}{\hbar}\int_{-\infty}^{\infty} L[q(t)]\,dt\right\}, \quad \left(N = \int\ldots\int\exp\left\{\frac{i}{\hbar}\int_{-\infty}^{\infty} L\,dt\right\}\prod_{-\infty}^{\infty} dq(t)\right) \tag{28}$$

This result in its conciseness reminds us of Gibbs' formula for the thermodynamic equilibrium distribution at one definite time. However, Eq. (28) includes a narrower of phenomena, as it refers only to the ground state which in thermo-dynamic language corresponds to the absolute zero. One can go over from the complex distribution (28) to the action functional probability corresponding to the ordering principle (6),

$$w^{(1)}[q] = N_1^{-1}\cos\left\{\frac{1}{\hbar}\int_{-\infty}^{\infty} L[q]\,dt\right\}, \tag{29}$$

4. JOINT DISTRIBUTIONS FOR P AND P* TRAJECTORIES

1. If we take into consideration the functional

$$\Theta[u(t), v(t)] = \left\langle \mathrm{P}^{*}\left(\exp\int q(t)v(t)\,dt\right)\mathrm{P}\left(\exp\int q(t)u(t)\,dt\right)\right\rangle, \tag{30}$$

we can use it to write for the characteristic functionals for the ordering principles P, P*, and R,

$$\Theta^{(P)}[u] = \Theta[u, 0];\ \Theta^{(P^*)}[u] = \Theta[0, u];$$
$$\Theta^{(R)}[u] = \Theta\left[\frac{u}{2}, \frac{u}{2}\right]. \tag{31}$$

The functional (30) will be interpreted as the characteristic functional $< \exp \int (ru + sv)\, dt >$ of the joint distribution of P-trajectories $r(t)$ and P*-trajectories $s(t)$. If $w[r(t), s(r)]$ is the density of this joint distribution, one can according to equations (31) obtain from it the distribution density of $q(t)$ for the different arrangement principles,

$$w^{(P)}[q(t)] = \int \ldots \int w[q(t), s(t)]\, \Pi\, ds(t); \quad (31)$$
$$w^{(P^*)}[q(t)] = \int \ldots \int w[r(t), q(t)]\, \Pi\, dr(t); \quad (32)$$
$$w^{(R)}[q(t)]$$
$$= \int \ldots \int w\left[q(t) + \frac{\sigma(t)}{2};\ q(t) - \frac{\sigma(t)}{2}\right] \Pi\, d\sigma(t). \tag{33}$$

These formulas express the fact that in order to find the distribution of P-trajectories one must take into account the P*-trajectories and vice versa, and also that the R-trajectories are equal to $(r(t) + s(t))/2$, *i.e.*, are the mean of the P- and the P*-trajectories.

By approximately the same methods as used to obtain (29) and (31) one finds easily for a chosen interval $[0, T]$

$$w_{0T}[r(t), s(t)] = N^{-1}\delta(r(T)$$
$$- s(T)) \exp\left\{\frac{i}{\hbar}\int_0^{T-\varepsilon}(L[r(t+\varepsilon), r(t)]\right. \tag{34}$$
$$\left. - L[s(t+\varepsilon), s(t)])\, dt\right\} \psi(r(0), 0)\, \psi^*(s(0), 0).$$

Hence the distributions (32) and (33), and also $w^{(1)}$ are obtained by integration.

2. The formulas found in the previous section are closely connected with the results of Refs. 3 and 7. However, it is impossible to consider the concepts of the present paper to be the same as those of the above mentioned papers. We can illustrate their difference, for instance, by calculating the probability W that in the interval $[0, T]$ the trajectory $q(t)$ shall lie within the limits $a(t) \leqslant q(t) \leqslant b(t)$. In the classical theory this probability is equal to

$$W = \left\langle \prod_0^T \int_{a(t)}^{b(t)} \delta(q(t) - x(t))\, dx(t) \right\rangle. \tag{35}$$

In quantum theory the $q(t)$ are operators and one must in Eq. (35) indicate the order of their arrangement,

$$W = \left\langle \Pr \prod_0^T \int_{a(t)}^{b(t)} \delta(q(t) - x(t))\, dx(t) \right\rangle \tag{36}$$

Different principles Pr give, generally speaking, different probabilities. According to (32) and (33) the principal ones of these are equal to

$$W^{(1)} = \frac{1}{2}\left\{\int_{a(t)}^{b(t)} \cdots \iint_{-\infty}^{\infty} \cdots \int + \int_{-\infty}^{\infty} \cdots \iint_{a(t)}^{b(t)} \cdots \int\right\} w[r, s]\, \delta r\, \delta s;$$
$$W^{(2)} = \int_{a(t)}^{b(t)} \cdots \iint_{-\infty}^{\infty} \cdots \int w\left[q + \frac{\sigma}{2},\ q - \frac{\sigma}{2}\right] \delta q\, \delta\sigma \quad (\delta x = \Pi\, dx(t)). \tag{37}$$

These quantities differ in the limits of integration from the quantity

$$W = \int_{a(t)}^{b(t)} \cdots \iint_{a(t)}^{b(t)} \cdots \int w[r, s]\, \delta r\, \delta s, \tag{38}$$

which was indicated in Refs. 3 and 7 and which represents the absolute square of the probability of the event considered. In our opinion expression (38) cannot be interpreted as a probability since there exists no arrangement principle ordering Pr such that expression(38) would follow from equation (36). Expression (38) is thus not connected with any complete statistical picture.

5. STATISTICAL INTERPRETATION BASED UPON THE R-ARRANGEMENT

1. Processes of time evolution described by the distributions $w^{(P)}[q(t)]$, $w^{(P^*)}[q(t)]$ are Markov processes, *i.e.*, the joint distribution density of the values $q(t_1), \ldots, q(t_n)$ can be written in the form

$$w(q(t_1), \ldots, q(t_n))$$
$$= V(q(t_n), t_n; q(t_{n-1}), t_{n-1}) \ldots$$
$$\ldots V(q(t_2), t_2; q(t_1), t_1)\, W(q(t_1), t_1). \tag{39}$$

Indeed, Eq. (39) agrees with Eq. (20) if we put

$$W(q, t) = \Psi^*(q, t)\,\Psi(q, t); \; V(q', t'; q; t) = \frac{\Psi^*(q', t')}{\Psi^*(q, t)}\, U(q', t'; q, t).$$

Unfortunately, the Markov transition probability V turns out to depend on the chosen state Ψ. The arrangements $\mathrm{Pr}^{(1)}$ and R do not lead to Markov processes, even in such a sense. However, the R arrangement corresponds to a "Markov process with derivatives", *i.e.*, the transition from a pair of values $q(t)$, $\dot{q}(t)$ to the same pair at a different time is a Markov process. Expressed differently, evolution in phase space is a genuine Markov process (with a transition probability independent of the state). To see this we consider the joint R-distribution of the quantities $q(t_1)$, $q(t_1 + \varepsilon)$, $q(t_2)$, $q(t_2 + \varepsilon), \ldots, q(t_n + \varepsilon)$ which we obtain by writing expression (33) in a discrete version instead of in a continuous one. It has the form

$$\begin{gathered} \int \ldots \int U(q_n', q_n + \tau_n)\, U^*(q_n', q_n - \tau_n)\, U(q_n + \tau_n, q_{n-1}' + \tau_{n-1}') \\ \times U^*(q_n - \tau_n, q_{n-1}' - \tau_{n-1}')\, U(q_{n-1}' + \tau_{n-1}', q_{n-1} + \tau_{n-1}) \\ \times U^*(q_{n-1}' - \tau_{n-1}', q_{n-1} - \tau_{n-1}) \ldots U(q_2 + \tau_2, q_1' + \tau_1') \times U^*(q_2 - \tau_2, q_1' - \tau_1') \\ \times U(q_1' + \tau_1', q_1 + \tau_1)\, U^*(q_1' - \tau_1', q_1 - \tau_1)\; R(q_1 + \tau_1, q_1 - \tau_1) \\ 2^{2n-1}\, d\tau_1 \ldots d\tau_n\, d\tau_1' \ldots d\tau_{n-1}', \end{gathered} \tag{40}$$

where $q_k = q(t_k)$, $q_k' = q(t_k + \varepsilon)$, $\tau_k = \sigma_k/2$, R is the density matrix, $U(q_k, q_{k-1}') = U(q(t_k), t_k; q(t_{k-1} + \varepsilon), t_{k-1} + \varepsilon)$ is the operator (21).

Taking it into account that for small values of ε

$$U(q_k', q_k) \approx c \exp\left\{\frac{i}{\hbar}\,\frac{m}{2\varepsilon}\,(q_k' - q_k)^2\right\}, \quad c = \left(\frac{im}{2\pi\hbar\varepsilon}\right)^{1/2}, \tag{41}$$

we write Eq. (40) in the form

$$\begin{gathered} |c|^{2n} \int \ldots \int \exp\left\{-\frac{im}{\hbar\varepsilon}(q_n' - q_n)\,\sigma_n\right\} U\left(q_n + \frac{\sigma_n}{2},\, q_{n-1}' + \frac{\sigma_{n-1}'}{2}\right) \\ \times U^*\left(q_n - \frac{\sigma_n}{2},\, q_{n-1}' - \frac{\sigma_{n-1}'}{2}\right) \exp\left\{\frac{im}{\hbar\varepsilon}(q_{n-1}' - q_{n-1})(\sigma_{n-1}' - \sigma_{n-1})\right\} \ldots \\ \ldots U\left(q_2 + \frac{\sigma_2}{2},\, q_1' + \frac{\sigma_1'}{2}\right) U^*\left(q_2 - \frac{\sigma_2}{2},\, q_1' - \frac{\sigma_1'}{2}\right) \\ \times \exp\left\{\frac{im}{\hbar\varepsilon}(q_1' - q_1)(\sigma_1' - \sigma_1)\right\} R\left(q_1 + \frac{\sigma_1}{2},\, q_1 - \frac{\sigma_1}{2}\right) d\sigma_1 \ldots d\sigma_n\, d\sigma_1' \ldots d\sigma_{n-1}'. \end{gathered} \tag{42}$$

The last expression splits into a product of functions. Since the Jacobian of the transformation from

$$q(t_1),\, q(t_1 + \varepsilon),\, \ldots,\, q(t_n),\, q(t_n + \varepsilon)$$

to the quantities

$$q(t_1),\, \dot{q}(t_1),\, \ldots,\, \dot{q}(t_n),\, \dot{q}(t_n) \quad \left(\dot{q}(t) = \frac{q(t + \varepsilon) - q(t)}{\varepsilon}\right)$$

is equal to ε^{-n} the density of the distribution of the latter quantities differs from expression (42) by that factor and is equal to

$$w^{(R)}(q(t_1), \dot{q}(t_1), \ldots, \dot{q}(t_n)) = K_{t_n t_{n-1}}(q_n, \dot{q}_n; q_{n-1}, \dot{q}_{n-1}) \ldots K_{t_2 t_1}(q_2, \dot{q}_2; q_1, \dot{q}_1)\, W_t(q_1, \dot{q}_1), \tag{43}$$

where

$$W_t(q, \dot{q}) = \frac{m}{2\pi\hbar}\int \exp\left\{-\frac{im}{\hbar}\dot{q}\sigma\right\} R\left(q+\frac{\sigma}{2},\ q-\frac{\sigma}{2}\right)d\sigma; \tag{44}$$

$$K_{t't}(q', \dot{q}'; q, \dot{q}) = \frac{m}{2\pi\hbar}\iint \exp\left\{-\frac{im}{\hbar}(\dot{q}'\sigma'-\dot{q}\sigma)\right\} U\left(q'+\frac{\sigma'}{2},\ q+\frac{\sigma}{2}\right)U^*\left(q'-\frac{\sigma'}{2},\ q-\frac{\sigma}{2}\right)d\sigma\, d\sigma' \tag{45}$$

are the corresponding Wigner distribution and Markov transition probability. Thus the evolution process is actually a Markov process in the case of the R arrangement.

The function (45) was considered by Moyal[1] as the operator defining the time evolution of the momentaneous distribution law (44). In particular, he derived a differential equation for it. We note that Moyal's statement that this evolution process is a Markov process is in his paper only a hypothesis inasmuch as the multiple distribution laws do not follow from the evolution of the momentaneous distribution law. As we have just shown, this hypothesis is justified for the R-arrangement of operators, but just for the $\mathrm{Pr}^{(s)}$ arrangement, which was used by Moyal as a basis to derive the Wigner distribution, it is not justified.

2. In many cases the integral (33) can be obtained from expression (34). A number of these cases correspond to quantum fields with localized interactions described by the usual form of the interaction Lagrangian. We consider as an example the relativistic case of the interaction of a neutral with a charged field. For the sake of simplicity we assume both fields to be scalar. Let the Lagrangian be of the form

$$L[\varphi, \psi] = \frac{1}{2}(\varphi_\lambda\varphi^\lambda - \mu^2\varphi^2) + \psi^*_\lambda\psi^\lambda - m^2\psi^*\psi + g\varphi\psi^*\psi. \tag{46}$$

The generalization of equations (33) and (34) for the case of the distribution of these fields within a four-dimensional region M is given by the equation

$$\begin{aligned} w^{(R)}[\varphi(x), \psi(x)] = N^{-1}\int\ldots\int \exp\Big\{\frac{i}{\hbar}\int_M dx\Big(L\Big[\varphi+\frac{\xi}{2},\ \psi+\frac{\eta}{2}\Big] \\ - L\Big[\varphi-\frac{\xi}{2},\ \psi-\frac{\eta}{2}\Big]\Big)\Big\}\prod_M d\xi(x)\, d\eta(x)\, d\eta^*(x). \end{aligned} \tag{47}$$

We have in this equation not written out explicitly the boundaries of the region M. From Eq. (46) we get

$$\begin{aligned} F(x) \equiv L\Big[\varphi+\frac{\xi}{2},\ \psi+\frac{\eta}{2}\Big] - L\Big[\varphi-\frac{\xi}{2},\ \psi-\frac{\eta}{2}\Big] = \varphi^\lambda\xi_\lambda - \mu^2\varphi\xi + g\psi^*\psi\xi \\ + \eta^*_\lambda\psi^\lambda - m^2\eta^*\psi + g\varphi\eta^*\psi + \psi^{*\lambda}\eta_\lambda - m^2\psi^*\eta + g\psi^*\eta + \frac{1}{4}g\xi\eta^*\eta. \end{aligned} \tag{48}$$

We subdivide the region M into cells of size Δ_j, containing the points x_j. We replace the integral in the exponent in expression (47) by the sum $\Sigma F(x_j)\Delta_j$, where $F(x_j)$ is defined by expression (48) in which the derivatives ξ_λ, η_λ are represented by the differences of the values of the $\xi(x_j)$, $\eta(x_j)$ in neighboring cells. After substituting this expression into the sum we combine all those terms in the exponent which contain the same variables $\xi(x_j)$, $\eta(x_j)$, and we get

$$\int\ldots\int \exp\Big\{\frac{i}{\hbar}\sum_j F_j\Delta_j\Big\}\prod_j d\xi_j\, d\eta_j\, d\eta^*_j = \prod_j \int \exp i\,\{\alpha_j\xi_j + \beta^*_j\eta_j + \beta_j\eta^*_j + \gamma_j\xi_j\eta^*_j\eta_j\}d\xi_j\, d\eta_j\, d\eta^*_j, \tag{49}$$

where

$$\alpha_j = \frac{\Delta_j}{\hbar}[\Box\varphi - \mu^2\varphi + g\psi^*\psi]_{x-x_j};\ \ \beta_j = \frac{\Delta_j}{\hbar}[(\Box - m^2 + g\varphi)\psi]_{x=x_j};$$

$$\gamma_j \doteq \Delta_j/4h;\ \xi_j = \xi(x_j),\ \ \eta_j = \eta(x_j).$$

The factors on the right hand side of (49) refer to those cells which are not near the boundary of the region considered. We have not written out explicitly the factors referring to the cells on the boundaries as they are more complicated. Integration over η_j and η_j^* in (49) means integrating both the real and the imaginary part from $-\infty$ to $+\infty$. Let $\eta_j = \rho + i\sigma$, $\beta_j = \rho_1 + i\sigma_1$; one can take each factor of the integral separately and we obtain

$$\int \exp i\,\{\alpha\xi + 2(\rho\rho_1 + \sigma\sigma_1) + \gamma\xi(\rho^2 + \sigma^2)\}\,d\xi\,d\rho\,d\sigma = \frac{2\pi^2}{\gamma} I_0\left(2\left[\frac{\alpha}{\gamma}(\rho_1^2 + \sigma_1^2)\right]^{1/2}\right), \tag{50}$$

where $I_0(x) = J_0(ix)$ is a Bessel function of the second kind. We have thus

$$w^{(R)}[\varphi(x), \psi(x)] = N_0^{-1}\prod_j I_0\left(2(\alpha_j\beta_j^*\beta_j/\gamma_j)^{1/2}\right)$$
$$= N_1^{-1}\left[\exp\left\{\frac{1}{2\hbar\sqrt{g}}\int[\Box\varphi - \mu^2\varphi + g\psi^*\psi]^{1/2}\,|(\Box - m^2 + g\varphi)\psi|\,z(x)\,dx\right\}\right]^{(2)}. \tag{51}$$

In this equation$^{(2)}$ indicates a symbolic square defined by the equation

$$\left[\sum_{\lambda,\mu,\ldots} a_{\lambda\mu\ldots}\, z_1^\lambda z_2^\mu \ldots\right]^{(2)} = \sum_{\lambda,\mu,\ldots}(a_{\lambda\mu\ldots})^2, \tag{52}$$

so that

$$[e^{az}]^{(2)} = I_0(2a);\ \ [e^{\Sigma a_j z_j}]^2 = \Pi\, I_0(2a_j).$$

If we write out in detail the factors in Eq. (51) referring to the interior points of the region we get in the limit $\hbar\sqrt{g} \to \infty$ the "classical" form

$$\prod_j \delta(\Box\varphi - \mu^2\varphi + g\psi^*\psi)\,\delta((\Box - m^2 + g\varphi)\psi)\,\delta\ \text{(compl. conj.)},$$
$$(\delta(\alpha + i\beta)\,\delta(\alpha - i\beta) \equiv \delta(\alpha)\,\delta(\beta)).$$

It is well known that one obtains the "classical" basis of evolution not only as $\hbar \to 0$, but also in the case of linear equations of motion (Sec. 2).

6. CONCLUDING REMARKS

We shall make several remarks about the connection between the statistical interpretation just developed and well-known methods of relativistic field theory.

1. Let $A(x)$ stand for all field operators (for instance, φ, ψ) and let $L[A]$ be the corresponding Lagrangian. For each arrangement principle there is for a given complete statistical picture a corresponding characteristic functional $\Theta = \langle S\rangle$ where

$$S = \Pr\exp\left\{i\int A(x)\,J(x)\,dx\right\}.$$

We remember that in the classical case [commuting $A(x)$] we have for every $F[A]$

$$F\left[\frac{\delta}{i\delta J(x)}\right]S = F[A(x)]\,S. \tag{53}$$

In quantum theory the operation of $F[\delta/i\delta J(x)]$ on S gives $\Pr\{F[A]S\}$ which, generally speaking, is different from $F[A]S$. We shall get a formula very similar to the classical expression (53) in the case of the P (and P*) arrangement. In this case after "disentangling" from $\mathrm{P}\{F[A]S\}$ the exponential factor[4] we shall have

$$F\,[\delta/i\delta J\,(x)]\,S = F\,[\widetilde{A}\,(x)]\,S, \tag{54}$$

where $\widetilde{A}(x)$ are the operators "in a different representation," more precisely the operators whose evolution is described by the Lagrangian $L\,[A] + AJ$ (we put $\hbar = 1$).

If one considers that the addition of AJ describes external sources, the fields $A\,(x)$, which evolve without sources, will be operators in the "interaction representation" (with respect to the "interaction" AJ). Also S will be the "scattering matrix" describing the action of external sources. The characteristic functional Θ in the P-arrangement can thus be interpreted dynamically as the probability amplitude for a $\Psi - \Psi$ transition under the action of external sources.

If $F_1\,[\widetilde{A}\,(x)] = F_2\,[J\,(x)]$ is the equation of motion of the fields with sources, then in virtue of (54) we can go over to the following equation for the characteristic functional describing fields without sources

$$F_1\,[\delta\,/\,i\delta J(x)]\,\Theta = F_2\,[J\,(x)]\,\Theta.$$

Equations of this form were used in Ref. 8 to derive Feynman's Lagrangian form and in Ref. 9 to derive Schwinger's equations. Our aim was to draw attention to the fact that Θ (Z in the notation of the above mentioned papers) can equally well be treated as a characteristic functional.

2. We define generalized moment and correlation (cumulative) functions by the equations

$$m_n\,(x_1, \ldots, x_n \,|\, J) = \frac{1}{\Theta}\,\frac{\delta}{i\delta J\,(x_1)} \cdots \frac{\delta}{i\delta J\,(x_n)}\,\Theta; \tag{55}$$

$$k_n\,(x_1, \ldots, x_n \,|\, J) = \frac{\delta}{i\delta J\,(x_1)} \cdots \frac{\delta}{i\delta J\,(x_n)}\,\ln\Theta. \tag{56}$$

The usual moment and correlation functions are defined analogously, but after performing the differentiations one puts $J\,(x) \equiv 0$. The difference between the functions (55) and (56) for $J \neq 0$ and the usual ones is essentially that the probability functional $w[A]$ which describes the field distribution, is replaced by a new functional

$$\exp\left(i\int AJ\,dx\right) w\,[A]\,\Big/\!\int \exp\left(i\int AJ\,dx\right) w\,[A]\,\delta A,$$

for which expressions (55) and (56) are the usual moment and correlation functions. The formulas in which expressions (55) and (56) occur will thus have the usual form.

In view of this all we see that the distribution functions introduced by Schwinger[10] for the general case when external sources are present are nothing but the correlation functions (56), and some equations involving then can be explained in a trivial manner. For instance, a formula typical for Ref. 10 of the form

$$\frac{\delta\,\langle A\,(x')\rangle}{i\delta J\,(x)} = \frac{\delta^2 \ln\Theta}{i\delta J\,(x)\,i\delta J\,(x')} = \langle \mathrm{P} A\,(x)\,A\,(x')\rangle - \langle A\,(x)\rangle\,\langle A\,(x')\rangle$$

is essentially an elementary formula from correlation theory

$$k_2\,(x,\,x') = m_2\,(x, x') - m_1\,(x)\,m_1\,(x').$$

3. Let the Lagrangian L be the sum of the Lagrangian of free fields L_0 and an interaction Lagrangian L_j. The ground state Φ_0 of the free fields and the ground state Ψ_0 of the interaction field correspond to different P-distributions (28), namely

$$w_0^{(P)}\,[A] = N_0^{-1} \exp\left\{i\int_{-\infty}^{\infty} L_0\,dx\right\};$$
$$w^{(P)}\,[A] = N^{-1} \exp\left\{i\int_{-\infty}^{\infty} L\,dx\right\}. \tag{57}$$

Hence we have

$$\int F\,[A]\,w\,\delta A = \frac{N_0}{N}\int F\,[A]\,\exp\left\{i\int L_J\,dx\right\} w_0\,\delta A. \tag{58}$$

Integrating over all w means averaging over the state Ψ_0 and over all w_0 averaging over the state Φ. Taking this into account we can go over to the quantum mechanical average, and if we furthermore compare expression (58) with itself, but with $F = 1$, and use the result, we get

$$(\Psi_0^*\,\mathrm{P}F\,(A)\,\Psi_0) = (\Phi_0^*\,\mathrm{P}\,(F\,[A]\,S)\,\Phi_0)/S_0;$$
$$S_0 = N/N_0 \tag{59}$$
$$\equiv \int \exp\left(i\int L\,dx\right)\delta A\,\Big/\int \exp\left(i\int L_0 dx\right)\delta A.$$

In this equation $S_0 = (\Phi_0^* S \Phi_0)$, and S is the scattering matrix produced by the interaction L_J. Thus the use of the distribution (57) makes it easier to derive the relations connected with the interaction representation.

We note that from equation (26) applied to Ψ_0 and Φ_0 we can derive the relation $\Psi_0 = N_0^{1/2} N^{-1/2}\,S(0,\,-\infty)\,\Phi_0$, which forms the contents of Gell-Mann and Low's theorem;[11] in our opinion it is necessary to introduce into L_0 and L an infinitely small dissipation in order to prove this theorem (Sec. 3).

[1] J. E. Moyal, Proc. Camb. Phil. Soc., 45, 99 (1949).

[2] R. L. Stratonovich, J. Exptl. Theoret. Phys. (U.S.S.R.) 31, 1012 (1956); Soviet Phys. JETP 4, 891 (1957).

[3] R. P. Feynman, Revs. Mod. Phys. 20, 467 (1948).

[4] R. P. Feynman, Phys. Rev. 84, 108 (1951).

[5] P. A. M. Dirac, Revs. Mod. Phys. 17, 195 (1945).

[6] R. P. Feynman, Phys. Rev. 97, 660 (1955).

[7] I. M. Gel'fand and A. M. Iaglom, Usp. Mat. Nauk 11, 77 (1956); translation scheduled for publication in Fortschr. d. Phys.

[8] I. M. Gel'fand and R. A. Minlos, Dokl. Akad. Nauk (U.S.S.R.) 97, 209 (1954).

[9] E. S. Fradkin, J. Explt. Theoret. Phys. (U.S.S.R.) 29, 121 (1955); Soviet Phys. JETP 2, 148 (1956).

[10] J. Schwinger, Proc. Nat. Acad. Sci. 37, 452 (1951).

[11] M. Gell-Mann and F. Low, Phys. Rev. 84, 350 (1951).

Translated by D. ter Haar
291

SOVIET PHYSICS JETP VOLUME 5, NUMBER 6 DECEMBER 15, 1957

The Surface Impedance of Metals in the Infrared Region

M. I. KAGANOV AND V. V. SLEZOV
Physico-Technical Institute, Ukranian Academy of Sciences

(Submitted to JETP editor November 2, 1956)
J. Exptl. Theoret. Phys. (U.S.S.R.) 32, 1496-1504 (June, 1957)

An expression has been obtained for the surface impedance of metals in the infrared region without making any special assumptions concerning the law of dispersion of the conduction electrons.

1. IN THE OPTICS OF METALS the most interesting region, it seems to us, is the infrared region in which the frequency of the electromagnetic field satisfies the condition

$$\nu_0 \ll \omega \ll \omega_a \qquad (1)$$

Here $\nu_0 = 1/\tau$ is the collision frequency (τ is the relaxation time), and ω_a is the limit of the internal photoeffect.* As shown in Ref. 1, for low temperatures and for pure metals this region is known to be essentially: $\nu_0 \sim 10^{11}$, $\omega_a \sim 10^{15}$ to 10^{16}. Thus we talk of working at wavelengths on the order of ten microns.

In this frequency region the electron gas is approximately described by the dielectric constant

$$\varepsilon = 1 - 4\pi Ne^2/m\omega^2 \qquad (2)$$

where N is the density of free electrons and m the effective mass.* In other words, the electron gas "behaves" like an electron plasma.

Since $\Omega^2 \approx 4\pi Ne^2/m \sim \omega_a^2$, then in the frequency region of interest to us the dielectric constant of the metal is negative ($\varepsilon < 0$), and, its modulus is considerably greater than 1, *i.e.*,

$$\varepsilon \approx -4\pi Ne^2/m\omega^2, \quad |\varepsilon| \gg 1.$$

The reflection of light from the surface of a metal in this case is, in principle, not connected with the ohmic loss and can be described by a purely imaginary surface impedance

---

* The internal photoeffect which is due to the interaction of electrons can occur at all frequencies; however, it principally occurs only for $\omega > \omega_a$ ($\hbar\omega_a$ is of the order of intervals between energy bands, $\sim 10^{-12}$ ergs).

* Note that according to the opinion of Ginzburg (*cf.* Ref. 1) we put in formula (2) the mass of the free electrons. All resultant changes in N/m are due to the change in the electron density N. This, of course, cannot lead to contradiction, but, it seems to us, causes trouble in comparing optically measured constants of the electron gas with results of other experiments (galvanomagnetic, specific heat, *etc.*). Moreover, if the calculation is carried out with the use of the kinetic equation, it is natural that in formula (2) there should appear precisely the effective mass (see below).

$$Z \approx iX = 4\pi i\omega / c\Omega \equiv i\sqrt{4\pi m\omega^2 / Ne^2c^2}. \qquad (3)$$

However, formula (2), and consequently also (3), are approximate. Ohmic loss, naturally, occurs but $R = \operatorname{Re} Z \ll X$.

The real part R of the impedance is essentially different in two cases, occurring for frequencies satisfying inequality (1): normal skin effect ($\delta \gg l$; $l = v\tau$, $\delta = c/\Omega$):

$$R = 2\pi\nu_0 / c\Omega; \qquad (4)$$

anomalous skin effect ($\delta \ll l$):

$$R = 3\pi v / 4c^2 \qquad (5)$$

(v is the limiting Fermi velocity).

Formulas (3) to (5) were obtained on the basis of an isotropic quadratic dispersion relation ($\varepsilon = p^2/2m$; ε, $\mathbf{p}$ — energy and quasi-momentum of the electron) without allowing for quantum mechanical effects. The latter are due to the fact that $h\omega$ for low temperatures not only is not less than kT, but may possibly be even considerably larger than kT. However, Wolfe[2] has shown that the results of quantum mechanical and classical calculations of ohmic loss connected with diffuse scattering of electrons on walls coincide. True, one must bear in mind (especially when comparing formulas of type (5) with experiment) that the surface loss is not always considerably larger than the volume loss.* For instance, according to Goldstein,[3] for $\hbar\omega \gg k\Theta$, kT (Θ is the Debye temperature) the quantum losses are of the same order as given by formula (5).

In the present article we obtain generalized formulas for the case of an arbitrary anisotropic dispersion law: $\varepsilon = \varepsilon(\mathbf{p})$. Just as in Refs. 1 and 4 to 8, the calculation is made with the aid of the classical kinetic equation.

2. Consider a plane monochromatic wave of frequency ω on a normally incident half-space $z > 0$ occupied by metal.

The complete system of equations describing the behavior of the electrons comprises the linearized kinetic equation

$$i\omega f + v_z \frac{\partial f}{\partial z} + \frac{f}{\tau} = -\frac{\partial f_0}{\partial \varepsilon} e\mathbf{E}\mathbf{v} \qquad (6)$$

and the Maxwell equations

$$\operatorname{curl} \mathbf{H} = 4\pi \mathbf{j}/c, \operatorname{curl} \mathbf{E} = -\frac{i\omega}{c}\mathbf{H};$$

$$\mathbf{j} = \frac{2e}{(2\pi\hbar)^3}\int \mathbf{v} f \, d\mathbf{p}, \qquad (7)$$

f is an addition to the equilibrium Fermi function and $v = \nabla_{\mathbf{p}}\varepsilon$. The boundary condition for Eq. (6) serves as the condition for diffusion of the surface electron from the metal-vacuum boundary

$$f = 0 \quad \text{for} \quad v_z > 0, \; z = 0 \qquad (8)$$

and for the vanishing of the non-equilibrium addition f inside the metal

$$f = 0 \quad \text{for} \quad z \to \infty. \qquad (9)$$

We shall solve the systems (6) and (7) by successive approximations. Assuming ω considerably larger than v/δ and $1/\tau$ we find the zeroth approximation for the distribution function f and the electric field E, neglecting the second and third terms in Eq. (6). From the obtained field we determine the first approximate distribution function, a knowledge of which allows us to calculate the real part R of the impedance (the imaginary part X of the impedance is calculated from the zeroth approximation). Thus, the zeroth approximation is:

$$i\omega f = -(\partial f_0 / \partial \varepsilon) e\mathbf{E}\mathbf{v}.$$

Considering that $\partial f_0/\partial\varepsilon = -\delta(\varepsilon - \varepsilon_0)$ we have

$$j_i = \frac{2e^2}{(2\pi\hbar)^3 \, i\omega}\oint v_i v_k \frac{dS}{v} E_k. \qquad (10)$$

Integration is over the surface $\varepsilon(\mathbf{p}) = \varepsilon_0$ where ε_0 is the Fermi limiting energy, and dS an area element on the Fermi surface. From the fact that the current density and the electric field are out of phase by $\pi/2$, it is evident that we deal here not with the ohmic current but with a polarized electron gas.

We eliminate from Eq. (7) the magnetic field and, by means of the condition $j_z = 0$, the z component of the electric field.* Then we obtain an equation for the electric field

---

*If we do not take into account quantum mechanical effects, then in the case of the anomalous skin effect of interest to us $R_{\text{surf}} \gg R_{\text{vol}}$. Actually, according to (4) and (5): $R_{\text{surf}}/R_{\text{vol}} \sim v\Omega/c\nu_0 \sim l/\delta \gg 1$.

*Condition $j_z = 0$ is equivalent to the equation of continuity $\operatorname{div} j = 0$. We have omitted the term $\partial\rho/\partial t$ (ρ is the electron density), which corresponds to disregarding displacement current (*cf.* Ref. 7).

$$\frac{d^2E_\alpha}{dz^2} - \frac{4\pi e^2}{c^2}\left(\frac{N}{m}\right)_{\alpha\beta} E_\beta = 0, \tag{11}$$

where we introduce the designation

$$\left(\frac{N}{m}\right)_{\alpha\beta} = \frac{2}{(2\pi\hbar)^3} \oint \left\{ \frac{v_\alpha v_\beta}{v}\, dS \right.$$

$$\left. - \oint \frac{v_\alpha v_z}{v}\, dS \oint \frac{v_z v_\beta}{v}\, dS \Big/ \oint \frac{v_z^2}{v}\, dS \right\} \tag{12}$$

(α, $\beta = x, y$). In the isotropic (quadratic) case

$$d^2E_\alpha/dz^2 - 4\pi Ne^2E_\alpha/mc^2 = 0. \tag{13}$$

The last equation is obtained from Eq. (11) if we assume $\varepsilon = p^2/2m$, $v = p/m$ and take into account that $N = (8\pi/3)p^3(2\pi\hbar)^{-3}$. We align the x and y axes with the principal axes of the tensor $(N/m)_{\alpha\beta}$. Then

$$E_x = E_x(0)\, e^{-z/\delta_x};\ E_y = E_y(0)\, e^{-z/\delta_y}, \tag{14}$$

where

$$\delta_x = c/\Omega_x;\ \delta_y = c/\Omega_y;$$
$$\Omega_x^2 = 4\pi e^2 (N/m)_x;\ \Omega_y^2 = 4\pi e^2 (N/m)_y \tag{15}$$

$(N/m)_x$, $(N/m)_y$ are the principal values of the tensor $(N/m)_{\alpha\beta}$. If the crystal is cubic then $\Omega_x = \Omega_y$.

The surface impedance in the zeroth approximation is pure imaginary

$$Z_x = 4\pi E_x(0)/cH_y(0) = 4\pi i\omega\delta_x/c^2 = 4\pi i\omega/c\Omega_x; \tag{16}$$

$$Z_y = -4\pi E_y(0)/cH_x(0) = 4\pi\omega i\delta_y/c^2 = 4\pi i\omega/c\Omega_y. \tag{17}$$

These formulas are natural generalizations of expression (3).

Note that if we do not take into account ohmic loss (to what degree this is valid will be shown further on), then we have two directions (axes x and y in our notation) in which the polarized reflected wave coincides with the incident one (we speak here of a plane polarized incident wave):

Assume for definiteness that a wave polarized longitudinal to the x axis falls on the metal. Then we have inside the metal a field (zeroth approximation):

$$E_x = E_x(0)\, e^{-z/\delta_x};\ E_y = 0;\ E_z = E_z(0)\, e^{-z/\delta_x};$$

$$E_z(0) = -E_x(0) \oint \frac{v_z v_x}{v}\, dS \Big/ \oint \frac{v_z^2}{v}\, dS. \tag{18}$$

The expression for E_z is obtained from the condition $j_z = 0$ (*cf.* above). Substituting expression (18) in Eq. (6) and integrating with allowance for boundary conditions (8) and (9) we find

$$f = -\frac{\partial f_0}{\partial \varepsilon}\, eE_x(0)\, \frac{v_x/v_z - \oint (v_z v_x/v)\, dS \Big/ \oint (v_z^2/v)\, dS}{(i\omega + \nu_0)/v_z - 1/\delta_x}$$
$$\times \left\{ \exp\left(-\frac{z}{\delta_x}\right) - A \exp\left(-\frac{i\omega + \nu_0}{v_z}\, z\right) \right\} \tag{19}$$

where

$$A = \begin{cases} 0, \text{ if } v_z < 0, \\ 1, \text{ if } v_z > 0. \end{cases}$$

Using (19) and the central symmetry of the Fermi surface, we calculate the total current flowing through the metal

$$J_\alpha = \int_0^\infty j_\alpha(z)\, dz = \frac{2e^2}{(2\pi\hbar)^3}\, E_x(0)\, \frac{\delta_x}{i\omega + \nu_0}$$

$$\times \oint \left(v_x v_\alpha - v_\alpha v_z \oint \frac{v_z v_x}{v}\, dS \Big/ \oint \frac{v_z^2}{v}\, dS \right) \tag{20}$$

$$\times \left(1 + \frac{1}{1 + (v_z/\delta_x)(i\omega + \nu_0)} \right) d/Sv.$$

Neglecting ν_0 compared with ω and $v_z/\delta_x\omega$ compared with unity, we obtain for the current a zeroth approximation which agrees with expression (10) if we substitute (18) for the field E_i. In particular, the y-component of the zeroth approximation for the current is equal to zero.

We are interested in the first approximation – that part of the current in phase with the field. As was indicated earlier, two cases are possible: *normal skin effect,* when

$$\nu_0/\omega \gg v/\delta\omega, \quad \text{or} \quad l \ll \delta, \tag{21}$$

and *anomalous skin effect,* when

$$\nu_0/\omega \ll v/\delta\omega, \quad \text{or} \quad l \gg \delta. \tag{22}$$

Prior to calculating the current in the first approximation we recall the inequalities which the frequency must satisfy for our analysis to be correct. It is assumed here that $\omega_a \sim \Omega$. Then from (1)

$$\nu_0 \ll \omega \ll \Omega,$$

and from $\omega \gg v/\delta$ (the path traversed by the electron during one period of the field is considerably less than the depth of penetration) we find that $\omega \gg \Omega v/c$. Thus

$$\Omega v / c \ll \omega \ll \Omega.$$

According to (21) and (22) we have finally: *normal skin effect*

$$\Omega v / c \ll \nu_0 \ll \omega \ll \Omega;$$

anomalous skin effect

$$\nu_0 \ll \Omega v / c \ll \omega \ll \Omega.$$

Both chains of inequalities can take place, since $v/c \sim 10^{-3}$.

Thus, in case of the normal skin effect we neglect in expression (20) the terms of order $v/\omega\delta$ and retain terms of order ν_0/ω.* For the surface impedance we obtain here

$$X_x = 4\pi\omega\delta_x / c^2; \; R_x = 2\pi\nu_0\delta_x / c^2. \tag{23}$$

Analogously, if the incident wave is polarized along the y axis:

$$X_y = 4\pi\omega\delta_y / c^2, \; R_y = 2\pi\nu_0\delta_y / c^2. \tag{23'}$$

To derive (23) and (23′) we used the relation between impedance and total current

$$Z_x = E_x(0) / J_x; \; Z_y = E_y(0) / J_y.$$

For the *anomalous skin effect*, neglecting the terms $\sim \nu_0/\omega$ and retaining the term $\sim v/\delta\omega$, we have from (20):

$$X_x = \frac{4\pi\delta_x\omega}{c^2}; \quad R_x = \frac{3\pi\widetilde{v}_x}{4c^2};$$

$$X_y = \frac{4\pi\delta_y\omega}{c^2}; \quad R_y = \frac{3\pi\widetilde{v}_y}{4c^2}. \tag{24}$$

Here (the prime stands for integration in the region $v_z > 0$)

$$\widetilde{v}_\alpha = \frac{16\oint' \left\{v_z v_\alpha^2 - v_\alpha v_z^2 \oint \frac{v_z v_\alpha}{v}\, dS \Big/ \oint \frac{v_z^2}{v}\, dS\right\} \frac{dS}{v}}{3\left\{\oint v_\alpha^2 \frac{dS}{v} - \left(\oint \frac{v_z v_\alpha}{v}\, dS\right)^2 \Big/ \oint \frac{v_z^2}{v}\, dS\right\}}. \tag{25}$$

In case of a quadratic isotropic dependence $\widetilde{v}_\alpha = v$, and we arrive at Eq. (5).

From expression (20) it is evident that even if the incident wave is polarized along one of the main axes of the tensor $(N/m)_{ik}$ the current is elliptically polarized. This, combined with the fact that in the presence of the anomalous skin effect the metal is characterized not by the conductivity tensor but the conductivity operator which obviously cannot be diagonalized at all points.

The presence of elliptical polarization of the current leads to "oblique" terms of surface impedance. Put*

$$\begin{aligned} E_x(0) / J_{yx} &= Z_{xy} \eqsim R_{xy}; \\ E_y(0) / J_{xy} &= Z_{yx} \eqsim R_{yx}. \end{aligned} \tag{26}$$

Here J_{yx} is the y component of the current, caused by the incidence of an electromagnetic wave polarized along the x axis. Analogously, J_{xy} is the x component of the current due to the electric field J_y.

From (20) and (26):

$$R_{xy} = \frac{\omega^2 (2\pi\hbar)^3}{2e^2} \times \left[\oint_{v_z>0} \left(v_y v_x v_z - v_y v_z^2 \oint \frac{v_z v_x}{v}\, dS \Big/ \oint \frac{v_z^2}{v}\, dS\right) \frac{dS}{v}\right]^{-1}, \tag{27}$$

$$R_{yx} = \frac{\omega^2 (2\pi\hbar)^3}{2e^2} \times \left[\oint_{v_z>0} \left(v_y v_x v_z - v_x v_z^2 \oint \frac{v_z v_y}{v}\, dS \Big/ \oint \frac{v_z^2}{v}\, dS\right) \frac{dS}{v}\right]^{-1}. \tag{27'}$$

If we assume that the anisotropy is on the order of unity, then from (27) it is easy to obtain an estimate of the "oblique" terms:

$$R_{xy} \sim \omega^2\delta^2 / c^2 v^2,$$

---

*It should be taken into account that in this approximation $\delta_{x,y} = \delta_{x,y}^{(0)}(1 - i\nu_0/2\omega)$ where $\delta_{x,y}^{(0)}$ is defined by (16). Equations (23) and (23′) contain $\delta_{x,y}^{(0)}$ (zeros omitted!).

*$X_{yx} = X_{xy} = 0$ (zeroth approximation!).

i.e.,

$$R_{xy}/X \sim \delta\omega/v = c\omega/v\Omega \gg 1.$$

Such an inequality is entirely natural since $|J_x| \gg |J_{yx}|$.

Formulas (23) – (25) and (27) solve the postulated problem – determination of expressions for the component of surface impedance in the case of an arbitrary dispersion of conduction electrons, usable in the region of infrared frequences.

3. Consider now the behavior of a wave reflected from a metal. If an electromagnetic wave polarized along the x axis is incident on a metal surface, the electromagnetic field outside the metal has the form

$$E_x = E_{\text{inc}} \cdot e^{-ikz} + E_{\text{ref}}\, e^{ikz};$$
$$H_y = E_{\text{inc}}\, e^{-ikz} - E_{\text{ref}}\, e^{ikz}; \qquad (28)$$
$$E_y = E_{yx} e^{ikz}; \quad H_x = E_{yx} e^{ikz}; \quad k = \omega/c.$$

The resultant y component of the electric field and x component of the magnetic field are due to the presence of the "oblique" terms in the surface impedance.

Equations (17) and (26) allow us to calculate the amplitudes of the reflected waves

$$E_{\text{ref}} = -E_{\text{inc}} \frac{1 - cZ_x/4\pi}{1 + cZ_x/4\pi};$$
$$E_{yx} = 2E_{\text{inc}} \frac{Z_x}{Z_{xy}} (1 + cZ_x/4\pi)^{-1};$$

and if we take into account that $|cZ_x/4\pi| \ll 1$, then

$$E_{\text{ref}} \approx -E_{\text{inc}}(1 - cZ_x/2\pi),$$
$$E_{yx} \approx 2E_{\text{inc}} Z_x/Z_{xy} \approx 2iE_{\text{inc}} X_x/R_{xy}. \qquad (29)$$

The relationship $E_{yx}/E_{\text{inc}} \sim v\Omega/c\omega$ measures the ellipticity of the reflected wave since Z_x and Z_{xy} have different components (Z_{xy} is real and Z_x almost pure imaginary).

4. Measurement of the surface resistance allows us in principle to obtain information about the form of the Fermi surface. However, the formulas obtained are very complicated, and, naturally, it is not possible to say much about a complete synthesis of the Fermi surface from these data. On the other hand it is possible to use certain simple assumptions about the character of the dispersion dependence, and attempt to make use of the quantity $Z = R + iX$ to determine the constants which describe the properties of the electron gas.

If we examine the isotropic quadratic dependence of energy on momentum*

$$\varepsilon = p^2/2m, \qquad (30)$$

then for the measured values of R and X (*cf.* Refs. 3 and 5)† it is possible to determine the effective electron mass m and the electron concentration N:

$$N = 9 \cdot 2^{-3/2} \pi^{5/2} (2\pi\hbar)^{3/2} \left(\frac{\omega}{ec^2}\right)^3 R^{-3/2} X^{-3};$$
$$m = 9 \cdot 2^{-7/2} \pi^{3/2} (2\pi\hbar)^{3/2} (\omega/ec^4)\, R^{-3/2} X^{-1}.$$

We use the fact that the limiting velocity of the electrons is determined by the electron concentration and the mass

$$\bar{v} = (3/8\pi)^{1/3} (2\pi\hbar/m) N^{1/3}.$$

If the static conductivity σ is known, then, in addition to determining N and m, it is possible to determine the collision frequency $\nu_0 = 4\pi\omega^2/c^2X^2\sigma$.

Let us turn attention to the following fact. It is very important to be certain that the formulas used to determine the characteristics of the electron gas [in our case (3) and (5)] are correct; *i.e.*, we must be satisfied that we are really in the plasma region (2) and therefore under the conditions of the anomalous skin effect. For this it is necessary that the ohmic loss be small, *i.e.*, we must have

$$R \ll X. \qquad (31)$$

If this condition is fulfilled, we know that we are in the plasma region. The determination of the character of the skin effect (normal or anomalous) is difficult since this character is connected with the relationship between the mean free path $l = v\tau$ and the depth of penetration $\delta = c/\Omega$.

---

* It is obviously possible to use this dependence for a description of the properties of a polycrystal.

† We, purposely, use only the formulas of the anomalous skin effect since the relaxation time τ (or the collision frequency ν_0) does not enter into them. On the other hand the formulas for the normal skin effect can indeed be used for determining the quantity ν_0 (and, of course, the ratio N/m). Actually from (3) and (4) we have: $\nu_0 = 2\omega R/X$; $N/m = 4\pi\omega^2/e^2c^2X^2$. The value of the static conductivity $\sigma = Ne^2/m\nu_0$ can be employed to check the determined values of N/m and ν_0. Note that in this case it is impossible to determine N and m individually, but only their ratio.

If the normal skin effect takes place ($l \ll \delta$) then by using the expression for the surface impedance

$$Z = R + iX = \sqrt{\frac{2\pi\omega}{c^2\sigma}}\,\{(\sqrt{\omega^2c^2+1}-\omega\tau)^{1/2}$$

$$+\, i\,(\sqrt{\omega^2\tau^2+1}+\omega\tau)^{1/2}\}$$

(*cf.*, for example, Ref. 4; $\sigma = Ne^2\tau/m$ is the static conductivity of the metal) it is easy to find an equation connecting R, X and σ:

$$XRc^2\sigma / 2\pi\omega = 1. \qquad (32)$$

The relation obtained can serve as a criterion for the normal skin effect since in that case when the mean free path $l = v\tau$ is considerably greater than the depth of penetration of the field, the parameter $\xi = XRc^2\sigma/2\pi\omega$ is also considerably greater than unity. Actually, if we use the expression for surface impedance in the radio-frequency region at low temperatures (the limit of the anomalous skin effect, *cf.*, for example, formula (4.19) of Ref. 1) we obtain

$$\xi \sim (l/\delta)^{2/3} \gg 1 \; (l \gg c/\sqrt{2\pi\sigma\omega}).$$

From (3) and (5) (infrared region, low temperatures) we have

$$\xi \sim l/\delta \gg 1 \; (l \gg c/\Omega).$$

Thus, if $\xi \gg 1$ we have the anomalous skin effect. If furthermore $R \ll X$, we deal with the "plasma" region.

Note that allowing for the polarization of the bound electrons (electrons of the ionic residues of the metal) does not change substantially the value of the parameter ξ. For instance, under the conditions of the normal skin effect we have for $\omega \ll \Omega$:

$$\xi = 1 + 2\varepsilon_0\omega^2/\Omega^2 \approx 1.$$

5. Generally in optical investigations we do not make use of the surface impedance, but use the idea of a complex coefficient of reflection $n - i\varkappa$. When the mean free path of the electron is much less than the depth of the skin layer ($l \ll \delta$, normal skin effect) the coefficient of reflection is connected in the usual manner with the complex dielectric constant

$$n - i\varkappa = \sqrt{\varepsilon'}; \quad \varepsilon' = \varepsilon(\omega) - \pi 4\sigma(\omega)\, i/\omega.$$

In particular, if the relaxation effect is described with the help of the relaxation time ($\sigma = \sigma_0/(1+i\omega\tau)$) and we do not take into account the ionic residues, then

$$\varepsilon(\omega) = 1 - \Omega^2/(\nu_0^2+\omega^2); \quad \sigma(\omega) = \sigma_0\nu_0^2/(\nu_0^2+\omega^2);$$

$$n = \left\{\frac{1}{2}\left(1-\frac{\Omega^2}{\nu_0^2+\omega^2}\right) + \frac{1}{2}\sqrt{\left(1-\frac{\Omega^2}{\nu_0^2+\omega^2}\right)^2+\left(\frac{\nu_0}{\omega}\frac{\Omega^2}{\nu_0^2+\omega^2}\right)^2}\right\}^{1/2};$$

$$\varkappa = \left\{\frac{1}{2}\left(\frac{\Omega^2}{\nu_0^2+\omega^2}-1\right) + \frac{1}{2}\sqrt{\left(1-\frac{\Omega^2}{\nu_0^2+\omega^2}\right)^2+\left(\frac{\nu_0}{\omega}\frac{\Omega^2}{\nu_0^2+\omega^2}\right)^2}\right\}^{1/2}.$$

The expression for the surface impedance, as is known,[1,9] may serve as a basis for introducing the effective dielectric constant ε_{eff}, and consequently n_{eff} and $\varkappa_{\text{eff}}$;*

$$n_{\text{eff}} = \frac{cR/4\pi}{(cR/4\pi)^2+(cX/4\pi)^2}, \qquad \varkappa_{\text{eff}} = \frac{cX/4\pi}{(cR/4\pi)^2+(cX/4\pi)^2}. \qquad (33)$$

For $R \ll X$ (of interest in our case)

$$n_{\text{eff}} = 4\pi R/cX^2, \quad \varkappa_{\text{eff}} = 4\pi/cX. \qquad (33')$$

For expression (33) to be considered as defining the effective coefficient of reflection, the impedance must depend weakly on the form of the incident wave, *i.e.*, on the angle of incidence and polarization.[1,9] In order to be satisfied that the concept of effective dielectric constant can be used also in the infrared region (under the conditions of the anomalous skin effect) we have examined the dependence of the surface impedance on the angle of incidence φ in that case when the vector of the electric field is polarized in the plane of incidence (p is the polarization). Assuming the quadratic dispersion law (30), we have obtained ($\omega/\Omega \ll 1$):

---

* For $\delta \gg l$, naturally, $n_{\text{eff}} = n$, $\varkappa_{\text{eff}} = \varkappa$.

$$X = \frac{4\pi}{c}\frac{\omega}{\Omega}\left(1 + \frac{v^2}{5c^2}\sin^2\varphi\right), \quad R = \frac{3\pi}{4}\frac{v}{c^2} \tag{34}$$

Thus, in this case it is not necessary to take into account the dependence on the angle of incidence, since $v^2/c^2 \sim 10^{-6}$, and we have discarded terms known to be larger to obtain formulas (3), (5), (23), (24), and (34).

Therefore, in the region of frequency and temperature under consideration we may introduce an effective index of reflection, which

$$n_{\text{eff}} = 3v\Omega^2/16c\omega^2; \quad \varkappa_{\text{eff}} = \Omega / \omega \tag{35}$$

[we have used (33′)]. Note that in this region one must satisfy a condition analogous to (31):

$$n_{\text{eff}} \ll \varkappa_{\text{eff}}, \tag{31′}$$

In the anisotropic case (particularly, when the ohmic resistance has "oblique" terms) introduction of an effective index of reflection is inconvenient and does not present great interest.

6. In the case of a single-crystal metal with anisotropic conductivity we use for the description of the electron gas a quadratic dispersion law with two effective masses:

$$\varepsilon = (p_1^2 + p_2^2) / 2m_1 + p_3^2 / 2m_3. \tag{36}$$

Assuming that the normal to the surface makes an angle α with the axis of the crystal, we obtain:

(1) The coordinate of the principal directions* on the surface of the metal

$$\mathbf{x} = [\mathbf{z} \times [\mathbf{z} \times \mathbf{n}]]/\sin\alpha; \quad \mathbf{y} = [\mathbf{z} \times \mathbf{n}]/\sin\alpha$$

($\mathbf{z}$ is the coordinate of the normal to the surface, $\mathbf{n}$ the coordinate of the axis of the crystal, and $\cos\alpha = (\mathbf{z} \cdot \mathbf{n})$.

(2) Principal values of the tensor $(N/m)_{ik}$:

$$\left(\frac{N}{m}\right)_{xx} = \frac{N}{m_1\cos^2\alpha + m_3\sin^2\alpha}; \quad \left(\frac{N}{m}\right)_{yy} = \frac{N}{m_1}$$

(3) Components of the surface impedance:

$$\begin{aligned} X_{xx} &= \left[\frac{4\pi\omega^2}{Ne^2c^2}(m_1\cos^2\alpha + m_3\sin^2\alpha)\right]^{1/2}, \\ X_{yy} &= \sqrt{\frac{4\pi\omega^2}{Ne^2c^2}m_1}, \\ R_{xx} &= R_{yy} = \frac{3\pi}{4c^2}\left[2\varepsilon_0\left(\frac{\cos^2\alpha}{m_3} + \frac{\sin^2\alpha}{m_1}\right)\right]^{1/2}; \\ \varepsilon_0 &= \left(\frac{3N}{8\pi}\right)^{2/3}\frac{(2\pi\hbar)^2}{2m_1^{2/3}m_3^{1/3}} \end{aligned} \tag{37}$$

(ε_0 is the limiting Fermi energy). The oblique terms of the surface impedance R_{xy} and R_{yx} in this case are equal to zero. This, obviously, is connected with the "isotropy" of R_{ik}. It should be borne in mind that the vanishing of the "oblique" terms of the ohmic resistance in this simple case does not at all indicate that they are equal to zero in reality. The point is that the selected dispersion law (36), although it also may describe, for example, the anisotropy of the conductivity, is known not to be useful for more complex effects (for example, galvanomagnetism, de Hass–van Alphen effect, *etc.*). Obviously, for the description of the formation of electric polarization at normal incidence a more complex dispersion law is necessary. For example, the assumption of some specially oriented ellipsoid (as in Bi)[10] leads to the expected effect.

Equations (37) allow us to determine the electron concentration N and both values of the effective mass (m_1, m_3):

$$N = \frac{9\pi^{5/2}}{2\sqrt{2}}(2\pi\hbar)^{3/2}\left(\frac{\omega}{ec^2}\right)^3\frac{1}{X_y^{5/2}X_x^{1/2}R^{3/2}}\,\frac{\sin^2\alpha}{1-(X_y/X_x)^2\cos^2\alpha};$$

$$m_1 = \frac{9\pi^{3/2}}{8\sqrt{2}}(2\pi\hbar)^{3/2}\frac{\omega}{ec^4}\frac{1}{X_y^{1/2}X_x^{1/2}R^{3/2}}\,\frac{\sin^2\alpha}{1-(X_y/X_x)^2\cos^2\alpha};$$

$$m_3 = (9\pi^{3/2}/8\sqrt{2})\,(2\pi\hbar)^{3/2}\,(\omega/ec^4)\,X_x^{3/2}/X_y^{5/2}R^{3/2}.$$

In conclusion the author expresses thanks to V. L. Ginzburg, L. D. Landau, I. M. Lifshitz, and K. D. Sinel'nikov for useful discussions of the points raised here.

I.e., the direction in which the tensor X_{ik} is diagonal (*cf.* Sec. 2).

[1] V. L. Ginzburg and G. P. Matulevich, Usp. Fiz. Nauk 55, 469 (1955).

[2] R. Wolfe, Proc. Phys. Soc. (London) 68 A, 121 (1955).

[3] T. Holstein, Phys. Rev. 96, 53 (1954).

[4] G. E. Reuter and E. H. Sondheimer, Proc. Roy. Soc. 195, 336 (1948).

[5] T. Holstein, Phys. Rev. **88**, 1427 (1952).

[6] R. B. Dingle, Physica **19**, 348 (1953).

[7] M. Ia. Azbel' and M. I. Kaganov, Dokl. Akad. Nauk SSSR **95**, 41 (1954).

[8] M. I. Kaganov and M. Ia. Azbel', Dokl. Akad. Nauk SSSR **102**, 49 (1955).

[9] E. Kaner, M. I. Kaganov, J. Exptl. Theoret. Phys. (U.S.S.R.) **31**, 459 (1956); Soviet Phys. JETP **4**, 393 (1957).

[10] V. Heine, Proc. Phys. Soc. (London) **69 A**, 505 (1956).

Translated by L. B. Leder
292

SOVIET PHYSICS JETP VOLUME 5, NUMBER 6 DECEMBER 15, 1957

Bremsstrahlung of Ultra-Relativistic Particles in a Central Field

A. G. SITENKO
Khar'kov State University

(Submitted to JETP editor November 19, 1956)
J. Exptl. Theoret. Phys. (U.S.S.R.) 32, 1505-1508 (June, 1957)

Bremsstrahlung of an ultra-relativistic particle of spin one-half in an arbitrary field with central symmetry is considered. A relation between the bremsstrahlung cross section and elastic scattering cross section is obtained for ultra-relativistic particles.

1. AS IS KNOWN, the bremsstrahlung in the collision of an ultra-relativistic charged particle with a nucleus occurs principally at large distances from the nucleus. The cross section for the process is therefore determined by the assymptotic form of the wave function of the particle in the nuclear field.[1-3] The assymptotic form of the particle wave functions may be found by describing the scattering effect of the nucleus by the scattering matrix. In the ultra-relativistic case, it is possible to establish a general relationship between bremsstrahlung and elastic scattering cross sections. This relationship does not depend on the character of the interaction between the particles and the scattering nuclear field.

Let us first of all consider the elastic scattering of fast particles with spin ½ in a field with central symmetry. The free motion of a spin-½ particle of momentum p is described by the spinor plane wave

$$\psi_0 = u_p e^{i\mathbf{pr}},$$

where u_p is the unit amplitude of the spinor wave. The scattering of particles in an external central field will be characterized by the scattering matrix S. The wave function describing the stationary states of the particles in the external field will then obviously be determined by the product of the matrix S by ψ_0

$$\psi_{\mathbf{p}}^{(+)} = S\psi_0. \tag{1}$$

At large distances from the center of the field, the wave function (1) will be of the form of a sum of a plane wave and an outgoing spherical wave. To verify this, let us use the Huygens principle as formulated by Akhiezer[4] for spinor waves. This principle establishes a relationship between the value of the wave function at a certain point and the value of the wave function on a closed surface surrounding this point. Let us choose for this surface an infinite plane perpendicular to the momentum of the impinging particle and passing through the center of the external field

$$\begin{aligned}\psi_{\mathbf{p}}^{(+)}(\mathbf{r}) &= \frac{1}{4\pi}\int\left(\gamma\frac{\partial}{\partial\mathbf{r}} - \gamma_4 E - m\right)\gamma\mathbf{n}\,\frac{\exp(ip\,|\mathbf{r}-\boldsymbol{\rho}|)}{|\mathbf{r}-\boldsymbol{\rho}|}\,S u_p e^{i\mathbf{p}\boldsymbol{\rho}}\,d\boldsymbol{\rho}\\ &= u_p e^{i\mathbf{pr}} - \frac{1}{4\pi}\int\left(\gamma\frac{\partial}{\partial\mathbf{r}} - \gamma_4 E - m\right)\gamma\mathbf{n}\,\frac{\exp(ip\,|\mathbf{r}-\boldsymbol{\rho}|)}{|\mathbf{r}-\boldsymbol{\rho}|}\,\{1-S\}\,u_p e^{i\mathbf{p}\boldsymbol{\rho}}\,d\boldsymbol{\rho}.\end{aligned} \tag{2}$$

Far from the center of the field ($r \to \infty$), this function has the form

$$\begin{gathered}\psi_{\mathbf{p}}^{(+)}(\mathbf{r}) \to u_p e^{i\mathbf{pr}} + f(\vartheta_e)\, u_{p_e} e^{ipr}/r,\\ f(\vartheta_e) = \frac{ip}{2\pi} u_{p_e}^{*} u_p \int \{1 - e^{2i\eta(\rho)}\} \exp\{-i(\mathbf{p}_e - \mathbf{p})\rho\}\, d\rho,\end{gathered} \tag{3}$$

where $\mathbf{p}_e = p\mathbf{r}/r$; the eigenvalues of the scattering operator S are expressed through the phase shifts $\eta(\rho)$. (It is assumed that the phase shift η is identical for $l + \frac{1}{2}$ and $l - \frac{1}{2}$, $l = \rho p$). The multiplier diverging wave $f(\vartheta_e)$ is the elastic-scattering amplitude.

Averaging the square of the modulus of the elastic-scattering amplitude over the initial polarizations, and summing it over the final polarizations, we obtain the following expression for the elastic scattering cross section of spin-½ particles

$$d\sigma_e = \left(1 - v^2 \sin^2 \frac{\vartheta_e}{2}\right) \left| \int_0^\infty \{1 - e^{2i\eta(\rho)}\}\, J_0(p \sin \vartheta_e \rho)\, \rho d\rho \right|^2 p^2 do_e. \tag{4}$$

This expression differs from the expression for elastic scattering cross section of particles without spin by an additional factor $[1 - v^2 \sin^2(\vartheta_e/2)]$. (We use a system of units where $c = \hbar = 1$.)

2. Let us now examine the scattering of a spin-½ particle with emission of a γ-quantum. Assuming the interaction between the charge and the electromagnetic field of the γ-quantum to be small we obtain the following expression for the transition matrix element

$$u_{i\to f} = -\frac{ie}{\sqrt{2\omega}} \int \psi_{\mathbf{p}'}^{(-)*} \gamma_4 \hat{e} e^{-i\mathbf{kr}} \psi_{\mathbf{p}}^{(+)}\, d\mathbf{r}, \tag{5}$$

where ω, $\mathbf{k}$ and $\mathbf{e}$ are the frequency, momentum and polarization of the emitted γ-quantum, and $\mathbf{p}'$ is the particle momentum after emission of the γ-quantum. At large distances from the center, the wave function of the particle in the final state $\psi_{\mathbf{p}'}^{(-)}$ has the form of a sum of a plane wave and a converging spherical wave

$$\psi_{\mathbf{p}'}^{(-)}(\mathbf{r}) = u_{p'} e^{i\mathbf{p}'\mathbf{r}} + \frac{1}{4\pi} \int \left(\gamma \frac{\partial}{\partial \mathbf{r}} - \gamma_4 E' - m\right) \gamma \mathbf{n}' \frac{\exp\{-ip' |\mathbf{r} - \rho|\}}{|\mathbf{r} - \rho|} \{1 - S^*\} u_{p'}\, d\rho. \tag{6}$$

In computing the matrix element (5), let us note that, in the ultra-relativistic case (E, $E' \gg m$), the spherical parts of the wave functions $\psi_{\mathbf{p}}^{(+)}$ and $\psi_{\mathbf{p}'}^{(-)}$ practically do not overlap. Noting also that, in the ultra-relativistic case, the main role is played by the small angles between $\mathbf{k}$, $\mathbf{p}'$ and $\mathbf{p}$, we obtain the matrix element in the form

$$u_{i\to f} = -\frac{2\pi i e}{\sqrt{2\omega}} \int_0^\infty \{1 - e^{2i\eta(\rho)}\}\, J_0(|k\boldsymbol{\vartheta} + p'\boldsymbol{\vartheta}'|\rho)\, \rho d\rho\; \bar{u}_{p'} \left\{ \frac{\hat{e}(i\hat{f}' - m)\hat{n}}{\mathbf{p}^2 - \mathbf{f}'^2} + \frac{\hat{n}'(i\hat{f} - m)\hat{e}}{\mathbf{p}'^2 - \mathbf{f}^2} \right\} u_p, \tag{5'}$$

where $f = p - k$, $f' = p' + k$ and the two-dimentional angular vectors $\boldsymbol{\vartheta}$ and $\boldsymbol{\vartheta}'$ are determined by the relations

$$\mathbf{p}' = (\mathbf{p}'\mathbf{n})\mathbf{n} + p'\boldsymbol{\vartheta}', \quad \mathbf{k} = (\mathbf{kn})\mathbf{n} + k\boldsymbol{\vartheta}.$$

The differential cross section for the emission of a γ-quantum by the particle is determined from the formula

$$d\sigma_\gamma = (2\pi/v)\, |u_{i\to f}|^2\, \delta(E - E' - \omega)\, d\mathbf{p}'\, d\mathbf{k}/(2\pi)^6, \tag{7}$$

where v is the velocity of the incident particle.

Averaging the cross section over the initial particle polarizations and summing it over the final particle polarizations and over polarizations of the emitted γ-quantum, we obtain

$$d\sigma_\gamma = \frac{e^2 p'}{2\omega p}\left|\int_0^\infty \{1 - e^{2i\eta(\rho)}\} J_0(|k\vartheta + p'\vartheta'|\rho)\rho\, d\rho\right|^2 \frac{1}{4}\,\mathrm{Sp}\, F\, \frac{\omega^2 d\omega}{(2\pi)^3}\, do\, do',$$

$$F = \left\{\frac{\hat{n}'(i\hat{f} - m)\gamma_i}{\mathbf{p}'^2 - \mathbf{f}^2} + \frac{\gamma_i(i\hat{f}' - m)\hat{n}}{\mathbf{p}^2 - \mathbf{f}'^2}\right\}(i\hat{p} - m)\left\{\frac{\gamma_i(i\hat{f} - m)\hat{n}'}{\mathbf{p}'^2 - \mathbf{f}^2} + \frac{\hat{n}(i\hat{f}' - m)\gamma_i}{\mathbf{p}^2 - \mathbf{f}'^2}\right\}(i\hat{p}' - m). \tag{8}$$

Calculating the trace the usual way, we finally obtain the following expression for the differential cross section for emission of a γ-quantum by an ultra-relativistic spin-½ particle in an external central field

$$d\sigma_\gamma = \frac{e^2 p'}{4\pi^3 p}\left|m\int_0^\infty \{1 - e^{2i\eta(\rho)}\} J_0(m|\mathbf{x} + \mathbf{y}|\rho)\rho\, d\rho\right|^2 \left\{\left(\frac{\mathbf{x}}{1 + x^2} + \frac{\mathbf{y}}{1 + y^2}\right)^2 + \frac{\omega^2}{2pp'}\frac{(\mathbf{x} + \mathbf{y})^2}{(1 + x^2)(1 + y^2)}\right\}\frac{d\omega}{\omega}\, d\mathbf{x}\, d\mathbf{y}, \tag{9}$$

where

$$\mathbf{x} = (p/m)\,\vartheta \text{ and } \mathbf{y} = (p'/m)(\vartheta' - \vartheta).$$

In the ultra-relativistic case ($E \gg m$), the elastic scattering will also principally occur at small angles; the cross section (4) can therefore be presented in the form

$$d\sigma_e = \sigma_e(u)\, d\mathbf{u}, \quad \sigma_e(u) = \left|m\int_0^\infty \{1 - e^{2i\eta(\rho)}\} J_0(mu\rho)\rho\, d\rho\right|^2,$$

where

$$\mathbf{u} = (p/m)\,\vartheta_e. \tag{10}$$

Comparing (9) and (10), one can establish the following general relationship between the elastic scattering cross section σ_e and bremsstrahlung from charged ultra-relativistic spin-½ particles:

$$d\sigma_\gamma = \sigma_e(|\mathbf{x} + \mathbf{y}|)\frac{e^2 p'}{4\pi^3 p}\left\{\left(\frac{\mathbf{x}}{1 + x^2} + \frac{\mathbf{y}}{1 + y^2}\right)^2 + \frac{\omega^2}{2pp'}\frac{(\mathbf{x} + \mathbf{y})^2}{(1 + x^2)(1 + y^2)}\right\}\frac{d\omega}{\omega}\, d\mathbf{x}\, d\mathbf{y}. \tag{11}$$

A similar relation holds for spin-zero particles†

$$d\sigma_\gamma^0 = \sigma_e^0(|\mathbf{x} + \mathbf{y}|)\frac{e^2 p'}{4\pi^3 p}\left(\frac{\mathbf{x}}{1 + x^2} + \frac{\mathbf{y}}{1 + y^2}\right)^2\frac{d\omega}{\omega}\, d\mathbf{x}\, d\mathbf{y}. \tag{12}$$

Integrating (11) over the angle x and y, we obtain the spectral distribution of the radiation

$$d\sigma_\gamma(\omega) = \frac{4e^2 p'\, d\omega}{\pi p\omega}\int_{q_m}^\infty \sigma_e(2q)\left\{\frac{2q^2 + 1}{q\sqrt{1 + q^2}}\ln(q + \sqrt{1 + q^2}) - 1 + \frac{\omega^2}{pp'}\frac{q}{\sqrt{1 + q^2}}\ln(q + \sqrt{1 + q^2})\right\} q\, dq, \tag{13}$$

where $q = \frac{1}{2}|\mathbf{x} + \mathbf{y}|$, and the minimum value q_m is determined by the conservation law: $q_m = m\omega/4EE'$.

3. As an illustration, let us apply the obtained formulas to the case of scattering of fast protons by absorbing nuclei.* In this case, the scattering matrix can be written in the form

---

* The relationship between $d\sigma_\gamma$ and the elastic scattering amplitude for spin zero particles was also obtained in Ref. 3.

† It should be noted that, in the case of a proton, a big role should be played by the radiation due to the anomalous magnetic moment; this effect has not been taken into account, however.

$$S=\begin{cases}0, & \rho\leqslant R\\ e^{2i\eta(\rho)}, & \rho>R,\end{cases}$$

where R is the nuclear radius, $\eta(\rho)\simeq n\ln p\rho\,(p\rho\gg 1)$ and $n=Ze^2E/4\pi p$.

The elastic scattering cross section is equal to

$$d\sigma_e=\left(1-v^2\sin^2\frac{\vartheta}{2}\right)\left|\frac{RJ_1(pR\sin\vartheta)}{\sin\vartheta}+\frac{2inR}{\sin\vartheta}\int\limits_1^\infty J_1(pR\sin\vartheta\zeta)\zeta^{2in}d\zeta\right|^2do. \tag{14}$$

In the limiting case $n\ll 1$

$$d\sigma_e=\left(1-v^2\sin^2\frac{\vartheta}{2}\right)\left\{\frac{R^2J_1^2(pR\sin\vartheta)}{\sin^2\vartheta}+\frac{4n^2}{p^2}\frac{J_0^2(pR\sin\vartheta)}{\sin^4\vartheta}\right\}do. \tag{15}$$

The first term in the braces describes the differential scattering of particles by an absolutely black nucleus. The second term describes the scattering of charged particles in the Coulomb field of a nucleus of finite dimensions.

The cross section for emission of a γ-quantum during scattering of a proton by an absorbing nucleus is, taking into account the Coulomb interaction, equal to

$$d\sigma_\gamma=\frac{e^2p'}{4\pi^3p}\left|\frac{RJ_1(m|\mathbf{x}+\mathbf{y}|R)}{|\mathbf{x}+\mathbf{y}|}+\frac{2in}{|\mathbf{x}+\mathbf{y}|}\int\limits_R^\infty e^{2i[\eta(\rho)-\eta(R)]}J_1(m|\mathbf{x}+\mathbf{y}|\rho)\,d\rho\right|^2$$
$$\times\left\{\left(\frac{\mathbf{x}}{1+x^2}+\frac{\mathbf{y}}{1+y^2}\right)^2+\frac{\omega^2}{2pp'}\frac{(\mathbf{x}+\mathbf{y})^2}{(1+x^2)(1+y^2)}\right\}\frac{d\omega}{\omega}d\mathbf{x}\,d\mathbf{y}.$$

Setting $R=0$ in (16) and noting that

$$\int\limits_0^\infty e^{2i[\eta(\rho)-\eta(0)]}J_1(m|\mathbf{x}+\mathbf{y}|\rho)\,d\rho=(2p)^{2in}/(m|\mathbf{x}+\mathbf{y}|)^{2in+1}, \tag{16}$$

we obtain the Bethe-Heitler formula for bremsstrahlung from a proton in the Coulomb field of a nucleus

$$d\sigma_\gamma^{\mathrm{B-H}}=\frac{n^2e^2}{\pi^3}\frac{p'}{p}\frac{1}{m^2|\mathbf{x}+\mathbf{y}|^4}\left\{\left(\frac{\mathbf{x}}{1+x^2}+\frac{\mathbf{y}}{1+y^2}\right)^2+\frac{\omega^2}{2pp'}\frac{(\mathbf{x}+\mathbf{y})^2}{(1+x^2)(1+y^2)}\right\}\frac{d\omega}{\omega}d\mathbf{x}\,d\mathbf{y}. \tag{17}$$

Setting $n=0$ in (16), we obtain the Akhiezer formula[4] for the diffraction radiation of γ-quanta by protons

$$d\sigma_\gamma^{\mathrm{A}}=\frac{e^2}{4\pi^3}\frac{p'}{p}\frac{R^2J_1^2(m|\mathbf{x}+\mathbf{y}|R)}{|\mathbf{x}+\mathbf{y}|^2}\left\{\left(\frac{\mathbf{x}}{1+x^2}+\frac{\mathbf{y}}{1+y^2}\right)^2+\frac{\omega^2}{2pp'}\frac{(\mathbf{x}+\mathbf{y})^2}{(1+x^2)(1+y^2)}\right\}\frac{d\omega}{\omega}d\mathbf{x}\,d\mathbf{y}. \tag{18}$$

Equation (16) describes bremsstrahlung due to Coulomb interaction as well as to the presence of diffraction. In the limiting case $n\ll 1$, this cross section is equal to

$$d\sigma_\gamma=\frac{e^2p'}{4\pi^3p}\left\{\frac{R^2J_1(m|\mathbf{x}+\mathbf{y}|R)}{|\mathbf{x}+\mathbf{y}|^2}+\frac{4n^2}{m^2}\frac{J_0^2(m|\mathbf{x}+\mathbf{y}|R)}{|\mathbf{x}+\mathbf{y}|^4}\right\}$$
$$\times\left\{\left(\frac{\mathbf{x}}{1+x^2}+\frac{\mathbf{y}}{1+y^2}\right)^2+\frac{\omega^2}{2pp'}\frac{(\mathbf{x}+\mathbf{y})^2}{(1+x^2)(1+y^2)}\right\}\frac{d\omega}{\omega}d\mathbf{x}\,d\mathbf{y}. \tag{19}$$

I express my deep gratitude to A. I. Akhiezer for discussing this work.

---

[1] L. D. Landau and I. Ia. Pomeranchuk, J. Exptl. Theoret. Phys. (U.S.S.R.) 24, 505 (1953).

[2] E. L. Feinberg, Uspekhi Fiz. Nauk 58, 193 (1956).

[3] Iu. A. Vdovin. Dokl. Akad. Nauk SSSR 105, 947 (1955).

[4] A. I. Akhiezer, Dokl. Akad. Nauk SSSR 94, 651 (1954).

Translated by E. S. Troubetskoy
293

SOVIET PHYSICS JETP VOLUME 5, NUMBER 6 DECEMBER 15, 1957

Quantum Theory of the Electrical Conductivity of Metals in a Magnetic Field

I. M. LIFSHITZ
Physico-Technical Institute, Academy of Sciences, U.S.S.R.

(Submitted to JETP editor November 22, 1956)
J. Exptl. Theoret. Phys. (U.S.S.R.) 32, 1509-1518 (June, 1957)

A consistent quantum mechanical theory of the electrical conductivity of metals in a magnetic field is constructed. The kinetic equation for the density matrix is derived on the basis of some general assumptions regarding the electron energy spectrum, and the transition to the classical limit is analyzed. The asymptotic values of the kinetic coefficients in a strong magnetic field are analyzed. On the basis of the relations established between the solutions to the quantum and classical equations quantum corrections, including oscillations of the conductivity, are found for the kinetic coefficients.

AS IS WELL KNOWN, the correct description of metallic conductivity is essentially quantum mechanical. Nevertheless, since the wavelength of the electron is small compared with its mean free path and, in the presence of a magnetic field, also compared with the radius of curvature of its trajectory, it is usually sufficient to treat the problem semiclassically. This means that the electron may be treated classically, as a quasi-particle satisfying Fermi statistics and a certain dispersion law

$$\varepsilon = \varepsilon_j(p_x, p_y, p_z) \tag{1}$$

($\varepsilon_j(\mathrm{p})$ is a periodic function with the period of the reciprocal lattice, and j is the band number). It was on this basis that the semiclassical theory of the galvanomagnetic effects in metals[1] was developed.

Such a treatment, however, fails to show up certain specific quantum effects (for instance the oscillation of the resistance with the magnetic field) related to the quantum levels. These effects are experimentally observed,[2] but their theoretical study[3] does not seem to us to be sufficiently consistent or satisfactory.

The present work is an attempt to construct a consistent quantum theory of metallic conduction in a magnetic field. The theory makes it possible to study the above-mentioned oscillatory quantum effects and the transition to the classical limit.

As has been shown,[4] the energy levels ε_n for a particle with the dispersion law of Eq. (1) and in a magnetic field H directed along the z axis are given in the quasi-classical approximation by the condition

$$S(\varepsilon_n, p_z) = (eh/c)H(n+\gamma), \quad n \gg 1, \quad 0<\gamma<1, \tag{2}$$

where $S(\varepsilon, p_z)$ is the area of the intersection between the surface of Eq. (1) and the plane p_z = const in quasi-momentum space.

According to Eq. (2), the separation between levels will be

$$\Delta\varepsilon_n = \varepsilon_{n+1} - \varepsilon_n = \hbar\omega^* = \mu^* H; \quad \mu^* = e\hbar/m^*c; \tag{3}$$

$$\omega^* = eH/m^*c; \quad m^* = (1/2\pi)\,\partial S/\partial\varepsilon; \quad m^* = m^*(\varepsilon, p_z). \tag{4}$$

Thus significant effects may be expected when $\hbar\omega^* \geqslant kT$. On the other hand, in order for the quasi-classical approximation to be valid and the dispersion law of Eq. (1) to be applicable, it is necessary that $\hbar\omega \ll \zeta$ (where ζ is the chemical potential). In what follows, we shall assume this condition to be fulfilled.

1. THE KINETIC EQUATION FOR THE DENSITY MATRIX

Assuming the electron to be in a homogeneous magnetic field **H** and a weak electric field **E**, let us write its Hamiltonian in the form

$$\hat{\mathscr{H}} = \hat{\mathscr{H}}_0 + \hat{U}; \quad \hat{U} = -e\mathbf{E}\hat{\mathbf{r}}, \tag{5}$$

where $\hat{\mathscr{H}}_0$ is the kinetic energy operator of the electron in the magnetic field. This operator, at least in the quasi-classical approximation, is obtained from $\varepsilon(\mathrm{p})$ by replacing the components of the momentum p by the components of the kinetic momentum operator $\hat{\mathbf{p}}$, and by suitable symmetrization whose exact meaning will not be of importance for us.

Since the kinetic momentum operators $\hat{p}_x$, $\hat{p}_y$, $\hat{p}_z$

with a magnetic field $H_z = H$ do not commute $\{\hat{p}_x, \hat{p}_y\} = eH/c$) we shall describe the states of the electron gas by a density matrix $\hat{f}$, rather than by a distribution function.

When there is no electric field ($\hat{U} = 0$), the operator $\hat{f} = \hat{f}^0$ is the equilibrium Fermi function

$$\hat{f}^0 = \hat{f}^0(\hat{\mathscr{H}}_0); \quad f^0(\varepsilon) = [1 + e^{(\varepsilon-\zeta)/\Theta}]^{-1}, \quad \Theta = kT \tag{6}$$

(where ζ is the chemical potential). In the presence of an electric field, we shall set

$$\hat{f} = \hat{f}^0 + \hat{f}^1. \tag{7}$$

In what follows we shall treat the operator $\hat{\mathscr{H}}_0$ in the representation in which n and p_z are diagonal, and then as will be seen, in the quasi-classical approximation we may consider $\hat{f}^1$ a matrix with respect to n and a number with respect to p_z (this is related to the fact that the momentum p_z is not quantized).

When dealing with several electron bands, the band number j enters into $\hat{f}$ as a parameter. This follows from the fact that in the classical motion of a particle, j remains constant. Therefore in the quasi-classical approximation, the parameter j can change only as a result of collisions, and this can be accounted for in the collision matrix. The situation is exactly similar with respect to the spin states s, whose treatment requires the introduction of an additional parameter s into $\hat{f}$, since the energy levels depend on s according to

$$\varepsilon_{ns} = \varepsilon_n(p_z) + s\mu_0 H; \quad s = \pm 1; \quad \mu_0 = e\hbar/2m_0c.$$

We shall henceforth suppress the indices j, s.

The kinetic equation for $\hat{f}^1$ can be written in the form

$$\{\hat{f}^0, \hat{\mathscr{H}}\} + \{\hat{f}^1, \hat{\mathscr{H}}\} + \widetilde{W}\hat{f}^1/t_0 = 0. \tag{8}$$

Here $\widetilde{W}/t_0$ is a certain linear transformation corresponding to the collision integral, t_0 is the characteristic relaxation time, and the curly brackets indicate quantum Poisson brackets. In order to make the analysis that will follow as clear as possible, let us start with the simplest case $\widetilde{W} = 1$.

Bearing in mind the obvious relation $\{\hat{f}^0, \hat{\mathscr{H}}_0\} = 0$ and neglecting the term $\{\hat{f}^1, \hat{U}\}$, which is quadratic in the electric field, we obtain

$$\{\hat{f}^1, \hat{\mathscr{H}}_0\} + \hat{f}^1/t_0 = -\{\hat{f}^0, \hat{U}\}. \tag{9}$$

Writing out the matrix elements and taking account of the fact that $\hat{\mathscr{H}}_0$ and $\hat{f}^0$ are diagonal, we have

$$i(\varepsilon_{n'} - \varepsilon_n) f^1_{nn'}/\hbar + f^1_{nn'}/t_0 = (f^0_{n'} - f^0_n)\cdot iU_{nn'}/\hbar. \tag{10}$$

From the equations of motion of the electron in a magnetic field, it follows that

$$-\{\hat{\mathscr{H}}_0, \hat{\mathbf{r}}\} = \dot{\hat{\mathbf{r}}} = \hat{\mathbf{v}}, \tag{11}$$

or, from Eq. (5),

$$(i/\hbar)(\varepsilon_n - \varepsilon_{n'}) U_{nn'} = e\mathbf{E}(\hat{\mathbf{v}})_{nn'}, \tag{11a}$$

where $\hat{\mathbf{v}}$ is the velocity operator corresponding to the classical quantity $\mathbf{v} = \partial\varepsilon/\partial\mathbf{p}$. This gives

$$\left\{\frac{i}{\hbar}(\varepsilon_{n'} - \varepsilon_n) + \frac{1}{t_0}\right\} f^1_{nn'} = -\frac{f^0_{n'} - f^0_n}{\varepsilon_{n'} - \varepsilon_n} e\mathbf{E}\mathbf{v}_{nn'}. \tag{12}$$

According to Eq. (3), we have $\varepsilon_n - \varepsilon_n = (n' - n)\hbar\omega^*$. Now setting

$$\hat{f}^1 = -et_0\mathbf{E}\hat{\boldsymbol{\psi}} \tag{13}$$

and dividing Eq. (12) by ω^*, we obtain

$$[i(n' - n) + \gamma]\hat{\boldsymbol{\psi}}_{nn'} = \gamma g_{nn'}\hat{\mathbf{v}}_{nn'},$$

$$\gamma = 1/t_0\omega^* = H_0^*/H; \quad H_0^* = m^*c/et_0; \tag{14}$$

$$g_{nn'} = (f^0_{n'} - f^0_n)/(\varepsilon_{n'} - \varepsilon_n).$$

Setting $n' - n = k$, we finally arrive at

$$(ik + \gamma)\boldsymbol{\psi}_k = \gamma g_k \mathbf{v}_k. \tag{15}$$

Here we have introduced the notation

$$\boldsymbol{\psi}_{n,\,n+k} = \boldsymbol{\psi}_k(\varepsilon_n, p_z); \quad \mathbf{v}_{n,\,n+k} = \mathbf{v}_k(\varepsilon_n, p_z), \tag{16}$$

$$g_k(\varepsilon_n) = g_{n,\,n+k} = g_{n+k,\,n}$$

$$= [f^0(\varepsilon_n + k\hbar\omega^*) - f^0(\varepsilon_n)]/k\hbar\omega^*. \tag{17}$$

When $k = 0$, the expression for g_k is indeterminate. Simple calculation† shows that

$$g_0(\varepsilon) = \partial f^0 / \partial \varepsilon. \tag{17a}$$

It is easily seen that as $\hbar\omega^* \to 0$ we have

$$g_k(\varepsilon) \to \partial f^0 / \partial \varepsilon, \tag{18}$$

and Eq. (15) becomes

$$\begin{gathered}(ik + \gamma)\psi_k = \gamma \frac{\partial f^0}{\partial \varepsilon} \mathbf{v}_k; \quad \psi_k = \psi_k(\varepsilon, p_z); \\ \mathbf{v}_k = \mathbf{v}_k(\varepsilon, p_z).\end{gathered} \tag{19}$$

This is just the classical kinetic equation for the Fourier components of the distribution function $\boldsymbol{\psi} = \boldsymbol{\psi}(\varepsilon, p_z, \varphi)$ (where φ is the angle variable on the particle trajectory in momentum space, and is proportional to the time of rotation), derived previously.[1] Here the $\mathbf{v}_k$ are the Fourier amplitudes of the classical velocity vector, namely

$$\mathbf{v}(\varepsilon, p_z, \varphi) = \sum \mathbf{v}_k e^{ik\varphi}; \quad \mathbf{v} = \partial \varepsilon / \partial \mathbf{p}, \tag{20}$$

$$\begin{gathered}\mathbf{v}_k = \frac{1}{2\pi} \int\limits_0^{2\pi} \frac{\partial \varepsilon}{\partial \mathbf{p}} e^{-ik\varphi} d\varphi; \quad \varphi = 2\pi \int \frac{dl}{v_\perp} \Big/ \oint \frac{dl}{v_\perp}, \\ dl = |d\mathbf{p}|; \quad v_\perp = \sqrt{v_x^2 + v_y^2}.\end{gathered} \tag{21}$$

Returning to the quantum mechanical equation (15), let us replace the $\mathbf{v}_k(\varepsilon_n, p_z)$ by their limiting values of Eq. (21) (which corresponds to the quasi-classical approximation for the matrix elements $\mathbf{v}_{nn'}$). A similar replacement ($g_k \to \partial f^0 / \partial \varepsilon$) cannot be performed for the g_k, since $f^0(\varepsilon)$ varies very rapidly in the neighborhood of the limiting energy ($\varepsilon - \zeta \sim \Theta$), and the whole effect we are attempting to find is related just to this fact.

Thus as a solution to Eq. (15) we obtain

$$\psi_k = \gamma g_k \mathbf{v}_k / (ik + \gamma). \tag{22}$$

Let us now return to the general kinetic equation (8), and set

$$(\widetilde{W} \hat{\psi})_{n, n+k} = \hat{W}_{kk'} \psi_{k'}, \tag{23}$$

where $\hat{W}_{kk'}$ is an operator acting on the variables ε_n and p_z and the functions $\boldsymbol{\psi}_k(\varepsilon_n, p_z)$ according to

$$\begin{gathered}\hat{W}_{kk'} \psi_{k'} = \sum_{\varepsilon'} \int W_{kk'}(\varepsilon, p_z; \varepsilon', p_z') \psi_{k'}(\varepsilon', p_z') \, dp_z \, \Delta\varepsilon' \\ (\varepsilon = \varepsilon_n, \quad \varepsilon' = \varepsilon_{n'}).\end{gathered} \tag{24}$$

(In taking account of transitions between different bands, the kernel $W_{kk'}$ also has the indices j and j'.) Then repeating all the previous considerations, we transform the original equation (8) to a form similar to (15), namely

$$ik\psi_k + \gamma \hat{W}_{kk'} \psi_{k'} = \gamma g_k \mathbf{v}_k. \tag{25}$$

Equation (25), just as (15), goes over to the classical equation (31) of Ref. 1 when $g_k(\varepsilon)$ is replaced by its value $\partial f^0 / \partial \varepsilon$ in the limit and in going over from summation in Eq. (24) to integration. Then in agreement with the correspondence principle, the $\hat{W}_{kk'}$ of Eq. (25) are the Fourier amplitudes of the collision operator in the classical Eq. (31) of Ref. 1.

Since the g_k, and therefore also the $\boldsymbol{\psi}_k$, are rapidly varying functions of ε_n and slowly varying functions of p_z (for fixed $\varepsilon_n = \varepsilon$), it is convenient to go over to integration over ε and summation over p_{zn} (*i.e.*, to the independent variables ε and n) in Eqs. (25) and (24). Solving Eq. (2) $n = n(\varepsilon, p_z)$ for p_z, we have

$$\begin{gathered}\sum_n \int F(\varepsilon_n, p_z) \, dp_z \, \Delta\varepsilon_n = \int \Big\{ \sum_{p_{zn}} F(\varepsilon, p_{zn}) \Delta p_{zn} \Big\} d\varepsilon; \\ p_{zn} = p_z(n, \varepsilon); \quad \Delta p_{zn} = \frac{\partial P_z}{\partial n} = \frac{ehH}{c} \Big/ \frac{\partial S}{\partial p_z}\end{gathered} \tag{26}$$

(the limits of summation over n now depend on ε!).

Thus, for instance, for elastic scattering impurities, we have

---

†From the fact that $\dot{\hat{\mathscr{H}}}_0 = e\mathbf{E}\hat{\mathbf{v}}$, we have

$$\{\hat{f}^0, \hat{U}\} = \dot{\hat{f}}^0 = \lim \frac{f^0(\hat{\mathscr{H}}_0 + e\mathbf{E}\hat{\mathbf{v}}\delta t) - f^0(\hat{\mathscr{H}}_0)}{\delta t}.$$

Since $\hat{\mathscr{H}}_0$ is diagonal,

$$\{(\hat{\mathscr{H}}_0 + e\mathbf{E}\hat{\mathbf{v}}\delta t)^m - \hat{\mathscr{H}}_0^m\} / \delta t \,|_{nn} = e\mathbf{E}\mathbf{v}_{nn} \varepsilon_n^{m-1} m,$$

for all m, and for an arbitrary function $f^0(\hat{\mathscr{H}}_0)$ we have

$$\{\hat{f}^0, \hat{U}\}_{nn} = e\mathbf{E}\mathbf{v}_{nn} \partial f^0 / \partial \varepsilon,$$

which corresponds to (17a).

$$\hat{W}_{kk'}\psi_{k'} = \sum_{\varepsilon'}\int w_{kp_z,\,k'p'_z}(\varepsilon)\,\delta\,(\varepsilon-\varepsilon')\,[\psi_k(\varepsilon,p_z)-\psi_{k'}(\varepsilon',p'_z)]\,dp'_z\,\Delta\varepsilon' = \sum_{p'_z} w_{kp_z,k'p'_z}(\varepsilon)\,[\psi_k(\varepsilon,p_z)-\psi_{k'}(\varepsilon,p'_z)]\,\Delta p'_z. \qquad (27)$$

Correspondingly, now the quantities $\boldsymbol{\psi}_k$, $\mathbf{v}_k$ and g_k in Eqs. (25) and (27) are considered functions of the continuous variable ε and the discrete variable $p_{zn} = p_z(n, \varepsilon)$:

$$\psi_k = \psi_k(\varepsilon, p_{zn}); \quad \mathbf{v}_k = \mathbf{v}_k(\varepsilon, p_{zn});$$

$$g_k = g_k(\varepsilon, p_{zn}) = [f^0(\varepsilon + k\hbar\omega^*) - f^0(\varepsilon)]\,/\,k\hbar\omega^*;$$

$$g_0 = \partial f^0 / \partial\varepsilon. \qquad (28)$$

For scattering by impurities, the parameter $\hbar\omega^*/kT$ does not enter into the kernel of the collision operator of Eq. (27), and therefore the kernel w can be replaced by its classical expression. For inelastic scattering by phonons, such a replacement would seem to be invalid.

As in the classical case, it is impossible to obtain an explicit solution of Eq. (25) for arbitrary fields and without any specific assumptions with regard to the collision integral. Thus our problem is first to study the asymptotic behavior of the conductivity σ_{ik} for strong fields ($\gamma \ll 1$), and second to clarify the connection between the quantum mechanical and classical expressions for σ_{ik} for arbitrary values of γ. In this second case we shall consider the classical problem solved, and shall describe the quantum effects in terms of the classical solution.

2. HIGH-FIELD ($\gamma \ll 1$) LIMIT OF THE CONDUCTIVITY

As has been previously mentioned,[1] the high-field limit of the conductivity is determined essentially by the topology of the Fermi surface. Since the equations are quantized only for the case of closed orbits (finite motion), all our quantum mechanical considerations pertain indeed to this case.

This means, in particular, that in view of the equation of motion in a magnetic field, we have

$$\{\hat{\mathbf{p}}, \hat{\mathscr{H}}_0\} = \frac{e}{c}\,[\mathbf{v}\mathbf{H}], \qquad (29)$$

which, in terms of matrix elements, can be written in the form

$$ik\mathbf{p}_k = m^*\,[\mathbf{v}_k\,\mathbf{n}]; \quad \mathbf{H} = H\mathbf{n}. \qquad (30)$$

The diagonal matrix elements of the velocity in the xy plane, perpendicular to the direction $\mathbf{n}$ of the magnetic field, vanish, so that

$$[\mathbf{v}_{nn}\,\mathbf{n}] = [\mathbf{v}_0\,\mathbf{n}] = 0. \qquad (31)$$

Let us introduce the components of the operator $\hat{\boldsymbol{\psi}}$ according to

$$[\hat{\psi}\,\mathbf{n}] = \hat{\boldsymbol{\varphi}}; \quad (\hat{\psi}\,\mathbf{n}) = \hat{\vartheta}. \qquad (32)$$

From (13) we have

$$\hat{f}^1 = et_0\,\{(\hat{\boldsymbol{\varphi}}\,[\mathbf{E}\mathbf{n}]) + \hat{\vartheta}\,(\mathbf{E}\mathbf{n})\}. \qquad (33)$$

Bearing (30) in mind, Eq. (25) leads to

$$ik\boldsymbol{\varphi}_k + \gamma\hat{W}_{kk'}\,\boldsymbol{\varphi}_{k'} = ik\gamma g_k\,\mathbf{p}_k\,/\,m^*. \qquad (34)$$

In order to expand $\boldsymbol{\varphi}_k$ in powers of γ, we must first eliminate $\boldsymbol{\varphi}_0$ from (34). Setting $k = 0$ in (34), we have

$$\boldsymbol{\varphi}_0 = -\hat{W}_{00}^{-1}\,\hat{W}_{0k'}\,\boldsymbol{\varphi}_{k'}; \quad k' \neq 0. \qquad (35)$$

From this we obtain

$$\boldsymbol{\varphi}_k - \gamma\hat{L}_{kk'}\,\boldsymbol{\varphi}_{k'} = \gamma g_k\,\mathbf{p}_k\,/\,m^*; \quad k, k' \neq 0, \qquad (36)$$

$$\hat{L}_{kk'} = (i/k)\,\{\hat{W}_{kk'} - \hat{W}_{k0}\,\hat{W}_{00}^{-1}\,\hat{W}_{0k'}\}; \quad k, k' \neq 0, \qquad (37)$$

and the solution is easily written in the form of a power series in γ, namely

$$\boldsymbol{\varphi}_k = (1 - \gamma\hat{L})_{kk'}^{-1}\,\gamma\,\frac{g_{k'}\,\mathbf{p}_{k'}}{m^*} = \gamma\,\frac{g_k\,\mathbf{p}_k}{m^*} + \gamma\hat{L}_{kk'}\,\gamma\,\frac{g_{k'}\,\mathbf{p}_{k'}}{m^*} + \cdots \qquad (38)$$

Similarly,

$$\vartheta_0 = \hat{W}_{00}^{-1}\,\{v_0^z\,\partial f^0/\partial\varepsilon - \hat{W}_{0k'}\,\vartheta_{k'}\}, \qquad (39)$$

whence

$$\vartheta_k - \gamma\hat{L}_{kk'}\,\vartheta_{k'} = \gamma h_k;$$

$$\frac{\gamma}{ik}\left\{g_k\,v_k^z - \hat{W}_{k0}\,\hat{W}_{00}^{-1}\,\frac{\partial f^0}{\partial\varepsilon}\,v_0^z\right\} = \gamma h_k, \qquad (40)$$

and therefore

$$\vartheta_k = \gamma h_k + \gamma \hat{L}_{kk'} \gamma h_{k'} = \cdots, \quad (k \neq 0), \tag{41}$$

$$\vartheta_0 = \hat{W}_{00}^{-1} \frac{\partial f^0}{\partial \varepsilon} v_0^z - \hat{W}_{00}^{-1} \hat{W}_{0k'} \gamma h_{k'} + \cdots \tag{41a}$$

We thus see that as in the classical case all the φ_k and ϑ_k, except ϑ_0, start with the first power of γ (of the order of $1/H$). Furthermore, the terms linear in γ in the expression for φ_k (with $k \neq 0$) do not depend on the collision integral.

The current in which we are interested is given by the expression

$$\mathbf{j} = e \operatorname{Sp} \hat{f}^1 \hat{\mathbf{v}}. \tag{42}$$

In view of the above, the terms linear in $\gamma \sim 1/H$ in the components σ^{xx}, σ^{xy}, and σ^{yy} of the conductivity tensor are not related to the collision integral, and an explicit expression for them is easily obtained. In order to find the components j^x and j^y, let us find the expression $[\mathbf{jn}]$. From (29) and (8) we have

$$\begin{aligned}[\mathbf{jn}] = e \operatorname{Sp} \hat{f}^1 [\hat{\mathbf{v}}\mathbf{n}] &= \frac{c}{H} \operatorname{Sp} \hat{f}^1 \{\hat{\mathbf{p}}, \mathscr{H}_0\} \\ &\hat{=} \frac{c}{H} \operatorname{Sp} \hat{\mathbf{p}} \{\hat{\mathscr{H}}_0, \hat{f}^1\} \\ = \frac{c}{H} \operatorname{Sp} \hat{\mathbf{p}} \{\hat{f}^0, \hat{U}\} &+ \frac{c}{H t_0} \operatorname{Sp} \hat{\mathbf{p}} \widetilde{W} \hat{f}^1.\end{aligned} \tag{43}$$

As follows from (33) and (38), retaining terms of order $1/H$, we have

$$(c/Ht_0) \operatorname{Sp} \hat{\mathbf{p}} \widetilde{W} \hat{f}^1 = (ec/H) E_z \operatorname{Sp} \hat{\mathbf{p}} \widetilde{W} \vartheta.$$

Terms proportional to E_x and E_y are given by the first term. Since $\hat{U} = -eE_j x^j$, we have

$$[\mathbf{jn}] = -\frac{ec}{H} E_i \operatorname{Sp} \hat{\mathbf{p}} \{\hat{f}^0, \hat{x}^i\}. \tag{44}$$

Going over to the components j^x and j^y of the current, up to terms of order $1/H^2$ we obtain

$$\sigma_{ik} = \sigma_{ik}^{(1)} + O(H^{-2}),$$

$$\sigma_{xx}^{(1)} = \frac{ec}{H} \operatorname{Sp} \hat{p}_y \{\hat{f}^0, \hat{x}\}, \quad \sigma_{yy}^{(1)} = -\frac{ec}{H} \operatorname{Sp} \hat{p}_x \{\hat{f}^0, \hat{y}\},$$

$$\sigma_{xy}^{(1)} = \frac{ec}{H} \operatorname{Sp} \hat{p}_x \{\hat{f}^0, \hat{x}\}. \tag{45}$$

From the equation

$$\operatorname{Sp} \hat{p}_y \{\hat{f}^0, \hat{x}\} = \operatorname{Sp} \hat{f}_0 \{\hat{x}, \hat{p}_y\} = 0$$

and a similar one for $\sigma_{yy}^{(1)}$, we have

$$\sigma_{xx}^{(1)} = \sigma_{yy}^{(1)} = 0. \tag{46}$$

In view of the relation $\{\hat{p}_x, \hat{x}\} = 1$, the expression for $\sigma_{xy}^{(1)}$ must be dealt with more carefully (it is not correct simply to change the order of the factors in the trace). Detailed calculations show that when all the isoenergetic surfaces of Eq. (1) in the neighborhood $|\varepsilon - \zeta| \sim \Theta$ are closed, we obtain the expressions

$$\begin{aligned}&\operatorname{Sp} \hat{p}_x \{\hat{f}^0, \hat{x}\} = \operatorname{Sp} \hat{f}^0 = N_+ \quad \text{for } \partial\varepsilon/\partial n > 0, \\ &\operatorname{Sp} \hat{p}_x \{\hat{f}^0, \hat{x}\} = \operatorname{Sp} (\hat{f}^0 - 1) = -N_- \\ &\qquad \text{for } \partial\varepsilon/\partial n < 0,\end{aligned} \tag{47}$$

for each band separately, where N_+ is the number of occupied states with $m^* > 0$ (number of "electrons"), and N_- is the number of occupied states with $m^* < 0$ (number of "holes"). Thus in this case we have

$$\sigma_{xy}^{(1)} = (ec/H) \left(\sum N_+ - \sum N_- \right), \tag{48}$$

which is the same as the previously obtained classical result. As in the classical case, when the topology of the Fermi surfaces is more complicated, Eq. (48) is not valid.

When the number of "holes" and "electrons" is equal,

$$\sigma_{xy}^{(1)} = 0. \tag{49}$$

We have thus shown that there are no quantum corrections to those terms the expansion of σ_{ik} in powers of γ which vanish in the classical case.

This means that, at least in the quasi-classical approximation, significant effects can be expected only in the temperature dependence of the conductivity and in the occurrence of quantum fluctuations. We shall now go on to a consideration of these questions.

3. THE RELATION BETWEEN THE QUANTUM MECHANICAL AND CLASSICAL EXPRESSIONS FOR THE CONDUCTIVITY IN A MAGNETIC FIELD

The expression for the conductivity tensor $\sigma^{xx'}$ is, according to (42) and (13),

$$\sigma^{xx'} = -e^2 t_0 \,\mathrm{Sp}\, \hat{v}^x \hat{\psi}^{x'}. \tag{50}$$

Noting that $\hat{v}$ and $\hat{\psi}$ are Hermitian and diagonal with respect to p_z, we have

$$\sigma^{xx'} = A\int \sum_{n,\, n'} v^x_{n'n} \psi^{x'}_{n'n}\, dp_z$$

$$= A\int \Big\{ \sum_n v^x_{nn} \psi^{x'}_{nn} + 2\mathrm{Re} \sum_{n'>n} v^x_{nn'} \psi^{x'}_{n'n} \Big\} dp_z$$

$$= A \sum_n \int \{ v^x_0 \psi^{x'}_0 + 2\mathrm{Re} \sum_{k=1}^{\infty} v^x_{-k} \psi^{x'}_k \}\, dp_z. \tag{51}$$

The normalizing constant A is most simply determined by comparison with the classical limit $\hbar\omega \to 0$ (see Eq. (42) of Ref. 1). Noting that $m^*\Delta\varepsilon_n = eH\hbar/c$, we have

$$A = -2\,(e^2 t_0 / h^3)\,(eHh/c). \tag{52}$$

The ψ^x_k to be substituted into Eq. (51) must be a solution of the kinetic equation (25). In view of the linearity of (25) and (51) with respect to ψ^x_k and g_k, the results of this substitution can be written in the form of a certain "scalar product"

$$\sigma^{xx'} = -2\frac{e\hbar H}{c}(\chi^{xx'}, g);$$

$$(\chi^{xx'}, g) = \sum_n \int \Big\{ \sum_{k=0}^{\infty} \chi^{xx'}_k g_k \Big\} dp_z; \quad \chi = \chi_k(\varepsilon_n, p_z). \tag{53}$$

Since v^x_0 and v^y_0 vanish, and the term g_0 enters only into the equation for ψ^z, none of the components of $\sigma^{xx'}$ containg $g_0 = \partial f^0/\partial\varepsilon$, except σ^{zz}:

$$\sigma^{xx'} = -2\int \sum_{p_{zn}} \Big\{ \sum_{k=1}^{\infty} \chi^{xx'}_k g_k \Big\} m^* \Delta p_{zn}\, d\varepsilon,$$

$$(x, x' \neq z, z), \tag{54}$$

$$\sigma^{zz} = -2\int \sum_{p_{zn}} \Big\{ \chi^{zz}_0 \frac{\partial f^0}{\partial\varepsilon} + \sum_{k=1}^{\infty} \chi^{zz}_k g_k \Big\} m^* \Delta p_{zn}\, d\varepsilon. \tag{55}$$

Thus, for instance, in the case $\tilde{W} = 1$ we have, according to (22),

$$\chi^{xx'}_k = \frac{2\pi e^2 t_0}{h^3} \mathrm{Re} \frac{2\gamma}{ik+\gamma} v^x_{-k} v^x_k. \tag{56}$$

In particular, for the diagonal components of σ^{xx}

$$\chi^{xx}_k = \frac{4\pi e^2 t_0}{h^3} \frac{\gamma^2}{k^2+\gamma^2} |v^x_k|^2. \tag{57}$$

Expressions (56) and (57) agree exactly with the classical ones, since as has already been indicated the $\mathbf{v}_k$ are the Fourier amplitudes of the classical velocity vector; in order to obtain the classical expression for $\sigma^{xx'}$ it is sufficient to replace g_k by $\partial f^0/\partial\varepsilon$ in (54) and (55), and to go from summation over n to integration over $d\varepsilon$.

In the general case, the $\chi^{xx'}$ can be expressed in terms of the Green function of the kinetic equation (25)

$$ik\mathfrak{G}_k + \gamma \hat{W}_{kk'} \mathfrak{G}_{k'} = \gamma\delta(\varepsilon - \varepsilon^0)\, \delta_{p_{zn},\, p_{zn^\circ}} \delta_{kk^\circ} / \Delta p_{zn};$$

$$\mathfrak{G}_k = \mathfrak{G}(\varepsilon^0 p^0_z k^0 \,|\, \varepsilon p_z k); \qquad p_z = p_{zn} = p_z(n, \varepsilon);$$

$$p^0_z = p_{zn^\circ} \tag{58}$$

by means of the equation

$$m^*(\varepsilon^0, p^0_z)\chi^{xx'}_{k^\circ}(\varepsilon^0, p^0_z) = \frac{2\pi e^2 t_0}{h^3} 2\mathrm{Re} \int \sum_{p_z} \Big\{ \sum_k v^x_{k_\circ}(\varepsilon^0, p^0_z)$$

$$\times\, \mathfrak{G}(\varepsilon^0 p^0_z k^0 \,|\, \varepsilon p_z k)\, v^{x'}_{-k}(\varepsilon, p_z) \Big\} m^*(\varepsilon, p_z)\, d\varepsilon\, \Delta p_z. \tag{59}$$

The classical "Green function" is a solution of the equation

$$ik\mathfrak{G}_k + \gamma \hat{W}_{kk'} \mathfrak{G}_{k'} = \gamma\delta(\varepsilon - \varepsilon^0)\delta(p_z - p^0_z)\, \delta_{kk^\circ}, \tag{60}$$

where $\hat{W}_{kk'}$ is the classical limit of the collision integral; in order to obtain $\chi^{xx'}$, one must go from summation to integration over p_z in Eq. (59).

When only elastic scattering by impurities is of importance, the collision integral does not contain the temperature. Therefore $\chi^{xx'}$ does not contain the parameter $\mu^* H/\Theta = \hbar\omega^*/\Theta$ and the transition to the classical limit for $\chi^{xx'}$ means just neglecting quantities of the order of $\hbar\omega^*/\zeta$ in comparison with $\hbar\omega^*/\Theta$ entering into the quantum effects through the expressions

$$g_k = [f^0(\varepsilon + k\hbar\omega^*) - f^0(\varepsilon)] / k\hbar\omega^*.$$

Thus in the case indicated, we may consider the $\chi^{xx'}_k$ in (54) and (55) to be equal to their classical analogs.

The classical expression for the conductivity is obtained by the substitution $g_k \to \partial f^0/\partial\varepsilon$ and transition to the integral

$$\sigma^{xx'} = -2\iint \frac{\partial f^0}{\partial\varepsilon} \chi^{xx'} m^*\, dp_z\, d\varepsilon; \quad x, x' \neq z, z;$$

$$\sigma^{zz} = -2\iint \frac{\partial f^0}{\partial\varepsilon} \{\chi^{zz}_0 + \chi^{zz}\} m^*\, dp_z\, d\varepsilon; \tag{61}$$

$$\chi^{xx'} = \sum_{k=1}^{\infty} \chi_k^{xx'}. \tag{62}$$

Noting that the fundamental part of the quantum corrections is due to neighborhoods in which the function f^0 is highly nonstationary (that is, where $\varepsilon_n \cong \zeta$), and the functions $m^*(\varepsilon, p_z)$ and $\chi(\varepsilon, p_z)$ are smoothly varying, with the same accuracy, according to (54) and (17), we obtain the difference between the quantum and classical expressions for $\sigma^{xx'}$ (for $x, x' \neq z, z'$):

$$-\frac{1}{2}(\sigma^{xx'} - \sigma^{xx'}_{\text{class}}) = \sum_{k=1}^{\infty}\int\sum_n \left\{\chi_k^{xx'} \frac{f^0(\varepsilon_n + k\hbar\omega^*)}{k\hbar\omega^*} - \chi_k^{xx'} \frac{f^0(\varepsilon_n)}{k\hbar\omega^*}\right\} \Delta\varepsilon_n \, dp_z$$

$$- \sum_{k=1}^{\infty}\iint \chi_k^{xx'} \frac{\partial f^0}{\partial\varepsilon} m^* \, d\varepsilon \, dp_z = \sum_{k=1}^{\infty}\int dp_z \left\{\sum_{n \geqslant k} m^* \chi_k^{xx'} (\varepsilon - k\hbar\omega^*) \frac{f_n^0}{k} - \right.$$

$$\left. - \sum_{n \geqslant 0} m^* \chi_k^{xx'}(\varepsilon_n) \frac{f_n^0}{k} - f^0(\varepsilon_0) m^*(\varepsilon_0, p_z) \chi_k^{xx'}(\varepsilon_0, p_z) + \int f^0 (\partial(\chi_k^{xx'} m^*)/\partial\varepsilon) \, d\varepsilon\right\}$$

$$= - \sum_{k=1}^{\infty}\int dp_z \left\{\sum_{\varepsilon_n} (\partial(\chi_k^{xx'} m^*)/\partial\varepsilon_n) f^0(\varepsilon_n) \Delta\varepsilon_n - \int (\partial(\chi_k^{xx'} m^*)/\partial\varepsilon) f^0 \, d\varepsilon\right\}.$$

Summing over k, we obtain

$$\sigma^{xx'} - \sigma^{xx'}_{\text{class}} = -2\iint f^0 (\partial(\chi^{xx'} m^*)/\partial\varepsilon) \, d\varepsilon \, dp_z + \int\sum_n f^0 (\partial(\chi^{xx'} m^*)/\partial\varepsilon) \Delta\varepsilon \, dp_z.$$

Let us now go over to integration over n, making use of the fact that $\partial\varepsilon/\partial n = \hbar\omega^* = \Delta\varepsilon$ and Poisson's formula

$$\sigma^{xx'} - \sigma^{xx'}_{\text{class}} = \int \varphi^{xx'}(n) \, dn - \sum \varphi^{xx'}(n) = -\frac{1}{2}\varphi^{xx'}(0) + \sum_k I_k^{xx'};$$

$$\varphi^{xx'}(n) = -2\int f^0 \left.\frac{\partial(\chi^{xx'} m^*)}{\partial\varepsilon}\right|_{\varepsilon=\varepsilon(n,\, p_z)} \hbar\omega^* \, dp_z;$$

$$I_k^{xx'} = 2\int \varphi^{xx'}(n) e^{2\pi ikn} \, dn.$$

The expression obtained for the quantum corrections contains both an oscillating part and terms varying smoothly with the field. In the latter, however, a large contribution comes from levels with small n (in particular, from $\varphi(0)$). For these levels the quasi-classical approximation is exact only for the quadratic dispersion law. In general we need maintain only the oscillating part of the conductivity, since the smoothly varying part merely contributes a small correction to the basic classical value. Thus

$$\sigma^{xx'} - \sigma^{xx'}_{\text{class}} = m \sum_{k=1}^{\infty} I_k;$$

$$I_k = 2\iint f^0 \frac{\partial(\chi^{xx'} m^*)}{\partial\varepsilon} \hbar\omega^* e^{2\pi ikn} \, dn \, dp_z \tag{63}$$

Noting that according to (55) the expression for σ^{zz} contains an additional term with $\chi_0^{zz}\partial f^0/\partial\varepsilon$, we obtain in a similar way

$$\sigma^{zz} - \sigma^{zz}_{\text{class}} = \sum I_k^{zz} - \sum L_k^{zz};$$

$$L_k^{zz} = 2\iint \frac{\partial f^0}{\partial\varepsilon} \chi_0^{zz} m^* \hbar \omega^* e^{2\pi ikn} \, dn \, dp_z. \tag{64}$$

The structure of Eqs. (63) and (64) is such that it is easy to separate out the oscillating terms in I_k and L_k. Their detailed analysis, and a discussion of the various aspects of the Shubnikov–de Haas effect, is taken up in a separate article.

[1] Lifshitz, Azbel', and Kaganov, J. Exptl. Theoret. Phys. (U.S.S.R.) 31, 63 (1956); Soviet Phys. JETP 4, 41 (1957).

[2] W. de Haas, *et al.*, Leid. Commun. 237 (1935).

[3] A. I. Akhiezer, J. Exptl. Theoret. Phys. (U.S.S.R.)

9, 426 (1939); B. I. Davydov and I. Ia. Pomeranchuk, J. Exptl. Theoret. Phys. 9, 1295 (1939); G. E. Zil'berman, J. Exptl. Theoret. Phys. (U.S.S.R.) 29, 762 (1955); Soviet Phys. JETP 2, 650 (1956).

[4] I. M. Lifshitz and A. M. Kosevich, J. Exptl. Theoret. Phys. (U.S.S.R.) 29, 730 (1955); Soviet Phys. JETP 2, 636 (1956).

Translated by E. J. Saletan
294

SOVIET PHYSICS JETP VOLUME 5, NUMBER 6 DECEMBER 15, 1957

Vacuum Polarization in Mesonic Atoms

G. E. PUSTOVALOV
Moscow State University

(Submitted to JETP editor November 26, 1956)
J. Exptl. Theoret. Phys. (U.S.S.R.) 32, 1519-1527 (June, 1957)

Level shifts in mesonic atoms due to vacuum polarization produced by the nuclear electric field are computed. The recursion relations between the meson wave functions are used to derive equations in closed form for the first six level shifts. The shifts for the first three levels of heavy mesonic atoms are computed with allowance for the finite volume of the nucleus.

1. INTRODUCTION

TO STUDY THE PROPERTIES of mesonic atoms it is important to know the position of the energy levels of the meson. In light mesonic atoms (up to $Z \sim 20$), the energy level is determined principally by nonrelativistic formulas of the Keppler problem of hydrogen-like atoms, in which the electron mass is replaced by a reduced meson mass.[1] The most significant corrections for these formulas are the relativistic corrections, the level shifts due to the vacuum polarization by the electric field of the nucleus,[2] the shift due to the distribution of the positive charge over the volume of the nucleus, and in π-mesoatoms also the shift due to nuclear interaction between the meson and the nucleons of the nucleus.[3] In heavy mesonic atoms the effect of the finite volume of the nucleus on the position of the levels is so considerable that it can no longer be considered a small perturbation. For example, when the volume of the nucleus is taken into account, the energy of the 1S muon in μ-meso-lead turns out to have half the value given by the equation for point-like nuclei.[1] In the case of heavy mesonic atoms it therefore becomes necessary to solve from the very beginning for the motion of the meson in the electric field of a nucleus occupying a finite volume. As to the remaining significant corrections to the energy levels of heavy mesonic atoms, to which one must add also the influence of the quadrupole electric moment of the nucleus[4,5] and the polarization (deformation) of the nucleus by the meson,[6,7] these do not exceed 1 – 2% of the level energy.

While in the hydrogen atom the Lamb shift of the electron energy levels is due fundamentally to the correction for the field electromagnetic mass, and approximately 1/25th of the shift is caused by vacuum polarization, the situation in mesonic atoms is different. The vacuum polarization of electrons and positrons changes the electrostatic potential of the nucleus at a distance on the order of the Compton wavelength of the electron ($\sim 10^{-11}$ cm), regardless of what particle, electron or meson, moves around the nucleus. Since the Bohr radius of the orbit is inversely proportional to the mass of the particle, the radii of the meson orbits are 200 – 300 times smaller than the radii of the electron orbits and their dimensions are on the order of $10^{-11} - 10^{-12}$ cm. As a result, the meson spends a greater part of its time in a region where the electrostatic potential of the nucleus is changed by the influence of the vacuum polarization, which leads to a considerable level shift. At the same time, the correction for the electromagnetic intrinsic mass, which is inversely proportional to the square of the mass of the moving particle, will be considerably smaller in mesonic atoms than the Lamb shift for electrons, as a consequence of the greater mass of the meson.

The energy level shift due to vacuum polarization is a substantial correction for all mesonic atoms ($\sim 0.1 - 2\%$ of the energy of the level). The influence of vacuum polarization is noticeable at small Z also for levels with greater orbital momenta l, where the effect of the volume of the nucleus is relatively small. For example, the shift of the $3D_{5/2}$ level of μ-meso-uranium due to vacuum polarization is approximately 10 kev, and that due to the finite volume of the nucleus is only approximately 5 kev. This is clearly seen in Fig. 1 for mesonic atoms with small Z.

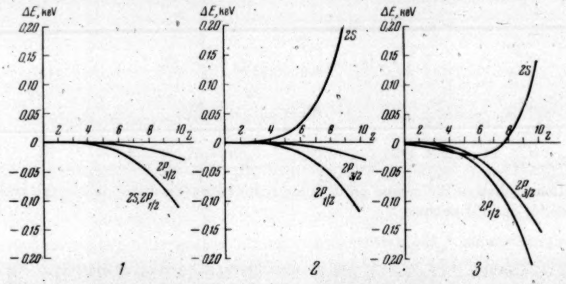

FIG. 1. Dependence of the splitting of the second level in light μ-mesonic atoms on Z, caused by various effects: 1 – relativistic splitting without allowance for the volume of the nucleus and vacuum polarization, 2 – with allowance for the volume of the nucleus, 3 – with additional allowance for vacuum polarization. The zero level represents the nonrelativistic level energy without allowance for the volume of the nucleus.

It is the purpose of this work to calculate the meson level shift due to vacuum polarization in the mesonic atom. For the first six levels, equations were derived for the shift in closed form. The effect of the nuclear volume is accounted for in the calculation of the level shift in heavy mesonic atoms.

2. CALCULATION OF THE LEVEL SHIFTS

To calculate the level shift due to vacuum polarization in mesonic atoms, let us take the Feynman form of the Fourier component of the effective polarization potential induced by an external electric field with a Fourier component of potential $\varphi_0(\mathbf{k})$ (see, for example, Ref. 8).

$$\varphi(\mathbf{k}) = \frac{\alpha}{\pi}\left[\frac{4k_0^2-2\mathbf{k}^2}{3\mathbf{k}^2}\left(1-\frac{\sqrt{4k_0^2+\mathbf{k}^2}}{|\mathbf{k}|}\sinh^{-1}\frac{|\mathbf{k}|}{2k_0}\right)+\frac{1}{9}\right]\varphi_0(\mathbf{k}), \tag{1}$$

where $k_0 = mc/\hbar$ (m is the electron mass), $\alpha = e^2/\hbar c$ is the fine-structure constant. For a concentrated point nucleus with a Coulomb potential

$$V(r) = eZ/r \tag{2}$$

the Fourier component of the potential will be

$$\varphi_0(\mathbf{k}) = eZ/2\pi^2 k^2. \tag{3}$$

In the coordinate representation we have for the polarization potential

$$\varphi(r) = \frac{4\alpha}{r}\int_0^\infty\left[\frac{4k_0^2-2k^2}{3k^2}\left(1-\frac{\sqrt{4k_0^2+k^2}}{k}\sinh^{-1}\frac{k}{2k_0}\right)+\frac{1}{9}\right]\varphi_0(k)\,k\sin kr\,dk. \tag{4}$$

The energy level shift will be determined by perturbation theory, averaging the polarization potential over the meson wave functions.

$$\Delta E_{nl} = -e\int |\psi_{nl}(r,\vartheta,\varphi)|^2 \varphi(r)\,d\tau = -e\int\limits_0^\infty R_{nl}^2(r)\,\varphi(r)\,r^2\,dr =$$

$$= -4\alpha e\int\limits_0^\infty I_{nl}(k)\,\varphi_0(k)\left[\frac{4k_0^2-2k^2}{3k^2}\left(1-\frac{\sqrt{4k_0^2+k^2}}{k}\operatorname{Arsh}\frac{k}{2k_0}\right)+\frac{1}{9}\right]k^2\,dk, \tag{5}$$

$$I_{nl}(k) = \frac{1}{k}\int\limits_0^\infty r R_{nl}^2(r)\sin kr\,dr. \tag{6}$$

Using the notation

$$x = k/2k_0,\quad \varepsilon = nk_0a/Z = nm/\alpha\mu Z,\quad y = kr \tag{7}$$

($a = \hbar^2/\mu e^2$ is the Bohr radius of the meson orbit, μ the reduced meson mass, and m the principal quantum number) expressions (5) and (6) become

$$\Delta E_{nl} = -\frac{4}{3}\alpha e\,(2k_0)^3\int\limits_0^\infty I_{nl}(\varepsilon x)\,\varphi_0(2k_0x)\left[(1-2x^2)\left(x-\sqrt{1+x^2}\sinh^{-1}x\right)+\frac{x^3}{3}\right]\frac{dx}{x}, \tag{8}$$

$$I_{nl}(\varepsilon x) = \frac{1}{k^3}\int\limits_0^\infty R_{nl}^2\left(\frac{an}{2Z\varepsilon x}y\right)y\sin y\,dy. \tag{9}$$

For a point concentrated nucleus, using the relation $\sinh^{-1}x = \ln(x+\sqrt{1+x^2})$ and Eq. (3), we can rewrite expression (8) for the level shift as

$$\Delta E_{nl} = -\frac{\alpha^2}{3\pi}mc^2 ZK_{nl}(\varepsilon), \tag{10}$$

$$K_{nl}(\varepsilon) = \frac{4}{\pi}\int\limits_0^\infty I_{nl}(\varepsilon x)\left\{(1-2x^2)\left[x-\sqrt{1+x^2}\ln\left(x+\sqrt{1+x^2}\right)\right]+\frac{x^3}{3}\right\}\frac{dx}{x^3}. \tag{11}$$

Taking for $R_{nl}(r)$ the expression for the radial portions of the wave functions of the Keppler problem of hydrogen-like atoms (see, for example, Ref. 9), we obtain, using the notation of (7)

$$\begin{aligned}
R_{10}^2 &= \frac{1}{2}\left(\frac{k}{\varepsilon x}\right)^3\exp\left\{-\frac{y}{\varepsilon x}\right\},\\
R_{20}^2 &= \frac{1}{8}\left(\frac{k}{\varepsilon x}\right)^3\left[4-4\frac{y}{\varepsilon x}+\left(\frac{y}{\varepsilon x}\right)^2\right]\exp\left\{-\frac{y}{\varepsilon x}\right\},\\
R_{21}^2 &= \frac{1}{24}\left(\frac{k}{\varepsilon x}\right)^3\left(\frac{y}{\varepsilon x}\right)^2\exp\left\{-\frac{y}{\varepsilon x}\right\},\\
R_{30}^2 &= \frac{1}{72}\left(\frac{k}{\varepsilon x}\right)^3\left[36-72\frac{y}{\varepsilon x}+48\left(\frac{y}{\varepsilon x}\right)^2-12\left(\frac{y}{\varepsilon x}\right)^3+\left(\frac{y}{\varepsilon x}\right)^4\right]\exp\left\{-\frac{y}{\varepsilon x}\right\},\\
R_{31}^2 &= \frac{1}{144}\left(\frac{k}{\varepsilon x}\right)^3\left[16-8\frac{y}{\varepsilon x}+\left(\frac{y}{\varepsilon x}\right)^2\right]\left(\frac{y}{\varepsilon x}\right)^2\exp\left\{-\frac{y}{\varepsilon x}\right\},\\
R_{32}^2 &= \frac{1}{720}\left(\frac{k}{\varepsilon x}\right)^3\left(\frac{y}{\varepsilon x}\right)^4\exp\left\{-\frac{y}{\varepsilon x}\right\}.
\end{aligned} \tag{12}$$

Noting that

$$\exp\{-y/\varepsilon x\} = 2\,(\varepsilon x/k)^3 R_{10}^2, \tag{13}$$

we obtain an expression for the squares of the wave functions of the higher state in terms of the square of the wave function of the 1S state and of its derivatives with respect to the parameter ε:

$$\begin{aligned} R_{20}^2 &= R_{10}^2 + \varepsilon \frac{dR_{10}^2}{d\varepsilon} + \frac{1}{4}\varepsilon^2 \frac{d^2R_{10}^2}{d\varepsilon^2}, \\ R_{21}^2 &= R_{10}^2 + \frac{2}{3}\varepsilon \frac{dR_{10}^2}{d\varepsilon} + \frac{1}{12}\varepsilon^2 \frac{d^2R_{10}^2}{d\varepsilon^2}, \\ R_{30}^2 &= R_{10}^2 + 2\varepsilon \frac{dR_{10}^2}{d\varepsilon} + \frac{4}{3}\varepsilon^2 \frac{d^2R_{10}^2}{d\varepsilon^2} + \frac{1}{3}\varepsilon^3 \frac{d^3R_{10}^2}{d\varepsilon^3} + \frac{1}{36}\varepsilon^4 \frac{d^4R_{10}^2}{d\varepsilon^4}, \\ R_{31}^2 &= R_{10} + \frac{16}{9}\frac{dR_{10}^2}{d\varepsilon}\varepsilon + \frac{19}{18}\varepsilon^2 \frac{d^2R_{10}^2}{d\varepsilon^2} + \frac{2}{9}\varepsilon^3 \frac{d^3R_{10}^2}{d\varepsilon^3} + \frac{1}{72}\varepsilon^4 \frac{d^4R_{10}^2}{d\varepsilon^4}, \\ R_{32}^2 &= R_{10}^2 + \frac{4}{3}\varepsilon \frac{dR_{10}^2}{d\varepsilon} + \frac{1}{2}\varepsilon^2 \frac{d^2R_{10}^2}{d\varepsilon^2} + \frac{1}{15}\varepsilon^3 \frac{d^3R_{10}^2}{d\varepsilon^3} + \frac{1}{360}\varepsilon^4 \frac{d^4R_{10}^2}{d\varepsilon^4}. \end{aligned} \tag{14}$$

If we now introduce into (11) the integrals (9), into which, in turn, we substitute expressions (14), and if we then interchange the order of integration with respect to x and y and the differentiation with respect to ε, we arrive, in the final analysis, to an expression for $K_{nl}(\varepsilon)$ in terms of $K_{10}(\varepsilon)$ and the derivatives of $K_{10}(\varepsilon)$ with respect to ε. Furthermore, the coefficients of the derivatives will coincide with the coefficients of the corresponding derivatives in (14). Thus, having determined the dependence of the shift of the 1S level on ε, we can obtain the shift of the remaining level by differentiating with respect to ε, thus facilitating the computations considerably.

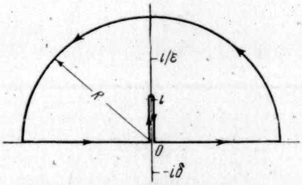

FIG. 2.

According to (9), we have for the 1S state

$$I_{10}(\varepsilon x) = [1 + (\varepsilon x)^2]^{-2}. \tag{15}$$

Then

$$K_{10}(\varepsilon) = \frac{4}{\pi}\int_0^\infty \left\{(1-2x^2)\left[x - \sqrt{1+x^2}\ln\left(x+\sqrt{1+x^2}\right)\right] + \frac{x^3}{3}\right\}\frac{dx}{x^3(1+\varepsilon^2x^2)^2}. \tag{16}$$

To calculate this integral let us consider the integral

$$K(\delta,\varepsilon) = \frac{4}{\pi\varepsilon^4}\int_C \frac{(1-2z^2)\left[z - \sqrt{1+z^2}\ln\left(z+\sqrt{1+z^2}\right)\right] + {}^1/_3(z+\delta i)^3}{(z+\delta i)^3(z+i/\varepsilon)^2(z-i/\varepsilon)^2}\,dz, \tag{17}$$

taken in the complex plane along the contour C, shown in Fig. 2, and so chosen that the branch point $z = i$ of the intergrand is located outside the contour. Let us assume that $\varepsilon < 1$, and then the intergrand has a second-order pole inside the contour at the point $z = i/\varepsilon$. Choosing the single-valued branch of the intergrand, we obtain with the aid of the residue theorem

$$\begin{aligned} \lim_{\delta\to 0} K(\delta,\varepsilon) &= 2\frac{4}{\pi\varepsilon^4}\int_0^\infty \frac{(1-2x^2)\left[x-\sqrt{1+x^2}\ln\left(x+\sqrt{1+x^2}\right)\right] + {}^1/_3x^3}{x^3(x^2+\varepsilon^{-2})^2}\,dx + \lim_{\delta\to 0}\frac{4i}{\varepsilon^4}\int_L \frac{(1-2z^2)\sqrt{1+z^2}}{(z+\delta i)^3(z^2+\varepsilon^{-2})^2}\,dz \\ &= \lim_{\delta\to 0} 2\pi i \operatorname{res}\left\{\frac{4}{\pi\varepsilon^4}\frac{(1-2z^2)\left[z-\sqrt{1+z^2}\ln\left(z+\sqrt{1+z^2}\right)\right] + {}^1/_3(z+\delta i)^3}{(z+\delta i)^3(z+i/\varepsilon)^2(z-i/\varepsilon)^2}\right\}_{z=i/\varepsilon} \end{aligned} \tag{18}$$

It was taken into account here that the integral along an arc of radius R tends to 0 as $R \to \infty$. The first integral equals $2K_{10}(\varepsilon)$. The integration path L of the second integral consists of the negative part of the real axis from $-\infty$ to 0 and the segment of the imaginary axis from 0 to i. This integral is calculated in a straightforward, although cumbersome, manner. As a result we obtain

$$2K_{10}(\varepsilon) - (3 + 4\varepsilon^2)\pi + \frac{2 - \varepsilon^2 - 4\varepsilon^4}{\varepsilon\sqrt{1 - \varepsilon^2}}\pi i = \frac{2}{\varepsilon}\left[-\frac{11}{3} - 4\varepsilon^2 + \frac{2 - \varepsilon^2 - 4\varepsilon^4}{\sqrt{1 - \varepsilon^2}}\left(\ln\frac{1 + \sqrt{1 - \varepsilon^2}}{\varepsilon} + \frac{\pi i}{2}\right)\right]. \tag{19}$$

Hence

$$K_{10}(\varepsilon) = \frac{1}{\varepsilon}\left[-\frac{11}{3} - 4\varepsilon^2 + \left(\frac{3}{2}\varepsilon + 2\varepsilon^3\right)\pi + \frac{2 - \varepsilon^2 - 4\varepsilon^4}{\sqrt{1 - \varepsilon^2}}\ln\frac{1 + \sqrt{1 - \varepsilon^2}}{\varepsilon}\right]. \tag{20}$$

If we now use Eq. (14), in which we substitute K_{nl} and the derivatives K_{10} in place of R^2_{nl} and the derivatives R^2_{10} with respect to ε, we obtain

$$\begin{aligned}
K_{20}(\varepsilon) &= \frac{1}{\varepsilon}\Big\{-\frac{16}{3} - 14\varepsilon^2 + \pi\left(\frac{3}{2}\varepsilon + 7\varepsilon^3\right) + \frac{3}{4}(1 - \varepsilon^2)^{-1} + \frac{9}{4}(1 - \varepsilon^2)^{-2} \\
&\quad + \left[\frac{13}{4} + 4\varepsilon^2 - 14\varepsilon^4 - \frac{9}{4}(1 - \varepsilon^2)^{-2}\right]\Phi(\varepsilon)\Big\}, \\
K_{21}(\varepsilon) &= \frac{1}{\varepsilon}\Big\{-\frac{14}{3} - 10\varepsilon^2 + \pi\left(\frac{3}{2}\varepsilon + 5\varepsilon^3\right) + \frac{5}{4}(1 - \varepsilon^2)^{-1} + \frac{3}{4}(1 - \varepsilon^2)^{-2} \\
&\quad + \Big[\frac{11}{4} + 2\varepsilon^2 - 10\varepsilon^4 - (1 - \varepsilon^2)^{-1} - \frac{3}{4}(1 - \varepsilon^2)^{-2}\Big]\Big)\Phi(\varepsilon)\Big\}, \\
K_{30}(\varepsilon) &= \frac{1}{\varepsilon}\Big\{-\frac{73}{9} - \frac{92}{3}\varepsilon^2 + \pi\left(\frac{3}{2}\varepsilon + \frac{46}{3}\varepsilon^3\right) + 2(1 - \varepsilon^2)^{-1} + \frac{77}{12}(1 - \varepsilon^2)^{-2} \\
&\quad - \frac{65}{6}(1 - \varepsilon^2)^{-3} + \frac{35}{4}(1 - \varepsilon^2)^{-4} + \Big[\frac{16}{3} + \frac{37}{3}\varepsilon^2 - \frac{92}{3}\varepsilon^4 - \frac{5}{12}(1 - \varepsilon^2)^{-1} \\
&\quad - \frac{37}{4}(1 - \varepsilon^2)^{-2} + \frac{55}{4}(1 - \varepsilon^2)^{-3} - \frac{35}{4}(1 - \varepsilon^2)^{-4}\Big]\Phi(\varepsilon)\Big\}, \\
K_{31}(\varepsilon) &= \frac{1}{\varepsilon}\Big\{-\frac{67}{9} - \frac{80}{3}\varepsilon^2 + \pi\left(\frac{3}{2}\varepsilon + \frac{40}{3}\varepsilon^3\right) + \frac{5}{2}(1 - \varepsilon^2)^{-1} \\
&\quad + \frac{37}{24}(1 - \varepsilon^2)^{-2} - \frac{35}{12}(1 - \varepsilon^2)^{-3} + \frac{35}{8}(1 - \varepsilon^2)^{-4} + \Big[\frac{29}{6} + \frac{31}{3}\varepsilon^2 - \frac{80}{3}\varepsilon^4 \\
&\quad - \frac{49}{24}(1 - \varepsilon^2)^{-1} - \frac{17}{8}(1 - \varepsilon^2)^{-2} + \frac{35}{8}(1 - \varepsilon^2)^{-3} - \frac{35}{8}(1 - \varepsilon^2)^{-4}\Big]\Phi(\varepsilon)\Big\}, \\
K_{32}(\varepsilon) &= \frac{1}{\varepsilon}\Big\{-\frac{55}{9} - \frac{56}{3}\varepsilon^2 + \pi\left(\frac{3}{2}\varepsilon + \frac{28}{3}\varepsilon^3\right) + \frac{19}{10}(1 - \varepsilon^2)^{-1} \\
&\quad + \frac{101}{120}(1 - \varepsilon)^{-2} + \frac{5}{12}(1 - \varepsilon^2)^{-3} + \frac{7}{8}(1 - \varepsilon^2)^{-4} + \Big[\frac{23}{6} + \frac{19}{3}\varepsilon^2 \\
&\quad - \frac{56}{3}\varepsilon^4 - \frac{37}{24}(1 - \varepsilon^2)^{-1} - \frac{5}{8}(1 - \varepsilon^2)^{-2} - \frac{1}{8}(1 - \varepsilon^2)^{-3} - \frac{7}{8}(1 - \varepsilon^2)^{-4}\Big]\Phi(\varepsilon)\Big\},
\end{aligned} \tag{21}$$

where

$$\Phi(\varepsilon)\,\frac{1}{\sqrt{1 - \varepsilon^2}}\ln\frac{1 + \sqrt{1 - \varepsilon^2}}{\varepsilon} \qquad (\varepsilon < 1). \tag{22}$$

These equations can be continued analytically to include the case when $\varepsilon > 1$. In this case (22) it becomes

$$\Phi(\varepsilon) = \frac{1}{\sqrt{\varepsilon^2 - 1}} \tan^{-1} \sqrt{\varepsilon^2 - 1}. \tag{23}$$

We finally determine the vacuum polarization shift of the first six energy levels of the meson in mesonic atoms with Eqs. (10) and (20) – (23). One need merely take into account that according to (7) ε has different values for states with different principal quantum numbers n. Figs. 3 and 4 show the Z-dependence of the level shifts for π and μ mesonic atoms, calculated with the aid of these equations.

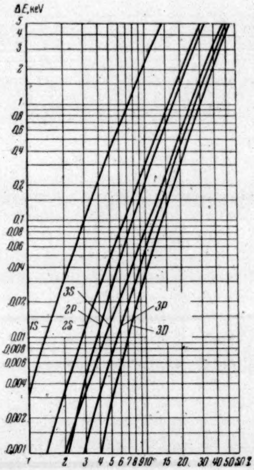

FIG. 3. Dependence of the value of the level shift of π-mesonic atoms on Z, caused by vacuum polarization. The mass of the pion is 272.5 m_e.

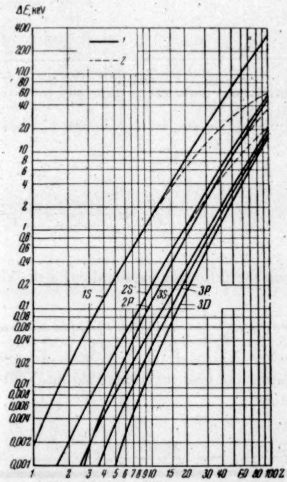

FIG. 4. Dependence of the value of the level shift of μ-mesonic atoms on Z, resulting from vacuum polarization: 1 – without allowance for the volume of the nucleus, 2 – with allowance for the volume of the nucleus.

3. ALLOWANCE FOR THE VOLUME OF THE NUCLEUS

Taking account of the volume distribution of the charge of the nucleus reduces considerably the effect of vacuum polarization in high-Z mesonic atoms (see Refs. 10 and 11). The fact that the nucleus is not concentrated in a point leads, on one hand, to a change in the potential of the electrostatic field of the nucleus, and on the other hand to a change in the meson wave functions. If we take the cause of vacuum polarization to be a nucleus with a charge uniformly distributed within a sphere of radius R_0, there will be an oscillator potential inside the nucleus and a Coulomb potential on the outside

$$\begin{aligned} V(r) &= \frac{eZ}{R_0}\left[\frac{3}{2} - \frac{1}{2}\left(\frac{r}{R_0}\right)^2\right] \quad (r < R_0), \\ V(r) &= eZ / r \quad (r > R_0). \end{aligned} \tag{24}$$

The Fourier component of such a potential will be

$$\varphi_0(k) = \frac{eZ}{2\pi^2 k^2} \frac{3}{R_0^2 k^2}\left(\frac{\sin kR_0}{kR_0} - \cos kR_0\right). \tag{25}$$

To account for the change in the meson wave functions, caused by the finite nuclear dimensions, let us turn to the variational method. Let us take for the states 1S, 2S, and 2P respectively orthonormalized trial wave functions

$$R_{10}(r) = 2\left(q\,\frac{Z}{a}\right)^{3/2} \exp\left\{-q\,\frac{z}{a}\,r\right\},$$

$$R_{20}(r) = \frac{2\sqrt{3}\,s\left(s\,\frac{Z}{a}\right)^{3/2}}{\sqrt{s^2 - sq + q^2}}\left[1 - \frac{1}{3}\,\frac{Z}{a}\,(s+q)\,r\right]\exp\left\{-s\,\frac{Z}{a}\,r\right\}, \tag{26}$$

$$R_{21}(r) = \frac{2}{\sqrt{3}}\left(t\,\frac{Z}{a}\right)^{5/2} r \exp\left\{-t\,\frac{Z}{a}\,r\right\}$$

with variational parameters q, s, and t. With the aid of the radial portion of the Schroedinger equation with potential (24)

$$\frac{d^2R}{dr^2} + \frac{2}{r}\,\frac{dR}{dr} + \left(\frac{2\mu}{\hbar^2}E + \frac{3Z}{aR_0} - \frac{Z}{aR_0^3}\,r^2 - \frac{l\,(l+1)}{r^2}\right)R = 0 \quad (r < R_0),$$

$$\frac{d^2R}{dr^2} + \frac{2}{r}\,\frac{dR}{dr} + \left(\frac{2\mu}{\hbar}\,E + \frac{2Z}{ar} - \frac{l\,(l+1)}{r^2}\right)R = 0 \quad (r > R_0), \tag{27}$$

we obtain the following expression for the energy

$$E = -\frac{\hbar}{2\mu}\left\{-\int_0^\infty\left[\left(\frac{dR}{dr}\right)^2 r^2 + l\,(l+1)\,R^2\right]dr + \int_0^{R_0}\left(\frac{3Z}{aR_0} - \frac{Z}{aR_0^3}\,r^2\right)R^2r^2dr + \int_{R_0}^\infty \frac{2Z}{a}\,R^2rdr\right\}. \tag{28}$$

Substituting the trial functions (26) into (28) leads to expressions for the energy in terms of the variational parameters

$$E_{10} = -\frac{\hbar^2}{2\mu}\left(\frac{Z}{a}\right)^2 q\left[-q + \frac{3}{pq} - \frac{3}{p^3q^3} + \left(\frac{3}{pq} + \frac{6}{p^2q^2} + \frac{3}{p^3q^3}\right)\exp\{-2pq\}\right],$$

$$E_{20} = -\frac{\hbar^2}{2\mu}\left(\frac{Z}{a}\right)^2\left\{\frac{3}{p} - \frac{s^2}{3} + \frac{s}{s^2 - sq + q^2}\left[-2s^3 - \frac{3s^2 + 15q^2}{2p^3s^3}\right.\right. \tag{29}$$

$$\left.\left. + \left(ps^3 + 2ps^2q + psq^2 - s^2 + 4sq + 5q^2 + \frac{12q^2 + 3sq}{ps} + \frac{15q^2 + 3s^2}{p^2s^2} + \frac{15q^2 + 3s^2}{p^3s^3}\right)\exp\{-2qs\}\right]\right\},$$

$$E_{21} = -\frac{\hbar^2}{2\mu}\left(\frac{Z}{a}\right)^2 t\left[-t + \frac{3}{pt} - \frac{15}{2p^3t^3} + \left(pt + 5 + \frac{12}{pt} + \frac{15}{p^2t^2} + \frac{15}{2p^3t^3}\right)\exp\{-2pt\}\right].$$

Here $p = R_0Z/a$. The values of the parameters q, s and t are found, as usual, from the minimum-energy condition. The transcendental equations thus obtained can be solved numerically. The table gives values for the variational parameters and for the energy levels of several μ-mesonic atoms (it was assumed in the calculation that the mass of a μ-meson is 270 m, and the nuclear radius $R_0 = 1.2 \times 10^{-13}\,A^{1/3}$ cm).

Using the functions (26) we obtain by means of formula (9) expressions for I_{nl} with allowance for the volume of the nucleus

$$I_{10} = 1\,/\,[1 + (\varepsilon_q x)^2]^2,$$

$$I_{20} = \frac{3s^2}{s^2 - sq + q^2}\left\{\frac{1}{[1+(\varepsilon_s x)^2]^2} - \frac{s+q}{3s}\,\frac{3 - (\varepsilon_s x)^2}{[1+(\varepsilon_s x)^2]^3} + \frac{(s+q)^2}{3s^2}\,\frac{1 - (\varepsilon_s x)^2}{[1+(\varepsilon_s x)^2]^4}\right\}, \tag{30}$$

$$I_{21} = [1 - (\varepsilon_t x)^2]\,/\,[1 + (\varepsilon_t x)^2]^4,$$

where

$$\varepsilon_q = k_0 a / qZ, \quad \varepsilon_s = k_0 a / sZ, \quad \varepsilon_t = k_0 a / tZ.$$

Element	Variational parameters			Energy, Mev				
				Point nucleus		Variational method		
	q	s	t	E_{10}	E_{20}, E_{21}	E_{10}	E_{20}	E_{21}
Si_{14}^{28}	0.9642	0.4918	0.5000	0.550	0.137	0,536	0.136	0.137
Zn_{30}^{65}	0.8376	0.4558	0.4994	2.530	0,632	2,202	0.590	0.632
Sb_{51}^{121}	0.6685	0.3938	0.4926	7.317	1.829	5,183	1.525	1,817
Pb_{82}^{208}	0.5003	0.3197	0.5480	18,923	4.731	9.986	3.316	4,511

The expressions for the level shifts are then obtained by inserting (25) and (30) into (18). The values of the level shifts, obtained therefrom by numerical integration with allowance for the volume of the nucleus, are shown dotted in Fig. 4. By way of an example let us indicate that for μ-meso-lead the shift in the 1S level, due to polarization of vacuum, is 217 kev without allowance for the volume of the nucleus, and nearly 53 kev with allowance for the volume of the nucleus; for the 2S and 2P levels the shifts are 37 and 33 kev respectively without allowance for the volume of the nucleus, and 17 and 28 kev with allowance for the nucleus.

To check how good the approximate solution obtained by the variational method is, we obtained for Eq. (27), by numerical integration by the Runge-Kutta method, the eigenvalue of the energy and the wave function of the 1S state of μ-meso-lead, for the same values of the meson mass and nuclear radius. The eigenvalue of the energy of the 1S level was found to be 10.412 Mev, *i.e.*, approximately 4% greater than the value obtained by the variational method. Fig. 5 shows that the variational wave function is a better approximation than the wave function of the Keppler problem.

It must be noted that in all the above calculations of the mesonic atom level shifts due to vacuum polarization, we took into consideration only terms of the order αZ. As shown in Ref. 12, accounting for terms of higher orders gives for a point nucleus, even in the case of μ-meso-uranium, a shift which amounts to less than 0.02% of the energy level. It is evident that allowance for the volume of the nucleus can only reduce this figure.

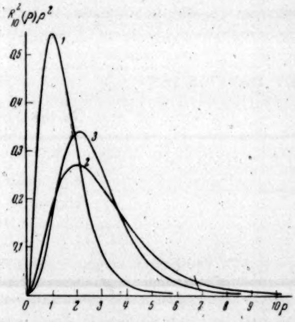

FIG. 5. Radial probability density of finding a meson in μ-meso-lead in state 1S, determined by various methods: 1 – without accounting for the volume of the nucleus [wave function of the Keppler problem $R(\rho) = 2e^{-\rho}$], 2 – with allowance for the volume of the nucleus [variational wave function $R(\rho) = 2q^{3/2}e^{-q\rho}$, $q = 0.5003$], 3 – with allowance for the volume of the nucleus (numerical solution); $\rho = rZ/a$.

The influence of vacuum polarization on the position of the energy levels in mesonic atoms was actually discovered experimentally. In many works on the determination of the masses of π- and μ-mesons using spectra of mesonic atoms it became necessary, to obtain mass values that are in agreement with data of other experiments to compare theory with experiment, to take into account the vacuum polarization level shift in the mesonic atoms.[13-14] Vacuum polarization is also accounted for in investigations of the interaction between the π-meson in the mesonic atom with the nucleons of the nucleus.[15]

In conclusion, the author expresses his gratitude to Professor D. D. Ivanenko for reviewing the manuscript.

---

[1] J. A. Wheeler, Revs. Mod. Phys. 21, 133 (1949).

[2] A. D. Galanin and I. Ia. Pomeranchuk, Dokl. Akad. Nauk SSSR 86, 251 (1952).

[3] Deser, Goldberger, Baumann, and Thirring, Phys. Rev. 96, 774 (1954).

[4] J. A. Wheeler, Phys. Rev. 92, 812 (1953).

[5] B. A. Jacobson, Phys. Rev. 96, 1637 (1954).

[6] W. Lakin and W. Kohn, Phys. Rev. 94, 787 (1954).

[7] L. N. Cooper and E. M. Henley, Phys. Rev. 92, 801 (1953).

[8] A. I. Akhiezer and V. B. Berestetskii, *Quantum Electrodynamics*, p. 376, Gostekhizdat, M. 1953.

[9] P. Gombas, *Many-Particle Problem in Quantum Mechanics*, (Russian transl.) p. 20, IIL, M. 1952.

[10] G. E. Pustovalov, J. Exptl. Theoret. Phys. (U.S.S.R.) 27, 758 (1954).

[11] A. B. Mickelwait and H. C. Corben, Phys. Rev. 96, 1145 (1954).

[12] E. H. Wichmann and N. M. Kroll, Phys. Rev. 101, 843 (1956).

[13] Koslov, Fitch, and Rainwater, Phys. Rev. 95, 291 (1954).

[14] Stearns, Stearns, de Benedetti, and Leipuner, Phys. Rev. 95, 1353 (1954).

[15] Stearns, Stearns, de Benedetti, and Leipuner, Phys. Rev. 97, 240 (1955).

Translated by J. G. Adashko
295

SOVIET PHYSICS JETP VOLUME 5, NUMBER 6 DECEMBER 15, 1957

On the Structure of the Front of Strong Shock Waves in Gases

IU. P. RAIZER
Academy of Sciences, U.S.S.R.

(Submitted to JETP editor November 29, 1956)
J. Exptl. Theoret. Phys. (U.S.S.R.) 32, 1528-1535 (June, 1957)

The internal structure of the front of strong shock waves is investigated, taking account of radiation. Approximate solutions of the equations of the mode are found. Profiles of the hydrodynamic quantities, density and radiation flux, are constructed.

ONE OF THE METHODS of study of shock waves in gases (in particular, in air) is photometric measurement of the brightness of the wave front. In a certain amplitude interval, the shock wave front radiates like a black body. Consequently, it is possible to determine the temperature behind the wave front directly, by photometry. Combined with the measurement of another parameter of the wave, for example, its velocity, this allows us to make some suppositions concerning the thermodynamic functions of the gas being studied. The question arises, up to what amplitudes does the visible temperature coincide with the temperature behind the shock wave, and what is its dependence on the actual temperature behind the front when the latter reaches tens and hundreds of thousands of degrees, since at the present time such powerful shock waves are becoming the subject of experimental investigation.[1] This question leads, first of all, to the problem of the internal structure of a shock wave front, taking account of radiation.

This problem was investigated by Prokof'ev,[2] who obtained correct integrals of the approximate equations in the separate regions in which the variables are continuous. However, as a result of an erroneous analysis of the equations, he joined these solutions in an incorrect way, which led to the continuity of the hydrodynamic variables in the wave. Prokof'ev's error was pointed out by Zel'dovich,[3] who gave a correct qualitative analysis of the approximate equations of the mode, and proved that there is a discontinuity of the hydrodynamic variables in the shock wave.

In the present article, approximate solutions are found of the equations of the mode, encompassing a broad interval of shock wave amplitudes, as well as the case of thermal waves, in which the propagation of energy in the gas takes place not hydrodynamically, but by means of radiant thermal conduction, as proposed by Zel'dovich and Kompaneets.[4]

The physical meaning of the regularities of the behavior of the hydrodynamic quantities and the quantities characterizing the radiation is made quite evident by the extreme simplicity of the approximate solutions, which conserve the fundamental qualitative characteristics of the phenomena and are sufficiently accurate.

In the following article, the theory presented here will be applied to the propagation of waves in air.

1. THE EQUATIONS OF HYDRODYNAMICS AND RADIATION TRANSFER, DESCRIBING THE INTERNAL STRUCTURE OF THE SHOCK WAVE FRONT

We consider a stationary mode in a system of coordinates moving with the wave front. The x-axis is in the direction of propagation of the wave. The undisturbed gas flows into the wave with velocity $-D$ $(D > 0)$, equal in modulus to the velocity of the front. The hydrodynamic equations can be integrated and yield the conditions of conservation of the fluxes of mass, momentum, and energy,

$$\rho v = -\rho_0 D, \quad p + \rho v^2 = \rho_0 D^2,$$
$$\rho v(\varepsilon + p/\rho + v^2/2) + S = -\rho_0 D^3/2. \qquad (1)$$

where p, ρ, v, ε and S are the pressure, density, velocity, specific internal energy and flux of radiant energy* at the point x. ρ_0 is the density of the initial gas. The wave is assumed to be strong, so that the pressure and internal energy of the undisturbed gas may be neglected.

The pressure and density of the radiant energy is negligibly small in comparison with the pressure and energy of matter for the wave amplitudes under consideration. Only the flux of radiation in the visible and near ultraviolet regions of the spectrum reaches "infinity", since air, like other gases, is opaque at higher frequencies. This flux is much smaller than the flux in the wave region that will be of interest to us, and we will omit it.

For the explanation of the general character of the behavior of the variables inside the wave, the heat capacity will for simplicity be considered constant. Then,

$$\varepsilon = p/(\gamma - 1)\rho = RT/(\gamma - 1), \qquad (2)$$

where T is the temperature, R is the gas constant, γ is the adiabatic exponent, (at high temperatures the effective magnitude of the adiabatic exponent, taking account of the ex[illegible]nditure of energy for ionization, is approximately 1.25).

Behind the wave front, at $x = -\infty$, the flux S becomes zero. All quantities at $x = -\infty$ will be denoted by the subscript 1.

By a simple calculation, we can obtain from Eqs. (1) and (2) expressions for the temperature and flux at a flowing point in terms of the reciprocal of the compression $\eta = \rho_0/\rho$ at that point*

$$T = T_1\eta(1 - \eta)/\eta_1(1 - \eta_1), \qquad (3)$$

$$S = \rho_0 DRT_1(1 - \eta)(\eta - \eta_1)/2\eta_1^2(1 - \eta_1),$$
$$\eta_1 = \rho_0/\rho_1 = (\gamma - 1)/(\gamma + 1), \qquad (4)$$

$\eta_1 = 0.111$ when $\gamma = 1.25$.

The curve $T(S)$ which is obtained from Eqs. (3) and (4) by eliminating η, has two branches: one $(\eta \to 1,\ T \to 0,\ S \to 0)$ corresponds to the region in front of the shock discountinuity, the other $(\eta \to \eta_1,\ T \to T_1,\ S \to 0)$ corresponds to the region behind the discontinuity.[3]

As an approximation, we will consider the angular distribution of radiation in the diffusion approximation, replacing the rigorous kinetic equation for the intensity by a pair of equations for the density and flux of radiation. As a further simplification, we introduce a mean (over the spectrum) absorption coefficient $\varkappa = 1/l$ (l is the free path), having integrated the diffusion equations over the whole spectrum.

Eliminating the explicit dependence of the absorption coefficient on the point by means of a transformation from the geometrical coordinate x to the optical thickness τ by the well known formula

---

*In general, S should include the flux of electron thermal conduction, which is considerably greater than atomic (ionic) thermal conduction, acting only inside the shock discontinuity. However, calculations presented in the following article indicate that in the first approximation, this flux may be neglected in comparison with the flux of radiant energy (in gases with normal initial density).

*These formulas were derived by Prokof'ev in Ref. 2.

$$d\tau = \varkappa dx,\ \tau = \int_0^x \varkappa dx, \tag{5}$$

(the origin of coordinates $x = 0$ is located at the shock discontinuity), we may write the diffusion equations in the form

$$dS / d\tau = c\,(U_p - U), \tag{6}$$

$$S = -(c/3)\,dU / d\tau. \tag{7}$$

where U is the density of radiant energy, c is the velocity of light,

$$U_{\text{eq}} = 4\sigma T^4/c \tag{8}$$

is the equilbrium radiation density, and σ is the Stefan-Boltzmann constant.

In the general case the procedure of averaging over the spectrum is not rigorous, since the coefficient of absorption is averaged differently in Eqs. (6) and (7). As will be evident in what follows, averaging has a well defined meaning only in two limiting cases. Nevertheless, as an approximation, we will consider Eqs. (6) and (7) to be always valid.

Eqs. (3), (4), (6), and (7), together with the natural boundary conditions*

$$\tau = +\infty:\ S = 0,\ U = 0,\ T = 0, \tag{9}$$

$$\tau = -\infty:\ S = 0,\quad U = U_{\text{eq}\,1} = 4\sigma T_1^4/c,\ T = T_1 \tag{10}$$

are the starting point of the present article, just as in Refs. 2 and 3.

The order of the system may be lowered by dividing Eqs. (6) and (7) by one another,

$$dS / dU = (c^2/3)\,(U - U_{\text{eq}}) / S. \tag{11}$$

2. APPROXIMATE SOLUTION OF THE EQUATIONS IN THE CASE OF AN "ORDINARY" SHOCK WAVE, $T_1 < T_k$

In the limit of weak waves, the role of radiation is negligibly small, and none of the hydrodynamic quantities depend on the coordinate, except for the discontinuity at the point $x = 0$. As the amplitude of the wave increases, the radiant flux $S^0 = \sigma T_1^4$, issuing from the surface of the discontinuity, and being absorbed by the layers lying in front of it, heats them more and more.

As was shown by Zel'dovich,[3] the greatest heating temperature T_- that exists at the point $x = 0$ in front of the discontinuity cannot exceed T_1; the greatest compression in the heating zone cannot exceed in this case $1/(1 - \eta_1)$ (equal to 1.13 at $\gamma = 1.25$). Expressing S in terms of T through Eqs. (3) and (4) to within small quantities of the second order with respect to η_1, we obtain the simple equation

$$S = D\rho_0 RT / (\gamma - 1) = D\rho_0\varepsilon, \tag{12}$$

signifying that the energy of the absorbed radiation goes only toward raising the internal energy of the gas in front of the discontinuity.* The maximum possible error in Eq. (12) is no more than 1.7%.

If S^0, the value of the flux at the point of the discontinuity, is used in Eq. (12), we find the temperature in front of the discontinuity

$$S^0 = D\rho_0 RT_- / (\gamma - 1). \tag{13}$$

In the case of sufficiently weak waves, $S^0 \approx \sigma T_1^4$ and T_- increases very rapidly with increasing wave amplitude.

When the temperature in the heating zone is small compared with T_1, the temperature behind the front, the radiation density at any point in it, which is determined by the initial flux $S^0 \sim T_1^4$, is considerably greater than the equilibrium density $U_{\text{eq}} \sim T^4$ at that point. In other words, the radiation generated in the heating zone itself, contributes a small amount to the total flux and density. Under these conditions, neglecting U_{eq} compared with U in Eqs. (6) and (11), it is easy to find the solution of the system in front of the discontinuity†

$$S = cU / \sqrt{3} = S^0 \exp(-\sqrt{3}\tau), \quad \tau > 0, \tag{14}$$

$$T = T_- \exp(-\sqrt{3}\tau), \quad \tau > 0. \tag{15}$$

Its limit of applicability is evidently the temperature T_k at which $U_{\text{eq}}(T_k) = U(T_k)$, or, using Eqs. (8), (12) and (14),

$$4\sigma T_k^4 / \sqrt{3} = D\rho_0 RT_k / (\gamma - 1). \tag{16}$$

---

* Of these six conditions, only two are independent, the remaining ones result from the equations.

*The work of compression and the change of kinetic energy, which are proportional to η_1, cancel each other to within η_1^2.

† Essentially, our approximation consists simply of spreading the limiting form of integral curves, which originate at a singular point of the saddle-point type at $\tau = +\infty$, over the entire heating region.

T_k is evidently the temperature at which the hydrodynamic and radiant fluxes are comparable. Since D does not depend strongly on T_1 (for $\gamma = \text{const}$, $D \sim T_1^{1/2}$), temperature T_k is practically independent of the strength of the wave, when the latter does not vary over too broad a range (for example, in air, $T_k \approx 300{,}000°$).

At the same time, as follows from Eq. (16), T_k is extremely close to that temperature behind the front T_1, at which T_- is comparable with T_1. When $T_1 \ll T_k$ we get $T_- \ll T_1 \ll T_k$ and the solution (14), (15) is valid over the entire heating zone.

Numerical integration of Eqs. (11) and (12) shows that the approximate solution is quite accurate up to values of T_- extremely close to T_k. This occurs because the accuracy is proportional to the third power of the ratio T_-/T_k. Thus, for example, at $T_- = T_k/2$, the greatest error (in front of the discontinuity) is 1.1%.

Now we will find the solution of the equations behind the discontinuity. The curve $U(S)$ has two branches, corresponding to the two branches of $T(S)$. As was shown in Ref. 3, the point at which these branches intersect also determines the position of the discontinuity (the flux and density of radiation are, of course, continuous in the wave).

In the limit of a weak wave, the compression and the temperature are constant behind the discontinuity. Assuming that the change of compression behind the discontinuity is small, we find, as before, the connection between the flux and the temperature from Eqs. (3) and (4) on the second branch, to within small quantities of the second order $\sim \eta_1^2$:

$$(T - T_1)\, D\rho_0 R\, (\gamma + 1)(3 - \gamma)/(\gamma - 1) = S. \tag{17}$$

We will obtain an approximate solution of the equations behind the discontinuity by assuming that the temperature in this region varies slowly, *i.e.*, by replacing $U_{\mathbf{eq}}$ by $U_{\mathbf{eq}1} = 4\sigma T_1^4/c$ in Eqs. (6) and (11). To this approximation, the system of equations is easily solved, and yields*

$$S = c\,(U_{\mathbf{eq}1} - U)/\sqrt{3} = S^0 \exp(\sqrt{3}\,\tau), \quad \tau < 0, \tag{18}$$

$$T - T_1 = (T_+ - T_1) \exp(\sqrt{3}\,\tau), \quad \tau < 0, \tag{19}$$

where T_+ is the temperature at the discontinuity on the upper side of the jump.

We will obtain the values of U^0, S^0 at the discontinuity by joining both branches of the $U(S)$ curves, Eqs. (14) and (18)*

$$U^0 = {}^1/_2\, U_{\mathbf{eq}1} = 2\sigma T_1^4, \tag{20}$$

$$S^0 = 2\sigma T_1^4/\sqrt{3}. \tag{21}$$

We will find the values of the temperature on both sides of the jump from Eqs. (13) and (17). Taking (16) into account, we obtain

$$T_-/T_k = {}^1/_2\,(T_1/T_k)^4, \tag{22}$$

$$(T_+ - T_1)/T_k = \frac{3 - \gamma}{2(\gamma + 1)}\,(T_1/T_k)^4. \tag{23}$$

As could be expected, the value of the peak temperature $\Delta T_+ = T_+ - T_1$ falls rapidly as the strength of the wave is decreased.

An estimate of the upper limit of the possible error in the approximate solution (18), (19) shows that just as in the heating zone, the accuracy of the approximation is good up to T_1, sufficiently close to T_k. Thus, for example, at $T_1 = T_k/2$, the error in ΔT_+ and S^0 is less than 10%.

Profiles of the dimensionless temperature Θ, flux Σ, and density j of the radiation are shown in Fig. 1. The units of these quantities are T_k, S_k

Profiles of the dimensionless temperature Θ, flux Σ, and density j of the radiation are shown in Fig. 1. The units of these quantities are T_k, $S_k = 4\sigma T_k^4/\sqrt{3}$, and $U_k = 4\sigma T_k^4/c$, respectively.

When the radiation is far from equilibrium $U \gg U_{\mathbf{eq}}$, as occurs in the heating zone, the mean of the absorption coefficient over the spectrum in the diffusion equations has a completely defined character. In this case, we may also easily integrate the spectral diffusion equations for the flux and density of the radiant energy of frequency ν, per unit frequency interval, $S_\nu U_\nu$, which may be written in the same way as intergrals (6) and (7). Letting $U_\nu \gg U_{\mathbf{eq}}$, where

$$U_{\mathbf{eq}\nu} = (8\pi h/c^3)\,[e^{h\nu/kT} - 1]^{-1}, \tag{24}$$

---

*Exactly as in the region in front of the discontinuity, this solution is the limiting form of an integral curve, originating at a singular point of the saddle-point type at $\tau = -\infty$.

*Note that the value of U^0 was obtained correctly, corresponding to the limiting case $T(\tau) = T_1$ at $\tau < 0$, and $T = 0$ at $\tau > 0$. S^0 is too large by a factor of $2/\sqrt{3}$. This is a consequence of the diffusion approximation.

$$S_\nu = cU_\nu / \sqrt{3} = S_\nu^0 \exp(-\sqrt{3}\tau_\nu), \quad \tau_\nu = \int_0^x \varkappa_\nu dx, \tag{25}$$

so that the law of averaging is the same in both equations.

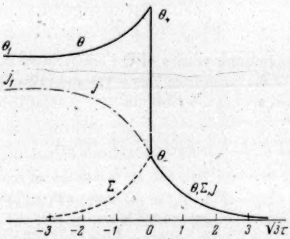

FIG. 1.

Integration over the spectrum of the spectral equation corresponding to Eq. (6) shows that $\varkappa_\nu = 1/l_\nu$ is averaged simply over the spectral density of radiation and the mean coefficient $\varkappa$ corresponds to the frequencies which give the greatest contribution to the flux and energy density of the radiation.

In the nonequilibrium zone we may obtain expressions for the flux and density, which in distinction to the diffusion approximation, take account rigorously of the angular distribution of the radiation. As is well known,[5] in the plane problem, S and U may be written in an integral form

$$S = \frac{c}{2}\int_{-\infty}^{\tau} U_{\text{eq}} E_2(\tau - \tau')\, d\tau' - \frac{c}{2}\int_{\tau}^{\infty} U_{\text{eq}} E_2(\tau' - \tau)\, d\tau', \tag{26}$$

$$U = \frac{1}{2}\int_{-\infty}^{\tau} U_{\text{eq}} E_1(\tau - \tau')\, d\tau' + \frac{1}{2}\int_{\tau}^{\infty} U_{\text{eq}} E_1(\tau' - \tau)\, d\tau', \tag{27}$$

where the functions E_1 and E_2 are special cases of integral exponentials

$$E_n(z) = \int_1^{\infty} e^{-xz} x^{-n} dx. \tag{28}$$

Since the radiation generated in the heating zone contributes very little to the total flux and density, we may, in Eqs. (26) and (27), neglect integrals over sources located in this zone, *i.e.*, integrals over τ from 0 to ∞. Using the well known properties of integral exponentials, we then obtain

$$S = S^0 2E_3(\tau), \quad U = U^0 E_2(\tau), \quad T = T_- 2E_3(\tau). \tag{29}$$

In the limit $T_+ - T_1 \ll T_1$ and $T(\tau) = T_1$ for $\tau < 0$, integrals (26) and (27) give, rigorously

$$S^0 = cU^0 / 2 = \sigma T_1^4. \tag{30}$$

3. APPROXIMATE SOLUTION OF THE EQUATIONS FOR THE CASES OF AN "ISOTHERMAL JUMP" $T_1 > T_k$ AND A THERMAL WAVE

At the lower edge of the heated zone of a strong shock wave with $T_1 > T_k$, in the region where $T < T_k$, the radiation is not in equilibrium, as before, and solutions of the type (14) and (15) are valid. When the temperature becomes of the order of T_k, the density U approaches equilibrium; moreover, as the temperature increases, the relative deviation of U from U_{eq} becomes less and less. This behavior is also indicated by the numerical integration of Eqs. (11) and (12). In this region, so called local equilibrium $U \approx U_{\text{eq}}$ occurs, which is the starting point of the radiant thermal conduction approximation. In the local equilibrium approximation, U_{eq} may be substituted into Eq. (7) in place of U. Combining the equation thus obtained with Eq. (12), we obtain an equation of the first order for the temperature, which is easily integrated.

This solution for the equilibrium part of the heating zone must be joined with the solution in the nonequilibrium part, Eqs. (14) and (15), at the point $\tau = \tau_k$, with temperature T_k, which effectively delimits both regions.

Using Eq. (16), which determines T_k, we find, after an elementary calculation, the solution in the heating zone:
in the nonequilibrium region

$$T / T_k = cU / 4\sigma T_k^4 = \sqrt{3}\, S / 4\sigma T_k^4 = \exp\{-\sqrt{3}(\tau - \tau_k)\}, \quad \tau > \tau_k \tag{32}$$

and in the equilibrium region

$$\frac{T}{T_k} = \frac{\sqrt{3} S}{4\sigma T_k^4} = \left(\frac{cU}{4\sigma T_k^4}\right)^{1/4} = \left[1 - \frac{3\sqrt{3}}{4}(\tau - \tau_k)\right]^{1/3}, \quad 0 < \tau < \tau_k, \tag{33}$$

where τ_k is expressed in terms of the greatest heating temperature

$$\tau_k = 4 \cdot 3^{-3/4} [(T_- / T_k)^3 - 1]. \tag{34}$$

Solution (33) is extremely close to the exact solution obtained by a numerical integration of Eqs. (11) and (12). Even at $T = 1.5\ T_k$ the error is less than 13%.

In the nonequilibrium region the more precise solution, Eqs. (29) – (31), is valid if in it we replace τ by $\tau - \tau_k$, and replace S^0, U^0, T_- by S_k, U_k, and T_k, respectively. In exactly the same way, the conclusions at the end of Sec. 2 regarding the law of averaging of the absorption coefficient are valid.

As regards the equilibrium region, since local equilibrium occurs, the free path l_ν is averaged according to Rosseland.[5] Here, the average free path l corresponds to high frequencies, lying in the Wien region ($h\nu \approx 6kT$ corresponds to $l_\nu \sim \nu^3 l$).

It was shown in Sec. 2 that as the amplitude of the wave increases, the temperature T_- in front of the jump becomes comparable with T_1, the temperature behind the front, when the latter reaches T_k. With further increase of T_1, T_- cannot become greater than T because otherwise the radiation density would decrease during the change behind the discontinuity from $U_- \approx 4\sigma T_-^4/c$ to $U_{\text{eq}1} = 4\sigma T_1^4/c$, the flux in this region would be directed toward the other side and density in the wave would not vary monotonically, which clearly does not make sense.*

Therefore, in the case of a sufficiently strong wave, where $T_- > T_k$, the temperature T_- in front of the discontinuity reaches the magnitude of the temperature T_1 behind the front, and with further increase of the amplitude of the wave, remains almost equal to it

$$T_- \approx T_1. \tag{35}$$

Because of the existence of local equilibrium in front of the discontinuity, the radiation density behind the discontinuity is almost independent of the coordinate, *i.e.*, the solution behind the discontinuity is

$$U(S) \approx U_{\text{eq}1} \approx U_- \equiv U^0. \tag{36}$$

The magnitude of the flux at the discontinuity is determined, in accordance with the general rule, from the conditions of intersection of both branches of the $U(S)$ curves. Using solutions (33) and (36), we find

$$S^0 = \frac{4\sigma T_k^4}{\sqrt{3}} \left(\frac{cU^0}{4\sigma T_k^4}\right)^{1/4} = \frac{4\sigma T_k^4}{\sqrt{3}} \left(\frac{T_1}{T_k}\right). \tag{37}$$

The temperature behind the discontinuity may be found from the approximate formula (17), or directly from the exact equations (3) and (4). The latter give*

$$T_+ = T_1 (3 - \gamma). \tag{38}$$

Had we also used the local equilibrium approximation behind the discontinuity, or, equivalently, the radiant thermal conduction approximation, then since the radiation density is constant, we would have obtained a constant temperature. Then the temperature would not undergo a discontinuity in the wave. This case is called the "isothermal jump".[6] Actually, an "isothermal jump" is never realized, as was noted in Ref. 3, because it contradicts the condition of continuity of flow.†

It is easy to evaluate the accuracy of solution (36). Substituting it into Eq. (11) as a zeroth approximation, and using Eq. (17) and the condition of flow boundedness which is a consequence of the hydrodynamic relations (3) and (4), we find after some straightforward calculations,

$$\frac{U_{\text{eq}1} - U^0}{U_{\text{eq}1}} < \frac{(\gamma + 1)^2}{16 (\gamma - 1)(3 - \gamma)} \left(\frac{T_k}{T_1}\right)^6. \tag{39}$$

We see that the relative deviation from $U_{\text{eq}1}$ of the radiation density behind the discontinuity decreases extremely rapidly as the amplitude of the wave increases.

We may estimate the upper limit of the optical thickness of the layer, in which the flux increases from zero to the maximum S^0 and which at the same time is the thickness $\Delta\tau$ of the temperature peak according to Eq. (7), in which as an approximation

---

* This simple physical result was obtained by Zel'dovich[3] from a purely mathematical analysis of the integral curves of the equations.

* The approximate formula yields $T_+ = 4T_1/(\gamma + 1)$. For $\gamma = 1.25$, the error is 1.7%, which attests to the great accuracy of Eq. (17).

† Indeed, in front of the discontinuity, at the point $x = 0$, S differs from zero and is proportional to T_- according to Eq. (13). But behind the discontinuity, in the local equilibrium approximation at the point $x = 0$,

$$S \sim dU/dx \approx dU_{\text{eq}}/dx \sim dT/dx = 0 \quad \text{for } T = \text{const}.$$

we replace $(dU/d\tau)^0$, the derivative at the discontinuity, by $(U_{\mathrm{eq}1} - U^0)/\Delta\tau$. Using Eqs. (37) and (39), we find that the thickness of the peak decreases rapidly with increasing amplitude of the wave,

$$\Delta\tau < \frac{\gamma+1}{4\sqrt{3}(3-\gamma)}\left(\frac{T_k}{T_1}\right)^3. \qquad (40)$$

Profiles of the nondimensional temperature, flux and density of radiation are shown in Fig. 2 for the case of an "isothermal jump". The realization of a strong "isothermal jump" requires special and rather artificial conditions, for example, a piston, "pushing" a strong shock wave ahead of it.

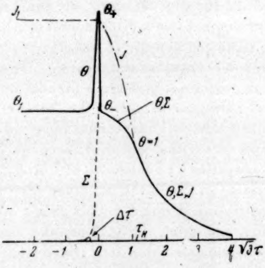

FIG. 2.

If we consider more real sources of such strong waves, such as a local discharge of very great energy, the early stages of the propagation of this energy from the source through the gas takes place not hydrodynamically, but by radiant heat conduction, as was envisaged in Ref. (4).

The radiant thermal conduction or thermal wave mode is essentially nonstationary. In Ref. 4, this mode was self-similar. However, the lowest edge of the wave is stationary in a system of coordinates moving with the velocity of a head wave. The thickness of the stationary layer is determined as follows: during the time that the wave progresses through a distance of the order of this thickness, its velocity D remains practically constant.

In the limiting case of a strong thermal wave, the role of hydrodynamics tends toward zero, and the wave propagates through a nonmoving gas. Under these conditions, the lower edge is described by the same equations, (3), (4), (6), and (7), as the heating zone in a strong shock wave. No conditions are imposed from above on the solution of the equations; it gradually transforms into the nonstationary solution, encompassing the whole space occupied by the wave (for example, in the self-similar solution of Zel'dovich and Kompaneets[4]). The solution of the equations clearly coincides with the solution in the heating zone, Eqs. (32) and (33), in which τ_k simply plays the role of a constant of integration. Since there is now no specially distinguished point in the wave (such as the point of discontinuity in the case of a shock wave), it is convenient to locate the coordinate origin $\tau = 0$ at the point delimiting the equilibrium and nonequilibrium regions, where $T = T_k$. Then the solution at the lower stationary edge of the thermal wave is written in the form

$$\frac{T}{T_k} = \frac{\sqrt{3}S}{4\sigma T_k^4} = \begin{cases} cU/4\sigma T_k^4 = \exp(-\sqrt{3}\tau) & \tau > 0, \\ (cU/4\sigma T_k^4)^{1/4} = (1-3\sqrt{3}\,\tau/4)^{1/3} & \tau < 0, \end{cases} \qquad (41)$$

where as previously, T_k is determined by Eq. (16), in which D is understood to represent the velocity of the head of the wave.

I take this opportunity to express deep thanks to Ia. B. Zel'dovich for his interest in the work, and valuable discussions and remarks.

---

[1] I. Sh. Model', J. Exptl. Theoret. Phys. (U.S.S.R.) **32**, 714 (1957), Soviet Phys. JETP **5**, 589 (1957).

[2] V. A. Prokof'ev, Uch. zap. MGU **172**, Mekhanika, p. 79, 1952.

[3] Ia. B. Zel'dovich, J. Exptl. Theoret. Phys. (U.S.S.R.) **32**, 1126 (1957), Soviet Phys. JETP **5**, 919 (1957).

[4] Ia. B. Zel'dovich and A. S. Kompaneets, Collection devoted to the 70th birthday of Academician A. F. Ioffe, Acad. of Sciences Press, 1950.

[5] A. Unsold, *Physics of Stellar Atmospheres*, (Russ. Transl.), IIL, 1949.

[6] L. Landau and E. Lifshits, *Mechanics of Continuous Media*, 2nd ed., p. 421, 1953.

Translated by D. Lieberman
296

SOVIET PHYSICS JETP VOLUME 5, NUMBER 6 DECEMBER 15, 1957

Angular Operators For Nuclear Reactions

V. I. RITUS
P. N. Lebedev Physical Institute, Academy of Sciences, U.S.S.R.

(Submitted to JETP editor March 14, 1957)
J. Exptl. Theoret. Phys. (U.S.S.R.) 32, 1536-1546 (June, 1957)

An orthogonal and normalized system of invariant angular operators is found; these are matrices in terms of which the scattering amplitude can be expressed. The angular operators correspond to transitions with definite total angular momentum and parity, and also definite values of other quantum numbers in the initial and final states, and they completely determine the angular distributions and polarizations of the particles in these transitions. The explicit form of the operators is presented for reactions in which the spin of the system is 0, ½, and 1, and for analogous reactions with γ-quanta, in particular for the scattering and energy loss of mesons against nucleons, for the scattering of photons and nucleons by nucleons, and for the reactions $\mathfrak{N} + \mathfrak{N} \rightarrow \pi + D$, $\gamma + D \rightarrow p + n$, and $\gamma + D \rightarrow \pi + D$.

1. INTRODUCTION

LET US CONSIDER in the center-of-mass system a reaction of the type $a + b \rightarrow a' + b'$, in which particle a with spin s is incident in the direction **k** on particle b with spin σ, the result being the formation of particle a' with spins s', emerging in the direction **k′**, and of particle b' with spin σ' (**k**, **k′** are unit vectors). The analysis of such a reaction can be conveniently carried out by means of the scattering matrix $S(\mathbf{k}'\alpha', \mathbf{k}\alpha)$, which takes the wave function $\psi_i(\mathbf{k}\alpha)$ of the initial state over into the wave function $\psi_f(\mathbf{k}'\alpha')$ of the final state

$$\psi_f(\mathbf{k}'\alpha') = S(\mathbf{k}'\alpha', \mathbf{k}\alpha)\,\psi_i(\mathbf{k}\alpha).$$

Hereinafter we shall be interested only in the angular and spin dependences of the scattering matrix, so that in S and in ψ_i, ψ_f there are written out only the angular variables **k**, **k′** and the spin variables α, α' of the initial and final states.

The complete theoretical calculation of the scattering matrix requires a knowledge of the detailed mechanism of interaction of the particles involved in the reaction. But by using the invariance of the Hamiltonian system with respect to rotations and reflections in space one can separate out those properties of the scattering matrix that do not depend on the mechanism of the interaction. For this purpose we expand S in terms of eigenfunctions* $\psi_{JM\pi\nu}(\mathbf{k}\alpha)$ of the operators for the total angular momentum, for one of its components, and for the reflection operator, in the initial and final states. Besides the total angular momentum J, its component M, and the parity π, these functions are characterized by further quantum numbers ν, since the operators for the total angular momentum, for its component, and for reflection can have several eigenfunctions for given $JM\pi$. In addition, we provide these functions with indices i, f, which determine the type and states of the particles in the initial and final channels of the reaction. Then

$$S(\mathbf{k}'\alpha', \mathbf{k}\alpha) = \sum_{J'M'\pi'\nu'}\sum_{JM\pi\nu}\psi^f_{J'M'\pi'\nu'}(\mathbf{k}'\alpha')\,S^{fi}_{J'M'\pi'\nu',\,JM\pi\nu}\,\psi^{i*}_{JM\pi\nu}(\mathbf{k}\alpha).$$

In virtue of the invariance of S under rotations and reflections the matrix elements of S are diagonal in J, M, and π and do not depend on M:

$$S^{fi}_{J'M'\pi'\nu';\,JM\pi\nu} = S^{f}_{J\pi\nu'\nu}\,\delta_{J'J}\,\delta_{M'M}\,\delta_{\pi'\pi}.$$

Thus

$$S(\mathbf{k}'\alpha', \mathbf{k}\alpha) = \sum_{J\pi\nu'\nu} S^{fi}_{J\pi\nu'\nu}\sum_{M}\psi^f_{JM\pi\nu'}(\mathbf{k}'\alpha')\,\psi^{i*}_{JM\pi\nu}(\mathbf{k}\alpha). \tag{A}$$

The matrix elements $S^{fi}_{J\pi\nu'\nu}$ are functions of the total energy of the system, and their calculation requires a knowledge of the detailed mechanism of the interaction. The operators

$$L^{fi}_{J\pi\nu'\nu}(\mathbf{k}'\alpha', \mathbf{k}\alpha) = \sum_{M}\psi^f_{JM\pi\nu'}(\mathbf{k}'\alpha')\,\psi^{i*}_{JM\pi\nu}(\mathbf{k}\alpha) \tag{1}$$

are functions of the angular variables **k**, **k′**, and ma-

---

*The functions $\psi_{JM\pi\nu}$ are quantities that transform on space rotations according to the $(2J + 1)$-dimensional irreducible representation of the three dimensional rotation group. We shall call them J-vectors. For $J = ½$ these are spinors, for $J = 1$, vectors, for $J = 2$, tensors of the second rank, *etc.* For the general definition and the properties of J-vectors see Ref. 1, where they are called L-vectors.

trices with respect to the spin variables α, α'. We shall call these operators $L^{fi}{}_{J\pi\nu'\nu}$ angular operators or polynomials of the reaction $a + b \rightarrow a' + b'$, since they completely determine the angular distribution and polarization of the particles in transitions with given $J\pi\nu'\nu$.[2,9] As can be seen from their definition, the angular operators are invariant under rotations and reflections in the ordinary space. In this connection it must be noted that the parity π of a state is determined not only by the orbital motion, but also by the intrinsic parity of the particles. Since the internal wave functions of the particles will not be written out explicitly, the operators L will be either scalars or pseudoscalars, depending on whether the product of the intrinsic parities of all particles taking part in the reaction is positive or negative. The angular operators are Hermitian:

$$L^{fi*}_{J\pi\nu'\nu}(\mathbf{k}'\alpha', \mathbf{k}\alpha) = L^{if}_{J\pi\nu\nu'}(\mathbf{k}\alpha, \mathbf{k}'\alpha').$$

Since the J-vectors $\psi^i{}_{JM\pi\nu}$ are orthogonal and normalized[1] by the condition

$$\sum_{\alpha}\int d\mathbf{k}\, \psi^{i*}_{J'M'\pi'\nu'}(\mathbf{k}\alpha)\, \psi^{i}_{JM\pi\nu}(\mathbf{k}\alpha) = 4\pi\delta_{J'J}\delta_{M'M}\delta_{\nu'\nu}$$

(and similarly for the $\psi^f{}_{JM\pi\nu}$), the angular polynomials are orthogonal and normalized in the following way

$$\sum_{\alpha'}\int d\mathbf{k}'\, L^{fi'*}_{J'\pi'\nu''\nu'''}(\mathbf{k}'\alpha', \mathbf{k}''\alpha'')\, L^{fi}_{J\pi\nu'\nu}(\mathbf{k}'\alpha', \mathbf{k}\alpha) = 4\pi\delta_{J'J}\delta_{\nu'\nu''}L^{i'i}_{J\pi''\nu'''\nu}(\mathbf{k}''\alpha'', \mathbf{k}\alpha). \tag{2}$$

We now consider two methods for analyzing the reaction $a + b \rightarrow a' + b'$, which differ in the choice of the quantum numbers ν, ν' which describe the system in its initial and final states. We shall distinguish the equations corresponding to these choices by the numbers I and II.

I. The initial state of the system is specified by the total angular momentum J, the parity π, the total angular momentum j of the incident particle a, and its orbital angular momentum l. The angular momentum J is the vector sum of the angular momentum j of particle a and the spin σ of particle b: $\mathbf{J} = \mathbf{j} + \boldsymbol{\sigma}$; the angular momentum j of the particle is the vector sum of its spin s and orbital angular momentum l: $\mathbf{j} = \mathbf{s} + \mathbf{l}$. The final state of the system is described by analogous quantities with primes. Thus $\nu \equiv jl$, $\nu' \equiv j'l'$.

II. The initial state of the system is specified by the total angular momentum J, the parity π, the spin S of the system, and the orbital angular momentum l. The angular momentum J is the vector sum of the spin S and the orbital angular momentum l: $\mathbf{J} = \mathbf{S} + \mathbf{l}$. The spin S of the system is the vector sum of the spins s and σ: $\mathbf{S} = \mathbf{s} + \boldsymbol{\sigma}$. The final state of the system is described by the analogous quantities with primes. Thus $\nu \equiv Sl$, $\nu' \equiv S'l'$.

For these two cases the J-vectors ψ can be represented in the form

$$\psi_{JMjl}(\mathbf{k}\alpha\gamma) = \sum_{\mu} C^{jM-\mu,\,\sigma\mu}_{JM} D_{jlM-\mu}(\mathbf{k}\gamma)\, Q_{\sigma\mu}(\alpha), \quad \psi_{JMSl}(\mathbf{k}\beta) = \sum_{\mu} C^{lM-\mu,\,S\mu}_{JM} Y_{lM-\mu}(\mathbf{k})\, Q_{S\mu}(\beta),$$

where $C^{jM-\mu,\sigma\mu}_{JM}$ are the Clebsch-Gordan coefficients, and Y_{lm}, D_{jlm}, $Q_{\sigma\mu}$, and $Q_{S\mu}$ are J-vectors that are eigenfunctions of the operators of the orbital angular momentum, the total angular momentum of the particle, the spin of the nucleus, and the spin of the system; Y_{lm} are ordinary spherical harmonics, and $D_{jlm}(\mathbf{k}\gamma)$ are spherical harmonics with spin

$$D_{jlm}(\mathbf{k}\gamma) = \sum_{\mu} C^{lm-\mu,\,s\mu}_{jm} Y_{lm-\mu}(\mathbf{k})\, Q_{s\mu}(\gamma) = \sum_{\mu} D^{s\mu}_{jlm}(\mathbf{k})\, Q_{s\mu}(\gamma), \tag{3}$$

$l = |j - s|, \ldots, j + s$; $Q_{\sigma\mu}$, $Q_{s\mu}$, and $Q_{S\mu}$ are spin functions depending on the respective spin variables α, γ, β. All of these functions are orthogonal and normalized in the following way:

$$\int Y^*_{l'm'}(\mathbf{k})\, Y_{lm}(\mathbf{k})\, d\mathbf{k} = 4\pi\delta_{l'l}\delta_{m'm},$$

$$\sum_{\gamma}\int D^*_{j'l'm'}(\mathbf{k}\gamma)\, D_{jlm}(\mathbf{k}\gamma)\, d\mathbf{k} = 4\pi\delta_{j'j}\delta_{l'l}\delta_{m'm}, \qquad \sum_{\alpha} Q^*_{\sigma\mu'}(\alpha)\, Q_{\sigma\mu}(\alpha) = \delta_{\mu'\mu}.$$

Consequently the angular operators for the transitions $Jjl \to Jj'l'$ and $JSl \to JS'l'$ are given by

$$L_{Jj'l'jl}(\mathbf{k}'\alpha'\gamma',\ \mathbf{k}\alpha\gamma) = \sum_{\mu'\lambda'\mu\lambda} L^{\mu'\lambda',\,\mu\lambda} Q_{\sigma'\mu'}(\alpha')\, Q_{s'\lambda'}(\gamma')\, Q^*_{\sigma\mu}(\alpha)\, Q^*_{s\lambda}(\gamma), \tag{4.I}$$

$$L_{JS'l'Sl}(\mathbf{k}'\beta',\ \mathbf{k}\beta) = \sum_{\mu'\mu} L^{\mu'\mu} Q_{S'\mu'}(\beta')\, Q^*_{S\mu}(\beta), \text{ or} \tag{4.II}$$

$$L^{\mu'\lambda',\,\mu\lambda}_{Jj'l'jl}(\mathbf{k}'\mathbf{k}) = \sum_M C^{j'M-\mu',\,\sigma'\mu'}_{JM} C^{jM-\mu,\,\sigma\mu}_{JM} D^{s'\lambda'}_{j'l'M-\mu'}(\mathbf{k}')\, D^{s\lambda^*}_{jlM-\mu}(\mathbf{k}), \tag{5.I}$$

$$L^{\mu'\mu}_{JS'l'Sl}(\mathbf{k}'\mathbf{k}) = \sum_M C^{l'M-\mu',\,S'\mu'}_{JM} C^{lM-\mu,\,S\mu}_{JM} Y_{l'M-\mu'}(\mathbf{k}')\, Y^*_{lM-\mu}(\mathbf{k}). \tag{5.II}$$

It is obvious that $L^{\mu'\lambda',\mu\lambda}$ and $L^{\mu'\mu}$ are matrix elements of the operators L in the spin-function representation and correspond to various components μ, μ', λ, λ', of the spins of the particles (I), or to various components μ, μ', of the spin of the system (II), in the initial and final states. The products of spin functions Q in (4) can be expressed in terms of the Hermitian operators $\mathbf{T}$ connecting the spin space of particles a, b with that of the particles a', b' (*cf.* Ref. 3, p. 70). Therefore Eqs. (4) and (5) make it possible to find the angular polynomials L in explicit form in terms of invariant products of these operators $\mathbf{T}$ and the vectors $\mathbf{k}$, $\mathbf{k}'$. This is done below for reactions with the spin of the system equal to 0, ½, and 1, and for analogous reactions with γ-quanta. For definiteness we shall talk about the scattering and photoproduction of mesons on nucleons, the scattering of photons and nucleons by nucleons, and also the reactions $\mathfrak{N} + \mathfrak{N} \to \pi + D$, $\gamma + D \to p + n$, and $\gamma + D \to \pi + D$.

2. SCATTERING OF MESONS BY NUCLEONS

For this reaction $S = S' = \tfrac{1}{2}$, so that for this reaction Eq. (5.II) is

$$L^{\mu'\mu}_{Jl'l}(\mathbf{k}'\mathbf{k}) = \sum_M C^{l'M-\mu';\ {}^1\!/_2\mu'}_{JM} C^{lM-\mu;\ {}^1\!/_2\mu}_{JM} Y_{l'M-\mu'}(\mathbf{k}')\, Y^*_{lM-\mu}(\mathbf{k}).$$

Since $Q_{{}^1\!/_2\mu}(\alpha) = \delta_{\alpha\mu}$, it is not hard to see that the angular polynomial $L_{Jl'l}(\mathbf{k}'\alpha', \mathbf{k}\alpha)$ can be put in the form

$$L = L^{{}^1\!/_2{}^1\!/_2} \frac{1}{2}(1+\sigma_z) + L^{{}^1\!/_2-{}^1\!/_2} \frac{1}{2}(\sigma_x + i\sigma_y) + L^{-{}^1\!/_2{}^1\!/_2} \frac{1}{2}(\sigma_x - i\sigma_y) + L^{-{}^1\!/_2-{}^1\!/_2} \frac{1}{2}(1-\sigma_z). \tag{6}$$

If we choose the z axis along $\mathbf{k}$, then $Y^*_{lM-\mu}(\mathbf{k}) \neq 0$ only for $M - \mu = 0$ (then $Y^*_{l0}(1) = \sqrt{2l+1}$), so that $M = \mu$, and $M - \mu' = \mu - \mu'$. Since μ and μ' take the values $\pm\tfrac{1}{2}$, we have $M - \mu' = 0, \pm 1$. This means that the matrix L contains $Y_{l'0}(\mathbf{k}')$ and $Y_{l',\pm 1}(\mathbf{k}')$. Let us choose the x axis in the plane of the vectors $\mathbf{k}$, $\mathbf{k}'$. Then

$$Y_{l'0} = \sqrt{2l'+1}\, P_{l'}(\mathbf{k}'\mathbf{k}),\ Y_{l',\pm 1} = \mp \sqrt{\frac{2l'+1}{l'(l'+1)}}\, k'_x P_{l'}(\mathbf{k}'\mathbf{k}).$$

The result is

$$\begin{aligned} L = {} & \frac{1}{2}(1+\sigma_z)\sqrt{(2l+1)(2l'+1)}\, C^{l'0;\ {}^1\!/_2{}^1\!/_2}_{J{}^1\!/_2} C^{l0;\ {}^1\!/_2{}^1\!/_2}_{J{}^1\!/_2} P_{l'} \\ & + \frac{1}{2}(\sigma_x + i\sigma_y)\sqrt{\frac{(2l+1)(2l'+1)}{l'(l'+1)}}\, C^{l'-1;\ {}^1\!/_2{}^1\!/_2}_{J-{}^1\!/_2} C^{l0;\ {}^1\!/_2-{}^1\!/_2}_{J-{}^1\!/_2} k'_x P'_{l'} \\ & - \frac{1}{2}(\sigma_x - i\sigma_y)\sqrt{\frac{(2l+1)(2l'+1)}{l'(l'+1)}}\, C^{l'1;\ {}^1\!/_2-{}^1\!/_2}_{J{}^1\!/_2} C^{l0;\ {}^1\!/_2{}^1\!/_2}_{J{}^1\!/_2} k'_x P'_{l'} \\ & + \frac{1}{2}(1-\sigma_z)\sqrt{(2l+1)(2l'+1)}\, C^{l'0;\ {}^1\!/_2-{}^1\!/_2}_{J-{}^1\!/_2} C^{l0;\ {}^1\!/_2-{}^1\!/_2}_{J-{}^1\!/_2} P_{l'}. \end{aligned} \tag{7}$$

According to the rules of vector addition l, l', and J can be related to each other in the following ways:

$$J = l + {}^1/_2 = l' + {}^1/_2,\ J = l + {}^1/_2 = l' - {}^1/_2,\ J = l - {}^1/_2 = l' + {}^1/_2,$$
$$J = l - {}^1/_2 = l' - {}^1/_2.$$

Furthermore, since the parity of the meson-nucleon system must be conserved, we have $(-1)^{l+1} = (-1)^{l'+1}$. Therefore only two cases are possible: $J = l + ½ = l' + ½$ and $J = l - ½\ l' - ½$. In both cases $l' = l$. Taking the Clebsch-Gordan coefficients for these two cases from tables[3] and substituting them into Eq. (7), we get

$$\begin{aligned} J = l + {}^1/_2 = l' + {}^1/_2,\ L &= (l+1) P_l + i\sigma_y k'_x P'_l = (l+1) P_l - i(\boldsymbol{\sigma}[\mathbf{k}'\mathbf{k}]) P'_l; \\ J = l - {}^1/_2 = l' - {}^1/_2,\ L &= lP_l - i\sigma_y k'_x P'_l = lP_l + i(\boldsymbol{\sigma}[\mathbf{k}'\mathbf{k}]) P'_l, \end{aligned} \tag{8}$$

since $\sigma_y k'_x = \sigma_y k'_x - \sigma_x k'_y = -[\boldsymbol{\sigma}\mathbf{k}']_z = -(\boldsymbol{\sigma}[\mathbf{k}'\mathbf{k}])$. It must be pointed out that the angular polynomials (8) were first obtained by Tamm, Gol'fand, and Fainberg[4] from other considerations. These polynomials correspond to the case in which the parity of the incident and scattered mesons is the same. It is not hard to show that if the parities of the incident and scattered mesons are different, the corresponding polynomials differ from those obtained above only by the factor $-(\boldsymbol{\sigma}\mathbf{k}')$:

$$\begin{aligned} J = l + {}^1/_2 = l' - {}^1/_2,\ L_{Jl'l}(\mathbf{k}'\mathbf{k}) &= -(\boldsymbol{\sigma}\mathbf{k}')[(l+1) P_l - i(\boldsymbol{\sigma}[\mathbf{k}'\mathbf{k}]) P'_l], \\ J = l - {}^1/_2 = l' + {}^1/_2,\ L_{Jl'l}(\mathbf{k}'\mathbf{k}) &= -(\boldsymbol{\sigma}\mathbf{k}')[lP_l + i(\boldsymbol{\sigma}[\mathbf{k}'\mathbf{k}]) P'_l]. \end{aligned} \tag{8'}$$

Since $(\boldsymbol{\sigma}\mathbf{k}')^2 = 1$, the differential cross-section remains invariant with respect to a change of parity of the incident or scattered mesons. This fact is known as Minami's theorem.[5]

3. THE PHOTOPRODUCTION OF MESONS ON NUCLEONS

In this case $\sigma = \sigma' = ½$, $s = 1$, $s' = 0$, so that $j' = l'$. Before applying Eq. (4.I), we note the following facts:

a) In the case under consideration, with $s = 1$, the tensor $D_{jlm}(\mathbf{k}, \gamma)$ which appeared in Eq. (4.I) is commonly called a spherical vector and denoted by $\mathbf{D}_{jlm}(\mathbf{k})$ (the components of this vector are the values of the tensor $D_{jlm}(\mathbf{k}, \gamma)$ at the three "points" γ). The state of a photon with momentum $\mathbf{k}$ and angular momentum j is described by a vector $\mathbf{D}_{jm}(\mathbf{k})$ which is in general a linear combination of three spherical vectors $\mathbf{D}_{jlm}(\mathbf{k})$, $l = j$, $j \pm 1$, given by Eq. (3). But the spherical vector $\mathbf{D}_{jm}(\mathbf{k})$ must satisfy the condition of transversality, $(\mathbf{D}_{jm}(\mathbf{k})\mathbf{k}) = 0$. It can be shown[1] that from the three spherical vectors $\mathbf{D}_{jlm}$ we can construct two transverse vectors $\mathbf{D}^{(0)}_{jm}$, $\mathbf{D}^{(1)}_{jm}$ and one longitudinal vector $\mathbf{D}^{(-1)}_{jm}$, with

$$\mathbf{D}^{(0)}_{jm} = \mathbf{D}_{jjm},\quad \mathbf{D}^{(1)}_{jm} = i[\mathbf{D}_{jjm}\mathbf{k}].$$

The tensors $\mathbf{D}^{(1)}_{jm}$ and $\mathbf{D}^{(0)}_{jm}$ have parities $(-1)^j$ and $(-1)^{j+1}$ [as can be seen from Eq. (3)] and correspond to states of electric and magnetic types. In connection with what has been said, in Eq. (4.I) one must understand the tensor $\mathbf{D}_{jlm}$ to mean the tensor $\mathbf{D}^{(1)}_{jm}$ or the tensor $\mathbf{D}^{(-1)}_{jm}$, depending on the parity of the state.

b) It is usually agreed to characterize the state of a photon not by the component of the spin along a chosen axis, but by the direction of a polarization vector $\mathbf{e} \perp \mathbf{k}$. Then in Eq. (4.I) instead of the product $D^{s\lambda}_{jlm} Q_{s\lambda}$ one must take $(\mathbf{D}^{(1)}_{jm}\mathbf{e})$ or $(\mathbf{D}^{(0)}_{jm}\mathbf{e})$ for the electric and magnetic radiations respectively. In connection with this, in the orthogonality-normalization condition (2), instead of summation over the variable γ' one must carry out an integration over the directions of the vector $\mathbf{e}'$, taking into account the statistical weight, *i.e.*, take the integral over $d\mathbf{e}' \cdot 2/4\pi$.

c) Finally, it can be shown that

$$\mathbf{D}^{(1)}_{jm}(\mathbf{k}) = \frac{1}{\sqrt{j(j+1)}}\left(\frac{\partial}{\partial \mathbf{k}} - \mathbf{k}\left(\mathbf{k}\frac{\partial}{\partial \mathbf{k}}\right)\right) Y_{jm}(\mathbf{k}),$$
$$\mathbf{D}^{(0)}_{jm}(\mathbf{k}) = -\frac{i}{\sqrt{j(j+1)}}\left[\mathbf{k}\frac{\partial}{\partial \mathbf{k}}\right] Y_{jm}(\mathbf{k}),$$

where the vector **k** is to be taken to be a unit vector

$$\begin{aligned}(\mathbf{eD}^{(1)}_{jm}) &= \frac{1}{\sqrt{j(j+1)}}\left(\mathbf{e}\,\frac{\partial}{\partial\mathbf{k}}\right)Y_{jm}\,(\mathbf{k}),\\ (\mathbf{eD}^{(0)}_{jm}) &= \frac{1}{\sqrt{j(j+1)}}\left(i\,[\mathbf{ke}]\,\frac{\partial}{\partial\mathbf{k}}\right)Y_{jm}\,(\mathbf{k}),\end{aligned} \tag{9}$$

In what follows we shall call the operator $(\mathbf{a}\partial/\partial\mathbf{k})$ the "polarization" operator. Then the construction of the operators for the reaction $\gamma + b \rightarrow a' + b'$ reduces to the "polarization" of the operators for the reaction $a + b \rightarrow a' + b'$, where a is a scalar or pseudoscalar particle with spin 0.

Thus we shall start with the formula

$$L^{\mu'\mu} = \frac{1}{\sqrt{j(j+1)}}\left(\mathbf{e}\,\frac{\partial}{\partial\mathbf{k}}\right)^{*}\sum_{M} C^{l'M-\mu';\ {}^{1}/_{2}\mu'}_{JM}\,C^{jM-\mu;\ {}^{1}/_{2}\mu}_{JM}\,Y_{l'M-\mu'}(\mathbf{k}')\,Y^{*}_{jM-\mu}(\mathbf{k}),$$

in which for the magnetic radiation one must replace **e** by $i[\mathbf{ke}]$. Therefore, if we recall the rule for vector addition: $J = j + \frac{1}{2} = l' + \frac{1}{2}$, $J = j - \frac{1}{2} = l' + \frac{1}{2}$, $J = j + \frac{1}{2} = l' - \frac{1}{2}$, $J = j - \frac{1}{2} = l' - \frac{1}{2}$, and the conservation of parity: $(-1)^{j} = (-1)^{l'+1}$, $(-1)^{j+1} = (-1)^{l'+1}$ for the electric and magnetic radiations respectively, the construction of the polynomials L reduces to the magnetic and electric "polarization" of the operators (8) and (8′) respectively. The angular polynomials have the following forms:

$$\begin{gathered} J = j + {}^{1}/_{2} = l' + {}^{1}/_{2},\\ \frac{1}{\sqrt{j(j+1)}}\{P'_j[-(\sigma[\mathbf{k}'\mathbf{s}]) - i(j+1)(\mathbf{k}'\mathbf{s})] - P''_j(\sigma[\mathbf{k}'\mathbf{k}])(\mathbf{k}'\mathbf{s})\},\\ J = j - {}^{1}/_{2} = l' + {}^{1}/_{2},\\ -\frac{1}{\sqrt{j(j+1)}}\{P'_j[(\sigma\mathbf{e}) + (j-1)(\sigma\mathbf{k}')(\mathbf{k}'\mathbf{e})] + P''_j[(\sigma\mathbf{k})(\mathbf{k}'\mathbf{e}) - (\sigma\mathbf{k}')(\mathbf{k}'\mathbf{e})(\mathbf{k}'\mathbf{k})]\},\\ J = j + {}^{1}/_{2} = l' - {}^{1}/_{2},\\ \frac{1}{\sqrt{j(j+1)}}\{P'_j[(\sigma\mathbf{e}) - (j+2)(\sigma\mathbf{k}')(\mathbf{k}'\mathbf{e})] + P''_j[(\sigma\mathbf{k})(\mathbf{k}'\mathbf{e}) - (\sigma\mathbf{k}')(\mathbf{k}'\mathbf{e})(\mathbf{k}'\mathbf{k})]\},\\ J = j - {}^{1}/_{2} = l' - {}^{1}/_{2},\\ \frac{1}{\sqrt{j(j+1)}}\{P'_j[(\sigma[\mathbf{k}'\mathbf{s}]) - ij(\mathbf{k}'\mathbf{s})] + P''_j(\sigma[\mathbf{k}'\mathbf{k}])(\mathbf{k}'\mathbf{s})\},\end{gathered} \tag{10}$$

where $\mathbf{s} = [\mathbf{ke}]$. From the conservation of parity it can be seen that the polynomials of the 1st and 4th types correspond to magnetic radiation, and those of the 2nd and 3rd types to electric radiation.

The angular distributions, averaged over the spins of the initial states and summed over the spins of the final states, are given by the quantity $\frac{1}{2}\,\mathrm{Sp}\,|L|^2$:

$$\begin{gathered} J = j + {}^{1}/_{2} = l' + {}^{1}/_{2},\\ \frac{1}{j(j+1)}\{[1 + j(j+2)(\mathbf{k}'\mathbf{s})^2]\,P'^2_j - j(j+1)(\mathbf{k}'\mathbf{s})^2 P_j P''_j\};\\ J = j - {}^{1}/_{2} = l' + {}^{1}/_{2},\\ \frac{1}{j(j+1)}\{[1 + (j^2-1)(\mathbf{k}'\mathbf{e})^2]\,P'^2_j - j(j+1)(\mathbf{k}'\mathbf{e})^2 P_j P''_j\};\\ J = j + {}^{1}/_{2} = l' - {}^{1}/_{2},\\ \frac{1}{j(j+1)}\{[1 + j(j+2)(\mathbf{k}'\mathbf{e})^2]\,P'^2_j - j(j+1)(\mathbf{k}'\mathbf{e})^2 P_j P''_j\};\\ J = j - {}^{1}/_{2} = l' - {}^{1}/_{2},\\ \frac{1}{j(j+1)}\{[1 + (j^2-1)(\mathbf{k}'\mathbf{s})^2]\,P'^2_j - j(j+1)(\mathbf{k}'\mathbf{s})^2 P_j P''_j\}.\end{gathered} \tag{11}$$

From these formulas it can be seen that the angular distributions with the same J and j differ only by rotation by 90° around the axis $\mathbf{k}$: in fact, on such a rotation $(\mathbf{k}'\mathbf{e})^2$ goes over into $(\mathbf{k}'\mathbf{s})^2$, and vice versa. On averaging over the polarizations

$$\overline{(\mathbf{k}'\mathbf{e})^2} = \overline{(\mathbf{k}'\mathbf{s})^2} = {}^1/_2\,(1-(\mathbf{k}'\mathbf{k})^2)$$

and the angular distributions of reactions with the same J and j are identical, as was noted by Feld in Ref. 6.

4. SCATTERING OF PHOTONS BY NUCLEONS

In this case $\sigma = \sigma' = 1/2$, $s = s' = 1$. In the construction of the polynomials of this type we shall start from Eq. (4.I) with the same changes as in the case of the photoproduction of mesons – namely, in place of the products $D^{s\lambda}_{jlm}\,Q_{s\lambda}$ we shall use the scalar products (9) for the electric and magnetic radiations respectively. Thus we shall start with the formula

$$L^{\mu'\mu} = \frac{1}{\sqrt{j'(j'+1)\,j(j+1)}}\left(\mathbf{e}'\,\frac{\partial}{\partial\mathbf{k}'}\right)\left(\mathbf{e}\,\frac{\partial}{\partial\mathbf{k}}\right)^{*}\sum_{M} C^{j'M-\mu';\ {}^1/_2\mu'}_{JM}\,C^{jM-\mu;\ {}^1/_2\mu}_{JM}\,Y_{j'M-\mu'}(\mathbf{k}')\,\overset{*}{Y}_{jM-\mu}(\mathbf{k})$$

(in this form it corresponds to the absorption and emission of electric radiation). The construction of the polynomials is carried out just as in Secs. 2 and 3, taking account of the vector addition of the angular momenta: $J = j = 1/2 = j' + 1/2$, $J = j - 1/2 = j' + 1/2$, $J = j + 1/2 = j' - 1/2$, $J = j - 1/2 = j' - 1/2$, and the conservation of parity. As the result we get for the polynomials corresponding to the absorption of electric quanta the following expressions

$$\begin{aligned}
&J = j + {}^1/_2 = j' + {}^1/_2,\quad \frac{1}{j(j+1)}\{[(j+1)(\mathbf{e}'\mathbf{e}) - i(\boldsymbol{\sigma}[\mathbf{e}'\mathbf{e}])]\,P'_j\\
&\quad + [(j+1)(\mathbf{k}'\mathbf{e})(\mathbf{e}'\mathbf{k}) + i(\boldsymbol{\sigma}\mathbf{k})(\mathbf{k}'[\mathbf{e}'\mathbf{e}]) + i(\boldsymbol{\sigma}\mathbf{k}')([\mathbf{e}'\mathbf{e}]\,\mathbf{k}) - i(\boldsymbol{\sigma}[\mathbf{k}'\mathbf{k}])(\mathbf{e}'\mathbf{e})\\
&\quad - 2i(\boldsymbol{\sigma}[\mathbf{e}'\mathbf{e}])(\mathbf{k}'\mathbf{k})]\,P''_j - i(\boldsymbol{\sigma}[\mathbf{k}'\mathbf{k}])(\mathbf{e}'\mathbf{k})(\mathbf{k}'\mathbf{e})\,P'''_j\};\\
&J = j - {}^1/_2 = j' + {}^1/_2,\quad \frac{i}{j\sqrt{j^2-1}}\{-(j-1)[(\boldsymbol{\sigma}\mathbf{s}')(\mathbf{k}'\mathbf{e}) + (\boldsymbol{\sigma}\mathbf{k}')(\mathbf{s}'\mathbf{e})]\,P'_j\\
&\quad + [-(i-2)(\boldsymbol{\sigma}\mathbf{k}')(\mathbf{s}'\mathbf{k})(\mathbf{k}'\mathbf{e}) - (\boldsymbol{\sigma}\mathbf{k})(\mathbf{s}'\mathbf{e}) - (\boldsymbol{\sigma}\mathbf{e})(\mathbf{s}'\mathbf{k}) + (\boldsymbol{\sigma}\mathbf{k}')(\mathbf{s}'\mathbf{e})(\mathbf{k}'\mathbf{k})\\
&\quad + (\boldsymbol{\sigma}\mathbf{s}')(\mathbf{k}'\mathbf{e})(\mathbf{k}'\mathbf{k})]\,P''_j - (\boldsymbol{\sigma}[[\mathbf{k}'\mathbf{k}]\,\mathbf{k}'])(\mathbf{k}'\mathbf{e})(\mathbf{s}'\mathbf{k})\,P'''_j\};\\
&J = j + {}^1/_2 = j' - {}^1/_2,\quad \frac{i}{(j+1)\sqrt{j(j+2)}}\{-(j+2)[(\boldsymbol{\sigma}\mathbf{s}')(\mathbf{k}'\mathbf{e}) + (\boldsymbol{\sigma}\mathbf{k}')(\mathbf{s}'\mathbf{e})]\,P'_j \qquad (12)\\
&\quad + [-(j+3)(\boldsymbol{\sigma}\mathbf{k}')(\mathbf{s}'\mathbf{k})(\mathbf{k}'\mathbf{e}) + (\boldsymbol{\sigma}\mathbf{k})(\mathbf{s}'\mathbf{e}) + (\boldsymbol{\sigma}\mathbf{e})(\mathbf{s}'\mathbf{k}) - (\boldsymbol{\sigma}\mathbf{k}')(\mathbf{s}'\mathbf{e})(\mathbf{k}'\mathbf{k})\\
&\quad - (\boldsymbol{\sigma}\mathbf{s}')(\mathbf{k}'\mathbf{e})(\mathbf{k}'\mathbf{k})]\,P''_j + (\boldsymbol{\sigma}[[\mathbf{k}'\mathbf{k}]\,\mathbf{k}'])(\mathbf{k}'\mathbf{e})(\mathbf{s}'\mathbf{k})\,P'''_j\};\\
&J = j - {}^1/_2 = j' - {}^1/_2,\quad \frac{1}{j(j+1)}\{[j(\mathbf{e}'\mathbf{e}) + i(\boldsymbol{\sigma}[\mathbf{e}'\mathbf{e}])]\,P'_j\\
&\quad + [j(\mathbf{k}'\mathbf{e})(\mathbf{e}'\mathbf{k}) - i(\boldsymbol{\sigma}\mathbf{k})(\mathbf{k}'[\mathbf{e}'\mathbf{e}]) - i(\boldsymbol{\sigma}\mathbf{k}')([\mathbf{e}'\mathbf{e}]\,\mathbf{k}) + i(\boldsymbol{\sigma}[\mathbf{k}'\mathbf{k}])(\mathbf{e}'\mathbf{e})\\
&\quad + 2i(\boldsymbol{\sigma}[\mathbf{e}'\mathbf{e}])(\mathbf{k}'\mathbf{k})]\,P''_j + i(\boldsymbol{\sigma}[\mathbf{k}'\mathbf{k}])(\mathbf{e}'\mathbf{k})(\mathbf{k}'\mathbf{e})\,P'''_j\}.
\end{aligned}$$

The polynomials corresponding to the absorption of magnetic quanta are obtained from (12) by the following replacements: in all the polynomials $\mathbf{e}$ is replaced by $-i[\mathbf{ke}]$, and in polynomials 1, and 4 $\mathbf{e}'$ is replaced by $i[\mathbf{k}'\mathbf{e}']$, while in polynomials 2 and 3 $i[\mathbf{k}'\mathbf{e}']$ is replaced by $\mathbf{e}'$.

The angular distributions for transitions of the 1st and 4th types, averaged over the spins of the initial states of the nucleon and summed over those of the final states, are given by

$$\frac{1}{j^2(j+1)^2}\{[j(j+2)(\mathbf{e}'\mathbf{e})^2+1]P_j'^2+2j(\mathbf{k}'\mathbf{e})(\mathbf{e}'\mathbf{k})(\mathbf{e}'\mathbf{e})P_j'P_j''$$

$$-j(j+1)(\mathbf{e}'\mathbf{k})^2(\mathbf{k}'\mathbf{e})^2P_j'P_j'''+[j(j+2)(\mathbf{k}'\mathbf{e})^2(\mathbf{e}'\mathbf{k})^2+1-(\mathbf{k}'\mathbf{k})^2]P_j''^2\};$$

$$\frac{1}{j^2(j+1)^2}\{[(j^2-1)(\mathbf{e}'\mathbf{e})^2+1]P_j'^2-2(j+1)(\mathbf{k}'\mathbf{e})(\mathbf{e}'\mathbf{k})(\mathbf{e}'\mathbf{e})P_j'P_j''$$

$$-j(j+1)(\mathbf{e}'\mathbf{k})^2(\mathbf{k}'\mathbf{e})^2P_j'P_j'''+[(j^2-1)(\mathbf{k}'\mathbf{e})^2(\mathbf{e}'\mathbf{k})^2+1-(\mathbf{k}'\mathbf{k})^2]P_j''^2\}.$$

The angular distributions for transitions of the 2nd and 3rd types are more cumbersome, and therefore are not written out here. We remark that the angular polynomials for the photoproduction of mesons and the scattering of photons by nucleons have been obtained previously in Ref. 2.

5. SCATTERING OF NUCLEONS BY NUCLEONS

In this case we shall use Eq. (4.II), in which $S = S' = 1$ for triplet transitions and $S = S' = 0$ for singlet transitions (as is well known, in the scattering of nucleons by nucleons the spin **S** of the system is conserved). The construction of the matrices L is again carried through as in Sec. 2; in doing so, we use instead of the matrices $\boldsymbol{\sigma}$ the matrices **S** of the spin of the system. Then the matrix L can be expressed in the form

$$L=L^{11}\frac{1}{2}(S_z^2+S_z)+L^{10}\frac{1}{\sqrt{2}}S_z(S_x+iS_y)+L^{1-1}\frac{1}{2}(S_x+iS_y)^2+$$

$$+L^{01}\frac{1}{\sqrt{2}}(S_x-iS_y)S_z+L^{00}(1-S_z^2)-L^{0-1}\frac{1}{\sqrt{2}}(S_x+iS_y)S+$$

$$+L^{-11}\frac{1}{2}(S_x-iS_y)^2-L^{-10}\frac{1}{\sqrt{2}}S_z(S_x-iS_y)+L^{-1-1}\frac{1}{2}(S_z^2-S_z).$$

By calculations taking account of the vector composition of angular momenta and of the conservation of parity we get:

A. *Triplet States*

$$J=l+1=l'+1,$$

$$\frac{1}{l+1}\{(l+1)P_l+[2(\mathbf{k}'\mathbf{k})-(\mathbf{S}\mathbf{k}')(\mathbf{S}\mathbf{k})-(l+1)i(\mathbf{S}\mathbf{n})]P_l'-(\mathbf{S}\mathbf{n})^2P_l''\};$$

$$J=l+1=l'-1,$$

$$\frac{1}{\sqrt{(l+1)(l+2)}}\{[-2(l+1)^2+(2l+3)(l+1)(\mathbf{S}\mathbf{k}')^2]P_l$$

$$+[-2(l+2)(\mathbf{S}\mathbf{k}')(\mathbf{S}\mathbf{k})+(2l+3)(\mathbf{S}\mathbf{k}')^2(\mathbf{k}'\mathbf{k})+(l+2)i(\mathbf{S}\mathbf{n})$$

$$+2(\mathbf{k}'\mathbf{k})]P_l'-(\mathbf{S}\mathbf{n})^2P_l''\};$$

$$J=l-1=l'+1, \tag{13}$$

$$\frac{1}{\sqrt{l(l-1)}}\{[-2l^2+(2l-1)l(\mathbf{S}\mathbf{k}')^2]P_l+[2(l-1)(\mathbf{S}\mathbf{k}')(\mathbf{S}\mathbf{k})$$

$$-(2l-1)(\mathbf{S}\mathbf{k}')^2(\mathbf{k}'\mathbf{k})-(l-1)i(\mathbf{S}\mathbf{n})+2(\mathbf{k}'\mathbf{k})]P_l'-(\mathbf{S}\mathbf{n})^2P_l''\};$$

$$J=l-1=l'-1,$$

$$\frac{1}{l}\{-lP_l+[2(\mathbf{k}'\mathbf{k})-(\mathbf{S}\mathbf{k}')(\mathbf{S}\mathbf{k})+li(\mathbf{S}\mathbf{n})]P_l'-(\mathbf{S}\mathbf{n})^2P_l''\};$$

$$J=l=l'.$$

$$\frac{2l+1}{l(l+1)}\{l(l+1)P_l+[(\mathbf{S}\mathbf{k}')(\mathbf{S}\mathbf{k})-2(\mathbf{k}'\mathbf{k})]P_l'+(\mathbf{S}\mathbf{n})^2P_l''\}.$$

In these formulas $\mathbf{n} = [\mathbf{k}'\mathbf{k}]$. For the singlet states Eq. (5.II) reduces to $\sum_M Y_{lM}^{*}(\mathbf{k})\, Y_{lM}(\mathbf{k}')$.

B. *Singlet States*

$$J = l = l',\ S = 0,\ L = (2l + 1)\, P_l. \tag{14}$$

6. THE REACTION $\mathfrak{N} + \mathfrak{N} \to \pi + D$

Just as in Sec. 5 we shall use Eq. (4.II), in which we have for the triplet → triplet transitions $S = S' = 1$, and for singlet → triplet transitions $S = 0$, $S' = 1$. For pseudoscalar π mesons we get from the conservation of angular momentum and of parity four varieties in the case of triplet → triplet transitions: $J = l + 1 = l'$, $J = l = l' + 1$, $J = l = l' - 1$, $J = l - 1 = l'$, and for the singlet → triplet transitions two varieties: $J = l = l' + 1$, $J = l = l' - 1$. For the triplet → triplet transitions the spin functions in Eq. (4.II) can be conveniently expressed in terms of the spin matrices **S**, as was done in Sec. 5.

Triplet → triplet:

$$\begin{gathered}
J = l + 1 = l', \\
\frac{1}{\sqrt{l+1}} \sqrt{\frac{2l+3}{l+2}} \{-(l+1)(\mathbf{S}\mathbf{k}')\, P_l - [(\mathbf{S}\mathbf{k}')(\mathbf{k}'\mathbf{k}) - i(l+2)(\mathbf{S}\mathbf{k}')(\mathbf{S}\mathbf{n})]\, P_l' - i(\mathbf{S}[\mathbf{n}\mathbf{k}'])(\mathbf{S}\mathbf{n})\, P_l''\}; \\
J = l = l' + 1, \\
\frac{1}{l} \sqrt{\frac{2l+1}{l+1}} \{[-(\mathbf{S}\mathbf{k}) + i(l-1)(\mathbf{S}\mathbf{n})(\mathbf{S}\mathbf{k}')]\, P_l' + i(\mathbf{S}\mathbf{n})(\mathbf{S}[\mathbf{n}\mathbf{k}'])\, P_l''\}, \\
J = l = l' - 1, \\
\frac{1}{l+1} \sqrt{\frac{2l+1}{l}} \{[-(\mathbf{S}\mathbf{k}) - i(l+2)(\mathbf{S}\mathbf{n})(\mathbf{S}\mathbf{k}')]\, P_l' + i(\mathbf{S}\mathbf{n})(\mathbf{S}[\mathbf{n}\mathbf{k}'])\, P_l\}, \\
J = l - 1 = l', \\
\frac{1}{l} \sqrt{\frac{2l-1}{l-1}} \{l(\mathbf{S}\mathbf{k}')\, P_l - [(\mathbf{S}\mathbf{k}')(\mathbf{k}'\mathbf{k}) + i(l-1)(\mathbf{S}\mathbf{k}')(\mathbf{S}\mathbf{n})]\, P_l' - i(\mathbf{S}[\mathbf{n}\mathbf{k}'])(\mathbf{S}\mathbf{n})\, P_l''\}.
\end{gathered} \tag{15}$$

Here $\mathbf{n} = [\mathbf{k}'\mathbf{k}]$. In the case of the singlet → triplet transitions the spin functions can be conveniently expressed in terms of the matrices **T** (*cf.* Ref. 3, p. 70), the elements of which correspond to singlet ⇄ triplet transitions.

Singlet → triplet

$$\begin{gathered}
J = l = l' + 1,\ \sqrt{\frac{2l+1}{l}} \{[(\mathbf{T}\mathbf{k}) - (\mathbf{T}\mathbf{k}')(\mathbf{k}'\mathbf{k})]\, P_l' + l(\mathbf{T}\mathbf{k}')\, P_l\}, \\
J = l = l' - 1,\ \sqrt{\frac{2l+1}{l+1}} \{[(\mathbf{T}\mathbf{k}) - (\mathbf{T}\mathbf{k}')(\mathbf{k}'\mathbf{k})]\, P_l' - (l+1)(\mathbf{T}\mathbf{k}')\, P_l\}.
\end{gathered} \tag{16}$$

For the reaction $\mathfrak{N} + \mathfrak{N} \to \pi + D$ with pseudoscalar mesons, in the case of the singlet → triplet transitions the type $J = l = l'$ is forbidden because of parity. For completeness, however, we write out the corresponding angular operator

$$J = l = l',\ -\frac{2l+1}{\sqrt{l(l+1)}}\, i(\mathbf{T}[\mathbf{k}'\mathbf{k}])\, P_l'. \tag{17}$$

With this inclusion, the operators written out in Secs. 5 and 6 form a complete set of angular operators for reactions in which the total spin of the initial and final states is equal to zero or unity.*

7. THE REACTIONS $\gamma + D \to p + n$ AND $\gamma + D \to \pi + D$

1. Using Eqs. (4) and (5) and also the considerations presented in Sec. 3, one can show without difficulty that the basic formula for the construction of the angular operators for the reactions $\gamma + D \to p + n$ and $\gamma + D \to \pi + D$ is

$$L_{Jl'S'j1}(\mathbf{k}'\mathbf{k}) = \frac{1}{\sqrt{j(j+1)}}\left(\mathbf{a}\frac{\partial}{\partial \mathbf{k}}\right)^{*} \sum_{M} C_{JM}^{l'M-\mu';\,S'\mu'} C_{JM}^{jM-\mu;\,1\mu}\, Y_{l'M-\mu'}(\mathbf{k}')\, Y^{*}_{jM-\mu}(\mathbf{k})\, Q_{S'\mu'}(\alpha')\, Q^{*}_{1\mu}(\alpha), \qquad (18)$$

where $S' = 0$ or 1 for transitions into singlet or triplet states, and $\mathbf{a} = \mathbf{e}$ and $i[\mathbf{ke}]$ respectively for electric and magnetic quanta. Apart from the "polarization" operator $[j(j+1)]^{-1/2}(\mathbf{a}\partial/\partial\mathbf{k})$ the right-hand member of Eq. (18) agrees exactly with the formula (4.II) used in Secs. 5 and 6 for the construction of the operators for the reactions $\mathfrak{N} + \mathfrak{N} \to \mathfrak{N} + \mathfrak{N}$ and $\mathfrak{N} + \mathfrak{N} \to \pi + D$, if we just make the replacement in the latter formula of the orbital angular momentum l by the total angular momentum j of the photon. Therefore the angular operators for the reactions $\gamma + D \to p + n$ and $\gamma + D \to \pi + D$ are obtained from the operators of Sections 5 and 6 by the simple application of the "polarization" operator $[j(j+1)]^{-1/2}(\mathbf{a}\partial/\partial\mathbf{k})^{*}$. Here, however, one remark must be made. Equations (16) and (17) correspond to the singlet → triplet case. Therefore for the reaction $\gamma + D \to p + n$ one must go over from these formulas to the triplet → singlet case. For this purpose we can use the Hermitian adjoint relation $[L_{Jl'S'lS}(\mathbf{k}'\mathbf{k})]^{+} L_{JlSl'S'}(\mathbf{k}\mathbf{k}')$ and the exchange of notations $lS\mathbf{k} \rightleftarrows l'S'\mathbf{k}'$. We get as the result:

Triplet → singlet

$$J = l + 1 = l'.\quad \sqrt{\frac{2l'+1}{l'}}\,\{[(\mathbf{Tk}') - (\mathbf{Tk})(\mathbf{k}'\mathbf{k})]\,P'_{l'} = l'(\mathbf{Tk})\,P_{l'}\},$$

$$J = l - 1 = l'.\quad \sqrt{\frac{2l'+1}{l'+1}}\,\{[(\mathbf{Tk}') - (\mathbf{Tk})(\mathbf{k}'\mathbf{k})]\,P'_{l'} - (l'+1)(\mathbf{Tk})\,P_{l'}\}, \qquad (19)$$

$$J = l = l' \cdot \frac{2l'+1}{\sqrt{l'(l'+1)}}\, i(\mathbf{T}\,[\mathbf{kk}'])\,P'_{l'}. \qquad (20)$$

Then, taking the conservation of parity into account for the reaction $\gamma + D \to p + n$, we get the angular operators in the form

$$\left.\begin{array}{ll} \frac{1}{\sqrt{j(j+1)}}\left(\mathbf{e}\,\frac{\partial}{\partial\mathbf{k}}\right)^{*} & (13)\ (\text{triplet} \to \text{triplet}) \\ \frac{1}{\sqrt{j(j+1)}}\left(\mathbf{e}\,\frac{\partial}{\partial\mathbf{k}}\right)^{*} & (20)\ (\text{triplet} \to \text{singlet}) \end{array}\right\}\ \text{absorption of an electric quantum}$$

$$\left.\begin{array}{ll} \frac{1}{\sqrt{j(j+1)}}\left(i\,[\mathbf{ke}]\,\frac{\partial}{\partial\mathbf{k}}\right)^{*} & (15)\ (\text{triplet} \to \text{triplet}) \\ \frac{1}{\sqrt{j(j+1)}}\left(i\,[\mathbf{ke}]\,\frac{\partial}{\partial\mathbf{k}}\right)^{*} & (19)\ (\text{triplet} \to \text{singlet}) \end{array}\right\}\ \text{absorption of a magnetic quantum}$$

and for the reaction $\gamma + D \to \pi + D$ we get them in the form

---

*If the spin of the system arises from the addition of the spins of particles of spin ½, then $\mathbf{S} = \frac{1}{2}(\boldsymbol{\sigma}_1 + \boldsymbol{\sigma}_2)$, $\mathbf{T} = \frac{1}{2}(\boldsymbol{\sigma}_1 - \boldsymbol{\sigma}_2)$.

$$\frac{1}{\sqrt{j(j+1)}}\left(\mathbf{e}\frac{\partial}{\partial \mathbf{k}}\right)^{*} \quad (15),$$

$$\frac{1}{\sqrt{j(j+1)}}\left(i\,[\mathbf{ke}]\,\frac{\partial}{\partial \mathbf{k}}\right)^{*} \quad (13).$$

We do not write these operators out in greater detail here.

8. CONCLUSION

A knowledge of the coefficients $S_{J\pi\nu'\nu}^{fi}$ in the expression of the scattering matrix in terms of the angular operators L [*cf.* the relation (A)] gives complete information about the scattering matrix. More complete evidence as to the behavior of these quantities can be obtained by the study of reactions with polarized particles. In this case the differential scattering cross-section is determined from the scattering matrix S by the formula

$$d\sigma/d\Omega = \mathrm{Sp}\,(S\rho S^{+}), \tag{21}$$

where ρ is the density matrix describing the polarization of the incident particles.[7,8] In the case of unpolarized particles $\rho = 1/(2s+1)$, and we have the usual definition of the differential cross-section. The polarization of the scattered particles is completely described by the density matrix ρ',

$$\rho' = S\rho S^{+}/\mathrm{Sp}\,(S\rho S^{+}), \tag{22}$$

so that the average value of any operator Ω in the spin space of the scattered particles is given by the relation

$$\langle\Omega\rangle' = \mathrm{Sp}\,(\rho'\Omega). \tag{23}$$

In virtue of the expansion (A) the differential cross-section $d\sigma/d\Omega$ and the average values of operators Ω can be obtained in terms of the coefficients $S^{fi}{}_{J\pi\nu'\nu}$ and known functions of the angles. Thus the coefficients $S^{fi}{}_{J\pi\nu'\nu}$ can be directly related to experimentally measured quantities.

The angular operators make it possible to carry out a generalized phase-shift analysis of the scattering amplitude (in this connection see Ref. 9), and to obtain the angular distributions and polarizations of the particles in the partial transitions. They are also very convenient for the separation of angular variables in various sorts of equations. For example, if the scattering amplitude obeys an integral equation of the Fredholm type, in which the integration is performed both over the energy and over angles, then, by expanding this amplitude, the kernel, and the inhomogeneous term of the equation in series of the angular operators and carrying out the integration over the angles, owing to the orthogonality condition (2) we obtain one-dimensional integral equations for the partial amplitudes.

---

[1] A. I. Akhiezer and V. B. Berestetskii, *Quantum Electrodynamics*, GITTL, 1953.

[2] V. I. Ritus, J. Exptl. Theoret. Phys. (U.S.S.R.) **27**, 660 (1954).

[3] E. U. Condon and G. H. Shortley, The Theory of Atomic Spectra, Cambridge Univ. Press, 1935.

[4] Tamm, Gol'fand, and Fainberg, J. Exptl. Theoret. Phys. (U.S.S.R.) **26**, 649 (1954).

[5] Bethe, de Hoffmann, and Schweber, Mesons and Fields, vol. 2.

[6] B. T. Feld, Phys. Rev. **89**, 330 (1953).

[7] R. H. Dalitz, Proc. Phys. Soc. **A65**, 175 (1952).

[8] L. Wolfenstein and J. Ashkin, Phys. Rev. **85**, 947 (1952).

[9] Iu. A. Gol'fand, J. Explt. Theoret. Phys. (U.S.S.R.) 31, 224 (1956); Soviet Phys. JETP 4, 103 (1957).

Translated by W. H. Furry
297

SOVIET PHYSICS JETP VOLUME 5, NUMBER 6 DECEMBER 15, 1957

Thermodynamic Theory of "Weak" Ferromagnetism In Antiferromagnetic Substances

I. E. DZIALOSHINSKII
Physical Problems Institute, Academy of Sciences, U.S.S.R.

(Submitted to JETP editor February 19, 1957)
J. Exptl. Theoret. Phys. (U.S.S.R.) 32, 1547-1562 (June, 1957)

A thermodynamic theory of "weak" ferromagnetism in α-Fe_2O_3, $MnCO_3$, and $CoCO_3$ is developed on the basis of Landau's theory of phase transitions of the second kind. It is shown that "weak" ferromagnetism is due to relativistic spin-lattice interaction and magnetic dipole interaction. A strong dependence of the properties of such "weak" ferromagnetics upon the magnetic symmetry of the crystal is noted. Their behavior in an external magnetic field is studied.

SOME ANTIFERROMAGNETIC crystals, for example α-Fe_2O_3 and the carbonates $MnCO_3$ and $CoCO_3$, exhibit a spontaneous magnetization. However, its magnitude is extremely small and varies from 10^{-2} to 10^{-5} of the nominal value. In α-Fe_2O_3 it amounts, according to measurements of Néel and Pauthenet,[1] to 0.02%; in the carbonates, according to measurements of A. S. Borovik-Romanov and M. P. Orlova,[2] to 0.2% for $MnCO_3$ and 2% for $CoCO_3$. The smallness of the spontaneous magnetization indicates that here we are not dealing with ordinary exchange ferromagnetism; for it, the spontaneous magnetization is equal in order of magnitude to the nominal value except in the vicinity of the Curie point.

In a recent work of Yin-Yuan Li,[3] this phenomenon is attributed to the existence of antiferromagnetic domains with magnetized boundaries. But as the author himself points out, the formation of such domains is energetically disadvantageous and would be possible only because of inhomogeneities and impurities in the crystal. Consequently the ferromagnetic properties of a crystal would depend greatly on its purity and homogeneity, would vary from specimen to specimen, and obviously would disappear completely in an ideal crystal.

Work[2] on very pure polycrystalline specimens indicates that the ferromagnetism remains even in this case; and by the same token, a connection between the "weak" ferromagnetism and any kind of nonequilibrium phenomenon appears very improbable. We shall show that many properties of such "weak" ferromagnetics are as immediate consequence of thermodynamics and can be fully explained by their magnetic symmetry, within the framework of the theory of phase transitions of the second kind developed by Landau.[4,5]

MAGNETIC SYMMETRY

Apart from the anomalous smallness of the spontaneous magnetic moment, "weak" ferromagnetism is characterized by great sensitivity to the symmetry of the crystal.

Consider, for example, the two isomorphic antiferromagnetics α-Fe_2O_3 and Cr_2O_3. They both belong to the rhombohedral system, and their arrangement of atoms has the symmetry of the space group D_{3d}^6.[6] In their unit cell are four Fe^{+3} or Cr^{+3} ions, located along a body diagonal of the rhombohedron (*cf.* Fig. 1). Neutronographic studies of Shull *et al.*[7] and of Brockhouse[8] have established that in the antiferromagnetic state, the magnetic and geometric unit cells coincide. The spins of ions 1, 2, 3, and 4 differ only in sign, and their sum over the cell is equal to zero; in α-Fe_2O_3, $\mathbf{s}_1 = -\mathbf{s}_2 = -\mathbf{s}_3 = \mathbf{s}_4$, and in Cr_2O_3, $\mathbf{s}_1 = -\mathbf{s}_2 = \mathbf{s}_3 = -\mathbf{s}_4$ (*cf.* Fig. 1 b; c). The direction of the spins with respect to the crystal axes in Cr_2O_3 has not been determined. α-Fe_2O_3 can exist in two different antiferromagnetic states, depending on the temperature: for $T < 250°K$ the spins point along the crystal axis (state I), and for $250° K < T < 950° K$ they lie in one of the vertical planes of symmetry at a small angle to the basal plane (111) (state II).

It is found that Cr_2O_3 in general possesses no ferromagnetism, and that α-Fe_2O_3 is ferromagnetic only in state II. With a lowering of the temperature, the spontaneous magnetic moment disappears when the transition occurs from state II to state I.

Suppose that we know the symmetry of the antiferromagnetic distribution of the spins, with their sum over the unit cell equal to zero. Then the question arises, does or does not the given symmetry permit ferromagnetism? In other words, is it possible to

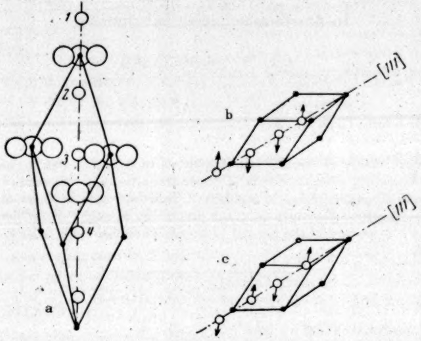

FIG. 1. (a) Unit cell of α-Fe_2O_3 and Cr_2O_3: the large circles denote oxygen ions, the small circles metallic ions. (b) Antiferromagnetic structure of α-Fe_2O_3. (c) Antiferromagnetic structure of Cr_2O_3.

change the directions or magnitudes of the spins, without disturbing the symmetry of their original distribution, in such a way as to make the sum of the spins over the unit cell different from zero?

For example, in state II of α-Fe_2O_3, ferromagnetism would appear if all the spins were to leave the planes of symmetry and turn toward one another (Fig. 2). The possiblity of such a rotation actually depends on whether the magnetic symmetry of state II and the symmetry of the state with rotated spins coincide.

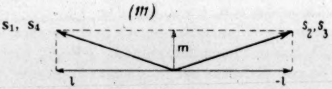

FIG. 2. Projection of the spins of the ions in α-Fe_2O_3 on the (111) plane.

The symmetry of a magnetic crystal is determined not only by the distribution of its atoms but also by the value of the mean spin $\mathbf{s}(x, y, z)$ at each point. As is known,[5] the vector quantity $\mathbf{s}(x, y, z)$ may possess, in addition to the usual symmetry transformations (that is, axes of rotation, planes of symmetry, and translations), also a singular element of symmetry R, consisting of a change of its sign: $\mathbf{s}(x, y, z) \to -\mathbf{s}(x, y, z)$. This is a consequence of the invariance of the equations of mechanics with respect to a simultaneous change of the sign of time and the sign of the magnetic field and the spins.

If the spin distribution by itself possesses the element R, then $\mathbf{s}(x, y, z) = -\mathbf{s}(x, y, z) = 0$, and the crystal will be paramagnetic. Any $\mathbf{s}(x, y, z)$ different from zero may, however, be invariant with respect to various combinations of R with axes of rotation, planes of symmetry, and translations. Therefore, along with the known 230 space groups, which describe all the possible types of symmetry of the distribution of atoms in a crystal, there arise new specifically "magnetic" space groups, which describe the symmetry of the distribution of spins.

The groups obtainable by this method have not yet all been constructed. However, in order to describe the symmetry of a ferromagnetic body it is not necessary to know the corresponding space group. The symmetry of the ferromagnetic properties, as in general of all macroscopic properties, is determined by the symmetry class, *i.e.*, by the point group that is obtained from the corresponding space group by replacing translations by identity transformations, and screw axes and glide planes by simple axes and planes. All the possible "magnetic" classes were constructed by Tavger and Zaitsev.[9] It was found that besides the usual 32 classes that by themselves contain the element R, there exist also 58 specifically "magnetic" classes.

We shall determine the symmetry classes of α-Fe_2O_3 and Cr_2O_3 in the antiferromagnetic state. As has already been mentioned, α-Fe_2O_3 can exist in two antiferromagnetic states: with the spins directed along the crystal axis (state I), and with the spins lying in one of the symmetry planes (state II). From symmetry considerations we must also examine one other possible orientation of the spins, namely along one of the twofold axes (state III).

By using the standard description of space group D^6_{3d},[10] it is easy to find to which class each of the states I, II, and III belongs for α-Fe_2O_3. We write the symmetry elements that generate the corresponding classes:*

$$\begin{array}{ll} \text{I} & 2C_3,\ 3U_2,\ I,\ 2S_6,\ 3\sigma_d, \\ \text{II} & U_2,\ I,\ \sigma_d, \\ \text{III} & U_2R,\ I,\ \sigma_dR. \end{array} \tag{1}$$

A spontaneous magnetic moment $\mathbf{m}$ can obviously exist only if it remains invariant under the action of all the symmetry transformations of the class. In state I, $\mathbf{m}$ is identically equal to zero, since the corresponding class contains a threefold axis and a twofold axis perpendicular to it. In states II and III, a spontaneous moment different from zero can exist; in II it is directed along a twofold axis, in III it lies in a symmetry plane.

Thus the experimental fact that α-Fe_2O_3 is ferromagnetic in state II and nonferromagnetic in state I is simply a consequence of the magnetic symmetry of the states. Furthermore, symmetry considerations permit determination of the direction of the spontaneous magnetic moment: it is directed along one of the twofold axes, perpendicular to the symmetry plane in which the antiferromagnetic components of the spins lie.

We turn to Cr_2O_3. As has already been mentioned, the spins of the Cr^{+3} ions differ only in sign, with $\mathbf{s}_1 = -\mathbf{s}_2 = \mathbf{s}_3 = -\mathbf{s}_4$. It is easy to see that such an antiferromagnetic structure possesses the symmetry element IR. From this it follows directly that Cr_2O_3 in general cannot be ferromagnetic. In fact, upon applying the element IR to the magnetic moment vector $\mathbf{m}$, we find $\mathbf{m} = -\mathbf{m} = 0$.

The considerations that we have presented enable us to tell whether ferromagnetism is possible for a given antiferromagnetic structure, and to find the directions of spontaneous magnetic moment that are allowed by its symmetry. However, symmetry does not impose any limitations on the magnitude of the magnetic moment. For example, in the case of α-Fe_2O_3 in state II it is possible, without violating the symmetry, to rotate the spins about the crystal axis toward one another in such a way that their directions coincide, and the crystal becomes a pure ferromagnetic. In order to explain the fact that the spontaneous magnetization is small and to show the intimate connection of "weak" ferromagnetism with antiferromagnetism, we must turn to the thermodynamic theory of phase transitions of the second kind.

LANDAU'S THEORY OF PHASE TRANSITIONS OF THE SECOND KIND

The state of a magnetic crystal is described by the mean density of the spin distribution, $\mathbf{s}(x, y, z)$. If there are in the unit cell several magnetic ions that cannot be transformed one to another by translations, then the mean spin of each type of ion will be described by its own function $\mathbf{s}_a(x, y, z)$. The symmetry of the magnetic crystal coincides with the symmetry of the vector function $\mathbf{s}(x, y, z)$ and is determined by one of the "magnetic" space groups.* In a phase transition of the second kind, the spin density $\mathbf{s}(x, y, z)$, that is the magnitude and orientation of the spins in the crystal, changes in a continuous manner, but its symmetry changes jumpwise; at the transition point itself, the symmetries of the two phases coincide,

Consider, for instance, a change from a paramagnetic to an antiferromagnetic state. In the paramagnetic phase $\mathbf{s}(x, y, z) = 0$, and its symmetry is described by one of the 230 "magnetic" groups that by themselves contain the element R.† In the antiferromagnetic phase $\mathbf{s}(x, y, z) \neq 0$ (but the integral of the spin density over the unit cell, $\int \mathbf{s}dV$, is equal to zero), and its symmetry coincides with the symmetry of the function $\mathbf{s}(x, y, z)$. The transition from the paramagnetic to the antiferromagnetic state in α-Fe_2O_3 and Cr_2O_3 proceeds without change of the unit cell. In this case the general theory of Landau[4,5] is considerably simplified. Namely, the magnetic structure of the crystals in question is now fully determined by assigning the mean spin of each of the four Fe^{+3} or Cr^{+3} ions, $\mathbf{s}_1$, $\mathbf{s}_2$, $\mathbf{s}_3$, and $\mathbf{s}_4$ (*cf.* Fig. 1). Near the transition point, the mean spins $\mathbf{s}_1$, $\mathbf{s}_2$, $\mathbf{s}_3$, and $\mathbf{s}_4$ of the ions are small, and the thermodynamic potential Φ can be expanded as a series in powers of their components. Only even powers will occur in the expansion, since Φ must obviously be invariant with respect to the transformation R, replacement of every **s** by $-$**s**. Further, the expansion must remain invariant under the action of all the symmetry transformations of the ordinary space group of the crystal, D_{3d}^6. However, since we deal here with a transition without change of the unit cell, all translations by a whole period of the lattice may be treated as identity transformations.

---

*Here C_3 denotes a vertical threefold axis, U_2 a horizontal twofold axis, σ_d a vertical symmetry plane, S_6 a sixfold rotation-reflection axis, and I the operation of inversion.

*The symmetry of the distribution of atoms is obtained from the symmetry of the distribution of mean spin by regarding the element R in the corresponding magnetic group as the identity transformation.

†If the ordinary space group of the crystal is G, then in the paramagnetic state its magnetic group is $G \times R$.

Instead of the vectors **s**, we introduce vectors **m**, $\mathbf{l}_1$, $\mathbf{l}_2$, and $\mathbf{l}_3$ determined by the equalities

$$\begin{aligned}
\mathbf{m} &= \mathbf{s}_1 + \mathbf{s}_2 + \mathbf{s}_3 + \mathbf{s}_4, & \mathbf{s}_1 &= {}^1/_4\,(\mathbf{m} + \mathbf{l}_1 + \mathbf{l}_2 + \mathbf{l}_3),\\
\mathbf{l}_1 &= \mathbf{s}_1 - \mathbf{s}_2 - \mathbf{s}_3 + \mathbf{s}_4, & \mathbf{s}_2 &= {}^1/_4\,(\mathbf{m} - \mathbf{l}_1 - \mathbf{l}_2 + \mathbf{l}_3),\\
\mathbf{l}_2 &= \mathbf{s}_1 - \mathbf{s}_2 + \mathbf{s}_3 - \mathbf{s}_4, & \mathbf{s}_3 &= {}^1/_4\,(\mathbf{m} - \mathbf{l}_1 + \mathbf{l}_2 - \mathbf{l}_3),\\
\mathbf{l}_3 &= \mathbf{s}_1 + \mathbf{s}_2 - \mathbf{s}_3 - \mathbf{s}_4, & \mathbf{s}_4 &= {}^1/_4\,(\mathbf{m} + \mathbf{l}_1 - \mathbf{l}_2 - \mathbf{l}_3).
\end{aligned}$$

The vector **m**, obviously, is simply the mean magnetic moment of the unit cell.[*]

It is now easy to write the most general form of the expansion of Φ consistent with the symmetry of the crystal. For the present we write only terms of the second order in the expansion of Φ:[†]

$$\begin{aligned}
\Phi = A_1\mathbf{l}_1^2 + A_2\mathbf{l}_2^2 + A_3\mathbf{l}_3^2 + B\mathbf{m}^2\\
+ \alpha_1 l_{1z}^2 + \alpha_2 l_{2z}^2 + \alpha_3 l_{3z}^2 \qquad (2)\\
+ bm_z^2 + \beta_1(l_{1x}m_y - l_{1y}m_x) + \beta_2(l_{2x}l_{3y} - l_{2y}l_{3x}).
\end{aligned}$$

In the expression (2) for the magnetic energy there are terms of different structure, corresponding to different types of spin interaction. The terms of the form $A\mathbf{l}^2$ do not depend on the orientation of the vector **l**, and by the same token of the spin **s**, with respect to the crystal axis; they represent exchange interactions. The terms of the form αl_z^2 and $\beta(l_x m_y - l_y m_x)$ arise because of relativistic spin-lattice interactions and magnetic dipole interaction and determine the magnetic anisotropy of the crystal. The ratio α/A of the magnetic anisotropy energy to the exchange energy is proportional to the square of the ratio of the speed of the electrons in the crystal to the speed of light, $(v/c)^2$, and ordinarily lies in the range 10^{-2} to 10^{-5}.

An important property of crystals of the symmetry under consideration is the presence, in the expansion of the thermodynamic potential, of the "mixed" terms $l_{1x}m_y - l_{1y}m_x$ and $l_{2x}l_{3y} - l_{2y}l_{3x}$. From the mathematical point of view they appear because the x and y components of the vectors **m** and $\mathbf{l}_1$ (or $\mathbf{l}_2$ and $\mathbf{l}_3$) transform according to identical representations. As we shall see, the first of these terms also leads to the ferromagnetism of α-Fe_2O_3.

In the paramagnetic phase every $A > 0$ and $B > 0$, and the minimum of the thermodynamic potential corresponds to the state in which all the **l**'s and **m** are equal to zero. A transition occurs at the point where one of the **A**'s becomes zero.[*] If the interaction of the spins in the crystal were purely exchange, then below the transition point only that vector **l** would be different from zero that has a negative A; consequently, in crystals of the contemplated symmetry there could arise one of the following three types of antiferromagnetic structure:

$$1)\ \mathbf{l}_1 \neq 0,\ \mathbf{l}_2 = \mathbf{l}_3 = \mathbf{m} = 0,\ \mathbf{s}_1 = -\mathbf{s}_2 = -\mathbf{s}_3 = \mathbf{s}_4,$$

α-Fe_2O_3 in fact has such a structure.

$$2)\ \mathbf{l}_2 \neq 0,\ \mathbf{l}_1 = \mathbf{l}_3 = \mathbf{m} = 0,\ \mathbf{s}_1 = -\mathbf{s}_2 = \mathbf{s}_3 = -\mathbf{s}_4,$$

this is the structure of Cr_2O_3;

$$3)\ \mathbf{l}_3 \neq 0,\ \mathbf{l}_1 = \mathbf{l}_2 = \mathbf{m} = 0,\ \mathbf{s}_1 = \mathbf{s}_2 = -\mathbf{s}_3 = -\mathbf{s}_4.$$

In actuality, however, because of the relativistic interactions that lead to the appearance of a term $l_{1x}m_y - l_{1y}m_x$, to the basic antiferromagnetic spin distribution in α-Fe_2O_3, described by the vector $\mathbf{l}_1$, there is added a small vector **m**, and the crystal becomes ferromagnetic. This ferromagnetism, clearly, is not of exchange but of relativistic nature.

For the same reason the antiferromagnetic structure of Cr_2O_3 will be determined jointly by the vectors $\mathbf{l}_2$ and $\mathbf{l}_3$ (on the structure of Cr_2O_3, *cf.* below).

THE FERROMAGNETISM OF α-Fe_2O_3

We shall study the magnetic structure of α-Fe_2O_3 in more detail. Near the transition point **l** and **m** are small, and for determining them it is sufficient to consider only second-order terms in the expansion of the thermodynamic potential, with the addition of an exchange term proportional to $\mathbf{l}_1^4$, since the other fourth-order terms are small in comparison with it. Then Φ takes the form

---

[*] It is easily seen that in all symmetry transformations, the vectors **l** and **m** transform independently of each other. The components m_z, l_{1z}, l_{2z}, l_{3z} transform according to the one-dimensional representations A_{2g}, A_{1g}, A_{1u}, A_{2u} of the point group D_{3d} (for tables of types of representation not cited *cf.*, for instance, Ref. 11). The x and y components of the vectors **m** and $\mathbf{l}_1$ transform according to the same two-dimensional representation E_g; of the vectors $\mathbf{l}_2$ and $\mathbf{l}_3$, according to E_u.

[†] We shall use a rectangular system of coordinates with the z axis along the crystal axis, and with the x axis along one of the twofold axes.

[*] We shall assume B always greater than zero; for in the contrary case the crystal would be an ordinary exchange ferromagnetic.

$$\Phi = \frac{A}{2}\mathbf{l}^2 + \frac{B}{2}\mathbf{m}^2 + \frac{\alpha}{2} l_z^2 + \frac{b}{2} m_z^2 + \beta(l_x m_y - l_y m_x) + \frac{C}{4}\mathbf{l}^4,$$

where we have omitted the index 1 on all the letters. The minimum of Φ for given $\mathbf{l}$ is determined by the equations

$$\beta m_y = \lambda l_x, \quad -\beta m_x = \lambda l_y, \quad \alpha l_z = \lambda l_z;$$

$$B m_x - \beta l_y = 0, \quad B m_y + \beta l_x = 0; \quad (B + b) m_z = 0;$$

$$l_x^2 + l_y^2 + l_z^2 = \mathbf{l}^2.$$

This system has two solutions:

$$\text{I)}\ \mathbf{m} = 0, \ l_x = l_y = 0;$$

$$\text{II)}\ l_z = 0, \ m_z = 0, \ m_x = (\beta/B)\, l_y,$$

$$m_y = -(\beta/B)\, l_x.$$

In the state I, the spins of the ions are directed along the crystal axis, and ferromagnetism is absent. In the state II, the spins lie in the (111) plane, and there appears a spontaneous magnetic moment perpendicular to the vector $\mathbf{l}$ and of magnitude $m = (|\beta|/B)l$. As we have already said, $|\beta|/B \sim 10^{-2}$ to 10^{-5}, whence it follows that $m/l \sim 10^{-2}$ to 10^{-5}, in agreement with the experimental value $m/l = 2 \times 10^{-4}$. Thus in the state II the spins $\mathbf{s}_1$, $\mathbf{s}_4$ and $\mathbf{s}_2$, $\mathbf{s}_3$ no longer compensate each other, but are turned with respect to each other through a small angle of order 10^{-4}, as is shown in Fig. 2.

The direction of the vector $\mathbf{l}$ in the (111) plane is not determined by second-order terms in the expansion of Φ. For this purpose it is necessary to consider the lowest-order invariant that can be constructed out of l_x and l_y. This is $(l_x + i l_y)^6 + (l_x - i l_y)^6$; and depending on its coefficient, $\mathbf{l}$ will lie either along one of the twofold axes or in one of the symmetry planes. All these results, of course, are in complete agreement with the results obtained above from symmetry considerations.

Of the two possible structures I and II, that one actually exists that corresponds to the minimum value of the thermodynamic potential. In case I

$$\Phi_{\mathrm{I}} = \frac{A}{2} l^2 + \frac{\alpha}{2} l^2 + \frac{C}{4} l^4,$$

and in case II

$$\Phi_{\mathrm{II}} = \frac{A}{2} l^2 - \frac{\beta^2}{2B} l^2 + \frac{C}{4} l^4.$$

On minimizing these with respect to l^2, we get

$$\Phi_{\mathrm{I}} = -\frac{(A+\alpha)^2}{4C}, \quad \Phi_{\mathrm{II}} = -\frac{(A - \beta^2/B)^2}{4C}, \quad l^2 \simeq -\frac{A}{C}.$$

Since $\alpha \sim \beta \sim (v/c)^2$, we finally get, by neglecting terms of order $(v/c)^2$,

$$\Phi_{\mathrm{I}} \simeq -A^2/4C - A\alpha/C, \quad \Phi_{\mathrm{II}} \simeq -A^2/4C.$$

Consequently, the one or the other modification emerges according to the sign of α. Shall *et al.* have established that for 250°K < T < 950° K the spins lie in the (111) plane, and that for T < 250° K they lie in the [111] direction; hence $\alpha > 0$ for 250° K < T_0 < 950° K (we recall that $A < 0$), and $\alpha < 0$ for T < 250° K.

To determine the dependence of l and m on temperature near the transition point, we set $A = \lambda(T - T_k)$ as usual, whence

$$l = \sqrt{\lambda(T_k - T)/C}, \quad m = (|\beta|/B)\sqrt{\lambda(T_k - T)/C}.$$

Far from the transition point, $\mathbf{l}$ is no longer small, and an expansion in its powers is, in general, incorrect. However, an expansion in powers of the unit vector $\boldsymbol{\gamma}$ in the direction of $\mathbf{l}$ still has meaning (it is easy to see that such an expansion is equivalent to an expansion in powers of $(v/c)^2$). An expansion in powers of $\mathbf{m}$, of course, is always possible in view of its smallness.

We write the invariants of fourth order in $\boldsymbol{\gamma}$ and $\mathbf{m}$ that contain $\mathbf{m}$ only in powers no higher than the second (invariants in which $\mathbf{m}$ enters to higher powers are negligibly small). Here as earlier we must distinguish the pure exchange invariants, the invariants of mixed nature, and finally the relativistic invariants. The ratio of the mixed-invariant energy to the exchange is proportional to $(v/c)^2$, and the ratio of the relativistic-invariant energy to the exchange is proportional to $(v/c)^4$; therefore we shall sometimes call the last "twice relativistic."

For a crystal with the symmetry of α-Fe_2O_3 there are always one exchange invariant of fourth order, $(\mathbf{m}\gamma)^2$, two mixed invariants, $(\mathbf{m}\gamma)m_z\gamma_z$ and $\gamma_z^2 m_z^2$, and five twice relativistic invariants,

$$[(\gamma_x + i\gamma_y)^3 - (\gamma_x - i\gamma_y)^3]\,\gamma_z,\ [(\gamma_y + i\gamma_y)^3 + (\gamma_x - i\gamma_y)^3]\,m_z,$$
$$\gamma_z^4,\ (\gamma_x m_y - \gamma_y m_x)^2,\ \gamma_z^2(\gamma_x m_y - \gamma_y m_x).$$

Of these, only the exchange invariant and the first three relativistic invariants will be important for us; the rest are small in comparison with them, as can be extablished *a posteriori*. In addition, we shall need one thrice relativistic invariant $(\gamma_x + i\gamma_y)^6 + (\gamma_x - i\gamma_y)^6$; the ratio of the energy corresponding to it to the exchange energy is proportional to $(v/c)^6$.

The thermodynamic potential Φ finally takes the form

$$\Phi = \frac{a}{2}\gamma_z^2 + \frac{B}{2}\mathbf{m}^2 + q(\gamma_x m_y - \gamma_y m_x) + \frac{b}{2}m_z^2 + \frac{D}{2}(\gamma\mathbf{m})^2 + \frac{d}{2i}[(\gamma_x + i\gamma_y)^3 - (\gamma_x - i\gamma_y)^3]\,\gamma_z$$
$$+ \frac{f}{2}[(\gamma_x + i\gamma_y)^3 + (\gamma_x - i\gamma_y)^3]\,m_z + \frac{e}{2}[(\gamma_x + i\gamma_y)^6 + (\gamma_x - i\gamma_y)^6] + \frac{g}{4}\gamma_z^4. \tag{3}$$

We shall determine the magnetic structure of α-Fe_2O_3 at temperatures between the point of transition to the paramagnetic state and the point of transition from state I to state II, but not too close to these points. In this region $a \gg d$, e, f, and g, since $d/a \sim f/a \sim g/a \sim (v/c)^2$, and since $e/a \sim (v/c)^4$. We rewrite the expression (3) for Φ, introducing polar coordinates for the vector γ and discarding the term $\frac{1}{4}g\gamma_z^4$, which – as can be established *a posteriori* – is unimportant in this region.

$$\Phi = \frac{a}{2}\cos^2\theta + \frac{B}{2}m^2 + q\sin\theta\,(m_y\cos\varphi - m_x\sin\varphi)$$
$$+ \frac{b}{2}m_z^2 + \frac{D}{2}[m_z\cos\theta + \sin\theta\,(m_x\cos\varphi + m_y\sin\varphi)]^2 \tag{3a}$$
$$+ d\cos\theta\sin^3\theta\sin 3\varphi + e\cos 6\varphi\sin^6\theta + fm_z\sin^3\theta\cos 3\varphi.$$

On minimizing Φ with respect to $\mathbf{m}$ for given values of the angles φ and θ, we find

$$m_x = \frac{q}{B}\sin\theta\sin\varphi,\quad m_y = -\frac{q}{B}\sin\theta\cos\varphi,\quad m_z = -\frac{f}{B}\cos 3\varphi\sin^3\theta. \tag{4}$$

For a minimum of the thermodynamic potential Φ there are three choices of the values of $\mathbf{m}$, θ, and φ:

$$\text{I)}\ \theta = 0,\ \mathbf{m} = 0.$$
$$\text{II)}\ \theta \approx \pi/2 - d/a,\ \varphi = \pi/2,\ m_x = q/B,\ m_y = m_z = 0.$$
$$\text{III)}\ \theta = \pi/2,\ \varphi = 0,\ m_y = -q/B,\ m_z = -f/B,\ m_x = 0. \tag{5}$$

Thus when a is not too small, and α-Fe_2O_3 crystal may be in any of three magnetic states. In state I, all the spins are directed along the [111] axis, and ferromagnetism is absent. In state II, the antiferromagnetic part of the spins lies in one of the symmetry planes at a small angle $[\sim d/a \sim (v/c)^2]$ to the (111) plane; a spontaneous magnetic moment $m_0 = |q|/B \sim (v/c)^2$ is directed along a twofold axis, perpendicular to the antiferromagnetic part of the spins. In state III, the antiferromagnetic part of the spins is directed along one of the twofold axes; the spontaneous magnetic moment has the same value as in state II, $m_0 = |q|/B$, and lies in a symmetry plane, perpendicular to the twofold axis mentioned, at a small angle [of order $f/q \sim (v/c)^2$] to the (111) plane.

It is easy to see that the solutions found are in complete agreement with the results obtained earlier from symmetry considerations.

According to the measurements of Néel and Pauthenet,[1] $m_0 = 0.4$ CGS emu, and $B = 5 \times 10^4$ (B is the reciprocal of the magnetic susceptibility in the paramagnetic phase*). Hence we get for q the value 2×10^4 CGS emu.

Actually, at a given temperature and pressure, the one of the three states realized is that corresponding to the smallest value of Φ. By use of (5), we find

$$\Phi_{\mathrm{I}} = a/2, \quad \Phi_{\mathrm{II}} = (-q^2/2B) - (d^2/4a) - e, \quad \Phi_{\mathrm{III}} = (-q^2/2B) + e.$$

In general $|a| \gg q^2/2B$, $d^2/4|a|$, and $|e|$; therefore for $a > 0$, state II is realized if $e > -d^2/8a$ (according to Ref. 7 this takes place for $250°\,\mathrm{K} < T < 950°\,\mathrm{K}$) and state III if $e < -d^2/8a$. For $a < 0$, state I is realized (according to Refs. 1 and 7 this takes place for $T < 250°\,\mathrm{K}$).

At some value of a near zero, a transition occurs between state I and state II (or III). The character of this transition can be determined on the basis of symmetry considerations, without resort to solution of the corresponding equations. In fact, from Landau's theory, presented above, it follows that a transition of the second kind is possible only between two states such that the symmetry group of the one is a subgroup of the symmetry group of the other. In the section on magnetic symmetry we found the symmetry classes of states I, II, and III. It is immediately evident that a transition of the second kind between states I and III or between states II and III is impossible. The symmetry class of state II is a subgroup of the symmetry class of state I. However, in order that a transition of the second kind between these states may actually occur, it is necessary that in the expansion of the thermodynamic potential near the transition point there be no third-order terms.[4,5] In the case of a transition from state I to state II, the small quantities in which Φ is expanded are the x and y components of the vector $\boldsymbol{\gamma}$. It is easily verified that the magnetic symmetry of state I requires the presence of the third-order invariant $(\gamma_x + i\gamma_y)^3 - (\gamma_x - i\gamma_y)^3$, and consequently the transition $\mathrm{I} \rightleftarrows \mathrm{II}$ is also a transition of the first kind.

Let us consider the behavior of an α-$\mathrm{Fe_2O_3}$ crystal near the transition point of the first kind from state II to state I. In this case it is sufficient to keep, in the expansion (3) of the thermodynamic potential, the terms

$$\Phi = \frac{a}{2}\gamma_z^2 + \frac{B}{2}m^2 + q(\gamma_x m_y - \gamma_y m_x) + \frac{D}{2}(\mathbf{m}\gamma)^2 + \frac{d}{2i}[(\gamma_x + i\gamma_y)^3 - (\gamma_x - i\gamma_y)^3]\gamma_z + \frac{g}{4}\gamma_z^4.$$

On expressing $\mathbf{m}$ in terms of $\boldsymbol{\gamma}$ and again introducing polar coordinates for $\boldsymbol{\gamma}$, we get

$$\Phi = -\frac{q^2}{2B} + {}^1\!/_2 a' \cos^2\theta + {}^1\!/_4 g \cos^4\theta + d\cos\theta\sin^3\theta\sin 3\varphi,$$

where $a' = a + q^2/B$. In state I, $\cos\theta = \pm 1$; and in state II, $\sin 3\varphi = \pm 1$. Therefore, assuming that $\theta < \pi/2$, we have

$$\Phi_{\mathrm{I}} = -\frac{q^2}{2B} + {}^1\!/_2 a' + {}^1\!/_4 g,$$

$$\Phi_{\mathrm{II}} = \Phi_{\mathrm{I}} - {}^1\!/_2 a' \cos^2\theta - {}^1\!/_4 g(1 + \cos^2\theta)\sin^2\theta - |d|\cos\theta\sin^3\theta.$$

The angle θ is determined by the equation

$$a'\cos\theta + g\cos^3\theta - |d|\sin^3\theta + 3|d|\cos^2\theta\sin\theta = 0$$

At the transition point itself, $\Phi_{\mathrm{I}} = \Phi_{\mathrm{II}}$ and $\partial\Phi_{\mathrm{II}}/\partial\theta = 0$, which gives the following two equations for determination of the angle θ_k and the quantity a'_k:

---

*Actually, in the paramagnetic phase the thermodynamic potential has the form $\Phi = {}^1\!/_2 Bm^2 + {}^1\!/_2 bm_z^2$. Hence, since $\partial\Phi/\partial\mathbf{m} = \mathbf{H}$, we have

$$m_x = H_x/B, \; m_y = H_y/B, \; m_z = H_z/(B+b),$$

with $b/B \ll 1$.

$$|d|\tan^3\theta_k - a'_k\tan^2\theta_k - 3|d|\tan\theta_k - a'_k - g = 0,$$
$$(a'_k + \tfrac{1}{2}g)\tan^2\theta_k + 2|d|\tan\theta_k + a'_k + a'_k + g = 0,$$

Hence

$$|d|\tan^2\theta_k + \tfrac{1}{2}g\tan\theta_k - |d| = 0,\ \tan\theta_k = -g/4|d| + \sqrt{(g/4d)^2 + 1}.$$

We further compute the value of the spontaneous magnetic moment m_k at the transition point and the entropy of the transition. By use of (4) we find

$$m_k = (|q|/B)\sin\theta_k, \quad \text{or} \quad \sin\theta_k = m_k/m_0,$$

where m_0 is the value of the magnetic moment far from the transition point. Further,

$$\Delta S = -\frac{\partial}{\partial T}(\Phi_{\rm I} - \Phi_{\rm II}) = -{}^1/_2\left(\frac{da'}{dT}\right)_k \sin^2\theta_k$$

and the heat of transition is

$$q = -{}^1/_2\, T_k\,(da'/dT)_k\,(m_k/m_0)^2.$$

Now we are able to describe completely the behavior of an α-Fe_2O_3 crystal with change of temperature. At temperatures $T > 950°$ K, the crystal is in the paramagnetic state. At the point $T = 950°$ K there occurs a transition to a state in which, to the first approximation, the spins of the Fe^{+3} ions differ only in sign, with $\mathbf{s}_1 = -\mathbf{s}_2 = -\mathbf{s}_3 = \mathbf{s}_4$, and are directed along the line of intersection of the (111) plane and of one of the symmetry planes. In the next approximation, the spins $\mathbf{s}_1$, $\mathbf{s}_4$ and $\mathbf{s}_2$, $\mathbf{s}_3$ are rotated toward one another about the crystal axis [111] by a small angle, of order 10^{-4}, as in Fig 2; in consequence of this there arises a spontaneous magnetic moment, amounting to 0.04% of the nominal moment and directed along a twofold axis.* Furthermore the spins actually do not lie in the (111) plane but make a small angle, of order $(v/c)^2$, with it (*cf.* Fig. 3). Upon cooling to $T = 250°$ K, the angle between the spins and the [111] axis begins to decrease rapidly. At $T = 250°$ K it reaches a certain critical value θ_k, and the spontaneous magnetic moment falls to a value m_k. At $T = 250°$ K there occurs a phase transition of the first kind, in which the spins change discontinuously to the [111] direction, and the spontaneous magnetic moment disappears. For $T < 250°$ K the crystal is in an antiferromagnetic state, with the spins oriented along the crystal axis; in this state ferromagnetism is absent.

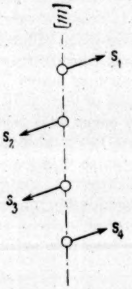

FIG. 3. Projection of the spins of α-Fe_2O_3 on a symmetry plane.

BEHAVIOR OF α-Fe_2O_3 IN A MAGNETIC FIELD

The greatest interest attaches to the behavior in a magnetic field of the ferromagnetic modification of α-Fe_2O_3; for its magnetic properties in the purely antiferromagnetic state I are the usual ones for any antiferromagnetic.

We restrict ourselves to the consideration of not-too-large magnetic fields, $H^2 \ll aB$; for at fields for which $H^2 \sim aB$, a transition from state II to state I may occur, with destruction of the ferromagnetism. The fields necessary for this, for the known antiferromagnetics at temperatures of the order of 100 degrees, have values from 10^5 to 10^6 Oersted.

---

*Such a representation of the origin of weak ferromagnetism in $MnCO_3$ and $CoCO_3$ was first proposed by Borovik-Romanov and Orlova.[2]

In the presence of an external magnetic field, the thermodynamic potential has the form*

$$\begin{aligned}\widetilde{\Phi} = \Phi - \mathbf{mH} = {}^1/_2\, a \cos^2\theta + {}^1/_2\, Bm^2 + {}^1/_2\, bm_z^2 + q \sin\theta\, (m_y \cos\varphi \\ - m_x \sin\varphi) + {}^1/_2\, D\, [m_z \cos\theta + \sin\theta\, (m_x \cos\varphi + m_y \sin\varphi)]^2 \\ + d \cos\theta \sin^3\theta \sin 3\varphi + e \cos 6\varphi \sin^6\theta + fm_z \sin^3\theta \cos 3\varphi - \mathbf{mH}.\end{aligned} \tag{6}$$

We examine first the limiting case of very weak fields, whose intensity is small in comparison with the anisotropy energy in the (111) plane. The latter is described by the terms $d \cos\theta \sin^3 \sin 3\varphi$ and $e \cos 6\varphi \sin^6\theta$. Under the condition $H^2 \ll aB$, $\cos\theta$ as before remains a small quantity of order d/a; therefore the anisotropy energy is in order of magnitude equal to $e + d^2/a$. The magnetic field energy consists basically of the energy $H|q|/B$ of the spontaneous magnetic moment $m_0 = |q|/B$ in the field. Thus the criterion for weakness of the field can be expressed in the following form:

$$\frac{H\,|q|}{B} \ll \frac{d^2}{a} + e \quad \text{or} \quad H \ll H_k = \frac{6B}{|q|}\left(e + \frac{d^2}{4a}\right)$$

(we have introduced directly for H_k a quantity convenient for later calculations).

In the absence of the field, the crystal is in state II. Then its spontaneous magnetic moment is directed along the x axis; $\varphi = \pi/2$, and $\theta = \pi/2 - d/a$. In a weak magnetic field the thermodynamic potential will be a quadratic function of the components of intensity, and the quantities $m_x - |q|/B$, m_y, m_z, $\pi/2 - \varphi$, and $\pi/2 - d/a - \theta$ will be linear functions of the intensity. We introduce the notation

$$m_x' = m_x - \frac{|q|}{B}, \quad \varkappa = \frac{\pi}{2} - \varphi, \quad \alpha = \frac{\pi}{2} - d/a - \theta$$

and expand $\widetilde{\Phi}$ to the second degree in these quantities:

$$\begin{aligned}\widetilde{\Phi} = -\frac{q^2}{2B} - \frac{d^2}{2a} - e + \frac{a}{2}\alpha^2 + \frac{dq}{a}\alpha m_x' + \left(\frac{q^2}{2B} + \frac{Dq^2}{2B^2} + \frac{9}{2}\frac{d^2}{a} + 18e\right)\varkappa^2 \\ + q\left(1 + \frac{D}{B}\right)\varkappa m_y + \left(\frac{Dqd}{Ba} - 3f\right)\varkappa m_z + \frac{B}{2} m_x'^2 + \frac{B+D}{2} m_y^2 \\ + \frac{B+b}{2} m_z^2 + \frac{Dd}{a} m_y m_z - H_x m_x' - H_y m_y - H_z m_z.\end{aligned}$$

We further introduce, instead of m_y, the quantity $m_y' = m_y + q\varkappa/B$. Then $\widetilde{\Phi}$ can be rewritten in the form

$$\begin{aligned}\widetilde{\Phi} = \frac{a}{2}\alpha^2 + \frac{dq}{a}\alpha m_x' + \frac{B}{2} m_x'^2 - H_x m_x' + \frac{B+D}{2} m_y'^2 \\ + \frac{B+b}{2} m_z^2 + \frac{Dd}{a} m_z m_y' - 3f\varkappa m_z + \frac{q}{B} H_y \varkappa + 18e'\varkappa^2 - H_z m_z - H_y m_y',\end{aligned}$$

where we have denoted the quantity $e + d^2/4a$ by e' and have dropped nonessential constant terms.

Upon using the condition that $\widetilde{\Phi}$ be a minimum to determine α, $\varkappa$, m_x', m_y', and m_z, we get the system of equations

$$a\alpha + \frac{dq}{a} m_x' = 0, \quad Bm_x' + \frac{dq}{a}\alpha - H_x = 0, \quad 36e'\varkappa + \frac{q}{B} H_y - 3fm_z = 0,$$

$$(B + D)\, m_y' + \frac{Dd}{a} m_z - H_y = 0, \quad (B + b)\, m_z + \frac{Dd}{a} m_y' - 3f\varkappa - H_z = 0,$$

hence, after some calculation, with retention only of the terms of largest order of magnitude, we find for $\varkappa$ and α

---

* Φ is the thermodynamic potential corresponding to variables p, T, and $\mathbf{m}$; the potential $\widetilde{\Phi}$ corresponds to the variables p, T, and $\mathbf{H}$. Therefore $(d\widetilde{\Phi})_{T,p} = -\mathbf{m}\, d\mathbf{H}$ and, in particular, $\widetilde{\Phi}$ must be a minimum for a given value of $\mathbf{H}$.

$$\varkappa = -\frac{q}{36e'B}H_y + \frac{f}{12e'B}H_z, \quad \alpha = -\frac{dq}{a^2B}H_x, \tag{7}$$

for the components of magnetic moment

$$\begin{aligned} m_x &= |q|/B + H_x/B, \\ m_y &= q^2H_y/36e'B^2 - qfH_z/12e'B^2, \\ m_z &= H_z/(B+b) - qfH_y/12e'B^2 \end{aligned} \tag{8}$$

and for the magnetic susceptibilities

$$\chi_{xx} = \frac{1}{B}, \quad \chi_{zz} = \frac{1}{B+b}, \quad \chi_{yy} = \frac{q^2}{36e'B^2}, \quad \chi_{yz} = -\frac{qf}{12e'B^2}.$$

It is to be noted that whereas χ_{xx}, χ_{zz}, and χ_{yz} are equal in order of magnitude to the susceptibility $1/B$ in the paramagnetic phase, χ_{yy} has – as is easily established – a much greater value, of order $(v/c)^{-2}$.

The vanishing of χ_{xy} and χ_{xz} is not accidental. The thermodynamic potential, as a function of the components of field intensity, must remain invariant with respect to all symmetry transformations of the crystal. We established above that the symmetry group of state II consists of the elements U_2, I, and σ_d. The most general combination of H_x, H_y, and H_z that is invariant with respect to these transformations is

$$\tilde{\Phi} = -m_0H_x - {}^1/_2\chi_{xx}H_x^2 - {}^1/_2\chi_{yy}H_y^2 - {}^1/_2\chi_{zz}H_z^2 - \chi_{yz}H_yH_z,$$

whence one obtains an expression of the type (8) for the magnetic moment.

We pass on to the opposite limiting case of a field $H \gg H_k$. In this case the anisotropy-energy terms in in the expression for the thermodynamic potential can be neglected. Furthermore, since we are assuming $H^2 \ll aB$, the small deviation of the angle θ from a right angle may be neglected. Then $\tilde{\Phi}$ can be written in the form

$$\tilde{\Phi} = \frac{B}{2}m^2 + \frac{b}{2}m_z^2 + q(m_y\cos\varphi - m_x\sin\varphi) + \frac{D}{2}(m_x\cos\varphi + m_y\sin\varphi)^2 - \mathbf{mH}.$$

We express the magnetic moment $\mathbf{m}$ in terms of the external field and the angle φ:

$$\begin{aligned} -q\sin\varphi + D(m_x\cos\varphi + m_y\sin\varphi)\cos\varphi + Bm_x &= H_x, \\ q\cos\varphi + D(m_x\cos\varphi + m_y\sin\varphi)\sin\varphi + Bm_y &= H_y, \\ (B+b)m_z &= H_z \end{aligned}$$

and furthermore

$$\begin{aligned} m_x &= \frac{q}{B}\sin\varphi + \frac{H_x}{B} - \frac{D}{B+D}(H_x\cos\varphi + H_y\sin\varphi)\cos\varphi, \\ m_y &= -\frac{q}{B}\cos\varphi + \frac{H_y}{B} - \frac{D}{B+D}(H_x\cos\varphi + H_y\sin\varphi)\sin\varphi, \\ m_z &= H_z/(B+b). \end{aligned}$$

In the xy plane, we introduce polar coordinates for H_x and H_y, $H_x = H_t\cos\psi$ and $H_y = H_t\sin\psi$, and we resolve m along and perpendicular to the direction of $\mathbf{H}_t$:

$$\begin{aligned} m_\parallel &= -\frac{q}{B}\sin(\psi-\varphi) + \frac{H_t}{B} - \frac{DH_t}{B(B+D)}\cos^2(\psi-\varphi), \\ m_\perp &= \frac{q}{B}\cos(\psi-\varphi) - \frac{DH_t}{B(B+D)}\cos(\psi-\varphi)\sin(\psi-\varphi), \\ m_z &= H_z/(B+b). \end{aligned} \tag{9}$$

We now eliminate m from the expression for the thermodynamic potential, and in it we drop the terms independent of φ:

$$\tilde{\Phi} = \frac{q}{B} H_t \sin(\psi - \varphi) + \frac{DH_t^2}{2B(B+D)} \cos^2(\varphi - \psi). \tag{10}$$

φ is determined as a function of H_t by the equation

$$\frac{\partial\tilde{\Phi}}{\partial\varphi} = -\frac{q}{B} H_t \cos(\psi - \varphi) + \frac{DH_t^2}{B(B+D)} \cos(\psi - \varphi)\sin(\psi - \varphi) = 0\,,$$

which has two solutions,

$$1)\ \cos(\psi - \varphi) = 0,$$
$$2)\ \sin(\psi - \varphi) = \frac{q(B+D)}{DH_t}.$$

To these correspond the values of the chemical potential

$$\tilde{\Phi}_1 = -\frac{|q|}{B} H_t \text{ and } \tilde{\Phi}_2 = \frac{DH_t^2}{2B(B+D)} + \frac{q^2(B+D)}{2BD}\,,$$

the sign of the difference

$$\tilde{\Phi}_2 - \tilde{\Phi}_1 = \frac{D}{2B(B+D)}\left(H_t + \frac{|q|(B+D)}{D}\right)^2.$$

coincides with the sign of D.

Thus in fields $H \gg H_k$, the crystal can be in either of two states, according to the sign of D. In the first,

$$D > 0,\ \varphi = \psi + \pi/2 \text{ and}$$
$$m_\parallel = |q|/B + H_t/B,\ m_\perp = 0,\ m_z = H_z/(B+b).$$

The spontaneous magnetic moment lies in the xy plane and is directed along the field; the antiferromagnetic components of the spins are directed perpendicular to it. In contrast to ordinary antiferromagnetics, the magnetic susceptibility is practically isotropic. This situation in α-Fe_2O_3 was encountered in the work of Néel and Pauthenet, a fact that affords evidence for the positiveness of D.

In the second state, $D < 0$. From (9) we get

$$m_\parallel = H_t/(B+D),\ m_\perp = 0,\ m_z = H_z/(B+b).$$

The susceptibility is sharply anisotropic in the direction of the crystal axis, and the spontaneous magnetic moment in general is absent; that is, the crystal behaves like an ordinary antiferromagnetic. Figs. 4 *a* and *b* depict schematically the dependence of $m_\parallel$ on the field for different signs of D.

Finally, we consider the range of magnetic fields $H \sim H_k$. In this case, as can be shown by simple but laborious calculations, expression (10) for the thermodynamic potential must be supplemented with a term $e'\cos 6\varphi$ representing anisotropy energy:

$$\tilde{\Phi} = \frac{q}{B} H_t \sin(\varphi - \varphi) + \frac{DH_t^2}{2B(B+D)} \cos^2(\psi - \varphi) + e' \cos 6\varphi\,. \tag{11}$$

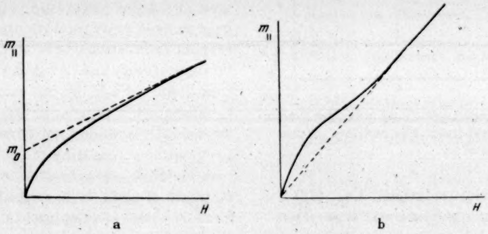

a b

FIG. 4. Magnetization curve: (a) in the base $D > 0$; (b) in the case $D < 0$.

Expression (9) for the magnetic moment remains valid as before.

When $H_t \sim H_k$, the second term in (11) is small in comparison with the first, since $H_k = 6Be'/|q|$ and $|q|H_k/B \sim (v/c)^6$, whereas $H_k^2/B \sim (v/c)^3$. Thus, finally, we can write the expression for Φ

$$\tilde{\Phi} = \frac{q}{B} H_t \sin(\psi - \varphi) + e' \cos 6\varphi \qquad (12)$$

and the equation that determines φ

$$qH_t \cos(\psi - \varphi) + 6e'B \sin 6\varphi = 0.$$

The last equation and the expression (12) can be put into dimensionless form by introducing, instead of H_t, the variable $h = H_t/H_k$:

$$\begin{gathered} \tilde{\Phi}/e = 6h \sin(\psi - \varphi) + \cos 6\varphi, \\ h \cos(\psi - \varphi) + \sin 6\varphi = 0. \end{gathered} \qquad (13)$$

Fig. 5 shows equilibrium magnetization curves obtained by numerical solution of Eq. (13). Plotted along the ordinate axis is the quantity $m_{\parallel} - H_t/B$, measured in units of the spontaneous magnetic moment $m_0 = |q|/B$.

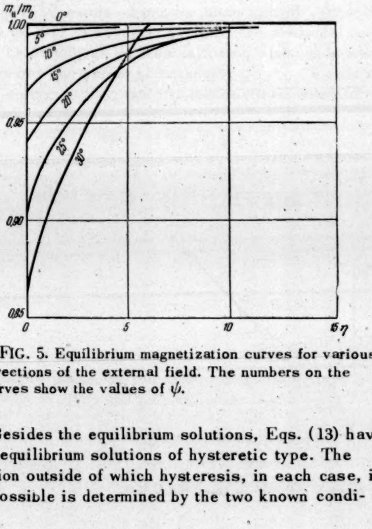

FIG. 5. Equilibrium magnetization curves for various directions of the external field. The numbers on the curves show the values of ψ.

Besides the equilibrium solutions, Eqs. (13) have nonequilibrium solutions of hysteretic type. The region outside of which hysteresis, in each case, is impossible is determined by the two known conditions $\partial\tilde{\Phi}/\partial\varphi = \partial^2\tilde{\Phi}/\partial\varphi^2 = 0$; this gives the equations of the limiting curve in the parametric form

$$\begin{gathered} h \cos(\psi - \varphi) + \sin 6\varphi = 0, \\ h \sin(\psi - \varphi) + 6 \cos 6\varphi = 0. \end{gathered} \qquad (14)$$

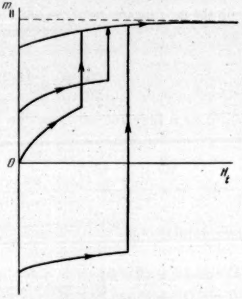

FIG. 6. Typical hysteresis curves.

In Fig. 6 are schematically represented typical hysteresis curves, given by Eqs. (13) and the conditions (14).

Cr_2O_3

We shall treat briefly the antiferromagnetic structure of Cr_2O_3. The distribution of the spins of the Cr^{+3} ions is described by the vectors $\mathbf{l}_2$ and $\mathbf{l}_3$. It was explained above that the components of $\mathbf{l}_2$ and $\mathbf{l}_3$ transform, in the symmetry transformations of the crystal, as do the $\mathbf{l}_1$ and $\mathbf{m}$ that describe the magnetic structure of α-Fe_2O_3, with this difference only: $\mathbf{l}_2$ and $\mathbf{l}_3$ change sign in the inversion transformation, whereas $\mathbf{l}_1$ and $\mathbf{m}$ do not. In the expansion of the thermodynamic potential, $\mathbf{l}_2$ and $\mathbf{l}_3$ enter only in even powers; therefore their properties with respect to inversion have no bearing on the form of this expansion, and Φ for Cr_2O_3 can be obtained from Φ for α-Fe_2O_3 by replacing $\mathbf{l}_1$ by $\mathbf{l}_2$ and $\mathbf{m}$ by $\mathbf{l}_3$. Therefore it is possible to describe the thermodynamically possible antiferromagnetic structures of Cr_2O_3 without repeating the calculations.

In the first approximation, the antiferromagnetic structure of Cr_2O_3 is described by the vector $\mathbf{l}_2$. All four Cr^{+3} ions have spins of the same magnitude and direction, except that $\mathbf{s}_1 = -\mathbf{s}_2 = \mathbf{s}_3 = -\mathbf{s}_4$ (*cf.* Fig. 1c). As before, three states are possible, with dif-

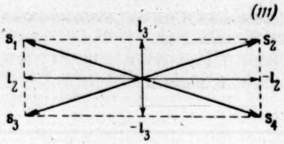

FIG. 7. Projection of the spins of Cr_2O_3 on the (111) plane

ferent directions of the spins **s** with respect to the crystalline axes. In state I, the spins are directed along the crystal axis [111]; in state II, the spins lie along the line of intersection of one of the symmetry planes with the (111) plane; and in state III, the spins are directed along one of the twofold axes.

In the next approximation, the spins $\mathbf{s}_1$ and $\mathbf{s}_2$ and the spins $\mathbf{s}_3$ and $\mathbf{s}_4$, in states II and III, are rotated toward one another through a small angle about the [111] axis, as is shown in Fig. 7. In this process, however, their sum remains equal to zero, so that ferromagnetism does not arise; more precisely,

$$\mathbf{s}_1 = {}^1/_4\,(\mathbf{l}_2 + \mathbf{l}_3), \quad \mathbf{s}_2 = {}^1/_4\,(-\mathbf{l}_2 + \mathbf{l}_3),$$

$$\mathbf{s}_3 = {}^1/_4\,(\mathbf{l}_2 - \mathbf{l}_3), \quad \mathbf{s}_4 = -{}^1/_4\,(\mathbf{l}_2 + \mathbf{l}_3),$$

that is

$$\mathbf{s}_1 = -\mathbf{s}_4, \quad \mathbf{s}_2 = -\mathbf{s}_3.$$

The magnetic properties of Cr_2O_3 will not differ from those of ordinary antiferromagnetics, and we will not dwell on them.

$MnCO_3$, $CoCO_3$, $FeCO_3$

The isomorphic antiferromagnetic crystals $MnCO_3$, $CoCO_3$, and $FeCO_3$ are also remarkable in this respect, that two – $MnCO_3$ and $CoCO_3$ – exhibit a "weak" ferromagnetism, while $FeCO_3$ is a pure antiferromagnetic.

The ferromagnetism of $MnCO_3$ and $CoCO_3$ was studied in detail by Borovik-Romanov and Orlova.[2] According to their measurements the spontaneous magnetic moment of $MnCO_3$ amounts to 0.2% of the nominal, and that of $CoCO_3$ to about 2%. $FeCO_3$ was investigated by Bizette;[12] it was found that in the antiferromagnetic state the spins of the Fe^{+2} ions are directed along the crystal axis [111].

These properties can be explained in a natural way by supposing that the antiferromagnetic transition occurs in these materials without change of the unit cell. $MnCO_3$, $CoCO_3$, and $FeCO_3$ belong to the rhombohedral system, and their symmetry is described by the space group D_{3d}^6 (Ref. 6) – that is, the same group as for α-Fe_2O_3 and Cr_2O_3. The unit cell contains two metallic ions located on the body diagonal of the rhombohedron at the sites (¼ ¼ ¼) and (¾ ¾ ¾).

As before, we shall describe their magnetic structure by means of the ionic spins $\mathbf{s}_1$ and $\mathbf{s}_2$. We introduce the vectors $\mathbf{m} = \mathbf{s}_1 + \mathbf{s}_2$ and $\mathbf{l} = \mathbf{s}_1 - \mathbf{s}_2$. It is easily verified that in all the symmetry transformations, **m** and **l** transform independently of each other; m_z and l_z transform according to the one-dimensional representations A_{2g} and A_{1g} of point group D_{3d}, and the x and y components transform according to the single representation E_g, that is according to the same representation as do the vectors **m** and $\mathbf{l}_1$ for α-Fe_2O_3.

Thus the magnetic symmetry properties of these crystals coincide completely with those of α-Fe_2O_3, and therefore all the results obtained for the latter may be carried over to this case.

In particular, the fact that $FeCO_3$ exhibits no ferromagnetism is fully explained by the fact that the spins of the Fe^{+2} ions are directed along the crystal axis (state I).

Contrariwise, from the presence of ferromagnetism in $MnCO_3$ and $CoCO_3$ we can and must conclude that they are in states with spins lying in the (111) plane (state II or III).

All the calculations relating to the magnetic properties of α-Fe_2O_3 are completely applicable to ferromagnetic $MnCO_3$ and $CoCO_3$.

I express my thanks to academicians L. L. Landau and E. M. Lifshitz for valuable advice and discussion of the results. The author is also grateful to A. S. Borovick-Romanov for helpful discussions.

---

[1] L. Néel and R. Pauthenet, Compt. rend. **234**, 2172 (1952).

[2] A. S. Borovik-Romanov and M. P. Orlova, J. Exptl. Theoret. Phys. (U.S.S.R.) **31**, 579 (1956); Soviet Phys. JETP **4**, 531 (1957).

[3] Yin-Yuan Li, Phys. Rev. **101**, 1450 (1956).

[4] L. Landau. J. Exptl. Theoret. Phys. (U.S.S.R.) **7**, 19 (1937).

[5] L. Landau and E. Lifshitz, *Statistical Physics* (M.–L., Gostekhizdat 1951).

[6] R. W. G. Wyckoff, *The Structure of Crystals* (Chemical Catalog Co., New York, 1931).

[7] Shull, Strauser, and Wollan, Phys. Rev. **83**, 333 (1951).

[8] B. N. Brockhouse, J. Chem. Phys **21**, 961 (1953).

[9] B. A. Tavger and V. M. Zaitsev, J. Exptl. Theoret. Phys. (U.S.S.R.) **30**, 564 (1956); Soviet Phys. JETP **3**, 430 (1956).

[10] Internationale Tabellen zur Bestimmung von Kristallstrukturen, Bd. 1 (Bornträger, Berlin, 1935).

[11] L. Landau and E. Lifshitz, *Quantum Mechanics* (M.–L., Gostekhizdat 1948).

[12] H. Bizette, J. phys. et radium **12**, 161 (1951).

Translated by W. F. Brown Jr.
298

SOVIET PHYSICS JETP VOLUME 5, NUMBER 6 DECEMBER 15, 1957

Electron-Positron Pair Production in Collisions Between Fast π-Mesons and Nucleons

E. M. RABINOVICH

(Submitted to JETP editor June 12, 1956)
J. Exptl. Theoret. Phys. (U.S.S.R.) **32**, 1563-1566 (June, 1957)

The cross section is calculated for pair production in collisions between high-energy π-mesons and nucleons.

LANDAU AND POMERANCHUK[1] have considered gamma-radiation processes in the collision of high-energy π-mesons with nucleons. Their method can be used also for treating electron-positron pair production.

The cross section for this process, naturally, will be α^2 times less than that for gamma-radiation. Owing, however, to the experimental difficulties in the detection and energy measurement of photons, it may be found experimentally simpler to deal with electron-positron pairs. Thus a theoretical investigation of electron-positron pair production is of interest.

The method used is based on the fact that at high π-meson energies the nucleon appears as an opaque sphere, so that the meson ψ-function outside the radius of action of the nuclear forces is a superposition of a plane wave and a diffracted wave. It turns out that in order to calculate the cross section for photon or pair production, it is sufficient to know the meson wave function outside the radius of action of the nuclear forces.

The two cases of pair production accompanying meson diffraction and absorption (stopping) must be considered separately. In the second case the final π-meson state is an ingoing wave, and we have a "sink" for particles. This leads to a situation in which the transition currents do not satisfy a continuity equation, and it becomes necessary to introduce an additional transition charge density in order to obtain charge conservation. This method was first applied by Tisza[2] to pair production in β-decay.

Landau and Pomeranchuk performed their calculation with the aid of a Green function. In the present work we make use of the transition-current method, since this makes it easier to account for the "disappearance" of charge. This "disappearance" effect does not have to be treated in considering gamma-radiation, since the interaction Hamiltonian of the meson and the electromagnetic field contains only the vector potential, so that the introduction of an additional transition charge density does not change its form.

The interaction of mesons with the electron-positron field is given by*

$$\hat{V} = e\left[(\boldsymbol{\alpha},\ \mathbf{A}(\mathbf{r})) - \varphi(\mathbf{r})\right], \tag{1}$$

where $\mathbf{A}$ and φ are the meson transition potentials.

The matrix element corresponding to production of a pair with total momentum $\mathbf{k}_0 = \mathbf{k} + \mathbf{k}'$ and total energy $\varepsilon_0 = \varepsilon + \varepsilon'$, is

$$U = e\left[(u_{k'}^{*}, \alpha \mathbf{A}_{k_0, \varepsilon_0} v_k) - (u_{k'}^{*}, v_k)\, \varphi_{k_0, \varepsilon_0}\right], \tag{2}$$

where A_{k_0, ϵ_0} and $\varphi_{k_0, \epsilon_0}$ are the Fourier components of the transition potentials, given by

$$\begin{aligned} \mathbf{A}_{k_0, \varepsilon_0} &= \int \mathbf{A}_{\varepsilon_0}(\mathbf{r})\, e^{-i\mathbf{k}_0\mathbf{r}}\, d\mathbf{r}, \\ \varphi_{k_0, \varepsilon_0} &= \int \varphi_{\varepsilon_0}(r)\, e^{-i\mathbf{k}_0\mathbf{r}}\, d\mathbf{r}; \end{aligned} \tag{3}$$

The index ε_0 indicates that the transition takes place between states whose energy difference is ε_0, and $u_{k'}$ and v_k are the electron and positron spinor amplitudes, respectively. The transition potentials are given in terms of the transition currents by the expression

---

* Throughout we have set $\hbar = c = 1$.

$$\mathbf{A}_{k_0,\,\varepsilon_0} = 4\pi \mathbf{j}_{k_0,\,\varepsilon_0} / (\varepsilon_0^2 - k_0^2);$$

$$\varphi_{k_0,\,\varepsilon_0} = 4\pi \rho_{k_0,\,\varepsilon_0} / (\varepsilon_0^2 - k_0^2). \qquad (4)$$

Finally,

$$\mathbf{j} = \frac{e}{4\pi i} (\nabla \psi_{p'}^* \psi_p - \psi_{p'}^* \nabla \psi_p),$$

$$\rho = \frac{e}{4\pi i} \left(\psi_{p'}^* \frac{\partial \psi_p}{\partial t} - \frac{\partial \psi_{p'}^*}{dt} \psi_p \right), \qquad (5)$$

where ψ_p and $\psi_{p'}$ are the wave functions of the initial and final meson states with momenta **p** and **p**$'$, respectively.

The probability for pair production is given by the expression (normalized for unit volume)

$$dw = 2\pi \,|U|^2 (2\pi)^{-9} d\mathbf{k}\, d\mathbf{k}'\, d\mathbf{p}' \delta (E - E' - \varepsilon - \varepsilon'), \qquad (6)$$

where E and E' are the initial and final meson energies. In order to integrate over the direction at which the electron is omitted, let us separate out the invariant $|U|^2 d\mathbf{k}'$ and go over to the center-of-mass system of the pair, where this integration is easily performed. Integrating over $d\mathbf{k}'$ and summing over spins, we obtain

$$dw = \frac{e^2}{3(2\pi)^7} \sqrt{1 - \frac{4m^2}{\varepsilon_0^2 - k_0^2}} \left(1 + \frac{2m^2}{\varepsilon_0^2 - k_0^2}\right)$$

$$\times (\varepsilon_0^2 - k_0^2)(A_{k_0,\,\varepsilon_0}^2 - \varphi_{k_0,\,\varepsilon_0}^2)\, d\mathbf{k}_0 p' E' d\varepsilon_0 d\Omega_{p'}. \qquad (7)$$

Let us first consider pair production with diffraction of the meson. Here

$$\psi_p = \sqrt{\frac{2\pi}{E}} \left[e^{i\mathbf{pr}} - \frac{p}{2\pi i} \int\limits_{\rho^2 \leqslant R^2} \frac{e^{ip|\mathbf{r}-\boldsymbol{\rho}|}}{|\mathbf{r}-\boldsymbol{\rho}|}\, d\boldsymbol{\rho} \right] e^{-iEt},$$

$$\psi_{p'} = \sqrt{\frac{2\pi}{E}} \left[e^{i\mathbf{p}'\mathbf{r}} + \frac{p'}{2\pi i} \int\limits_{\rho^2 \leqslant R^2} \frac{e^{-ip'|\mathbf{r}-\boldsymbol{\rho}|}}{|\mathbf{r}-\boldsymbol{\rho}|}\, d\boldsymbol{\rho} \right] e^{-iE't}. \qquad (8)$$

The integrals are taken over planes passing through the nucleus and perpendicular to **p** and **p**$'$, respectively; R is the radius of the nucleon. The calculation is exactly the same as that of Landau and Pomeranchuk,[1] who used the Green function, and we shall therefore present only the result:

$$d\sigma = \frac{e^4 R^2}{3\pi^3} \frac{p'}{p} \sqrt{1 - \frac{4m^2}{x}} \left(1 + \frac{2m^2}{x}\right) \frac{dx}{x} \frac{dk_0}{k_0} \frac{J_1^2(|p'\theta' + k_0\theta|R)}{|p'\theta' + k_0\theta|^2}$$

$$\times \left\{ \frac{(p'\theta' + k_0\theta)^2}{(\alpha^2 + \theta^2)(\alpha'^2 + (\theta - \theta')^2)} - \frac{\mu^2}{p^2 p'^2} \left[\frac{p^2}{\alpha^2 + \theta^2} - \frac{p^2}{\alpha'^2 + (\theta' - \theta)^2} \right]^2 \right. \qquad (9)$$

$$\left. + \frac{k_0(p + p')}{2pp'} \left[\frac{p'^2}{\alpha^2 + \theta^2} - \frac{p^2}{\alpha'^2 + (\theta' - \theta)^2} \right] \right\} d\theta\, d\theta'.$$

Here we have introduced the notation

$$\alpha = \mu / p, \quad \alpha' = \mu / p', \quad x = \varepsilon_0^2 - k_0^2,$$

$$\mathbf{p}' = (\mathbf{pp}')\,\mathbf{p} / p^2 + p'\boldsymbol{\theta}', \quad \mathbf{p} = (\mathbf{pk}_0)\,\mathbf{p} / p^2 + k_0\boldsymbol{\theta}. \qquad (10)$$

The variable x characterizes the angle of divergence of the pair, and is related to it by the expression

$$x = kk' \left(\frac{m^2 k_0^2}{k^2 k'^2} + \vartheta^2 \right).$$

In calculating the matrix elements, the distance

$$r_{\text{eff}} \sim pp' / \mu^2 k_0;$$

is of importance, and when $p \gg \mu$ and the energy of the pair is not too large, $r_{\text{eff}} \gg R$, which verifies the validity of using free-particle wave functions.

The spectral distribution of the pairs produced is given by the expression

$$d\sigma = \frac{2e^4 R^2}{3\pi} \frac{p'}{p} \left(\ln \frac{k_0}{m} - \frac{5}{6} \right) \frac{dk_0}{k_0} G(\mu R), \qquad (11)$$

where G is defined by the integral

$$G(\mu R) = \int\limits_0^\infty \frac{J_1^2(2\mu R x)}{x^2} \left\{ [\sinh^{-1}(x(4x^2 + 3)) + \sinh^{-1} x] \frac{1 + 2x^2}{\sqrt{1 + x^2}} - 4x \right\} dx \qquad (12)$$

$$G(\mu R) \cong \frac{2{,}6}{\mu R} \quad (\text{for} \quad \mu R \gg 1); \quad G(1) = 2.$$

Finally, we present the total cross section for pair production:

$$\sigma = \frac{e^4 R^2}{3\pi} G(\mu R)\left(\ln\frac{p}{m}\right)^2\left[1 - \frac{11}{3\ln(p/m)}\right] \tag{13}$$

Let us now consider pair production with stopping of the meson. For the initial wave function let us take a plane wave, since the whole process takes place in the region of space in front of the nucleus. We shall describe the final state as a converging wave; since dimensions much larger than the nuclear radius are of importance, it is natural to consider only *s*-waves:

$$\psi_p = \sqrt{\frac{2\pi}{E}}\, e^{i\mathbf{pr}} e^{-iEt}, \quad \psi_{p'} = \sqrt{\frac{2\pi}{E'}}\, \frac{e^{-ip'r}}{4\pi r} e^{-iE't}. \tag{14}$$

The Fourier components of the transition current are given by

$$\mathbf{j}_{k_0,\varepsilon_0} = \frac{2\pi e}{\sqrt{EE'}} \frac{2\mathbf{p} - \mathbf{k}_0}{|\mathbf{p} - \mathbf{k}_0|^2 - p'^2},$$

$$\rho_{k_0,\varepsilon_0} = \frac{2\pi e}{\sqrt{EE'}} \frac{2E - \varepsilon_0}{|\mathbf{p} - \mathbf{k}_0|^2 - p'^2}. \tag{15}$$

We shall show that the model we have chosen leads to exactly the same results as the Green function calculation in the case of photon production.

The interaction Hamiltonian of mesons and the electromagnetic field is

$$\hat{V} = (\mathbf{A}_{\text{phot}}\, \mathbf{j}_{\text{mes}}).$$

The matrix element for photon production is

$$U = \sqrt{2\pi/k}\,(\mathbf{e}\mathbf{j}_k),$$

where **e** is the polarization vector of the photon, and $\mathbf{j}_k$ is the Fourier component of the meson transition current. The photon production probability is given by

$$dw = 2\pi |U|^2 (2\pi)^{-3} d\mathbf{k} - (2\pi)^{-3} 4\pi p'^2 dp' \delta(E),$$

and the cross section by

$$d\sigma = \frac{e^2}{4\pi} R^2 \frac{(\mathbf{pe})^2}{(|\mathbf{p} - \mathbf{k}|^2 - p'^2)} \frac{k\,dk}{pp'}\, d\boldsymbol{\theta},$$

where θ is the angle between **k** and **p**. This expression is exactly the same as Equation (45) of Landau and Pomeranchuk.[1]

The transition current and charge as given by expression (15) do not satisfy a continuity equation. Let us calculate the additional transition charge density ρ' which must be introduced to preserve charge conservation. To do this let us integrate the continuity equation

$$\operatorname{div}\mathbf{j} - i\varepsilon_0(\rho + \rho') = 0 \tag{16}$$

over a sphere surrounding the origin and then go to the limit as the radius of the sphere approaches zero. Here j and ρ are given by Equation (5), where ψ_p and $\psi_{p'}$ are taken from (14). The only point at which ψ_p has a singularity is the origin, so that $\rho' = \rho_0'\delta(r)$. Since $\int \rho dr = 0$ when $R \to 0$, we have

$$\rho_0' = \frac{1}{i\varepsilon_0}\int \mathbf{j}\, d\mathbf{S} = -\frac{2\pi e}{\varepsilon_0\sqrt{EE'}} \qquad (R \to 0).$$

The corrected expressions for the transition current and charge are

$$\mathbf{j}_{k_0,\varepsilon_0} = \frac{2\pi e}{\sqrt{EE'}} \frac{2\mathbf{p} - \mathbf{k}_0}{|\mathbf{p} - \mathbf{k}_0|^2 - p'^2},$$

$$\rho_{k_0,\varepsilon_0} = \frac{2\pi e}{\sqrt{EE'}} \left\{\frac{2E - \varepsilon_0}{|\mathbf{p} - \mathbf{k}_0|^2 - p'^2} - \frac{1}{\varepsilon_0}\right\}. \tag{17}$$

The differential cross section for pair production with stopping of the meson is given by

$$d\sigma = \frac{2e^4R^2}{3\pi^2}\left(1 - \frac{k_0}{p}\right)\left(\ln\frac{k_0}{m} - \frac{5}{6}\right) \times \frac{dk_0}{k_0}\left\{\frac{1}{(\mu^2/p^2) + \theta^2} - \frac{\mu^2/p^2}{(\mu^2/p^2 + \theta^2)^2} - \frac{1}{4}\right\} d\boldsymbol{\theta}; \tag{18}$$

where θ is the angle between $\mathbf{k}_0$ and **p**.

The pair spectrum is given by

$$d\sigma = \frac{4e^4R^2}{3\pi}\left(1 - \frac{k_0}{p}\right)\left(\ln\frac{k_0}{m} - \frac{5}{6}\right)\left(\ln\frac{p}{\mu} - 1\right)\frac{dk_0}{k_0}. \tag{19}$$

Finally, the total cross section is

$$\sigma = \frac{2e^4R^2}{3\pi}\ln\frac{p}{\mu}\left(\ln\frac{p}{m}\right)^2\left(1 - \frac{11}{3\ln(p/m)}\right) \times \left(1 - \frac{1}{\ln(p/\mu)}\right). \tag{20}$$

Landau and Pomeranchuk note that the interaction of a meson with the nucleon background should lead to the "smearing out" of the charge over a region of dimensions $\sim 1/\mu$. This leads to the occurrence of a form factor F, which accounts for the finite dimensions of the π-meson, in all the expressions for the cross sections. Comparison of experiment and the theory based on the assumption of a point meson should give some information on the "structure" of the particle interacting with the vacuum.

It was shown by Landau and Pomeranchuk that if $k_0 \ll p$, $\theta' < \mu/2p$ and $\theta \ll \mu^2/pk_0\theta'$, the form-factor depends only on $k_0\theta^2$, and can be written

$$F = F(pk_0\theta^2/2\mu^2).$$

The form-factor is equal to unity when its argument is small, and approaches zero as its argument increases.

In conclusion, the author takes this opportunity to express his gratitude to Professor I. Ia. Pomeranchuk for his constant attention and direction.

---

[1] L. D. Landau, I. Ia. Pomeranchuk, J. Exptl. Theoret. Phys. (U.S.S.R.) **24**, 5 (1953).

[2] L. Tisza, Physik. Z. Sowjetunion 11, 425 (1937).

Translated by E. J. Saletan
299

Letters to the Editor

On Bubble Chambers

P. V. VAVILOV

(Submitted to JETP editor November 29, 1956)
J. Exptl. Theoret. Phys. (U.S.S.R.) **32**, 1567-1568
(June, 1957)

THE MECHANISM of bubble formation incident to the passage of particles through a superheated liquid still remains unclear. Many authors (see for example Bertanza *et al.*[1]) consider that the bubbles are due to electrostatic repulsion of positive ions produced by the ionizing particle and that the thermal process in the formation of the bubble can be neglected. In this communication we assume that the thermal process is the predominant one in bubble formation.

Let us examine a superheated liquid. It is known that for every metastable phase there exist certain minimal dimensions which an accumulation of another phase must attain in order for the latter to be more stable than the initial one. During the passage of a charged particle through matter there form δ-electrons of different energies, which lose their energy over a relatively short section of path. Let us assume that the entire energy of the δ-electron is released in the form of heat; then for the formation of a bubble we must have localization of a certain amount of energy $E_{\min}$ in a region commensurate with the dimensions of the bubble. If we further assume that the formation of the bubble occurs isothermally, then for $E_{\min}$ we obtain

$$E_{\min} = Nq + pV + 4\pi r_{\min}^2 \alpha. \tag{1}$$

If the liquid is weakly superheated, we can use for $r_{\min}$ the familiar expression[2]

$$r_{\min} = 2\alpha/(p_0 - p).$$

To determine the number N of vapor molecules we can make use of the equation of state for an ideal gas. Finally we obtain for $E_{\min}$

$$E_{\min} = [16\pi\alpha^3/(p_0 - p)^2]$$
$$\times [1 + 2p_0(p/p_0 + q/kT)/3(p - p_0)], \tag{2}$$

where α is the surface tension, p_0 is the pressure with a plane interface, p is the pressure in the superheated liquid, q is the heat of evaporation per molecule, and T is the temperature of the superheated liquid.

The δ-electrons of different energies will produce bubbles having different radii; finally at some energy E' the δ-electron will be capable of forming several bubbles; however, since such electrons form visible tracks branching off from the track of the ionizing particle they can be disregarded. Thus the problem is to find the number of δ-electrons of energy $E_{\min} \leq E \leq E'$; this number, on the basis of our assumption, will be equal to the number of bubbles formed. It can readily be shown that the number of δ-electrons per unit length is given by the expression

$$g(\beta) = \frac{e^2}{\pi v^2 \hbar}$$
$$\times \sum_j \int\limits_{\omega_j + E_{\min}/\hbar}^{\infty} \frac{\operatorname{Im} \varepsilon}{|\varepsilon|^2} \left[\ln \frac{2mv^2 E'}{(\hbar\omega)^2 |1 - \beta^2 \varepsilon|} - \beta^2 \operatorname{Re} \varepsilon \right] d\omega, \tag{3}$$

where

$$\varepsilon = 1 + \frac{4\pi N e^2}{m} \sum_j \frac{f_j}{\omega_j^2 - \omega^2 - i g_j \omega},$$

and the other symbols are in the conventional notation. If we consider small superheats, then $E_{\min} \gg \omega_j \hbar$ (here $\hbar\omega_j$ is the ionization potential of the atom). Assuming that $g_j \ll \omega_j$, we obtain

$$g(\beta) = \frac{2Ne^4}{mv^2} \frac{\varepsilon^0}{E_{\min}^2} \left[\ln \frac{2mv^2 E'}{E_{\min}^2 D(\beta^2)} - \beta^2 \right], \tag{4}$$
$$D(\beta^2) = 1 - \beta^2 + \beta^2 (4\pi N e^2 \hbar^2 / E_{\min}^2 m), \quad \varepsilon_0 = \sum_j f_j h g_j.$$

A characteristic feature of (4) is the strong dependence of $g \sim (p_0 - p)^6$ on the superheat. The value of E' is determined from the conditions of the experiment (E' is of the order of $10^4 - 10^5$ ev), although actually the choice of E' does not substantially affect the results.

---

[1] Bertanza, Martelli, and Zacutti, Nuovo cimento **9**, 487 (1955).

[2] L. Landau and E. Lifshitz, *Statistical Physics*, M., 1951.

Translated by E. J. Rosen
300

Concerning One Method of Measuring the Lifetimes of Excited States of Atomic Nuclei

A. F. TULINOV
Moscow State University

(Submitted to JETP editor February 17, 1957)
J. Exptl. Theoret. Phys. (U.S.S.R.) 32, 1568-1570
(June, 1957)

IN THE PRESENT LETTER the possibility is considered of using a new method for the measurement of the lifetimes τ of excited states of light nuclei, ranging from 10^{-12} to 10^{-14} sec.

We will consider the nuclear reaction occuring in a thin target acted upon by a beam of monoenergetic particles. Let the counters, connected in the circuit, detect both component products of reaction (the light component and the recoil nucleus). If we fix the direction of emergence of the light component, angular distribution of the recoil nuclei corresponding to this light component will be represented by a system of peaks, each of which will relate to a definite energy level of the final nucleus.[1] The peaks corresponding to the excited states, in general, will be broad, since the recoil nuclei, besides the momenta acquired in the reaction, will receive additional momenta from the γ-quanta at the instant of radiation. The width of each peak will be determined by the ratio of the γ-quantum momentum to the initial momentum of the recoil nucleus. If along the path of motion of the nuclei directly behind the target we place a layer of substance, so that the recoil nuclei will be partially retarded in it, then the width of the peak will depend on how much the recoil nucleus has been retarded at the instant of radiation, in other words, on the rate of retardation and on the time interval between the formation of the recoil nucleus and its γ-radiation. Thus a comparison of the shapes of the peaks obtained with and without a retarding layer can provide information regarding the value τ.

In order to establish quantitative relationships we will consider the case in which the recoil nucleus, having been produced in an excited state, goes over into the ground state with emission of a single γ-quantum of energy E_γ. Since the degree of anisotropy of the emission of γ-quanta does not exceed a few percent, we will consider the emission as isotropic. In addition, we will assume that the relationship $p_\gamma / p_n \ll 1$, where p_γ and p_n are the momenta of the γ-quantum and of the recoil nucleus, will hold. This condition is practically always fulfilled. Finally, let the diaphragm in front of the counter of the recoil nuclei be adequately narrow and high. From geometric considerations it can be easily shown that, under the conditions formulated above, for a thin target without a retarding layer the angular distribution of the recoil nuclei, pertaining to the excited state under consideration, will have a rectangular form with a total width $\Gamma_1 = 2p_\gamma / p_n$ (see Fig. 1a). If we place directly behind the target a retarding layer of matter of thickness d (the lining can serve as such a layer), then the total angular distribution will consist of two parts, I and II (Fig. 1b). Part I will be dependent on the nuclei whose radiation takes place inside the retarding layer, and part II – after the passage through the layer. Let the range R of the recoil nuclei in the retarding substance be related to the velocity v by $R = \alpha v^2$, where α is a coefficient dependent on the nature of the recoil nuclei and of the retarding substance. Then the velocity with which the nuclei leave the retarding layer, will be $v_d = v_0(1 - d/R)$, where v_0 is the initial velocity of the recoil nucleus, and, therefore, the width of part II of the distribution will be given by $\Gamma_2 = \Gamma_1/(1 - d/R)$. Taking into account the exponential character of radiation, it can be shown that the angular distribution of the fissioning nuclei in this case will be given by

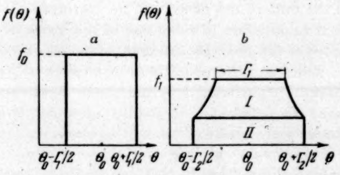

FIG. 1

$$f(\theta-\theta_0)=\frac{1}{(1+\lambda\alpha)\Gamma_1}\left\{\lambda\alpha\left(\frac{\Gamma_{1/2}}{|\theta-\theta_0|}\right)^{\lambda\alpha-1}+\left(1-\frac{d}{R}\right)^{\lambda\alpha+1}\right\} \text{ for } \frac{\Gamma_1}{2}\leqslant|\theta-\theta_0|\leqslant\frac{\Gamma_2}{2}, \qquad (1) \qquad (1)$$

$$f(\theta-\theta_0)=\frac{1}{(1+\lambda\alpha)\Gamma_1}\left\{\lambda\alpha+\left(1-\frac{d}{R}\right)^{\lambda\alpha+1}\right\} \text{ for } |\theta-\theta_0|\leqslant\frac{\Gamma_1}{2},$$

where $\lambda = \ln 2/\tau$. The function f is normalized so that the area under the curve (Fig. 1b) is unity. At $\lambda\alpha \gg 1$ we have $f = 1/\Gamma_1$ for $|\theta - \theta_0| \leq \Gamma_1/2$ and $f = 0$ for $|\theta - \theta_0| > \Gamma_2/2$, *i.e.*, rectangular distribution of nuclei is obtained, corresponding to the case when they radiate before passing through the retarding layer.

For the case $\lambda\alpha \ll 1$ we obtain $f = (1/\Gamma_1)(1 - d/R)$ for $|\theta - \theta_0| \leq \Gamma_2/2$ and $f = 0$ for $|\theta - \theta_0| > \Gamma_2/2$, *i.e.*, we again have a rectangular distribution of the nuclei whose radiation takes place after they have passed the retarding layer. Thus, all the information regarding τ is contained in the form of the curve at $\Gamma_1/2 < |\theta - \theta_0| < \Gamma_2/2$ and in the value of the function $f(\theta)$ at $|\theta - \theta_0| < \Gamma_1/2$. To obtain precise values for τ from an analysis of the form of the curve at $\Gamma_1/2 < |\theta - \theta_0| < \Gamma_2/2$ is apparently impossible, for owing to the effect of multiple scattering and to other causes (final target thickness, inhomogeneity of the beam with respect to energy, *etc.*) the form of the curve will be distorted. However, it is possible to make use of the value of the ordinate at the peak for the determination of τ, since under definite conditions this value will not be affected significantly by the above-mentioned causes. To determine the conditions under which the latter statement will hold, it is sufficient to take into account only the multiple scattering, since the effect of the other factors can be made insignificant. If we assume the multiple scattering to have a Gaussian distribution with a mean square deviation angle of $\overline{\Phi^2}$ and the distribution shown in Fig. 1b to be rectangular with a width Γ_1, the value of the ordinate at the peak will be determined by the expression $f(\theta_0)P(\Gamma_2/2\sqrt{2\overline{\Phi^2}})$, where P is the probability integral. The multiple scattering can be neglected when the value P is close to unity. We shall assume that $P > 0.95$, corresponding to the inequality $\sqrt{\overline{\Phi^2}} < \Gamma_1/4$. From the theory of multiple scattering,[3] it can be shown that this inequality will hold for γ-radiation levels with sufficiently high excitation energy. For the actual evaluations it is necessary to know the magnitude of α. Unfortunately, the literature contains practically no data on this quantity for the passage of multi-charged particles through solid substances. Ia. A. Teplova (Moscow State University) has carried out recently tentative measurements of α for the passage of light nuclei (Be^9, C^{12}, N^{14}) through organic films. These values were found to differ little for the various nuclei and at the energy of ~ 1 Mev are approximately equal to 6×10^{-13} sec^{-1}. If we assume that the recoil nuclei lose half their velocity in the organic lining, which acts like a retarding layer, the calculation carried out for light recoil nuclei ($A \approx 15$) yields $E_\gamma > 1.8\,Z^{1/3}$, where Z is the charge of the recoil nucleus and E_γ is expressed in Mev. If this relationship is not satisfied, it is necessary to introduce a corresponding correction for the effect of multiple scattering.

It is convenient to determine $\delta = f_1/f_0$ directly from experiment (see Fig. 1), using alternate rotation of the target with the corresponding lining through 180°. It can be easily shown that the following relationship will hold:

$$\delta = \frac{1}{1+\lambda\alpha}\left\{\lambda\alpha + \left(1 - \frac{d}{R}\right)^{\lambda\alpha+1}\right\}, \qquad (2)$$

from which we can obtain $\lambda\alpha$. Fig. 2 shows the dependence of δ on $\lambda\alpha$ for various values of d/R. It is evident that δ is more sensitive to changes in $\lambda\alpha$ at $\lambda\alpha < 5$. Hence, for each substance of the lining exists a range of λ which is more favorable for measurements. Since the values of α for various substances range from 10^{-12} to 10^{-14} sec^{-1}, these limits also determine the range of values of τ which can be measured.

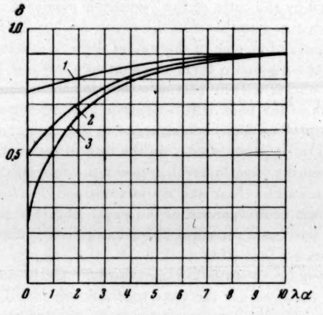

FIG. 2. Curve $1 - d/R = 1/4$; $2 - d/R = 1/2$; $3 - d/R = 3/4$.

In conclusion, I wish to express my gratitude to S. S. Vasil'ev for valuable discussion of this work.

---

[1] A. F. Tulinov, J. Exptl. Theoret. Phys. (U.S.S.R.) 31, 698 (1956); Soviet Phys. JETP 4, 596 (1957).

[2] P. M. S. Blackett and C. H. Lees, Proc. Roy. Soc. A **134**, 658 (1932).

[3] N. Bohr, *Passage of Atomic Particles Through Matter*, (Russ. Transl.), IIL, Leningrad, 1950.

Translated by Esther Rabkin
301

Scattering of Photons by Protons

A. M. BALDIN AND V. A. PETRUN'KIN

(Submitted to JETP editor January 17, 1957)
J. Exptl. Theoret. Phys. (U.S.S.R.) 32, 1570-1572
(June, 1957)

IN CONNECTION with the beginning of experimental investigation of the scattering of photons by protons,[1] we feel it would be of interest to examine this process, starting from the general properties of the S-matrix and elementary physical considerations. The purpose of the present note is to obtain information on the structure of the S-matrix and the minimum number of parameters necessary for describing the process in question.

We shall use the following approach to the problem. We write out the S-matrix in the representation in which its properties are most simply expressed, *i.e.*, in the representation of the total momentum I and its projection M, the total isotopic spin T and its projection T_z, and the parity Π. All the quantities are defined in the center-of-mass system

$$S_{\mu\nu} = (m'\alpha' \mid S^{J\Pi} \mid m\alpha)\ \delta_{(J'J)}\,\delta(M'M)\,\delta(\Pi'\Pi)\,\delta(T'_zT_z), \tag{1}$$

where the m's are the other variables characterizing the channel α. The S-matrix is examined on an energy surface. Next we enumerate all the open channels with the given energy (we restrict our examination to the region of energies under 300 Mev) and all quantum numbers characterizing these channels. In our analysis we shall examine only the following α channels: γ-quantum and proton (γ) and π-meson and nucleon (π). Taking account of the other channels would not substantially affect our results. It must be noted, however, that the channel with the formation of an electron-positron pair is an exception; the matrix element of the S-matrix describing the transition in this channel is not small.

Actually the process of pair formation leads to so-called scattering in the Coulomb field. However, this process, as has been shown by Bethe and Rohrlich,[2] is characterized by a sharply limited forward angular distribution. It can be shown that if we do not consider scattering angles of the order of m_ec^2/E_γ this effect can be neglected.

Let us impose the requirements of unitarity and symmetry on the S-matrix.

$$SS^+ = 1,\ S_{\mu\nu} = S_{\nu\mu};\ S_{\mu\nu} = r_{\mu\nu}e^{i\varphi_{\mu\nu}}. \tag{2}$$

Each of the indices μ and ν goes through eight values. The first condition in (2) is of course approximated with an accuracy equal to the value of the matrix elements describing the transitions in the rejected channels. The second condition in (2) is a consequence of the reciprocity theorem[3] and of the fact that the selected representation does not comprise projections of spins and directions of velocities. These conditions represent the system of transcendental equations which $\alpha_{\mu\nu}$ and $r_{\mu\nu}$ must satisfy. Before attempting to solve the system, we make two simple assumptions which actually follow from experiment: (1) we use the long-wave approximation, whereby we consider the interaction of only dipole quanta (electric and magnetic) with the proton and (2) we assume that the moduli of the matrix elements linking channels γ and γ', γ and π and π with π' are related, respectively, as

$$e^2/\hbar c : \sqrt{e^2/\hbar c} : 1. \tag{3}$$

Part of the S-matrix describing the meson scattering contains isotopic invariant terms regarding which we also assume that they are of the order of $e^2/\hbar c$. The first assumption follows, for example, from experiments on electron-nucleon scattering which show that the dimensions of a nucleon are less than $\hbar/\mu c$ (*i.e.*, smaller than the photon wavelength at the energies under consideration) and also from experiments on scattering and photoproduction of mesons.

The last approximation makes it possible to solve the system of equations by the method of successive approximations, expressing $\alpha_{\mu\nu}$ and $r_{\mu\mu}$ in terms $\alpha_{\mu\mu}$ and $r_{\mu\nu}$, where $\mu \neq \nu$. The ratios between the scattering and photoproduction matrix element obtained in the calculations agree within the limit of small corrections with analogous ratios obtained by Watson.[4] In order to obtain the angular distribution of the scattered photons one must bring the S-matrix to the angular representation, square its modulus, average over the initial and sum over the final spin states of the nucleons and polarizations of the photons. However, we can make direct use of the results of Morita, Sugie and Yoshida[5] who deduced a general expression for the differential cross section for photon scattering from a particle with an arbitrary spin, but without examining the conditions of (2):

$$\frac{d\sigma}{d\Omega}=\frac{1}{32k_{\gamma}^{2}}\{[4\,|X|^{2}-2\,\mathrm{Re}\,X^{*}Y+7\,|Y|^{2}+4\,|Z|^{2}-2\,\mathrm{Re}\,Z^{*}Y+7\,|W|^{2}]$$

$$+4\,\mathrm{Re}\,[X^{*}(2Z+W)+Y^{*}(Z+5W)]\cos\theta+3\,[2\,\mathrm{Re}\,X^{*}Y+|Y|^{2}+2\,\mathrm{Re}\,Z^{*}W+|W|^{2}]\cos^{2}\theta\}, \qquad (4)$$

$$X=(11\ \gamma\,|\,R^{1/2-}\,|\,11\ \gamma),\ Y=(11\ \gamma\,|\,R^{3/2-}\,|\,11\ \gamma),\ Z=(10\ \gamma\,|\,R^{1/2+}\,|\,10\ \gamma),$$

$$W=(10\,\gamma\,|\,R^{3/2+}\,|\,10\,\gamma), \qquad (4a)$$

$$R=S-1. \qquad (4b)$$

Here X, Y, Z and W are the matrix element of the matrix $(L'p'\alpha'\,|\,R^{J\,\mathrm{II}}\,|\,Lp\alpha)$, where L is the total moment of the photon, p is a parity symbol which has a value of 0 for magnetic radiation, and a value of 1 for electric radiation. The remaining notation is clear from what has been said above.

Solution of the system of equations yields the following expressions for the matrix elements:

$$\begin{aligned}X+1&=\sqrt{1-r_1^2-r_2^2e^{i\gamma}}\approx 1-{}^1/_2\,r_1^2-{}^1/_2\,r_2^2+i\gamma,\\ Y+1&=\sqrt{1-\rho_1^2-\rho_2^2e^{i\delta}}\approx 1-{}^1/_2\,\rho_1^2-{}^1/_2\,\rho_2^2+i\delta,\\ Z+1&=\sqrt{1-r_3^2-r_4^2e^{i\alpha}}\approx 1-{}^1/_2\,r_3^2-{}^1/_2\,r_4^2+i\alpha,\\ W+1&=\sqrt{1-\rho_3^2-\rho_4^2e^{i\beta}}\approx 1-{}^1/_2\,\rho_3^2-{}^1/_2\,\rho_4^2+i\beta,\end{aligned} \qquad (5)$$

where α, β, γ and δ are real parameters and r_i and ρ_k are moduli of the matrix elements of meson photoproduction. At γ-quanta energies below the photoproduction thresholds, they vanish:

$$r_1=\left|\left(11\gamma\,|\,S^{1/2-}\,|\,0\,\tfrac{1}{2}\,\pi\right)\right|,\quad r_2=\left|\left(11\gamma\,|\,S^{1/2-}\,|\,0\,\tfrac{3}{2}\,\pi\right)\right|,\quad r_3=\left|\left(10\gamma\,|\,S^{1/2+}\,|\,1\,\tfrac{1}{2}\,\pi\right)\right|,$$

$$r_4=\left|\left(10\gamma\,|\,S^{1/2+}\,|\,1\,\tfrac{3}{2}\,\pi\right)\right|$$

$$\rho_1=\left|\left(11\gamma\,|\,S^{3/2-}\,|\,2\,\tfrac{1}{2}\pi\right)\right|,\quad \rho_2=\left|\left(11\gamma\,|\,S^{3/2-}\,|\,2\,\tfrac{3}{2}\,\pi\right)\right|, \qquad (5a)$$

$$\rho_3=\left|\left(10\gamma\,|\,S^{3/2+}\,|\,1\,\tfrac{1}{2}\,\pi\right)\right|\quad \rho_4=|(10\,\gamma\,|\,S^{3/2+}\,|\,1\tfrac{3}{2}\,\pi)\,|.$$

The arrangement of indices in Eqs. (5a) is the following: $S_{m'm}=(Lp\alpha'\,|\,S^{J\,\mathrm{II}}\,|\,lT\alpha)$, where l is the relative orbital momentum in channel α. Expansion of the exponents and roots is allowable inasmuch as it is known from experiments that the total cross section for the Compton effect on protons is of the order of 10^{-31} cm^2. It is interesting to note that the differential cross section for the process under consideration subdivides into two parts $f_1(\theta)$ and $f_2(\theta)$, of which the former depends on α, β, γ, and δ, and the latter on r_i and ρ_k. This follows directly from formula (5) and the general expression for the differential cross section (4). Thus, by determining experimentally the coefficients A, B and C characterizing the angular distribution of the photons,

$$d\sigma\,/\,d\Omega=(1\,/\,32\ k_{\gamma}^{2})\,(A+B\cos\vartheta+C\cos^{2}\theta). \qquad (6)$$

we will not be able to find α, β, γ and δ inasmuch as we will obtain three equations with four unknowns. We assume that r_i and ρ_k can be determined from experimental data on photomeson production on nucleons. Consequently, for unambiguous determination of the parameters α, β, γ and δ we must have additional data. These can be obtained from experiments with polarized particles. We might also call attention to another possible effect, *viz.* the interference of ordinary scattering with scattering in the Coulomb field. This effect might be detected in investigating small angle scattering of photons.

It would be expedient to examine separately the case of small energies, *i.e.*, the region in which the cross section differs little from the cross section given by Thomson's formula. In this case we can write

$$\alpha = \Delta_1, \ \beta = \Delta_2, \ \gamma = \Delta_3 + a, \ \delta = \Delta_4 + a. \qquad (7)$$

If $\Delta_i = 0$, Eq. (4) with $a^2 = (16/9)k_\gamma^2(e^2Mc^2)$ goes over into Thomson's formula

$$d\sigma/d\Omega = {}^1/_2(e^2/Mc^2)^2(1+\cos^2\theta). \qquad (8)$$

If we express X, Y, Z and W in (4) in terms of Δ_i and a and neglect the terms $\Delta_i\Delta_k$, we obtain

$$d\sigma / d\Omega$$

$$= (1/32\,k_\gamma^2)[(9a^2 + 6\bar{X}a)(1+\cos^2\theta) + 12\,a\bar{Y}\cos\theta]. \qquad (9)$$

Here $$\bar{X} = \Delta_3 + 2\Delta_4, \ \bar{Y} = \Delta_1 + 2\Delta_2. \qquad (9a)$$

Comparison of Eq. (9) with experiment should make it possible to check the assumptions made in deriving it and enable us to determine $\bar{X}$ and $\bar{Y}$, which is important inasmuch as $\bar{X}$ is expressed only through quantities connected with electric radiation, while $\bar{Y}$ is expressed only through quantities connected with magnetic radiation.

[1] C. L. Oxley and V. L. Telegdi, Phys. Rev. **100**, 435 (1955); Govorkov, Gol'danskii, Karpukhin, Kutsenko and Pavlovskaia, Dokl. Akad. Nauk SSSR **111**, 988 (1956).

[2] H. Bethe and F. Rohrlich, Phys. Rev. **86**, 10 (1952).

[3] J. Blatt and V. Weisskopf *Theoretical Nuclear Physics*, (Russ. Transl.), IIL, 1954.

[4] K. Watson, Phys. Rev. **95**, 228 (1954).

[5] Morita, Sugie and Yoshida, Prog. Theor. Phys. **12**, 713 (1954).

Translated by E. J. Rosen
302

Use of a Mixture of Two Liquids in Bubble Chambers

G. A. BLINOV, IU. S KRESTNIKOV,
M. F. LOMANOV AND IA. IA. SHALAMOV

(Submitted to JETP editor February 8, 1957)
J. Exptl. Theoret. Phys. (U.S.S.R.) **32**, 1572-1573
(June, 1957)

AS THE SIZE of bubble chambers is increased, the technical difficulties involved in their operation become ever greater in view of the necessity of producing and maintaining the temperatures and pressures approprite to the liquid employed. These difficulties could be largely obviated if it were possible to work at close to room temperature. Of the substances employed in bubble chambers hitherto, the two having a working temperature closest to room temperature are propane ($t_{\text{work}} \approx 64°$ C) and Freon-13 ($t_{\text{work}} \approx 0°$ C). We assumed that a convenient working temperature could be obtained by using appropriate mixtures of two liquids.

For the purpose of exploring the possibility of employing mixtures we carried out a series of experiments with a bubble chambe filled with a mixture of Freon-12 (CCl_2F_2) and Freon-13 ($CClF_3$). For Freon-12 the critical temperature and pressure are 111.5° C and 39.6 atmospheres; for Freon-13 the respective values are 28.8° C and 39.4 atmospheres. The chamber described in an earlier communication[1] was used for the tests. Inasmuch as this chamber has a pressure-actuated device for limiting the expansion, the sensitivity of the chamber was controlled by varying the lower level of the pressure drop at constant temperature. With a Co^{60} γ-source mounted in front of the chamber window it was possible to observe and photograph the electron tracks and establish at what temperature, pressures and concentrations observation of the tracks was feasible.

We used two different mixtures, containing about 40 and 75 percent molar Freon-12. In the first case the pressure of the saturated vapor of the mixture was 21 atmospheres at 19° C; in the second case 21.6 atmospheres at 43° C. The temperatures and pressures at which particle tracks could be observed in each case are shown in Fig. 1. The tests were carried out at temperatures ranging from 19 to 38° C for the first mixture and from 43 to 52° C for the second. Curves 1 and 5 in the figure are drawn through the points corresponding to the sensitivity threshold. With pressure drops to a lower level there was observed an increase in sensitivity (shaded areas in figure). Curves 3 and 6 denote the lower boundary of the pressure drops. At these pressures fog was

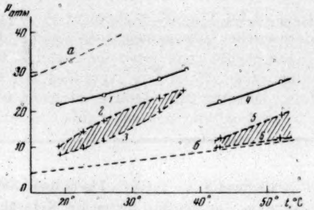

Dash lines – pressures of the unsaturated vapors of pure: (a) Freon-13, (b) Freon-12. Solid curves – same for the mixtures: (1) 40% Freon-12, (4) 75% Freon-12. Curves 2 and 3 bound the working region for the first mixture; curves 5 and 6 bound the region for the second mixture.

observed in the chamber at temperatures of 34 and 38° C for the first mixture and 52° C for the second mixture; at other temperatures there was no fog formation since it was impossible to realize a greater pressure drop due to boiling of the mixture in the separator.

The chamber was expanded every 10 sec. In all experiments the pressure in the chamber between expansions was 35 atmospheres. The sensitivity time was determined from photographs exposed with different delays relative to the beginning of pressure relief. The sensitivity time was found to be 40 microseconds.

Thus satisfactory operation of a bubble chamber is possible with a mixture which at room temperature has a saturated vapor pressure of about 21 atmospheres. The suggested mixture by virtue of its high density (~ 1.0 g/cm³) is convenient for many nuclear investigations. The use of mixtures makes it easier to select the best "working substance" for a given physical problem. Of particular interest would be hydrogen-containing mixtures, for example, a mixture of methane with propane, which has been used in a "gas" bubble chamber,[2] or a mixture of ethane and propane.

---

[1] Blinov, Krestnikov, and Lomanov, J. Exptl. Theoret. Phys. (U.S.S.R.) **31**, 762 (1956), Soviet Phys. JETP **4**, 661 (1957).

[2] P. E. Argan and A. Gigli, Nuovo cimento **4**, 953 (1956).

Translated by E. J. Rosen
303

Two-Electron Green Function in the Bloch–Nordsieck Approximation

R. V. TEVIKIAN
Erevan State University

(Submitted to JETP editor February 20, 1957)
J. Exptl. Theoret. Phys. (U.S.S.R.) 32, 1573-1574 (June, 1957)

THE ELECTRON GREEN FUNCTION in the Bloch–Nordsieck approximation[2] has been considered in an earlier work.[1] As is well known, the Bloch–Nordsieck approximation, in which the matrix γ^μ is replaced by the c-number u^μ, allows a consideration of the interaction of an electron with long-wave photons. In the present work we consider the two-electron Green function in this same approximation.

In the Bloch–Nordsieck approximation the Schwinger equation[3] has the following form:

$$\begin{gathered}\left\{iu^\mu \frac{\mu\partial}{\partial x^\mu} - m + \sqrt{4\pi}\, eu^\mu A_\mu(x) + i\sqrt{4\pi}\, eu^\mu \int D_{\mu\nu}(x,\xi)\frac{\delta}{\delta A_\nu(\xi)}\, d\xi\right\} G(x, x'; y, y' \mid A) \\ = \delta(x-y')\, G(x', y \mid A) - \delta(x-y)\, G(x', y' \mid A), \qquad (1) \\ u^2 = (u^0)^2 - \mathbf{u}^2 = 1, \qquad m \to m - i\varepsilon\,(\varepsilon > 0,\ \varepsilon \to 0).\end{gathered}$$

In this case the one-electron Green function satisfies the equation

$$F_x G(x, y \mid A) = -\delta(x-y), \tag{2}$$

where F_x is the operator which appears in the curly brackets in the left-hand part of Eq. (1).

The solution of Eq. (1) is given by

$$G(x, x'; y, y' \mid A) = G(x, y \mid A)\, G(x', y' \mid A) - G(x, y' \mid A)\, G(x', y \mid A) + G_{12}(x, x'; y, y' \mid A) - G_{12}(x, x'; y', y \mid A) \tag{3}$$

and for the function G_{12} we get the following equation:

$$F_x G_{12}(x, x'; y, y' \mid A) = -i\sqrt{4\pi}\, eu^{\mu} \int D_{\mu\nu}(x, \xi) \frac{\delta G(x', y' \mid A)}{\delta A_{\nu}(\xi)} G(x, y \mid A)\, d\xi. \tag{4}$$

To solve this equation we use the same method as in the earlier work. The following expressions follow from the homogeneity of space and time:

$$\begin{gathered} G_{12}(x, x'; y, y' \mid A) = G_{12}(x' - x, y - x, y' - x \mid T_x A), \\ G(x, y \mid A) = G(y - x \mid T_x A), \qquad D_{\mu\nu}(x, \xi) = D_{\mu\nu}(\xi - x) \end{gathered} \tag{5}$$

where $T_x A_{\mu}(\xi) = A_{\mu}(\xi + x)$.

Using these relations we can write Eq. (4) in momentum space in the form

$$\begin{aligned} &\Big\{(up_1) + (up_2) + (up_3) - m - \int (uk)\, A_{\mu}(\kappa) \frac{\delta}{\delta A_{\mu}(k)} dk + \sqrt{4\pi} \frac{eu^{\mu}}{(2\pi)^2} \int A_{\mu}(k)\, dk \\ &\qquad + i\sqrt{4\pi} \frac{eu^{\mu}}{(2\pi)^2} \int D_{\mu\nu}(k) \frac{\delta}{\delta A_{\nu}(k)} dk \Big\} G_{12}(p_1, p_2, p_3 \mid A) \\ &= -i\sqrt{4\pi} \frac{eu^{\mu}}{(2\pi)^2} \int D_{\mu\nu}(k) \left[\frac{\delta G(p_3 \mid A)}{\delta A_{\nu}(k)}\right]_{A \to T_x A} \cdot G(p_2 \mid A)\, e^{i(k - p_1 - p_3)x} dx\, dk, \end{aligned} \tag{6}$$

where $T_x A_{\mu}(k) = e^{ikx} A_{\mu}(k)$.

Using the proper-time method of Fock,[4] Eq. (6) can be solved exactly; the solution has the form

$$\begin{aligned} G_{12}(p_1, p_2, p_3 \mid A) = &-\sqrt{4\pi} \frac{eu^{\mu_1}}{(2\pi)^2} \int_0^{\infty} d\nu e^{-\varepsilon\nu} e^{-i(m - up_1 - up_2 - up_3)\nu + f(\nu)} \exp\left\{-\sqrt{4\pi} \frac{eu^{\mu}}{(2\pi)^2} \int \frac{e^{-i(up)\nu} - 1}{(up)} A_{\mu}(p)\, dp\right\} \\ &\times \int D_{\mu_1\nu_1}(k) \left\{\left[\frac{\delta G(p_3 \mid A)}{\delta A_{\nu_1}(k)}\right]_{A \to T_x A} G(p_2 \mid A)\right\}_{A \to A^{T_\nu}} e^{i(k - p_1 - p_3)x} dx\, dk, \end{aligned} \tag{7}$$

$$\begin{gathered} A_{\mu}^{T_\nu}(k) = A_{\mu}(k)\, e^{-i(uk)\nu} - i\sqrt{4\pi} \frac{eu^{\sigma}}{(2\pi)^2} D_{\sigma\mu}(k) \frac{e^{-i(uk)\nu} - 1}{(uk)}, \\ f(\nu) = -i \frac{e^2}{4\pi^3} \int_0^{\nu} d\nu \int_0^{\nu} d\nu \int e^{-i(uk)\nu} u^{\mu} u^{\rho} D_{\mu\rho}(k)\, dk. \end{gathered} \tag{8}$$

In the Bloch–Nordsieck approximation there is no vacuum polarization; whence it follows that:

$$\begin{gathered} D_{\mu\nu}(k) = -g^{\mu\nu} / (k^2 + i\varepsilon) - g^{\mu\nu} / (M^2 - k^2 - i\varepsilon) \qquad (M \to \infty) \\ g^{\mu\nu} = 0\ (\mu \neq \nu), \qquad g^{00} = -g^{11} = -g^{22} = -g^{33} = 1, \end{gathered} \tag{9}$$

where M is the Pauli–Villars auxiliary mass. Carrying out the indicated integrations in (8) we find

$$f(\nu) = -i \frac{e^2}{2} M\nu + \frac{e^2}{\pi} \ln \frac{M}{m'} + \frac{e^2}{\pi} \ln m'\nu, \tag{10}$$

and from the previous work we have

$$G(p_1 \mid A) = i \int_0^{\infty} d\nu e^{-\varepsilon\nu} e^{-i(m - up_1)\nu + f(\nu)} \exp\left\{-\sqrt{4\pi} \frac{eu^{\mu}}{(2\pi)^2} \int \frac{e^{-i(up)\nu} - 1}{(up)} A_{\mu}(p)\, dp\right\}. \tag{11}$$

The divergence which appears in the function in (7) can be removed by renormalization. The first term in (10), which contains the auxiliary mass M, is removed by mass renormalization

$$m' = m + e^2 M / 2, \tag{12}$$

where m' is the observed mass of the electron. The other terms which contain M go into the renormalized constant in the Green function.

Using the present method it is also possible to determine Green functions for three and more electrons in the Bloch–Nordsieck approximation; in these cases, however, the expressions are much more complicated.

---

[1] R. V. Tevikian, J. Exptl. Theoret. Phys. (U.S.S.R.) 30, 949 (1956); Soviet Phys. JETP 3, 967 (1957).

[2] F. Bloch and A. Nordsieck, Phys. Rev. 52, 54 (1937).

[3] J. Schwinger, Proc. Nat. Acad. Sci. 37, 452 (1951).

[4] V. A. Fock, Z. Phys. Sowjetunion 12, 404 (1937).

Translated by H. Lashinsky
304

Green Function in Scalar Electrodynamics In The Boch-Nordsieck Approximation

R. V. TEVIKIAN
Ereven State University

(Submitted to JETP editor February 20, 1957)
J. Exptl. Theoret. Phys. (U.S.S.R.) 32, 1575 (June, 1957)

A METHOD WHICH HAS been applied earlier[1] is used to consider the Green function in scalar electrodynamics in the Boch-Nordsieck approximation,[2] *i.e.*, when the particle recoil can be neglected. As is well known, the infra-red catastrophe does not arise in this case.

The Green function is scalar electrodynamics satisfies the equation

$$\left\{m^2 - \left[i\frac{\partial}{\partial x^\mu} + \sqrt{4\pi}\, eA_\mu(x) + i\sqrt{4\pi}e\int D_{\mu\nu}(x,\xi)\frac{\delta}{\delta A_\nu(\xi)}d\xi\right]^2\right\} G(x, y \mid A) = \delta(x-y). \tag{1}$$

Using the invariance of the Green function against translation, in the momentum representation Eq. (1) can be written in the form

$$\left\{m^2 - \left[p_\mu - \int k_\mu A_\nu(k)\frac{\delta}{\delta A_\nu(k)}dk + \sqrt{4\pi}\frac{e}{(2\pi)^2}\int A_\mu(k)\,dk + i\sqrt{4\pi}\frac{e}{(2\pi)^2}\int D_{\mu\nu}(k)\frac{\delta}{\delta A_\nu(k)}dk\right]^2\right\} G(k \mid A) = 1. \tag{2}$$

In the Boch-Nordsieck approximation Eq. (2) assumes the form

$$\left\{m^2 - \left[u^\mu\left(p_\mu - \int k_\mu A_\nu(k)\frac{\delta}{\delta A_\nu(k)}dk + \sqrt{4\pi}\frac{e}{(2\pi)^2}\int A_\mu(k)\,dk + i\sqrt{4\pi}\frac{e}{(2\pi)^2}\int D_{\mu\nu}(k)\frac{\delta}{\delta A_\nu(k)}dk\right)\right]^2\right\} G(p \mid A) = 1;$$

$$u^\mu = p^\mu / |p|, \quad m \to m - i\varepsilon \quad (\varepsilon > 0, \varepsilon \to 0). \tag{3}$$

In this same approximation the photon Green function is

$$\begin{gathered} D_{\mu\nu}(k) = -g^{\mu\nu}/(k^2 + i\varepsilon) - g^{\mu\nu}/(M^2 - k^2 - i\varepsilon) \quad (M \to \infty). \\ g^{\mu\nu} = 0 \ (\mu \neq \nu), \ g^{00} = -g^{11} = -g^{22} = -g^{33} = 1, \end{gathered} \tag{4}$$

where M is the Pauli-Villars auxiliary mass.

Using the proper-time method of Fock,[3] Eq. (3) can be solved exactly. Terms containing the auxiliary mass M are removed by renormalization and the following expression is found for the renormalized Green function $G' = (M/m')^{e^2/\pi}G$:

$$G'(p \mid A) = -\int_0^\infty d\nu \int_0^\infty d\mu e^{-\varepsilon(\nu+\mu)} \exp\{-i(m'-up)\nu - i(m'+up)\mu\} (m' \mid \nu+\mu \mid)^{e^2/\pi} \times \exp\left\{-\sqrt{4\pi}\frac{eu^\mu}{(2\pi)^2}\int \frac{\exp\{-i(uk)(\nu-\mu)\}-1}{(uk)} A_\mu(k)\,dk\right\}, \tag{5}$$

where $m' = m + e^2M/2$ is the observed mass. In particular, for $A = 0$, we have:[4]

$$G'(p/0) = \frac{1}{m'^2 - p^2}\left|\frac{m'^2}{m'^2-p^2}\right|^{e^2/\pi}. \tag{6}$$

Applying the Green function,[5] we calculate the probability of the following process. A particle is scattered in the external field and radiates an arbitrary number of long-wave photons with energies less than ε' and n additional photons with energies from E_1 to E_2. It is assumed that the energy and momentum of the radiated photons are small compared with the energy and the change of momentum of the particles in scattering, *i.e.*, $\varepsilon' \ll m'$ and $E_1 > \varepsilon'$. The probability of this process is given by the following expression:

$$dw = dw_0\left(\frac{\varepsilon'}{m'}\right)^{2e^2/\pi}\frac{1}{n!}\left\{\frac{2e^2}{\pi}\ln\frac{E_2}{E_1}\right\}^n, \tag{7}$$

where dw_0 is the scattering probability in the zeroth perturbation theory approximation.

If the condition $(2e^2/\pi)\ln(m'/\varepsilon') \ll 1$ is satisfied, Eq. (7) assumes the form

$$dw = dw_0\frac{1}{n!}\left\{\frac{2e^2}{\pi}\ln\frac{E_2}{E_1}\right\}^n.$$

---

[1] R. V. Tevikian, J. Exptl. Theoret. Phys. (U.S.S.R.) 30, 949 (1956); Soviet Phys. JETP 3, 967 (1957).

[2] F. Bloch and A. Nordsieck, Phys. Rev. 52, 54 (1937).

[3] V. A. Fock, Z. Phys. Sowjetunion 12, 404 (1937).

[4] A. A. Logunov, J. Exptl. Theoret. Phys. (U.S.S.R.) 29, 871 (1955); Soviet Phys. JETP 2, 337 (1956).

Translated by H. Lashinsky
305

Coherent Scattering and Radiation of Electromagnetic Waves by a Plasma in an Inhomogeneous Magnetic Field

G. A. ASKARIAN

(Submitted to JETP editor February 25, 1957)
J. Exptl. Theoret. Phys. (U.S.S.R.) 32, 1576-1577
(June, 1957)

IN VIEW OF THE INTEREST in the potentialities of the intense radiative acceleration interaction in a plasma[1] and the difficulty involved in the formation of stable plasma bunches which provide effective coherent radiation scattering, we propose another possible method for enhancing radiation scattering in a plasma, *viz.* the application to the plasma of local magnetic fields.

It is well known that the presence of a magnetic field in a plasma causes a change in its electromagnetic properties, in particular, in the dielectric constant ε; this change depends not only on the magnitude of the field but also on its direction. Furthermore, the use of an inhomogeneous magnetic field can bring about an inhomogeneous plasma density distribution because of the dependence of the ionization efficiency of a given ionizing agency, for example a high-frequency wave, on magnetic field. Hence, regions of the plasma in which the magnetic field differs noticeably in magnitude or direction are analagous to "optical inhomogeneities."

If the dimensions of the localized region of a given magnetic field are considerably smaller than the wavelength of the incident radiation, the radiation associated with the particles of the plasma is coherent; if there is no strong shielding of the field in the external region (small difference in dielectric constants in the internal and external regions) the radiation is proportional to the square of the number of particles.

For purposes of illustration, we consider coherent scattering of a quasi-plane wave of frequency ω propagating in a wave guide filled with plasma to which there is applied a longitudinal magnetic field to bring about colinear motion of the particles. If the plasma density falls off sharply between the axis of the wave guide and the walls, an effective scattering region may be formed by the application of a supplementary local field having, for example, a localized longitudinal component. The quantities which characterize the average values of the plasma parameters inside and outside the region of effective scattering will be denoted in the following by the subscripts i and a. For simplicity we will assume that $\varepsilon_a \approx \varepsilon_i \approx 1$ and $|1 - \varepsilon_i| \gg |1 - \varepsilon_a|$. Then the effective cross-section for radiation scattering (of wavelength λ) in the region of inhomogeneous magnetic field, which we will assume to be quasi-spherical and of dimensions $l \ll \lambda$, is

$$\sigma \approx \frac{2\pi^5}{3}\frac{l^6}{\lambda^4}\left(\frac{\varepsilon_i - 1}{\varepsilon_i + 2}\right)^2 \approx \frac{2\pi^5}{3^3}\frac{l^6}{\lambda^4}\left\{\frac{\omega_0^2(n_i)}{\Delta\omega^2(H_{zi})}\right\}^2,$$

where the plasma frequency $\omega_0 = (4\pi e^2 n/m)^{1/2}$; n is the electron density in the plasma, e and m are the charge and mass of the electron, and $\Delta\omega^2(H_i) \approx \omega^2 - \omega_H^2(H_i)$, where the Larmor frequency is given by $\omega_{Hi} = eH_{zi}/mc$. For $\Delta\omega^2 \sim \omega^2$, $\sigma_i \approx 8\pi r_0^2 N^2/3$ (r_0 is the classical electron radius and N is the total number of electrons in the scattering region) and the intensity of the field equivalent to the radiation force acting on the electron in the region is $\mathbf{E}_{\mathrm{eff}} \approx \sigma_i \mathbf{S}/Nec$. For example, with a radiation flux $S \approx 300\,\mathrm{kw/cm^2}$ and $N \sim 3 \times 10^{12}$; these crude calculations yield $E_{\mathrm{eff}} \sim 100$ v/cm.

The multiplication of the radiation force acting on each particle which participates in scattering can be used, in practice, for the formation of intense coherent fluxes of plasma particles. In fact a judicious choice of the periodicity of the spatial distribution of the localized-field regions can provide coherent radiation by the different plasma regions and by increasing the number of inhomogeneous field regions it may be possible for the radiation mechanism to provide continuous (in transition) acceleration of the particles as they travel from one acceleration zone to another. Furthermore, the application of a localized magnetic field in the plasma can be used to inhibit undesired radiation propagation in the wave guide and to enhance conversion in a resonator. In this case, with a given power input, it is possible to achieve much higher radiation pressures and interactions at resonance than is possible in scattering by traveling waves.

As an interesting example of the inverse problem we consider the coherent radiation of a bunch in an electron plasma which travels through a spatially-periodic, axially-symmetric magnetic field ("longitudinal undulator") comprising, for example, a system of magnetized rings of alternating longitudinal polarity or a succession of magnetic lenses or coils in which the direction of current flow is alternated. (Undulators in which transverse fields are employed are discussed in Refs. 2 and 3.)

The radiation of a bunch which travels along the axis of such a system arises by virtue of the change in the induced moment of the bunch. The appearance of a magnetic moment in the bunch and the effect of the focusing forces due to the external field and the induced motion of the electrons themselves can be interpreted and evaluated most simply in a coordinate system which moves with the center of the bunch. In this system the fixed sinusoidal distribution of axially-symmetric magnetic field in the laboratory system can be considered an axially-symmetric wave whose effect on a bunch (if the coherence conditions apply and if the change of dimensions of the bunch is neglected) is that of a quasi-homogeneous sinusoidally varying magnetic field on a quasi-cylindrical or quasi-spherical section of the medium (the expression for the field is given, for example, in Ref. 4). An estimate of the average ponderomotive force indicates that over a wide range of the plasma parameters, which are of practical interest, the plasma tends to focus the bunches; there is a longitudinal focusing effect which arises as a result of the attraction between the induced currents flowing in the same direction. This effect may make possible the use of compact hollow rings or intense solid bunches for relatively long periods of time.

It would be of interest to investigate the dissipation of the alternating component of the energy of a plane quasi-neutral plasma when it is penetrated by periodic or otherwise inhomogeneous axially-symmetric fields.

---

[1] V. I. Veksler, *Proceedings of the CERN Symposium on High-Energy Accelerators and Pion Physics, Geneva, June, 1956* (CERN, 1956) p. 80.

[2] H. Motz, J. Appl. Phys. **22**, 527 (1951).

[3] Motz, Thon, and Whitehurst, J. Appl. Phys. **24**, 826 (1953).

[4] M. A. Divil'kovskii, J. Exptl. Theoret. Phys. (U.S.S.R.) **9**, 343 (1939).

Translated by H. Lashinsky
306

Investigations of the Equation of State by Mechanical Measurements

IA. B. ZEL'DOVICH
*P. N. Lebedev Institute of Physics,
Academy of Sciences, U.S.S.R.*

(Submitted to JETP editor March 6, 1957)
J. Exptl. Theoret. Phys. (U.S.S.R.) **32**, 1577-1578
(June, 1957)

RECENT YEARS have seen successful investigations of the properties of matter at high pressures obtained by explosive means. By this procedure pressures of the order of a million atmospheres are readily attained. However, a distinctive feature of the explosive method is the short duration of the high pressure. Because of this the measurements are limited to determining the velocity of the shock wave (D), the rate of displacement (u) of the material compressed by the shock wave, or the density attained in compression ($\rho = 1/v$, where v is the specific volume). These quantities are related by the expression $D\rho_0 = (D - u)\rho$. In addition to the measurements pertaining to the material compressed by the shock wave, it is also feasible to make certain measurements in the course of the subsequent adiabatic expansion of the material.

A common characteristic of investigations carried out by the explosive procedure is determination of mechanical quantities – the velocities, density, pressure (in the shock wave $p = p_0 + \rho_0 Du$), and energy of the material. In the shock wave $E = E_0 + (v_0 - v)(p + p_0)/2$. The thermal processes and equalizations of temperature do not have time to attain equilibrium, hence conventional temperature measurements prove impossible. Optical measurement of the temperature of the shock wave is possible only in transparent materials, primarily in gases and then only in a temperature range bounded both from below (absence of radiation and transparency of the compressed gas) and from above (formation of a heated layer in front of the shock wave[1]).

Thus in the typical case of investigation of the equation of state by the explosive method, experiments give only information on the energy, pressure and density. By varying the initial state of the material, in particular, by compressing the material in the form of a finely dispersed powder with a reduced initial density by means of the shock wave, one can obtain the different adiabatic curves for shock compression and fill in an entire region in the p, v plane.

In the case of adiabatic (isenotropic) expansion the following relationships hold: $dp = \rho c\,du$; $dp = c^2\,d\rho$ and $dE = p\rho^{-2}\,d\rho$, where c is the velocity of sound. By measuring the velocity and pressure attained during expansion one can also find $E(p, v)$ along an isentrope. Finally in detonation waves and in the expansion of the products of the explosion itself measurements of the rates of detonation and displacement makes it possible to find $E(p, v)$. Thus in principle one can find the function of two variables $p(E, v)$ or $E(p, v)$ at high pressures.

In the present note we examine the problem of how, knowing $E(p, v)$, one can obtain the full thermodynamic characteristic of the material, *i.e.*, find the temperature T and entropy S at the high pressures that can be attained only by the explosive method.

Knowing $E(p, v)$ one can plot the lines of constant entropy. From

$$dE = TdS - pdv = E_p dp + E_v dv \tag{1}$$

we obtain for the isentrope ($dS = 0$):

$$(dp / dv)\,|_S = -(E_v + p) / E_p \tag{2}$$

(the subscripts at E denote partial derivatives).

However, the absolute value of the entropy cannot be determined from mechanical measurements alone, *i.e.*, from the function $E(p, v)$. The entropy can be determined only in the case when the measurements of the mechanical quantities in the shock wave and in the process of expansion can be linked with the region of low density where calculation or calorimetric measurement of the entropy is possible. Obviously if a constant-entropy line in the p, v plane is known and the value of the entropy at the lower end of this line is known, we will have S for the entire line. It can readily be shown that this also pertains to temperature: if the temperature at one end of an adiabatic curve is known, then when $E(p, v)$ is known, we can calculate the temperature over the entire adiabatic curve.

Let us imagine that we have two neighboring adiabatic lines $p_1(v)$ and $p_2(v)$ drawn in the p, v plane and that the energy E is known over the entire length of the adiabatic lines. If in the region of low pressures and low densities the temperature $T = T_0$ is known at some point of $v \doteq v_0$ [or more accurately, let $T_0 = (T_1 + T_2)/2$], then the entropy difference on the two adiabatic curves is given by

$$S_1 - S_2 = \{E[p_1(v_0), v_0] - E[p_2(v_0), v_0]\}\,/T_0. \tag{3}$$

In this case the temperature between the two neighboring adiabatic curves at a high pressure and a corresponding density (low specific volume v) is given by

$$T = \frac{E[p_1(v),\ v] - E[p_2(v),\ v]}{S_1 - S_2}$$

$$= T_0 \frac{E[p_1(v),\ v] - E[p_2(v),\ v]}{E[p_1(v_0),\ v_0] - E[p_2(v_0),\ v_0]}. \qquad (4)$$

Consequently, if mechanical measurements giving $E(p,\ v)$ have been made, all the thermodynamic quantities can be determined along the adiabatic curves extended to where they join the region in which these quantities (T and S) can be determined by calculation or experimentally.

Let us carry out the formal operations substantiating this conclusion and leading to more convenient expressions for the temperature. Determining dS from (1), we then obtain

$$\frac{\partial^2 S}{\partial p \partial v} = \frac{\partial}{\partial v}\left(\frac{E_p}{T}\right) = \frac{\partial}{\partial p}\left(\frac{E_v + p}{T}\right) \qquad (5)$$

Equation (5) is a partial differential equation for the absolute temperature; after elementary operations we obtain

$$(E_v + p)\, \partial T / \partial p - E_p \partial T / \partial v = T. \qquad (6)$$

The characteristics of this equation are lines, whose differential equation is

$$dp / dv = -(E_v + p) / E_p \qquad (7)$$

i.e., adiabatic lines [compare with Eq. (2)]. Along these lines Eq. (6) gives

$$dT / dv |_S = -T / E_p, \qquad (8)$$

whence

$$T = T_0 \exp\left(-\int_{v_0}^{v} \frac{dv}{E_p}\right) = T_0 \exp\left(\int_{p_0}^{p} \frac{dp}{E_v + p}\right), \qquad (9)$$

where the integrals are taken along the adiabatic line. Just as in Eq. (4), the temperature in Eq. (9) is everywhere proportional to the given value T_0 at the end of the adiabatic line.

In the present note we do not examine the question of the accuracy with which it is necessary to make the initial measurements of D and u, as well as of the velocities attained in adiabatic expansion, in order to be able to carry out the calculations for $E(p,\ v)$, the adiabatic lines, and finally the temperatures according to formulas (4) or (9).

In conclusion I wish to express my gratitude to L. V. Al'tshuler, S. M. Volosov, and N. A. Dmitriev for valuable discussions.

---

[1] Ia. B. Zel'dovich, J. Exptl. Theoret. Phys. (U.S.S.R.) 32, 1126 (1957); Soviet Phys. JETP 5, 919 (1957).

Translated by E. J. Rosen
307

Beta-Emission From Polarized Nuclei

G. R. KHUTSISHVILI
Institute of Physics, Academy of Sciences, Georgian SSR

(Submitted to JETP editor March 8, 1957)
J. Exptl. Theoret. Phys. (U.S.S.R.) 32, 1578-1580 (June, 1957)

1. THE ANGULAR DISTRIBUTION of β-radiation from oriented nuclei has been investigated theoretically by Cox and De-Groot[1] and the writer.[2] However, it was assumed in these investigations that parity is conserved in β-decay. Recently it has been found that conservation of parity is violated in β-decay.[3,4] In view of this, the results obtained in the aforementioned investigations[1,2] are valid only for aligned nuclei, but are not valid for polarized nuclei.

In the general case the distribution of the β-particles in energy and in angle should be

$$W(E,\ \vartheta) = a_0 + a_1 f_1 P_1(\cos\vartheta) + \cdots + a_n f_n P_n(\cos\vartheta), \qquad (1)$$

where $n \leq 2l + 1$ and $n \leq 2I$ (here I is the spin of the initial nucleus and l is the maximum orbital momentum carried off by the leptons), ϑ is the angle between the direction of the β-particle and the quantization axis, $a_0, \ldots, a_n$ are quantities dependent on the nuclear spin, on the type of β-transition and on the energy of the β-particle, and $f_1 \ldots, f_n$ are parameters characterizing the degree of orientation of the nuclei (see, for example, Ref. 5), normalized so that their maximum values will equal unity.

It is well known that β-interaction is a mixture of scalar and tensor forms of interaction. Lee and Yang[3] compute the angular distribution of β-radiation from polarized nuclei for allowed $\Delta I = \pm 1$ (no) β-transitions. Such transitions are due only to tensor interaction. It should also be of interest to examine allowed β-transitions of the $\Delta I = 0$ (no) type. By comparing the theoretical results for such transitions with the experimental data it should be possible to draw certain conclusions regarding the ratio of the β-interaction constants.

We note that all our calculations were carried out in the Born approximation.

2. We take the density of the matrix element for the β^--transition in the form

$$H = (\psi_p^+ \beta \psi_n) [C_S (\psi_e^+ \beta \psi_\nu) + C'_S (\psi_e^+ \beta \gamma_5 \psi_\nu)] + (\psi_p^+ \beta \boldsymbol{\sigma} \psi_n) [C_T (\psi_e^+ \beta \boldsymbol{\sigma} \psi_\nu) + C'_T (\psi_e^+ \beta \boldsymbol{\sigma} \gamma_5 \psi_\nu)] \tag{2}$$

(the notation here is that of Lee and Yang[3]). The relativistic term of the tensor interaction is not included here since it plays no part in these transitions.

Let us first examine allowed β-transitions with $\Delta I = 0 \pm 1$ (no). For the energy and angular distribution of the β-particles we obtain

$$\begin{aligned} W(E, \vartheta) = K \Big\{ \Big| \int 1 \Big|^2 (|C_S|^2 + |C'_S|^2) + \Big| \int \boldsymbol{\sigma} \Big|^2 (|C_T|^2 + |C'_T|^2) \\ + (2\mathbf{p} / E) [\mathbf{L} \operatorname{Re} (C_T C'^*_T) + \mathbf{Q} \operatorname{Re} (C_S C'^*_T + C'_S C^*_T) + \mathbf{R} \operatorname{Im} (C_S C'^*_T + C'_S C^*_T)] \Big\}, \end{aligned} \tag{3}$$

where

$$K = 4\pi (2\pi)^{-5} pEq^2,$$

Q, **L**, and **R** are the vectors introduced by Talhoek and De-Groot:[6]

$$\mathbf{L} = i \Big[\Big(\int \boldsymbol{\sigma} \Big) \Big(\int \boldsymbol{\sigma} \Big)^* \Big], \quad \mathbf{Q} = \frac{1}{2} \Big\{ \Big(\int 1 \Big) \Big(\int \boldsymbol{\sigma} \Big)^* + \Big(\int 1 \Big)^* \Big(\int \boldsymbol{\sigma} \Big) \Big\},$$

$$\mathbf{R} = \frac{i}{2} \Big\{ \Big(\int 1 \Big) \Big(\int \boldsymbol{\sigma} \Big)^* - \Big(\int 1 \Big)^* \Big(\int \boldsymbol{\sigma} \Big) \Big\}.$$

In the expression for **L** summation over the directions of spin of the final nucleus is implied. The other designations in formula (3) are standard. According to Talhoek and De-Groot[6] we obtain (after averaging over the nuclei)

$$\mathbf{L} = \Big| \int \boldsymbol{\sigma} \Big|^2 g f_1 \boldsymbol{\eta},$$

where $\boldsymbol{\eta}$ is a unit vector along the axis of quantization (z-axis) and the value of g is given by the expressions

$$g = 1/(I + 1);\ 1;\ -I/(I + 1),$$

respectively, for the $I \to I$, $I \to I - 1$ and $I \to I + 1$ transitions. Further, one can readily obtain

$$\mathbf{Q} = \sqrt{\Big| \int 1 \Big|^2 \Big| \int \boldsymbol{\sigma} \Big|^2} \sqrt{I / (I + 1)}\, f_1 \boldsymbol{\eta} \cos \alpha, \quad \mathbf{R} = \sqrt{\Big| \int 1 \Big|^2 \Big| \int \boldsymbol{\sigma} \Big|^2} \sqrt{I / (I + 1)}\, f_1 \boldsymbol{\eta} \sin \alpha,$$

wherein α is determined by the formula

$$\exp(2i\alpha) = \Big(\int 1 \Big)^* \Big(\int \sigma_z \Big) \Big/ \Big(\int 1 \Big) \Big(\int \sigma_z \Big)^*.$$

Finally we obtain

$$W(E,\vartheta)=K\left\{\left|\int 1\right|^2(|C_S|^2+|C'_S|^2)+\left|\int \boldsymbol{\sigma}\right|^2(|C_T|^2+|C'_T|^2)+\frac{2p}{E}f_1\cos\vartheta\left[g\left|\int\boldsymbol{\sigma}\right|^2\mathrm{Re}\,(C_TC'^*_T)\right.\right.$$
$$\left.\left.+\sqrt{I/I+1}\sqrt{\left|\int 1\right|^2\left|\int\boldsymbol{\sigma}\right|^2}(\cos\alpha\,\mathrm{Re}\,(C_SC'^*_T+C'_SC^*_T)+\sin\alpha\,\mathrm{Im}\,(C_SC'^*_T+C'_SC^*_T)\right]\right\}. \qquad (4)$$

At present the results of investigations of β-spectra and $\beta-\gamma$ angular correlation have made it possible to determine the numerical values of $|C_S|^2+|C'_S|^2$ and $|C_T|^2+|C'_T|^2$. By making measurements of the angular distribution in the case of a β-transition with $\Delta I=\pm 1$ (no) one can determine the value of $\mathrm{Re}(C_TC'^*_T)$ from comparison with theory. Further carrying out measurements of the angular distribution for a $\Delta I=0$ (no) type β-transition for which $\int 1$ and $\int\boldsymbol{\sigma}$ can be computed, we can obtain through comparison with theory the numerical value of still another expression containing C_S, C'_S, C_T and C'_T. Thus investigation of β-radiation from polarized nuclei makes it possible to draw certain conclusions regarding the β-interaction constants.

If we assume that there is conservation of combined parity[7] the results are simplified for in this case all the constants C are real. Comparison with experiment makes it possible to determine the numerical values of the quantities $C_TC'_T$ and $C_SC'_T+C'_SC_T$. Knowing also $C_S^2+C_S'^2$ and $C_T^2+C_T'^2$, it should be possible to determine the coefficients C.

For the above method of comparing theory with experiment it is necessary to calculate the matrix elements $\int 1$ and $\int\boldsymbol{\sigma}$. These calculations are simplest in the case of a β-transition between the corresponding states of neighboring mirror isobars.

3. Let us also examine β-transitions of the $\Delta I=\pm 2$ (yes) type. As a result of these calculations we obtain

$$W(E,\vartheta)=\frac{K}{4}\left\{(|C_T|^2+|C'_T|^2)\,T_{ik}\left(p_ip_k+\frac{q^2}{3}\delta_{ik}\right)\right.$$
$$\left.+2\mathrm{Re}\,(C_TC'^*_T)\frac{1}{E}\left(S_{ikt}\,p_ip_kp_t+\frac{q^2}{3}S_{iit}p_t\right)\right\}, \qquad (5)$$

where

$$T_{ik}=B_{ni}B^*_{nk},\quad S_{ikt}=i\varepsilon_{nmt}B_{ni}B^*_{mk}, \qquad (6)$$

here B_{ik} is the known symmetric tensor with trace zero:

$$B_{ik}=\int\left(\sigma_ix_k+\sigma_kx_i-\frac{2}{3}\sigma_tx_t\delta_{ik}\right) \qquad (7)$$

(everywhere in the above repeated indices imply summation, in (6) summation is implied over the direction of spin of the final nucleus).

Carrying out the calculation of the matrix elements, we finally obtain

$$W(E,\vartheta)=\frac{K}{12}T_{nn}\left\{(|C_T|^2+|C'_T|^2)\,[p^2+q^2-af_2p^2P_2(\cos\vartheta)]+\right.$$
$$\left.+\mathrm{Re}\,(C_TC'^*_T)\frac{6p}{5E}\left[bf_1\left(p^2+\frac{5}{3}q^2\right)P_1(\cos\vartheta)-cf_3p^2P_3(\cos\vartheta)\right]\right\} \qquad (8)$$

here $a=b=c=1$ for $I\to I-2$ transitions while for $I\to I+2$ transitions

$$a=I(2I-1)/(I+1)(2I+3),\quad b=-I/(I+1),$$
$$c=-I(I-1)(2I-1)/(I+1)(I+2)(2I+3).$$

We note that for these transitions the role of Coulomb effects is negligible.

Transitions with $\Delta I=\pm 2$ (yes) give nothing new as compared with allowed transitions as regard determination of the interaction constants. Further data on the interaction constants can be obtained by investigating the shape of the β-spectra associated with $\Delta I=0,\ \pm 1$ (yes) transitions.[8] Investigation of these β-spectra should make it possible to determine the value of $\mathrm{Re}(C_SC^*_T+C'_SC'^*_T)$.

---

[1] J. A. M. Cox and S. R. De-Groot, Physica **19**, 683 (1953).

[2] G. R. Khutsishvili, J. Exptl. Theoret. Phys. (U.S.S.R) **25**, 763 (1953); **28**, 370 (1955); Soviet Phys. **1**, 376 (1955); Trudy, Institute of Physics, Academy of Sciences, Georgian SSR **4**, 3 (1956).

[3] T. D. Lee and C. N. Yang, Phys. Rev. **104**, 254 (1956).

[4] C. S. Wu *et al*, Phys. Rev. (in press).

[5] G. R. Khutsishvili, J. Exptl. Theoret. Phys. (U.S.S.R.) **28**, 496 (1955), Soviet Phys. JETP **1**, 390(1955).

[6] N. A. Talhoek and S. R. De-Groot, Physica 17, 81 (1951).

[7] L. D. Landau, J. Exptl. Theoret. Phys. (U.S.S.R.) 32, 405 (1957); Soviet Phys. JETP 5, 336 (1957).

[8] D. L. Pursey, Phil. Mag. 42, 1193 (1951); Morita, Fujita, and Yamada, Progr. Theor. Phys. 10, 630 (1953).

Translated by E. J. Rosen
308

Electronic Resonance in Current-Carrying Solutions

A. A. GALKIN, IA. L. SHAMFAROV
AND A. V. STEFANISHINA
Institute of Radiophysics and Electronics,
Academy of Sciences, U.S.S.R.

(Submitted to JETP editor March 23, 1957)
J. Exptl. Theoret. Phys. (U.S.S.R.) 32, 1581-1582
(June, 1957)

AS IS KNOWN, electronic resonance is observed in ammonia solutions of alkali metals.[1,2] This effect is due to the fact that in ammonia solutions the atoms of the alkali metals dissociate into electrons and positive ions. The positive ions have a noble gas electron structure and are diamagnetic, while the electrons, having a magnetic moment, are responsible for the electron resonance effect.

It must be noted that solutions of alkali metals in liquid ammonia are colored, the coloring being explained by the presence of "free" electrons in the solution.[3]

It was shown by Gordon and Broude[4] that coloring is observed in an initially colorless solution of table salt in ammonia when a current is passed through the solution. The developing color is reminiscent of that characteristic of ammonia solutions of alkali metals. These investigators also noted the deflection of the colored streams in a magnetic field, which, according to these authors, is indicative of the electronic character of the conduction.

We felt that deflection of streamlines in a magnetic field is not in itself a convincing argument in favor of electron conduction. Hence we undertook a series of experiments on detection of electronic resonance in solutions of NaCl in ammonia on the assumption that in the case of electronic conduction, electronic resonance incident to the passage of current should be observed. Obviously, the electronic resonance line in this case should have a shape and spectroscopic splitting factor analogous to those of the line observed in solutions of Na in NH_3.

For observation of electronic resonance at a frequency of 9000 Mc the ampoule containing the ammonia solution of NaCl was placed in the rectangular cavity (H_{102} mode) of a sensitive radiospectrometer. The ampoule had two sealed-in platinum electrodes.

As usual the cavity was placed in a constant magnetic field, modulated by a field having a frequency of 50 cps. The intensity of the constant field was selected so as to satisfy the condition $g\mu H = h\nu$, where g is the radio-spectroscopic splitting factor for the solution, μ is the magnetic moment of the electron and ν is the frequency of the radiospectrometer generator. The investigation showed that under ordinary conditions no electronic resonance is observed when there is no current through the salt solution. When a current is passed through the solution an electronic resonance line appears at approximately the same place as the line associated with Na in liquid NH_3 (see Fig. 1). The intensity of the line depends on the strength of the current. When the current is switched off the intensity of the absorption line gradually decreases.

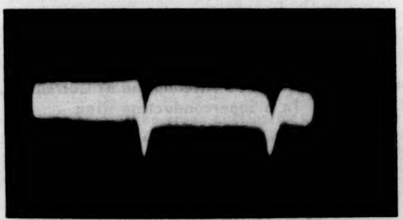

FIG. 1. Oscillogram of electronic resonance of a solution during passage of current.

Thus it is possible to observe electronic resonance only when electrons associated with the passage of current through the solution are present; this substantiates the electronic character of the conduction in these solutions.

If at the time of passage of current through the ampoule the solution is frozen in liquid nitrogen, the color of the solution is retained (there is no recombination of the electrons with the chlorine) and it is possible to observe electronic resonance even in the absence of a current (Fig. 2). In this manner it is possible to produce a medium with an easily controlled number of free electrons.

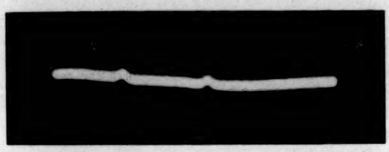

FIG. 2. Oscillogram of electronic resonance of a frozen solution.

The concentration of electrons can readily be determined from the intensity of the electronic resonance line.

We believe that the electronic resonance method described above may prove useful in determining the nature of different solutions.

[1] C. A. Hutchison, Phys. Rev. 75, 1769 (1949).

[2] A. Clyde and J. Hutchison, J. Phys. Chem. 57, 546 (1953).

[3] C. A. Kraus, J. Frankl. Inst., 212, 537 (1931).

[4] B. E. Gordon and V. L. Broude, Zhur. fiz. khim. 24, 409 (1950).

Translated by E. J. Rosen
309

Discontinuous Attenuation of Current In a Superconducting Ring

A. A. GALKIN, IA. S. KAN AND B.G. LAZAREV
Physico-Technical Institute, Academy of Sciences, Ukrainian SSR

(Submitted to JETP editor March 13, 1957)
J. Exptl. Theoret. Phys. (U.S.S.R.) 32, 1582
(June, 1957)

IN AN EARLIER INVESTIGATION, devoted to the kinetics of the transition from the normal state to the superconducting one, it was shown that the resistance of the specimen is a non-monotonic function of the temperature and fluctuates between zero and the normal value as the temperature is gradually decreased.[1,2] These fluctuations of resistance were related, in particular, with the kinetics of formation of an intermediate state arising in the process of destruction of the superconductivity by the current. It was assumed that an analogous but reverse effect might be observed during transition of a superconducting ring in which a current was induced to the normal state, *i.e.*, that the current would attenuate in jumps with gradually increasing temperature.

The experiments described herein were set up for the purpose of investigating the process. The apparatus consisted of a 10 mm radius lead ring made of 1 mm diameter wire and a coil of 8000 turns of copper wire mounted coaxially with the ring. By means of this coil it was possible to measure both the full current in the ring (by turning the coil about an axis in the plane of the ring) and the change in current ΔI (from the change in the induced emf produced by ΔI). In the first case the coil was connected to a ballistic galvanometer, in the second to a short-period galvanometer.

The coil and ring were enclosed in a copper cup immersed in liquid helium. By filling the cup with gaseous helium at a pressure of 1 – 2 mm Hg, the system could be cooled to the temperature of the helium bath. By applying a magnetic field $H > H_k$ and then cutting it off, a current $I = I_k$ was induced in the ring. After this the helium was pumped out of the cup to a residual pressure of $10^{-6} - 10^{-7}$ mm Hg and the ring slowly and gradually warmed. The rate of heating could be regulated and in most cases was $10^{-4} - 10^{-5}$ degrees/sec.

Part of the curve characterizing the variation with time of the emf in the measurement coil while the ring with the initially induced current was heated is shown in the accompanying figure. It will be seen that the current in the ring does not attenuate gradually, but falls off in jumps of several seconds duration; in the intervals between jumps the emf equals zero, *i.e.*, the current does not change during the interval.

From the $E(t)$ curves one can determine the relative change in current $\Delta I/I$ occurring during each jump. In the vicinity of 4.2° K the average value of $\Delta I/I$ for the lead ring is 10^{-4}.

Knowing $\Delta I/I$, the self-inductance of the ring, $L \approx 40$ cm, and the current attenuation time τ, one can evaluate the effective resistance responsible for the damping:

$$R_{\text{eff}} = (\Delta I/I)\,L/\tau \approx 10^{-11} \text{ ohm}.$$

Inasmuch as the total resistance of the ring in the normal state was $\sim 10^{-7}$ ohm, we can say that, re-

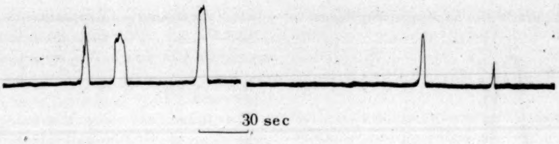

gardless of the specific character of the intermediate state during the attenuation of the current, only an insignificant part of the volume of the superconductor is in the normal state.

---

[1] A. A. Galkin and B. G. Lazarev, Dokl. Akad. Nauk. SSSR 59, 1017 (1948).

[2] Galkin, Kan, and Lazarev, J. Exptl. Theoret. Phys. (U.S.S.R.) 20, 865 (1950).

Translated by E. J. Rosen
310

Calculation of the Polarization of Neutrons on the Basis of the Diffused Edge Nuclear Model

P. E. NEMIROVSKII AND IU. P. ELAGIN
Academy of Sciences, U.S.S.R.

(Submitted to JETP editor March 16, 1957)
J. Exptl. Theoret. Phys. (U.S.S.R.) 32, 1583
(June, 1957)

THE RESULTS OF EXPERIMENTS on the polarization of 400-kev neutrons have been examined by Adair[1] on the basis of the optical nuclear model with a rectangular potential well. In the examination the spin-orbit potential was assumed to be constant inside the nucleus. However, this examination does not take into account the basic properties of spin-orbit interaction which must actually exist only on the surface of the nucleus, as may be concluded from analogy with electromagnetic interaction.

In view of the above it is logical to assume that the spin-orbit interaction is proportional to

$$\frac{1}{r}\frac{dV}{dr}(\mathbf{l}\boldsymbol{\sigma}), \tag{1}$$

where V is the depth of the potential well inside the nucleus. In this case, as can readily be seen, the magnitude of the spin-orbit interaction depends on the dimensions of the nucleus; this circumstance could not be taken into account in Adair's calculations.

In our calculations the selected form of the potential was

$$\begin{aligned} V &= V_0(1+i\zeta) = \text{const} \quad \text{for } r \leqslant r_0, \\ V &= V_0 e^{-\alpha(r-r_0)}(1 + c\alpha / r_0) \quad \text{for } r \geqslant r_0. \end{aligned} \tag{2}$$

With this choice of potential there is a small discontinuity at $r = r_0$; this however is unimportant inasmuch as $c\alpha/r_0 < 1$. For the purpose of simplifying the solution, the factor $1/r$ in (1) was replaced by the constant $1/r_0$, which is a satisfactory approximation for heavy nuclei in which the thickness of the boundary layer is $d \ll r_0$. This substitution greatly facilitates calculations, since it makes it possible to use the procedure developed in Ref. 2.

The spin-orbit coupling coefficient c was assumed equal to 3.3×10^{-27} cm^2 in accordance with the data of Levintov[3] obtained in investigating light nuclei.

The polarization was computed according to familiar formulas which were derived on the assumption that the spin of the target nucleus is zero. It was assumed that the cross section for elastic scattering is due to optical elastic scattering and resonance elastic scattering. The latter makes no contribution to the polarization since the individual levels with different values of l do not interfere with each other.

The calculations were carried out on the assumption that only the s- and p-phases differ from zero. Inasmuch as we considered nuclei close to the maximum of the p-wave ($A \sim 100$), the d-phase in this region had a minimum as a function of A and, according to the calculations of one of the present authors, was close to zero.

In the calculations we assumed the following parameters:

$$r_0 = 1.28\ A^{1/3},\ V_0 = 42 \text{ Mev};\ \zeta = 0.05 \text{ and } \zeta = 0.1;$$
$$1/\alpha = 0.7 \cdot 10^{-13} \text{ cm}.$$

We investigated polarization with scattering at an angle of 90° to the direction of the incident beam.

The results are shown in the accompanying figure.

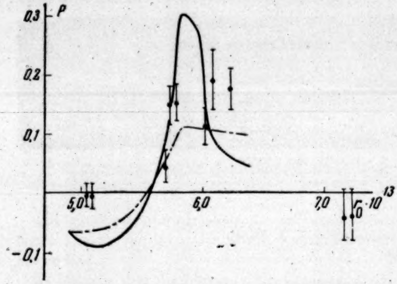

Dependence of the polarization of neutrons on the nuclear radius.

As may be seen from the figure, the experimental points lie in the region of the maximum between the theoretical curves, which would indicate that the closest agreement with experiments is obtained with $0.05 < \zeta < 0.1$. This conclusion is also in good agreement with data on the values of the parameter ζ, obtained in investigating[2] the total cross sections and Γ_n/D.

Thus it has been shown that using one and the same value of the spin-orbit interaction constant one can describe scattering both from light and from heavy nuclei. This coefficient is somewhat smaller than that given by Ross and coworkers in connection with their investigation of the splitting of the ground level of magic number nuclei.

---

[1] R. K. Adair, S. E. Darden, and K. E. Fields, Phys. Rev. **96**, 503 (1954).

[2] P. E. Nemirovskii, J. Exptl. Theoret. Phys. (U.S.S.R.) **32**, 1143 (1957); Soviet Phys. JETP **5**, 932 (1957).

[3] I. I. Levintov, Dokl. Akad. Nauk SSSR, **107**, 240 (1956).

Translated by E. J. Rosen
311

Unitarity Relationships for Elastic Collisions of Particles with Arbitrary Spins

R. M. RYNDIN AND IA. A. SMORODINSKII
Joint Institute for Nuclear Studies

(Submitted to JETP editor March 20, 1957)
J. Exptl. Theoret. Phys. (U.S.S.R.) **32**, 1584-1585
(June, 1957)

LET US CONSIDER the collisions of particles without spin. Let the energy of the impinging particles be such that only elastic scattering is possible. Then as Glauber and Schomaker[1] have shown the scattering amplitude $f(\vartheta)$ obeys the following integral relation

$$4\pi \operatorname{Im} f(\vartheta) = k \int f^*(\vartheta'') f(\vartheta') \, d\omega(\mathbf{k}''). \tag{1}$$

Here ϑ is the angle between the vectors of the initial $\mathbf{k}$ and final $\mathbf{k}'$ momenta; ϑ' is the angle between $\mathbf{k}$ and a variable vector $\mathbf{k}''$; ϑ'' is the angle between $\mathbf{k}'$ and $\mathbf{k}''$ ($k = k' = k''$, c. m. s.); and the integration is carried out over all directions of $\mathbf{k}''$. From (1) with $\vartheta \to 0$, we obtain the so-called optical theorem: the relation between the imaginary part of the scattering amplitude forward and the total cross section σ. Below we shall generalize (1), extending it to the case of elastic collision of particles with arbitrary spins s_1 and s_2 and shall show that in addition to the optical theorem there can be deduced from (1) a series of other relations connecting scattering matrix elements that do not vanish when $\mathbf{k}' \to \mathbf{k}$ with different spin characteristics.

The process of elastic scattering is fully described by the matrix $M(\mathbf{k}, \mathbf{k}')$ in $(2s_1 + 1)(2s_2 + 1)$-dimensional spin space, determining the amplitude of the scattered wave

$$\Psi_{\mathbf{k}}(\mathbf{r} \to \infty) \sim \varphi_{\mathbf{k}'}^{\text{incid}} + \varphi_{\mathbf{k}}^{\text{scat}} = e^{ikr}\chi + M(\mathbf{k}, \mathbf{k}')\chi e^{ikr}/r. \tag{2}$$

The indices of the total spin of the system and its projection at the spin functions χ are omitted for simplicity of notation. In view of unitarity of S-matrix the wave functions $\Psi_{\mathbf{k}}$ satisfy the same requirements of orthogonality and normalization as the initial functions of the incident wave and form, when $r \to \infty$, a complete system of functions with respect to the angular variables

$$\int \varphi_{\mathbf{k}'}^{+\,\text{incid}} \varphi_{\mathbf{k}}^{\text{incid}} \, d\omega = \int \Psi_{\mathbf{k}'}^{+} \Psi_{\mathbf{k}} \, d\omega. \tag{3}$$

The + sign, as usual, denotes Hermitian conjugates.

Utilizing expression (2), the asymptotic representation of plane wave

$$\varphi_{\mathbf{k}}^{\text{incid}} \sim \frac{i}{k}\,\delta\left(1+\frac{\mathbf{kr}}{kr}\right)e^{-ikr}/r-\frac{i}{k}\,\delta\left(1-\frac{\mathbf{kr}}{kr}\right)e^{ikr}/r$$

and the completeness of system of spin functions, one can readily obtain from (3) the sought integral relation for the scattering matrix

$$2\pi\left[M(\mathbf{k},\mathbf{k}')-M^{+}(\mathbf{k}',\mathbf{k})\right]$$
$$=ik\int M^{+}(\mathbf{k}',\mathbf{k}'')\,M(\mathbf{k},\mathbf{k}'')\,d\omega(\mathbf{k}''), \qquad (4)$$

From (4) there immediately follow the integral relations for the coefficients of expansion of $M(\mathbf{k},\mathbf{k}')$ in terms of the invariant spin matrices given in Ref. 2 for nucleon-nucleon scattering and applied therein to the analysis of the full set of trials aimed at reestablishment of the scattering matrix.

If with $\mathbf{k}'=\mathbf{k}$ we utilize the expansion of $M(\mathbf{k},\mathbf{k}) = \sum_{\mu} \alpha_{\mu} S_{\mu}$ in the orthogonal and normalized Hermitian operators S_{μ} [the operators are orthogonal and normalized if $\mathrm{Sp}\, S_{\mu} S_{\nu} = (2s_1+1)(2s_2+1)\delta_{\mu\nu}$], then from (4) we can obtain the following relation

$$4\pi\,\mathrm{Im}\,\alpha_{\nu}(2s_1+1)(2s_2+1)=4\pi\,\mathrm{Im}\,\mathrm{Sp}\,S_{\nu}M(\mathbf{k},\mathbf{k})$$
$$=k\int \mathrm{Sp}\,S_{\nu}M^{+}(\mathbf{k},\mathbf{k}'')\,M(\mathbf{k},\mathbf{k}'')\,d\omega(\mathbf{k}''). \qquad (5)$$

In particular, assuming S_{ν} to be unity, we obtain the extension of the optical theory to the case of particles with spins

$$4\pi\,\mathrm{Im}\,\mathrm{Sp}\,M(\mathbf{k},\mathbf{k})=k(2s_1+1)(2s_2+1)\,\sigma.$$

From the last relation there follows the inequality[3] $\sigma(0) \geq (k/2\pi)^2\sigma^2$, limiting the value of the cross section for elastic scattering to 0°. With $S_{\nu} \neq I$ the relations (5) connect $\mathrm{Im}\,\alpha_{\nu}$ with the integral with respect to $\mathrm{Sp}\,S_{\nu}M^{+}M$, determining the addition

$$(2s_1+1)^{-1}(2s_2+1)^{-1}\langle S_{\nu}\rangle_{\text{incid}}\,\mathrm{Sp}\,S_{\nu}M^{+}M$$

to the cross section for scattering of a nonpolarized beam from a nonpolarized target, due to the initial polarization of the colliding particles (in the initial state the mean value of $\langle S_{\nu}\rangle_{\text{incid}}$ of the quantity S_{ν} differs from zero).

The number of relations (5) is equal to the number of coefficients α_{ν} that are not zero for $\mathbf{k}'=\mathbf{k}$. Thus in the case of scattering of mesons from nucleons we obtain only the optical theorem [the coefficient at $(\sigma\mathbf{n})$ in the expansion of the scattering amplitude vanishes when $\mathbf{k}'\to\mathbf{k}$]. In the case of nucleon-nucleon scattering we obtain three relations. In this case for S_{ν} one should select operators

$$I,\ 2^{-1/2}\left[(\sigma_1,\sigma_2)-(\sigma_1\mathbf{l})(\sigma_2\mathbf{l})\right],\ (\sigma_1\mathbf{l})(\sigma_2\mathbf{l})$$

(it is impossible to construct a greater number of scalar expressions from the vectors σ_1, σ_2 and $\mathbf{l}=\mathbf{k}/k$). In view of the invariance of the scattering matrix $M(\mathbf{k},\mathbf{k}')$ relative to time reversals, the traces containing the operators

$$2^{-1/2}\left[(\sigma_1\sigma_2)-(\sigma_1\mathbf{l})(\sigma_2\mathbf{l})\right],\ (\sigma_1\mathbf{l})(\sigma_2\mathbf{l})$$

and determining the additions to the cross section, can be expressed[2] in terms of the components of the tensor of correlation of the polarization arising incident to collisions of nonpolarized nucleons.

The author desires to thank L. I. Lapidus who read the manuscript and made a number of valuable suggestions.

---

[1] R. Glauber and V. Schomaker, Phys. Rev. 89, 667 (1953).

[2] L. Puzikov, R. Ryndin, and Ia. Smorodinskii, J. Exptl. Theoret. Phys. (U.S.S.R.) 32, 592 (1956); Soviet Physics JETP 5, 489 (1957).

[3] G. Wick, Phys. Rev. 75, 1459 (1949).

Translated by E. J. Rosen
312

Gadolinium Isotope with Mass 146

I. A. GUSEV, O. M. LILOVA, A. N. MURIN,
B. K. PREOBRAZHENSKII, AND
V. A. IAKOVLEV
Radium Institute, Academy of Sciences, U.S.S.R.

(Submitted to JETP editor March 21, 1957)
J. Exptl. Theoret. Phys. (U.S.S.R.) 32, 1585
(June, 1957)

WHEN TANTALUM is bombarded with 660 Mev protons there are formed new isotopes of gadolinium[1] hitherto unreported in the literature. Upon decay, these isotopes in a number of cases form known isotopes of europium, from which it is possible to determine the mass number of the parent substances – the new gadolinium isotopes. In fractions of europium separated from pure fractions of gadolinium (obtained 32 hours after cessation of bombardment) we observed a radioactive isotope that decays with a period of 1.6 days in accord with the tabular data for Eu^{146}. On the basis of measurements of this isotope from the time of its separation from the gadolinium fraction we evaluated the period of the parent substance Gd^{146} to be 12 ± 4 hours. It should be noted that the mass number of Gd^{146} was determined with the same degree of reliability as that of the daughter europium isotope, which belongs, according to Seaborg's[2] tables, in class C (mass number "reliable or probable").

[1] Gorodinskii, Pokrovskii, Preobrazhenskii, Murin, and Titov, Dokl. Akad. Nauk, SSSR 112, 405 (1957); Soviet Phys. "Doklady" 2, 39 (1957).

[2] Seaborg, Perlman, and Hollander, Table of Isotopes, (M., 1956).

Translated by E. J. Rosen
313

Possibility of Constructing a Chain of Equations for Model Operators

V. M. ELEONSKII
Ural' Polytechnic Institute

(Submitted to JETP editor March 21, 1957)
J. Exptl. Theoret. Phys. (U.S.S.R.) 32, 1585-1587 (June, 1957)

THE THEORY OF MODEL TRANSFORMATIONS[1] is characterized by the fact that the model operator M_n transforming the model state

$$|\varphi_1 \ldots \varphi_n\rangle = \prod_{\gamma=1}^{n} \varphi(\gamma)$$

into the real state of the system $|\Psi\rangle = \Psi(1 \ldots n)$, is an operator function of all the dynamic variables of the system. To reduce the many-particle problem to a single-particle problem, let us introduce the sequence of generalized transition amplitudes

$$\langle\varphi_1 \ldots \varphi_n|\Psi\rangle;\ \langle\varphi_1 \ldots \varphi_{\alpha-1}, \varphi_{\alpha+1} \ldots \varphi_n|\Psi\rangle \equiv \langle \ldots (\varphi_\alpha) \ldots |\Psi\rangle, \ldots, \langle\varphi_\alpha \varphi_\beta|\Psi\rangle;\ \langle\varphi_\alpha|\Psi\rangle;\ |\Psi\rangle,$$

where, for example,

$$\langle \ldots (\varphi_\alpha) \ldots |\Psi\rangle = \int \frac{d\tau}{d\tau_\alpha} \prod_{\gamma \neq \alpha} \overset{+}{\varphi}(\gamma)\, \Psi(1 \ldots n).$$

Assuming that the real and model states of the system are described by the wave equations

$$i\partial_t |\Psi\rangle = \Big\{\sum_\alpha T(\alpha) + \sum_{\alpha\beta} H(\alpha\beta)\Big\} |\Psi\rangle, \quad i\partial_t \varphi_\alpha = \{T(\alpha) + U(\alpha)\}\, \varphi_\alpha,$$

we obtain a system of equations

$$i\partial_t \langle\varphi_1 \ldots \varphi_n|\Psi\rangle = \sum_{\alpha\beta} \langle\varphi_\alpha \varphi_\beta|H(\alpha\beta)|\langle \ldots (\varphi_\alpha \varphi_\beta) \ldots |\Psi\rangle\rangle - \sum_\alpha \langle\varphi_\alpha|U(\alpha)|\langle \ldots (\varphi_\alpha) \ldots |\Psi\rangle\rangle,$$

$$\ldots\ldots\ldots\ldots\ldots\ldots\ldots\ldots\ldots\ldots,$$

$$\Big\{i\partial_t - \sum_{\alpha\neq\gamma} T(\alpha) - \sum_{\alpha\beta\neq\gamma} H(\alpha\beta)\Big\} \langle\varphi_\gamma|\Psi\rangle = \langle\varphi_\gamma\Big| \sum_{\alpha\neq\gamma} H(\alpha\gamma) - U(\gamma)|\Psi\rangle,$$

similar to the system of equations for a density matrix.[2] In the stationary case the system assumes the form

$$\Big\{E-\sum_{\alpha}E_\alpha\Big\}\langle E_1\ldots E_n\,|\,E\rangle=\sum_{\alpha\beta}\langle E_\alpha E_\beta\,|\,H(\alpha\beta)|\,\langle\ldots(E_\alpha E_\beta)\ldots|\,E\rangle\rangle-\sum_{\alpha}\langle E_\alpha|U(\alpha)|\,\langle\ldots(E_\alpha)\ldots|\,E\rangle\rangle;$$

$$\Big\{E-\sum_{\alpha\neq\gamma}E_\alpha-T(\gamma)\Big\}\langle\ldots(E_\gamma)\ldots|\,E\rangle=\sum_{\alpha\beta\neq\gamma}\langle E_\alpha E_\beta\,|\,H(\alpha\beta)|\langle\ldots(E_\alpha E_\beta E_\gamma)\ldots|\,E\rangle\rangle$$
$$+\sum_{\alpha\neq\gamma}(E_\alpha\,|\,H(\gamma\alpha)-U(\alpha)|\langle\ldots(E_\alpha E_\gamma)\ldots|\,E\rangle\rangle; \tag{1}$$
$$\ldots\ldots\ldots\ldots\ldots\ldots\ldots\ldots\ldots;$$
$$\Big\{E-E_\gamma-\sum_{\alpha\neq\gamma}T(\alpha)-\sum_{\alpha\beta\neq\gamma}H(\alpha\beta)\Big\}\langle E_\gamma\Big|E\rangle\Big|=\langle E_\gamma\Big|\sum_{\alpha\neq\gamma}H(\alpha\gamma)-U(\gamma)\Big|E\rangle.$$

System (1) jointly with the equations

$$\Big\{E-\sum_{\alpha}T(\alpha)-\sum_{\alpha\beta}H(\alpha\beta)\Big\}\,|\,E\rangle=0,\quad \{E_\alpha-T(\alpha)-U(\alpha)\}\,|\,E_\alpha\rangle=0.$$

determines the single-particle potential U on the surface of constant energy $\Big(E-\sum_{\alpha}E_\alpha=0\Big)$ and is equivalent to the model transformation $|\,E\rangle=M_n\,|\,E_1\ldots E_n\rangle$. The last assertion becomes obvious, if we introduce the sequence of model operators

$$\langle\ldots(E_\alpha)\ldots|\,E\rangle=M_1(\alpha)|\,E_\alpha\rangle;$$
$$\langle\ldots(E_\alpha E_\beta)\ldots|\,E\rangle=M_2(\alpha\beta)|\,E_\alpha E_\beta\rangle;$$
$$\ldots\ldots\ldots\ldots\ldots\ldots\ldots;$$
$$\langle E_\alpha\,|\,E\rangle=M_{n-1}(\ldots\alpha-1,\alpha+1,\ldots)|\,E_1,\ldots E_{\alpha-1}E_{\alpha+1}\ldots E_n\rangle;$$
$$|\,E\rangle=M_n\,|\,E_1\ldots E_n\rangle$$

and find the operator equations for M_p.

Consideration of stationary transitions on a constant energy surface corresponds in this case to examination of such single-particle states which satisfy the requirement $\partial_t\langle\varphi_1\ldots\varphi_n\,|\,\Psi\rangle=0$, that is an analogue of the usual condition of normalization of $\partial_t\langle\Psi\,|\,\Psi\rangle=0$.

---

[1] R. I. Eden and N. C. Francis, Phys. Rev. 97, 1366 (1955).

[2] N. N. Bogoliubov, *Lectures on Quantum Statistics*, Kiev, 1949.

Translated by E. J. Rosen
314

Some Remarks on Slow Processes of Transformation of Elementary Particles

L. OKUN' AND B. PONTECORVO
Joint institute for Nuclear Research

(Submitted to JETP editor March 26, 1957)
J. Exptl. Theoret. Physics (U.S.S.R.) 32, 1587-1588
(June, 1957)

AS IS KNOWN, there are two types of slow processes:

(a) lepton:

$$n\to e+\bar{\nu}+p,\ \mu\to e+\nu+\bar{\nu},\ \mu+p\to n+\nu,\ \pi\to\mu+\nu,$$
$$K\to\mu+\nu,\ K\to\mu+\nu+\pi,\ K\to e+\nu+\pi,$$

(b) non-lepton:

$$K\to 2\pi,\ K\to 3\pi,\ \Lambda(\Sigma)\to N+\pi,\ \Xi\to\Lambda+\pi.$$

The constants of the interactions responsible for these processes in units of $\hbar=\mu=c=1$ (where μ is the π-meson mass) are of the same order of magnitude as $G^2=10^{-14}-10^{-12}$. This suggests that the same mechanism (for example, the universal Fermi interaction[1]) may lie at the basis of all* these processes. This idea is supported by the fact that parity is not conserved in all these processes.[2] In the case of lepton processes (a) the non-conservation of parity can be interpreted as following from the concept of the longitudinal neutrino.[3] It is tempting to speculate that this property of the neutrino could also explain the non-conservation of parity in the other slow processes (b) in which no neutrino is emitted. Inasmuch as processes (a) and (b) have comparable probabilities, it would be natural to assume that they are all second order processes as regards neutrino interactions. In this case first order processes will be interactions with the participation of a neutrino and an X baryon with a mass greater than the hyperons mass. The coefficient g^2 of such a first order interaction must be of the order of $10^{-6} - 10^{-7}$ in $\hbar = \mu = c = 1$ units ($g^2 = G$). The lifetime of the X baryon for decay into two leptons and a baryon must then be of the order of 10^{-17} sec and the cross section for its formation in collisions (for example, of fast electrons with nucleons) must be approximately 10^{-34} cm^2.

---

*Non-conservation of parity in the decay of hyperons, although it has not yet been proved experimentally, almost inescapably follows from the established parity non-conservation in the decay of K-mesons.

Obviously, one can image other schemes describing universal non-conservation of parity in slow processes.

The close connection between processes (a) and (b), on the one hand, and the signal lack of success of attempts to extend the concepts of isotopic spin T and strangeness S to leptons, on the other, make it very desirable to evaluate the applicability of these concepts to slow processes of type (b) as well. We have in mind here the selection rules $|\Delta T| = \frac{1}{2}$ and $|\Delta S| = 1$ for slow non-lepton processes which have been examined by a number of authors.[4] Actually all the well-studied processes of type (b) are characterized by $|\Delta S| = 1$. However, in any of these processes (except decay of Ξ-hyperons) there occurs disintegration of particles with $S = 1$ into particles with $S = 0$ and it is difficult to see how the change in strangeness could differ from 1. We note, incidentally, that for the K_1^0 and K_2^0 mesons introduced by Gell-Mann and Pais[5] the concept of strangeness is not unambiguous. Thus, the only argument remaining in favor of the $|\Delta S| = 1$ rule is that based on the fact that the Ξ-hyperon, the strangeness of which in the scheme of Gell-Mann equals -2, does not decay into $n + \pi^-$ but rather into $\Lambda^0 + \pi^-$ (Ref. 6). However, from the experimental viewpoint the Ξ-hyperon is determined precisely as a particle decaying into $\Lambda^0 + \pi^-$. In view of the fact that there have been very few observations of Ξ-hyperons the $\Xi^- \to n + \pi^-$ decay could simply have escaped identification so far.

In view of what has been said above it may be of interest to examine some of the consequences following from the assumption that slow processes with $|\Delta S| = 1$ and $|\Delta S| > 1$ can have comparable probabilities.

1. If there exist K-fragments – nuclear fragments containing a K-meson – then for them in accord with the $|\Delta S| = 1$ selection rule only so-called mesonic and nonmesonic decays are possible.[7] However, under the assumption that processes with $|\Delta S| = 2$ have a probability comparable to that for other slow processes, the decay of K-fragments with the emission of a hyperon becomes possible. In this case one could also except to observe a "cascade fragment" effect, when the K-fragment in decaying emits an ordinary Λ-fragment. The observation of even one case of emission of a hyperon from a nuclear fragment or one case of "fragment cascade" would invalidate the $|\Delta S| = 1$ rule.

2. Let us consider the Gell-Mann – Pais – Piccioni effect.[5,8] The equations describing K^0 and $\tilde{K}^0$-mesons in vacuum have the form

$$-i\partial\psi(K^0)/\partial t = m_0\psi(K^0) + H\psi(\tilde{K}^0),$$
$$-i\partial\psi(\tilde{K}^0)/\partial t = m_0\psi(\tilde{K}^0) + H\psi(K^0),$$

where $\psi(K^0)$ and $\psi(\tilde{K}^0)$ are wave functions, m_0 is the mass of the K^0 and $\tilde{K}^0$-particles, and H is the matrix element of the $K^0 \to K^0$ transition. The masses of the symmetric combination K_1^0 and antisymmetric combination K_2^0 are, respectively, $m_0 + H$ and $m_0 - H$. It is usually assumed[5,9] that the transformation $K^0 \to \tilde{K}^0$ is due to processes of the

$$K^0 \xrightarrow{|\Delta S|=1} \pi + \pi \xrightarrow{|\Delta S|=1} \tilde{K}^0$$

type *i.e.*, two successive transitions in each of which $|\Delta S| = 1$. This leads to the mass difference $\Delta m = 2H$ between K_1^0 and K_2^0 being $\sim G^2 m \sim 10^{-11} m_e$. In this case the time of the transition $K^0 \rightleftarrows K^0$ is equal to $T = 2\pi\hbar/\Delta m \approx 10^{-10}$ sec and is comparable with the lifetimes of K_1^0 and K_2^0-mesons ($\tau_1 \sim 10^{-10}$ sec and $\tau_2 \geq 3 \times 10^{-9}$ sec).[10]

If it be assumed that the $K^0 \to \tilde{K}^0$ transition can be due to interaction with $|\Delta S| = 2$, for example, that it can proceed according to the scheme.

$K_0 \xrightarrow{|\Delta S|=0}$ antihyperon + nucleon $\xrightarrow{|\Delta S|=2}$ hyperon + antinucleon $\xrightarrow{|\Delta S|=0} \tilde{K}^0$, then the matrix element H will be proportional to G and not to G^2. In this case the mass difference $\Delta m'$ between the K_1^0- and K_2^0-mesons proves to be $\sim Gm \approx 10^{-5} m_e$. Accordingly, the transformation $K^0 \rightleftarrows \tilde{K}^0$ in vacuum will occur with a characteristic transition time $T' = 2\pi\hbar/\Delta m' \approx 10^{-16}$ sec, a time that is appreciably shorter than the lifetime of K_1^0 and K_2^0-mesons.

The distance R from the K^0 particle source, at which the numbers of K^0 and $\widetilde{K}^0$ particles become comparable, will no longer be of the order of centimeters, but of the order of 10^{-6} cm. The smallness of the distance R may lead to apparent violations of conservation of strangeness in processes resulting in the formation of strange particles. The formation of K^--mesons at energies below the threshold for the formation of K-meson pairs ($K^0 \to \widetilde{K}^0$ transitions in vacuum and $\widetilde{K}^0 - K^-$ transitions in matter) have been discussed by Lande *et al.*[10] who assumed that the time of the $K^0 \rightleftarrows \widetilde{K}^0$ transition is close to τ_1. Accurate measurements of the mechanism of formation of K^--mesons in thin targets as a result of nuclear collisions of nucleons or π-mesons having energies below the threshold for K-meson pair formation could resolve the question of the time of the $K^0 \rightleftarrows \widetilde{K}^0$ transition. This however presents certain difficulties connected with the fact that the nuclear range even in dense material is not only $\gg cT'$ but even $> cT$.

[1] B. Pontecorvo, Phys. Rev. 72, 246 (1947). G. Puppi, Nuovo cimento 6, 3 (1949). J. Tiomno and J. Wheeler, Revs. Mod. Phys. 21, 153 (1949). G. Costa and N. Dallaporta, Nuovo cimento 2, 519 (1955). M. Gell-Mann, *Proceedings of the 6th Rochester Conference*, 1956.

[2] T. Lee and C. Yang, Phys. Rev. 104, 254 (1956). C. Wu *et al*, Phys. Rev. 105, 1413 (1957). L. Leberman *et al*, Phys. Rev. 105, 1415 (1957).

[3] L. Landau, J. Exptl. Theoret. Phys. (U.S.S.R.) 32, 405 (1957); Soviet Phys. JETP 5, 336 (1957). T. Lee and C. Yang, Phys. Rev. 105, 4 (1957). A Salam, Phys. Rev. (in press).

[4] M. Gell-Mann, *International Conference, Pisa*, 1955. R. Gatto, Nuovo cimento 3, 319 (1956). L. Okun', J. Exptl. Theoret. Phys. (U.S.S.R.) 31, 333 (1956); Soviet Phys. JETP 4, 284 (1957). G. Wentzel, Phys. Rev. 101, 1215 (1956).

[5] M. Gell-Mann and A. Pais, Phys. Rev. 97, 1387 (1955).

[6] Cowan, Anderson, *et al*, Phys. Rev. 92, 1089 (1953). E. Cowan, Phys. Rev. 94, 161 (1954). W. Fretter and E. Friesen, Phys. Rev. 96, 853 (1954). W. Arnold *et al*, Phys. Rev. 98, 838 (1955). M. Gell-Mann, *International Conference, Pisa*, 1955.

[7] A. Pais and R. Serber, Phys. Rev. 99, 1551 (1955).

[8] A. Pais and O. Piccioni, Phys. Rev. 100, 1487 (1955).

[9] Ia. Zel'dovich, J. Exptl. Theoret. Phys. (U.S.S.R.) 30, 1168 (1956); Soviet Phys. JETP 3, 989 (1957).

[10] Lande, Impeduglia and Lederman, Phys. Rev. 103, 1901 (1956).

[11] M. Danysh and B. Pontecorvo, J. Exptl. Theoret. Phys. (U.S.S.R.) 32, 398 (1957); Soviet Phys. JETP 5, 325 (1957).

Translated by E. J. Rosen
315

Anomalous Decay of a Hypernucleus

A. P. GRIGOR'EV, E. P. TOPORKOVA
AND A. I. FESENKO
Moscow Engineering-Physical Institute

(Submitted to JETP editor March 26, 1957)
J. Exptl. Theoret. Physics (U.S.S.R.) 32, 1589
(June, 1957)

A CASE OF AN UNUSUAL decay of a hypernucleus has been observed in an emulsion chamber (Type "R" NIKFI film) exposed to cosmic radiation in the stratosphere.

The hypernucleus was emitted from a type $10+0n$ star and, after traveling a distance of 2930 μ, disintegrated in flight into three charged particles which were stopped in the emulsion chamber. A microphotograph of this event is reproduced in Fig. 1; the decay products are listed in the table below.

The masses of the decay products were determined by the grain density-range method (with reference to π-mesons). The charge and residual range of the hypernucleus in the emulsion, as determined from the δ-electron density along the residual path, proved to be $2e$ and $600 \pm 100\,\mu$, respectively.

Inasmuch as the mass of particle (2) proved to be $850 \pm 300\ m_e$, it was natural to assume that this particle is K-meson. On the other hand, inasmuch as the charge of the hypernucleus, which was determined with great accuracy, equals $2e$, it could be assumed that the K-meson is negative (the absence of decay products for the K-meson also points to its charge being negative).

The non-coplanarity of the decay products of the hypernucleus indicates the emission of at least one neutron, the energy of which was determined from the momentum vector diagram. Thus it may be assumed that the decay of the hypernucleus occurs according to the scheme

$$(\mathrm{He}_2^5)^* \to \mathrm{H}_1^1 + K^- + n + \mathrm{He}_2^3 + (103 \pm 5)\ \mathrm{Mev},$$

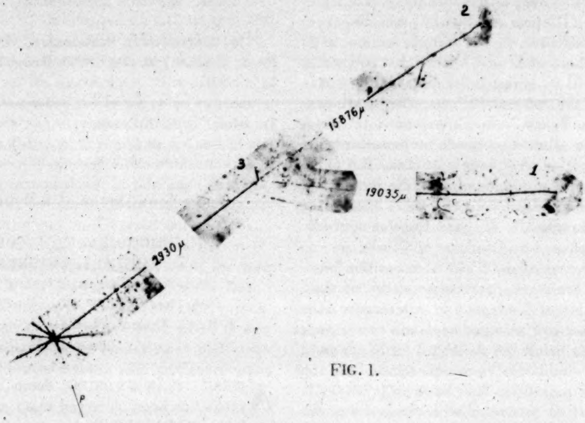

FIG. 1.

Track	Range, μ	Angle relative to hypernucleus track	Depth angle	Mass, m_e	Energy, Mev
1	19035	45°	1°	2100±700	76.0
2	15876	2°	40′	850±300	50.0
3	10	65°	5°30′	He_2^3	3.0
				He_2^4	3.2

or the scheme

$$(He_2^6)^* \rightarrow H_1^1 + K^- + n + He_2^4 + (110 \pm 6)\ \text{Mev}.$$

For determining the energies, the mass of the K-meson was taken as 966.7 m_e. If it be assumed that the decay of the hypernucleus occurs as a result of the decay of a bound hyperon, the mass of this hyperon would appear to be of the order of 3000 m_e.

The estimated lifetime of the hyperon is 5×10^{-11} sec.

A more detailed analysis of the described event is now being performed.

Translated by E. J. Rosen
316

Hall Effect and Susceptibility of Gold

N. E. ALEKSEEVSKII AND IU. P. GAIDUKOV
Institute of Physical Problems,
Academy of Sciences, U.S.S.R.

(Submitted to JETP editor March 28, 1957)
J. Exptl. Theoret. Physics (U.S.S.R.) 32, 1589-1591
(June, 1957)

IN AN EARLIER communication[1] we noted that the anomalous behavior of the resistivity of gold at low temperatures [the presence of a minimum on the $r(T)$ curve] disappeared when the variation of r as a function of T was measured in a constant magnetic field stronger than a certain critical value H_c.

We felt it would be of interest to investigate the effect of magnetic fields on other properties of gold. In the present note we describe the preliminary results of an investigation of the Hall effect in and the magnetic susceptibility of gold. For measuring the Hall effect we took two gold samples of the same size (0.5 × 14 × 30 mm); sample Au-1 was prepared of the lot of gold for which the anomaly in the $r(T)$ curve was observed, while sample Au-4 was prepared from a lot of gold characterized by a normal $r(T)$ curve.

The design of the apparatus used for measuring the Hall effect at $T < 1°$ K has already been described.[1] (The temperature dependence of the resistivity of the samples Au-1 and Au-4 was also measured on the same apparatus.) The measurements were carried out by means of a potentiometer connected to a two-stage photoelectric amplifier with a sensitivity of 2×10^{-9} volts. Measurements of the temperature dependence of r for the Au-1 sample showed that $T_{\min} \approx 4°$ K and that the increase in r is proportional to log $(1/T)$; the value of $\Delta r/r_{\min}$ at $T = 0.07°$ K was found to be 15 percent. Measurements of the value of $\Delta r = r_{0.07} - r_{\min}$ as a function of the magnetic field led to a value of about 8500 oersted for H_c.

No anomaly was detected for the Au-4 sample.

Fig. 1 shows the dependence of the Hall field E_y on the magnetic field at $T = 1.45°$ K. Analogous dependences were obtained at 0.07°, 4.2°, 10°, 20.4°, 77° and 295° K.

The jump-like change in the Hall angle at $H \approx 8500$ oersted, which coincides with the field value at which Δr becomes zero, naturally led us to assume that the magnetic properties of this gold sample may also change in this field. To clarify this we undertook a series of preliminary measurements of the magnetic susceptibility of a sample of gold from the same lot as Au-1. The measurements were carried out by the Faraday method; the balance had a sensitivity of 0.01 mg. The specimen was prepared in the form of a cylinder of gold foil 0.05 mm thick. The cylinder diameter was 8 mm, the length 8 mm, and the weight 5.06 grams.

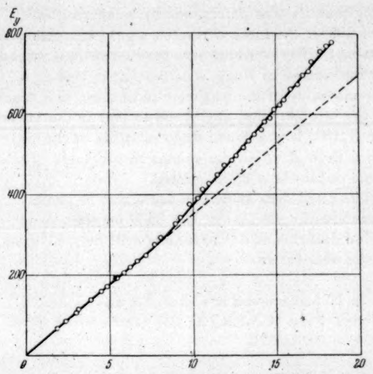

FIG. 1.

The measurements showed that the susceptibility χ remained diamagnetic in the temperature range from 295° to 1.45° K; at 1.45° K its value is 0.7 that at $T = 295°$ K.

The values of the force F acting on the specimen as a function of $H(dH/dx)$ are shown in Fig. 2. The

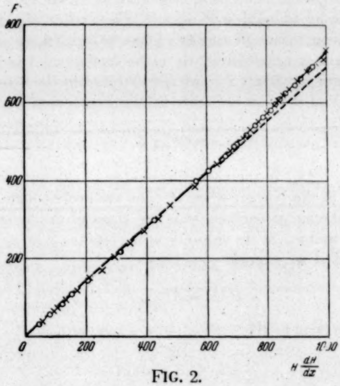

FIG. 2.

last quantity was determined by measuring at $T = 295°$ K the force acting on a gold specimen, the susceptibility of which was previously determined by the method of Huey. It will be seen that at a certain value of the magnetic field there is a break in the straight line, analogous to that in the curve for $E_y(H)$. It was found that the value of the magnetic field at which the change in the angle of the force occurs is ~ 8500 oersted.

The cited data show that some sort of phase transformation occurs at $H \approx 8500$ oersted. A detailed description of the results will be published in the near future.

[1] N. E. Alekseevskii and Iu. P. Gaidukov, J. Exptl. Theoret. Phys. (U.S.S.R.) 31, 947 (1956); Soviet Phys. JETP 4, 807 (1957).

Translated by E. J. Rosen
317

Ejection of Electrons from Metals by Fast Molecules

A. M. FURMAN

(Submitted to JETP editor August 28, 1956)
J. Exptl. Theoret. Phys. (U.S.S.R.) 32, 1591-1593
(June, 1957)

IZMAILOV AND THE AUTHOR[1] have examined the question of ejection of electrons from metals by molecules of neutral gases. It was shown that the mechanism of "potential" ejection of electrons from metals by molecules of neutral gases takes place for those values of energy of gas molecules, at which they are sufficiently close to the metal at a distance x_0. The value of x_0 is related to the kinetic energy of the gas molecule by the expression

$$U(x_0) = mv_\infty^2/2, \tag{1}$$

where $U(x_0)$ is the potential energy of the repulsive force at the instant when the gas molecules stop near the metal surface, m is the mass of the molecule, and v_∞ is its velocity at a distance $x \gg x_0$. In Ref. 1 we expressed $U(x)$ as

$$U(x) = B/x^p. \tag{2}$$

From (1) and (2) we obtain

$$x_0 = (2B/mv_\infty^2)^{1/p}. \tag{3}$$

In the absence of reliable data on the values of the constant B and exponent p in expression (2) we are forced, as in Ref. 1, to restrict ourselves to an expression of the form $N = f(x_0)$ for the number of electrons N ejected from one cm² of metal surface by a stream of gas molecules. At the present time it seems possible to estimate the parameters in (2) and, consequently, to express N in terms of macroscopic parameters of the gas stream.

From Ref. 1 it is possible to obtain an expression for the charging of the gas stream

$$\frac{N}{n} = \frac{2\pi}{3}\left(\frac{\pi}{10p}\right)^{1/2}\frac{Q^2C}{B}\,mv_\infty^2\,x_0^{p-7}\,\lambda^{-1/2}e^{-\lambda}. \tag{4}$$

$$C = (e^2/4\pi^2\hbar^2)\,(w_i^{1/2}/w_a\varphi_0^{1/2}), \tag{4a}$$

$$\lambda = \left[\frac{2}{3}\left(2m_0\varphi_0^3\right)^{1/2}/\hbar e^2\alpha\right]x_0^5 = \beta x_0^5/2Q,\quad Q = e\alpha, \tag{4b}$$

where n is the concentration of gas molecules, e and m_0 the charge and mass of the electron, φ_0 the work function of the electrons in the metal, w_a the potential barrier on the metal surface, w_i the Fermi level, and α the polarizability of the gas molecules.

Substituting in (4) the value of x_0 from (3) and expressing it in terms of the velocity and of the parameter B, we obtain for $p = 7$

$$N/n = K_1\,(v_\infty/B)^{19/14}\exp\left(-K_2B^{5/7}/v_\infty^{10/7}\right), \tag{5}$$

$$K_1 = (4\pi/3)\,(\pi/70)^{1/2}\,Q^2C\,(2Q/\beta)^{1/2}\,(m/2)^{19/14}, \tag{5a}$$

$$K_2 = (\beta/2Q)\,(2/m)^{5/7}. \tag{5b}$$

The quantities entering in (5a) and (5b) can be determined for a given metal and gas from the tables of physical constants. The quantities appearing in (2) can be estimated. We do not know of any reliable data for the potential of the repulsive force between the solid and the gas. To determine the potential between the metal and the gas we proceed from the following premises: (1) The potential can be either a power or an exponential function. (2) If the parameters of the potential are known for each phase separately, the interphase potential is determined as an average[2] in the following form

$$\begin{gathered} B_{12} = (B_{11}B_{22})^{1/2},\quad p_{12} = {}^1/_2\,(p_{11} + p_{22}), \\ (x_{12})_0 = {}^1/_2\,[(x_{11})_0 + (x_{22})_0], \end{gathered} \tag{6}$$

where the symbols correspond to those in (2) and (3). (3) The value of the energy of interaction between the gas molecules and the metal and their equilibrium internuclear distance x_0 serve as a starting point for determining the parameters of the potential (2) from the relation

$$B = U_0 x_0^7. \qquad (7)$$

U_0 for metals corresponds to the heat of sublimation of the atoms[3] reduced to 0° K; $(x_{11})_0$ corresponds to the internuclear distance for closely packed atoms. It is possible to assume for $(x_{11})_0$ a value double the atomic radius. For the particular case of O_2/Fe interaction it is possible to obtain from Ref. 4 $(U_{O_2})_0 = 1.697 \times 10^{-14}$ ergs, $(x_{O_2})_0 = 3.5$ A. For iron, according to Ref. 5, $(U_{Fe})_0 = 6.46 \times 10^{-12}$ ergs, $(x_{Fe})_0 = 2.88$ A, from which, according to (6) and (7), $U_{O_2/Fe} = 3.29 \times 10^{-13}$ ergs, $(x_{O_2/Fe})_0 = 3.19$ A and $B = 1.22 \times 10^{-65}$.

For other metals with other values of heat of sublimation we get $U_0 \sim 1 \times 10^{-11}$ to 1×10^{-12} ergs, and for gases $U_0 \sim 1 \times 10^{-14}$ to 1×10^{-15} ergs. It is therefore possible to expect that for other gas–metal cases $B \sim 1 \times 10^{-64}$ to 1×10^{-66}.

The constants for Fe according to Ref. (6) and the values of K_1 and K_2 calculated from (5a) and (5b) follow:

$$w_a = 11.9 \text{ ev}, \; w_i = 7.13 \text{ ev}, \; \varphi_0 = 4.77 \text{ ev},$$
$$C = 3.75 \times 10^{17}, \; \beta = 2.48 \times 10^6, \; \alpha = 1.76 \times 10^{-24}.$$
$$Q^2C = 2.68 \times 10^{-49}, \; B = 1 \times 10^{-64},$$
$$K_1 = 1.5 \times 10^{-99}, \; K_2 = 1.94 \times 10^{55}.$$

The table lists the values of N/n as functions of the velocity v_∞. From these it is evident that at a relative velocity of the O_2 molecule to the Fe surface of $v_\infty = 4$ km/sec there appears an appreciable probability of ejection of electrons from the metal. Starting with a velocity $v_\infty = 10$ km/sec nearly all the gas molecules that collide with the surface of the metal are ionized. In Fig. 1 we show a family of curves $\log N/n = f(\log v_\infty)$ for intermediate values of $B = 1 \times 10^{-66}$ to $B = 5 \times 10^{-64}$. From the figure it is also evident that for $B = 1 \times 10^{-66}$, which corresponds to a low value of U_0, ionization occurs for too low values of velocity; this indicates that the values of B should be 1×10^{-66} or larger. With the exception of the rare gases, the above theory is applicable to all gases with appreciable electronegative properties. In analogy to the preceding, it is possible to calculate N/n for any other combination of gas and metal.

v_∞ km/sec	N/c
3.0	$3.59 \cdot 10^{-22}$
3.5	$1.01 \cdot 10^{-17}$
4.0	$9.44 \cdot 10^{-14}$
4.5	$2.32 \cdot 10^{-11}$
5.0	$6.68 \cdot 10^{-9}$
5.5	$4.78 \cdot 10^{-6}$
7.5	$3.9 \cdot 10^{-3}$
10	0.75

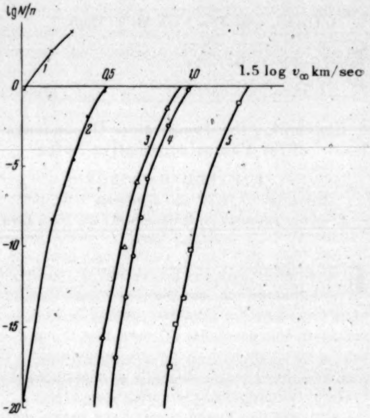

FIG. 1. Values of B for curves: 1 – 1×10^{-66}; 2 – 1×10^{-65}; 3 – 7.5×10^{-65}; 4 – 1×10^{-64}; 5 – 5×10^{-64}.

In conclusion we note that this mechanism of charging, along with others, may possibly explain the production of ionized regions in the atmosphere upon the entry of meteors. The velocity of meteors ranges from 8 to 100 km/sec,[7,8] the maximum number of cases being with $v = 40$ km/sec.

---

[1] C. V. Izmailov and A. M. Furman, J. Exptl. Theoret. Phys. (U.S.S.R.) 20, 729 (1950).

[2] E. A. Mason and W. E. Rice, J. Chem. Phys. 22, 522 (1954).

[3] D. K. C. MacDonald and S. K. Roy, Phys. Rev. 97, 671 (1955).

[4] E. Lennard-Jones, Physica 4, 941 (1937).

[5] D. Kaye, T. Laby, *Handbook of Physical Experimentation* Moscow, I. I. L. (1949).

[6] B. M. Tsarev, *Contact Potential Differences*, M.–L., (1955).

[7] N. Herlofson, Reports Prog. Phys. 11, 444 (1948).

[8] A. Lovell, Usp. Fiz. Nauk 61, 9 (1950).

Translated by L. B. Leder
318

Concerning the Temperature Dependence of the Photoelectromotive Force

F. F. KODZHESPIROV

(Submitted to JETP editor November 10, 1956)
J. Exptl. Theoret. Phys. (U.S.S.R.) 32, 1593-1594
(June, 1957)

EXPERIMENTAL INVESTIGATIONS of the crystal photoeffect[1] and photoelectromotive force, occurring when the capacitor method is used to investigate semiconductors,[2] show that these effects have a maximum with respect to temperature. This maximum, however, is difficult to explain on the basis of the proposed theoretical formulas.

Lashkarev and Kosonogova[3] have shown that the dependence of the non-barrier-layer photoelectric force in copper oxide on the intensity of light is described by the formula

$$V = (kT / e) \ln (1 + BJ). \tag{1}$$

By comparing (1) for small intensity with the theoretical formulas obtained by Lashkarev[4] it is possible to assume that for the crystal photoeffect $BJ \approx \Delta\sigma_- / \sigma_T$.

Thus both effects (non-barrier photoelectromotive force and photoelectric force in the capacitor method) may be described by relations (1) of like form but of somewhat different content. It is essential that in the case of the crystal photoeffect $\Delta\sigma_-$ (light-induced increment of conductivity at the base of the anti-barrier layer or on the boundary of the neutral contact) is due to the minority carriers, while in the capacitor method there is no need for restriction to the minority carriers.

The experimenter usually deals with samples of finite thickness, and therefore (1) can be written more precisely as

$$V = (kT / e) [\ln (1 + B_1 J) - \ln (1 + B_2 J)]. \tag{2}$$

But since the factor B_2, which must take into account the absorption of light in the sample and possibly also the diffusion of the minority carriers toward the second electrode, is very small, the second logarithm in Eq. (2) does not exert a notable influence on the intensity dependence of the photoelectromotive force. In this case Eq. (1) is satisfied to a good degree.

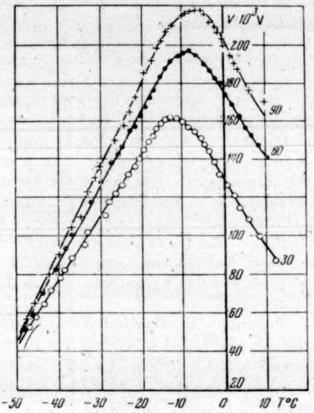

Matters are different in temperature investigations. It is shown in Refs. 1 and 2 that Eq. (1) cannot give even a qualitative explanation of the existence of a maximum in the photoelectromotive force *vs.* temperature curve. Ryvkin,[2] to reconcile the experimental data with Eq. (1) makes assumptions that are far from obvious concerning the mechanism of recombination at low temperatures. The need for such a reconciliation between the experimental data and the theoretical ones disappears if one takes into account the finite thickness of the sample. Making the same assumptions concerning the temperature dependence of σ_T and $\Delta\sigma$ it is possible to rewrite Eq. (2) in the form

$$\vartheta = T \ln \frac{1 + a_1 x}{1 + a_2 x}, \tag{3}$$

where

$$\vartheta = Ve / k, \; a_{1,2} = \mathrm{const}\,(T), \; b = W / k, \; x = e^{b/T}, \; a_1 > a_2.$$

Let us test Eq. (3) for an extremum. It is necessary for us to determine the temperature for which

$$\frac{d\vartheta}{dT} = \ln \frac{1 + a_1 x}{1 + a_2 x} - \frac{(a_1 - a_2)\, x \ln x}{(1 + a_1 x)(1 + a_2 x)} = f(x) - \varphi(x) = 0. \tag{4}$$

Since $a_1 > a_2$ and $x \geq 1$, then $f(x) > 0$ and $\varphi(x) \geq 0$. The function $f(x)$ increases monotonically and is different from zero over the entire range of variation of x, while $\varphi(x)$ vanishes at the end of the interval. Equation (4) is satisfied for two values of x, corresponding to two extremal points of Eq. (3). The character of the extremum (sign of the second derivative) depends on the sign of the difference $(1 - a_1a_2x^2)$.

Since Eq. (4) in its general form is not solvable, we attempt to approximate it. Solving Eq. (4) for specific values of a_1 and a_2 shows that an intersection of $f(x)$ and $\varphi(x)$ takes place for $a_{1,2}x \ll 1$ and $a_1x \gg 1$; $a_2x > 1$. In the first case Eq. (4) yields approximately $\ln x_1 \approx 1$. Near the second root, with satisfactory approximation, it is possible to represent Eq. (4) as

$$\ln (a_1 / a_2) - (a_1 - a_2) \ln x_2 / a_1 a_2 x_2 = 0.$$

Subject to a certain error, it is possible to assume that $\ln x_2 \approx - \ln a_2$ and $a_1 \gg a_2$, whence

$$x_2 = 1 / [a_2 (1 - \ln a_1 / \ln a_2)].$$

The root $x = x_1$ corresponds to a minimum of the function $\vartheta(T)$ and the root $x = x_2$ to a maximum.

The temperature maximum (T_M) and minimum (T_m) are determined from the relation

$$T_{M,\,m} = W / k \ln x_{2,1}, \tag{5}$$

i.e., for low temperatures we have a maximum, for high ones a minimum. The position of the maximum depends on the thickness of the sample and on the intensity of the illumination. With increase in the thickness of the specimen, a_2 quickly decreases, and the maximum moves towards the lower temperatures.

It is possible to obtain the dependence of the position of the maximum on the illumination intensity by assuming $a_{1,2} = a'_{1,2}J$. We then obtain for the shift of the maximum ΔT

$$\Delta T = cT_1^2 / (1 - cT_1),\ c = (k_2 / W) \ln (J_2 / J_1), \tag{6}$$

T_1 is the temperature of the maximum for intensity J_1. With increase in intensity $[\ln (J_2/J_1) > 0]$ the maximum moves to the side of higher temperatures.

It has been established by us[5] that when amorphous selenium is exposed to x-rays there is developed an electromotive force similar to the crystal-photoeffect and described by relation (2). The figure shows the temperature dependence of the emf for different intensities of x-ray exposure of amorphous selenium (the number under the curve gives the intensity of radiation in dosimeter pulses per second). With change in temperature we actually observe a maximum whose position moves to the side of higher temperature with increasing intensity, as follows from Eq. (6).

---

[1] A. V. Ioffe and A. F. Ioffe, J. Tech. Phys. (U.S.S.R.) 5, 111 (1935).

[2] S. M. Ryvkin, J. Tech. Phys. (U.S.S.R.) 18, 1521 (1948).

[3] V. E. Lashkarev and K. M. Kosonogov, J. Exptl. Theoret. Phys. (U.S.S.R.) 18, 927 (1948).

[4] V. E. Lashkarev, J. Exptl. Theoret. Phys. (U.S.S.R.) 18, 917 (1948).

[5] F. I. Kolomoitsev and F. F. Kodzhespirov, J. Tech. Phys. (U.S.S.R.) 27, 5 (1947).

Translated by L. B. Leder

319

Author Index to Volume 5

References with L are Letters to the Editor

Abrikosov, A. A. On the Magnetic Properties of Superconductors of the Second Group – 1174.

— (see **Khalatnikov, I. M.**) – 745.

— **and I. M. Khalatnikov.** Theory of Kinetic Phenomena in Liquid He^3 – 887.

Agranovich, V. M. and A. S. Davydov. Optical Model of the Interaction of Nucleons with Nuclei in the Resonance Region of the Compound Nucleus – 1164.

Akhiezer, A. I., M. I. Kaganov, and G. Ia. Liubarskii. Ultrasonic Absorption in Metals – 685.

— **and A. G. Sitenko.** Diffraction Scattering of Fast Deuterons by Nuclei – 652.

Aleksandrov, Iu. A. (see **Brashenkov, V. S.**) – 144L.

Aleksandrov, Iu. A. Covariant Equation for Two Annihilating Particles – 696.

Alekseeva, K. I. and N. L. Grigorov. Inelastic Interaction of Protons Having Energies above 7 Bev with Carbon and Hydrogen Nuclei – 339L.

Alekseevskii, N. E. and Iu. P. Gaidukov. Hall Effect and Susceptibility of Gold – 1301L.

Alikhanian, A. I. and A. O. Vaisenberg. Spectrum and Positive Excess of the Hard Component in the $(0.3-17) \times 10^9$ ev/c Momentum Range at an Altitude of 3250 Meters – 349.

Alikhanov, A. I., G. P. Eliseev, V. A. Liubimov, and B. V. Ershler. Polarization of Electrons in β-Decay – 1097.

Ali-Zade, S. A. (see **Nikol'skii, B. A.**) – 93.

Anastasevich, V. S. Derivation of the Formula for the Cross Section for Formation of High Energy Neutrons in Deuteron-Nuclei Collisions – 520L.

Andronikashvili, E. L. and M. F. Bibilashvili. The Spatial Distribution of the Penetrating Component of Wide Atmospheric Showers – 341L.

Ankudinov, V. A. (see **Fogel', Ia. M.**) – 382.

Antonov, Iu. N., Iu. N. Vavilov, G. T. Zatsepin, A. A. Kutuzov, Iu. V. Skvortsov, and G. B. Khristiansen. Structure of the Periphery of Extensive Atmospheric Cosmic Ray Showers – 172.

Askar'ian, G. A. Coherent Scattering and Radiation of Electromagnetic Waves by a Plasma in an Inhomogeneous Magnetic Field – 1285L.

— Some New Possibilities of Ionic Phenomena in Metastable Liquids – 1011L.

Azbel', M. Ia. On the Theory of Skin Effect in Metals – 1027L.

— **V. I. Gerasimenko, and I. M. Lifshitz.** Paramagnetic Resonance and Polarization of Nuclei in Metals – 986.

— **M. I. Kaganov, and I. M. Lifshitz.** Thermal Conductivity and Thermoelectric Phenomena in Metals in a Magnetic Field – 967.

— **and E. L. Kaner.** Theory of Cyclotron Resonance in Metals – 730.

Baboshkin, S. A., A. S. Karamian, and G. N. Flerov. Interaction of Nitrogen and Gold Nuclei – 1055.

Baiukov, Iu. D., M. S. Kozodaev, and A. A. Tiapkin. Investigation of the Energy and Angle Distribution of Neutral Pions Produced by 470 and 660 Mev Protons in Carbon – 552.

— **Iu. Ts. Oganesian, and A. A. Tiapkin.** Absorption of γ-Quanta of 500 Mev Mean Energy in Lead, Copper, and Aluminum – 151L.

— **A. N. Sinaev, And A. A. Tiapkin.** Experimental Comparison of the Energy Spectra of γ-Quanta from the Decay of π^0-Mesons Formed on Carbon and Lead Nuclei by 660 Mev Protons – 299L.

— **and A. A. Tiapkin.** Energy Spectrum of γ-Quanta from the Decay of π^0-Mesons Produced by 660 Mev Protons on Hydrogen Nuclei – 779.

Balashov, V. V. (see **Shirokov, Iu. M.**) – 136L.

Baldin, A. M. and V. A. Petrun'kin. Scattering of Photons by Protons – 1279.

Baranskii, K. N. (see **Iakovlev, I. A.**) – 762L.

Barashenkov, V. S. Concerning Some Possibilities of Formulation of a Relativistically Invariant Theory of Extended Particles – 470.

— The Construction of a Phenomenological Scattering Matrix with Nonlocal Interaction – 313L.

— **I. P. Stakhanov, and Iu. A. Aleksandrov.** Elastic Small Angle Scattering of Neutrons by Heavy Nuclei – 144L.

Bass, F. G. On the Possible Mechanism for the Increase in the Conductivity of Atomic Semiconductors in a Strong Electric Field – 705.

— **and M. I. Kaganov.** Concerning the Saturation of the Hall "Constant" in Semiconductors in Strong Magnetic Fields – 1002.

Baz', A. I. Charge Invariance in Nuclear Reactions – 403.

— Polarization in Reverse Reactions – 521L.

Bazarov, I. P. Equations with Variational Derivatives in Statistical Equilibrium Theory – 872.

— Statistical Theory of Systems of Charged Particles with Account of Short Range Forces of Repulsion – 946.

Bekeshko, V. A. and E. I. Kondorskii. Temperature Dependence of the Overhauser Effect in Metallic Lithium – 505L.

Belenkii, S. Z. Relation Between Scattering and Multiple Particle Production – 952.

— **and N. M. Gerasimova.** On the Absorption of High Energy Nuclear-Active Particles – 456.

Berestetskii, V. B. and Iu. A. Bychkov. Scattering of *K*-Mesons with Change of Intrinsic Parity – 105L.

Berlovich, E. E. and G. V. Dubinkin. Some Cases of Very Small Life Times of Low Nuclear Levels – 164.

Bibilashvili, M. F. (see **Andronikashvili, E. L.**) – 341L.

Bilen'kii, S. M. Level Shift of π-Mesonic Atoms – 517L.

Blank, V. Z. Application of a Renormalization Group to Different Problems of Scattering in Quantum Electrodynamics – 759L.

Blinov, G. A., Iu. S. Krestnikov, M. F. Lomanov, and Ia. Ia. Shalamov. Use of a Mixture of Two Liquids in Bubble Chambers – 1281.

Blokhintsev, D. I. Scattering of Fast Protons on Protons – 284.

— Some Remarks on the Validity of the Hydrodynamic Description of Quantum States – 286.

Bochagov, B. A., A. P. Komar, and G. E. Kocharov. Fine Structure of the α-spectra of U^{234} and U^{238} – 1026.

Bogdankevich, L. S. Motion of a Charge Parallel to the Axis of a Cylindirical Channel in a Dielectric – 1157.

Bolotovskii, B. M. Skin Effect in Thin Films and Wires – 465.

— (see **Bogdankevich, L. S.**) – 1157.

Bonch-Bruevich, [illegible] On the Exciton Mechanism of Capture of Current Carriers in Homopolar Semiconductors – 1196.

— Remarks on the Theory of the Electron Plasma in Semiconductors – 894.

Borovik-Romanov, A. S. and M. P. Orlova. Magnetic Properties of the Oxides of Manganese at Temperatures from 20 to 300° K – 1023L.

Brodskii, A. M. On the Derivation of the Low Equation in the Theory of Meson Scattering – 509L.

Buimistrev, V. M. and S. I. Pekar. Quantum States of Particles Coupled to a Harmonically Oscillating Continuum with Arbitrarily Strong Interaction, I. Case of Absence of Translational Symmetry – 970.

Bunkin, F. V. On Radiation in Anisotropic Media – 277.

— Thermal Radiation from an Anisotropic Medium – 665.

Bychkov, Iu. A. (see **Berestetskii, V. B.**) – 150L.

Chavchanidze, V. V. (see **Mirianashvili, V. V.**) – 1005L.

Cheishvili, O. D. Polarization of Deuterons in Elastic Scattering – 1009L.

Cherepanov, V. (see **Sokolov, A. V.**) – 777L.

Chernikov, N. A. The Effect of a Longitudinal Magnetic Field on the Multiple Scattering of Particles – 320L.

Chernysheva, M. A. (see **Indenbom, V. L.**) – 575.

Chilashvili, G. A. (see **Mamasakhlisov, V. I.**) – 661.

Chukichev, M. V. (see **Vavilov, V. A.**) – 579.

Chuvilo, I. V. and V. G. Shevchenko. Angular and Energy Distributions of Photoprotons from Be^9 and O^{12} – 1090.

Danysh, M. and B. Pontecorvo. The Threshold of "Creation" and the Threshold of "Generation" of Negative *K*-Particles – 325L.

Davydov, A. S. (see **Agranovich, V. M.**) – 1164.

— **and G. F. Filippov.** Moment of Inertia of a System of Interacting Particles – 676.

— **and G. F. Filippov.** Quadrupole Moments and the Zero-Point Surface Vibrations of Axially Symmetrical Nuclei – 773L.

— **and D. M. Mel'nichenko.** On the Second Approximation in the Problem of Slow Neutron Scattering by Bound Protons – 769L.

Deev, Iu. S. (see **Krongauz, A. N.**) – 828.

Deigen, M. F. and V. L. Vinetskii. Quantum States and Optical Transitions of the F_2^+ Center Electron – 226.

— **and V. L. Vinetskii.** Interaction Between Current Carriers and *F*-Centers and Acoustical of the Lattice in Ionic Crystals – 1125.

Deineko, A. S., A. Ia. Taranov, and A. K. Val'ter. Measurement of the C^{12} (p, γ) and C^{12} (d, n) Effective Cross Sections for Low Energy Bombarding Particles – 201.

Deliagin, N. M. and V. S. Shpinel'. Concerning Even-Even Nuclei Having the Characteristic 2^+ for the Second Excited State – 309L.

D'erdi (Gyorgi), G. A Physical Model of the Hyperon – 152L.

Diatlov, I. T., V. V. Sudakov, and K. A. Ter-Martirosian. Asymptotic Meson-Meson Scattering Theory – 631.

Dmitriev, I. S. Electron Loss Probabilities for Multiply-Charged Ions – 473.

— (see **Nikolaev, V. S.**) – 789.

— (see **Teplova, Ia. A.**) – 797.

Dolginov, A. Z. The Character of Nucleonic Forces – 506L.

Dolinskii, E. I. (see Shapiro, I. S.) – 129L.

Dovzhenko, O. I., B. A. Nelepo, and S. I. Nikol'skii. Energy Spectrum of μ-Mesons in Extensive Atmospheric Cosmic Ray Showers – 391.

Druin, V. A., S. M. Polikanov, and G. N. Flerov. Fission of Nuclei under the Influence of Accelerated Nitrogen Nuclei – 1059.

Drukarev, G. F. Energy Dependence of the Effective Cross Section of Inelastic Scattering of Particles Near the Threshold – 496L.

Dubinkin, G. V. (see **Berlovich, E. E.**) – 164.

Dukel'skii, V. M. and V. M. Sokolov. Negative Ions of Silicon, Germanium, Tin, and Lead – 306L.

Dzhelepov, V. P., K. O. Oganesian, and V. B. Fliagin.

Production of Neutral Pions by Neutrons on Deuterons and Complex Nuclei – 560.

Dzialoshinskii, I. E. Thermodynamical Theory of "Weak" Ferromagnetism in Antiferromagnetic Substances – 1259.

Elagin, Iu. P. (see **Nemirovskii, P. E.**) – 1293L.

Eleonskii, V. M. Possibility of Constructing a Chain of Equations for Model Operators – 1296L.

— and P. S. Zyrianov. Contribution to the Theory of Collective Motion of Particles in Quantum Mechanical Systems – 432.

Eliseev, G. P. (see **Alikhanov, A. I.**) – 1097.

Ershler, B. V. (see **Alikhanov, A. I.**) – 1097.

Estulin, I. V., L. F. Kalinkin, and A. S. Melioranskii. Soft γ-Rays Emitted by Nuclei in the Capture of Thermal Neutrons – 801.

Evstigneev, Iu. F. (see **Vavilov, Iu. N.**) – 1078.

Fadeev, V. I. (see **Zhernovoy, A. I.**) – 563.

Fain, V. M. (see **Ginzburg, V. L.**) – 123L.

— Natural Line Widths of Microwaves – 501L.

Fainberg, Ia. B. and N. A. Khizhniak. Energy Loss of a Charged Particle Passing Through a Laminar Dielectric, I. – 720.

Fateeva, L. N. (see **Nikolaev, V. S.**) – 789.

— (see **Teplova, Ia. A.**) – 797.

Fesenko, A. I. (see **Grigor'ev, A. P.**) – 1299L.

Fikhtengolts, I. G. On the Dependence of the Motion of Bodies in a Gravitational Field on Their Mass – 898.

— Application of the Dirac-Fock-Podol'skii Method to a Mechanical Many-Body Problem – 1144.

Filimonov, G. F. Level Shifts in Helium – 192.

— and Iu. M. Shirokov. Multiple Interaction Hamiltonians in Quantum Electrodynamics – 84.

Filippov, G. F. (see **Davydov, A. S.**) – 676.

— (see **Davydov, A. S.**) – 773L.

Firsov, Iu. A. On the Structure of the Electron Spectrum in Lattices of the Tellurium Type – 1101.

Firsov, O. B. Interaction Energy of Atoms for Small Nuclear Separations – 1192.

Flerov, G. N. (see **Baboshkin, S. A.**) – 1055.

— (see **Druin, V. A.**) – 1059.

Fliagin, B. B. (see **Dzhelepov, V. P.**) – 560.

Fliagin, V. B. (see **Kiselev, V. S.**) – 786.

Fogel', Ia. M. The Applicability of the Relation of Detailed Balance for a Cluster of Ions of Stationary Composition – 499L.

— V. A. Ankudinov, and R. E. Slabospitskii. Loss of Two Electrons in Single Collisions Between Negative Hydrogen Ions and Molecules of Gases – 382.

Fomenko. D. E. (see **Skliarevskii, V. V.**) – 220.

Fradkin, E. E. Particle with Spin $3/2$ in an Electromagnetic Field – 298L.

— On the Rarita–Schwinger Method in the Theory of Particles of Half-Integral Spin – 1203.

Fradkin, E. S. Contribution to the Theory of Transport Processes in a Plasma Located in a Magnetic Field – 956.

Furman, A. M. Ejection of Electrons from Metals by Fast Molecules – 1302L.

Gaidukov, Iu. P. (see **Alekseevskii, N. E.**) – 1301L.

Galanin, A. D. On the Possibility of Formulating a Meson Theory with Several Fields – 460.

Galkin A. A., Ia. S. Kan, and B. G. Lazarev. Discontinuous Attenuation of Current in a Superconducting Ring – 1292L.

— Ia. L. Shamfarov, and A. V. Stefanishina. Electron Resonance in Current-Carrying Solutions – 1291L.

Gal'perin, F. M. s–d Exchange in Ferromagnetic Metals – 321L.

Garif'ianov, N. S. Double Absorption Peaks in Electron Resonance at Saturation – 503L.

~~— Paramagnetic Reso~~nance in Alkali Metals – 111L.

Geilikman, B. T. Magnetic Interaction of Electrons and Anomalous Diamagnetism – 981.

Gerasimenko, V. I. (see **Azbel', M. Ia.**) – 986.

Gerasimova, N. M. (see **Belen'kii, S. Z.**) – 456.

Gerasimova, R. I. (see **Varfolomeev, A. A.**) – 792.

Ginzburg, V. L. and V. M. Fain. On Quantum Effects Occurring on Interaction of Electrons with High Frequency Fields in Resonant Cavities – 123L.

Giterman, M. Sh. and K. B. Tolpygo. Band Structure of the Polaron Energy Spectrum – 713.

Glebashev, G. Ia. On the Shape of Resonance Paramagnetic Absorption Curves in Crystals – 38.

Goldin, L. L. (see **Novikova, G. I.**) – 832.

Gorbunov, B. V. (see **Vertsner, V. N.**) – 782.

Gor'kov, L. P. Two Limiting Momenta in Scalar Electrodynamics – 167.

Gramenitskii, I. M., G. B. Zhdanov, E. A. Zamchalova, and M. N. Shcherbakova. Nuclear Interaction in a Photoemulsion at an Energy of 8×10^{13} ev – 763L.

Grechukhin, D. P. Electric Monopole Transitions of Atomic Nuclei – 846.

— On the Angular Distribution of Deuterons from the $\mathrm{Be}_4^9\,(p, d)\,\mathrm{Be}_4^8$ Reaction – 1188.

Gribov, V. N. Excitation of Rotational States in the Interaction Between Neutrons and Nuclei – 688.

— Effect of Diffuseness of the Nuclear Boundary on Neutron Scattering – 537.

Grigor'ev, A. P., E. P. Toporkova, and A. I. Fesenko. Anomalous Decay of a Hypernucleus – 1299L.

Grigor'ev, E. L. (see **Mitin, N. A.**) – 378.

Grigor'ev, V. I. Quantum Field Theoretical Solutions without Perturbation Theory – 109L.

Grigorov, N. L. (see **Alekseeva, K. I.**) – 399L.

Gubkin, A. N. and G. I. Skanavi. Some New Electrets from Inorganic Dielectrics – 140L.

Gumeniuk, V. S. (see **Mitropan, I. M.**) – 157.

Gurevich, A. V. Simplification of the Equations for the Distribution Function of Electrons in a Plasma – 1006L.

Gurevich, V. L. and Iu. N. Obraztsov. The Effect of the Entrainment of Electrons by Phonons on Thermomagnetic Effects in Semiconductors – 302L.

Gusev, I. A., O. M. Lilova, A. N. Murin, B. K. Preobrazhenskii, and V. A. Iakovlev. Gadolinium Isotope with Mass 146 – 1295L.

Guzhavin, V. V. and G. T. Zatsepin. Altitude Dependence of the Elementary Act of Nuclear Collisions – 312L.

Gyorgi (D'erdi) G. (see **D'erdi, G.**) – 152L.

Iakovlev, I. A., T. S. Velichkina and K. N. Baranskii. Absorption of Sound in a Phase Change in Rochelle Salt – 762L.

Iakovlev, V. A. (see **Gusev, I. A.**) – 1295L.

Iampol'skii, P. A. (see **Leipunskii, O. I.**) – 305L.

Iankov, V. V. Ponderomotive Forces in a Localized Plasma in the Electromagnetic Field of a Plane Wave – 753L.

Iavor, I. P. (see **Komar, A. P.**) – 508L.

Indenbom, V. L. and M. A. Chernyasheva. Construction of the Thermodynamic Potential of Rochelle Salt from Results of Optical Investigation of Domains – 575.

Ioffe, B. L. Two Possible Schemes of Non-Conservation of Parity in Weak Interactions – 1015L.

— **L. B. Okun', and A. P. Rudik.** The Problem of Parity Non-Conservation in Weak Interactions – 328L.

Itskevich, E. S. and V. M. Kontorovich. Heat Capacity of Laminar Structures at Low Temperatures – 147L.

— **and P. G. Strelkov.** Heat Capacity of Laminar Lattices at Low Temperatures – 394.

Itskovich, F. I. (see **Zil'berman, G. E.**) – 119L.

Iur'ev, B. A. (see **Teplov, I. B.**) – 134L.

Ivanchik, I. I. On the Absolute Value of the Stripping Cross Section and Cross Section for Diffraction Disintegration of the Deuteron – 133L.

Ivanenko, I. P. Equilibrium Spectrum of Electrons and Photons with Account of Scattering – 204.

— The Energy Spectrum of Cascade Electrons in Lead – 413.

— **and M. A. Malkov.** Energy Spectrum of Cascade Photons in Light Substances – 112L.

Ivanter, I. G. and L. B. Okun'. On the Theory of Scattering of Particles by Nuclei – 340L.

Izhak, I. A. Contribution to the Thermodynamical Theory of Ferroelectrics – 121L.

Iziumov, Iu. A. Extension of the Spin Wave Model to the Case of Several Electrons Surround Each Site – 866.

Kadomtsev, B. B. Fluctuations in Gases – 771L.

Kaganov, M. I. (see **Akhiezer, A. I.**) – 685.

— (see **Azbel', M. Ia.**) – 967.

— (see **Bass, F. G.**) – 1002.

— **I. M. Lifshitz, and K. D. Sinel'nikov.** On the Possibility of Observing the Variation of the Chemical Potential of Electrons of a Metal in a Magnetic Field – 500L.

— **and V. V. Slezov.** Surface Impedance of Metals in the Infrared Region – 1216.

Kaipov, D. K. and Zh. S. Takibaev. Generation of Slow π-Mesons by Cosmic Ray Particles – 569.

Kalinkin, L. F. (see **Estulin, I. V.**) – 801.

Kan, Ia. S. (see **Galkin, A. A.**) – 1292L.

Kaner, E. A. (see **Azbel', M. Ia.**) – 730.

Karamian, A. S. (see **Baraboshkin, S. A.**) – 1055.

Karpman, V. I. On the Theory of "Strange" Particles – 767L.

Kel'man, V. M., V. A. Romanov, R. Ia. Metskhvarishvili, and V. A. Koliunov. Investigation of Conversion Lines in the β-Spectrum of a Eu^{152}–Eu^{154} Mixture – 24.

Kerimov, B. K. Nuclear Saturation and Levy–Klein Potential of Pseudoscalar Meson Theory – 326L.

Kertes, I. (see **Zhuravlev, N. N.**) – 1073.

Khaidarov, A. A. (see **Zhdanov, G. B.**) – 583.

Khalatnikov, I. M. Hydrodynamics of Solutions of Two Superfluid Liquids – 542.

— On Magnetohydrodynamic Waves and Magnetic Tangential Discontinuities in Relativistic Hydrodynamics – 901.

— **and A. A. Abrikosov.** The Thermodynamics of Liquid He^3 – 745.

— **and V. N. Zharkov.** Theory of Diffusion and Thermal Conductivity of Dilute Solutions of He^3 in Helium II – 905.

— (see **Abrikosov, A. A.**) – 887.

Khizhniak, N. A. (see **Fainberg, Ia. B.**) – 720.

Khokhlov, Iu. K. Some Sum Rules for the Cross Sections of Electric Quadrupole Transitions in the Nuclear Photoeffect – 88.

Khokhlov, R. V. (see **Klimontovich, Iu. L.**) – 937.

Khristiansen, G. B. (see **Antonov, Iu. N.**) – 172.

Khromchenko, I. M. Investigation of the Energy Levels of the F^{20} Nucleus by Magnetic Analysis – 231.

Khutsishvili, G. R. Beta Emission from Polarized Nuclei – 1288L.

Kikoin, A. K. (see **Likhter, A. I.**) – 772L.

Kirzhnits, D. A. Contribution to Field Theory Involving a Cut-off Factor – 445.

— Quantum Corrections to the Thomas–Fermi Equation – 64.

Kiselev, V. S. and V. B. Fliagin. Energy Distribution of Neutrons Emitted from Beryllium Bombarded by 680 Mev Protons – 786.

Kitova, A. I. (see **Toropov, A. P.**) – 315L.

Kliarfeld, B. N. (see **Pokrovskaia-Soboleva, A. S.**) – 812.

Klimontovich, Iu. L. and R. V. Khoklov. Contribution to the Theory of the Molecular Generator – 937.

Kobzarev, I. Iu. On the Problem of K^0 Decays – 125L.

— and L. B. Okun'. Simultaneous Creation of λ and θ Particles – 761L.

Kocharov, G. E. (see **Bochagov, B. A.**) – 1026L.

Kodzheepirov, F. F. Concerning the Temperature Dependence of the Photoelectromotive Force – 1304L.

Kogan, A. V. and L. I. Rusinov. Neutron Emission by Excited RaD Nuclei – 365.

Kolesnikov, N. N. (see **Teodorovich, E. V.**) – 304L.

Koliumov, V. A. (see **Kel'man, V. M.**) – 24.

Komar, A. P. and I. P. Iavor. Photodisintegration of Neon Nuclei – 508L.

— and V. N. Shrednik. Investigation of the Allotropic Transformation $\alpha \rightleftarrows \beta$ Zr with the Aid of an Electronic Projector – 127L.

— (see **Bochagov, B. A.**) – 1026L.

— (see **Vorob'ev, A. A.**) – 516L.

Kondorskii, E. I. and A. S. Pakhomov. The Theory of Ferromagnetism of Metals and Alloys at Low Temperatures – 269.

— (see **Bekeshko, V. A.**) – 505L.

Kondrat'ev, L. N. (see **Novikova, G. I.**) – 832.

Koniukov, M. V. On Low-Frequency Oscillations in the Plasmas of Electronegative Gases – 429.

Konorova, E. A. Statistical Retardation in Dielectric Breakdown of Solid Dielectrics – 497L.

— and L. A. Sorokina. Dependence of Dielectric Strength of Alkali Halide Crystals on Temperature – 143L.

Kontorovich, V. M. (see **Itskevich, E. S.**) – 147L.

Kopaleishvili, T. I. Nuclear Photoeffect in Be^9 at High Energies – 1018L.

Korolev, V. A. (see **Vorob'ev, A. A.**) – 516L.

Kozel, S. M. On the Fluctuation Resolution Limit of an Optical Modulation Interferometer – 609.

Kozodaev, M. S. (see **Baiukov, Iu. D.**) – 552.

Kresnin, A. A. and L. N. Rozentsveig. Polarization Effects in the Scattering of Electrons and Positrons by Electrons – 288.

— (see **Visotskii, G. L.**) – 883.

Krestnikov, Iu. S. (see **Blinov, G. A.**) – 1281.

Krisiuk, E. M. (see **Zhernovoy, A. I.**) – 563.

Krivoglaz, M. A. Theory of Diffuse Scattering of X-rays and Thermal Neutrons in Solid Solutions. II. Microscopic Theory – 1115.

Krongauz, A. N., Iu. S. Duv, and V. K. Liapidevskii. Photoconductivity of Cuprite – 828.

Kucher, T. I. Characteristic Frequencies and Amplitudes of Free Normal Oscillations in KCl Crystals – 418.

— Heat Capacity of KCl – 114L.

Kudrin, L. P. (see **Nikol'skii, B. A.**) – 93.

Kulakov. Iu. I. Inelastic Proton–Proton Scattering – 477.

Kunin, P. E. and I. M. Taksar. Some Relativistic Properties of the Behavior of Spin-½ Particles – 426.

Kurdgelaidze, D. P. On the Nonlinear Generalization of the Meson and Spinor Field Equations – 941.

Kurushin, A. I. Paramagnetic Absorption at High Frequencies in Gadolinium Salts in Parallel Fields – 601.

— Paramagnetic Absorption in Some Manganese Salts in Parallel Fields at Super-High Frequencies – 766L.

Kutuzov, A. A. (see **Antonov, Iu. N.**) – 172.

Kuznetsov, V. M. Separation of Helium Isotopes by Rectification and Thermo-Osmosis – 819.

Landau, L. D. Conservation Laws in Weak Interactions – 336L.

— Oscillations in a Fermi Liquid – 101.

— Possible Properties of the Neutrino Spin – 337L.

— and E. M. Lifshitz. Hydrodynamic Fluctuations – 512L.

Lapidus, L. I. Contribution to the Theory of Exchange Collisions Between Fast Nucleons and Deuterons – 1170.

Latyshev, G. D. (see **Zhernovoy, A. I.**) – 563.

Lazarev, B. G. (see **Galkin, A. A.**) – 1292L.

Lazareva, L. E. (see **Zatsepina, G. N.**) – 21.

Lebedev, S. V. Explosion of a Metal by an Electric Current – 243.

— Reply to Critical Remarks of I. F. Kvartskhava Concerning our Papers $^{2-6}$ – 126L.

Leipunskii, O. I., A. M. Morozov, Iu. V. Makarov, and P. A. Iampol'skii. New Short-Lived Isomers in the Millisecond Range – 305L.

Leksin, G. A. Elastic and Quasi-Elastic Scattering of 660 Mev Protons by Deuterons – 371.

Levin, B. A. (see **Voitovetskii, V. K.**) – 184.

Levintov, I. I., A. V. Miller, and V. N. Shamshev. A New Method for Measurement of Polarization of Medium Energy Neutrons and the Phase Shift Analysis of n-He^4 Scattering – 258.

— A. V. Miller, E. Z. Tarumov, and V. N. Shamshev. Dependence of the Polarization of (D + D) Neutrons on the Energy of the Deuterons – 310L.

Liapidevskii, V. K. (see **Krongauz, A. N.**) – 828.

Lifshitz, I. M. Quantum Theory of the Electrical Conductivity of Metals in a Magnetic Field – 1227.

— (see **Azbel', M. Ia.**) – 967.

— (see **Azbel', M. Ia.**) – 986.

— (see **Kaganov, M. I.**) – 500L.

— (see **Landau, L. D.**) – 512L.

Likhachev, V. M. and Iu. P. Merekov. Charge and Momentum Analysis of Relativistic Particles by the Nuclear Emulsion Technique in Pulsed Magnetic Fields – 31.

Likhter, A. I. and A. K. Kikoin. Effect of Neutron Irradiation on the Compressibility of Metals – 772L.

— and L. F. Vereshchagin. The Hall Effect in Bismuth under Pressures up to 30,000 kg/cm² – 511L.

Lilova, O. M. (see **Gusev, I. A.**) – 1295L.

Liubarskii, G. Ia. (see **Akhiezer, A. I.**) – 685.

Liubimov, V. A. (see **Alikhanov, A. I.**) – 1097.

Logunov, A. A. and A. N. Tavkhelidze. Dispersion Relations for Photoproduction of Pions on Nucleons – 1134.

Lomanov, M. F. (see **Blinov, G. A.**) – 1281.

Loskutov, Iu. M. (see **Sokolov, A. A.**) – 523L.

Lozhkin, O. V. On the Nautre of the Cone-Like Shape of Tracks of Multi-charged Ions in Nuclear Emulsions – 293.

Magalinskii, V. B. and Ia. P. Terletskii. The Application of the Microcanonical Distribution to the Statistical Theory of Multiple Production of Particles – 483.

Makharov, Iu. V. (see **Leipunskii, O. I.**) – 305L.

Maksimenko, V. M. and I. L. Rozental'. Some Problems Related to the Statistical Theory of Multiple Production of Particles – 546.

Maksimov, M. Z. (see **Viktorov, D. V.**) – 42.

Malkov, M. A. (see **Ivanenko, I. P.**) – 112L.

Mamaladze, Iu. G. (see **Mirianashvili, V. V.**) – 1005L.

Mamasakhlisov, V. I. and G. A. Chilashvili. Disintegration of Light Nuclei in a Coulomb Field – 661.

Marchenko, B. V. (see **Voitovetskii, V. K.**) – 184.

Markelova, T. N. (see **Teplov, I. B.**) – 134L.

Mashkevich, V. S. Electrical, Optical, and Elastic Properties of Diamond-Type Crystals, II. Lattice Vibrations with Calculation of Atomic Dipole Moments – 707.

— and K. B. Tolpygo. Electrical, Optical and Elastic Properties of Diamond-Type Crystals. I – 435.

Matinian, S. G. Non-Conservation of Parity and Hyperon Decay – 1017L.

— On the Energy Spectrum of μ-Mesons in $K_{\mu 3}$ Decay – 757L.

— On Strong Interaction between the K-Particle and the π-Particle – 758L.

Medvedev, B. V. On the Construction of the Scattering Matrix. II. The Theory with Nonlocal Interaction – 48.

Melikian, E. G. Internal Compton Effect in Pair Conversion – 331L.

Melioranskii, A. S. (see **Estulin, I. V.**) – 801.

Mel'nichenko, D. M. (see **Davydov, A. S.**) – 769L.

Merekov, Iu. P. (see **Likhachev, V. M.**) – 31.

Meshkovski, A. G., Iu. S. Pligin, Ia. Ia. Shalamov, V. A. Shebanov. Pion Production in Zero Isotopic Spin Nuclei – 1085.

Metskhavishvili, R. Ia. (see **Kel'man, V. M.**) – 24.

Migdal, A. B. The Momentum Distribution of Interacting Fermi Particles – 333L.

— Bremsstrahlung and Pair Production at High Energies in Condensed Media – 527.

Mikhailov, I. N. Decay of the τ-Meson – 265.

Miller, A. V. (see **Levintov, I. I.**) – 258.

— (see **Levintov, I. I.**) – 310L.

Minarik, E. V. and V. A. Novikov. Fission of U, Th, Bi, and Tl Induced by High Energy γ-Quanta – 253.

Mints, M. Ia. Force Fluctuations in an Electron Gas – 319L.

Mirianashvili, M. M., V. V. Chavchanidze and Iu. G. Mamaladze. The Nautre of Field Fluctuations – 1005L.

Mironov, E. S. and L. M. Nemenov. Investigation of Slow Electron Emission by High Energy Protons – 188.

Mishakova, A. P. (see **Shapiro, I. S.**) – 129L.

Mitin, N. A. and E. L. Grigor'ev. Elastic Scattering of 360 Mev Positive π-Mesons by Protons – 378.

Mitropan, I. M. and V. S. Gumeniuk. Emission of Negative Ions from Metallic Surfaces Bombarded with Positive Hydrogen Ions – 157.

Model', I. Sh. Measurement of High Temperatures in Strong Shock Waves in Gases – 589.

Morozov, A. I. Radiation from a Point Charge, Moving Uniformly Along the Surface of an Isotropic Medium – 1028L.

— The Acceleration of Plasma by a Magnetic Field – 215.

Morozov, A. M. (see **Leipunskii, O. I.**) – 305L.

Murin, A. N. (see **Gusev, I. A.**) – 1295L.

Neganov, B. S. and O. V. Savchenko. Production of π^+-Mesons in p–p Collisions at 480 – 660 Mev – 1033.

Nelepo, B. A. (see **Dovzhenko, O. I.**) – 391.

Nemenov, L. M. (see **Mironov, E. S.**) – 188.

Nemilov, Iu. A. and A. N. Pisarevskii. Investigation of γ-Rays from Po–Li and Po–Mg Neutron Sources – 115L.

Nemirovskii, P. E. Model of a Semi-transparent Nucleus with a Diffuse Boundary. II – 932.

— and Iu. P. Elagin. Calculation of the Polarization of Neutrons on the Basis of the Diffused Edge Nuclear Model – 1293L.

Nikolaev, V. S., L. N. Fateeva, I. S. Dmitriev, and Ia. A. Teplova. Equilibirum Distribution of Nitrogen Ion Charges – 789.

— (see **Teplova, Ia. A.**) – 797.

Nikol'skii, B. A., L. P. Kudrin, and S. A. Ali-Zade. Inelastic Scattering of 160 Mev Pions on Emulsion Nuclei – 93.

Nikol'skii, S. I. and V. M. Seleznev. Distribution of the Electron-Photon Component on the Periphery of Extensive Air Showers in Cosmic Rays – 1019L.

— (see **Dovzhenko, O. I.**) – 391.
— (see **Vavilov, Iu. N.**) – 1078.
Novikov, V. A. (see **Minarik, E. V.**) – 253.
Novikova, G. I., L. N. Kondrat'ev, Iu. N. Sobolev, and L. L. Goldin. The Alpha Decay of Pu^{239} – 832.
Novozhilov, Iu. V. Reduction of the Two-Nucleon Problem to a Single-Nucleon Problem in the Nonrelativistic Range – 1030L.
— Scale Transformation and the Virial Theorem in Quantum Field Theory – 138L.
Obraztsov, Iu. N. (see **Gurevich, V. L.**) – 302L.
Obreimov, I. V. and E. S. Trekhov. Optical Contact of Polished Glass Surfaces – 235.
Oganesian, Iu. Ts. (see **Baiukov, Iu. D.**) – 151L.
Oganesian, K. O. (see **Dzhelepov, V. P.**) – 560.
Oksman, Ia. A. (see **Vertsner, V. N.**) – 782.
Okun', L. B. The μ-Decay of K-Mesons and Hyperons – 334L.
— (see **Ioffe, B. L.**) – 328L.
— (see **Ivanter, I. G.**) – 340L.
— (see **Kobzarev, I. Iu.**) – 761L.
Okun', L. and B. Pontecorvo. Some Remarks on Slow Processes of Transformation of Elementary Particles – 1297L.
— **and A. Rudik.** Possible Correlation in π-μ-e-Decay – 520L.
Orlov, Iu. F. Excitation of Betatron Oscillations by Synchrotron Momentum Oscillations in a Strong Focusing Accelerator – 45.
— Nonlinear Theory of Betatron Oscillations in a Strong Focusing Synchrotron – 195.
Orlova, M. P. (see **Borovik-Romanov, A. S.**) – 1023L.
Osokina, R. M. and B. S. Ratner. Investigation of the (γ, p) Reaction in Zinc. – 1.
Ostroumov, V. I. Disintegration of Silver and Bromine Nuclei by High Energy Protons – 12.
Pafomov, V. E. Peculiarities of Cerenkov Radiation in Anisotropic Media – 307L.
— Radiation of a Point Charge, Moving Along the Boundary Between Two Media – 504L.
Pakhomov, A. S. (see **Kondorskii, E. I.**) – 269.
Pekar, S. I. (see **Buimistrov, V. M.**) – 970.
Peker, L. K. and L. A. Silva. Electric Monopole Transitions in Nuclei with Odd Mass Numbers – 515L.
Perel', V. I. Calculation of the Drift Velocity of Ions in the Electric Field in Their Gas – 440.
Perlin, Iu. E. Capture of Conduction Electrons by Charged Defects in Ionic Crystals – 71.
Peshkov, V. P. and K. N. Zinov'eva. Visual Observation of the Stratification of Solutions of He^3-He^4 – 1024L.
Petrun'kin, V. A. (see **Baldin, A. M.**) – 1279.
Petukhov, V. A. Concerning the Possibility for an Experimental Investigation of the Structure of the Electron – 317L.
Pisarevskii, A. N. (see **Nemilov, Iu. A.**) – 115L.
Pligin, Iu. S. (see **Meshkovskii, A. G.**) – 1085.
Pokrovskaia-Soboleva, A. A. and B. N. Kliarfled. Ignition of the High Voltage Discharge in Hydrogen at Low Pressures – 812.
Polikanov, S. M. (see **Druin, V. A.**) – 1059.
Pontecorvo, B. M. (see **Danysh, M.**) – 325L.
Pontecorvo, B. (see **Okun', L.**) – 1297L.
Popov, Iu. M. Scattering of π-Mesons on Nucleons in Higher Approximations of the Tamm–Dancoff Method – 131L.
Popovici, A. Nonlinearity of the Field in Conformal Reciprocity Theory – 642.
Pospelov, A. N. (see **Zatsepina, G. N.**) – 21.
Preobrazhenskii, B. K. (see **Gusev, Ia. A.**) – 1295L.
Prokoshkin, Iu. D. and A. A. Tiapkin. Investigation of the Excitation Functions for the Reactions $C^{12}(p, pn)C^{11}$, $Al^{27}(p, 3pn)Na^{24}$ and $Al^{27}(p, 3p3n)Na^{22}$ in the 150–660 Mev Energy Range – 148L.
— **and A. A. Tiapkin.** π^0-Meson Production in p–p and p–n Collisions in the 390–660 Mev Energy Region – 618.
Pustovalov, G. E. Vacuum Polarization in Mesonic Atoms – 1234.
Puzikov, L., R. Ryndin, and Ia. Smorodinskii. Reconstructuion of the Scattering Matrix of a Two-Nucleon System – 489.
Rabinovich, E. M. Electron-Positron Pair Production in Collisions between Fast π-Mesons and Nucleons – 1272.
Raizer, Iu. P. On the Structure of the Front of Strong Shock Waves in Gases – 1242.
Ratner, B. S. (see **Osokina, R. M.**) – 1.
Remennyi, A. G. (see **Zhernovoy, A. I.**) – 563.
Riazanov, M. I. Phenomenological Study of the Effect of a Nonconducting Medium in Quantum Electrodynamics – 1013L.
Ritus, V. I. Angular Operators for Nuclear Reactions – 1249.
Romankevich, A. V. Concerning the Lifetime of the Two Forms of the π^0-Meson – 509L.
Romanov, V. A. (see **Kel'man, V. M.**) – 24.
Rozental', I. L. (see **Maksimenko, V. M.**) – 546.
Rozentsveig, L. N. (see **Kresnin, A. A.**) – 288.
— (see **Sitenko, A. G.**) – 330L.
— (see **Visotskii, G. L.**) – 883.
Rudik, A. P. (see **Ioffe, B. L.**) – 328L.
— (see **Okun', L.**) – 520L.
Rusinov, L. I. (see **Kogan, A. V.**) – 365.
Ruzevich, Z. Concerning the Letter to the Editor by N.

A. Kraskokutskii "Light from Aluminum Melts in an Electrolytic Bath." – 111L.

Ryndin, R. (see **Puzikov, L.**) – 489.

Ryndin, R. M. and Ia. A. Smorodinskii. Minami Transformation for Nucleon-Nucleon Scattering – 976.

— and Ia. A. Smorodinskii. Unitarity Relationships for Elastic Collisions of Particles with Arbitrary Spins – 1294L.

Sakharov, A. D. (see **Zel'dovich, Ia. B.**) – 775L.

Savchenko, O. V. (see **Neganov, B. S.**) – 1033.

Seleznev, V. M. (see **Nikolskii, S. I.**) – 1019L.

Selivanenko, A. S. The Exciton State of an Imperfect Molecular Crystal – 79.

Seliverstov, D. M. (see **Vorob'ev, A. A.**) – 516L.

Sergeev, A. G. (see **Zhernovoy, A. I.**) – 563.

Shafranov, V. D. Structure of Shock Waves in a Plasma – 1183.

Shalamov, Ia. Ia. (see **Blinov, G. A.**) – 1281.

— (see **Meshkovskii, A. G.**) – 1085.

Shamfarov, Ia. L. (see **Galkin, A. A.**) – 1291L.

Shamshev, V. N. (see **Levintov, I. I.**) – 258.

— (see **Levintov, I. I.**) – 310L.

Shapiro, I. S., E. I. Dolinskii, and A. P. Mishakova. On the Question of the Spin and Parity of the τ-Meson – 129L.

Shcherbakova, M. N. (see **Gramenitskii, I. M.**) – 763L.

Shebanov, V. A. (see **Meshkovski, A. G.**) – 1085.

Shevchenko, V. G. (see **Chuvilo, I. V.**) – 1090.

Shirokov, Iu. M. (see **Filimonov, G. F.**) – 84.

— V. V. Balashov, and K. A. Tumanov. On a Method of Direct Computation of the Nucleon-Nucleon Interaction Hamiltonian on the Basis of Experimental Values for the Levels of Light Nuclei – 136L.

Shirokov, M. I. Reactions Involving Polarized Particles – 835.

Shpetnyi, A. I. Energy and Angular Distribution of Neutrons Emitted in the $Be^9(d, n)B^{10}$ Reaction – 357.

Shpinel', V. S. (see **Deliagin, N. M.**) – 309L.

Shrednik, V. N. (see **Komar, A. P.**) – 127L.

Shut'ko, A. V. (see **Zaretskii, D. F.**) – 323L.

Sinayev, A. N. (see **Baiukov, Iu. D.**) – 299L.

Sinel'nikov, K. D. (see **Kaganov, M. I.**) – 500L.

Sitenko, A. G. Bremsstrahlung of Ultra-Relativistic Particles in a Central Field – 1223.

— (see **Akhiezer, A. I.**) – 652.

— and L. N. Rozentsveig. Diffractive Production of Photon-Antiproton Pairs by High Energy Photons – 330L.

Skanavi, G. I. (see **Gubkin, A. N.**) – 140L.

Skliarevskii, V. V., D. E. Fomenko, and E. P. Stepanov. Investigation of U^{235} Fission γ-Rays in the Energy Region up to 250 kev – 220.

Skvortsov, Iu. V. (see **Antonov, Iu. N.**) – 172.

Slabospitskii, R. E. (see **Fogel', Ia. M.**) – 382.

Slezov, V. V. (see **Kaganov, M. I.**) – 1216.

Sliv, L. A. (see **Peker, L. K.**) – 515L.

Smirnitskii, V. (see **Vaisenberg, A. O.**) – 607.

— (see **Vaisenberg, A. O.**) – 1093.

Smirnov, L. S. (see **Vavilov, V. S.**) – 579.

Smorodinskii, Ia. (see **Puzikov, L.**) – 489.

— (see **Ryndin, R. M.**) – 976.

— (see **Ryndin, R. M.**) – 1294L.

Sobolev, Iu. P. (see **Novikova, G. I.**) – 832.

Sokolov, A. A. and Iu. M. Loskutov. Polarization of Cerenkov Radiation – 523L.

Sokolov, A. V. and V. I. Cherepanov. Correction to the Articles "Dispersion Formulas of the Quantum Optics of Metals in the Many-Electron Theory" – 777L.

Sokolov, S. N. Photon Green Function Accurate to e^4 – 1029L.

Sokolov, V. M. (see **Dukel'skii, V. M.**) – 306L.

Solov'ev, V. G. Investigation of a Model in Quantum Field Theory – 859.

Sorokina, L. A. (see **Konorova, E. A.**) – 143L.

Soroko, L. M. Resonant Pion-Nucleon Interaction and Production of Pions by Nucleons – 927.

Spitsyn, A. V. (see **Vavilov, V. S.**) – 579.

Stakhanov, I. P. (see **Barashenkov, V. S.**) – 144L.

Stratonovich, R. L. On the Statistical Interpretations of Quantum Theory – 1206.

Stefanishina, A. V. (see **Galkin, A. A.**) – 1292L.

Stepanov, E. P. (see **Skliarevskii, V. V.**) – 220.

Strelkov, P. G. (see **Itskevich, E. S.**) – 394.

Strutinskii, V. M. Excitation of Rotational States in α-Decay of Even-Even Nuclei – 1150.

Sudakov, V. V. (see **Diatlov, I. T.**) – 631.

Sumbaev, O. I. Measurement of the Relative Intensities of γ-Lines by a Two-Meter Crystal Diffraction γ-Spectrometer – 170.

— Reflection of Gamma Rays from Bent Quartz Plates – 1042.

Surkov, V. Z. Electron Emission from Dielectric Films Bombarded by Positive Hydrogen Ions – 7.

Takibaev, Zh. S. (see **Kaipov, D. K.**) – 569.

— and P. A. Usik. Account of Primary α-Particles in the Development of a Nucleon Shower in the Stratosphere – 752L.

Taksar, I. M. (see **Kunin, P. E.**) – 426.

Tamm, I. E. On the Structure of Nucleons – 154L.

Taranov, A. Ia. (see **Deineko, A. S.**) – 201.

Tarumov, E. Z. (see **Levintov, I. I.**) – 310L.

Tavkhelidze, A. N. (see **Logunov, A. A.**) – 1134.

Teodorovich, E. V. and N. N. Kolesnikov. The Role of Three-Particle Forces in the Three-Body Problem – 304L.

Teplov, I. B., B. A. Iur'ev, and T. N. Markelova. Angular Distribution of the Products of the $S^{32}(d, p)S^{33}$ Reaction – 134L.

Teplova, Ia. A., I. S. Dmitriev, V. S. Nikolaev, and L. N. Fateeva. On the Interaction Between Lithium Ions and Matter – 792.

— (see **Nikolaev, V. S.**) – 789.

Terletskii, Ia. P. Motion of a Rarefied Plasma in a Variable Magnetic Field – 755L.

— Production of Very Strong Magnetic Fields by Rapid Compression of a Conducting Shell – 301L.

— (see **Magalinskii, V. B.**) – 483.

Ter-Martirosian, K. A. (see **Diatlov, I. T.**) – 631.

Tevikian, R. V. Green Function in Scalar Electrodynamics in the Bloch–Nordsieck Approximation – 1284L.

— Two-Electron Green Function in the Bloch–Nordsieck Approximation – 1282L.

Tiapkin, A. A. (see **Baiukov, Iu. D.**) – 151L.

— (see **Baiukov, Iu. D.** – 299L.

— (see **Baiukov, Iu. D.**) – 552.

— (see **Baiukov, Iu. D.**) – 779.

— (see **Prokoshkin, Iu. D.** – 148L.

— (see **Prokoshkin, Iu. D.**) – 618.

Tishkov, P. G. Second Relaxation in a Spin System at Room Temperature – 514L.

Tkalich, V. S. Possibilities of Focusing in a Linear Accelerator with the Aid of Traveling Waves – 518L.

Tolpygo, K. B. (see **Mashkevich, V. S.**) – 435.

— (see **Giterman, M. Sh.**) – 713.

Toporkova, E. P. (see **Grigor'ev, A. P.**) – 1299L.

Toropov, A. P. and A. I. Kitova. An Experiment on the Measurement of the Viscosity of an Expanded Liquid – 315L.

Trekhov, E. S. (see **Obreimov, I. V.**) – 235.

Tret'iakova, M. I. Determination of Mass of Slow Charged Particles in Photographic Plates – 1045L.

Tserkovnikov, Iu. A. Stability of Plasma in a Strong Magnetic Field – 58.

Tulinov, A. F. Concerning One Method of Measuring Lifetimes of Excited States of Atomic Nuclei – 1277L.

Tumanian, V. A. (see **Varfolomeev, A. A.**) – 792.

Tumanov, K. A. (see **Shirokov, Iu. M.**) – 136L.

Usik, P. A. (see **Takibaev, Zh. S.**) – 752L.

Vaisenberg, A. O. Momentum Spectrum of the Cosmic Radiation and the Positive Excess in the $(0.1-2.5)\times10^9$ ev/c Range at an Altitude of 3250 m – 352.

— (see **Alikhanian, A. I.**) – 349.

— **and V. A. Smirnitskii.** Correlation in π-μ-e-Decays – 1093.

— **and V. A. Smirnitskii.** Mesonic Decay of a Tritium Hyperfragment – 607.

Val'ter, A. K. (see **Deineko, A. S.**) – 201.

Varfolomeev, A. A., R. I. Gerasimova, and V. A. Tumanium. Multiple Electron Production in a High Energy Electron-Photon Shower – 792.

Vavilov, Iu. N. (see **Antonov, Iu. N.**) – 172.

— **Iu. F. Evstigneev, and S. I. Nikol'skii.** The Penetrating Component of Extensive Cosmic Ray Air Showers in the Atmosphere – 1078.

Vavilov, P. V. Ionization Losses of High Energy Heavy Particles – 749.

— On Bubble Chambers – 1276L.

— The interaction Cross Sections of π-Mesons and Nucleons at High Energies – 768L.

Vavilov, V. S., A. V. Spitsyn, L. S. Smirnov, and M. V. Chukichev. The Effect of Fast Neutron Irradiation on Recombination of Electrons and Holes in Germanium Crystals – 579.

Vdovin, Iu. A. Production of Proton-Antiproton Pairs by High Energy γ-Quanta – 452.

Velichkina, T. S. (see **Iakovlev, I. A.**) – 762L.

Vereshchagin, L. F. (see **Likhter, A. I.**) – 511L.

Verkin, B. I. Concerning the Temperature Dependence of the Magnetic Susceptibility of the Elements – 117L.

Vertsner, V. N., B. V. Gorbunov, and Ia. A. Oksman. Structural Characteristics of Antimony Sulfide Layers – 782.

Veselago, V. G. Dipole Moment of the HDSe Molecule – 513L.

Viktorov, D. V. and M. Z. Maksimov. Dependence of the Taper Length of Emulsion Tracks on Particle Charge – 42.

Vinetskii, V. L. (see **Deigen, M. F.**) – 226.

— (see **Deigen, M. F.**) – 1125.

Visotskii, G. L., A. A. Kresnin, and L. N. Rozentsveig. Bremsstrahlung of Polarized Electrons – 883.

Vladimirskii, V. V. On the Mechanism of Fission of Heavy Nuclei – 673.

Voitovetskii, V. K., B. A. Levin, and E. V. Marchenko. Soft 15–800 Kev Radiation Accompanying the Thermal Neutron Fission of Uranium – 184.

Vorob'ev, A. A., V. A. Korolev, A. P. Komar and D. M. Seliverstov. Internal Conversion Coefficient of the 53 kev Gamma Radiation on the L Shell of Th^{230} – 516L.

Zamchalova, E. A. (see **Gramenitskii, I. M.**) – 763L.

Zaretskii, D. F. and A. V. Shut'ko. Quasi-Magnetic Interaction of the Spin of a Nucleon with the Rotation of the Nucleus – 323L.

Zatsepin, G. T. (see **Antonov, Iu. N.**) – 172.

— (see **Guzhavin, V. V.**) – 312L.

Zatsepina, G. N., L. E. Lazareva, and A. N. Pospelov. Angle–Energy Distribution of Photoneutrons from Bi – 21.

Zavoiskii, E. K. A Source of Polarized Nuclei for Accelerators – 603.

— Concerning a Possible Method for the Polarization of a Proton Beam – 338L.

Zel'dovich, Ia. B. Investigations of the Equation of State by Means of Mechanical Measurements – 1287L.

— Shock Waves of Large Amplitude in Air – 919.

— **and A. D. Sakharov.** Reactions Produced by μ-Mesons in Hydrogen – 775L.

Zharkov, V. N. (see **Khalatnikov, I. M.**) – 905.

Zhdanov, G. B. (see **Gramenitskii, I. M.**) – 763L.

— **and A. A. Khaidarov.** Investigation of the Penetrating Component of Electron-Nuclear Showers by the Delayed Coincidence Method in Conjunction with a Hodoscope – 583.

Zhernovoy, A. I., E. M. Krisyuk, G. D. Latyshev, A. S. Remennyi, A. G. Sergevev, and V. I. Fadeev. Internal Conversion Electron Spectrum of Radiothorium II – 563.

Zhirnov, N. N. On Quasiclassical Single-Electron Wave Functions – 1021L.

Zhuravlev, N. N. Structure of Superconductors. X. Thermal, Microscopic, and X-Ray Investigation of the Bismuth-Palladium System – 1064.

— **and I. Kertes.** Structure of Superconductors. XI. Investigation of Alloys of Bismouth with Platinum, Ruthenium, Osmium, and Iridium – 1073.

Zil'berman, G. E. and F. I. Itskovich. Temperature Dependence of the Magnetic Susceptibility of Electrons in Metals – 119L.

— Behavior of an Electron in a Periodic Electric and Uniform Magnetic Field – 208.

Zimin, A. G. Application of Correlation Polarization in the Phase Analysis of p–p Scattering – 1008L.

— Polarization Correlation in Nucleon-Nucleon Scattering – 996.

Zinov'eva, K. N. (see **Peshkov, V. P.**) – 1024L.

Zyrianov, P. S. (see **Eleonskii, V. M.**) – 432.

SOVIET PHYSICS JETP VOLUME 5, NUMBER 6 DECEMBER 15, 1957

Analytic Subject Index to Volume 5

References with L are Letters to the Editor. Items are listed under the following categories:

- Acoustics
- Astrophysics
- Atomic and Molecular Beams
- Atomic Mass and Abundance
- Atomic Structure and Spectra
- Chemical Effects and Properties
- Constants, Standards, and Units
- Cosmic Radiation
- Crystalline State
- Dielectrics and Dielectric Properties
- Diffraction
- Diffusion
- Editorial
- Electrical Conductivity and Resistance
- Electrical Discharges
- Electrical Properties
- Electromagnetic Theory and Electromagnetics
- Electrons and Positrons
- Elementary Particle Interactions
- Errata
- Field Theory
- Films, Properties
- Fluid Dynamics
- Gamma Rays
- Gases
- Geophysics
- Helium, Liquid
- Imperfections in Solids
- Ionization
- Ions
- Ions and Electrons, Mobility
- Liquids
- Luminescence
- Magnetic Properties
- Magnetic Resonance
- Mathematical Methods
- Mechanics
- Mesons and Hyperons
- Methods and Instruments
- Microwaves
- Miscellaneous
- Molecular Aggregates
- Molecular Structure and Spectra
- Noise
- Nuclear Fission
- Nuclear Moments and Spin
- Nuclear Photoeffects
- Nuclear Reactions, General
- Nuclear Reactions Induced by α-Particles and He^3
- Nuclear Reactions Induced by Deuterons and Tritons
- Nuclear Reactions Induced by Mesons
- Nuclear Reactions Induced by Neutrons
- Nuclear Reactions Induced by Protons
- Nuclear Spectra
- Nuclear Structure Theory
- Optical Properties
- Quantum Electrodynamics
- Quantum Mechanics
- Radiation
- Radioactivity
- Range and Energy Loss of Particles
- Relativity and Gravitation
- Scattering, General
- Scattering of α-Particles
- Scattering of Deuterons
- Scattering of Electrons and Positrons
- Scattering of Mesons
- Scattering of Neutrons
- Scattering of Protons
- Statistical Mechanics and Thermodynamics
- Superconductivity
- Thermal Properties
- X-Rays

Absorption of Radiation (see Radiation)

Acoustics

- Absorption of Sound in a Phase Change in Rochelle Salt. I. A. Iakovlev, T. S. Velichkina and K. N. Baranskii—762L.
- Shock Waves of Large Amplitude in Air. Ia. B. Zel'dovich—919.
- Ultrasonic Absorption in Metals. A. I. Akhiezer, M. I. Kaganov and G. Ia. Liubarskii—685.

Afterglow (see Electrical Discharges)

Alloys (see Crystalline State)

Annihilation (see Electrons and Positrons)

Antiferroelectric Phenomena (see Dielectrics and Dielectric Properties)

Antiferromagnetism (see Magnetic Properties)
Arcs (see Electric Discharges)
Astrophysics
  Thermal Radiation from an Anisotropic Medium. F. V. Bunkin—665.
Atomic and Molecular Beams
  A Source of Polarized Nuclei for Accelerators. E. K. Zavoiskii—603.
  Concerning a Possible Method for the Polarization of a Proton Beam. E. K. Zavoiskii—338L.
  Contribution to the Theory of the Molecular Generator. Iu. L. Klimontovich and R. V. Khokhlov—937.
  Loss of Two Electrons in Single Collisions between Negative Hydrogen Ions and Molecules of the Gas. Ia. M. Fogel', V. A. Ankudinov, and R. E. Slabopitskii—382.
Atomic Structure and Spectra
  Electric Monopole Transitions of Atomic Nuclei. D. P. Grechukhin—846.
  Interaction Energy of Atoms for Small Nuclear Separations. O. B. Firsov—1192.
  Internal Conversion Electron Spectrum of Radiothorium II. A. I. Zhernovoi, E. M. Krisiuk. G. D. Latyshev, A. S. Remennyi, A. G. Sergeev and V. I. Fadeev—563.
  Level Shifts in Helium. G. F. Fillimonov—192.
Auger Effect (see Atomic Structure and Spectra)
Barkhausen Effect (see Magnetic Properties)
Biographical Material
  Grigorii Samuilovich Landsberg—345.
Boson Theory (see Radiation)
Broadening of Spectral Lines (see Atomic Structure and Spectra; Spectra, General)
Capture Cross Sections (see Electrons and Positrons; Nuclear Reactions, General; Radiation)
Cerenkov Effect (see Radiation)
Chemical Effects and Properties
  Discontinuous Attenuation of Current in a Superconducting Ring. A. A. Galkin, Ia. S. Kan, and B. G. Lazarev— 1292L.
  On the Possibility of Observing the Variation of the Chemical Potential of Electrons of a Metal in a Magnetic Field. M. I. Kaganov, I. M. Lifshitz, and K. D. Sinel'nikov—500L.
Chemiluninescence (see Luminescence)
Cold Emission (see Electrical Properties)
Compton Effect (see Radiation)
Conductivity, Electrical (see Electrical Conductivity and Resistance)
Cosmic Radiation
  Account of Primary α-Particles in the Development of a Nucleon Shower in the Stratosphere. Zh. S. Takibaev and P. A. Usik—752L.
  Altitude Dependence of Broad Atmospheric Showers According to the Various Models of the Elementary Act of Nuclear Collisions. V. V. Guzhavin and G. T. Zatsepin—312L.
  Anomalous Decay of a Hypernucleus. A. P. Grigor'ev, E. P. Toporkova, and A. I. Fesenko— 1299L.
  Concerning the Temperature Dependence of the Photoelectromotive Force. F. F. Kodzhespirov— 1304L.
  Distribution of the Electron-Photon Component on the Periphery of Extensive Air Showers of Cosmic Rays. S. I. Nikol'skii and V. M. Seleznev—1019L.
  Energy Spectrum of Casdade Photons in Light Substances. I. P. Ivanenko and M. A. Malkov—112L.
  Energy Spectrum of Muons in Extensive Atmospheric Cosmic Ray Showers. O. I. Dvozhenko, B. A. Nelepo, and S. I. Nikol'skii—391.
  Inelastic Interaction of Protons with Energies Greater than 7 Bev with Carbon and Hydrogen Nuclei. K. I. Alekseeva and N. L. Grigorov—339L.
  Investigation of the Penetrating Component of Electron-Nuclear Showers by the Delayed Coincidence Method in Conjugation with a Hodoscope. G. B. Zhadanov and A. A. Khaidarov—583.
  Momentum Spectrum of the Cosmic Radiation and the Positive Excess in the $(0.1-2.5)\times 10^9$ ev/c Range at an Altitude of 3250 m. A. O. Vaisenberg—352.
  Nuclear Interaction in a Photoemulsion at an Energy of 8×10^{13} ev. I. M. Gramenitskii, G. B. Zhdanov, E. A. Zamchalova and M. N. Shcherbakova—763L.
  On the Absorption of High Energy Nuclear Active Particles. S. Z. Belen'kii and N. M. Gerasimova—456.
  Spectrum and Positive Excess of the Hard Component in the $(0.3-17)\times 10^9$ ev/c Momentum Range at an Altitude of 3250 m. A. L. Alikhanian and A. O. Vaisenberg—349.
  The Energy Spectrum of Cascade Electrons in Lead. I. P. Ivanenko—413.
  Generation of Slow π-Mesons by Cosmic Ray Particles. D. K. Kaipov and Zh. S. Takibaev—569.
  The Penetrating Component of Extensive Cosmic-Ray Showers in the Atmosphere. Iu. N. Vavilov, Iu. F. Evstigneev, and S. I. Nikol'skii—1078.
  The Spatial Distribution of the Penetrating Component of Wide Atmospheric Showers. E. I. Andronikashvili and M. F. Bibilashvili—341L.
Cosmology (see Relativity and Gravitation)
Critical Potentials (see Atomic Structure and Spectra)
Cross Section (see Electrons and Positrons; Nuclear Reactions; Radiation; Scatter, General)
Crystal Counters (see Methods and Instruments)
Crystalline State (see also Electrical Properties; Magnetic Properties; Semiconductors, etc.)

Absorption of Sound in a Phase Change in Rochelle Salt. I. A. Iakovlev, T. S. Velichkina and K. N. Baranskii—762L.

Band Structure in the Polaron Energy Spectrum. M. Sh. Gitterman and K. B. Toplygo—713.

Capture of Conduction Electrons by Charged Defects in Ionic Crystals. Iu. E. Perlin—71.

Concerning the Temperature Dependence of the Photoelectromotive Force. F. F. Kodzhespirov— 1304L.

Construction of the Thermodynamical Potential of Rochelle Salt from the Results of the Optical Investigation of Domains. V. L. Indenbom and M. A. Chernysheva—575.

Corrections to the Articles "Dispersion Formulas of the Quantum Optics of Metals in the Many-Electron Theory." A. V. Sokolov and V. I. Cherepanov—777L.

Effect of Fast Neutron Irradiation on Recombination of Electrons and Holes in Germanium Crystals. V. S. Vavilov, A. V. Spitsyn, L. S. Smirnov, and M. V. Chukichev—579.

Electrical, Optical and Elastic Properties of Diamond Type Crystals. II. V. S. Mashkevich—707.

Energy Loss by a Charged Particle Passing Through a Laminar Dielectric. Ia. B. Fainberg and N. A. Khizhniak—720.

Extension of the Spin Wave Model to the Case of Several Electrons Surrounding Each Site. Iu. A. Iziumov—866.

Heat Capacity of Laminar Lattices at Low Temperatures. E. S. Itskevich and P. G. Strelkov—147L.

Interaction Between Current Carriers and F-Centers and the Acoustical Vibrations of the Lattice in Ionic Crystal. M. F. Deigen and V. L. Vinetskii—1125.

Investigation of the Penetrating Component of Electron-Nuclear Showers by the Delayed Coincidence Method in Conjunction with a Hodoscope. G. B. Zhdanov and A. A. Khaidarov—583.

On the Exciton Mechanism of Capture of Current Carriers in Homopolar Semiconductors. V. L. Bonch-Bruevich—1196.

On the Structure of the Electron Spectrum in Lattices of the Tellurium Type. Iu. A. Firsov—1101.

On the Theory of Skin Effect in Metals. M. Ia. Azbel'—1027L.

Quantum States and Optical Transitions of the F^{2+} Center Electron. M. F. Deigen and V. L. Vinetskii—226.

Quantum States of Particles Coupled to a Harmonically Oscillating Continuum with Arbitrary Strong Interaction. I. V. M. Buimistrov and S. I. Pekar—970.

Structural Characteristics of Antimony Sulfide Layers. V. N. Vertsner, B. V. Gorbunov, and Ia. A. Oksman—782.

Structure of Superconductors. X. N. N. Zhuravlev—1064.

Structure of Superconductors. XI. N. N. Zhuravlev and L. Kertes—1073.

Surface Impedance of Metals in the Infrared Region. M. I. Kaganov and V. V. Slezov—1216L.

Thermal Conductivity and Thermoelectric Phenomena in Metals in a Magnetic Field. M. Ia. Azbel, M. I. Kaganov, and I. M. Lifshitz—967.

Diamagnetism (see Magnetic Properties)

Dielectrics and Dielectric Properties

Absorption of Sound in a Phase Change in Rochelle Salt. I. A. Iakovlev, T. S. Velichkina and K. N. Baranskii—762L.

Construction of the Thermodynamical Potential of Rochelle Salt from the Results of the Optical Investigation of Domains. V. L. Indenbom and M. A. Chernysheva—575.

Electron Emission From Dielectric Films Bombarded by Positive Hydrogen Ions. V. Z. Surkov—7.

Motion of a Charge Parallel to the Axis of a Cylindrical Channel in a Dielectric. L. S. Bogdankevich and B. M. Bolotovskii—1157.

Peculiarities of Cerenkov Radiation in Anisotropic Media. V. E. Pafomov—3076.

Radiation of a Point Charge Moving Along the Boundary Between Two Media. V. E. Pafomov—504L.

Statistical Retardation in the Electric Sparking in Solid Dielectrics. E. A. Konorova—497L.

The Effect of Fast Neutron Irradiation on Recombination of Electrons and Holes in Germanium Crystals. V. S. Vavilov, A. V. Spitsyn, L. S. Smirnov, and M. V. Chukichev—579.

Diffraction

Diffractive Production of Proton-Antiproton Pairs by High-Energy Photons. A. G. Sitenko and L. N. Rozentsveig—330L.

Electrical, Optical, and Elastic Properties of Diamond-Type Crystals II. Lattice Vibrations with Calculation of Atomic Dipole Moments. V. S. Mashkevich—707.

Energy Loss by a Charged Particle Passing Through a Laminar Dielectric. I. Ia. B. Fainberg and N. A. Khizhniak—720.

Diffusion

Theory of Diffusion and Thermal Conductivity of Dilute Solutions of He^3 in Helium II. I. M. Khalatnikov and V. N. Zharkov—905.

Elasticity and Plasticity

An experiment on the Measurement of the Viscosity of an Expanded Liquid. A. P. Toropov and A. I. Kitova—315L.

Electrical, Optical and Elastic Properties of Diamond Type Crystals. II. V. S. Mashkevich—707.

Energy Loss by a Charged Particle Passing Through a Laminar Dielectric. I. Ia. B. Fainberg and N. A. Khizhniak—720.

Effect of Neutron Irradiation on the Compressibility of Metals. A. I. Likhter and A. I. Kikoin—772L.

Electrical Breakdown (see **Dielectrics and Dielectric Properties; Electrical Discharges**)

Electrical Conductivity and Resistance (see also **Electrical Properties; Semiconductors; Superconductivity**)

Electronic Resonance in Current-Carrying Solutions. A. A. Galkin, Ia. L. Shamfarov, and A. V. Stefanishina. – 1291L.

Explosion of a Metal by an Electric Current. S. V. Lebedev—243.

On the Possibility of Observing the Variation of the Chemical Potential of Electrons of a Metal in a Magnetic Field. M. I Kaganov, I. M. Lifshitz and K. D. Sinel'nikov—500L.

On the Theory of the Skin Effect in Metals. M. Ia. Azbel'—1027L.

Paramagnetic Resonance and Polarization of Nuclei in Metals. M. Ia. Azbel', V. I. Gerasimenko, and I. M. Lifshitz—967.

Quantum Theory of the Electrical Conductivity of Metals in a Magnetic Field. I. M. Lifshitz— 1227.

Surface Impedance of Metals in the Infrared Region. M. I. Kaganov and V. V. Slezov— 1216.

The Hall Effect in Bismuth under Pressures up to 30,000 kg/cm^2. A. I. Likhter and L. F. Vereshchagin—511L.

The Photoconductivity of Cuprite. A. N. Krongauz, V. K. Liapidevskii, and Iu. S. Deev—828.

The Problem of Saturation of the Hall "Constant" in Semiconductors in Strong Magnetic Fields. F. G. Bass and M. I. Kaganov—1002.

The Thermodynamics of Liquid He^3. I. M. Khalatnikov and A. A. Abrikosov—745.

Theory of Cyclotron Resonance in Metals. M. Ia. Azbel' and E. A. Kaner—730.

Thermal Conductivity and Thermoelectric Phenomena in Metals in a Magnetic Field. M. Ia. Azbel', M. I. Kaganov, and I. M. Lifshitz—967.

Electrical Discharges

Calculation of the Drift Velocity of Ions in the Electric Field in Their Gas. V. I. Perel'—440.

Coherent Scattering and Radiation of Electromagnetic Waves by a Plasma in an Inhomogenous Magnetic Field. G. A. Askarian— 1285L.

Ignition of the High Voltage Discharge in Hydrogen at Low Pressures. A. S. Pokrovskaia-Soboleva and B. N. Kliarfel'd—812.

Motion of a Rarefied Plasma in a Variable Magnetic Field. Ia. P. Terletskii—755L.

On Low-Frequency Oscillations in the Plasmas of Electronegative Gases. M. V. Koniukov—429.

Ponderomotive Forces in a Localized Plasma in the Electromagnetic Field of a Plane Wave. V. V. Iankov—753L.

Simplification of the Equations for the Distribution Function of Electrons in a Plasma. A. V. Gurevich—1006L.

Some New Possibilities of Ionic Phenomena in Metastable Liquids. G. A. Askar'ian—1011L.

Electrical Properties (see also **Dielectrics and Dielectric Properties; Electrical Conductivity and Resistance; Semiconductors; Superconductivity**)

Capture of Conduction Electrons by Charged Defects in Ionic Crystals. Iu. E. Perlin—71.

Concerning the Temperature Dependence of the Photoelectromotive Force. F. F. Kodzhespirov— 1304L.

Construction of the Thermodynamical Potential of Rochelle Salt from the Results of the Optical Investigation of Domains. V. L. Indenbom and M. A. Chernysheva—575.

Contribution to the Theory of Collective Motion of Particles in Quantum Mechanical Systems. V. M. Eleonskii and P. S. Zyrianov—432.

Corrections to the Articles "Dispersion Formulas of the Quantum Optics of Metals in the Many-Electron Theory." A. V. Sokolov and V. I. Cherepanov—777L.

Effect of Fast Neutron Irradiation on Recombination of Electrons and Holes in Germanium Crystals. V. S. Vavilov, A. V. Spitsyn, L. S. Smirnov, and M. V. Chukichev—579.

Ejection of Electrons from Metals by Fast Molecules. A. M. Furman— 1302L.

Electrical, Optical and Elastic Properties of Diamond Type Crystals. II. V. S. Mashkevich—707.

Electron Emission from Dielectric Films Bombarded by Positive Hydrogen Ions. V. Z. Surkov—7.

Energy Loss by a Charged Particle Passing Through a Laminar Dielectric. Ia. B. Fainberg and N. A. Khizhniak—720.

Explosion of a Metal by an Electric Current. S. V. Lebedev—243.

Interaction Between Current Carriers and F-Centers and the Acoustic Vibrations of the Lattices in Ionic Crystals. M. F. Deigen and V. L. Vinetskii—1125.

Investigation of Slow Electron Emission Induced by High Energy Protons. E. S. Mironov and L. M. Nemanov—188.

On the Possible Mechanism for the Increase in the Conductivity of Atomic Semiconductors in a Strong Electric Field. F. G. Bass—705.

On the Theory of the Skin Effect in Metals. M. Ia. Azbel'—1027L.

Quantum Theory of the Electrical Conductivity of Metals in a Magnetic Field. I. M. Lifshitz— 1227.
Some New Possibilities of Ionic Phenomena in Metastable Liquids. G. A. Askar'ian—1011L.
The Problem of Saturation of the Hall "Constant" in Semiconductors in Strong Magnetic Fields. M. I. Kaganov and F. G. Bass—1002.
Thermal Conductivity and Thermoelectric Phenomena in Metals in a Magnetic Field. M. Ia. Azbel', M. I. Kaganov, and I. M. Lifshitz—967.

Electrodynamics (see **Electromagnetic Theory and Electrodynamics**)

Electromagnetic Theory and Electrodynamics (see also **Microwaves**)
Application of the Dirac-Fock-Podolskii Method to a Mechanical Many-Body Problem. I. G. Fikhtengol'ts—1144.
Behavior of an Electron in a Periodic Electric and Uniform Magnetic Field. G. E. Zil'berman—208.
Coherent Scattering and Radiation of Electromagnetic Waves by a Plasma in an Inhomogeneous Magnetic Field. G. A. Askarian— 1285L.
Diffractive Production of Proton-Antiproton Pairs by High-Energy Photons. A. G. Sitenko and L. N. Rozentsveig—330L.
Energy Loss of a Charged Particle Passing Through a Laminar Dielectric. I. Ia. B. Fainberg and N. A. Khizhniak—720.
Internal Compton Effect in Pair Conversion. E. G. Melikian—331L.
Motion of a Charge Parallel to the Axis of a Cylindrical Channel in a Dielectric. L. S. Bogdankevich and B. M. Bolotovskii—1157.
Motion of a Rarefied Plasma in a Variable Magnetic Field. Ia. P. Terletskii—755L.
Multiple Interaction Hamiltonians in Quantum Electrodynamics. G. F. Filimonov and Iu. M. Shirokov—84.
On Magnetohydrodynamic Waves and Magnetic Tangential Discontinuities in Relativistic Hydrodynamics. I. M. Khalatnikov—901.
Particle with Spin $\frac{3}{2}$ in an Electromagnetic Field. E. E. Fradkin—298L.
Peculiarities of Cerenkov Radiation in Anisotropic Media. V. E. Pafomov—307L.
Polarization Effects in the Scattering of Electrons and Positrons on Electrons. A. A. Kresnin and L. N. Rozentsveig—288.
Ponderomotive Forces in a Localized Plasma in the Electromagnetic Field of a Plane Wave. V. V. Iankov—753L.
Production of Very Strong Magnetic Fields by Rapid Compression of a Conducting Shell. Ia. P. Terletskii—301L.
Radiation From a Point Charge, Moving Uniformly Along the Surface of an Isotropic Medium. A. I. Morozov—1028L.
Simplification of the Equations for the Distribution Function of Electrons in a Plasma. A. V. Gurevich—1006L.
Theory of Cyclotron Resonance in Metals. M. Ia. Azbel' and E. L. Kaner—730.
Thermal Radiation from an Anisotropic Medium. F. V. Bunkin—665.
Two Limiting Momenta in Scalar Electrodynamics. L. P. Gor'kov—167.

Electron Diffraction (see **Scattering of Electrons and Positrons**)

Electron Optics (see **Methods and Instruments**)

Electrons and Positrons (see also **Electromagnetic Theory and Electrodynamics; Elementary Particle Interactions; Scattering of Electrons and Positrons**)
Beta Emission from Polarized Nuclei. G. R. Khutsishivili— 1288L.
Concerning the Possibility of an Experimental Investigation of the Structure of the Electron. V. A. Petukhov—317L.
Correlations in $\pi \rightarrow \mu \rightarrow e$-Decay. A. O. Vaisenberg and V. A. Smirnitskii—1093.
Effect of the Diffuseness of the Nuclear Boundary on Neutron Scattering. V. N. Gribov—537.
Equilibrium Spectrum of Electrons and Photons with Account of Scattering. I. P. Ivanenko—204.
Force Fluctuations in an Electron Gas. M. Ia. Mints—319L.
Internal Compton Effect in Pair Conversion. E. G. Melikian—331L.
Internal Conversion Election Spectrum of Radiothorium II. A. I. Zhernovoi, E. M. Krisiuk. G. D. Latyshev, A. S. Remennyi, A. G. Sergeev and V. I. Fadeev—563.
Multiple Electron Production in a High Energy Electron-Photon Shower. A. A. Varfolomeev, R. I. Gerasimova, and V. A. Tumanian—792.
Polarization Effects in the Scattering of Electrons and Positrons on Electrons. A. A. Kresnin and L. N. Rozentsveig—288.
Polarization of Electrons in β Decay. A. I. Alikhanov, G. P. Eliseev, V. A. Liubimov and B. V. Ershler—1097.
Some Relativistic Properties of the Behavior of Spin-$\frac{1}{2}$ Particles. P. E. Kunin and I. M. Taksar—426.

Electrons, Scattering of (see **Scattering of Electrons and Positrons**)

Electrons, Secondary (see **Electrical Properties**)

Electro-Optical Effects (see **Optical Properties**)

Electrostriction (see **Dielectrics and Dielectric Properties**)

Elementary Particle Interactions
A Physical Model of the Hyperon. Gesa D'erdi (Gyorgi)—152L.
Absorption of γ-Quanta of 500 Mev Mean Energy in Lead, Copper, and Aluminum. Iu. D. Baiukov, Iu. Ts. Oganesian, and A. A. Tiapkin—151L.
Application of a Renormalized Group to Different Scattering Problems in Quantum Electrodynamics. V. Z. Blank—759L.
Calculation of the Polarization of Neutrons on the Basis of the Diffused Edge Nuclear Model. P. E. Nemirovskii and Iu. P. Elagin.
Concerning a Possible Method for the Polarization of a Proton Beam. E. K. Zavoiskii—338L.
Concerning Some Possibilities of Formulation of a Relativistically Invariant Theory of Extended Particles. V. S. Barashenkov—470.
Concerning the Possibility of an Experimental Investigation of the Structure of the Electron. V. A. Petukhov—317L.
Conservation Laws in Weak Interactions. L. D. Landau—336L.
Correlations in $\pi \to \mu \to e$-Decay. A. O. Vaisenberg and V. A. Smirnitskii—1093.
Covariant Equation for Two Annihilating Particles. A. I. Alekseev—696.
Diffractive Production of Proton-Antiproton Pairs by High-Energy Photons. A. G. Sitenko and L. N. Rozentsveig—330L.
Dispersion Relations for Photoproduction of Pions on Nucleons. A A. Logunov and A. N. Tavkhelidze—1134.
Effect on the Diffuseness of the Nuclear Boundary on Neutron Scattering. V. N. Gribov—537.
Elastic and Quasi-Elastic Scattering of 660 Mev Protons by Deuterons. G. A. Leksin—371.
Elastic Scattering of 360 Mev Positive π-mesons by Protons. N. A. Mitin and E. L. Grigor'ev—378.
Electric Monopole Transitions of Atomic Nuclei. D. P. Grechukhin—846.
Electron-Positron Pair Production in Collisions Between Fast Mesons and Nucleons. E. M. Rabinovich—1272.
Energy Spectrum of γ-Quanta from the Decay of π^0-Mesons Produced by 660 Mev Protons on Hydrogen Nuclei. Iu. D. Baiukov and A. A. Tiapkin.—779.
Excitation of Rotational States in the Interaction Between Neutrons and Nuclei. V. N. Gribov—688.
Inelastic Interaction of Protons Having Energies Above 7 Bev with Carbon and Hydrogen Nuclei. K. I. Alekseeva and N. L. Grigorov—339L.
Inelastic Proton-Proton Scattering. Iu. I. Kulakov—477.
Investigation of a Model in Quantum Field Theory. V. G. Solov'ev—859.
Investigation of the Energy and Angle Distribution of Neutral Pions Produced by 470 and 660-Mev Protons in Carbon. Iu. D. Baiukov, M. S. Kozodaev and A. A. Tiapkin—552.
Loss of Two Electrons in Single Collisions Between Negative Hydrogen Ions and Molecules of Gases. Ia. M. Fogel', V. A. Ankudinov and R. E. Slabospitskii—499L.
Moment of Inertia of a System of Interacting Particles. A. S. Davydov and G. F. Filippov—676.
Non-Conservation of Parity and Hyperon Decay. S. G. Matinian—1017L.
On the Construction of the Scattering Matrix II. The Theory with Nonlocal Interaction. B. V. Medvedev—48.
On the Possibility of Formulating a Meson Theory with Several Fields. A. D. Galanin—460.
On the Problem of K Decays. I. Iu. Kobzarev—125L.
On the Question of the Spin and Parity of the t-Meson. I. S. Shapiro, E. I. Dolinskii and A. P. Mishakova—129L.
On the Rarita–Schwinger Method in the Theory of Particles of Half-Integral Spin. E. E. Fradkin—1203.
On the Structure of Nucleons. I. E. Tamm—154L.
On the Theory of Scattering of Particles by Nuclei. I. G. Ivanter and L. B. Okun'—340L.
Photon Green Function Accurate to e^4. S. N. Sokolov—1029L.
Polarization of Electrons in β-Decay. A. I. Alikhanov, G. P. Eliseev, V. A. Liubimov and B. V. Ershler—1097.
Possible Correlation in $\pi \to \mu \to e$-Decay. L. Okun' and A. Rudik—520L.
Possible Properties of the Neutrino Spin. L. D. Landau—337L.
Production of Neutral Pions by Neutrons on Deuterons and Complex Nuclei. V. P. Dzhelepov, K. O. Oganesian and V. B. Fliagin—560.
Production of π^+ Mesons in $p-p$ Collisions at $480-660$ Mev. B. S. Neganov and O. V. Savchenko—1033.
Resonant Pion-Nucleon Interaction and Production of Pions by Nucleons. L. M. Soroko—927.
Scattering of K-Mesons with Change of Intrinsic Parity. V. B. Berestetskii and Iu. A. Bychkov—150L.
The μ-Decay of K-Mesons and Hyperons. L. B. Okun'—334L.
The Nature of Field Fluctuations. M. M. Mirianashvili, V. V. Chavchanidze, and Iu. G. Mamaladze—1005L.
The Problem of Parity Non-Conservation in Weak Interactions. B. L. Ioffe, L. B. Okun' and A. P. Rudik—328L.

The Threshold of "Creation" and the Threshold of "Generation" of Negative K-Particles. M. Danysh and B. Pontecorvo—325L.

Two Possible Schemes of Non-Conservation of Parity in Weak Interactions. B. L. Ioffe—1015L.

Elements (see Atomic Mass and Abundance)

Energy Loss of Particles (see Range and Energy Loss)

Energy States of Atoms (see Atomic Structure and Spectra)

Energy States of Nucleus (see Nuclear Reactions; Nuclear Spectra; Nuclear Structure)

Errata

Corrections to the Articles "Dispersion Formulas of the Quantum Optics of Metals in the Many-Electron Theory." A. V. Sokolov and V. I. Cherepanov—777L.

Evaporation (see Liquids)

Excitation of Atoms (see Atomic Structure and Spectra)

Excitation of Nucleus (see Nuclear Reactions; Nuclear Spectra; Nuclear Structure)

Faraday Effect (see Optical Properties)

Ferroelectric Phenomena (see Dielectrics and Dielectric Properties)

Field Emission (see Electrical Properties)

Field Theory (see also Quantum Electrodynamics)

Asymptotic Meson-Meson Scattering Theory. I. T. Diatlov, V. V. Sudakov, and K. A. Ter-Martirosian—631.

Concerning Some Possibilities of Formulation of a Relativistically Invariant Theory of Extended Particles. V. S. Barashenkov—470.

Conservation Laws in Weak Interactions. L. D. Landau—336L.

Contribution to Field Theory Involving a Cut-off Factor. D. A. Kirzhnits—445.

Covariant Equation for Two Annihilating Particles. A. I. Alekseev—696.

Energy Spectrum of μ-Mesons in $K_{\mu 3}$ Decay. S. G. Matinian—757L.

Green Function in Scalar Electrodynamics in the Bloch-Nordsieck Approximation. R. V. Tevikian— 1284L.

Internal Compton Effect in Pair Conversion. E. G. Melikian—331L.

Investigation of a Model in Quantum Field Theory. V. G. Solov'ev—859.

Level Shifts in Helium. G. Filimonov—192.

Multiple Electron Production in a High Energy Electron-Photon Shower. A. A. Varfolomeev, R. I. Gerasimova, and V. A. Tumanian—792.

Non-Conservation of Parity and Hyperon Decay. S. G. Matinian—1017L.

Nonlinearity of the Field in Conformal Reciprocity Theory. A. Popovici—642.

Nuclear Saturation and The Levy-Klein Potential of Pseudoscalar Meson Theory. B. K. Kerimov—326L.

On Magnetohydrodynamic Waves and Magnetic Tangential Discontinuities in Relativistic Hydrodynamics. I. M. Khalatnikov—901.

On Strong Interaction Between the k-Particle and the π-Particle. S. G. Martinian—758L.

On the Construction of the Scattering Matrix II. The Theory with Nonlocal Interaction. B. V. Medvedev—48.

On the Energy Spectrum of μ-Mesons from $K_{\mu 3}$ Decay. S. G. Matinian—757L.

On the Nonlinear Generalization of the Meson and Spinor Field Equations. D. F. Kurdgelaidze—941.

On the Possibility of Formulating a Meson Theory with Several Fields. A. D. Galanin—460.

On the Statistical Interpretations of Quantum Theory. R. L. Stratonovich— 1206.

Photon Green Function Accurate to e^4. S. N. Sokolov—1029L.

Possible Correlations in $\pi \rightarrow \mu \rightarrow e$-Decay. L. Okun' and A. Rudik—520L.

Reduction of the Two Nucleon Problem to a Single Nucleon Problem in the Nonrelativistic Range. Iu. V. Novozhilov—1030L.

Scale Transformation and the Virial Theorem in Quantum Field Theory. Iu. V. Novozhilov—138L.

The Nature of Field Fluctuations. M. M. Mirianashvili, V. V. Chavchanidze, and Iu. G. Mamaladze—1005L.

The Problem of Parity Non-conservation in Weak Interactions. B. L. Ioffe, L. B. Okun', and A. P. Rudnik — 328L.

Two-Electron Green Function in the Bloch-Nordsieck Approximation. R. V. Tevikian— 1284L.

Two Limiting Momenta in Scalar Electrodynamics. L. P. Gor'kov—167.

Two Possible Schemes of Non-Conservation of Parity in Weak Interactions. B. L. Ioffe—1015L.

Use of a Mixture of Two Liquids in Bubble Chambers. G. A. Blinov, Iu. S. Krestnikov, M. F. Lamanov, and Ia. Ia. Shalamov— 1281L.

Films, Properties

Concerning a Possible Method for the Polarization of a Proton Beam. E. K. Zavoiskii—328L.

Nuclear Interaction in a Photoemulsion at an Energy of 8×10^{13} ev. I. M. Gramenitskii, G. B. Zhdanov, E. A. Zamchalova and M. N. Shcherbakova—763L.

Structural Characteristics of Antimony Sulfide Layers. V. N. Vertsner, B. V. Gerbunov, and Ia. A. Oksman—782.

Fine Structure (see Atomic Structure and Spectra)

Fission of Nucleus (see Nuclear Fission)

Fluctuation Phenomena (see Noise)

Fluid Dynamics

- Explosion of a Metal by an Electric Current. S. V. Lebedev—243.
- Hydrodynamic Fluctuations. L. D. Landau and E. M. Lifshitz—512L.
- Hydrodynamics of Solutions of Two Superfluid Liquids. I. M. Khalatnikov—542.
- On Magnetohydrodynamic Waves and Magnetic Tangential Discontinuities in Relativistic Hydrodynamics. I. M. Khalatnikov—901.
- On the Structure of the Front of Strong Shock Waves in Gases. Iu. P. Raizer— 1242.
- Shock Waves of Large Amplitude in Air. Ia. B. Zel'dovich—919.
- Some New Possibilities of Ionic Phenomena in Metastable Liquids. G. A. Askar'ian—1011L.
- Structure of a Shock Wave in a Plasma. V. D. Shafranov—1183.

Fluorescence (see Luminescence)

Galvanomagnetic Effect (see Magnetic Properties)

Gamma Rays

- Diffractive Production of Proton-Antiproton Pairs by High-Energy Photons. A. G. Sitenko and L. N. Rozentsveig—330L.
- Experimental Comparison of the Energy Spectra of γ-Quanta from the Decay of π^0-Mesons Formed on Carbon and Lead Nuclei by 660 Mev Protons. Iu. D. Baiukov, A. N. Sinaev and A. Tiapkin—299L.
- Fission of U, Th, Bi and Tl Induced by High Energy γ-Quanta. E. V. Minarik and V Novikov—253.
- Investigation of the Energy and Angle Distribution of Neutral Pions Produced by 470 and 660 Mev Protons in Carbon. Iu. D. Baiukov, M. S. Kozodaev, and A. A. Tiapkin—552.
- Investigation of U^{235} Fission γ-Rays in the Energy Region up to 250 kev. V. V. Skliarevskii, D. E. Fomenko and E. P. Stepanov—220.
- Measurement of the Relative Intensities of γ-Lines by a Two-Meter Crystal Diffaction γ-Spectrometer. O. I. Sumbaev—170.
- Nuclear Photoeffect in Be^9 at High Energies. T. I. Kopaleishvili—1018L.
- Photodisintegration of Neon Nuclei. A. P. Komar and I. P. Iavor—508L.
- Production of Neutral Pions by Neutrons on Deuterons and Complex Nuclei. V. P Dzhelepov, K. O. Oganesian, and V. B. Fliagin—560.
- Soft 15 – 800 Kev Radiation Accompanying the Thermal Neutron Fission of Uranium. V. K. Voitovetskii, B. A. Levin and E. V. Marchenko—184.

Gases

- Contribution to the Theory of Transport Processes in a Plasma Located in a Magnetic Field. E. S. Fradkin—956.
- Explosion of a Metal by an Electric Current. S. V. Lebedev—243.
- Ignition of the High Voltage Discharge in Hydrogen at Low Pressures. A. S. Pokrovskaia-Soboleva and B. N. Kliarfel'd—812.
- Measurement of High Temperatures in Strong Shock Waves in Gases. I. Sh. Model'—589.
- On Magnetohydrodynamic Waves and Magnetic Tangential Discontinuities in Relativistic Hydrodynamics. I. M. Khalatnikov—901.
- On the Structure of the Front of Strong Shock Waves in Gases. Iu. P. Raizer— 1242.
- Shock Waves of Large Amplitude in Air. Ia. B. Zel'dovich—919.
- Structure of a Shock Wave in a Plasma. V. D. Shafranov—1183.

Gravitation (see Relativity and Gravitation)

Gyromagnetization (see Magnetic Properties)

Hall Effect (see Electrical Conductivity and Resistance; Semiconductors)

Helium, Liquid

- Hydrodynamics of Solutions of Two Superfluid Liquids. I. M. Khalatnikov—542.
- Oscillations in a Fermi Liquid. L. D. Landau—101.
- Separation of Helium Isotopes by Rectification and Thermo-Osmosis. V. M. Kuznetsov—819.
- The Thermodynamics of Liquid He^3. I. M. Khalatnikov and A. A. Abrikosov—745.
- Theory of Diffusion and Thermal Conductivity for Dilute Solutions of He^3 in Helium II. I. M. Khalatnikov and V. N. Zharkov—905.
- Theory of Kinetic Phenomena in Liquid He^3. A. A. Abrikosov and L. M. Khalatnikov—887.
- Visual Observation of the Stratification of Solutions of $He^3 - He^4$ Solutions. V. P. Peshkov and K. N. Zinov'eva—1024L.

High Voltage Tubes and Machines (see Methods and Instruments)

Hyperfine Structure (see Atomic Structure and Spectra; Nuclear Moments and Spin)

Hyperons (see Mesons and Hyperons)

Imperfections in Solids

- Investigation of the Penetrating Component of Electron-Nuclear Showers by the Delayed Coincidence Method in Conjunction with a Hodoscope. G. B. Zhdanov and A. A. Khaidarov—583.
- On the Exciton Mechanism of Capture of Current Carriers in Homopolar Semiconductors. V. L. Bonch-Bruevich—1196.
- Photoconductivity of Cuprite. A. N. Krongauz. V. K. Liapidevskii, and Iu. S. Deev—828.

Quantum States and Optical Transitions of the F^{2+} Center Electron. M. F. Deigen and V. L. Vinetskii—226.

Quantum States of Particles Coupled to a Harmonically Oscillating Continuum with Arbitrarily Strong Interaction, I. V. M. Buimistrov and S. J. Pekar—970.

Remarks on the Theory of the Electron Plasma in Semiconductors. V. L. Bonch-Bruevich—894.

The Effect of Fast Neutron Irradiation on the Recombination of Electrons and Holes in Germanium Crystals. V. S. Vavilov, A. V. Spitsyn, L. S. Smirnov and M. V. Chukichev—579.

Inelastic Scattering (see Nuclear Reactions; Scattering)

Instruments (see Methods and Instruments)

Internal Conversion (see Nuclear Spectra)

Ionization (see also Electrical Discharges, Range and Energy Loss of Particles)

Application of a Renormalized Group to Different Scattering Problems in Quantum Electrodynamics. V. Z. Blank—759L.

Calculation of the Drift Velocity of Ions in the Electric Field in Their Gas. V. I. Perel'—440.

Concerning a Possible Method for the Polarization of a Proton Beam. E. K. Zavoiskii—338L.

Electron Loss Probabilities for Multiply-Charged Ions. I. S. Dmitriev—473.

Ignition of the High Voltage Discharge in Hydrogen at Low Pressures. A. S. Pokrovskaia-Soboleva and B. N. Kliarfel'd—812.

Investigation of Slow Electron Emission Induced by High Energy Protons. E. S. Mironov and L. M. Nemenov—188.

Loss of Two Electrons In Single Collisions Between Negative Hydrogen Ions and Molecules of the Gas. Ia. M. Fogel', V. A. Ankudinov and R. E. Slabospitskii—382.

Measurement of High Temperatures in Strong Shock Waves in Gases. I. Sh. Model'—589.

On Magnetohydrodynamic Waves and Magnetic Tangential Discontinuities in Relativistic Hydrodynamics. I. M. Khalatnikov—901.

Some New Possibilities of Ionic Phenomena in Metastable Liquids. G. A. Askar'ian—1011L.

Structure of a Shock Wave in a Plasma. V. D. Shafranov—1183.

The Spatial Distribution of the Penetrating Component of Wide Atmospheric Showers. E. L. Andronikashvili and M. F. Bibilashvili—341L.

Ionization Potentials of Atoms (see Atomic Structure and Spectra)

Ions (see also Electrical Discharges)

Calculation of the Drift Velocity of Ions in the Electric Field in Their Gas. V. I. Perel'—440.

Concerning a Possible Method for the Polarization of a Proton Beam. E. K. Zavoiskii—338L.

Ejection of Electrons from Metals by Fast Molecules. A. M. Furman— 1302L.

Electron Loss Probabilities for Multiply-Charged Ions. I. S. Dmitriev—473.

Fission of Nuclei Under the Influence of Accelerated Nitrogen Ions. V. A. Druin, S. M. Polikanov and G. N. Flerov—1059.

Ignition of the High Voltage Discharge in Hydrogen at Low Pressures. A. S. Pokrovskaia-Soboleva and B. N. Kliarfel'd—812.

Investigation of Slow Electron Emission Induced by High Energy Protons. E. S. Mironov and L. M. Nemenov—188.

Loss of Two Electrons in Single Collisions Between Negative Hydrogen Ions and Molecules of the Gas. Ia. M. Fogel', V. A. Ankudinov and R. E. Slabospitskii—382.

On Low-Frequency Oscillations in the Plasmas of Electro-Negative Gases. M. V. Koniukov—429.

On the Interaction Between Lithium Ions and Matter. Ia. A. Teplova, I. S Dmitriev, V. S. Nikolaev, and L. N. Fateeva—797.

Some New Possibilities of Ionic Phenomena in Metastable Liquids. G. A. Askar'ian—1011L.

Structure of a Shock Wave in a Plasma. V. D. Shafranov—1183.

The Applicability of the Relation of Detailed Balance for a Cluster of Ions of Stationary Composition. Ia. M. Fogel'—499L.

Ions and Electrons, Mobility

Contribution to the Theory of Transport Processes in a Plasma Located in a Magnetic Field. E. S. Fradkin—956.

Investigation of Slow Electron Emission Induced by High Energy Protons. E. S. Mironov and L. M. Nemenov—188.

Motion of a Rarefied Plasma in a Variable Magnetic Field. Ia. P. Terletskii—755L.

Ponderomotive Forces in a Localized Plasma in the Electromagnetic Field of a Plane Wave. V. V. Iankov—753L.

Simplification of the Equations for the Distribution Function of Electrons in a Plasma. A. V. Gurevich—1006L.

Isobars (see Atomic Mass and Abundance)

Isomers, Nuclear (see Nuclear Spectra)

Isotopes (see Atomic Mass and Abundance; Radioactivity)

Kerr Effect (see Optical Properties)

Liquid Helium (see Helium, Liquid)

Liquids
An Experiment on the Measurement of Viscosity of an Expanded Liquid. A. P. Toropov and A. I. Kitova—315L.
Hydrodynamics of Solutions of Two Superfluid Liquids. I. M. Khalatnikov—542.
Oscillations in a Fermi Liquid. L. D. Landau—101.
Some New Possibilities of Ionic Phenomena in Metastable Liquids. G. A. Askar'ian—1011L.
Theory of Kinetic Phenomena in Liquid He^3. A. A. Abrikosov and L. M. Khalatnikov—887.
Luminescence
Structural Characteristics of Antimony Sulfide Layers. V. M. Vertsner, B. V. Gorbunov, and Ia. A. Oksman—782.
Magnetic Fields (see Electromagnetic Theory and Electrodynamics)
Magnetic Properties
Concerning a Possible Method for the Polarization of a Proton Beam. E. K. Zavoiskii—328L.
Concerning the Saturation of the Hall "Constant" in Semiconductors Located in Strong Magnetic Fields. F. G. Bass and M. I. Kaganov—1002.
Dependence of the Polarization of $(D + D)$-Neutrons on the Energy of the Deuterons. I. I. Levintov, A. V. Miller, E. Z. Tarumov, and V. N. Shamshev—310L.
Extension of the Spin-Wave Model to the Case of Several Electrons Surrounding Each Site. Iu. A. Iziumov—866.
Magnetic Interaction of Electrons and Anomalous Diamagnetism. B. T. Geilikman—981.
Magnetic Properties of the Oxides of Manganese at Temperatures from 20 to 300°K. A. S. Borovik-Romanov and M. P. Orlova—1023L.
On the Magnetic Properties of Superconductors of the Second Group. A. A. Abrikosov—1174.
On the Mechanism of Fission of Heavy Nuclei. V. V. Vladimirskii—673.
Paramagnetic Absorption in Some Manganese Salts in Parallel Fields at Super-High Frequencies. A. I. Kurushin—766L.
Quantum Theory of the Electrical Conductivity of Metals in a Magnetic Field. I. M. Lifshitz— 1227.
s–d Exchange in Ferromagnetic Metals. F. M. Gal'perin—321L.
The Hall Effect in Bismuth at Pressures up to 30,000 kg/cm^2. A. I. Likhter and L. F. Vereshchagin—511L.
The Theory of Ferromagnetism of Metals and Alloys at Low Temperatures. E. I. Kondorskii and A. S. Pakhomov—269.
The Thermodynamics of Liquid He^3. I. M. Khalatnikov and A. A. Abrikosov—745.
Theory of Cyclotron Resonance in Metals. M. Ia. Azbel' and E. A. Kaner—730.
Thermal Radiation from an Anisotropic Medium. F. V. Bunkin—665.
Thermodynamical Theory of "Weak" Ferromagnetism in Antiferromagnetic Substances. I. E. Dzialoshinkii—1259.
Magnetic Resonance
Double Absorption Peaks in Electron Resonance at Saturation. N. S. Garif'ianov—503L.
On the Possibility of Observing the Variation of the Chemical Potential of Electrons of a Metal in a Magnetic Field. M. I. Kaganov, I. M. Lifshitz and K. D. Sinel'nikov—500L.
Paramagnetic Absorption at High Frequencies in Gadolinium Salts in Parallel Fields. A. I. Kurushin—601.
Paramagnetic Resonance and Polarization of Nuclei in Metals. M. Ia. Azbel', V. I. Gerasimenko, and I. M. Lifshitz—986.
Second Relaxation in a Spin System at Room Temperature. P. G. Tishkov—514L.
Temperature Dependence of the Overhauser Effect in Metallic Lithium. N. A. Bekeshko and E. I. Kondorskii—505L.
The Thermodynamics of Liquid He^3. I. M. Khalatnikov and A. A. Abrikosov—745.
Theory of Cyclotron Resonance in Metals. M. Ia Azbel' and E. A. Kaner—730.
Magneto-Optical Effects (see Optical Properties)
Magnetoresistance (see Electrical Conductivity and Resistance; Semiconductors)
Magnetostriction (see Magnetic Properties)
Mass Spectroscopy (see Methods and Instruments)
Mathematical Methods
Angular Operators for Nuclear Reactions. V. I. Ritus— 1249.
Contribution to the Theory of Collective Motion of Particles in Quantum Mechanical Systems. V. M. Eleonskii and P. S. Zyrianov—432.
Electrical, Optical and Elastic Properties of Diamond Type Crystals. I. V. S. Mashkevich and K. B. Tolpygo—435.
Equations with Variational Derivatives in Statistical Equilibrium Theory. I. P. Bazarov—872.
Green Function in Scalar Electrodynamics in the Bloch-Nordsieck Approximation. R. V. Tevikian—1284L.
Minani Transformation for Nucleon-Nucleon Scattering. R. M. Ryndin and Ia. A. Snerodinskii—976.
Multiple Interaction Hamiltonians in Quantum Electrodynamics. G. F. Filimonov and Iu. M. Shirokov—84.

On the Construction of the Scattering Matrix II. The Theory with Nonlocal Interaction. B. V. Medvedev—48.
On the Nonlinear Generalization of the Meson and Spinor Field Equations. D. F. Kurdgelaidze—941.
Polarization Correlation in Nucleon-Nucleon Scattering. A. G. Zimin—996.
Possibility of Constructing a Chain of Equations for Model Operators. V. M. Eleonskii.
Simplification of the Equations for the Distribution Function of Electrons in a Plasma. A. V. Gurevich—1006L.
The Construction of a Phenomenological Scattering Matrix with Nonlocal Interaction. V. S. Barashenkov—313L.
Two-Electron Green Function in the Bloch-Nordsieck Approximation. R. V. Tevikian— 1282L.
Measurements (see Methods and Instruments)
Mechanics
An Experiment on the Measurement of Viscosity of an Expanded Liquid. A P. Toropov and A. I. Kitova—315L.
Application of the Dirac-Fok-Podolskii Method to a Mechanical Many-Body Problem. I. G. Fikhtengolts—1144.
Moment of Inertia of a System of Interacting Particles. A. S. Davydov and G. F. Filippov—676.
On the Dependence of the Motion of Bodies in a Gravitational Field on Their Mass. I. G. Fikhtengolts—898.
On the Theory of Scattering of Particles by Nuclei. I. G. Ivanter and L. B. Okun'—340L.
Optical Contact of Polished Glass Surfaces. I. V. Obreimov and E. S. Trekhov—235.
Some Relativistic Properties of the Behavior of Spin-½ Particles. P. E. Kunin and I. M. Taksar—426.
Mechanics, Quantum (see Quantum Mechanics)
Mechanics, Quantum – Atomic Structure and Spectra (see Atomic Structure and Spectra)
Mechanics, Quantum – of Solid Bodies (see Crystalline State)
Mechanics, Statistical (see Statistical Mechanics and Thermodynamics)
Meson Field Theory (see Field Theory)
Mesons and Hyperons (see also Cosmic Radiation; Elementary Particle Interactions; Nuclear Reactions Induced by Meson; Scattering of Mesons)
A Physical Model of the Hyperon. Gesa D'erdi (Gyorgi)—152L.
Angular and Energy Distributions of Photoprotons from Be^9 and 0^{12}. I. V. Chuvilo and V. G. Shevchenko—1090.
Anomalous Decay of a Hypernucleus. A. P. Grigor'ev, E. P. Toporkova, and A. I. Fesenko— 1299L.
Asymptotic Meson-Meson Scattering Theory. I. T. Diatlov, V. V. Sudakov, and K. A. Ter-Martirosian—631.
Conservation Laws in Weak Interactions. L. D. Landau—336L.
Correlations in $\pi \to \mu \to e$-Decay. A. O. Vaisenberg and V. A. Smirnitskii—1093.
Decay of the τ-Meson. I. N. Mikhailov—265.
Derivation of the Low Equation in the Theory of Meson Scattering. A. M. Brodskii—509L.
Determination of Mass of Slow Charged Particles in Photographic Plates. M. I. Tret'iakova—1045.
Dispersion Relations for Photoproduction of Pions on Nucleons. A. A. Logunov and A. N. Tavkhelidze—1134.
Elastic Scattering of 360 Mev Positive π-mesons by Protons. N. A. Mitin and E. L. Grigor'ev—378.
Electron-Positron Pair Production in Collisions Between Fast Pions and Nucleons. E. M. Rabinovich—1272.
Energy Spectrum of μ-Mesons in Extensive Atmospheric Cosmic Ray Showers. O. I. Dovzhenko. B. A. Nelepo and S. I. Nikol'skii—391.
Experimental Comparison of the Energy Spectra of γ-Quanta From the Decay of π^0-Mesons Formed on Carbon and Lead Nuclei by 660 Mev Protons. Iu. D. Baiukov, A. N. Sinaev and A. Tiapkin—299L.
Generation of Slow Mesons by Cosmic Ray Particles. D. K. Kaipov and Zh. S. Takibaev—569.
Inelastic Proton-Proton Scattering. Iu. I. Kulakov—477.
Investigation of the Energy and Angle Distribution of Neutral Pions Produced by 470 and 660-Mev Protons in Carbon. Iu. D. Baiukov, M. S. Kozodaev and A. A. Tiapkin—552.
Investigation of the Penetrating Component of Electron-Nuclear Showers by the Delayed Coincidence Method in Conjunction with a Hodoscope. G. B. Zhdanov and A. A. Khaidarov—583.
Measurement of the Relative Intensities of γ-Lines by a Two-Meter Crystal Diffraction γ-Spectrometer. O. I. Sumbaev—170.
Mesonic Decay of a Tritium Hyperfragment. A. O. Vaisenberg and V. A. Smirnitskii—607.
Momentum Spectrum of the Cosmic Radiation and the Positive Excess in the $(0.1-2.5) \times 10^9$ ev/c Range at an Altitude of 3250 m. A. O. Vaisenberg—352.
Nuclear Interaction in a Photoemulsion at an Energy of 8×10^{13} ev. I. M. Gramenitskii, G. B. Zhdanov, E. A. Zamchalova and M. N. Shcherbakova—763L.
On the Energy Spectrum of μ-Mesons in $K_{\mu 3}$ Decay. S. G. Matinian—757L.
Non-conservation of Parity and Hyperon Decay. S. G. Matinian—1017L.
On the Nonlinear Generalization of the Meson and Spinor Field Equations. D. F. Kurgelaidze—941.

On the Problem of K^0 Decays. I. Iu. Kobzarev—125L.

On the Question of the Spin and Parity of the τ-Meson. I. S. Shapiro, I. E. Dolinskii and A. P. Mishakova—129L.

On the Structure of Nucleons. I. E. Tamm—154L.

On the Theory of Scattering of Particles by Nuclei. I. G. Ivanter and L. B. Okun—340L.

On the Theory of "Strange" Particles. V. I. Karpman—767L.

Pion Production in Zero Isotopic Spin Nuclei. A. G. Meshkovskii, Iu. S. Pligin, Ia. Ia. Shalamov, and V. A. Shebanov—1085.

Polarization of Electrons in β-Decay. A. I. Alikhanov, G. P. Eliseev, V. A. Liubimov, and B. V. Ershler—1079.

Possible Correlations in $\pi\to\mu\to e$-Decay. L. Okun' and A. Rudik—520L.

Possible Properties of the Neutrino Spin. L. D. Landau—337L.

Production of Neutral Pions by Neutrons on Deuterons and Complex Nuclei. V. P. Dzhelepov, K. O. Oganesian and V. B. Fliagin—560.

Production of π^+-Mesons in p–p Collisions at 480–660 Mev. B. S. Neganov and O. V. Savchenko—1033.

Reactions Produced by μ-Mesons in Hydrogen. Ia. B. Zel'dovich and A. D. Sakharov—775L.

Resonant Pion-Nucleon Interaction and Production of Pions by Nucleons. L. M. Soroko—927.

Scattering of K-Mesons with Change of Intrinsic Parity. V. B. Bereststskii and Iu. A. Bychkov—150L.

Scattering of π-Mesons on Nucleons in Higher Approximations of the Tamm–Dancoff Method. Iu. M. Popov—131L.

Scattering of Photons by Protons. A. M. Baldin and V. A. Petrun'kin— 1279L.

Simultaneous Creation of λ and θ Particles. I. Iu. Kobzarev and L. B. Okun'—761L.

Some Remarks on Slow Processes of Transformation of Elementary Particles. L. Okun' and B. Pontecorvo — 1297L.

Structural Characteristics of Antimony Sulfide Layers. V. N. Vertsner, B. V. Gerbunov, and Ia. A. Oksman—782.

The μ-Decay of K-Particles and Hyperons. L. B. Okun'—334L.

The Lifetime of the Two Forms of the π^0-Meson. A. V. Romankevich—509L.

The Penetrating Component of Extensive Cosmic-Ray Showers in the Atmosphere. Iu. N. Vavilov, Iu. F. Evstigneev, and S. I. Nikol'skii—1078.

The Problem of Parity Non-conservation in Weak Interaction. B. L. Ioffe, L. B. Okun' and A. P. Rudik—328L.

The Threshold of "Creation" and the Threshold of "Generation" of Negative K-Particles. M. Danysh and B. Pontecorvo—325L.

Two Possible Schemes of Non-conservation of Parity in Weak Interactions. B. L. Ioffe—1015L.

Vacuum Polarization in Mesonic Atoms. G. E. Pustovalov— 1234.

Metals (see Crystalline State)

Metastable Atoms (see Atomic Structure and Spectra)

Methods and Instruments

An Experiment on the Measurement of Viscosity of an Expanded Liquid. A. P. Toropov and A. I. Kitova—315L.

Coherent Scattering and Radiation of Electromagnetic Waves by a Plasma in an Inhomogeneous Magnetic Field. G. A. Askarian— 1285L.

Determination of Mass of Slow Charged Particles in Photographic Plates. M. I. Tret'iakova—1045.

Fission of Nuclei Under the Influence of Accelerated Nitrogen Ions. V. A. Druin, S. M. Polikanov and G. N. Flerov—1059.

Heat Capacity of Laminar Lattices at Low Temperatures. E. S. Itskevich and P. G. Strelkov—394.

Investigation of the Penetrating Component of Electron-Nuclear Showers by the Delayed Coincidence Method in Conjunction with a Hodoscope. G. D. Zhdanov and A. A. Khaidarov—583.

Investigation of U^{235} Fission γ-Rays in the Energy Region up to 250 kev. V. V. Skliarevsky, D. E. Fomenko, and E. P. Stepanov—220.

Measurement of High Temperatures in Strong Shock Waves in Gases. I Sh. Model'—589.

Measurement of the $C^{12}(p, \gamma)$ and $C^{12}(d, n)$ Effective Cross Sections for Low Energy Bombarding Particles. A. S. Deineko, A. Ia. Taranov and A. K. Val'ter—201.

Neutron Emission by Excited RaD Nuclei. A. V. Kogan and L. I. Rusinov—365.

On Bubble Chambers. P. V. Vavilov— 1276L.

On the Nature of the Cone-Like Shape of Tracks of Multi-Charged Ions in Nuclear Emulsions. O. V. Lozhkin—293.

Paramagnetic Absorption at High Frequencies in Gadolinium Salts in Parallel Fields. A. I. Kurushin—601.

Possibilities of Focusing in a Linear Accelerator with the Aid of Traveling Waves. V. S. Tkalich—518L.

Production of Very Strong Magnetic Fields by Rapid Compression of a Conducting Shell. Ia. P. Terletskii—301L.

Reflection of Gamma Rays from Bent Quartz Plates. G. I. Sumbaev—1042.

Separation of Helium Isotopes by Rectification and Thermo-Osmosis. V. M. Kuznetsov—819.

Some New Possibilities of Ionic Phenomena in Metastable Liquids. G. A. Askar'ian—1011L.

The Effect of Fast Neutron Irradiation on the Recombination of Electrons and Holes in Germanium Crystals. V. S. Vavilov, A. V. Spitsyn, L. S. Smirnov and M. V. Chukichev—579.

Use of a Mixture of Two Liquids in Bubble Chambers. G. A. Blinov, Iu. S. Krestnikov, M. F. Lomanov, and Ia. Ia. Shalamov— 1281L.

Microwaves

Energy Loss of a Charged Particle Passing Through a Laminar Dielectric, I. Ia. B. Fainberg and N. A. Khizhniak—720.

Theory of Cyclotron Resonance in Metals. M. Ia. Azbel' and E. L. Kaner—730.

Natural Line Widths of Microwaves. V. M. Fain—501L.

Miscellaneous

Dependence of the Taper Length of Emulsion Tracks on Particle Charge. C. V. Viktorov and M. Z. Maksimov—42.

Ejection of Electrons from Metals by Fast Molecules. A. M. Furman— 1302L.

Electron Emission from Dielectric Films Bombarded by Positive Hydrogen Ions. V. Z. Surkov—7.

Energy Distribution of Neutrons Emitted from Beryllium Bombarded by 680 Mev Protons. V. Kiselev and V. B. Fliagin—786.

Equilibrium Distribution of Nitrogen Ion Charges. V. S. Nikolaev, L. N. Fateeva, I. S. Dmitriev, and Ia. A. Teplova—789.

Excitation of Betatron Oscillations by Synchrotron Momentum Oscillations in a Strong Focusing Accelerator. Iu. F. Orlov—45.

Excitation of Rotational States in α-Decay of Even-Even Nuclei. V. M. Strutinski—1150.

Level Shift of π-Mesonic Atoms. S. M. Bilen'kii—517L.

Nonlinear Theory of Betatron Oscillations in a Strong Focusing Synchrotron. Iu. F. Orlov—195.

On the Fluctuation Resolution Limit of an Optical Modulation Interferometer. S. M. Kozel—609.

Optical Contact of Polished Glass Surfaces. I. V. Obreimov and R. S. Trekhov—235.

Possibilities of Focusing in a Linear Accelerator with the Aid of Traveling Waves. V. S. Tkalich—518L.

Production of Proton-Antiproton Pairs by High Energy γ-Quanta. Iu. A. Vdovin—452.

Some Remarks on the Validity of the Hydrodynamic Description of Quantum States. D. I. Blokhintsev—286.

Structural Characteristics of Antimony Sulfide Layers. V. N. Vertsner, B. V. Gorbunov and Ia. A. Oksman—782.

Molecular Aggregates

Reactions Produced by μ-Mesons in Hydrogen. Ia. B. Zel'dovich and A. D. Sakharov—775L.

Molecular Structure and Spectra

Dipole Moment of the HDSe Molecule. V. G. Veselago —513L.

Measurement of High Temperatures in Strong Shock Waves in Gases. I. Sh. Model'—589.

Moments, Nuclear (see **Nuclear Moments and Spin**)

Neutrino

Correlation in $\pi\to\mu\to e$-Decays. A. O. Vaisenberg and V. A. Smirnitskii—1093.

Polarization Effects in the Scattering of Electrons and Positrons by Electrons. A. A. Kresnin and L. N. Rosentsveig—288.

Polarization of Electrons in β-Decay. A. I. Alikhanov, G. P. Eliseev, V. A. Liubimov, and B. V. Ershler—1097.

Possible Properties of the Neutrino Spin. L. D. Landau —337L.

The μ-Decay of K-Particles and Hyperons. L. B. Okun' —334L.

The Problem of Parity Non-conservation in Weak Interaction. B. L. Ioffe, L. B. Okun' and A. P. Rudik—328L.

Neutrons (see **Elementary Particle Interaction**)

Noise

On the Fluctuation Resolution Limit of an Optical Modulation Interferometer. S. M. Kozel—609.

Nuclear Fission

Concerning One Method of Measuring the Lifetimes of Excited States of Atomic Nuclei. A. F. Tulinov—1277L.

Fission of Nuclei Under the Influence of Accelerated Nitrogen Ions. V. A. Druin, S. M. Polikanov and G. N. Flerov—1059.

Interaction of Nitrogen and Gold Nuclei. S. A. Baraboshkin, A. S. Karamian and G. N. Flerov—1055.

Investigation of U^{235} Fission γ-Rays in the Energy Region up to 250 kev. V. V. Skliarevsky, D. E. Fomenko and E. P. Stepanov—220.

Measurement of the Relative Intensities of γ-Lines by a Two-Meter Crystal Diffraction-Spectrometer. O. I. Sumbaev—170.

Moment of Inertia of a System of Interacting Particles. A. S. Davydov and G. F. Fillipov—676.

Neutron Emission by Excited RaD Nuclei. A. V. Kogan and L. I. Rusinov—365.

On the Mechanism of Fission of Heavy Nuclei. V. V. Vladimirskii—673.

Soft 15 – 800 Kev Radiation Accompanying the Thermal Neutron Fission of Uranium. V. K. Voitovsetskii, B. A. Levin, and E. V. Marchenko—184.

Nuclear Forces (see **Elementary Particle Interactions; Field Theory; Nuclear Structure Theory**)

Nuclear Induction (see **Magnetic Resonance**)

Nuclear Moments and Spin

Concerning Even-Even Nuclei Having the Characteristic 2+ for the Second Excited State. N. N. Deliagin and V. S. Shipnel'—309L.

Conservation Laws in Weak Interactions. L. D. Landau—336L.

Dependence of the Polarization of (D^+D) Neutrons on the Energy of the Deuterons. I. I. Levintov, A. V. Miller, E. Z. Tarumov and V. N. Shamshev—310L.

Moment of Inertia of a System of Interacting Particles. A. S. Davydov and G. F. Filippov—676.

On the Structure of Nucleons. I. E. Tamm—154L.

Particle with Spin $^3/_2$ in an Electromagnetic Field. E. E. Fradkin—298L.

Reactions Produced by μ-Mesons in Hydrogen. Ia. B. Zel'dovich and A. D. Sakharov—775L.

Nuclear Photoeffects

Angle-Energy Distribution of Photoneutrons From Bi. G. N. Zatsepin, L. I. Lazareva and A. N. Pospelov—21.

Angular and Energy Distribution of Photoprotons from Be^9 and C^{12}. I. V. Chuvilo and V. G. Shevchenko—1090.

Pion Production in Zero Isotopic Spin Nuclei. A. G. Meshkovski, Iu. S. Pligin, Ia. Ia. Shalamov, and V. A. Shebanov—1085.

Dispersion Relations for Photoproduction of Pions on Nucleons. A. A. Logunov and A. N. Tavkhelidze—1134.

Investigation of the (γ, p) Reaction in Zinc. R. M. Osokina and B. S. Ratner—1.

Measurement of the Relative Intensities of γ-Lines by a Two-Meter Crystal Diffraction γ-Spectrometer. O. I. Sumbaev—170.

Neutron Emission by Excited RaD Nuclei. A. V. Kogan and L. I. Rusinov—365.

Nuclear Photoeffect in Be^9 at High Energies. T. I. Kopaleishvili—1018L.

Photodisintegration of Neon Nuclei. A. P. Komar and I. P. Iavor—508L.

Some Sum Rules for the Cross Sections of Electric Quadrupole Transitions in the Nuclear Photoeffect. Iu. K. Khokhlov—88.

Nuclear Reactions, General

Angular Operators for Nuclear Reactions. V. I. Ritus—1249.

Angular Distribution of the Products of the $S^{32}(d, p)S^{33}$ Reaction. I. B. Teplov, B. A. Iur'ev, and T. N. Markelov—134L.

Concerning One Method of Measuring the Lifetimes of Excited States of Atomic Nuclei. A. F. Tulinov—1277L.

Dependence on the Polarization of (D^+D) Neutrons on the Energy of the Deuterons. I. I. Levintov, A. V. Miller, E. Z. Tarumov and V. N. Shamshev—310L.

Distintegration of Light Nuclei in a Coulomb Field. V. I. Mamasakhlisov and G. A. Chilashvili—661.

Disintegration of Silver and Bromine Nuclei by High Energy Protons. V. I. Ostroumov—12.

Fission of Nuclei Under the Influence of Accelerated Nitrogen Ions. V. A. Druin, S. M. Polikanov and G. N. Flerov—1059.

Inelastic Interaction of Protons Having Energies Above 7 Bev with Carbon and Hydrogen Nuclei. K. I. Alekseeva and N. L. Grigorov—339L.

Interaction of Nitrogen and Gold Nuclei. S. A. Baraboshkin, A. S. Karamian, and G. N. Flerov—1055.

Investigation of Conversion Lines in the β-Spectrum of a $Eu^{152} - Eu^{154}$ Mixture. V. M. Kel'man, V. A. Romanov, R. Ia. Metskhvarishvili, and V. A. Koliunov—24.

Investigation of the Excitation Functions for the Reactions $C^{12}(p, pn)C^{11}$, $Al^{29}(p, 3pn)Na^{24}$, and $Al^{29}(p, 3p3n)Na^{22}$ in the 150 – 660 Mev Energy Range. Iu. D. Prokoshkin and A. A. Tiapkin—148L.

Investigation of U^{235} Fission γ-Rays in the Energy Region up to 250 kev. V. V. Skliarevsky, D. E. Fomenko and E. P. Stepanov—220.

Measurement of the $C^{12}(p, \gamma)$ and $C^{12}(d, n)$ Effective Cross Sections for Low Energy Bombarding Particles. A. S. Deineko, A. Ia. Taranov and A. K. Val'ter—201.

On the Angular Distribution of Deuterons from the $Be^9_4(p, d)Be^8_4$ Reaction. D. D. Grechukhin—1188.

On the Absolute Value of the Stripping Cross Section for Diffraction Disintegration of the Deuteron. I. I. Ivanchik—133L.

Photodisintegration of Neon Nuclei. A. P. Komar and I. P. Iavor—508L.

Polarization in Reverse Reactions. A. I. Baz'—521L.

Relation Between Scattering and Multiple Particle Production. S. Z. Belenkii—952.

Reactions Involving Polarized Particles. M. I. Shirokov—835.

Some Problems Related to the Statistical Theory of Multiple Production of Particles. V. M. Maksimenko and I. L. Rozental'—546.

The Application of the Microcanonical Distribution to the Statistical Theory of Multiple Production of Particles. V. B. Magalinskii and Ia. P. Terletskii—483.

Nuclear Reactions Induced by α-Particles and He^3

Neutron Emission by Excited RaD Nuclei. A. V. Kogan and L. I. Rusinov—365.

On the Angular Distribution of Deuterons from the $Be^9_4(pd)Be^8_4$ Reaction. D. P. Grechukhin—1188.

Nuclear Reactions Induced by Deuterons and Tritons

A New Method for Measurement of Polarization of Medium Energy Neutrons and the Phase Shift Analysis of n-He^4. I. I. Levintov, A. V. Miller and V. N. Shamshev—258.

Angular Distribution of the Products of the $S^{32}(d, p)S^{33}$ Reaction. I. B. Teplov, B. A. Iur'ev and T. N. Markelova—134L.

Derivation of the Formula for the Cross Section for Formation of High Energy Neutrons in Deuteron-Nuclei Collisions. V. S. Anastasevich—520L.

Energy and Angular Distribution of Neutrons Emitted in the $Be^9(d, n)B^{10}$ Reaction. A. I. Shpetnyi—357.

Hydrodynamics of Solutions of Two Superfluid Liquids. I. M. Khalatnikov—542.

Investigation of the Energy Levels of the F^{20} Nucleus by Magnetic Analysis. L. M. Khromchenko—231.

Measurement of the $C^{32}(p, \gamma)$ and $C^{12}(d, n)$ Effective Cross Sections for Low Energy Bombarding Particles. A. S. Deineko, A. Ia. Taranov and A. K. Val'ter—201.

On the Absolute Value of the Stripping Cross Section for Diffraction Disintegration of the Deuteron. I. I. Ivanchik—133L.

Nuclear Reactions Induced by Mesons (see also **Elementary Particle Interactions; Scattering of Mesons**)

Reactions Produced by μ-Mesons in Hydrogen. Ia. B. Zel'dovich and A. D. Sakharov—775L.

Some Problems Related to the Statistical Theory of Multiple Production of Particles. V. M. Maksimenko and I. L. Rozental'—546.

Nuclear Reactions Induced by Neutrons

Bremmstrahlung and Pair Production at High Energies in Condensed Media. A. B. Migdal—527.

Excitation of Rotational States in the Interaction Between Neutrons and Nuclei. V. N. Gribov—688.

Fission of Nuclei Under the Influence of Accelerated Nitrogen Ions. V. A. Druin, S. M. Polikanov, and G. N. Flerov—1059.

Fission of U, Th, Bi and Tl Induced by High Energy γ-Quanta. E. V. Minarik and V. A. Novikov—253.

Generation of Slow Mesons by Cosmic Ray Particles. D. K. Kaipov and Zh. S. Takibaev—569.

Investigation of the Penetrating Component of Electron-Nuclear Showers by the Delayed Coincidence Method in Conjunction with a Hodoscope. G. B. Zhdanov and A. A. Khaidarov—583.

Model of a Semi-Transparent Nucleus with a Diffuse Boundary. II. P. E. Nemirovskii—932.

Optical Model of the Interaction of Nucleons with Nuclei in the Resonance Region of the Compound Nucleus. V. M. Agranovich and A. S. Davydov—1164.

Production of Neutral Pions by Neutrons on Deuterons and Complex Nuclei. V. P. Dzhelepov, K. O. Oganesin and V. B. Fliagin—560.

Soft γ-Rays Emitted by Nuclei in the Capture of Thermal Neutrons. I. V. Estulin, L. F. Kalinkin and A. S. Melioranskii—801.

Soft 15 – 800 Kev Radiation Accompanying the Thermal Neutron Fission of Uranium. V. K. Voitovetskii, B. A. Levin and E. V. Marchenko—184.

The Effect of Neutron Irradiation on the Compressibility of Metals. A. I. Likhter and A. I. Kikoin—772L.

Nuclear Reactions Induced by Protons

Angular and Energy Distributions of Protons Produced in the Photodisintegration of Be^9 and O^{12}. I. V. Chuvilo and V. G. Shevchenko—1090.

Disintegration of Silver and Bromine Nuclei by High Energy Protons. V. I. Ostroumov—12.

Experimental Comparison of the Energy Spectra of γ-Quanta from the Decay of π^0-Mesons Formed on Carbon and Lead Nuclei by 660 Mev Protons. Iu. D. Baiukov, A. N. Sinaev and A. Tiapkin—299L.

Generation of Slow Mesons by Cosmic Ray Particles. D. K. Kaipov and Zh. S. Takibaev—569.

Inelastic Interaction of Protons Having Energies Above 7 Bev with Carbon and Hydrogen Nuclei. K. I. Alekseeva and N. L. Grigorov—339L.

Investigation of the Energy and Angle Distributions of Neutral Pions Produced by 470 and 660 Mev Protons in Carbon. Iu. D. Baiukov, M. S. Kozodaev and A. A. Tiapkin—552.

Investigation of the Excitation Functions for the Reactions $C^{12}(p, pn)C^{11}$, $Al^{27}(p, 3pn)Na^{24}$, and $Al^{27}(p, 3p3n)Na^{22}$ in the 150 – 660 Mev Energy Range. Iu. D. Prokoshkin and A. A. Tiapkin—148L.

Investigation of the Penetrating Component of Electron-Nuclear Showers by the Delayed Coincidence Method in Conjunction with a Hodoscope. G. B. Zhdanov and A. A. Khaidarov—583.

Measurement of the $C^{12}(p, \gamma)$ and $C^{12}(d, n)$ Effective Cross Sections for Low Energy Bombarding Particles. A. S. Deineko, A. Ia. Taranov and A. K. Val'ter—201.

On the Angular Distribution of Deuterons from the $Be^9_4(pd)Be^8_4$ Reaction. D. D. Grechukhin—1183.

Pion Production in Zero Isotopic Spin Nuclei. A. G. Meshkovskii, Iu. S. Pligin, Ia. Ia. Shalamov, and V. A. Shebanov—1085.

Polarization Correlation in Nucleon-Nucleon Scattering. A. G. Zimin—996.

Reactions Produced by μ-Mesons in Hydrogen. Ia. B. Zel'dovich and A. D. Sakharov—775L.

Resonant Pion-Nucleon Interaction and Production of Pions by Nucleons. L. M. Soroko—927.

Nuclear Scattering (see Scattering)

Nuclear Spectra (see also Nuclear Reactions; Radioactivity)

- Application of Correlation Polarization in the Phase Analysis of p–p Scattering. A. G. Zimin—1008L.
- Electric Monopole Transitions in Nuclei with Odd Mass Numbers. L. K. Peker and L. A. Sliv—515L.
- Energy and Angular Distribution of Neutrons Emitted in the $Be^9(d, n)B^{10}$ Reaction. A. I. Shpetnvi—357.
- Fine Structure of the α-Spectra of U^{234} and U^{238}. B. A. Bochagov, A. P. Komar, and G. E. Kocharov—1026L.
- Hydrodynamics of Solutions of Two Superfluid Liquids. I. M. Khalatnikov—542.
- Internal Conversion Coefficient of the 53 kev Gamma Radiation on the L Shell of Th^{230}. A. A. Vorob'ev, V. A. Korolev, A. P. Komar, and D. M. Seliverstov—516L.
- Internal Conversion Electron Spectrum of Radiothorium. II. A. I. Zhernovoi, E. M. Krisiuk, G. D. Latyshev, A. S. Remennyi, A. G. Sergeyev, and V. I. Fadeev—563.
- Investigation of Conversion Lines in the β-Spectrum of a $Eu^{132}-Eu^{154}$ Mixture. V. M. Kel'man, V. A. Romanov, R. Ia. Metskhvarishvili, and V. A. Kol'unov—24.
- Investigation of the Energy Levels of the F^{20} Nucleus by Magnetic Analysis. L. M. Khromchenko—231.
- Investigation of U^{235} Fission γ-Rays in the Energy Region up to 250 kev. V. V. Skliarevsky, D. E. Fomenko and E. P. Stepanov—220.
- On a Method of Direct Computation of the Nucleon-Nucleon Interaction Hamiltonian on the Basis of Experimental Values for the Levels of Light Nuclei. Iu. M. Shirokov, V. V. Balashov, and K. A. Tumanov—136L.
- On the Interaction Between Lithium Ions and Matter. Ia. A. Teplova, I. S. Dmitriev, V. S. Nikolaev, and L. N. Fateeva—792.
- Soft 15 – 800 Kev Radiation Accompanying the Thermal Neutron Fission of Uranium. V. K. Voitovetskii, B. A. Levin and E. V. Marchenko—184,
- Soft γ-Rays Emitted by Nuclei in the Capture of Thermal Neutrons. I. V. Estulin, L. F. Kalinkin and A. S. Melioranskii—801.
- The Alpha Decay of Pu^{239}. G. I. Novikova, L. N. Kondrat'ev, Iu. P. Sobolev, and L. L. Gol'din—832.

Nuclear Structure Theory

- Angle-Energy Distribution of Photoneutrons from Bi. G. N. Zatsepina, L. E. Lazareva, and A. N. Pospelov—21.
- Concerning Even-Even Nuclei Having the Characteristic 2^+ for the Second Excited State. N. N. Deliagin and V. S. Shipnel'—309L.
- Disintegration of Light Nuclei in a Coulomb Field. V. I. Mamasakhlisov and G. A. Chilashvili—661.
- Excitation of Rotational States in the Interaction Between Neutrons and Nuclei. V. N. Gribov—688.
- Investigation of Conversion Lines in the β-Spectrum of a $Eu^{152}-Eu^{154}$ Mixture. V. M. Kel'man, V. A. Romanov, R. Ia. Metskhvarishvili, and V. A. Koliunov—24.
- Model of a Semi-Transparent Nucleus with a Diffuse Boundary. II. P. E. Nemirovskii—932.
- Moment of Inertia of a System of Interacting Particles. A. S. Davydov and G. F. Fillipov—676.
- Neutron Emission by Excited RaD Nuclei. A. V. Kogan and L. I. Rusinov—365.
- Nuclear Saturation and the Levy–Klein Potential of Pseudoscalar Meson Theory. B. K. Kerimov—326L.
- On a Method of Direct Computation of the Nucleon-Nucleon Interaction Hamiltonian on the Basis of Experimental Values for the Levels of Light Nuclei. Iu. M. Shirokov, V. V. Balashov, and K. A. Tumanov—136L.
- On the Mechanism of Fission of Heavy Nuclei. V. V. Vladimirskii—673.
- On the Theory of Scattering of Particles by Nuclei. I. G. Ivanter and L. B. Okun'—340L.
- Quadrupole Momenta and the Zero-Point Surface Vibrations of Axially Symmetrical Nuclei. A. S. Davydov and G. F. Filippov—773L.

Optical Instruments (see Methods and Instruments)

Optical Properties (see also Luminescence)

- Electrical, Optical and Elastic Properties of Diamond Type Crystals. I. V. S. Mashkevich and K. B. Tolpygo—435.
- Energy Loss by a Charged Particle Passing Through a Laminar Dielectric, I. Ia. B. Fainberg and N. A. Khizhniak—720.
- Measurement of High Temperatures in Strong Shock Waves in Gases. I. Sh. Model'—589.
- On Radiation in Anisotropic Media. F. V. Bunkin—277.
- Optical Contact of Polished Glass Surfaces. I. V. Obreimov and E. S. Trekhov—235.
- Peculiarities of Cerenkov Radiation in Anisotropic Media. V. E. Pafomov—307L.
- Reflection of Gamma Rays from Bent Quartz Plates. O. I. Sumbaev—1042.
- Some New Possibilities of Ionic Phenomena in Metastable Liquids. G. A. Askar'ian—1011L.
- Surface Impedance of Metals in the Infrared Region. M. I. Kaganov and V. V. Slezov—1216.

Pair Production (see Electrons and Positrons)

Phosphors and Phosphorescence (see Luminescence; Semiconductors)

Photoconductivity (see **Electrical Conductivity and Resistance**)

Photodisintegration (see **Nuclear Photoeffects**)

Photoelectric Effect (see **Electrical Properties**)

Photography and Photographic Emulsions (see **Methods and Instruments; Optical Properties**)

Photometry (see **Methods and Instruments; Optical Properties**)

Photons (see **Radiation**)

Photovoltaic Effect (see **Electrical Properties; Semiconductors**)

Piezoelectric Effect (see **Dielectrics and Dielectric Properties**)

Polarization, Electrical (see **Dielectrics and Dielectric Properties**)

Positrons (see **Electrons and Positrons**)

Probability (see **Mathematical Methods**)

Protons (see **Elementary Particle Interaction**)

Quantum Electrodynamics (see also **Field Theory**)

- Application of a Renormalized Group to Different Scattering Problems in Quantum Electrodynamics. V. Z. Blank—759L.
- Bremsstrahlung of Polarized Electrons. G. L. Visotskii, A. A. Kresnin, and L. N. Rozentsveig—883.
- Bremsstrahlung of Ultra-Relativistic Particles in a Central Field. A. G. Sitenko—1223.
- Diffractive Production of Proton-Antiproton Pairs by High-Energy Photons. A. G. Sitenko and L. N. Rozentsveig—330L.
- Dispersion Relations for Photoproduction of Pions on Nucleons. A. A. Logunov and A. N. Tavkhelidze—1134.
- Electric Monopole Transitions of Atomic Nuclei. D. P. Grechukhin—846.
- Green Function in Scalar Electrodynamics in the Bloch-Nordsieck Approximation. R. V. Tevikain—1284L.
- Internal Compton Effect in Pair Conversion. E. G. Melikian—331L.
- Investigation of Conversion Lines in the β-Spectrum of a $Eu^{152}-Eu^{154}$ Mixture. V. M. Kel'man, V. A. Romanov, R. Ia. Metskhvarishvili, and V. A. Koliunov—24.
- Magnetic Interaction of Electrons and Anomalous Diamagnetism. B. T. Geilikman—981.
- Multiple Electron Production in a High Energy Electron-Photon Shower. A. A. Varfolomeev, R. I. Gerasimova, and V. A. Tumanian—792.
- Multiple Interaction Hamiltonians in Quantum Electrodynamics. G. F. Filimonov and Iu. M. Shirokov—84.
- On the Nonlinear Generalization of the Meson and Spinor Field Equations. D. F. Kurgelaidze—941.
- Phenomenological Study of the Effect of Nonconducting Medium in Quantum Electrodynamics. M. I. Riazanov—1013L.
- Photon Green Function Accurate to e^4. S. N. Sokolov—1029L.
- Polarization of Cerenkov Radiation. A. A. Sokolov and Iu. M. Loskutov—523L.
- Scale Transformation and the Virial Theorem in Quantum Field Theory. Iu. V. Novozhilov—138L.
- Two-Electron Green Function in the Bloch-Nordsieck Approximation. R. V. Tevikian—1282L.
- Vacuum Polarization in Mesonic Atoms. G. E. Pustovalov—1234.

Quantum Mechanics

- Contribution to the Theory of Collective Motion of Particles in Quantum Mechanical Systems. V. M. Eleonskii and P. S. Zyrianov—432.
- Diffraction Scattering of Fast Deuterons by Nuclei. A. I. Akhiezer and A. G. Sitenko—652.
- Electric Monopole Transitions of Atomic Nuclei. D. P. Grechukhin—846.
- Interaction Energy of Atoms for Small Nuclear Separations. O. B. Firsov—1192.
- Investigation of Conversion Lines in the β-Spectrum of a $Eu^{152}-Eu^{154}$ Mixture. V. M. Kel'man, V. A. Romanov, R. Ia. Metskhvarishvili and V. A. Koliunov—24.
- On Quantum Effects Occurring on Interaction of Electrons with High Frequency Fields in Resonant Cavities. V. L. Ginzburg and V. M. Fain—123L.
- On Quasi-Classical Single-Electron Wave Functions. N. I. Zhirnov—1021L.
- On the Construction of the Scattering Matrix II. The Theory with Nonlocal Interaction. B. V. Medvedev—48.
- On the Rarita–Schwinger Method in the Theory of Particles of Half-Integral Spin. E. E. Fradkin—1203.
- On the Statistical Interpretations of Quantum Theory. R. L. Stratonovich—1206.
- Quantum States of Particles Coupled to a Harmonically Oscillating Continuum with Arbitrarily Strong Interaction, I. V. M. Buimistrov and S. I. Pekar—970.
- Quantum Theory of Electrical Conductivity of Metals in a Magnetic Field. I. M. Lifshitz—1227.
- Some Problems Related to the Statistical Theory of Multiple Production of Particles. V. M. Maksimenko and I. L. Rozental'—546.
- Some Relativistic Properties of the Behavior of Spin-½ Particles. P. E. Kunin and I. M. Taksar—426.
- The Theory of Ferromagnetism of Metals and Alloys at Low Temperatures. E. I. Kondorskii and A. S. Pakhomov—269.

Quenching of Radiation (see **Radiation**)

Radar (see **Methods and Instruments; Radiation**)

Radiation (see also **Range and Energy Loss of Particles**)

- Bremsstrahlung of Polarized Electrons. G. L. Visotskii, A. A. Kresnin and L. N. Rozentsveig—883.

Concerning One Method of Measuring the Lifetimes of Excited States of Atomic Nuclei. A. F. Tulinov —1277L.

Effect of the Diffuseness of the Nuclear Boundary of Neutron Scattering. V. N. Gribov—537.

Electrical, Optical, and Elastic Properties of Diamond-Type Crystals II. Lattice Vibrations with Calculation of Atomic Dipole Moments. V. S. Mashkevich—707.

Energy Loss by a Charged Particle Passing Through a Laminar Dielectric. I. Ia. B. Fainberg and N. A. Khizhniak—720.

Fission of U, Th, Bi and Tl Induced by High Energy γ-Quanta. E. V. Minarik and V. A. Novikov—253.

Inelastic Interaction of Protons Having Energies Above 7 Bev with Carbon and Hydrogen Nuclei. K. I. Alekseeva and N. L. Grigorov—339L.

Investigation of the Penetrating Component of Electron-Nuclear Showers by the Delayed Coincidence Method in Conjunction with a Hodoscope. G. B. Zhdanov and A. A. Khaidarov—583.

On Radiation in Anisotropic Media. F. V. Bunkin—277.

On the Mechanism of Fission of Heavy Nuclei. V. V. Vladimirskii—673.

On the Structure of the Front of Strong Shock Waves in Gases. Iu. P. Raizer—1242.

Peculiarities of Cerenkov Radiation in Anisotropic Media. V. E. Pafomov—307L.

Polarization of Cerenkov Radiation. A. A. Sokolov and Iu. M. Loskutov—523L.

Radiation from a Point Charge, Moving Uniformly Along the Surface of an Isotropic Medium. A. I. Morozov—1028L.

Radiation of a Point Charge Moving Along the Boundary Between Two Media. V. E. Pafomov—504L.

Soft 15 – 800 Kev Radiation Accompanying the Thermal Neutron Fission of Uranium. V. K. Voitovetskii, B. A. Levin and E. V. Marchenko—184.

Structure of a Shock Wave in a Plasma. V. D. Shafranov—1183.

The Effect of Fast Neutron Irradiation on the Recombination of Electrons and Holes in Germanium Crystals. V. S. Vavilov, A. V. Spitsyn, L. S. Smirnov and M. V. Chukichev—579.

The Spatial Distribution of the Penetrating Component of Wide Atmospheric Showers. E. L. Andronikashvili and M. F. Bibilashvili—341L.

Thermal Radiation from an Anisotropic Medium. F. V. Bunkin—665.

Radioactivity (see also Nuclear Spectra)

Fine Structure of the α-Spectra of U^{234} and U^{238}. B. A. Bochagov, A. P. Komar, and G. E. Kocharov—1026L.

Fission of U, Th, Bi and Tl Induced by High Energy γ-Quanta. E. V. Minarik and V. A. Novikov—253.

Gadolinium Isotope with Mass 148. Ia. A. Gusev, O. M. Lilova, A. N. Murin, B. K. Breobrazhenskii, and V. A. Iakovlev—1295L.

Internal Conversion Electron Spectrum of Radiothorium. II. A. I. Zhernovoi, E. M. Krisiuk, G. D. Latyshev, A. S. Remennyi, A. G. Sergeev, and V. I. Fadeyev—563.

Neutron Emission by Excited RaD Nuclei. A. V. Kogan and L. I. Rusinov—365.

On the Interaction Between Lithium Ions and Matter. Ia. A. Teplova, I. S. Dmitriev, V. S. Nikolaev and L. N. Fateeva—792.

The Alpha Decay of Pu^{239}. G. I. Novikova, L. N. Kondrat'ev, Iu. P. Sobolev, and L. L. Gol'din—832.

Range and Energy Loss of Particles

Application of a Renormalization Group to Different Problems of Scattering in Quantum Electrodynamics. V. Z. Blank—759L.

Concerning a Possible Method for the Polarization of a Proton Beam. E. K. Zavoiskii—338L.

Effect of the Diffuseness of the Nuclear Boundary on Neutron Scattering. V. N. Gribov—5

Electron Loss Probabilities for Multiply-Charged Ions. I. S. Dmitriev—473.

Energy Loss of a Charged Particle Passing Through a Laminar Dielectric. I. Ia. B. Fainberg and N. A. Khizhniak—720.

Generation of Slow Mesons by Cosmic Ray Particles. D. K. Kaipov and Zh. S. Takibaev—569.

Inelastic Interaction of Protons Having Energies Above 7 Bev with Carbon and Hydrogen Nuclei. K. I. Alekseeva and N. L. Grigorov—339L.

Investigation of Slow Electron Emission Induced by High Energy Protons. E. S. Mironov and L. M. Nemenov—188.

Investigation of the Penetrating Component of Electron-Nuclear Showers by the Delayed Coincidence Method in Conjunction with a Hodoscope. G. B. Zhdanov and A. A. Khaidarov—583.

Ionization Losses of High Energy Heavy Particles. P. V. Vavilov—749.

Motion of a Charge Parallel to the Axis of a Cylindrical Channel in a Dielectric. L. S. Bogdankevich and B. M. Bolotovskii—1157.

On the Nature of the Cone-Like Shape of Tracks of Multi-Charged Ions in Nuclear Emulsions. O. V. Lozhkin—293.

Theory of Cyclotron Resonance in Metals. M. Ia. Azbel' and E. L. Kaner—730.

Rectifiers (see Electrical Conductivity and Resistance; Semiconductors)

Relativity and Gravitation

The Spatial Distribution of the Penetrating Component of Wide Atmospheric Showers. E. L. Andronikashvili and M. F. Bibilashvili—341L.

On the Dependence of the Motion of Bodies in a Gravitational Field on Their Mass. I. G. Fikhtengol'ts—898.

Application of the Dirac–Fock–Podolskii Method to a Mechanical Many-Body Problem. I. G. Fikhtengol'ts—1144.

On Magnetohydrodynamic Waves and Magnetic Tangential Discontinuities in Relativistic Hydrodynamics. I. M. Khalatnikov—901.

Nonlinearity of the Field in Conformal Reciprocity Theory. A. Popovici—642.

Resistance, Electrical (see Electrical Conductivity and Resistance)

Resonance Radiation (see Radiation)

Scattering, General (see also Elementary Particle Interactions; Nuclear Reactions; Range and Energy Loss of Particles)

Angular Operators for Nuclear Reactions. V. I. Ritus—1249.

Application of Correlation Polarization in the Phase Analysis of *p–p* Scattering. A. G. Zimin—1008L.

Coherent Scattering and Radiation of Electromagnetic Waves by a Plasma in an Inhomogeneous Magnetic Field. G. A. Askarian—1285L.

Concerning a Possible Method for the Polarization of a Proton Beam. E. K. Zavoiskii—338L.

Contribution to the Theory of Exchange Collisions Between Fast Nucleons and Deuterons. L. I. Lapidus—1170.

Elastic Small Angle Scattering of Neutrons by Heavy Nuclei. V. S. Barashenkov, I. P. Stakhanov, and Iu. A. Aleksandrov—144L.

Equilibrium Spectrum of Electrons and Photons with Account of Scattering. I. P. Ivanenko—204.

Inelastic Interaction of Protons Having Energies Above 7 Bev with Carbon and Hydrogen Nuclei. K. I. Alekseeva and N. L. Grigorov—339L.

Minami Transformation for Nucleon-Nucleon Scattering. R. M. Ryndin and Ia. A. Smorodinskii—976.

On the Theory of Scattering of Particles by Nuclei. I. G. Ivanter and L. B. Okun'—340L.

Polarization Correlation in Nucleon-Nucleon Scattering. A. G. Zimin—996.

Polarization in Reverse Reactions. A. I. Baz'—521L.

Polarization of Deuterons in Elastic Scattering. O. D. Cheishvili—1009L.

Relation Between Scattering and Multiple Particle Production. S. Z. Belenkii—952.

Scattering of Photons by Protons. A. M. Baldin and V. A. Petrun'kin—1279L.

The Character of Nucleonic Forces. A. Z. Dolginov—506L.

The Construction of a Phenomenological Scattering Matrix with Nonlocal Interaction. V. S. Barashenkov—313L.

The Effect of a Longitudinal Magnetic Field on the Multiple Scattering of Particles. N. A. Chernikov—320L.

Theory of Diffuse Scattering of X-Rays and Thermal Neutrons. M. A. Krivoglaz—1115.

Unitarity Relationships for Elastic Collisions of Particles with Arbitrary Spins. R. M. Ryndin and Ia. A. Smorodinskii—1294L.

Scattering of Deuterons

Diffraction Scattering of Fast Deuterons by Nuclei. A. I. Akhiezer and A. G. Sitenko—652.

Elastic and Quasi-Elastic Scattering of 660 Mev Protons by Deuterons. G. A. Leksin—371.

On the Absolute Value of the Stripping Cross Section for Diffraction Disintegration of the Deuteron. I. I. Ivanchik—133L.

Polarization of Deuterons in Elastic Scattering. O. D. Cheishvili—1009L.

Scattering of Electrons and Positrons (see also Electrons and Positrons)

Correlations in $\pi\rightarrow\mu\rightarrow e$-Decay. A. O. Vaisenberg and V. A. Smirnitskii—1093.

Elastic Small Angle Scattering of Neutrons by Heavy Nuclei. V. S. Barashenkov, I. P. Stakhanov, and Iu. A. Aleksandrov—144L.

Effect of the Diffuseness of the Nuclear Boundary on Neutron Scattering. V. N. Gribov—537.

On the Structure of Nucleons. I. E. Tamm—154L.

Polarization Effects in the Scattering of Electrons and Positrons on Electrons. A. A. Kresnin and L. N. Rozentsveig—288.

Polarization of Electrons in β-Decay. A. I. Alikhanov, G. P. Eliseev, V. A. Liubimov and B. V. Ershler—1097.

Scattering of Mesons (see also Nuclear Reactions Induced by Mesons)

Asymptotic Meson-Meson Scattering Theory. I. T. Diatlov, V. V. Sudakov, and K. A. Ter-Martirosian—631.

Dispersion Relations for Photoproduction of Pions on Nucleons. A. A. Logunov and A. N. Tavkhelidze—1134.

Elastic Scattering of 360 Mev Positive π-Mesons by Protons. N. A. Mitin and E. L. Grigor'ev—378.

On the Derivation of the Low Equation in the Theory of Meson Scattering. A. M. Brodskii—509L.

On the Theory of Scattering of Particles by Nuclei. I. G. Ivanter and L. B. Okun'—340L.

Electron-Positron Pair Production in Collisions Between Fast π-Mesons and Nucleons. E. M. Rabinovich—1272.

- Relation Between Scattering and Multiple Particle Production. S. Z. Belenkii—952.
- Scattering of K-Mesons with Change of Intrinsic Parity. V. B. Bereststskii and Iu. A. Bychkov—150L.
- Scattering of π-Mesons on Nucleons in Higher Approximations of the Tamm–Dancoff Method. Iu. M. Popov—131L.
- The Interaction Cross Section of π-Mesons and Nucleons at High Energies. P. V. Vavilov—768L.

Scattering of Neutrons (see also **Nuclear Reactions Induced by Neutrons**)
- A New Method for Measurement of Polarization of Medium Energy Neutrons and the Phase Shift Analysis of n-He^4 Scattering. I. I. Levintov, A. V. Miller and V. N. Shamshev—258.
- Bremsstrahlung and Pair Production at High Energies in Condensed Media. A. B. Migdal—527.
- Calculation of the Polarization of Neutrons on the Basis of the Diffused Edge Nuclear Model. P. E. Nemirovskii and Iu. P. Elagin—1293L.
- Elastic Small Angle Scattering of Neutrons by Heavy Nuclei. V. S. Barashenkov, I. P. Stakhanov and Iu. A. Aleksandrov—144L.
- Magnetic Interaction of Electrons and Anomalous Diamagnetism. B. T. Geilikman—981.
- Model of a Semi-Transparent Nucleus with a Diffuse Boundary II. P. E. Nemirovskii—932.
- On the Second Approximation in the Problem of Slow Neutron Scattering by Bound Protons. A. S. Davydov and D. M. Mel'nichenko—769L.
- Optical Model of the Interaction of Nucleons with Nuclei in the Resonance Region of the Compound Nucleus. V. M. Agranovich and A. A. Davydov—1164.
- π^0-Meson Production in p–p and p–n Collisions in the 390–660 Mev Energy Region. Iu. D. Prokoshkin and A. A. Tiapkin—618.
- Production of Neutral Pions by Neutrons and Deuterons and Complex Nuclei. V. P. Dzhelepov, K. O. Oganesian and V. B. Fliagin—562.
- Reconstruction of the Scattering Matrix of a Two-Nucleon System. L. Puzikov, R. Ryndin and Ia. Smorodinskii—489.
- Theory of Diffuse Scattering of X-Rays and Thermal Neutrons. M. A. Krivoglaz—1115.

Scattering of Protons (see also **Nuclear Reactions Induced by Protons**)
- Application of Correlation Polarization in the Phase Analysis of p–p Scattering. A. G. Zimin—1008L.
- Concerning a Possible Method for the Polarization of a Proton Beam. E. K. Zavoiskii—338L.
- Elastic and Quasi-Elastic Scattering of 660 Mev Protons by Deuterons. G. A. Leksin—371.
- Elastic Scattering of 360 Mev Positive π-Mesons by Protons. N. A. Mitin and E. L. Grigor'ev—378.
- Inelastic Interaction of Protons Having Energies Above 7 Bev with Carbon and Hydrogen Nuclei. K. I. Alekseeva and N. L. Grigorov—339L.
- Inelastic Proton-Proton Scattering. Iu. I. Kulakov—477.
- Investigation of the Energy and Angle Distributions of Neutral Pions Produced by 470 and 660 Mev Protons in Carbon. Iu. D. Baiukov, M. S. Kozodaev, and A. A. Tiapkin—552.
- Minami Transformation for Nucleon-Nucleon Scattering. R. M. Ryndin and Ia. A. Smorodinskii—976.
- π^0-Meson Production in p–p and p–n Collisions in the 390–660 Mev Energy Region. Iu. D. Prokoshkin and A. A. Tiapkin—618.
- Polarization Correlation in Nucleon-Nucleon Scattering. A. G. Zimin—996.
- Production of π^+-Mesons in p–p Collisions at 480–660 Mev. B. S. Neganov and O. V. Savchenko—1033.
- Reconstruction of the Scattering Matrix of a Two-Nucleon System. L. Puzikov, R. Ryndin and Ia. Smorodinskii—489.
- Scattering of Fast Protons on Protons. D. I. Blokhintsev—284.
- The Character of Nucleonic Forces. A. Z. Dolginov—506L.

Scattering of Radiation (see **Radiation**)

Scintillation Counters (see **Methods and Instruments**)

Secondary Emission (see **Electrical Properties**)

Semiconductors
- Electrical, Optical and Elastic Properties of Diamond-Type Crystals. I. V. S. Mashkevich—435.
- Energy Loss by a Charged Particle Passing Through a Laminar Dielectric. Ia. B. Fainberg and N. A. Khizhniak—720.
- Investigation of the Penetrating Component of Electron-Nucleon Showers by the Delayed Coincidence Method in Conjunction with a Hodoscope. G. B. Zhdanov and A. A. Khaidarov—583.
- On the Possible Mechanism for the Increase of Conductivity of Atomic Semiconductors in a Strong Electric Field. F. G. Bass—705.
- On the Exciton Mechanism for Capture of Current Carriers in Homopolar Semiconductors. V. L. Bonch-Bruevich—1196.
- On the Structure of the Electron Spectrum in Lattices of the Tellurium Type. Iu. A. Firsov—1101.
- Remarks on the Theory of the Electron Plasma in Semiconductors. V. L. Bonch-Bruevich—894.
- Structural Characteristics of Antimony Sulfide Layers. V. N. Vertsner, B. V. Gorbunov and Ia. A. Oksman—782.

The Effect of Fast Neutron Irradiation on the Recombination of Electrons and Holes in Germanium Crystals. V. S. Vavilov, A. V. Spitsyn, L. S. Smirnov and M. V. Chukichev—579.
The Photoconductivity of Cuprite. A. N. Krongauz, V. K. Liapidevskii, and Iu. S. Deev—828.
The Problem of Saturation of the Hall "Constant" in Semiconductors in Strong Magnetic Fields. F. G. Bass and M. I. Kaganov—1002.

Solid State (see Crystalline State)

Solutions (see Liquids)

Sound (see Acoustics)

Spallation (see Nuclear Reactions)

Spark Discharge (see Electrical Discharges)

Spectra, Atomic (see Atomic Structure and Spectra)

Spectra, General

Application of Correlation Polarization in the Phase Analysis of p–p Scattering. A. G. Zimin—1008L.
Electrical, Optical and Elastic Properties of Diamond-Type Crystals II. Lattice Vibrations with Calculation of Atomic Dipole Moments. V. S. Mashkevich—707.
Energy Loss by a Charged Particle Passing Through a Laminar Dielectric. Ia. B. Fainberg and N. A. Khizhniak—720.
Measurement of High Temperatures in Strong Shock Waves in Gases. I. Sh. Model'—589.
Investigation of Fission γ-Rays in the Energy Region up to 250 kev. V. V. Skliarevskii, D. E. Fomenko and E. P. Stepanov—220.
Natural Line Widths of Microwaves. V. M. Fain—501L.

Spectra, Nuclear (see Nuclear Spectra)

Spectroscopy Technique (see Methods and Instruments)

Spinor Fields (see Field Theory)

Stark Effect (see Atomic Structure and Spectra)

Statistical Mechanics and Thermodynamics

Bremsstrahlung of Polarized Electrons. G. L. Visotskii, A. A. Kresnin, and L. N. Rozentsveig—883.
Construction of the Thermodynamical Potential of Rochelle Salt from the Results of the Optical Investigation of Domains. V. L. Indenbom and M. A. Chernysheva—575.
Equations with Variational Derivatives in Statistical Equilibrium Theory. I. P. Bazarov—872.
Fluctuations in Gases. B. B. Kadomtsev—771L.
Investigations of the Equation of State by Mechanical Measurements. Ia. B. Zel'dovich—1287L.
Photoconductivity of Cuprite. A. N. Krongauz, Iu. S. Deev and V. K. Liapidevskii—828.
Reflection of Gamma Rays by Bent Plates. O. I. Sumbaev—1042.
Simplification of the Equations for the Distribution Function of Electrons in a Plasma. A. V. Gurevich—1006L.
Soft 15–800 Kev Radiation Accompanying the Thermal Neutron Fission of Uranium. V. K. Voitovetskii, B. A. Levin and E. V. Marchenko—184.
Some Problems Related to the Statistical Theory of Multiple Production of Particles. V. M. Maksimenko and I. L. Rozental'—546.
Statistical Theory of Systems of Charged Particles with Account of Short Range Forces of Repulsion. I. P. Bazarov—946.
Structure of Superconductors, X. N. N. Zhuravlev—1064.
Structure of Superconductors, XI. N. N. Zhuravlev and L. Kertes—1073.
Theory of Diffuse Scattering of X-Rays and Thermal Neutrons in Solid Solutions. II. M. A. Krivoglaz—1115.
Thermodynamical Theory of Weak Ferromagnetism in Antiferromagnetic Substances. I. E. Dzialoshinskii—1259.

Statistical Methods (see Mathematical Methods)

Superconductivity

Calculation of the Drift Velocity of Ions in the Electric Field in Their Gas. V. I. Perel'—440.
Discontinuous Attenuation of Current in a Superconducting Ring. A. A. Galkin, Ia. S. Kan, and B. G. Lazarev—1292L.
Effect of Fast Neutron Irradiation on Recombination of Electrons and Holes in Germanium Crystals. V. S. Vavilov, A. V. Spitsyn, L. S. Smirnov and M. V. Chukichev—579.
Equations with Variational Derivatives in Statistical Equilibrium Theory. I. P. Bazarov—872.
Fluctuations in Gases. B. B. Kadomtsev—771L.
Force Fluctuations in an Electron Gas. M. Ia. Mints—319L.
Hall Effect and Susceptibility of Gold. N. E. Alekseevskii and Iu. P. Gaidukov—1301L.
Hydrodynamic Fluctuations. L. D. Landau and E. M. Lifshitz—512L.
On the Magnetic Properties of Superconductors of the Second Group. A. A. Abrikosov—1174.
Simplification of the Equations for the Distribution Function of Electrons in a Plasma. A. V. Gurevich—1006L.
Statistical Theory of a System of Charged Particles with Account of Short Range Repulsion Forces. I. P. Bazarov—946.
Structure of Superconductors, XI. Investigation of Alloys of Bismuth with Platinum, Ruthenium, Osmium and Iridium. N. N. Zhuravlev and I. Kertes—1073.
The Application of the Microcanonical Distribution to the Statistical Theory of Multiple Production of Particles. V. B. Magalinskii and Ia. P. Terletskii—483.

The Momentum Distribution of Interacting Fermi Particles. A. B. Migdal—333L.
Thermodynamical Theory of "Weak" Ferromagnetism in Antiferromagnetic Substances. I. E. Dzialoshinsky—1259.

Thermal Properties
Absorption of Sound in a Phase Change in Rochelle Salt. I. A. Iakovlev, T. S. Velichkina and K. N. Baranskii—762L.
Concerning the Temperature Dependence of the Photoelectromotive Force. F. F. Kodzhespirov—1304L.
Construction of the Thermodynamical Potential of Rochelle Salt from the Results of the Optical Investigation of Domains. V. L. Indenbom and M. V. Chernysheva—575.
Electrical, Optical, and Elastic Properties of Diamond-Type Crystals II. V. S. Mashkevich—707.
On the Structure of the Front of Strong Shock Waves in Gases. Iu. P. Raizer—1242.
On the Theory of Skin Effect in Metals. M. Ia. Azbel'—1027L.
Structure of Superconductors, X. N. N. Zhuravlev—1064.
The Structure of a Shock Wave in a Plasma. V. D. Shafranov—1183.
Theory of Diffusion and Thermal Conductivity for Dilute Solutions of He^3 in Helium II. I. M. Khalatnikov and V. N. Zharkov—905.
Thermal Conductivity and Thermoelectric Phenomena in Metals in a Magnetic Field. M. Ia. Azbel', M. I. Kaganov, and I. M. Lifshitz—967.
Thermal Radiation from an Anisotropic Medium. F. V. Bunkin—665.

Thermionic Emmission (see Electrical Properties)
Thermodynamics (see Statistical Mechanics and Thermodynamics)
Thermoelectric Effect (see Electrical Properties; Semiconductors)
Thermoluminescence (see Luminescence)
Total Cross Sections (see Electrons and Positrons; Nuclear Reactions)
Uncertainty Principle (see Quantum Mechanics)
Vacuum Tubes (see Methods and Instruments)
Viscosity (see Liquids)
Wave Mechanics (see Quantum Mechanics)
Work Function (see Electrical Properties)

X-Rays
Bremsstrahlung of Polarized Electrons. G. L. Visotskii, A. A. Kresnin, and L. N. Rozentsveig—883.
Concerning the Temperature Dependence of the Photoelectromotive Force. F. F. Kodzhespirov—1304L.
Effect of Fast Neutron Irradiation on Recombination of Electrons and Holes in Germanium Crystals. V. S. Vavilov, A. V. Spitsyn, L. S. Smirnov and M. V. Chukichev—579.
Energy Loss by a Charged Particle Passing Through a Laminar Dielectric. Ia. B. Fainberg and N. A. Khizhniak—720.
Explosion of a Metal by an Electric Current. S. V. Lebedev—243.
Heat Capacity of KCl. T. I. Kucher—114L.
Heat Capacity of Laminar Lattices at Low Temperatures. E. S. Itskevich and P. G. Strelkov—394.
On the Mechanism of Fission of Heavy Nuclei. V. V. Vladimirskii—673.
On the Structure of the Front of Strong Shock Waves in Gases. Iu. P. Raizer—1242.
Reflection of Gamma Rays from Bent Quartz Plates. O. I. Sumbaev—1042.
Structure of Shock Waves in a Plasma. V. D. Shafranov—1183.
Structure of Superconductors, X. N. N. Zhuravlev—1064.
Structure of Superconductors, XI. Investigation of Alloys of Bismuth with Platinum, Ruthenium, Osmium and Iridium. N. N. Zhuravlev and I. Kertes—1073.
The Photoconductivity of Cuprite. A. N. Krongauz, V. K. Liapidevskii, and Iu. S. Deev—828.
Theory of Diffuse Scattering of X-Rays and Thermal Neutrons in Solid Solutions. II. M. A. Krivoglaz—1115.
Theory of Diffusion and Thermal Conductivity of Dilute He^3 Solutions in Helium II. I. M. Khalatnikov and V. N. Zharkov—905.
Theory of Skin Effect in Metals. M. Ia. Azbel'—1027L.
Thermal Conductivity and Thermoelectric Phenomena in Metals in a Magnetic Field. M. Ia. Azbel', M. I. Kaganov, and I. M. Lifshitz—967.

SOVIET PHYSICS JETP VOLUME 5, NUMBER 6 DECEMBER 15, 1957

ERRATA TO VOLUME 5

We are indebted to Mr. D. A. Kirzhnits of the P. N. Lebedev Physics Institute, Academy of Sciences, U.S.S.R. for calling our attention to a few regrettable errors in the translation of his article "Quantum Corrections to the Thomas–Fermi Equation" [Soviet Phys. JETP 5, 64–71 (August, 1957); original in J. Exptl. Theoret. Phys. (U.S.S.R.) 32, 115–123 (January, 1957)].

P. 66, column 1 – the text following Eq. (11) **should read**

> Concrete form of this function should be given additionally. Thus, if we are interested in a non-degenerate Fermi gas, then
>
> $$\hat{\rho} = 2\left[\exp\left(\frac{\hat{H} - E_0}{kT}\right) + 1\right]^{-1}.$$
>
> In the case of a degenerate gas, which will be considered below
>
> $$\hat{\rho} = 1 - \varepsilon(\hat{H} - E_0), \quad \varepsilon(x) = x / |x|. \qquad (12)$$

Additional errata are:

P. 68, column 1, 9 lines above Eq. (23)	**reads**	$Z^{-1/3}$	**should read**	$Z^{-2/3}$
P. 68, column 2, first line after Eq. (26)	**reads**	$Z^{-3/2}$	**should read**	$Z^{-2/3}$
P. 68, column 2, 14th line from bottom	**reads**	$E = -0.769\, Z^{7/2}$	**should read**	$E = -0.769\, Z^{7/3}$
P. 68, column 2, 10th line from bottom	**reads**	$r^{-2/3}$	**should read**	$r^{-3/2}$

P. 69, column 2, the following table was omitted

Atomic Number Z	δ, Thomas–Fermi	δ, Thomas–Fermi–Dirac	δ, Thomas–Fermi–Dirac with Weizsaecker correction	δ, from Eq. (27)	Variational parameters	
					β	$\lambda \cdot 10^{-8}$
10	−28	−36	+34	−7	4.0	0.24
18	−25	−30	+29	−6	4.3	0.56
36	−21	−25	+24	−6	4.7	3.5
54	−20	−23	+21	−5	5.0	7.6

Other Errata

Page	Column	Line	Reads	Should Read
		Volume 4		
38	1	Eq. (3)	$\ldots\frac{\pi r^2\rho^2\rho^2_n}{\rho_s^2},$	$\ldots\frac{\pi r^2\rho^2\rho_n}{\rho_s^2},$
196		Date of submittal	May 7, 1956	May 7, 1955
377	1	Caption for Fig. 1	$\delta_{35}=\eta-21\cdot\eta^5$	$\delta_{35}=-21^\circ\eta^5$.
377	2	Caption for Fig. 2	$\alpha_3=6.3^\circ\ \eta$	$\alpha_3=-6.3^\circ\eta$
516	1	Eq. (29)	$s^2/c^2\ldots$	s/c
516	2	Eqs. (31) and (32)	Replace A_1s^2/c^2 by A_1	
497		Date of submittal	July 26, 1956	July 26, 1955
900	1	Eq. (7)	$\ldots\frac{i}{4\pi}\sum_{c,\,\alpha}\frac{\partial w_a(t,P)}{\partial P^\alpha}\ldots$	$\ldots\ 2\pi^2 i\sum_{c,\,\alpha}\ldots$
			(This causes a corresponding change in the numerical coefficients in the expressions that result from the calculation of the effects of the plasma particles on each other).	
804	2	Eq. (1)	$\ldots\ \exp\{-(\overline{T}-V')\}$	$\ldots\ \exp\{-(\overline{T}-V')\tau^{-1}\}$
		Volume 5		
59	1	Eq. (6)	$v_l(1\partial F_0/\partial \mathrm{x})+\ldots$ where E_l is the projection of the electric field E on the direction 1	$\overline{(\mathrm{v}\partial F_0/\partial \mathrm{x})}+\ldots$ where the bar indicates averaging over the angle θ and E_l is the projection of the electric field E along the direction 1
91	2	Eq. (26)	$\Lambda=0.84\,(1+22/A)$	$\Lambda=0.84/(1+22/A)$
253		First line of summary	$\mathrm{Tl}^{204,\ 206}$	$\mathrm{Tl}^{203,\ 205}$
318	1	Figure caption	$\ldots\ e^2mc^2=2.8\cdot10^{-23}$ cm,	$\ldots e^2/mc^2=2.8\cdot10^{-13}$ cm,
398		Figure caption	... to a cubic relation. A series of points etc.	... to a cubic relation, and in the region 10 – 20°K to a quadratic relation. A series of points ●, coinciding with points ○, have been omitted in the region above 10°K.

CONTENTS – *continued*

Russian Reference

Bremsstrahlung of Ultra-Relativistic Particles in a Central Field . . . . . . A. G. Sitenko 1223 32, 1505

Quantum Theory of the Electrical Conductivity of Metals in a Magnetic Field . . . . . . I. M. Lifshitz 1227 32, 1509

Vacuum Polarization in Mesonic Atoms . . . . . . G. E. Pustovalov 1234 32, 1519

On the Structure of the Front of Strong Shock Waves in Gases . . . . . . Iu. P. Raizer 1242 32, 1528

Angular Operators for Nuclear Reactions . . . . . . V. I. Ritus 1249 32, 1536

Thermodynamical Theory of "Weak" Ferromagnetism in Antiferromagnetic Substances. . . . . . . I. E. Dzialoshinskii 1259 32, 1547

Electron-Positron Pair Production in Collisions between Fast π-Mesons and Nucleons. . . . . . . E. M. Rabinovich 1272 32, 1563

Letters to the Editor

On Bubble Chambers . . . . . . P. V. Vavilov 1276 32, 1567

Concerning One Method of Measuring the Lifetimes of Excited States of Atomic Nuclei. . . . . . . A. F. Tulinov 1277 32, 1568

Scattering of Photons by Protons . . . . . . A. M. Baldin and V. A. Petrun'kin 1279 32, 1570

Use of a Mixture of Two Liquids in Bubble Chambers . . . . . . G. A. Blinov, Iu. S. Krestnikov, M. F. Lomanov, and Ia. Ia. Shalamov 1281 32, 1572

Two-Electron Green Function in the Bloch-Nordsieck Approximation . . . . . . R. V. Tevikian 1282 32, 1573

Green Function in Scalar Electrodynamics in the Bloch-Nordsieck Approximation . . . . . . R. V. Tevikian 1284 32, 1575

Coherent Scattering and Radiation of Electromagnetic Waves by a Plasma in an Inhomogeneous Magnetic Field . . . . . . G. A. Askarian 1285 32, 1576

Investigations of the Equation of State by Mechanical Measurements . . . . . . Ia. B. Zel'dovich 1287 32, 1577

Beta Emission from Polarized Nuclei . . . . . . G. R. Khutsishvili 1288 32, 1578

Electronic Resonance in Current-Carrying Solutions . . . . . . A. A. Galkin, Ia. L. Shamfarov, and A. V. Stefanishina 1291 32, 1581

Discontinuous Attenuation of Current in a Superconducting Ring . . . . . . A. A. Galkin, Ia. S. Kan, and B. G. Lazarev 1292 32, 1582

Calculation of the Polarization of Neutrons on the Basis of the Diffused Edge Nuclear Model . . . . . . P. E. Nemirovskii and Iu. P. Elagin 1293 32, 1583

Unitarity Relationships for Elastic Collisions of Particles with Arbitrary Spins . . . . . . R. M. Ryndin and Ia. A. Smorodinskii 1294 32, 1584

Gadolinium Isotope with Mass 148 . . . . . . Ia. A. Gusev, O. M. Lilova, A. N. Murin, B. K. Breobrazhenskii, and V. A. Iakovlev 1295 32, 1585

Possibility of Constructing a Chain of Equations for Model Operators . . . . . . V. M. Eleonskii 1296 32, 1585

Some Remarks on Slow Processes of Transformation of Elementary Particles . . . . . . L. Okun' and B. Pontecorvo 1297 32, 1587

Anomalous Decay of a Hypernucleus . . . . . . A. P. Grigor'ev, E. P. Toporkova, and A. I. Fesenko 1299 32, 1589

Hall Effect and Susceptibility of Gold . . . . . . N. E. Alekseevskii and Iu. P. Gaidukov 1301 32, 1589

Ejection of Electrons from Metals by Fast Molecules . . . . . . A. M. Furman 1302 32, 1591

Concerning the Temperature Dependence of the Photoelectromotive Force . . . . . . F. F. Kodzhespirov 1304 32, 1593

Author Index to Volume 5 . . . . . . 1306 32, 1595

Analytic Subject Index to Volume 5 1316

SOVIET PHYSICS JETP VOLUME 5, NUMBER 6 DECEMBER 15, 1957

CONTENTS

Russian Reference

Production of π^+-Mesons in $p-p$ Collisions at 480 – 660 Mev . . . B. S. Neganov and O. V. Savchenko 1033 32, 1265
Reflection of Gamma Rays from Bent Quartz Plates . . . O. I. Sumbaev 1042 32, 1276
Determination of Mass of Slow Charged Particles in Photographic Plates . . . M. I. Tret'iakova 1045 32, 1280
Interaction of Nitrogen and Gold Nuclei . . . S. A. Baboshkin, A. S. Karamian, and G. N. Flerov 1055 32, 1294
Fission of Nuclei under the Influence of Accelerated Nitrogen Nuclei . . . V. A. Druin, S. M. Polikanov, and G. N. Flerov 1059 32, 1298
Structure of Superconductors, X. Thermal, Microscopic, and X-ray Investigation of the Bismuth-Palladium System . . . N. N. Zhuravlev 1064 32, 1305
Structure of Superconductors, XI. Investigation of Alloys of Bismuth with Platinum, Ruthenium, Osmium and Iridium . . . N. N. Zhuravlev and I. Kertes 1073 32, 1313
The Penetrating Component of Extensive Cosmic Ray Showers in the Atmosphere . . . Iu. N. Vavilov, Iu. F. Evstigneev, and S. I. Nikol'skii 1078 32, 1319
Pion Production in Zero Isotopic Spin Nuclei . . . A. G. Meshkovskii, Iu. S. Pligin, Ia. Ia. Shalamov, and V. A. Shebanov 1085 32, 1328
Angular and Energy Distribution of Photoprotons from Be^9 and C^{12} . . . I. V. Chuvilo and V. G. Shevchenko 1090 32, 1335
Correlations in $\pi\rightarrow\mu\rightarrow e$-Decay . . . A. O. Vaisenberg and V. A. Smirnitskii 1093 32, 1340
Polarization of Electrons in β-Decay . . . A. I. Alikhanov, G. P. Eliseev, V. A. Liubimov, and B. V. Ershler 1097 32, 1344
On the Structure of the Electron Spectrum in Lattices of the Tellurium Type . . . Iu. A. Firsov 1101 32, 1350
Theory of Diffuse Scattering of X-Rays and Thermal Neutrons in Solid Solutions. II. Microscopic Theory . . . M. A. Krivoglaz 1115 32, 1368
Interaction between Current Carriers and F-Centers and the Acoustic Vibrations of the Lattice in Ionic Crystals . . . M. F. Deigen and V. L. Vinetskii 1125 32, 1382
Dispersion Relations for Photoproduction of Pions on Nucleons . . . A. A. Logunov and A. N. Tavkhelidze 1134 32, 1393
Application of the Dirac-Fock-Podol'skii Method to a Mechanical Many-Body Problem . . . I. G. Fikhtengol'ts 1144 32, 1404
Excitation of Rotational States in α-Decay of Even-Even Nuclei . . . V. M. Strutinskii 1150 32, 1412
Motion of a Charge Parallel to the Axis of a Cylindrical Channel in a Dielectric . . . L. S. Bogdankevich and B. M. Bolotovskii 1157 32, 1421
Optical Model of the Interaction of Nucleons with Nuclei in the Resonance Region of the Compound Nucleus . . . V. M. Agranovich and A. S. Davydov 1164 32, 1429
Contribution to the Theory of Exchange Collisions between Fast Nucleons and Deuterons . . . L. I. Lapidus 1170 32, 1437
On the Magnetic Properties of Superconductors of the Second Group . . . A. A. Abrikosov 1174 32, 1442
The Structure of a Shock Wave in a Plasma . . . V. D. Shafranov 1183 32, 1453
On the Angular Distribution of Deuterons from the $\text{Be}^9_4(pd)\text{Be}^8_4$ Reaction . . . D. P. Grechukhin 1188 32, 1460
Interaction Energy of Atoms for Small Nuclear Separations . . . O. B. Firsov 1192 32, 1464
On the Exciton Mechanism for Capture of Current Carriers in Homopolar Semiconductors . . . V. L. Bonch-Bruevich 1196 32, 1470
On the Rarita-Schwinger Method in the Theory of Particles of Half-Integral Spin . . . E. E. Fradkin 1203 32, 1479
On the Statistical Interpretations of Quantum Theory . . . R. L. Stratonovich 1206 32, 1483
Surface Impedance of Metals in the Infrared Region . . . M. I. Kaganov and V. V. Slezov 1216 32, 1496

(Contents continued on inside back cover)